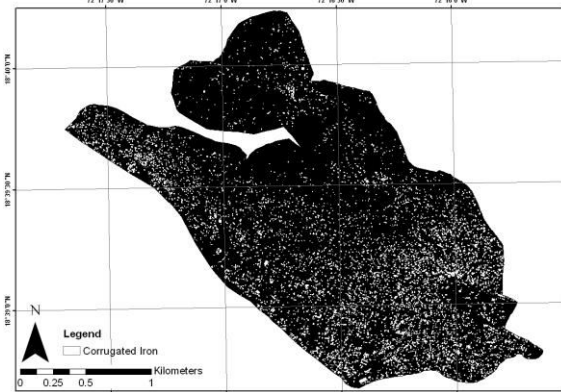
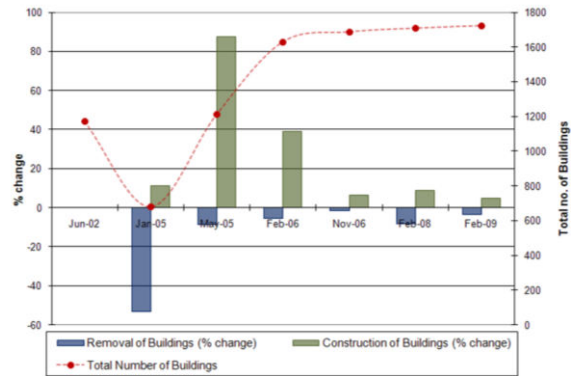
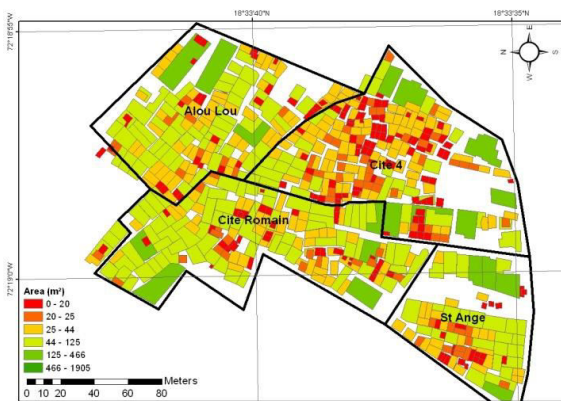


# THE USE OF GEOSPATIAL TOOLS TO SUPPORT, MONITOR AND EVALUATE POST-DISASTER RECOVERY



Daniel Michael Brown

Magdalene College

Department of Architecture

University of Cambridge

This dissertation is submitted for the degree of

*Doctor of Philosophy*

March 2017

## Cover Page

The illustrations on the cover page demonstrate the diverse ways geospatial tools were used to support post-disaster recovery throughout this research.

Top-left: Residents of the Delmas 19 slum in Port-au-Prince, Haiti using maps as part of the Participatory Approach for Safe Shelter Awareness (PASSA) after the 2010 Haiti earthquake.

Top-right: Quantification of building numbers and construction rates overtime in Ban Nam Khem, Thailand following the 2004 Indian Ocean tsunami.

Bottom-left: Rapid manual aerial assessment of building size in the Delmas 19 slum, Port-au-Prince after the 2010 Haiti earthquake.

Bottom-right: Semi-automated mapping of spontaneous settlement processes for UN-Habitat after the 2010 Haiti earthquake.

## Abstract

The aim of this research is to test the feasibility of using remote sensing-based information products and services to support the planning, monitoring and evaluation of recovery after disaster. The thesis begins by outlining the process of post-disaster recovery, what it entails and who is involved. The data and information needs at different stages of the disaster cycle are introduced and the importance of monitoring and evaluating post-disaster recovery is discussed.

The literature review introduces the high-spatial-resolution remote sensing market and the technology focusing on current sensors' capabilities. This is followed by a review of previous attempts to measure post-disaster recovery by practitioners and academics. At the end of the chapter a list of recovery indicators, suitable for remote sensing analysis, are presented and assessed through a user needs survey.

In chapter 3, the six recovery categories and thirteen indicators identified in the literature review form a framework for the retrospective analysis of recovery in Thailand and Pakistan. A selection of results is presented to demonstrate the usefulness of remote sensing as a recovery monitoring tool. To assess its reliability, the results from the satellite image analysis are triangulated against narratives and datasets acquired on the ground.

The next two chapters describe work done whilst providing real-time support to two humanitarian agencies operating in Port-au-Prince one-and-a-half years after the 2010 Haiti earthquake. Chapter 4 describes how geospatial tools were used to support a British Red Cross integrated reconstruction project for 500 households living in an informal settlement. The chapter describes how geospatial tools were used as a rapid assessment tool, and to support cadastral and enumeration mapping and the community participatory process. While previous chapters focus on the *manual* analysis of satellite imagery, chapter 5 reports how *semi-automatic* analyses of satellite imagery were used to support UN-Habitat by monitoring a planned camp and large-scale instances of spontaneous settlement.

The conclusion to the thesis summarises the key lessons learnt from the retrospective analysis of recovery in Thailand and Pakistan and the real-time application in Haiti. Recommendations are then made on how to effectively use remote sensing in support of post-disaster recovery focussing on what to measure, when and how. Recognising that a mixed-method approach can best monitor recovery, recommendations are also made on how to integrate remote sensing with existing tools.

## Table of Contents

<b>Chapter 1</b>	<b>Introduction</b>	<b>1-1</b>
1.1	Post-disaster Recovery	1-5
1.2	Data after Disasters	1-8
1.3	Recovery Project Operational Phases	1-8
1.4	The Need for Monitoring and Evaluating (M&E) Post-Disaster Recovery	1-10
1.5	Current Tools	1-13
1.6	Aims of Thesis	1-14
1.7	EPSRC Recovery Project (2008-2011) and EPSRC Follow-up Project (2011-2012)	1-16
1.8	Thesis Content and Layout	1-16
<b>Chapter 2</b>	<b>Literature Review and Development of Recovery Indicators</b>	<b>2-1</b>
2.1	Introduction: Aims and Content of the Chapter	2-1
2.2	The Science behind Remote Sensing	2-1
2.3	Review of High-Spatial-Resolution Satellite Optical Sensors and Operators	2-3
2.4	Sensors' Technical Capabilities	2-6
2.5	Image Classification	2-9
2.6	Remote Sensing and the Disaster Management Cycle	2-10
2.7	Guidelines and Monitoring Systems for Post-Disaster Response and Recovery	2-14
2.8	Donors and Aid Agencies – Common Approaches to Monitoring and Evaluation	2-16
2.9	Academic Approaches to Measuring Recovery	2-18
2.10	Need for more Longitudinal Studies	2-21
2.11	Recovery Project User-needs Survey	2-22
2.12	Recovery Indicator Table	2-24
<b>Chapter 3</b>	<b>Using Geospatial Tools to Retrospectively Monitor and Evaluate Recovery in Ban Nam Khem, Thailand after the 2004 Indian Ocean Tsunami</b>	<b>3-1</b>
3.1	Introduction: Aims and Content of the Chapter	3-1
3.2	Case Study Sites	3-2
3.3	Methodology	3-6
3.4	Auxiliary Datasets	3-15
3.5	Case Study Results	3-20
	Section 1: Accessibility	3-20
	Indicator 1: Road Length (Km)	3-24
	Indicator 2: Network Analysis	3-27
	Indicator 3: Reconstruction of Bridges and Public Transport Facilities	3-31
	Indicator 4: Presence of Vehicles	3-34
	Section 2: Buildings	3-39
	Indicator 5: Removal and Construction of Buildings	3-39
	Indicator 6: Change in Urban Layout and Morphology	3-51
	Indicator 7: Quality of Dwelling Reconstruction	3-57
	Section 3: Transitional Settlement/Displaced Population	3-66
	Indicator 8: Transitional Settlement	3-67
	Indicator 9: Displaced Population	3-82
	Section 4: Natural Environment	3-86

	Indicator 10: Land Cover and Urban Green Space Analysis	3-88
	Section 5: Livelihoods	3-102
	Indicator 11: Recovery of Livelihoods	3-102
	Section 6: Services and Utilities	3-116
	Indicator 12: Services and Facilities	3-116
	Indicator 13: Utilities – Power, Water and Sanitation	3-122
3.6	Conclusion	3-127

<b>Chapter 4</b>	<b>Mapping the Use of Geospatial Tools During the Planning and Implementation of a British Red Cross (BRC) Integrated Recovery Programme after the 2010 Haiti Earthquake</b>	<b>4-1</b>
4.1	Introduction: Aims and Content of the Chapter	4-1
4.2	The 2010 Haiti Earthquake	4-2
4.3	The Recovery Process in Haiti	4-4
4.4	Study Site: Delmas 19	4-6
4.5	BRC's Integrated Recovery Programme	4-8
4.6	Mapping the Decision-Making Processes	4-9
4.7	Remote Sensing in Support of Post-Disaster Needs Assessment	4-12
4.8	MTPTC Building Safety Ground Assessment	4-15
4.9	BRC's Baseline Survey in Delmas 19	4-20
4.10	Remote Sensing Assessment of Delmas 19	4-21
4.11	Selecting Appropriate Geospatial Analyses with BRC	4-23
4.12	Accessibility	4-25
4.13	Building Database	4-30
4.14	GIS Enumeration and Cadastral Survey	4-41
4.15	Photographic Survey	4-44
4.16	Integration and Analysis of Data in ArcGIS	4-45
4.17	Monitoring of Project Progress	4-57
4.18	Maps to Support the Participation Process	4-60
4.19	Conclusion	4-62

<b>Chapter 5</b>	<b>Comparing the use of manual and semi-automated remote sensing techniques to monitor camps and spontaneous settlement for UN-Habitat after the 2010 Haiti earthquake</b>	<b>5-1</b>
5.1	Introduction: Aims and Content of the Chapter	5-1
5.2	Study Background	5-3
5.3	Methodology	5-8
	<b>Study 1: The mapping and enumeration of spontaneous settlement across a large geographic extent using semi-automatic analysis of high-spatial-resolution satellite imagery</b>	<b>5-10</b>
5.4	Introduction	5-10
5.5	Ground Survey Results	5-12
5.6	Manual Analysis of Aerial Imagery Corresponding to the Ground Survey Site	5-15
5.7	Spectral Analysis of Satellite Imagery	5-19
5.8	Study 1 Method: Mapping Corrugated-Iron and Concrete Using the Semi-Automatic Maximum Likelihood Classifier	5-23
5.9	Sampling Approach to Estimate the Number of Corrugated-Iron Roofs	5-26
5.10	Manual Identification of Building Walls and Foundations	5-30
5.11	Results	5-30

5.12	Accuracy of the Maximum Likelihood Classifier	5-35
5.13	Conclusion	5-37
	<b>Study 2: The Mapping and Enumeration of Planned Camps using Semi-Automatic Analysis High-Spatial-Resolution Satellite Imagery: Comparing Spectral, Morphological and Object-Based Approaches</b>	<b>5-39</b>
5.14	Corail Planned Camp	5-40
5.15	Spatial Characteristics of Corail Camp	5-41
5.16	Spectral Characteristics of Camp Features	5-42
5.17	Method 1: Spectral Angle Mapper (spectral analysis)	5-45
5.18	Method 2: Top-Hat Transformation (mathematical morphology analysis)	5-47
5-19	Method 3: Object-Based Image Analysis	5-53
5.20	Results	5-61
5.21	Discussion	5-72

<b>Chapter 6</b>	<b>Conclusion</b>	<b>6-1</b>
6.1	Introduction: Aims and Content of the Chapter	6-1
6.2	The Need for Monitoring and Evaluation of Post-Disaster Recovery	6-2
6.3	Recovery Indicator Table	6-2
6.4	The Application of Indicators to Ban Nam Khem, Thailand: Review of Technical Methodology (What To Measure)	6-3
6.5	When to Purchase Images	6-5
6.6	What Tools to Use	6-8
6.7	Operationalisation of Remote Sensing and Overcoming Users' Uncertainties	6-14
6.8	Transferability	6-15
6.9	Reliability/Accuracy	6-17
6.10	Assumptions and Limitations	6-18
6.11	Work at Multiple Scales	6-19
6.12	Monitoring Large Areas	6-19
6.13	Time Requirements	6-21
6.14	Financial Requirements	6-22
6.15	Collectors of Data	6-23
6.16	Dissemination	6-23
6.17	Responsibility and Accountability of Data Management	6-24
6.18	Data Security and Legalities	6-24
6.19	Summary Statement	6-25
6.20	Further Research	6-26

Appendix A	Household Survey Form	
Appendix B	Key Informant Survey Form	
Appendix C	Building Typology used with UN-Habitat in Chapter 5	

## List of Figures

Figure 1-1: Thesis framework showing the key contribution of each of the chapters.	1-4
Figure 1-2: Urban recovery model developed by Kates & Pijawka (1977) and applied to 2005 hurricane Katrina (Kates et al. 2006).	1-6
Figure 1-3: Different users and uses of monitoring and evaluation data.	1-11
Figure 2-1: DigitalGlobe's fleet of current and past high-spatial-resolution satellites.	2-4
Figure 2-2: Earth Observation Data. Global demand by Sector in 2013.	2-6
Figure 2-3: The concept of Instantaneous Field of View (IFOV) (from Avery and Berlin, 1985).	2-7
Figure 2-4: The Disaster Management Cycle (from Sillah, 2015).	2-10
Figure 2-5: Yuka Karatani compared recovery indices ( $Si_1$ ) to assumed variation based on observations from outside the affected area ( $Si_0$ ).	2-20
Figure 3-1: Map of Ban Nam Khem, Phang Nga Province, Thailand in February 2009.	3-4
Figure 3-2: FLAASH atmospheric correction model graphic-user interface.	3-9
Figure 3-3: Pilot household surveys conducted in Ban Nam Khem in February 2009.	3-17
Figure 3-4: GPS Photomapper used to simultaneously view satellite imagery and GPS photographs. Each red dot represents a single GPS photograph.	3-19
Figure 3-5: The VIEWS system deployed in Ban Nam Khem, Thailand (left) and Sichuan Province, China (right).	3-19
Figure 3-6: Debris and inland water in Ban Nam Khem (left) and pumping equipment (right).	3-21
Figure 3-7: The army resurfaced the main road (left) but an estimated 34% of houses were still accessible by earth-road (right).	3-21
Figure 3-8: Road types identified in Ban Nam Khem.	3-22
Figure 3-9: Road damage classification after the 2004 Indian-Ocean tsunami.	3-24
Figure 3-10: Damage to the transport infrastructure in Ban Nam Khem.	3-25
Figure 3-11: Road status in Ban Nam Khem on 21 April 2005, four months after the 2004 Indian-Ocean tsunami.	3-26
Figure 3-12: Total length of functioning road in Ban Nam Khem by road type.	3-27
Figure 3-13: Best route from six housing developments to Ban Nam Khem school (red star) showing the shortest distance.	3-28
Figure 3-14: Distance (metres) from six housing developments to fishing-piers in Ban Nam Khem.	3-29
Figure 3-15: Road maps of Ban Nam Khem before the tsunami and after reconstruction.	3-30
Figure 3-16: The destruction and construction of a bridge near Ban Nam Khem linking shrimp ponds to the mainland.	3-32
Figure 3-17: Analysis of the ferry pier in Ban Nam Khem.	3-33
Figure 3-18: The Kho Khoa ferry (left) and in satellite imagery functioning one week after the tsunami (right).	3-33
Figure 3-19: Traffic analysis of the post-disaster satellite image acquired on 02 January 2005.	3-35
Figure 3-20: Length of functioning road in Ban Nan Khem and Chella Bandi.	3-38
Figure 3-21: Total number of buildings in Ban Nam Khem.	3-41
Figure 3-22: Building point database showing the construction and removal of buildings at different stages of the recovery process.	3-43
Figure 3-23: Building construction curves for eight 250 m grid cells. The plots show the number of buildings in each grid over time.	3-44
Figure 3-24: Buildings constructed within 30 m of the ocean after the 2004 tsunami.	3-45
Figure 3-25: Areas of building construction coded grey and bare ground coded yellow	3-46

using maximum likelihood classification (left) correlate well with a map of building construction produced manually (right).	
Figure 3-26: Omission and commission errors in Ban Nam Khem.	3-47
Figure 3-27: The urban extent normalised to the pre-disaster state measured manually and with Maximum Likelihood classifier.	3-49
Figure 3-28: Number of buildings in Ban Nan Khem and Chella Bandi.	3-51
Figure 3-29: Building density maps (left) and building density change between 2002 and 2009 (right).	3-54
Figure 3-30: Some areas near to the coast experienced a decrease in building density (top row), while some army-built areas saw an increase in building density (bottom row).	3-55
Figure 3-31: Landscape metrics were applied to building footprints delineated in a 250 m subset in the centre of Ban Nam Khem.	3-56
Figure 3-32: Different Stages of the building development cycle observed at different sites across Ban Nam Khem	3-59
Figure 3-33: Fifty households were analysed in detail across Ban Nam Khem using remote sensing and the household survey.	3-60
Figure 3-34: Building extensions were common features in the post-construction landscape.	3-62
Figure 3-35: Proportion of buildings at different stages of development throughout the recovery process.	3-63
Figure 3-36: Tents (left) and relief supplies (right) at Bang Muang camp.	3-66
Figure 3-37: Transitional shelters at Bang Muang Camp (left) and emergency shelters donated by the Friend-in-Need foundation (right).	3-67
Figure 3-38: Four planned camps in Bang Muang sub-district.	3-70
Figure 3-39: The number of buildings present at four planned camps.	3-71
Figure 3-40: Layout of the BNK School camp mapped using information from both remote sensing and local officials.	3-74
Figure 3-41: Layout of the Bang Muang camp mapped using information from both remote sensing and local officials.	3-75
Figure 3-42: Shelter dimensions and layout measured in satellite imagery.	3-76
Figure 3-43: Near-infrared false-colour-composite images showing removal of transitional shelters and restoration of playing field at Ban-Nam-Khem School Camp.	3-77
Figure 3-44: Map of Bang Muang Camp derived on the ground (left) and using satellite imagery (right).	3-79
Figure 3-45: The dispersed settlement approach used in Pakistan (left) was more difficult to reliably monitor than the planned camp approach used in Thailand (right).	3-80
Figure 3-46: Comparative recovery trends in transitional shelter numbers in Ban Nam Khem and Chella Bandi.	3-81
Figure 3-47: Transitional shelters used in planned camps across Phang Nga province.	3-83
Figure 3-48: Estimated population living in transitional settlement estimated by remote sensing and the Department of Disaster Prevention and Mitigation.	3-84
Figure 3-49. Mangroves species such as <i>Rhizophora apiculata</i> and <i>Avicennia alba</i> were widely distributed around Ban Nam Khem. Photo: Daniel Brown (February 2009).	3-86
Figure 3-50: Six Maximum Likelihood classification images showing the effect of the tsunami and the recovery process on land cover.	3-89
Figure 3-51: Proportion of land-cover in Ban Nam Khem, extracted from Maximum Likelihood classification images.	3-90
Figure 3-52: Change detection map of Ban Nam Khem showing at least three areas of <u>new development</u> : (a). New army-built housing (b). Phase 2 housing and (c). Ban Nam Khem school.	3-92

Figure 3-53: Change detection map of Ban Nam Khem showing areas of <u>reconstruction and repair</u> including (a). Fishing Piers (b). Army-built houses and (c). Resurfaced roads.	3-93
Figure 3-54: Green mangrove forest at different stages of the recovery process (left) and areas of mangrove forest gained and lost between June-2002 and February-2009 (right).	3-94
Figure 3-55: The area of Mangrove forest is seen to recover beyond the extent observed before the tsunami by 10%.	3-95
Figure 3-56: A Median filter was applied to the urban green space maps to remove noise and smooth the object shapes, which ultimately improved the reliability of the spatial metric results.	3-96
Figure 3-57: Green Space in Ban Nam Khem classified using NDVI Threshold technique.	3-97
Figure 3-58: Comparative trends in land cover for Ban Nam Khem and Chella Bandi.	3-101
Figure 3-59: Sources of livelihood identified on a walking-survey of Ban-Nam-Khem in February-2009.	3-103
Figure 3-60: Livelihood map of Ban Nam Khem populated using satellite image analysis and ground survey observations acquired in February-2009.	3-103
Figure 3-61: Shrimp farming. Derelict shrimp hatcheries (left) and functioning grow-out ponds (right) in Ban Nam Khem.	3-104
Figure 3-62: Shrimp hatcheries in Ban Nam Khem mapped with satellite imagery.	3-105
Figure 3-63: A medium-scale hatchery in Ban Nam Khem in June 2002 (left) and January 2005 (right).	3-106
Figure 3-64: Derelict shrimp hatcheries identified in satellite imagery and verified in field photographs in February-2009.	3-107
Figure 3-65: Classification of shrimp ponds full with water.	3-108
Figure 3-66: Area of functioning shrimp ponds.	3-109
Figure 3-67: Piers monitored in June-2002 and February-2009.	3-110
Figure 3-68: Pier length in Ban Nam Khem, calculated from Remote Sensing.	3-110
Figure 3-69: Long-tail boats and trawlers in ground photography and satellite imagery in February-2009.	3-111
Figure 3-70: Boat density in Ban Nam Khem throughout the recovery process, calculated from visual observation of satellite imagery.	3-112
Figure 3-71: The location of boats observed in satellite imagery acquired in February-2009: site (a). long-tail boats, (b). large trawlers and (c). mangrove fishers and boat repair yard.	3-113
Figure 3-72: The number of fishers and the length of pier after the 2004 tsunami normalized to the pre-disaster state.	3-115
Figure 3-73: Ban Nam Khem's service and facility database.	3-118
Figure 3-74 Site of Ban Nam Khem temple (left) and school (right) surveyed with satellite imagery and ground photography.	3-119
Figure 3-75: Time-line of events at Ban Nam Khem School.	3-120
Figure 3-76: Building analysis of Ban Nam Khem School site throughout the recovery process shows the construction of permanent and temporary structures.	3-121
Figure 3-77: Features required for power-supply observed using aerial imagery of Port-au-Prince after the 2010 Haiti Earthquake.	3-123
Figure 3-78: Annual composite night-time light data over Ban Nam Khem before and after the 2004 tsunami.	3-124
Figure 3-79: Average night-time lights in Ban Nam Khem and Chella Bandi normalised for pre-disaster condition.	3-125
Figure 4-1: USGS Shakemap of the 2010 Haiti earthquake	4-4
Figure 4-2: Location of the British Red Cross Integrated Recovery Programme. Delmas 19 is split into four zones marked by blue lines.	4-7
Figure 4-3: Panoramic photograph of Delmas 19 slum characterized by small buildings and	4-8

narrow access-ways.	
Figure 4-4: Key monitoring and evaluation activities in a Red Cross programme cycle (IFRC, 2011b).	4-9
Figure 4-5: Flow diagram showing how geospatial tools were used at each stage of a British Red Cross project in Haiti.	4-12
Figure 4-6: Acquisition and analysis of imagery in the first three months after the 2010 Haiti earthquake.	4-13
Figure 4-7: Result of a rapid damage assessment across the Port-au-Prince metropolitan area using remote sensing technology by the European Union's Joint Research Centre.	4-15
Figure 4-8: MTPTC-tagged buildings re-assigned tags by BRC engineers in September 2011.	4-17
Figure 4-9: Comparison of the proportion of MTPTC tags in Delmas 19 recorded in the MTPTC database and the BRC's enumeration survey.	4-18
Figure 4-10: Spatial analysis of MTPTC database (points) and MTPTC tags recorded on the ground by BRC (polygons).	4-19
Figure 4-11: Two aerial images acquired after the earthquake vary in their contrast and clarity.	4-22
Figure 4-12: Oblique Pictometry imagery was used to observe the facades of buildings.	4-23
Figure 4-13: The road database created using the manual analysis of aerial imagery.	4-26
Figure 4-14: Length of blocked roads in four neighbourhoods of Delmas 19 measured using aerial imagery.	4-27
Figure 4-15: The road network used to measure the distance from each building to the nearest road surface (left) and the shortest route to water wells and other facilities (right).	4-28
Figure 4-16 Validation of remote mapping of roads in Delmas 19 slum using aerial imagery.	4-29
Figure 4-17: Highways and asphalt roads were delineated with high confidence in the aerial imagery but narrow lanes were often missed.	4-30
Figure 4-18: Comparison of building database created using aerial imagery (points) and ground GPS surveying (polygons).	4-31
Figure 4-19: Comparison of structural damage results from engineer retrofittability survey, remote assessment and ground-derived MTPTC tags.	4-33
Figure 4-20: Number of buildings with structural damage derived on the ground and remotely.	4-34
Figure 4-21: Surface Elevation Model (left) and Hill-Shade Image (right) representing building height were both derived from RIT's Lidar data.	4-35
Figure 4-22: Three-dimensional model of Delmas 19 derived from Lidar height data.	4-36
Figure 4-23: Comparison of building height model derived using Lidar data and ground survey.	4-37
Figure 4-24: Comparison of the number of buildings with 1, 2 or 3 storeys derived with Lidar and ground survey.	4-38
Figure 4-25: Comparison of building size estimates derived using aerial imagery and ground survey.	4-39
Figure 4-26: The number of buildings disaggregated by size estimated using aerial imagery and ground survey.	4-39
Figure 4-27: Comparison of building density statistics derived remotely and using ground survey.	4-41
Figure 4-28: Cadastral and enumeration surveys were linked in the GIS to produce maps of the target area.	4-42
Figure 4-29: Pictometry was used to confirm the presence of three structures in the centre of Delmas 19 that had since been demolished.	4-44
Figure 4-30: GPS photographs of each building plot were shared and viewed internationally using Google Earth.	4-45

Figure 4-31: Amount of covered living space (m <sup>2</sup> per person).	4-49
Figure 4-32: Location of plots containing more than 2.5%, 5%, 10% and 20% of dependents as a percentage of the owner's total household size shaded in pink.	4-50
Figure 4-33: Livelihood indicators from the baseline survey linked to Shelter's GIS database. Households in-debt or receiving credit are shaded red.	4-51
Figure 4-34: Soil bearing capacity was mapped to highlight high-risk zones.	4-53
Figure 4-35: A sample of plots that met the selection criteria analysis.	4-56
Figure 4-36: Satellite imagery and maps provided throughout the session are used as prompts for discussion and to give the participants something they can compare their own map against.	4-61
Figure 4-37: The abstract community maps (left) were converted to real plans of the community to support the community action plan (right).	4-62
Figure 4-38: The common components of a reconstruction programme (adapted from Da Silva, 2010). Blue stars represent components of the BRC project that were assisted with geospatial tools.	4-63
Figure 5-1: Building-by-building survey techniques used by International Organisation for Migration in Canaan to count shelter numbers.	5-6
Figure 5-2: The bi-monthly cycle undertaken at each camp site to collect and update the DTM dataset lasted about six weeks.	5-7
Figure 5-3: Results of the DTM were published online at the CCCM website.	5-7
Figure 5-4: Canaan is located west of the Corail planned camps, 12 miles north of central Port-au-Prince.	5-11
Figure 5-5: Makeshift shelters in Canaan.	5-12
Figure 5-6: GPS-encoded photographs were taken for each building surveyed along a 1 km route and are displayed here as red dots.	5-13
Figure 5-7: The proportion of building-types surveyed in the Canaan subset in October 2011.	5-14
Figure 5-8: The location of concrete and non-concrete structures identified in aerial imagery representing a subset of Canaan in November 2010.	5-16
Figure 5-9: Different building classes visible in Canaan aerial imagery.	5-18
Figure 5-10: Retrieved surface reflectance for 3 roof materials in Canaan.	5-19
Figure 5-11: Corrugated-iron and concrete roof in four bands of a Worldview-2 satellite image.	5-20
Figure 5-12: Scatter-plot of class points displaying the separability between four classes in Worldview-2's four bands.	5-22
Figure 5-13: Probability density functions for 4 land cover classes in Canaan calculated using the class mean and standard deviation statistics.	5-24
Figure 5-14: Location of the 73 randomly-selected grid cells.	5-27
Figure 5-15: Comparison between automatically-derived number of structures and visually-counted number of structures for the 73 randomly selected cells across Canaan.	5-29
Figure 5-16: 175,230 m <sup>2</sup> of corrugated-iron in Canaan automatically mapped using the maximum likelihood classifier.	5-31
Figure 5-17: Map of exposed concrete in Canaan automatically mapped using maximum likelihood classifier.	5-32
Figure 5-18: Examples of exposed concrete in Canaan: piles of concrete material near to a construction site (left) and a vacant building with concrete-slab roof (right).	5-33
Figure 5-19: Map of incomplete concrete structures (foundations and walls) in Canaan mapped manually using Worldview-2 satellite imagery.	5-34
Figure 5-20: Density of corrugated iron, concrete and incomplete concrete structures. Measured using a kernel 178.41 m radius (100,000m <sup>2</sup> area) and 15 m cell size.	5-35

Figure 5-21: How to calculate correctly-identified pixels, commission and omission errors by directly comparing manually-delineated polygons (grey) and automatically-delineated polygons (blue).	5-36
Figure 5-22: A typical streetview in Corail camp.	5-40
Figure 5-23: Aerial image of Corail camp on 5 June 2010 shows structures in regular rows and blocks with large spaces between them.	5-41
Figure 5-24: Floor plan and elevation of the transitional shelter used in Corail planned camp.	5-42
Figure 5-25: Reflectance of shelter roofs and background land cover estimated from a Worldview-2 image using the FLAASH Atmospheric Model.	5-43
Figure 5-26: Detailed view of transitional shelters in Worldview-2 satellite imagery.	5-44
Figure 5-27: Spectral Angle Mapping compares the vector for an unknown feature type to a known material spectral vector.	5-46
Figure 5-28: SAM grey-scale rule image. White shades are pixels that have a close spectral similarity to corrugated-iron reference pixels.	5-47
Figure 5-29: Mathematical morphology workflow used to extract sunny and shaded roof panels in Corail planned camp.	5-48
Figure 5-30: The Opening operator applied to the blue band of a Worldview-2 image using a square structural element of varying size.	5-50
Figure 5-31: Erosion and dilation filters applied to blue and near-infrared Worldview-2 bands respectively.	5-51
Figure 5-32: Opening and closing filters applied to blue and near-infrared Worldview-2 bands respectively.	5-51
Figure 5-33: Top-hat processing applied to the results of the opening and closing filters.	5-52
Figure 5-34: Object Based Image Analysis workflow applied to transitional shelters. In this example two different shelter shapes have been extracted and coded red and blue.	5-54
Figure 5-35: Groups of pixels were converted to image objects using an edge-detection algorithm.	5-55
Figure 5-36: Three spatial indices applied to objects representing Corail camp.	5-56
Figure 5-37: Fuzzy rules for the main direction defined.	5-58
Figure 5-38: Nearest neighbour classification in the two-dimensional feature space.	5-60
Figure 5-39: The classification of Corail camp using four semi-automatic workflows.	5-62
Figure 5-40: Types of commission and omission errors.	5-66
Figure 5-41: Examples of commission error 1 in Corail camp.	5-66
Figure 5-42: Commission errors shown in black across Corail camp and in purple on the bottom row.	5-68
Figure 5-43: Omission errors shown in black across Corail camp and in orange on the bottom row.	5-70
Figure 5-44: Transitional shelters with different reflectance values contributed to omission errors.	5-71
Figure 6-1: Estimated timing and duration of key recovery activities and processes.	6-7
Figure 6-2: Direct observation and social-audit datasets may be integrated and used to supplement each other throughout the recovery process.	6-13
Figure 6-3: Recovery curves for the two case study sites, produced by normalising the number of buildings present using the pre-disaster building number.	6-17
Figure 6-4: The average percentage of access, housing, environment and power recovery according to key informants plotted against appropriate remote sensing-derived indices.	6-29

## List of Tables

Table 2-1: The organisations that responded to the Recovery Project’s User Needs Survey.	2-23
Table 2-2: Provisional list of Recovery Indicators with the average scores and ranking from the Recovery Project’s User Needs Survey (Platt, 2008).	2-24
Table 2-3: The TRIAMS Indicators, with the indicators that may be monitored using Remote Sensing highlighted in grey by the author.	2-26
Table 2-4: The Recovery Project indicators developed by the author.	2-27
Table 2-5: Comparison between the Recovery Project Categories and other methods of categorising recovery and disaster impact.	2-29
Table 3-1: Time-series of high-spatial-resolution satellite images acquired of Ban Nam Khem, Thailand.	3-7
Table 3-2: The methodology used both manual and semi-automated remote sensing techniques to map features related to the recovery process.	3-12
Table 3-3: Forms of spatial analysis used to study features related to post-disaster recovery.	3-15
Table 3-4: Landscape Metrics from McGarigal & Marks (1994) applied to building polygon maps.	3-53
Table 3-5: Changes in building structure and associated features in Ban Nam Khem.	3-61
Table 3-6: Recommended camp standards: UNHCR, Sphere Project and Norwegian Refugee Council.	3-68
Table 3-7: Attributes of transitional settlement that can be monitored using remote sensing.	3-69
Table 3-8: Tents and transitional shelters used at planned camps in Phang Nga Province.	3-73
Table 3-9: Accuracy of remote sensing compared to official statistics for Bang Muang Camp.	3-78
Table 3-10: Spatial metrics used to characterise the size, distribution and fragmentation of urban green spaces.	3-96
Table 3-11: Physical attributes used to indicate building use.	3-117
Table 4-1: Cluster groups and cluster coordinators operating in Haiti two years after the earthquake.	4-6
Table 4-2: A list of proposed techniques given to BRC based on the indicator table introduced in Chapter 2 and preliminary discussions with the team.	4-24
Table 4-3: Comparison of building height statistics derived using Lidar data and ground survey.	4-37
Table 4-4: Comparison of building dimensions measured on the ground and using satellite imagery.	4-40
Table 4-5: Number of plots that meet the selection criteria disaggregated by plot-type.	4-54
Table 5-1: A summary of the camp characteristics and techniques applied to each camp.	5-3
Table 5-2: Attributes contained in the DTM v2.0 dataset. Source: (CCCM, 2011b).	5-5
Table 5-3: Worldview-2 image attributes.	5-9
Table 5-4: Contingency matrix comparing 58 ground observations to manual aerial image analysis.	5-17
Table 5-5: Omission and commission errors for each building category	5-17
Table 5-6: Two regression results show the relationship between the number of manually-counted buildings and 1) number of automatically-delineated buildings and 2) area of corrugated-iron automatically-delineated.	5-28
Table 5-7: The number and area of shelters estimated by each classification method.	5-63
Table 5-8: Summary of the overlay analysis results. Errors of commission and omission in terms of the number of pixels are presented in parentheses.	5-65

Table 6-1: Forms of spatial analysis used to study features related to post-disaster recovery	6-5
---	-----

## Chapter 1: Introduction

The main objective of this thesis is to assess the feasibility of using remote sensing and geographical information systems to support the spatial analysis, planning and monitoring of post-disaster recovery. To do this it will be necessary to 1) thoroughly test the reliability of currently-available geospatial techniques to monitor recovery indicators over time, over large spatial areas and in differing contexts and 2) to better understand the information needs and decisions being made by potential users and to establish where remote sensing can support this decision-making process.

This is the first time that geospatial science has been used in the context of post-disaster recovery. This thesis will adopt an inductive approach to test a thesis statement resulting in a set of recommendations and a framework for both practitioners and scientists. The thesis hypothesis is as follows:

*Geospatial science is a reliable and timely data-source useful for decision-makers and is expected to offer a systematic method of collecting independent and quantitative datasets rapidly and non-intrusively for the purpose of assisting post-disaster recovery.*

To test this statement a systematic list of indicators, useful for practitioners and scientists alike, will first be developed based on existing humanitarian frameworks and a preliminary assessment of satellite imagery. The development of such a framework, based on a user needs' survey and a review of existing humanitarian frameworks, will be an important contribution to science as it will allow practitioners and analysts to make standardised comparisons between different stages of recovery and also between disasters (Chang, 2009).

The framework will be tested throughout the rest of the thesis across four case study sites that vary in their urban structure, the user involved and the type of study (e.g. retrospective or real-time study). A number of techniques and protocols will be developed for each indicator and first applied retrospectively to case studies in Thailand and Pakistan and later in real-time humanitarian operations in Haiti. The retrospective analysis of recovery in Thailand will allow the ability of remote sensing to monitor recovery over time to be assessed while the real-time analysis of recovery in Haiti will focus more on the spatial capabilities and limitations of existing geospatial science in a recovery context. It is important to note here that the objective of this thesis is not to develop new

techniques but instead to test the feasibility of using remote sensing in a new context, post-disaster recovery.

In Chapter 3, retrospective time-series analysis of recovery in Thailand will be used to test the ability of geospatial science to monitor recovery over time. Detailed recovery narratives and quantitative recovery curves will be produced that describe the speed and the quality of recovery over time in a standardised manner. Recovery in Thailand and Pakistan will also be quantitatively compared using indicators developed in Chapter 2. This will be the first time this has been done using remote sensing, allowing community recovery to be mapped and analysed remotely for the first time. Previous attempts to produce recovery curves have relied on regional-scale social and economic indicators. The work in this chapter will also allow the longitudinal recovery in Ban Nam Khem to be recorded in-detail at a time when recovery case studies are still scarce, under-recorded and much-requested by the scientific community.

The beginning of chapter 4 continues the investigation of recovery over time by mapping the information needs and decision-making processes of an aid agency - in particular, showing how recovery monitoring fits with existing operational processes such as needs assessment, recovery planning and cadastral mapping. This work will provide a unique insight into the sector and will show how the proposed framework in Chapter 2 aligns with current operational thinking. This is deemed important to ensure suitability and uptake of any proposed indicators or framework. This chapter will also contribute knowledge to the mapping of humanitarian decision-making, which is an important and growing area of scientific interest in itself (e.g. Darcy et al. 2013; Altay and Labonte, 2014).

While chapter 3 looks at the process of recovery over time, subsequent chapters will focus on exploring how geospatial science can be used in real-time post-disaster situations. Specifically this will involve testing the spatial capabilities and the limitations of remote sensing in different recovery contexts: 1) a complex urban slum, 2) a planned camp and 3) a large area of spontaneous settlement.

The accuracy and reliability of the geospatial techniques will be tested thoroughly throughout the thesis in chapters 3, 4 and 5. Chapter 4 verifies remote sensing analysis of a complex urban slum by comparing the results to accurate cadastral maps created on the ground. While chapter 5 will report how three semi-automatic analyses of satellite imagery were used to support UN-Habitat (instead of

manual methods, which are the focus of previous chapters). This chapter will summarise the accuracies, strengths and weaknesses of each semi-automatic technique with recommendations of what to use and when.

To conclude this thesis, lessons learnt from all of the chapters will be synthesised to produce a framework for the measurement of recovery (in particular, providing guidance to users on what to measure, when and how). Operational considerations will also be reviewed including a look at its reliability and a discussion on the appropriate techniques and scale of analysis. This will be useful to users like international and national NGOs and other decision makers, as well as the scientific community.

The main contribution of each chapter is summarised in Figure 1-1 on page 1-4. The illustration shows how the chapters focus on either the temporal or spatial capabilities of geospatial science. The chapters test remote sensing at two different geographic scales: neighbourhood- and urban-scale.

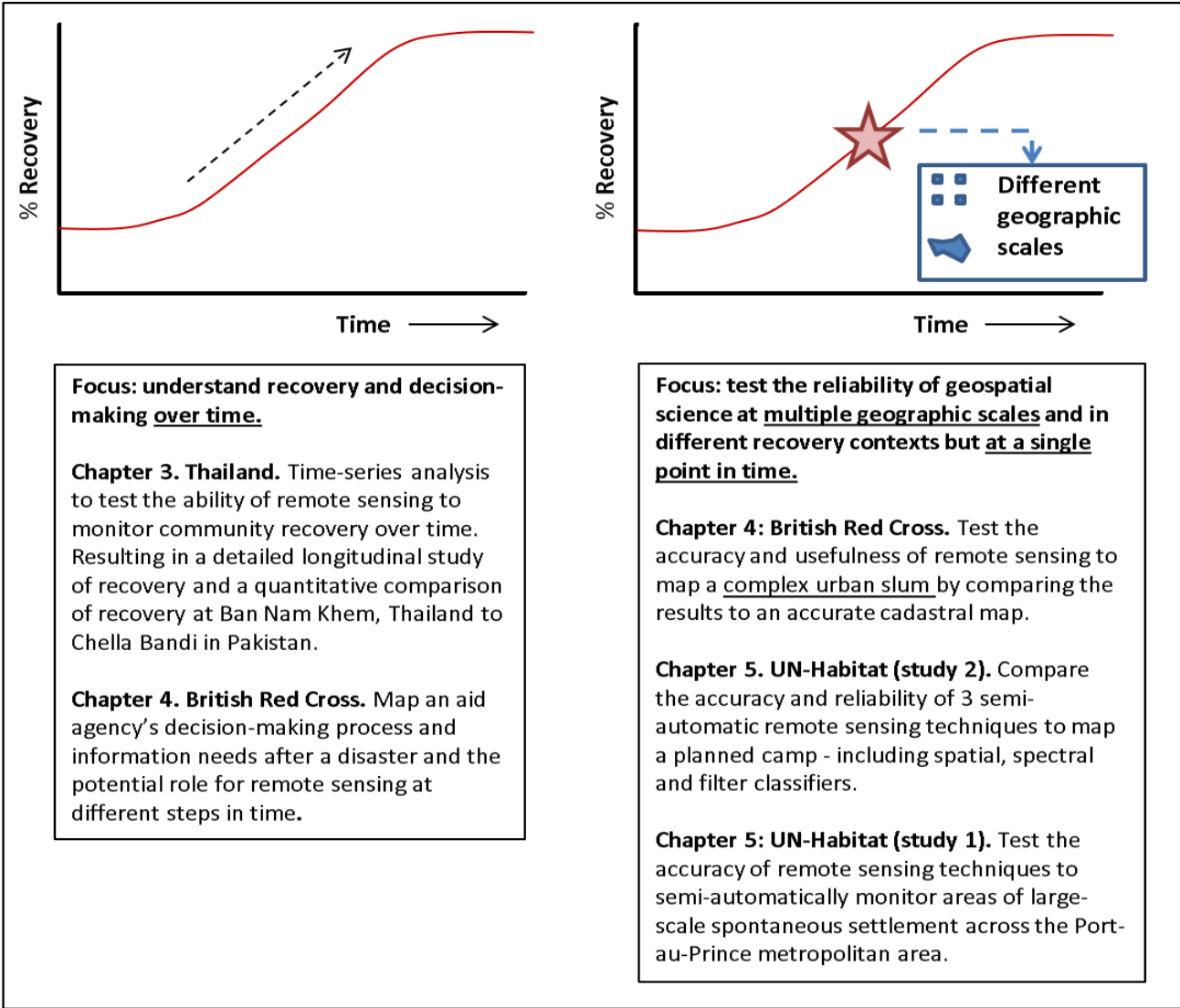
The focus of this thesis is the process of recovery and reconstruction that takes place following a disaster and in particular, the delivery of remote sensing-based information products and services to support the planning, monitoring and evaluation of the recovery process. The term *remote sensing* is used here to refer to the analysis of aircraft or satellite-derived data including high-spatial-resolution optical imagery, radar and lidar datasets. This chapter begins by outlining the process of post-disaster recovery, what it entails and who is involved. The data and information needs at different stages of the disaster cycle are then introduced and the importance of monitoring and evaluation post-disaster recovery is discussed. The chapter concludes by outlining the aims of the thesis and the layout of the subsequent chapters.

**Chapter 2: Indicator development.**

Based on a user needs' survey and review of humanitarian frameworks.

Provides indicators that are tested in subsequent chapters.

Such a framework will be important for the standardised monitoring of recovery.



**Chapter 6: Conclusion**

Provide recommendations on what to measure, when and how.

Discuss the reliability, manageability and transferability of the techniques.

Discuss other operational considerations.

Figure 1-1: Thesis framework showing the key contribution of each of the chapters.

## 1.1. Post-disaster Recovery

After a vulnerable community has been affected by a large natural or man-made disaster it can take years, and often decades, to redevelop its physical, social and economic systems and to rehabilitate the people living there. The process is often costly and complex, with roles and responsibilities encompassing many sectors and stakeholders (Da Silva, 2010; Olshansky & Johnson, 2010).

Households must repair and rebuild houses, deal with psycho-social issues whilst maintaining their livelihood; while businesses and government must replace assets, repair and rebuild infrastructure and re-employ staff (Miles and Chang, 2006).

Early research identified a linear sequence of recovery phases that a community was thought to undergo following a disaster. In Chapter 1 of the book *Reconstruction following Disaster*, Kates & Pijawka (1977) laid-out a conceptual framework for urban disaster recovery that describes how priorities shift as time passes through four overlapping stages (see figure 1-2). The identification of these phases is very useful for the practical allocation of funds and resources and to inform strategic decision-making at different points in the recovery process (Davis and Alexander, 2015), but as research has developed, the phases of recovery are now increasingly conceptualised as dynamic and interactive, as opposed to static and linear (Nigg, 1995).

After the emergency, life-saving phase, the short-term objectives of recovery often include the restoration of shelter, key lifelines and livelihood solutions so the affected population may be self-sufficient again (Quarantelli, 1999). At government and administrative level, efforts focus on the activation and restoration of appropriate governance and funding systems so that effective decision-making can be made again. In the years thereafter, recovery activities likely involve the development of land-use plans and the eventual reconstruction and monitoring of the built environment, transport network, utilities and services. Throughout this whole process, cross-cutting issues are commonly addressed, such as supporting vulnerable groups, risk reduction, sustainability, community participation and environmental protection.

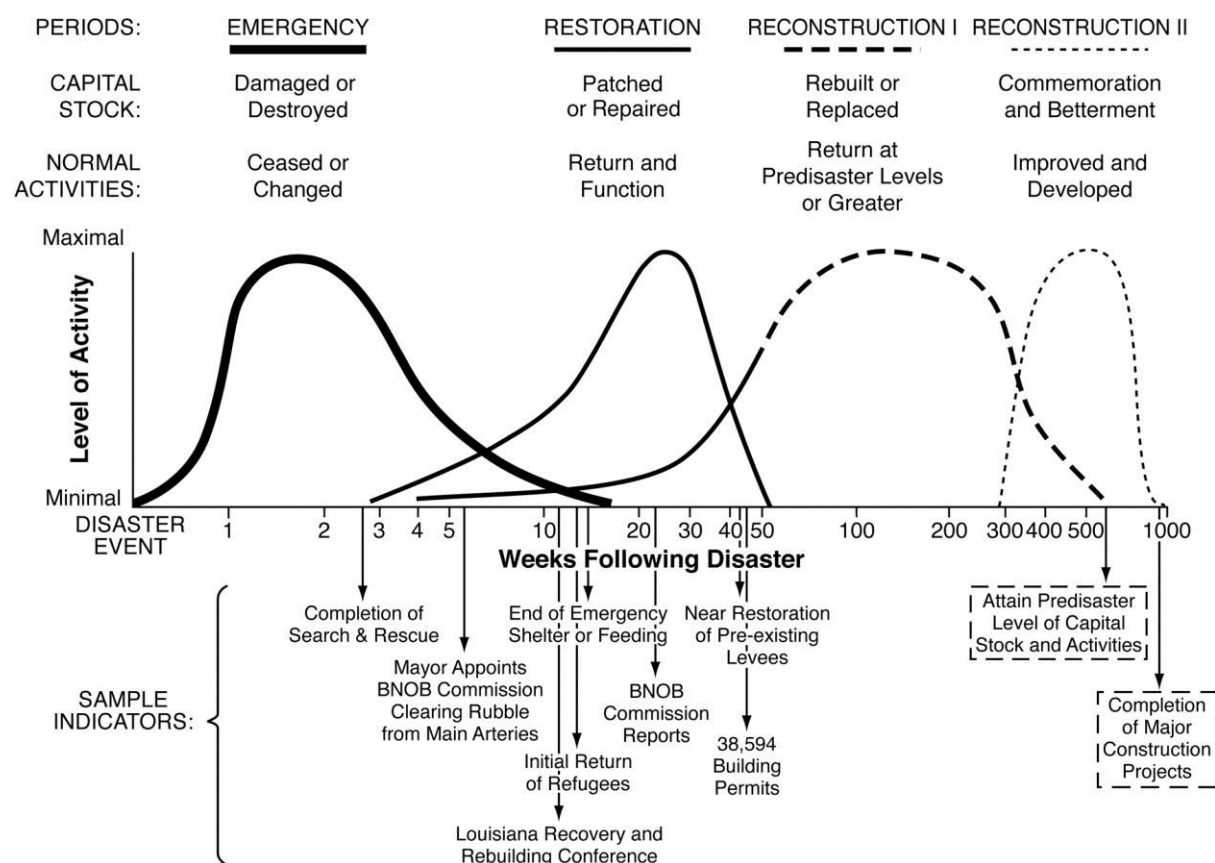


**Figure 1-2: Urban recovery model developed by Kates & Pijawka (1977) and applied to 2005 hurricane Katrina (Kates et al. 2006).**

Much of the research on recovery to-date has focused on the inequalities that are created by disasters and the subsequent recovery process. In particular, the recovery process has been shown to vary over *time* and *space* due to socioeconomic and political factors, and because of a multitude of decisions that are made before, during and after a disaster by different levels of authority, from individual households to central Governments (Hirayama, 2000; Olshansky, Johnson and Topping, 2006). There are subsequently similarities between recovery and social vulnerability theories, which suggest that vulnerable groups may be more susceptible to losses and have more difficulty recovering (Hewitt, 1997; Miles and Chang, 2003; Wisner et al. 2004).

A lack of finance or difficulties distributing funding effectively are some of many reoccurring factors preventing or slowing down reconstruction projects. The *Mind the Gap* report, produced for the Royal Institute of Chartered Surveyors, found that a disproportionate amount of funding and resources were often allocated to post-disaster emergency response efforts instead of long-term reconstruction (Lloyd-Jones, 2006). This is not surprising as money raised by emergency appeals often has to be spent within a pre-determined timeframe of being allocated (Da Silva, 2010).

Research has also focussed on the strategic decision-making that is made after a disaster, such as the provision of transitional shelters, and the decisions that can lead to its high cost, late delivery or its inappropriate location which can have severe repercussions on peoples' lives and on subsequent recovery activities (Davis, 1977; Johnson, 2007). There are now numerous guideline and 'lessons learnt' documents available to assist those agencies working in post-disaster recovery. The *Sphere Handbook* for example, provides a set of common principles and universal minimum standards on humanitarian response activities (Sphere Project, 2011). The *International Recovery Platform (IRP)* provides a comprehensive source of on-line information and documentation on post-disaster recovery and a partnership involving the *Active Learning Network for Accountability and Performance (ALNAP)* and the *ProVention Consortium* have also produced a series of excellent briefing papers summarising key lessons learnt from past earthquakes and flooding events (e.g. ProVention Consortium, 2008; Alam, 2008).

More recently, the World Bank's handbook on post-disaster reconstruction titled *Safer Homes, Stronger Communities* lists 10 *guiding principles of recovery* that are based around the key concepts of participation, collaboration, sustainability and risk reduction (Jha et al. 2010). These principles and other 'lessons learnt' documents now more often than not recognise that recovery offers a unique opportunity to improve conditions and to incorporate mitigation measures. In practice though, planners often find themselves having to balance time-sensitive needs and funding sources against opportunities for sustainable community improvement (Gardoni & Murphy, 2008; Olshansky & Chang, 2009).

There are a number of widely-recognised strategies that Governments might adopt which help guide the overall process of recovery. The World Bank lists 5 such approaches to housing reconstruction that differ chiefly in the amount of control the household has over the process, ranging from agency-driven reconstruction to the owner-driven approach (Jha et al. 2010). The owner-driven method is regarded as the most empowering, sustainable and cost-effective approach in many post-disaster situations (IFRC, 2007; IFRC, 2010). Social capital and community organisations with strong leadership are considered crucial to ensure a fast recovery and to provide maximum satisfaction to the community (Fujieda et al. 2004). It is argued that successful national recovery programs must be flexible and incorporate local opinion (Berke, Kartez, and Wenger, 1993) whilst also providing adequate guidance and technical support (Yu, 2004).

The stakeholders involved in recovery vary substantially according to the type and magnitude of the disaster and the capacity of the existing systems to respond. In most cases, recovery is coordinated by the Government or Regional Administration of the affected country and where necessary, assistance is provided by the military and national and local nongovernmental organisations. After particularly large disasters a separate Ministry or Reconstruction Agency may be created to coordinate recovery and associated activities. The government may request national or international assistance when their capacity to govern is exceeded. Assistance might then be provided by UN agencies, humanitarian agencies and sometimes private entities. When required, these agencies are coordinated by the *Cluster Approach* which arranges organisations into sector groups with lead agencies for each<sup>1</sup>.

## 1.2. Data after Disasters

The World Bank's book *Data Against Natural Disasters* illustrates the need to establish effective information systems after disasters through five case studies. The book in particular demonstrates how timely, reliable data is required for a number of applications: such as, describing damage to physical infrastructure, locating the displaced population and tracking incoming resources and supplies (Amin & Goldstein, 2008). This is now increasingly recognised across the humanitarian community. The Inter-Agency-Standing-Committee (IASC) for example, now calls for cluster lead agencies to take charge of information management to ensure agencies are working with the same information and baseline data and that the information is relevant, timely and accurate (IASC working group, 2008). In 2005 the UN General Assembly Resolution 59/212 also called upon States, the United Nations and other relevant actors to assist in addressing knowledge gaps in disaster management and risk reduction by identifying ways of improving systems and networks for the collection and analysis of information on disasters.

## 1.3. Recovery Project Operational Phases

A specific aim of this thesis is to develop and test remote sensing-based analyses which can be used to assist agencies working in post-disaster recovery; as such, it is useful to describe recovery here in terms of the agencies' likely project workflow. Despite the complexity of the recovery process as a whole, agencies working in recovery, including the World Bank and Red Cross, recognise that most recovery programmes pass through a similar project-cycle to that of non-disaster development

---

<sup>1</sup> See the UNOCHA website for more information on how the Cluster system works.

projects. The stages in chronological order often include: 1. Damage and loss assessment, 2. Planning, 3. Project design, 4. Implementation/monitoring and 5. Evaluation (Amin & Goldstein, 2008; Jha et al. 2010; IFRC, 2010; Da Silva, 2010).

### 1.3.1. *Damage and Loss Assessment*

Damage and Loss Assessments (DaLAs) after a disaster are needed to establish the extent and magnitude of losses and needs, the results of which are fed into subsequent reconstruction planning and policy. A standardised methodology - often based on the *Handbook for Estimating the Socio-Economic and Environmental Effects of a Disaster* (ECLAC, 2003) and the United Nation's Human Recovery Needs Assessment (HRNA) - is used to estimate the effects of the disaster. The assessments often account for both the *direct damage* to physical assets and *indirect losses* caused by disruption to population and the temporary absence of production flows and services. Some of the disaster impacts are quantifiable (e.g. loss of life, building damage, economic losses) and others are less easily measured (e.g. change in culture, loss of opportunities) (UNDRO, 1991). The assessments can be labour-intensive and the results are usually required within several months or even weeks to inform donor pledges and resource procurement. There is often a trade-off in this phase of disaster management between timeliness and accuracy; remote sensing has proved itself to be particularly useful as a tool to provide a rapid overview of the situation in the immediate aftermath of a disaster, thus greatly accelerating the initial decisions being made (Haiti PDNA, 2010; UNDP, 2013). The focus of this thesis though is on the use of this technology to support the longer-term processes of recovery and reconstruction that happen after the needs and losses have been quantified.

### 1.3.2. *Planning*

After the damage and losses have been established detailed understanding of the local context is necessary to identify the different options for reconstruction. This stage of the process will likely involve the creation of different land-use options that meet the economic and social needs of the people. As a result, planning often involves the analysis of physical, social and economic constraints on land-use and the interests of multiple stakeholders. Sometimes planners in a post-disaster context will plan for long-term development and make physical changes to the built environment that weren't possible before the disaster. Planning after a disaster offers a unique opportunity to produce more efficient and safer communities, but should hopefully be achieved in a manner that is

sustainable and sensitive to the surrounding environment. To make effective decisions during this process, physical plans and maps are usually required that show the terrain and geology of the area, the availability of open land for relocation, and the existing road and building-plot layout and land-use zones (World Bank, 2008; Jha et al. 2010). As planning moves into the design phase agencies require information to select eligible beneficiaries and to calculate the logistical needs of the proposed plans.

### 1.3.3. *Monitoring and Evaluation*

Agencies working in disaster-recovery are now increasingly likely to conduct monitoring and evaluation activities throughout the development and implementation of their project to support accountability, project management and learning. *Monitoring* is the routine, regular assessment of on-going activities and progress, and it is used to inform on-going decision-making and to track progress of the work against set plans and established standards; while *evaluation* is the periodic, often retrospective, assessment of overall achievements (Jha et al. 2010; Mackay, 2007; White, 2009). Evaluation is likely to focus on different aspects of the project in addition to its overall outcomes and impacts such as its finances, organisational efficiency and beneficiary perceptions. While monitoring looks at what is being done and should enable a continuous feedback on the status of program implementation, evaluation examines what has been achieved or what impact has been made. This is often achieved in the form of a midterm evaluation and/or final evaluation on completion of the project.

## 1.4. **The Need for Monitoring and Evaluating (M&E) Post-Disaster Recovery**

Monitoring and evaluation of post-disaster recovery is necessary to inform and assist on-going work and decision-making on the ground, to improve future aid policy and to uphold accountability and compliance. It can also provide beneficiaries with an opportunity to provide feedback as the work progresses. Although many organisations and institutions are involved in the recovery process, with different functions and data requirements, they may be divided into three broad groups based on their differing data needs: 1. Executing agencies 2. Coordinating agencies and 3. Donors.

*Executing agencies* conduct the development and logistical work and require data for operational reasons, to inform day-to-day management decision-making and situational understanding. They are the group most-likely to be collecting regular data on the ground. Timely and reliable data helps

these agencies identify issues as they arise so they may adapt to changing circumstances and ultimately improve project performance. For example, gap analysis may be conducted to identify discrepancies between the progress of recovery and the needs of the affected population. Monitoring data can also ensure that spatial or sectoral inequalities are not maintained or created by the recovery process (TRIAMS, 2007).

Agencies providing direct support on the ground are now often stipulated by law and/or their funders to monitor and evaluate their own programmes. Often the data from multiple executing agencies is collated by a single *coordinating agency*, which may be a government department or cluster coordination group. This ensures executing agencies are aware of each other’s work and progress. Executing agencies also collect and report data to their donors. The *donors* fund the work conducted by the executing agencies. Donors require data to provide accountability and transparency to their stakeholders and to ensure their objectives are being met on time and to budget. Future funding decisions are also likely to be based on an analysis of this data. Donors also include insurance companies that provide payment after a disaster.

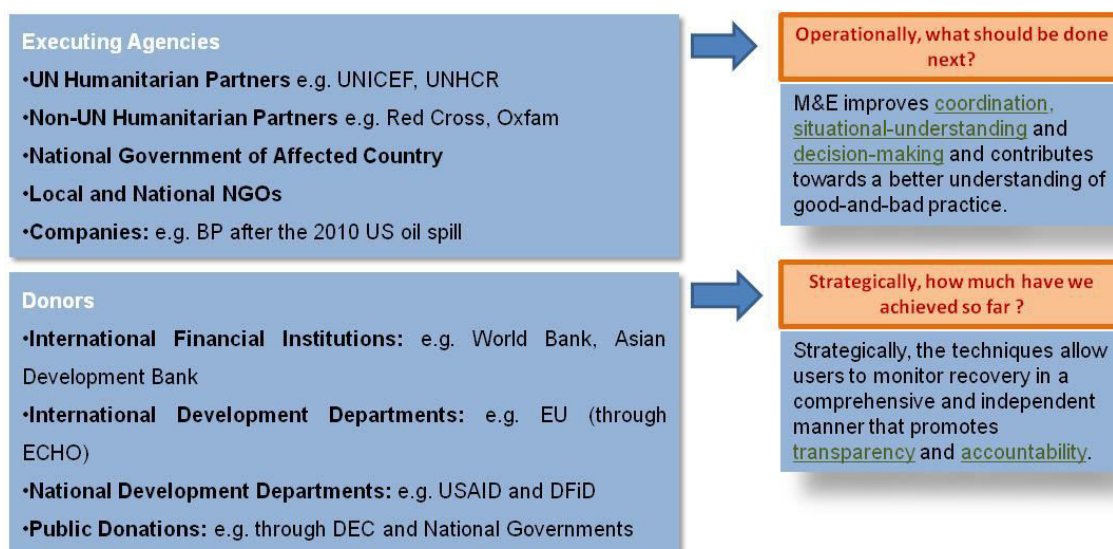


**Figure 1-3: Different users and uses of monitoring and evaluation data.**

Billions of dollars are often pledged to assist reconstruction after large natural disasters. The amount pledged to support the relief and recovery after the 2004 Indian Ocean tsunami eventually reached US\$14 billion. More recently, US\$9.9 billion was pledged to provide immediate and long-term aid to Haiti after the 2010 earthquake and US\$4.1 billion was pledged following the 2015 Gorkha earthquake. The governments of affected countries also tend to invest heavily in the recovery process. For example, after the 2004 tsunami the Government of India set aside approximately

US\$1.4 billion in tsunami-related funds and the Government of Indonesia set aside US\$2.0 billion<sup>2</sup>. International financial institutions, such as the International Monetary Fund (IMF), the Inter-American Development Bank and the World Bank, have become regular donors to long-term recovery. The World Bank is one of the largest funding agencies of disaster recovery and reconstruction in developing countries. Since 1984, the Bank has financed US\$ 26 billion in disaster activities in over 600 disaster responses. It provided US\$710 million after the 2008 Wenchuan earthquake to reconstruct infrastructure, US\$448 million after the 2005 Pakistan Earthquake to support livelihoods and reconstruction, and US\$650 million to Indonesia after the 2004 tsunami (World Bank, 2010).

Despite the large sums of money aiding recovery efforts and the complexity and importance of the work being conducted there are currently no standard frameworks or methodologies that can be adopted to monitor and evaluate the process. In May 2006, a Shelter meeting of the aid community in Geneva identified an urgent need for basic and applied research into the long-term recovery process (Shelter Centre, 2006). In particular, they noted the lack of a standard, independent and replicable approach to measure, monitor and evaluate the relief and recovery process. More recently, the *Active Learning Network for Accountability and Performance in Humanitarian Action* (ALNAP) called for “further research on the mix of impact-assessment methods most appropriate in the different emergency phases of relief, recovery and reconstruction” (Proudlock et al. 2009) and Lord Ashdown’s review of Humanitarian Emergency Response for the UK government called for initiatives to improve accountability and to “develop the most up-to-date innovations for disaster response, including satellite mapping to track the movement of people” (Ashdown, 2011). This call for continued improvements in accountability and transparency were repeated in the UK Government’s Humanitarian Reform Policy (DFID, 2017).

Long term recovery is often cited as one of the most poorly understood phases of the disaster management cycle (Rubin et al. 1985; Haas et al. 1997; Olshansky, 2005). In the past decade, there appears to have been increasing recognition within the academic community of the importance of measuring and monitoring recovery. Olshansky and Chang (2009) call for continued collection of recovery case studies and synthesis of comparative cases. Dr. Stephanie Chang acquired a thorough understanding of post-disaster recovery in the U.S. after she and Scott Miles developed a sophisticated agent-based model of households, businesses and lifelines (Miles & Chang, 2003; Miles & Chang, 2006). She used this knowledge to devise a measurement framework for recovery which

---

<sup>2</sup> Financial Tracking Service (FTS). UN Office for Coordination of Humanitarian Affairs (OCHA). <http://fts.unocha.org/>

provides important guidance on the use of time-series statistical data (Chang, 2009). Chang (2009) suggests that a systematic framework is needed to measure disaster recovery at the community scale. The use of quantitative indicators will allow analysts to measure and compare the progress of recovery across disaster and within disaster (Comerio, 2005; Chang, 2009; Davis, 2012). Comparing across disasters allows analysts to draw up a knowledge base and to start examining factors affecting recovery in different contexts.

There are a number of reasons why a full post-disaster recovery framework has not yet been developed. First, in practical terms developing indicators and data collection methodologies is rarely a priority for workers in the aftermath of a disaster. There has also been a lack of consensus among academics on a definition of recovery and in particular when the process is thought to end. Recovery is increasingly conceptualised as a complex set of on-going processes (Mileti, 1999; Olshansky, 2005), corresponding to the many facets of community life including housing, demography and the economy, which is a difficult prospect to have to represent with a small number of indices.

### **1.5. Current Tools**

Stakeholders use an assortment of tools and data collection techniques to collect data, including formal surveys, interviews, group discussions and direct observations (USAID, 1996; Proudlock, 2009). This is in agreement with the DAC Evaluation Criteria, which recommends analysts use a mixture of field interviews, surveys and literature reviews. These methods are often time-consuming and expensive to apply across large geographic regions, subjective and prone to inconsistencies in data quality. In extreme cases - when access is denied, security a critical issue, or donors not welcome – monitoring and evaluation has been all but absent (e.g. when the World Bank was unable to send operatives to Burma after the 2004 Indian Ocean tsunami and the 2008 cyclone Nargis). An assessment of 30 evaluation reports published in 2004, based on an ALNAP pro forma tool, found that just over 27% used international principles - such as the Sphere minimum standards - in a satisfactory manner, and that only 59% used appropriate evaluation methods (ALNAP, 2005; Wiles, 2005). The TRIAMS project further highlighted weaknesses in the current data collection frameworks, concluding that they were overly complicated or not standardised, and that recovery data is often lacking and not timely (TRIAMS, 2007).

Recent technological advances present the opportunity to enhance and support existing field-based tools and overcome many of the issues associated with passive frameworks and techniques. Remote

sensing, in particular, the manual and semi-automatic analysis of satellite imagery, is a proven data source for assisting disaster prevention efforts, mitigation, and relief, as well as damage and needs assessments (Li, Zlatanova and Fabri, 2007; Showalter and Lu, 2010). The post-disaster scenario can be confusing and dangerous, and collecting data is often challenging with numerous agencies working across large, disaster-stricken areas. Remote Sensing offers a systematic method of collecting independent and quantitative datasets rapidly and non-intrusively across large, dynamic geographic regions. The World Bank and DFID recognise the potential of remote sensing as a tool to monitor aspects of recovery (Jha et al. 2010; Ashdown, 2011), but there are currently no proven methodologies or protocols in which to analyse the data in support of post-disaster recovery.

## 1.6. Aims of Thesis

The main objective of this PhD is to assess the feasibility of using remote sensing and geospatial tools to support the spatial analysis, planning and monitoring of post-disaster recovery and reconstruction. The term '*geospatial tools*' is used here to refer both to the use of satellite imagery as a primary data source to directly observe processes on the ground and the use of geographical information systems (GIS) as a spatial platform to integrate and analyse remote sensing and other ground-derived datasets. To test the hypothesis that remote sensing and GIS can be used to support post-disaster recovery a series of techniques and protocols will be developed and applied retrospectively to case study sites in Thailand and Pakistan and later in real-time humanitarian operations in Haiti. Because it is important for users of the data to understand the reliability of the data they are using, the accuracy of the remote sensing results will be carefully verified by directly comparing them to GPS-encoded ground observations and narratives of recovery captured using social-audit techniques such as household surveys and focus-group meetings. Recognising that a mixed-method approach is likely necessary to effectively monitor recovery, recommendations will be made on how remote sensing may support other available tools at different stages of the disaster cycle.

Researchers have repeatedly shown that the process of recovery varies considerably over time and space due to a number of physical, social-economic and political factors. The analysis of multi-temporal remote sensing datasets is expected to be a suitable method of measuring recovery by mapping many of the physical aspects of the process. Quantifying and visualising the speed and quality of recovery under different circumstances is expected to provide a better understanding of the process as a whole and help understand why discrepancies in the process might occur. The

analysis will also help to answer some of the more logistical questions stakeholders involved in post-disaster recovery are likely to ask during the planning and implementation of a project, for example: 1) How much recovery has been achieved? and 2) Where do new interventions need to be focussed to encourage recovery and development?

Standardised indicators can be used to quantify certain issues and provide a means to measure and communicate progress over time and allow comparisons to be made across different disaster responses. A specific aim of this research is therefore to develop and test a suite of indicators and remote sensing analysis techniques and protocols that will allow donors and executing agencies to plan, monitor and evaluate post-disaster recovery and reconstruction. The indicators will be expected to meet the SMART criteria and therefore be *specific, measurable, attainable, relevant and time-bound* (Doran, 1981). To increase the likelihood that the indicators may be adopted by stakeholders the data also needs to be timely and reliable and the methods flexible enough to be applicable irrespective of the disaster type and the recovery strategy being used. The World Bank's *Data against Disasters* report states that one of the greatest challenges with new data systems is fitting them to existing operational systems. It can also be difficult for users to actively engage with any new technology, especially in a post-disaster context. This research will therefore seek to ground these analyses by fitting them to existing humanitarian approaches, such as the Post-Disaster Needs Assessment (PDNA) and the Humanitarian Cluster Framework, and according to the needs of the users, affected communities and appropriate stakeholders, who will be surveyed and interviewed at each of the case study sites.

To further test the indicators and to better understand how remote sensing may be used in an operational environment the indicators will be used to support real-time projects led by the British Red Cross and UN-Habitat in Haiti one-and-a-half years after the 2010 earthquake. This will provide a further test for the indicators and the technology to establish if and how it may be used to support on-going reconstruction programmes in a complex urban environment. Where appropriate, some of the analyses will be scaled-up which is likely to involve the semi-automatic analysis of satellite imagery across large geographic areas. The value of the indicators in this context will be evaluated by analysing how they were used by the agencies and whether they were judged to have made the projects more efficient in terms of time and financial cost. By mapping decision-making during these projects this work will establish when remote sensing is useful and how it can be connected to existing uses of the data such as needs assessment immediately after a disaster.

### **1.7. EPSRC Recovery Project (2008-2011) and EPSRC Follow-up Project (2011-2012)**

The first three years of the author's PhD studentship formed a substantial contribution to the *Recovery Project*, funded by the Engineering and Physical Sciences Research Council (EPSRC) and involving colleagues at the University of Cambridge, Cambridge Architectural Research Ltd. and Imagecat Ltd. The aim of the Recovery Project was to '*develop indicators of recovery that can exploit the wealth of data now available, including those from satellite imagery, internet-based statistics and advanced field survey techniques*' (Recovery Project, 2008). A summary of the author's contribution to this project, through the development and testing of remote sensing indicators using case studies in Thailand and Pakistan, forms the basis for Chapter 3 of this thesis. Colleagues at the three institutions listed above helped the author to select appropriate recovery indicators in the first year of the project. Dr. Steve Platt also designed and implemented the user-needs survey presented in Chapter 2 and assisted with the design of the household survey and key informant interviews implemented in Thailand and Pakistan and used to verify the work presented in Chapter 3.

On completion of the Recovery Project, a further years funding was received from EPSRC to explore how the previously developed remote sensing techniques and protocols may be operationalised. The author worked full-time on this project and provided remote geospatial support to a British Red Cross reconstruction project in Haiti from April-2011 and was subsequently invited to Haiti between September and November-2011 to establish and test the remote sensing and GIS systems further. This provided the author with an opportunity to test the indicators in an operational setting following the 2010 Haiti earthquake with both the British Red Cross and UN-Habitat – the results of which are presented in Chapters 4 and 5 of this thesis respectively.

### **1.8. Thesis Content and Layout**

#### *Chapter 2*

The literature review is split into three sections: Part 1 introduces the high-spatial-resolution remote sensing market and the technology, focusing on current sensors' capabilities and in particular, their spatial, spectral and temporal resolutions. In part 2 there is a review of previous attempts to measure post-disaster recovery by practitioners and academics. This section examines the main issues and considerations raised by these attempts. And finally in part 3 a list of recovery indicators – suitable for remote sensing analysis - is developed, and then ranked and assessed through a survey

## *Chapter 1: Introduction*

of users' needs. The output from this chapter is a table of recovery indicators which are to be tested using case study sites in Thailand and Pakistan, the results of which are presented in Chapter 3.

## *Chapter 3*

Six categories of recovery - identified in chapter 2 – form a framework for the retrospective analysis of recovery at two case study sites: Ban Nam Khem, Thailand and Chella Bandi, Pakistan, which at the time of the study were recovering from the 2004 Indian Ocean tsunami and 2005 Kashmir earthquake respectively. Remote sensing is used to extract information on each of the six categories. Each section of the chapter describes the methodology used to extract and analyse the appropriate data and presents a selection of results to demonstrate the usefulness of the proposed techniques. To verify the results and to measure the reliability of remote sensing, the results from the satellite image analysis are integrated into a geo-database and triangulated against narratives and datasets acquired on the ground.

## *Chapter 4*

The next two chapters describe work conducted by the author whilst providing real-time support to two agencies operating in Port-au-Prince one-and-a-half years after the 2010 Haiti earthquake. Chapter 4 describes how geospatial tools were used to support a British Red Cross integrated reconstruction project - involving shelter, livelihood and water-sanitation components - for 500 households living in an informal settlement in the Delmas area of Port-au-Prince. The chapter maps the key government and agency decisions after the earthquake and describes how geospatial tools were used at each stage of the British Red Cross project focusing on the use of 1) remote sensing as a rapid assessment tool, 2) GIS as a planning and monitoring tool in support of cadastral and enumeration mapping and 3) Community mapping as a tool to support the participatory process. As in chapter 3, the results of the remote sensing analysis are verified in detail by comparing them to a cadastral database created with ground-derived data; this further highlights the practical strengths and weaknesses of remote sensing as a tool to support different sectors of recovery.

## *Chapter 5*

In 2011 UN-Habitat was a coordinating agency in Haiti overseeing various shelter and camp components of recovery – as a result, they had very different data needs to the British Red Cross

project and so provided a very different operational context in which to test remote sensing analysis – one of the key differences was that UN-Habitat required monitoring data over a much larger geographical extent. While previous chapters focus on *manual* analysis of satellite imagery, chapter 5 reports how *semi-automatic* analyses of satellite imagery were used to support UN-Habitat by monitoring a planned camp and large-scale instances of spontaneous settlement. The chapter is split into two studies which compare spectral, mathematical morphology and object-based image analysis approaches to semi-automatically map tents, makeshift shelters and transitional shelters. The chapter concludes by summarising the strengths and weaknesses of each semi-automatic analysis technique and recommends in what context each may be most appropriately used.

## Chapter 6

The conclusion to the thesis summarises the key lessons learnt from the retrospective analysis of recovery in Thailand and Pakistan and the real-time application of the technology in Haiti. The strengths and weaknesses of remote sensing compared to existing data-collection tools is discussed by comparing their relative costs and effectiveness. Recommendations are then made on how to effectively use remote sensing in support of post-disaster recovery focussing on what to measure, when and how. Other important considerations that are important for the adoption of remote sensing as a tool to support post-disaster recovery are covered including appropriate delivery mechanisms and security of data in a post-disaster environment. The chapter will conclude with a section providing suggestions for further research to build on the work described here.

## Bibliography

Alam, K. (2008). *Flood disasters. Learning from previous relief and recovery operations*. ProVention Consortium. Active Learning Network for Accountability and Performance (ALNAP).

ALNAP (2005). *Assessing the quality of humanitarian evaluations. The ALNAP Quality Proforma 2005 (v. 02/03/05)*. Available at: <http://www.alnap.org/pool/files/QualityProforma05.pdf>

Altay, N. and Labonte, M. (2014). Challenges in humanitarian information management and exchange: evidence from Haiti. *Disasters*: **38** (s1), S50-S72.

Amin, S. and Goldstein, M. (2008). *Data against natural disasters: Establishing effective systems for relief, recovery, and reconstruction*. World Bank, Washington.

Ashdown, P. Lord. (2011). *Humanitarian emergency response review*. 28 March 2011. Available at: [https://www.gov.uk/government/uploads/system/uploads/attachment\\_data/file/67579/HERR.pdf](https://www.gov.uk/government/uploads/system/uploads/attachment_data/file/67579/HERR.pdf)

Barnett, M. (2005). Humanitarianism transformed. *Perspectives on Politics*: **4**, 723-740.

Berke, P.R., Kartez, J. and Wenger, D. (1993). Recovery after disaster: achieving sustainable development, mitigation and equity. *Disasters*: **17** (2), 93-109.

Chang, S. (2009). Urban disaster recovery: a measurement framework with application to the 1995 Kobe earthquake. *Disasters*: **34** (2), 303-327.

Comerio, M. (2005). Key elements in a comprehensive theory of disaster recovery. *First International Conference on Urban Disaster Reduction*. Kobe, Japan.

Dabelstein, N. (2006). *Evaluating humanitarian action using the OECD-DAC criteria. An ALNAP guide for humanitarian agencies*. ALNAP, London.

DANIDA (2006). *Evaluation Policy*. Evaluation Department Report. Danish International Development Agency, Copenhagen.

Darcy, J., Stobaugh, H., Walker, P. and Maxwell, D. (2013). The use of evidence in humanitarian decision making. ACAPS Operational Learning Paper. Tufts University, Massachusetts, USA.

Da Silva, D. (2010). *Lessons from Aceh. Key considerations in post-disaster reconstruction*. Practical Action Publishing, Warwickshire.

Davis, I. (1977). Emergency shelter. *Disasters*: **1**, 23–40.

Davis, I. (2012). *What is the vision for sheltering and housing in Haiti?* Summary of observations of reconstruction progress following the Haiti earthquake of January 12th 2010. Available at: <http://www.alnap.org/pool/files/1379.pdf>

Davis, I. and Alexander, D. (2015). *Recovery from Disaster*. Routledge Studies in Hazards, Disaster Risk and Climate Change, London.

DFID. (2017). *Saving lives, building resilience, reforming the system: the UK Government's Humanitarian Reform Policy*. Department for International Development. September 2017.

Doran, G.T. (1981). There's a S.M.A.R.T. way to write management's goals and objectives. *Management Review*. November 1981.

ECLAC. (2003). *Handbook for estimating socio-economic and environmental effects of disasters*. Economic Commission for Latin America and the Caribbean, Chile.

Fujieda, A., Nakagawa, R.Y., Shaw, R., Kobayashi, H. and Kobayashi, M. (2004). Roles of social capital and community organizations in the recovery process: Experience from Kobe and Gujarat Earthquakes. *1st International Conference of Urban Disaster Reduction*. Kobe, Japan.

Gardoni, P., and Murphy, C. (2008). Recovery from natural and man-made disasters as capabilities restoration and enhancement. *International Journal of Sustainable Development and Planning: 3* (4), 317-333.

Haiti PDNA. (2010). *Haiti earthquake PDNA: assessment of damage, losses, general and sectoral needs*. Annex to the Action Plan for National Recovery and Development of Haiti.

Haas, J., Kates, R., and Bowden, M. (1977). *Reconstruction Following Disaster*. MIT Press, Cambridge, Massachusetts.

Hewitt, K. (1997). *Regions of Risk: A geographical introduction to disasters*. Addison Wesley Longman Limited, London.

Hirayama, Y. (2000). Collapse and reconstruction: housing recovery policy in Kobe after the Hanshin great earthquake. *Housing Studies: 15* (1), 111–128.

IASC working group (2008). *Operational guidance of sector cluster leads and OCHA in Information Management v3.0*. Inter-Agency Standing Committee. Geneva.

IFRC. (2007). *Case study: rebuilding after hurricane Mitch, housing reconstruction in Honduras and Nicaragua*. International Federation of Red Cross and Red Crescent Societies, Geneva.

IFRC. (2010). *Owner-driven housing reconstruction guidelines*. International Federation of Red Cross and Red Crescent Societies, Geneva.

Jha, K., Barenstein, J.D., Phelps, P.M., Pittet, D. and Sena, S. (2010). *Safer homes, stronger communities. A handbook for reconstructing after natural disasters*. Global Facility for Disaster Reduction and Recovery. The World Bank, Washington.

Johnson, C. (2007). Strategic planning for post-disaster temporary housing. *Disasters*: **31** (4), 435–458.

Kates, R. and Pijawka, D. (1977). Chapter 1. From rubble to monument: the pace of reconstruction. In: Haas, J., Kates, R., and Bowden, M. (1977). *Reconstruction Following Disaster*. MIT Press, Cambridge, Massachusetts.

Kates, R.W., Colten, C.E., Laska, S. and Leatherman, S.P. (2006). Reconstruction of New Orleans after Hurricane Katrina: A research perspective. *Proceedings of the National Academy of Sciences of the United States of America*: **103** (40), 14653-14660.

Li, J., Zlatanova, S. and Fabri, A. (2007). *Geomatics solutions for disaster management*. Springer-Verlag, Berlin.

Lloyd-Jones, T. (2006). *Mind the Gap! Post-disaster reconstruction and the transition from humanitarian relief*. Max Lock Centre at the University of Westminster, London.

Mackay, K. (2007). *How to build M&E systems to support better government*. Independent Evaluation Group. World Bank, Washington D.C.

Miles, S.B. and Chang, S.E. (2003). *Urban disaster recovery: a framework and simulation model*. Technical Report MCEER 03-0005. Multidisciplinary Center for Earthquake Engineering Research, University of Buffalo, New York.

Miles, S.B. and Chang, S.E. (2006). Modelling community recovery from earthquakes. *Earthquake Spectra*: **22** ( 2), 439-458.

Mileti, D. (1999). *Disasters by Design: A reassessment of natural hazards in the United States*. Joseph Henry Press, Washington, D.C.

Mosse, R. and Sontheimer, L.E. (1996). *Performance monitoring indicators handbook*. Technical Paper No. 334. World Bank, Washington D.C.

Nigg, J. M. (1995). *Disaster recovery as a social process*. Preliminary paper #219. Disaster Research Center. University of Delaware.

OECD-DAC (1999). *Guidance for Evaluating Humanitarian Assistance in Complex Emergencies*. Organisation for Economic Co-operation and Development (OECD), London.

OECD (2010). *Development evaluation resources and systems – A study of network members*. Development Co-operation Directorate. Development Assistance Committee. The DAC Network on Development Evaluation, London.

Olshansky, R. (2005). Toward a theory of community recovery from disaster: A review of existing literature. *First International Conference of Urban Disaster Reduction*. Kobe, Japan.

Olshansky, R.B. and Chang, S.E. (2009). Planning for disaster recovery: emerging research needs and challenges. *Progress in Planning*: **72**, 195-250.

Olshansky, R.B. and Johnson, L.A. (2010). *Clear as Mud: Planning for the Rebuilding of New Orleans*. American Planning Association, Chicago.

Olshansky, R.B., Johnson, L.A. and Topping, K.C. (2006). Rebuilding communities following disaster: lessons from Kobe and Los Angeles. *Built Environment*: **32** (4), 354-374.

Proudlock, K., Ramalingam, B. and Sandison, P. (2009). Improving humanitarian impact assessment: bridging theory and practice. In: ALNAP's *8th Review of Humanitarian Action*. Active Learning Network for Accountability and Performance (ALNAP), London.

ProVention Consortium. (2008). *Responding to earthquakes 2008. Learning from earthquake relief and recovery operations*. ProVention Consortium. Active Learning Network for Accountability and Performance (ALNAP), London.

Quarantelli, E.L. (1999). *The disaster recovery process: what we know and do not know from research*. Preliminary Paper #286. Disaster Research Center. University of Delaware.

Recovery Project (2008). *Indicators for measuring, monitoring and evaluating post-disaster recovery. EPSRC Recovery Project – Case for Support*.

Rubin, C.B. (1985). The community recovery process in the United States after a major natural disaster. *International Journal of Mass Emergencies and Disasters*: **3**, 9-28.

Shelter Centre (2006). *Shelter Training Workshop*. Co-hosted by UN-Habitat and CARE International. 15 – 17 November 2006. Geneva.

Showalter, P.S. and Lu, Y. (2010). *Geospatial techniques in urban hazard and disaster analysis*. Springer, London.

Sphere Project. (2011). *The sphere handbook. Humanitarian charter and minimum standards in humanitarian response*. Practical Action Publishing, Rugby.

TRIAMS (2007). *Tsunami Recovery Impact Assessment and Monitoring System (TRIAMS)*. Second regional TRIAMS workshop. Bangkok, 21-23 March 2007.

UNDP (2009). *Handbook on planning, monitoring and evaluating for development results*. United Nations Development Programme, New York.

UNDP (2013). *Post disaster needs assessment. Guidelines. Volume A. United Nations Development Programme.*

UNDRO (1991). *Mitigating Natural Disasters: Phenomena, Effects and Options.* Geneva.

USAID (1996). *Performance monitoring and evaluation tips. Conducting a participatory evaluation.* USAID Centre for Development Information and Evaluation. 1996, Number 1.

White, H. (2009). Theory-based impact evaluation: principles and practice. *Journal of Development Effectiveness: 1 (3), 271-284.*

Wiles, P. (2005). *Meta-Evaluation.* In ALNAP's Review of humanitarian action in 2004. Active Learning Network for Accountability and Performance (ALNAP). Available at: <http://www.alnap.org/pool/files/rha04-c4meta.pdf>

Wisner, B., Blaikie, P., Cannon, T. and Davis, I. (2004). *At risk. Natural hazards, people's vulnerability and disasters.* 2<sup>nd</sup> edition. Routledge, London.

World Bank (2002). *Monitoring and evaluation: some tools, methods and approaches.* The World Bank. Washington D.C.

World Bank. (2008). *Planning for urban and township settlements after the earthquake. Good Practice Notes.* The World Bank. Washington D.C.

World Bank (2010). Mobilizing Post-Disaster Help. In: *Haiti, bank team prepares for damage assessment, recovery plan.* Available at: <http://www.worldbank.org/en/news/feature/2010/01/15/haiti-bank-team-prepares-for-damage-assessment-recovery-plan>

Yu, C.C. (2004). *Could home be re-built? – Lesson learned from Taiwan 1999 Chi-Chi earthquake recovery.* 1st International Conference of Urban Disaster Reduction. Kobe, Japan. 19 January 2004.

## **Chapter 2: Literature Review and Development of Recovery Indicators**

### **2.1. Introduction: Aims and Content of the Chapter**

The aim of this chapter is to review both the technical capabilities of satellite sensors and previous attempts by practitioners and academics to analyse recovery. A table of recovery indicators is developed based on the results of this literature review and is presented at the end of the chapter. The literature review is split into three sections: Part 1 introduces remote sensing technology, focusing on current sensors' spatial, spectral and temporal resolutions. Part 2 reviews previous attempts to measure post-disaster recovery and considers the main issues raised by these attempts. And part 3 describes the process to develop a list of recovery indicators – suitable for remote sensing analysis - and to rank and assess the indicators through a survey of users' needs. The output from this chapter is a table of recovery indicators which are applied to the Thailand case study, presented in chapter 3. As outlined in the framework in chapter 1, the development of an indicator table will form an important contribution to science as it will allow practitioners and analysts to make standardised comparisons between different stages of recovery and also between disasters.

### **Part 1: Remote Sensing - Technical Literature Review**

### **2.2. The Science behind Remote Sensing**

In 1988, the American Society for Photogrammetry and Remote Sensing (ASPRS) defined photogrammetry and remote sensing as the 'art, science, and technology of obtaining reliable information about physical objects and the environment, through the process of recording, measuring and interpreting imagery and digital representations of energy patterns derived from non-contact sensor systems' (Colwell, 1997, page 33-48). These sensors vary dramatically in size and range from handheld reflectance measurement devices through to platforms orbiting the planet. A background to the science behind remote sensing and the sensors currently available is provided below.

Most remote sensing instruments record *Electromagnetic radiation (EMR)*: a form of energy conceptualised in the 1860s by James Clerk Maxwell as a wave which travels through a vacuum at the speed of light, comprising of both oscillating electric and magnetic fields (Maxwell, 1865). EMR is classified according to the frequency or wavelength of its oscillations. The electromagnetic

spectrum, in order of increasing wavelength, consists of gamma rays, x-rays, ultraviolet radiation, visible light, infrared radiation, microwaves and radio waves (Lillesand & Kiefer, 1999). This thesis will focus on the use of energy in the visible and near infrared parts of the EMR spectrum due to the availability of these spectral bands on current satellite sensors.

Different properties of light can be explained using wave and particle theories, light is therefore said to have wave-particle duality. In 1690 Christiaan Huygens published a wave-based theory to explain the velocity of light through a substance known as 'ether'. Thomas Young (1801) later showed Huygen's Principle using the *double-slit experiment*: when shining light-waves through a screen with two slits equally spaced, two wave fronts eventually overlapped each other, leading to interference where light was enhanced and diminished on different parts of the screen. Though Isaac Newton was aware of light's wave-like characteristics he was one of the forbearers of the particle theory of light. In 1704 Newton explained numerous optical phenomena, including rectilinear propagation and reflection, by assuming light was made of tiny particles (corpuscles) travelling in straight lines.

The development of the Quantum Theory of EMR in the 20<sup>th</sup> century significantly shaped our current understanding of light. In 1890 Max Planck understood - through the study of blackbodies - that energy is emitted or absorbed in discrete packets of energy, known as Quanta (now called photons). Five years later, Albert Einstein developed Planck's ideas to explain the photoelectric effect, a phenomenon where metals emit electrons when radiation is shone upon them. The interaction between light and matter can now be described as follows: when an atom absorbs energy its electrons are excited and jump to higher orbits of the atom. When they drop back down EMR is released as photons.

We now know that all objects above absolute zero (-273 °C or 0 K) emit EMR and that most of the energy that is intercepted by remote sensing instruments on or around the earth originates from the sun. The sun produces a continuous spectrum of EMR with a dominant wavelength of 0.48 µm. The EMR travels through the vacuum of space where it interacts with the earth's atmosphere through the processes of refraction, scattering, absorption and reflectance (Jensen, 2007). Once the energy reaches the Earth's surface it is then reflected or emitted by ground features and passed through the atmosphere again before reaching the satellite sensor.

### 2.3. Review of High-Spatial-Resolution Satellite Optical Sensors and Operators

The focus of this thesis and the rest of this literature review is the use of optical satellite sensors with a maximum spatial resolution of 1.0 m<sup>1</sup>; this spatial resolution was deemed necessary so that buildings and other urban features could be delineated (Jensen, 2007).

These sensors commonly use a 'linear array pushbroom' system that records image data along a swath beneath an aircraft or satellite. A linear array of very small charge-coupled devices (CCDs), orientated at right angles to the flight direction is commonly used. A two-dimensional image is built up by recording successive scan lines. Each CCD is sub-divided into tens of thousands of cells by electrodes; the intensity of energy recorded at each cell is represented by a pixel in the resultant image. The pixels' brightness is quantized to 11-bits, which means each pixel contains a digital number ranging from 0 to 2,048.

Private companies were first permitted to enter the satellite imaging business after the Land Remote Sensing Policy Act was passed in 1992. This resulted in the creation of commercial groups including Orbimage, DigitalGlobe and ImageSat International. Since then, the market has grown substantially. 162 Earth Observation (EO) satellites were launched by civil government and commercial entities between 2004 and 2013 (Euroconsultant, 2014). And the global market for remote sensing technologies and hardware is expected to reach \$12.1 billion by 2019; which would represent an increase of \$4.5 billion (59%) since 2013 (BCC Research, 2013).

#### 2.3.1. DigitalGlobe

Two companies currently control more than 50% of the EO data sales: Airbus Defence & Space<sup>2</sup> and DigitalGlobe. All of the images used in this thesis were purchased from DigitalGlobe because of image availability and affordability so they are the focus of this review.

DigitalGlobe now has the largest fleet of high-spatial-resolution satellite sensors. Ikonos and Geoeye-1 were contributions from the GeoEye company<sup>3</sup>, while Quickbird, Worldview-1, Worldview-2 and Worldview-3 were originally developed by DigitalGlobe. Ikonos, launched in 1999, was the first commercially-available satellite with one metre spatial resolution and Quickbird was the first

---

<sup>1</sup> Hence referred to as 'high-spatial-resolution satellite sensors'.

<sup>2</sup> ADS own the following satellites: SPOT, Pléiades, TerraSAR-X and TanDEM-X.

<sup>3</sup> Geoeeye's contract was cancelled in 2012 which led to their merger with DigitalGlobe.

commercial satellite with sub-metre spatial resolution. DigitalGlobe now owns a fleet of four satellites with sub-metre spatial resolution, high geo-location accuracy, rapid control gyros for flexible positioning and an increasing number of spectral bands.

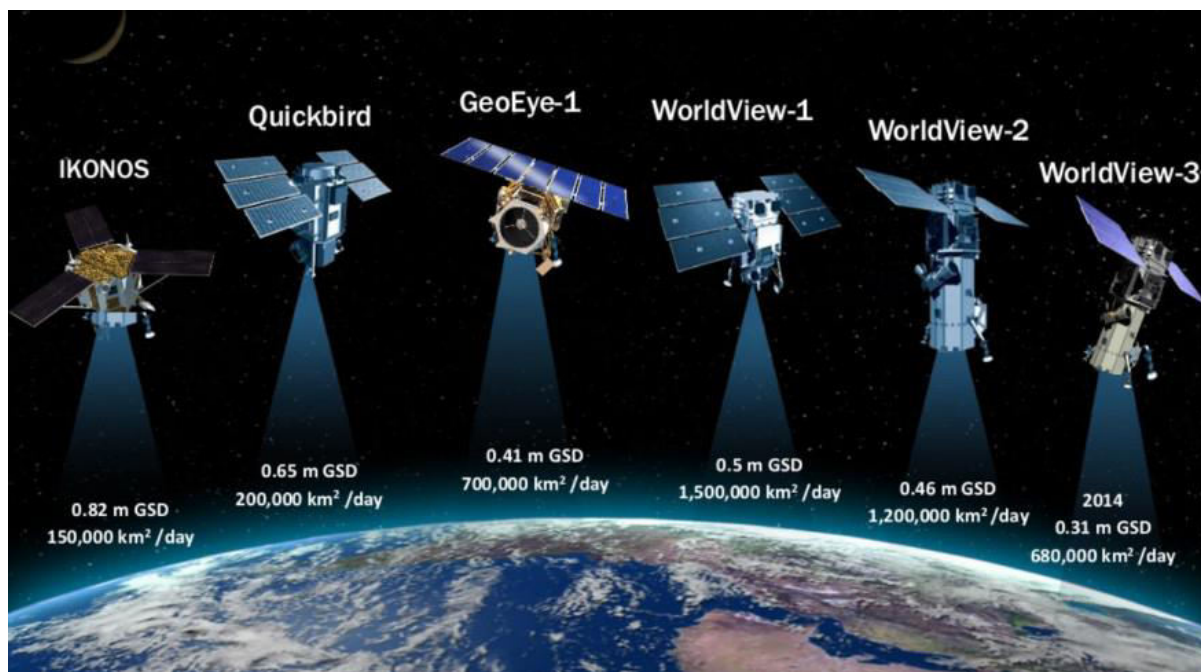


Figure 2-1: DigitalGlobe's fleet of current and past high-spatial-resolution satellites.

**Note: Ikonos and Quickbird were used in this study but have since been decommissioned.**

DigitalGlobe's partnership with the U.S. Government and in particular, the National Geospatial-Intelligence Agency (NGA) has contributed substantially towards the company's development. In particular, a series of NGA Service Level Agreements – including the EnhancedView contracts said to be worth \$7.3 billion over 10 years - have helped cost-share the development and launch of DigitalGlobe satellites (including WorldView 1, 2 and 3). The U.S. government now reportedly accounts for 85% of the use of WorldView-1 and about 50% of WorldView-2 capacity (Selding, 2015).

### 2.3.2. New Start-up Companies

While DigitalGlobe are likely to continue to dominate the provision of sub-metre spatial resolution satellite imagery, there have been some signs of change in other parts of the market. Last year, NGA announced plans to begin exploring the use of imagery products from new commercial satellite operators (Gruss, 2015). In particular, they intend to take advantage of new start-up companies – such as Skybox Imaging and PlanetLabs - that are currently launching their own constellations of small satellites. This constellation approach has helped to drive down the cost of satellite

manufacture and launch. These satellite systems offer daily acquisition of satellite imagery with a spatial resolution of 3-5 m, at a competitive price, which is particularly useful for change detection applications.

### *2.3.3. Data Market*

As shown in figure 2-2, the commercial remote sensing data market totalled \$1.5 billion in 2013. The U.S. Government has been a key customer to-date, but 2013 marked the first year of reduced spending with the Enhanced View service-level agreement. Despite this, spending has grown in other parts of the market, especially by non-US defence users. Defence represented the largest market for commercial data in 2013 (59%, \$880 million).

Non-defence markets have been slower to develop, possibly due to austerity and uncertainty about the cost-benefit of remote sensing solutions amongst potential customers. A report by Euroconsultant (2014) identified other key uses of EO data, these include meteorology and climate studies, land management and monitoring, agriculture, energy and urban planning. Imagery is also increasingly being used to support location-based applications and online services.

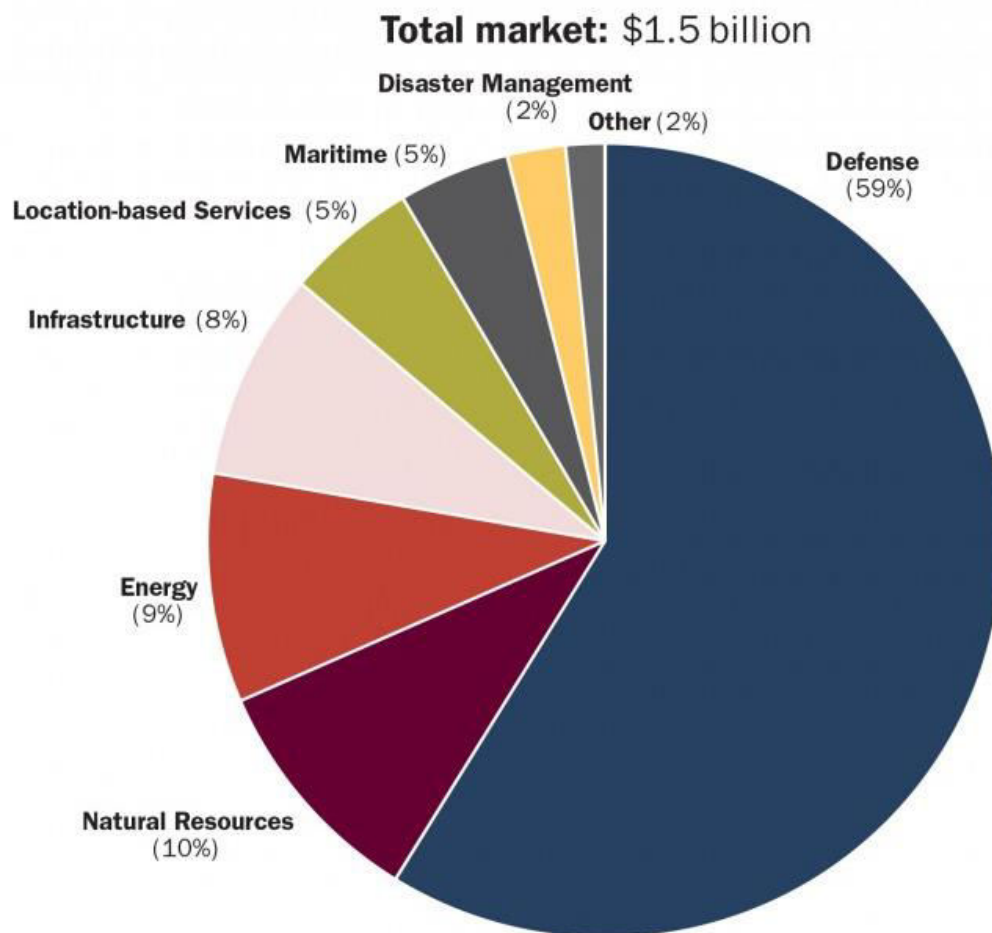


Figure 2-2: Earth Observation Data. Global demand by Sector in 2013. Source: Euroconsultant (2014).

## 2.4. Sensors' Technical Capabilities

The following three sections review the spatial, temporal and spectral abilities of the satellite sensors used in this thesis.

### 2.4.1. Spatial Resolution

The *spatial resolution* is 'a measure of the smallest angular or linear separation between two objects that can be resolved by the remote sensing system' (Jensen, 2007). Put simply, it defines the smallest object identifiable in an image. Literature often quotes the *nominal* spatial resolution of a remote sensing system which equates to the dimensions of the ground represented by an image's single pixel e.g. Quickbird panchromatic band has a nominal spatial resolution of 0.6 x 0.6 m.

Most satellites with high-spatial-resolution use optics that have a constant angle through which the detector is sensitive to radiation (this is known as the instantaneous-field-of-view (IFOV), as shown in figure 2-3). The diameter of the ground-projected IFOV beneath the satellite determines the spatial resolution and is a function of the IFOV angle multiplied by the altitude of the satellite. This means that as the altitude of the satellite increases the diameter of the IFOV increases and the spatial resolution decreases. A satellite can provide a higher spatial resolution in lower altitude but more frequent re-booster are required due to atmospheric drag (Scott, 2016).

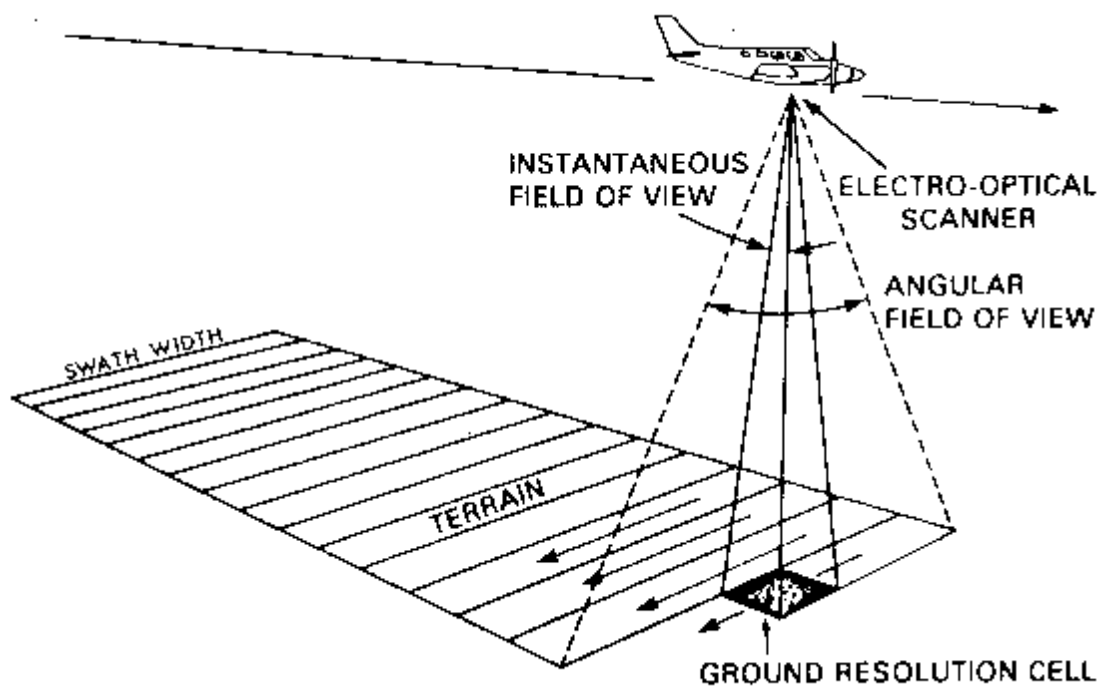


**Figure 2-3: The concept of Instantaneous Field of View (IFOV) (from Avery and Berlin, 1985).**

The spatial resolution is commonly thought to be the most important issue in urban remote sensing because it determines what size objects can be identified (Welch, 1992). Jensen (2007) states that the nominal spatial resolution should be less than half the size of the feature measured in its smallest dimension. A nominal spatial resolution of at least 1.0 m is therefore recommended to detect buildings and roads and for most urban applications. Up to 0.25 m is recommended for detailed work, such as to obtain building footprint perimeter information (Cowen & Jensen, 1998), to check road conditions (Stoeckleler, 1979) and to inventory transmission towers and utility poles (Jadkowski, 1994).

The Ikonos and Quickbird satellites offer 1.0 m and 0.6 m spatial resolution respectively.

DigitalGlobe's Worldview satellites 1, 2 and 3 all provide sub-0.50 m spatial resolution imagery with

the latest, Worldview-3, offering 0.31 m. Until June 2014 commercial satellite owners could only sell imagery with more than 0.5 m spatial resolution. Since then, the US Department of Commerce have provided permission to collect and sell satellite imagery at the best available spatial resolution. Specifically, six months after WorldView-3 was operational DigitalGlobe were permitted to sell imagery with a spatial resolution up to 0.25 m panchromatic and 1.0 m multispectral.

#### 2.4.2. Temporal Resolution

The frequency that satellites can collect new images has vastly improved by utilising innovative technology such as bidirectional scanning. DigitalGlobe's satellite fleet currently collects almost 3.5 million Km<sup>2</sup> of high-spatial-resolution satellite imagery a day and can collect a new image of a location every 1-3 days. The *revisit time* reflects how often an image of a particular location may be acquired. It is determined by the latitude of the target and each satellite's swath width, orbit-type, look angle and agility to shoot at multiple targets (Hubing, 2012).

The DigitalGlobe satellites all have sun-synchronous orbits that cross the equator between 10-10:30 am solar time so the satellites are in constant sunlight. They revolve around the earth in 90-100 minutes, which equates to approximately 15 resolutions of the earth every 24 hours (DigitalGlobe, 2016a).

Satellites now have increasingly more advanced Control Moment Gyros (CMGs) to orientate the direction that the sensor is facing. Satellite imagery is not collected directly below the satellite (known as being 'at nadir') but at an angle called the off-nadir angle. The maximum off-nadir angle is typically around 30 degrees but lower is required to minimise the amount buildings and other tall features appear to lean in the imagery. Customers must therefore consider a trade-off between spatial and temporal resolutions: a higher off-nadir angle shortens the revisit time but increases the spatial resolution. For example, Worldview-2 has a revisit time of 1.1 days at 1.0 m spatial resolution and 3.7 days at 20° off-nadir or less (0.52 m spatial resolution) (Hubing, 2012).

#### 2.4.3. Spectral Resolution

Remote sensing sensors are commonly designed with a number of *spectral bands* that measure the energy received within a pre-determined range of the electromagnetic spectrum. *Spectral resolution* refers to the number and width of the spectral bands that the sensor can collect reflected radiance.

The location of the bands in the electromagnetic spectrum determines what can be sensed. Further to the red, green, blue and near infrared bands on-board the Ikonos and Quickbird satellites, WorldView-2 and 3 have a number of additional bands. These include *coastal blue* (designed for bathymetric studies and atmospheric correction), *yellow* (which sits between green and red and measures water turbidity and vegetation health) and *red edge* (useful for determining plant health) (DigitalGlobe, 2010). This thesis will focus on the use of red, green, blue and near infrared spectral data collected by the Ikonos and Quickbird satellites at the time the research was conducted.

## Section 2.5. Image Classification

A range of techniques exist to classify satellite imagery including parametric supervised classifications (e.g. Maximum Likelihood), unsupervised classifications (e.g. ISODATA) and machine learning algorithms. In recent years there has been increased interest in ensemble classifiers such as Random Forest which work by producing multiple decision trees using a randomly selected subset of training samples and variables (Belgui and Drăguț, 2016). This technique has been shown to produce improved classification accuracies on its own, and with the use of multi-seasonal texture (Rodriguez-Galiano et al. 2012).

Random Forest has repeatedly been shown to improve the overall accuracy compared to other commonly-used algorithms such as Maximum Likelihood. The improvement is usually no more than 10% from around 80% to 90% (Bedawi, S.M. and Kamel, M.S. 2015; Jhonnerie et al. 2015).

In Chapters 3 and 4 manual analysis was predominantly used as this is the most accurate method of classifying buildings, roads and other small urban features (e.g. Pushparaj and Hegde, 2017). Commonly available, easy-to-use semi-automatic techniques were used in Chapter 5 including Maximum Likelihood, Spectral Angle Mapper, Top-Hat Transformation and Object-based Image Analysis. These algorithms were selected to represent a range of different methodologies including spectral classification, mathematical morphology and object classification. Random Forest and other recently developed techniques were not used as they are still not widely available, and the potential improvement in classification accuracy was not deemed necessary for this study as the focus is not to find the best technique but to test the currently available ones in a real, practical setting.

## 2.6. Remote Sensing and the Disaster Management Cycle

The value of geospatial technologies to support decision-making in all phases of the disaster management cycle is now increasingly recognised (Showalter and Lu, 2009). The disaster management cycle illustrates the general on-going process by which governments, businesses and civil society, plan-for and reduce the impact of disasters, react during and immediately following a disaster, and take steps to recover after a disaster has occurred (Coppola, 2015).

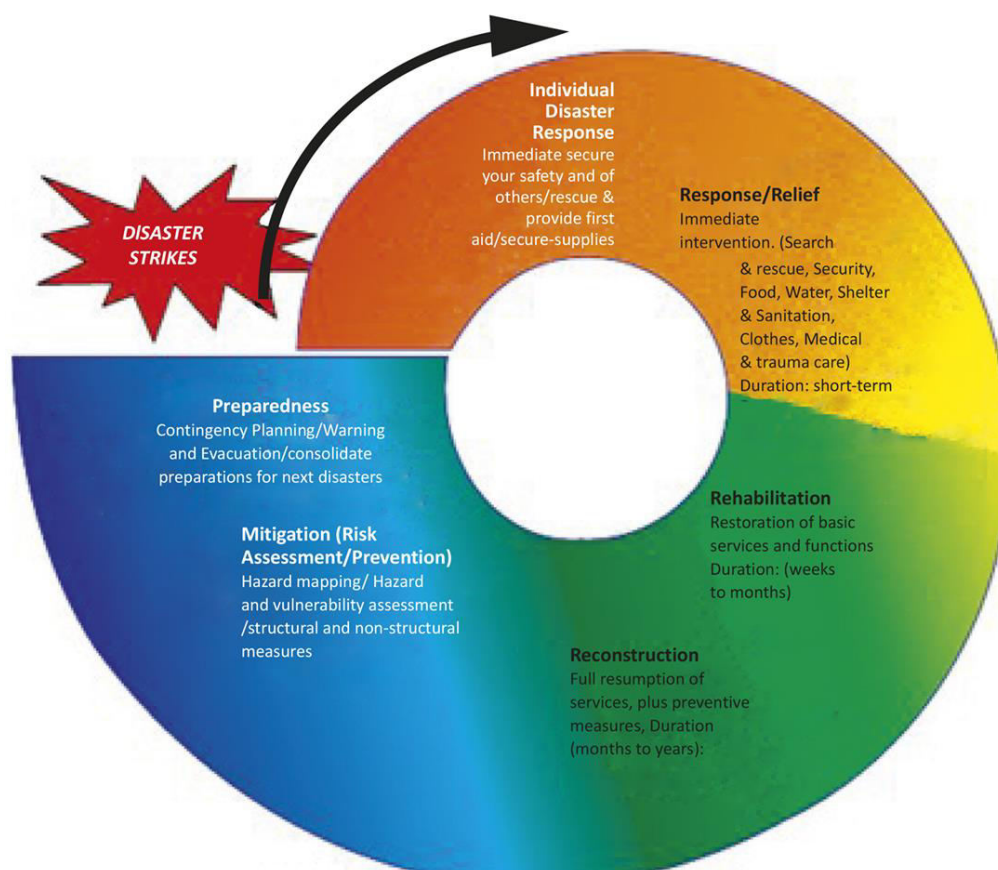


**Figure 2-4: The Disaster Management Cycle (from Sillah, 2015).**

Before a disaster occurs remote sensing and GIS can be used to support mitigation work and preparedness activities. In particular, information from satellite images has been used to support the modelling of vulnerability (Taubenbock et al. 2008) and risk assessment (Deichmann et al. 2011), the results of which can be used to inform mitigation planning (e.g. Patel and Srivastava, 2013). Remote sensing has also been used to support preparedness by modelling hazard events so early-warnings can be issued based on near real-time data (Intrieri et al. 2012; Sorooshian et al. 2014) and by providing maps and information for contingency and logistics planning (Pisano, 2006; Amna, 2013).

Since the introduction of one metre spatial resolution commercial sensors in 1999, academics and practitioners have been testing the use of satellite imagery for damage assessment after disaster (Saito, 2009; Dell'Acqua and Gamba, 2012; World Bank/GFDRR/Imagecat, 2013). There is now an increasing awareness of the usefulness of remote sensing to support relief activities (Kidd, McCallum and Ishadamy, 2010; IFRC, 2011) and subsequent recovery work (Hill et al. 2006; Showalter and Lu, 2009).

Geospatial technologies have been mainly used to-date to support ex-ante phases of the disaster management cycle (risk assessment and risk modelling, contingency planning) as well as ex-post damage assessments more than they have been used to support recovery and reconstruction (Gähler, 2008). This is reflected in the literature – for example, *Geomatics Solutions for Disaster Management* focuses on risk modelling and crisis response (Li, Zlatanova and Fabbri, 2007) and the World Bank's reconstruction handbook *Safer Homes, Safer Communities* includes a chapter on the use of remote sensing to support damage assessment but no guidance on how it might be used to support recovery (Jha et al. 2010)<sup>4</sup>.

The growing awareness of the usefulness of geospatial technologies in support of risk assessments and emergency response is also reflected in relevant policy and legislation; specifically the Sendai Framework for Disaster Risk Reduction 2015-2030 that highlights the importance of creating, updating and sharing location-based disaster risk information (United Nations, 2015) and the Sustainable Development Goals (SDGs) that acknowledge the role of remote sensing to monitor relevant indicators (DigitalGlobe, 2016b). The International Charter on Space and Major Disasters, initiated in 1999, also describes the intent by space agencies to supply data for the anticipation and management of potential crises. Note though that the Charter cannot be used for long-term recovery, only for emergency response (for 30 days after the emergency has been declared by the government) (Disaster Charter, 2000).

Additionally, a number of services have been established over the past 15 years with a particular focus on supporting crisis response and damage assessment, including the UN's Operational Satellite Applications Programme (UNOSAT), Sentinel Asia which monitors natural hazards focussing on Asia and Pacific regions and the European Union's Joint Research Centre's (JRC) Copernicus Emergency Management Service. *Crisis mapping* has also risen to prominence in recent years, especially since the 2010 Haiti earthquake. Crisis mapping uses a range of data including the results of social-media

---

<sup>4</sup> On page 260, the Handbook provides a reference to the Recovery Project and Brown et al. 2008 as an example of a project working to develop remote sensing tools and protocols in support of recovery.

and satellite image analysis to provide information during crisis (Meier, 2015). GEO-CAN is a global crowdsourcing approach that was used to assess damage using remote sensing after the 2010 Haiti earthquake (Corbane et al. 2011) and the 2011 Christchurch earthquake (Foulser-Piggott, Spence and Brown, 2013 )<sup>5</sup>.

A full review of the use of remote sensing in the different stages of the disaster management cycle is beyond the scope of this thesis but is available as a paper on the Cambridge Architectural Research Ltd. website (Brown, 2017).

### *2.6.1. Remote Sensing and Recovery*

Remote sensing's use in the recovery phase has been surprisingly absent. Hodgson et al. (2010) conducted a survey of U.S. state-level Emergency Management Agencies (EMAs). They found that prior to 2005 Hurricane Katrina, 88% of EMAs considered GIS to be beneficial but only 40% considered the same of remote sensing. But when offered specific remote sensing products 90% said they would use them, indicating unfamiliarity with the technology. Factors contributing to the lack of uptake include cost/time constraints and staff technical limitations (Hodgson et al. 2010).

Laituri and Kodrich (2008) noted that the use of geospatial technologies for disaster management is still in the development stage. There is still uncertainty with this group of technologies that has to be overcome - for example, Harwell (2002) warn that remote assessments may mask local equity and social welfare issues. Cutter, Boruff and Shirley (2003) believe some of the issues with geospatial technology arise because of a lack of understandable graphical interfaces and a lack of willingness to adopt new technology amongst users.

Researchers are now beginning to consider what elements of the recovery process could be assessed through the analysis of remote sensing imagery (Joyce et al. 2009). To-date such work on recovery has focussed predominantly on relief and emergency response. Hill et al. (2006) for example showed that physical evidence of recovery, such as blue tarpaulins, could be identified in Quickbird imagery after Hurricane Katrina.

---

<sup>5</sup> The author worked closely with colleagues at University of Cambridge, Cambridge Architectural Research Ltd. and ImageCat on this damage assessment work. Specifically he was involved in testing Imagecat's Virtual Disaster Finder after the 2008 Wenchuan earthquake; conducting remote damage assessment for EEFIT following the 2009 South Pacific Islands earthquake and as part of the GEO-CAN team after the 2010 earthquake and the 2011 Christchurch earthquake; testing the use of Pictometry data after the 2010 Haiti earthquake and validating the Haiti and Christchurch GEO-CAN results.

Non-Government Organisations such as the International Federation of Red Cross (IFRC) are also beginning to recognise aerial imagery and maps as an important secondary data source, but don't go as far as providing indicators for how it may be used (IFRC, 2011). UNHCR, the lead UN organisation for refugees, recognises remote sensing as a useful tool for camp planning (UNHCR, 2007). A review by the Overseas Development Institute (ODI) recommends remote sensing is used to provide information on land cover, topography, access, and the context of proposed camp locations (Chalinder, 1998).

Kidd, McCallum and Ishadamy (2010) analysed the use of an aerial optical image and digital terrain model (DEM) following the 2004 Indian Ocean tsunami. Their work showed that the data, which cost 1.43 million euros, was used directly by 99 users and indirectly by 635 users to support projects worth 28 million euro. The data was used across a number of sectors including transport, environmental protection, agriculture and research. UNDP for example used the data to map and plan the removal of waste including heavy deposits of sand, silt and debris. NGOs were the biggest group of users and they used it mainly for urban and rural planning purposes.

There are very few examples of remote sensing being used to monitor post-disaster recovery. The military have started to use remote sensing to monitor reconstruction in hard-to-reach conflict zones. The Special Inspector General for Iraq Reconstruction (SIGIR) was set-up to monitor the U.S. Congress' funds for Iraq relief and reconstruction. According to the SIGIR final report, 923 aerial assessments were used to monitor the reconstruction in Iraq<sup>6</sup>.

Murao (2004) created a recovery database after the 1999 Chi Chi earthquake using an Ikonos image as a base map. Spatial information was digitised (e.g. buildings, railways, roads, rivers, administrative districts and parks) and combined with field survey data including building damage status. Maki et al. (2007) developed a recovery process monitoring system using twice daily images of disaster impacted areas collected by a series of roof-top located camera systems. A GIS was created with this system showing reconstruction of buildings after the 2007 Noto earthquake.

In 2014 the Recovery Observatory Oversight Team was created with representatives from the satellite data providers, the international recovery stakeholder community and value-added

---

<sup>6</sup> A copy of all SIGIR assessment reports can be viewed at the SIGIR website:  
<http://cybercemetery.unt.edu/archive/sigir/20131001083050/http://www.sigir.mil/index.html>

providers. It oversees the development of basic infrastructure, monitors international events for potential triggering and has established several recovery pilots in Malawi and Nepal in 2016.

## **Part 2: Monitoring and Evaluation of Post-Disaster Recovery**

### **2.7. Guidelines and Monitoring Systems for Post-Disaster Response and Recovery**

Very few humanitarian organizations thought to measure the consequence of their actions until the 1990s, as it was largely assumed that their interventions were beneficial to the recipients (Barnett 2005). In the past 20 years though, a number of systems and projects have arisen that address the need for post-disaster monitoring and evaluation. The Sphere Handbook, for example, has provided minimum standards and guidance to humanitarian relief workers since it was devised in 1997 (Sphere Project, 2011). Due to the complex nature of post-disaster situations, the report provides guidance notes on how signs of bad practice may be identified, as well a series of potential indicators that agencies may want to adopt. The focus of the Sphere Project is on assisting emergency relief work as opposed to long-term recovery. The report is divided into four sections: 1. Water, sanitation and hygiene promotion 2. Food security, nutrition and food aid 3. Shelter, settlement and non-food items 4. Health services (Sphere Project, 2011).

Another approach to monitoring recovery has been to develop information systems capable of collating, storing and displaying statistics on damage and loss, the displaced population and the provision of humanitarian supplies. The World Bank's *Data against Natural Disasters* (2008) reviewed six such information systems. The simplest, known as a Logistics Support System (LSS), is used to organise the receipt, storage and distribution of supplies and donations. The main value of the system is the transparency and accountability it offers across the whole supply chain. The management of the system in Guatemala, after 2005 Hurricane Stan, by a permanent national organization dedicated to disaster response was deemed essential to ensuring the participation of the government and international organisations (Amin and Goldstein, 2008).

The Development Assistance Database (DAD) is a web-based aid management system that has been used to track the provision of aid in more than 35 countries. *Data Against Disasters* reviewed the World Bank's use of the system to track the pledge and allocation of funds in Aceh and Nias following the 2004 Indian Ocean tsunami (Amin and Goldstein, 2008). The DAD system provided an overview of the funding activities and was used for high-level decision-making and reporting by the

government and donors. The needs and loss assessment data formed a baseline for the system. Throughout recovery, implementing agencies regularly submitted concept notes to the World Bank describing their current projects, budgets and target sectors. The system used a simple, manual methodology and was cost-effective – requiring only four data analysts. Though users were obliged to submit data to the system by a presidential decree; most stakeholders presented their data on-time without pressure from the government – in part, because of the simplicity and regularity of the data reporting, and also because agencies were able to see the value of the data they were submitting through the dissemination of regular outputs and products.

While DAD was designed to predominantly track financial data, the Relief and Information Systems for Earthquake Pakistan (RISEPAK) was developed to monitor the outcomes of recovery after the 2005 Kashmir earthquake. Its aim was to provide information on needs and response at village-level for gap analysis. This was achieved by collating pre-earthquake maps and data - mainly from census data - and post-disaster information on access, damage and relief activities. The system was ambitious and innovative but not sustainable for a number of reasons. Humanitarian agencies were not effective at inputting data because they apparently didn't see clear benefits from the system to warrant their effort; so information was instead collected directly by RISEPAK volunteers in the field which was only sustainable for the first year of response. The system also suffered because it was not anchored in an appropriate institutional context, such as a recovery management agency and because the system was set-up *during* the response and not before. Suitable Information management systems and datasets should ideally be produced as part of disaster preparedness work prior to the disaster and institutionalised. Mapping consistent geographic locations and baselines in vulnerable areas using standardised geospatial datasets across the ministries and external organizations contributing to the recovery efforts is a particularly important task to ensure important datasets are available in the first hours and days of a response.

The Tsunami Recovery Impact Assessment and Monitoring System (TRIAMS) was one of the largest and most comprehensive attempts to monitor post-disaster recovery to date (TRIAMS, 2007). The framework endorsed by the Global Consortium for Tsunami-Affected Countries (India, Indonesia, the Maldives, Sri Lanka and Thailand) defined, promoted and supported the tracking of post-disaster recovery after the 2004 Indian Ocean tsunami. TRIAMS real innovation though was in the creation of output and outcome indicators categorised into four areas: vital needs, basic social services, infrastructure and livelihoods. The Tsunami Recovery Indicator Package (TRIP) is part of TRIAMS and now contains over 200 social, economic, environmental and demographic indicators (TRIP, 2007).

One of the key concerns raised by TRIAMS was the lack of a standardized method of data collecting. They noted that the monitoring capabilities of different countries affected by the Asian tsunami varied dramatically and that there was a need to find suitable methodologies and modalities to collect and analyse the TRIAMS core indicators in a systematic and periodic way (TRIAMS, 2007). When the author spoke to agencies that had responded to the tsunami in Thailand he was told that they commonly suffered from time and resource pressure and that many of the TRIAMS indicators required data that was unavailable and/or unreliable. In particular, there was a lack of good pre-disaster baseline data.

## **2.8. Donors and Aid Agencies - Common Approaches to Monitoring and Evaluation**

Alongside these systems, most international Non-Governmental Organisations (NGOs) and fund-providers now increasingly require their own internal Monitoring & Evaluation (M&E) policies and methods. The Disaster Emergency Committee (DEC) for example, which brings together 13 UK leading aid agencies, is reviewed at key milestones by independent consultants conducting short field missions and by full evaluations that are commissioned at the end of an appeal's expenditure period.

Some of the large donors have their own independent evaluation units, such as the World Bank's Independent Evaluation Group (IEG), to better understand what works and to deepen their evidence base. A review of the evaluation procedures of 24 bilateral donors and 7 multilateral institutions estimated US\$148 million was spent on development evaluation in 2009 by those agencies alone (OECD, 2010). The World Bank Group spent the most on evaluation with a budget of US\$31 million, while the UK's Department for International Development (DFID) had a budget of US\$9 million.

Most evaluating departments now use a *programme logic framework* approach, based on a clear theory of change – also known as a results-chain - and a set of clearly-defined inputs, activities, outputs and outcomes (Kusek and Rist, 2004). When an agency intends to establish a programme they will initially set clear objectives for it based on an analysis of the problem and the need on the ground. They then link these to immediate results and appropriate performance indicators and monitor progress towards the objectives.

It's useful to make the distinction here between the terms monitoring and evaluation. The International Federation of Red Cross (IFRC) defines them as follows:

*Monitoring*: 'is the routine collection and analysis of information in order to track progress, check compliance and make informed decisions for project/programme management',

*Evaluation*: 'is an assessment, as systematic and objective as possible of an on-going or completed project, programme or policy, its design, implementation and results' (IFRC, 2010).

Basic monitoring can provide regular information on the speed and timing of project activities and decisions. The *Handbook on owner-driven housing reconstruction* by the IFRC recommends teams also monitor programme management, programme design and collaborations with partners, as well as the participatory process and in particular, the inclusion of vulnerable households (IFRC, 2010).

Project-level evaluations commonly consist of a mid-term review and an end-of-project review. Many lessons can be learnt from the evaluation of developmental projects in a non-disaster context. In the book, *Evaluating the Impact of Development Projects on Poverty*, Judy Baker suggests that comprehensive project evaluations consist of real-time monitoring and the evaluation of service delivery, cost-effectiveness and impact (Baker, 2000).

Recently, there has been increased interest in impact evaluation (ALNAP, 2009), which attempts to measure 'lasting or significant changes – positive or negative, intended or not – in people's lives brought about by a given action or series of actions (Roche, 1999). Impact Evaluations are notoriously challenging and costly to conduct as they are designed to establish how individuals would fair in the absence of the program and therefore require a valid comparison group who were not in the program.

The ALNAP report '*Improving humanitarian impact assessment: bridging theory and practice*' identified a number of issues with impact assessments, including: weak or non-existent baselines; a focus on quantitative process and outputs indicators and not on the larger outcomes of a programme; and a lack of collective and coordinated approach to data collection (Proudlock, Ramalingam and Sandison, 2009).

A substantial amount of guidance material has been produced by agencies to support M&E work and is available publicly (Mosse and Sontheimer, 1996; World Bank, 2002; Dabelstein, 2006; Daniba, 2006; UNDP, 2009), much of which is based on the Development Assistance Committee evaluation criteria (OECD-DAC, 1999). The *DAC criteria* provide guidance to encourage evaluators to consider each programme's *relevance, effectiveness, efficiency, impact and sustainability* (Dabelstein, 2006). The criteria are now considered an essential reference for those wishing to evaluate developmental-based programmes and projects.

## 2.9. Academic Approaches to Measuring Recovery

Academic researchers have developed their own novel and interesting approaches to measuring recovery. Detailed studies of businesses and households by academic teams have tended to rely on data from a combination of interviews, observations, archival documents and surveys, using both cross-sectional and macro approaches, and to a lesser extent, longitudinal studies. Webb, Tierney & Dahlhamer (2000) used a cross-sectional approach to survey 5,000 private entities recovering from four disasters - the 1989 Loma Prieta earthquake, 1992 Hurricane Andrew, 1993 Midwest floods and 1994 Northridge earthquake - and they concluded that differential impacts upon business recovery were observed due to the severity of the losses, size of the business and damage to the surrounding areas. They recommend that businesses develop pre-disaster plans and help to promote higher resistance in their community as a whole.

Regional approaches to measuring recovery provide a convenient and useful means of measuring as the data collection frameworks are often already in place and conducted routinely (Karatani & Hayashi, 2007). Recovery after the 1995 Great Hanshin-Awaji earthquake was measured by analysing electricity consumption, with regions adjacent to the impact area exhibiting an increase in activity (Takashima & Hayashi, 1999; Takashima and Masasuke, 2007) and regional economic statistics, which showed a 3-4 year boost during reconstruction activities (Chang, 2009). Building construction has been measured with the use of house permit datasets (Wu & Lindell, 2003) and census and tax appraisal data (Lu et al. 2007). Rathfon et al. (2012) notes some of the limitations of using building permit data - for example, 1) homeowners might undertake repair without permits and 2) work permits only show that permission for work has been granted, not that the work has actually taken place.

### 2.9.1. Time-series Analysis

Time-series analysis of appropriate indicators allows the speed and stability of a process to be monitored along with the level of the variable at static points in time. As outlined by Chang (2009), monitoring the level or the stability of an index requires two different types of indicator. The measurement of a variable relative to the pre-disaster condition or to a projected recovery level involves the use of *stock indicators* which measure the quantity of something at a particular state in time. This might be the population or number of buildings. While the level of stability of an index may be measured using *flow indicators* which measure change over a unit of time.

### 2.9.2. Stock Indicators

Yuka Karatani and researchers at Meijo University began assessing time-series data after the 1995 Great Hanshin-Awaji earthquake using these two different approaches. First the stock indicator approach was used, the indices were standardised to the assumed variation of each index if the disaster hadn't occurred (Karatani et al. 2000, 2003, 2004). The concept behind this method is shown in figure 2-5,  $Si_1$  represents the actual measured variation of an index after the disaster and  $Si_0$  is the assumed variation of the index if the disaster had not occurred. The assumed variation in this method was estimated using data from outside the affected region over the same period of time and it assumes there is no spill-over effect from the disaster. Other researchers have normalised data points using series of data-points collected in the affected area before the disaster (Beniya, 2007).

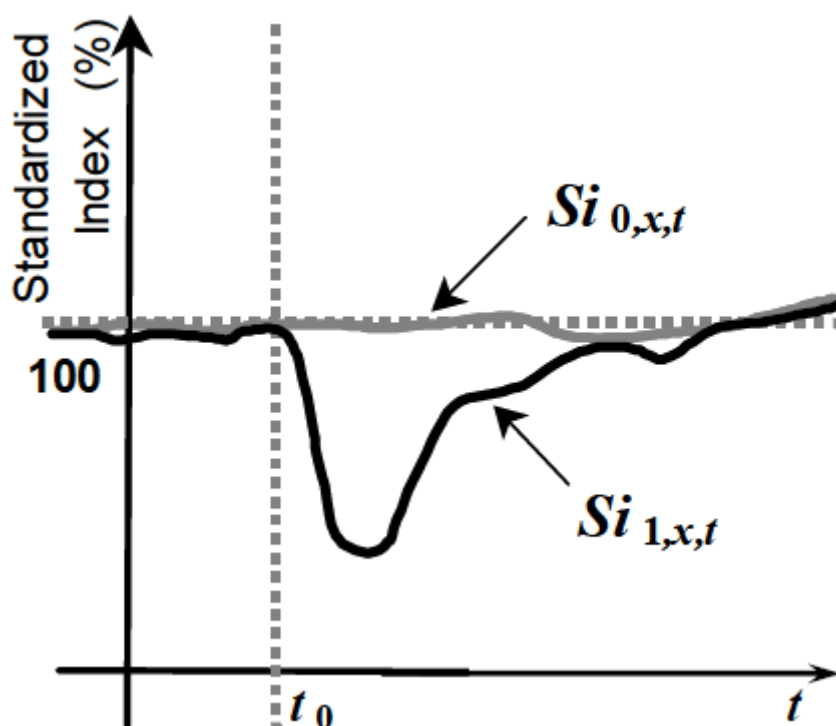


Figure 2-5: Yuka Karatani compared recovery indices ( $S_{i_1}$ ) to assumed variation based on observations from outside the affected area ( $S_{i_0}$ ).

### 2.9.3. Flow Indicators

A couple of years later Yuka Karatani tested another technique to analyse time-series data, this time by extracting trends, seasonal variation and noise from the data and comparing those to trends in pre-disaster time-series data (Karatani et al. 2007). This is advantageous as it does not require a reference region to be identified but it does require a large amount of pre-disaster data and assumes that pre-disaster data can be used to project trends that would occur without the influence of the disaster. The research identified 12 recovery patterns or scenarios based on the resumption of trends, seasonal variation and random variation. The return of seasonal trends is assumed to represent the restoration of stable social conditions and a reduction in noise is interpreted as a return to stability.

### 2.9.4. Recovery Scenarios and the End of Recovery

The work with time-series analysis raises interesting questions regarding the trajectory of recovery and in particular, when the process of recovery is deemed to have ended. The consensus is that the minimum goal is to replace lost housing stock and to return to pre-disaster economic function

(Olshansky, Johnson, and Topping, 2003). When an indicator, such as gross domestic product (GDP) or number of buildings, is plotted during recovery we see that there are several trajectories it might follow: 1) return to pre-disaster conditions (Schwab et al. 1998) 2) attaining what would have occurred without the disaster and 3) reaching a new stable state (Quarantelli, 1999). As such, there are several ideas about what constitutes a completed recovery. Alesch (2004) suggests that cities are self-organising systems and that recovery from catastrophic events will often involve finding a new stable state that may differ from the pre disaster stable state. Quarantelli (1999) states that recovery is the process of bringing the post-disaster situation to a level of acceptability.

Many researchers warn that bringing a community back to where it was before the disaster can recreate conditions of vulnerability to future disasters (Blaikie et al., 1994; Hewitt, 1997; Wu and Lindell, 2004). Disasters should, where possible, be seen as opportunities to improve pre-disaster conditions. Some recovery programs have successfully improved upon pre-disaster conditions by revitalizing urban areas, reducing vulnerability and preserving historic buildings (Tyler, O'Prey, and Kristiansson, 2002).

In some cases, disasters have created reconstruction booms that allow community reconstruction and re-planning projects to commence that were urgently required before the disaster allowing communities to 'build back better' (Clinton, 2006). Cosgrave (2008) warn though, that whilst there are limited opportunities for promoting change, a single disaster response cannot undo decades of underdevelopment. Despite all good intentions, aid agencies and governments must be realistic about what they can achieve.

### **2.10. Need for more Longitudinal Studies**

Implementing surveys in the field can consume a lot of time and resources, and research grants must often be used within a stipulated timeframe; as a result, researchers of recovery have had to limit the number of visits they might make, which subsequently affects the type of research they conduct. This was recognised at a 1996 Boulder workshop session attended by leading US-based researchers on recovery titled "*what is known and trends for improving recovery and reconstruction following disasters*". The researchers – including Joanne Nigg, Trish Bolton, Claire Rubin and Phil Berke – described existing studies of recovery as 'overly descriptive, fragmented and short-term oriented'. They also identified the need to "shift the conceptualisation of recovery from linear and outcome based to seeing it as an on-going and long-term process" (Tatsuki et al. 2005).

Soon after the Boulder meeting Dr. Daniel Alesch and colleagues at the University of Wisconsin-Madison began one of the longest-running longitudinal studies of recovery to-date. Over a period of 15 years the researchers tracked over two dozen communities, again in the US, the results of which are discussed in the book *'Managing for long-term community recovery in the aftermath of disaster'* (Alesch, Arendt and Holly . 2009). Their results suggest that the factors affecting resilience and the vulnerability of businesses are multidimensional and complex, but that businesses are more likely to recover successfully if they are willing and able to adapt to the new post-event environment (Alesch, 2001).

### **Part 3: Development of Recovery Indicators**

#### **2.11. Recovery Project User-needs Survey**

A key objective of the Recovery Project was to create a list of recovery indicators, informed by appropriate literature and a user needs survey of relevant stakeholders. A user needs survey of the national and international aid community was therefore carried out to assess the perceived requirements for indicators of monitoring recovery.

The survey was designed by Dr. Stephen Platt at Cambridge Architecture Research Ltd. and emailed to 41 organisations using contacts that were obtained from a UNDP Emergency Shelter Cluster Work Plan and a meeting in May 2008, hosted in Brussels by the United Nations Development Programme, the World Bank and the European Commission to discuss Post Disaster Needs Assessment and Recovery Planning (PDNA, 2008). The Survey had a response rate of 41% after 17 responses were received. Due to the low number of responses, the results were assessed with caution, but because the responses were received from a wide range of organisations they still provide a useful insight into the users' requirements. Table 2-1 lists the names of the organisations that responded to the survey, they include academic and governmental departments, and sections of the United Nations and the World Bank.

<ul style="list-style-type: none"> <li>• Department for International Development (DFID)</li> <li>• EuropeAid</li> <li>• European Commission</li> <li>• Food and Agriculture Organization of the UN (FAO)</li> <li>• International Labour Organization (ILO)</li> </ul>	<ul style="list-style-type: none"> <li>• International Recovery Platform</li> <li>• Office for the Coordination of Humanitarian Affairs (OCHA)</li> <li>• UN Development Group</li> <li>• UN Development Programme</li> <li>• UN Environment Programme</li> <li>• UN Population Fund</li> </ul>	<ul style="list-style-type: none"> <li>• University of Memphis</li> <li>• UNOSAT</li> <li>• World Food Programme (WFP)</li> <li>• World Bank – Head Quarters</li> <li>• World Bank – Indonesia</li> </ul>
---	---	---

**Table 2-1: The organisations that responded to the Recovery Project’s User Needs Survey.**

The survey asked the users to specify what information they required, what data they lacked and what indicators of recovery they would like to see mapped. A significant proportion of the agencies had conducted some form of monitoring in the past: 90% had used field surveys and statistics and 76% had used satellite imagery.

When asked to score a set of indicators proposed by the Recovery Project, the users scored them all highly, suggesting that all of the indicators are equally as important as each other (see table 2-2). Furthermore, all but one (93%) of the respondents indicated that they would prefer a ‘comprehensive’ approach to monitoring recovery as opposed to a ‘simple’ approach, which would involve monitoring less than 3 sectors. These results support the creation of a comprehensive list of indicators covering several different aspects of recovery, i.e. housing, infrastructure, services, livelihood, environment, social/security, risk reduction (Platt, 2008).

Selected comments from the survey respondents suggest donors such as the World Bank and Department for International Development would like a holistic overview of the situation, while agencies such as UNEP may have specialised areas of interest:

**Josef Leitmann - World Bank – Indonesia, Disaster Management Coordinator** “We lack good information about damage to housing and infrastructure; impact on access; land cover change. It would be very useful to have these indicators of recovery mapped as overlays onto satellite imagery”

**Anne-Cécile Vialle – UNEP, Associate Programme Officer** “We need maps of agricultural damage,

crop loss, forest loss, industrial and environmental sites, the location of displaced people and the sites where rubble/waste is being transported”.

**Dan Ayliffe - DIFD, Response Officer** “It would be useful to map population movements; rehabilitation of homes; rehabilitation of infrastructure, including roads, camps and medical centres; uptake of agricultural activities and other livelihoods”.

<b>Criteria</b>	<b>Indicator</b>	<b>Average Score</b>	<b>Rank Order</b>
Housing	Relief shelter	3.9	16=
	Transitional housing	4.2	8=
	Housing reconstruction	4.6	2
	New urban development	4.1	13
Infrastructure	Temporary road access	4.2	8=
	Road reconstruction	4.3	5=
	Power supply	3.7	21=
	Drinking water	4.3	5=
	Waste water disposal	3.9	16=
	Debris removal	4.0	14=
Health	Health – relief services	4.0	14=
	Health – recovery	4.2	8=
Education	Schools – relief	3.2	24
	Schools – recovery	3.8	18=
Agriculture	Crops / livestock / fisheries	4.4	4
	Food supply	3.8	18=
	Administration	3.7	21=
Economic	Livelihoods	4.8	1
	Tourism	3.6	23
	Business/Manufacturing	3.8	18=
Environment	Floodwater removal	4.3	5=
	Sand/debris removal	4.2	8=
	Vegetation	4.2	8=
	Water quality	4.5	3

**Table 2-2: Provisional list of Recovery Indicators with the average scores and ranking from the Recovery Project’s User Needs Survey (Platt, 2008).**

### 2.12. Recovery Indicator Table

An early list of recovery indicators was produced by Professor Robin Spence and Dr. Arleen Hill following the Recovery Project’s first steering committee meeting on 5 March 2008. The list was created based on Robin and Arleen’s experience of working in post-disaster environments. Part of

Arleen's previous work identified surface features associated with different phases of the disaster cycle (Hill et al. 2006), which provided an appropriate starting point for the creation of the indicator list, as it gave an indication of the types of features that may be identified.

The author spent much of the first year of the PhD creating a definitive list of indicators that represented all of the different aspects of recovery, but that remained practical. The User Needs Survey also contributed to the compilation of the indicators by asking the users *what indicators they would find useful to see mapped?* Five major categories were identified: 1. Livelihoods 2. Housing 3. Water 4. Environment and 5. Access. The respondents also identified several new indicator groups that were not already included in the list, including population movement, contamination, risk and vulnerability.

A review of relevant literature also informed the development of the recovery indicator list. The Tsunami Recovery Impact Assessment and Monitoring System (TRIAMS) and the Tsunami Recovery Indicator Package (TRIPS) were particularly useful resources. TRIPS provides one of the most comprehensive lists of indicators, with over 280 individual indicators. But with so many potential indicators to choose from, it was important to only select indicators that would accurately represent the progress of recovery and be monitored in a practical-manner. As an example, table 2-3 shows the TRIAMS indicators, with those indicators that are measurable with remote sensing highlighted in grey by the author. All eight indicators were incorporated into the Recovery Project indicator list if they were not already present.

<b>Vital needs in relief and recovery</b>	% of tsunami-affected and/or overall population with access to water from an improved source, by admin.
	% of tsunami-affected and/or overall population without basic sanitation facilities, by admin.
	proportion of tsunami-affected and/or overall population with housing damaged/destroyed living in emergency shelter/temporary houses/permanent houses, by admin., by time period
	measles immunization coverage, by admin.
	# titles to land given, by gender, by admin. (modified by specific country definition)
	% of housing built meeting applicable hazard-resistance standards, by admin.
<b>Basic Social Services</b>	# primary schoolchildren per school, by admin.
	# primary schoolchildren per teacher, by admin.
	# hospital beds per 10,000 population (inpatient & maternity), by admin.
	# of physicians, nurses and midwives per 10,000 population, by admin.
	# outpatient consultations/person/year, by admin.
	% of one-year-olds immunized with DPT3, by admin.
	# of health facilities with emergency obstetric care per 10,000 population, by admin.
# trained workers providing psychosocial support per 10,000 population, by admin.	
<b>Infrastructure</b>	# km of repaired/new road by type of road, by district
	# bridges repaired by district
	# harbours/jetties rehabilitated by type, by district
	# of new/rebuilt/rehabilitated schools, by category, by admin.
	# of new/ rebuilt schools by category that meet the applicable hazard resistance standards, by admin.
	# of new/rebuilt/rehabilitated health facilities by category, by admin.
	# of new/rebuilt health facilities by category that meet applicable hazard-resistance standards, by admin.
	# sq km of natural habitat restored, by type
# km of coastal protection constructed/repared, by type (bio-fencing, seawalls, quay walls, breakwaters), by admin.	
<b>Livelihoods</b>	% of tsunami-affected and/or overall population who have received loans, by type of loan, by gender, by admin.
	% of tsunami-affected and/or overall population enrolled in social protection programmes, by type, by gender, by admin.
	# people employed by different sectors, by gender, by admin.
	% of boats damaged/destroyed repaired/replaced, by use (fishing, tourism, ferrying and other income-generating activities) and by district

**Table 2-3: The TRIAMS Indicators, with the indicators that may be monitored using Remote Sensing highlighted in grey by the author.**

Other significant sources of literature include Stephanie Chang's object-based model of recovery, which identified important aspects of business and household recovery (Miles and Chang, 2003; 2006). The Economic Commission for Latin America and the Caribbean (ECLAC) also published a comprehensive loss assessment toolkit called the *Handbook for Estimating the Socio-economic and Environmental Effects of Disasters*, which provided a useful insight into the impact a disaster can have on a community (ECLAC, 1991). Other development indicators were also referred to, such as the United Nation's Millennium Development Goals (MDG, 2008) and the World Development

Indicators (WDI, 2008). The Sphere Guidelines also provided an important insight into the post-disaster situation from the agencies perspective. Not only does it suggest potential indicators and survey designs, but it also highlights minimum standards and provides guidance notes on how different elements of disaster relief should be monitored (Sphere Project, 2011).

An EPSRC-funded field reconnaissance trip to China, six months after the 2008 Sichuan Earthquake, was also fundamental in the design of the indicators, as it allowed the author to witness the recovery process first-hand, to identify signs of recovery and to talk to people about their recovery experiences. A considerable amount of geocoded photography and video footage was taken along a 34km transect that captured the state of the affected region 6 months after the earthquake. This technique was used to show the disparity in the recovery process across urban and rural areas. An in-depth study of damage and recovery was also conducted in the town of Yingxiu by analysing Quickbird imagery for signs of recovery including road clearance and the presence of tents and transitional shelters (Brown et al. 2012).

The table of indicators developed in this chapter is presented in table 2-4. As requested by the user-needs survey respondents, the table is small and manageable yet encompasses a wide range of categories. Users may pick-and-choose indicators according to their own needs and resources. Despite its relatively small size the table is still meant to be comprehensive and represent most of the information extractable from remote sensing that is related to the monitoring of post-disaster recovery.

Category	Indicator	Description
Accessibility	1. Road length (km)	Monitors the transport network, identifying damaged or broken sections immediately after the disaster, and cleared, resurfaced or reconstructed sections at intervals through the recovery process.
	2. Network Analysis	Monitors changes in the accessibility of the transport network in terms of travel time and distance brought about by damage to the network or relocation of homes and services. It can also identify households and businesses with inadequate access to key facilities and services.
	3. Bridge and public	Monitors the reconstruction of bridges and public

	transport	transport facilities.
	4. Presence of vehicles	Monitors the presence of vehicles and traffic activity to determine if roads and facilities are in use.
<b>Buildings</b>	5 Removal and Construction of Buildings	Tracks the construction and removal of buildings by monitoring their presence and absence throughout the recovery process.
	6. Change in Urban Land Use and Morphology	Monitors changes to the urban form and morphology of a region. Quantifies changes to the total built-up area and monitors the average size and shape of the buildings.
	7. Quality of Dwelling Reconstruction	Monitors changes to the size, shape, arrangement, location and context of buildings and to the natural and built environment surrounding them. Describes the timing and quality of the building construction process.
<b>Transitional Settlement / Displaced Population</b>	8. Transitional Settlement	A suite of analyses designed to identify temporary accommodation and to measure its longevity, infrastructure placement and environmental impact.
	9. Displaced Population	An estimate of the population living in transitional settlement based on the number of tents, makeshift shelters and transitional shelters, and an estimation of the population living in permanent accommodation based on the number of residential buildings.
<b>Natural Environment</b>	10. Land Cover and Urban Green Space	Identifies areas of vegetation gain and loss associated with processes such as land degradation, erosion and deforestation.
<b>Livelihoods</b>	11 Recovery of Livelihoods	Monitors changes in the main economic sectors in the disaster-affected areas, for example agriculture, fisheries and tourism.
<b>Services &amp; Utilities</b>	12. Services and Facilities	Describes the location and status of services and facility buildings across the affected region.
	13. Utilities - Power, water and sanitation	Maps features associated with the supply of key utilities including power, water and sanitation.

**Table 2-4: The Recovery Project indicators developed by the author.**

Table 2-5 shows the overlap between the Recovery Categories and categorisations used by three of the key sources of literature: ECLAC, the Sphere Guidelines and TRIAMS. The Recovery Project table has been designed to be generic and non country-specific by using a comprehensive and diverse range of sources. The indicators will be tested in Chapter 3 by applying them to recovery in two case study sites: Ban Nam Khem, Thailand following the 2004 Indian Ocean tsunami and Chella Bandi, Pakistan after the 2005 Kashmir earthquake.

Recovery Project Categories		ECLAC	Sphere Guidelines	TRIAMS
Physical Indicators	Accessibility	Transport and communications		Infrastructure
	Environment	Environment		Infrastructure
	Buildings	Affected population and Housing and Human Settlements	Shelter, Settlement and Non-Food Items	Vital needs Infrastructure
	Safety and Vulnerability			Infrastructure
Services and Amenities Indicators	Administration and Local Services			
	Education	Education and culture		Basic Social Services
	Healthcare	Health sector	Health Services	Vital needs Basic Social Services
	Power	Energy		
	Water and Sanitation	Drinking water and sanitation	Water, Sanitation and Hygiene Promotion	Vital needs
Socio-Economic Indicators	Food Aid and Food Security		Food Security, Nutrition and Food Aid	
	Livelihood	Employment and income Agriculture Trade and industry Tourism		Livelihoods

**Table 2-5: Comparison between the Recovery Project Categories and other methods of categorising recovery and disaster impact.**

## Bibliography

Alesch, D.J. (2001). *A quantitative and qualitative analysis of small organization survival and recovery following a natural hazard event*. A session summary (recorded by C.L. Reiss). The 2001 Hazards Research and Applications Workshop.

Alesch, D.J. (2004). Complex urban systems and extreme events: towards a theory of disaster recovery. *1st International Conference of Urban Disaster Reduction*. Kobe, Japan. 19 January 2004.

Alesch, D.J., Arendt, L.A. and Holly, J.N. (2009). Managing for long-term community recovery in the aftermath of disaster. Public Entity Risk Institute, Vancouver.

ALNAP (2009). *Re-thinking Humanitarian Impact Assessment: theory and practice*. OCHA Joint Review of Inter-Agency Evaluations. Geneva.

Amin, S. and Goldstein, M. (eds.) (2008). Data against natural disasters. Establishing effective systems for relief, recovery and reconstruction. The World Bank. Washington, DC.

Amna, S. (2013). Logistics support and its management during disaster relief operations. *International Journal of Scientific Footprints: 1(1)*, 1-12.

Avery, T.E. and Berlin, G.L. (1985). *Interpretation of Aerial Photographs (fourth edition)*. Burgess Publishing Company, Minneapolis.

Baker, J.L. (2000). *Evaluating the Impact of Development Projects on Poverty. A Handbook for Practitioners*. The World Bank. Washington, D.C.

Barnett, M. (2005). *Humanitarianism Transformed*. University of Minnesota.

BCC Research (2013). *Remote sensing technologies and global markets*. September 2013. Available at: <http://www.bccresearch.com/market-research/instrumentation-and-sensors/remote-sensing-technologies-ias022d.html>

Bedawi, S.M. and Kamel, M.S. (2015). Road detection in urban areas using random forest tree-based ensemble classification. *International Conference Image Analysis and Recognition*. 499-505.

Belgiu, M. and Drăguț, L. (2016). Random forest in remote sensing: a review of applications and future directions. *Remote Sensing*: **114**, 24-31.

Beniya, S. 2007. The evaluation of the status of disaster areas by using recovery indicators (in the case of the Great Hanshin-Awaji earthquake). *2<sup>nd</sup> International Conference on Urban Disaster Reduction*. November 27-29.

Blaikie, P., T. Cannon, I. Davis & B. Wisner. (1994). *At Risk: Natural hazards, People's vulnerability, and disasters*. Routledge, London.

Brown, D., Saito, K., Liu, M., Spence, R., So, E. and Ramage, M. (2012). The use of remotely sensed data and ground survey tools to assess damage and monitor early recovery following the 12.5.2008 Wenchuan earthquake in China. *Bulletin of Earthquake Engineering*: **10 (3)**, 741-764.

Brown, D. *Remote Sensing and Disasters* (2017). Cambridge Architectural Research Ltd.

Chalinder, A. (1998). Temporary Human Settlement Planning for Displaced Populations in Emergencies. *6th Good Practice Review*: January 1998. Overseas Development Institute, London.

Chang, S. (2009). Urban disaster recovery: a measurement framework and its application to the 1995 Kobe earthquake. *Disasters*: **34 (2)**, 303-327.

Clinton, W. (2006). *Lessons learned from Tsunami Recovery. Key propositions for building back better*. A Report by the United Nations Secretary-General's Special Envoy for Tsunami Recovery. Office of the UN Secretary-General's, Special Envoy for Tsunami Recovery.

Colwell, R.N. (1997). History and place of photographic interpretation. In: W.R. Philpson (ed.) *Manual of Photographic Interpretation (2nd edition)*. Bethesda, Maryland. American Society for Photogrammetry and Remote Sensing.

Coppola, D.P. (2015). *Introduction to international disaster management*. Elsevier, London.

Corbane, C, Saito, K, Dell’Oro, L, Gill, SPD, Piard, E, Huyck, CK., Kemper, T, Lemoine, G, Spence, RJS, Shankar, R, Senegas, O, Ghesquiere, F, Lallemand, D, Evans, GB, Gartley, RA, Toro, J, Ghosh, S, Svekla, WD, Adams, BJ, and Eguchi, R (2011). A Comprehensive Analysis of Building Damage in the 12 January 2010 MW7 Haiti Earthquake using High Resolution Satellite and Aerial Imagery. *Photogrammetric Engineering & Remote Sensing*: **77(10)**, 997-1009.

Cosgrave, J.(2008). *Responding to earthquakes. Learning from earthquake relief & recovery operations*. Provention Consortium & Alnap

Cowen, D.J. and Jensen, J.R. (1998). Extraction and modelling of urban attributes using remote sensing technology. In: D. Liverman, E.F. Moran, R.R. Rindfuss and P.C. Stern (eds.). *People and Pixels*. National Academy Press, Washington D.C.

Cutter, S. L., Boruff, B. J., & Shirley, W. L. (2003). Social vulnerability to environmental hazards. *Social Science Quarterly*: **84**, 242–261.

Dabelstein, N. (2006). *Evaluating humanitarian action using the OECD-DAC criteria. An ALNAP guide for humanitarian agencies*. ALNAP.

Daniba (2006). *Evaluation Policy*. Danish International Development Agency. Evaluation Department Report.

Deichmann, U., Ehrlich, D., Small, C. and Zeug, G. (2011). *Using high resolution satellite data for the identification of urban natural disaster risk*. European Union and the World Bank.

Dell’Acqua, F. and Gamba, P. (2012). Remote sensing and earthquake damage assessment: experiences, limits and perspectives. *Proceedings of the IEEE*: **100 (10)**. 2876-2890.

DigitalGlobe (2010). *The benefits of the eight spectral bands of Worldview-2*. DigitalGlobe Whitepaper, March 2010.

DigitalGlobe. (2016a). *The DigitalGlobe Constellation*. DigitalGlobe, Colorado.

DigitalGlobe. (2016b). *Transforming our world. Geospatial information key to achieving the 2030 agenda for sustainable development*. DigitalGlobe, Colorado.

Disaster Charter. (2000). *Charter on cooperation to achieve the coordinated use of space facilities in the event of natural or technological disasters*. International Charter Space and Major Disasters.

ECLAC. (1991). *Manual for estimating the socio-economic effects of natural disasters*. Economic Commission for Latin America and the Caribbean Programme Planning and Operations Division. Santiago, Chile.

Euroconsult (2014). *Satellite-Based Earth Observation: Market Prospects to 2023*. See their website at: [euroconsult-ec.com](http://euroconsult-ec.com)

Foulser-Piggott, R., Spence, R. and Brown, D. 2013. The use of remote sensing for building damage assessment following the 22<sup>nd</sup> February 2011 Christchurch earthquake: the GEOCAN study and its validation. Cambridge Architectural Research Ltd. Report for Global Earthquake Model (GEM). <http://www.carltd.com/sites/carwebsite/files/GEOCAN%20Christchurch%20Report.pdf>

Gähler M. (2008). Disaster Management with Remote Sensing. In: Schiewe J., Michel U. (eds). *Geoinformatics Paves the Highway to Digital Earth*. pp. 24–29. Osnabrück, Germany.

Gruss, M. (2015). NGA seeks info from new imagery companies. Spacenews. 12 May 2015. Available at: <http://spacenews.com/nga-seeks-info-from-new-imagery-companies/>

Harwell, E. (2002). Remote sensibilities: discourses of technology and the making of Indonesia's natural disaster. *Development and Change*: **31 (1)**, 307-340.

Hewitt, K. (1997). *Regions of Risk: A Geographical Introduction to Disasters*. Longman, Essex.

Hill, A. A., Keys-Mathews, L. D., Adams, B. J. and Podolsky, D. (2006). Remote sensing and recovery: a case study on the Gulf Coasts of the United States. *Proceedings of the Fourth International Workshop on Remote Sensing for Post-Disaster Response*. Cambridge, UK

Hodgson, M.E., Davis, B.A. and Kotelenska, J. (2009). Remote sensing and GIS data/information in the emergency response/recovery phase. In: Showalter, P.S. and Lu, Y. (Eds.) (2009). *Geospatial techniques in urban hazard and disaster analysis*. Springer Science and Business Media, London.

Hubing, N. (2012). Buying optical satellite imagery? *Earth Imaging Journal*. June 12, 2012. Available at: <http://eijournal.com/print/articles/buying-optical-satellite-imagery>

IFRC. (2010). *Project/programme planning. Guidance manual*. International Federation of Red Cross and Red Crescent Societies, Geneva.

IFRC. (2011). *Project/programme monitoring and evaluation (M&E) guide*. International Federation of Red Cross and Red Crescent Societies, Geneva.

Intrieri, E, Gigli, G., Mugnai, F., Fanti, R. and Casagli, N. (2012). Design and implementation of a landslide early warning system. *Engineering geology*: **147-148**, 124-136.

Jadkowski, M.A. (1994). EOAP funding develops aerial imaging system for pipeline infrastructure management. *Earth Observation Magazine*: **3**, 29-32.

Jensen, J.R. (2007). *Remote sensing of the environment. An earth resource perspective*. Pearson Prentice Hall. New Jersey.

Jha, J.K., Barenstein, J.D., Phelps, P.M., Pittet, D. and Sena, S. (2010). *Safer Homes, Stronger Communities : A Handbook for Reconstructing after Natural Disasters*. World Bank, Washington DC.

Jhonnerie, R., Siregar, V.P., Nababan, B., Prasetyo, L.B. and Wouthuyzen, S. (2015). Random forest classification for mangrove land cover mapping using Landsat 5 TM and ALOS PALSAR imageries. *Procedia Environmental Sciences*: **25**, 215-221.

Joyce, K.E., Belliss, S.E., Samsonoc, S.V., McNeill, S.J. and Glassey, P.J. (2009). A review of the status of satellite remote sensing and image processing techniques for mapping natural hazards and disasters. *Progress in Physical Geography*: **33(2)**, 183-207.

Karatani, Y., Hayashi, H., and Kawata, Y. (2000). Proposal of Hanshin Awaji Earthquake Disaster Recovery Indices (RI) using Kobe City Socioeconomic Statistics. *Institute of Social Safety Science: No.2*, pp. 213-222 (in Japanese).

Karatani, Y. and Hayashi, H. (2003). Development of Socioeconomic Recovery Index based on Kobe Statistics to Monitor the Recovery from the 1995 Kobe Earthquake. Disaster Resistant California, The Governor's Office of Emergency Services and The Collaborative for Disaster Mitigation, CD-ROM.

Karatani, Y. and Hayashi, H. (2004). Verification of Recovery Process under the Great Hanshin-Awaji Earthquake Disaster Based on The Recovery Index (RI). *13th World Conference on Earthquake Engineering*. Vancouver, B.C., Canada, CD-ROM.

Karatani, Y. and Hayashi, H. (2007). Quantitative Evaluation of Recovery Process in Disaster-Stricken Areas Using Statistical Data. *Journal of Disaster Research: 2(6)*, 453-464.

Kidd, R.A., McCallum, I. and Ishadamy, M.Y. (2010). The benefit of high resolution aerial imagery for topographic mapping and disaster recovery: lessons learnt from the 2004 Indonesian tsunami. In: Altan, O., Backhaus, R., Boccardo, P. and Zlatanova, S. (Eds.) *Geoinformation for disaster and risk management*. Joint Board of Geospatial Information Societies, Copenhagen.

Kusek, J.Z. and Rist, R.C. (2004). *Ten steps to a results-based monitoring and evaluation system. A handbook for development practitioners*. The World Bank, Washington.

Laituri, M. and Kodrich, K. (2008). On-line disaster response community: people as sensors of high magnitude disasters using internet GIS. *Sensors: 8*, 3037-3055.

Li, J., Zlatanova, S. and Fabbri, A. (2007). *Geomatics Solutions for Disaster Management*. Lecture Notes in Geoinformation and Cartography. Springer-Verlag, Berlin Heidelberg.

Lillesand, T. and Kiefer, R.W. (1999). *Remote sensing and image interpretation (4<sup>th</sup> edition)*. John Wiley & Sons, New Jersey.

Lu, J-C., Peacock, W. G., Zhang, Y. and Dash, N. (2007). Long-Term Housing Recovery: Does type really make a difference? *Proceedings of 2nd International Conference on Urban Disaster Reduction*. pp 1-8. Taipei, Taiwan.

Maki, N., Kawakata, H., Yoshitomi, P., Urakawa, G., Chan, K., Matsuura, H., Tatsumi, K., Hara, T., Inokuchi, M., Higashida, M. Hayashi, H. and Kawata, Y. (2007). Building an integrated database system of information on disaster hazard, risk, and recovery process – cross-media database. *Annals of Disas. Prev. Res. Inst., Kyoto Univ., No. 50 C, 2007./*

Maxwell, J.C. (1865). A dynamical theory of the electromagnetic field. *Philosophical Transactions of the Royal Society of London: 155*, 459-512.

Meier, P. (2015). *Digital humanitarians. How big data is changing the face of humanitarian response*. CRC Press, London.

Miles, S.B. and Chang, S.E. (2003). *Urban disaster recovery: A framework and simulation model*. MCEER-03-0005. 29 July 2003.

Miles, S. B., and Chang, S.E., (2006). Modeling community recovery from earthquakes. *Earthquake Spectra: 22(2)*, 439 - 458.

Mosse, R. and L.E. Sontheimer (1996). *Performance Monitoring Indicators Handbook*. Technical Paper No. 334. World Bank, Washington DC.

Murao, O. (2004). Description of building reconstruction process of Chi-Chi area using image archives after the 1999 Chi-Chi earthquake, Taiwan. *1st International Conference of Urban Disaster Reduction*. Kobe, Japan. 19 January 2004.

OECD (2010). *Development Evaluation Resources and Systems – A Study of Network Members*. Development Co-operation Directorate. Development Assistance Committee. The DAC Network on Development Evaluation.

OECD-DAC (1999). *Guidance for Evaluating Humanitarian Assistance in Complex Emergencies*. OECD, Paris.

Olshansky, R., L. Johnson and K. Topping (2003). Post-disaster redevelopment: lessons from Kobe and Northridge. Final Report, NSF Award No. CMS-9730137, July 11 2003.

Patel, D.P. and Srivastava, P.K. (2013). Flood hazards mitigation analysis using remote sensing and GIS: correspondence with town planning scheme. *Water Resources Management: 27 (7)*, 2353-2368.

PDNA (2008). *Developing a Common Framework for Post-Disaster Needs Assessment and Recovery Planning: Towards the Recovery Results Framework*. Post-Disaster Needs Assessments (PDNA). United Nations Development Programme, The World Bank and the European Commission. Brussels, May 19-21, 2008.

Pisano, F. (2006). Using satellite imagery to improve emergency relief. *Humanitarian Exchange. Number 32*. Humanitarian Practice Network (HPN). Overseas Development Institute (ODI). December 2005.

Platt, S. (2008). *Recovery User Needs Survey. Interim Report*. Cambridge Architectural Research Ltd. Cambridge. 5 August 2008.

Proudlock, K., Ramalingam, B. and Sandison, P. (2009). *Improving humanitarian impact assessment: bridging theory and practice*. ALNAP, London

Pushparaj, J. and Hegde, A.V. (2017). A comparative study on extraction of buildings from Quickbird-2 satellite imagery with and without fusion. *Cogent Engineering: 4 (1)*.

Quarantelli, E.L. (1999). *The disaster recovery process: what we know and do not know from research*. Preliminary Paper #286. University of Delaware. Disaster Research Center.

Rathfon, D., Davidson, R., Bevington, J., Vicini, A. and Hill, A. (2012). Quantitative assessment of post-disaster housing recovery: a case study of Punta Gorda, Florida, after Hurricane Charley. *Disasters: 37 (2)*, 333-355.

Roche, C. (1999). *Impact Assessment for Development Agencies: Learning to Value Change. Development Guidelines*. Oxford, Oxfam.

Rodriguez-Galiano, V.F., Chica-Olma, M., Abarca-Hernandez, F., Atkinson, P.M. and Jeganathan, C. (2012). Random forest classification of Mediterranean land cover using multi-seasonal imagery and multi-seasonal texture. *Remote Sensing of Environment*: **121**, 93-107.

Saito, K.(2009). *High-resolution optical satellite images for post-earthquake damage assessment*. Doctoral Thesis. Department of Architecture. University of Cambridge.

Scott, D.W. (2016). Frequently asked questions about WorldView-2. DigitalGlobe, Colorado, USA.

Schwab, J. (1998). *Planning for post-disaster recovery and reconstruction*. American Planning Association, Chicago.

Selding, P.B. (2015). *For DigitalGlobe, government business steady but commercial disappoints*. News article in SpaceNews. 30 October 2015. Available at: <http://spacenews.com/for-digitalglobe-government-business-steady-but-commercial-disappoints/>

Showalter, P.S. and Lu, Y. (Eds.) (2009). *Geospatial techniques in urban hazard and disaster analysis*. Springer Science and Business Media, London.

Sillah, R.M. (2015). A call to establish a child-centred disaster management framework in Zimbabwe. *Journal of Disaster Risk Studies*: **7 (1)**. 7 pages.

Soroosh, S., Nguyen, P., Sellars, S., Braithwaite, D., AghaKouchak, A. and Hsu, K. (2014). Chapter 8. Satellite-based remote sensing estimation of precipitation for early warning systems. In: Ismail-Zadeh, A., Fucugauchi, J.U., Kijko, A., Takeuchi, K. and Zaliapin, I (eds.) *Extreme natural hazards, disaster risks and societal implications*. Special publications of the international union of geodesy and geophysics. Cambridge University Press.

Sphere Project (2011). *Humanitarian Charter and Minimum Standards in Disaster Response*. The Sphere Project. Oxford, OXFAM Publishing.

Stoechleler, E.G. (1979). Use of aerial color photography for pavement evaluation studies. *Highway Research Record*: **319**, 40-57.

Takashima, M. and Hayashi, H. (1999). Quantitative Grasping Method for Recovery Status Using Electricity Consumption Time Series Data – Application to The Great Hanshin-Awaji Earthquake. *Japan Society for Natural Disaster Science*. No. 18-3, 355-367 (in Japanese).

Takashima, H. and Masasuke, T. (2007). Monitoring recovery using energy consumption indices. *Journal of Disaster Research*: 2 (6), 445-452.

Tatsuki, S., Hayashi, H., Yamori, K., Noda, T., Tamura, K. and Kimura, R. (2005). Long-term life recovery processes of the survivors of the 1995 Kobe Earthquake: Casual Modelling Analysis of the Hyogo Prefecture Life Recovery Panel Survey Data. *1st International Conference on Urban Disaster Reduction*. Kobe. January 18-21, 2005.

Taubenböck, H., Post, J., Roth, A., Zosseder, K., Strunz, G. and Dech, S. (2008). A conceptual vulnerability and risk framework as outline to identify capabilities of remote sensing. *Natural Hazards Earth Systems Science*: 8, 409-420.

TRIAMS (2007). Tsunami Recovery Impact Assessment and Monitoring System (TRIAMS). Second regional TRIAMS workshop. Bangkok, 21-23 March 2007.

TRIP (2007). *2nd Tsunami Recovery Indicator Package (TRIP) Report for Aceh and Nias. How far have we come? Where do we go from here?* Tsunami Recovery Indicator Package (TRIP). UNORC-IAS.

Tyler, M.B., O'Prey, K. and Kristiansson, K. (2002). Redevelopment after earthquakes. Spangle Associates, California.

UNDP (2009). *Handbook on Planning, Monitoring and Evaluating for Development Results*. United Nations Development Programme. Geneva.

UNHCR. (2007). *Handbook for emergencies (3rd edition)*. UNHCR. The UN Refugee Agency, Geneva.

United Nations. (2015). *Sendai framework for disaster risk reduction 2015-2030*. United Nations. Available at: [http://www.preventionweb.net/files/43291\\_sendaiframeworkfordrren.pdf](http://www.preventionweb.net/files/43291_sendaiframeworkfordrren.pdf)

WDI (2008). *World Development Indicators 2008*. The World Bank. Washington, D.C.

Webb, G., Tierney, K. and Dahlhamer, J. (2000). Businesses and disasters: empirical patterns and unanswered questions. *Natural Hazards Review*: **1**, 83-90.

Welch, R. (1982). Spatial resolution requirements for urban studies. *International Journal of Remote Sensing*: **3**, 139-146.

Wu, J. Y. and Lindell, M.K. (2003). Housing reconstruction after two major earthquakes: The 1994 Northridge earthquake in the United States and the 1999 Chi-Chi earthquake in Taiwan. *Disasters*: **28(1)**, 63-81.

World Bank (2002). *Monitoring and Evaluation: Some tools, methods and approaches*. The World Bank. Washington D.C.

World Bank/GFDRR/ImageCat (2013). *Final Report: 2010 Haiti Earthquake – Post-Disaster Building Damage Assessment using Satellite and Aerial Imagery Interpretation, Field Verification and Modeling Techniques*. Report produced for the World Bank/GFDRR by ImageCat, Inc.

## **Chapter 3: Using geospatial tools to retrospectively monitor and evaluate recovery in Ban Nam Khem, Thailand after the 2004 Indian Ocean tsunami**

### **3.1. Introduction: Aims and Content of the Chapter**

A full table of indicators for monitoring and evaluating post-disaster recovery using high-spatial-resolution satellite imagery is presented in chapter 2. It was created after reviewing existing humanitarian frameworks and consulting affected communities and relevant stakeholders through a user-needs survey and a series of focus-group meetings. The indicator table consists of six categories: accessibility, buildings, transitional settlement/displaced population, natural environment, livelihoods and services. Relevant satellite image analysis techniques and protocols were developed for each category and tested by applying them retrospectively to two case study sites: Ban Nam Khem, Thailand that was affected by the 2004 Indian Ocean tsunami and Chella Bandi, Pakistan that was hit by the 2005 Kashmir earthquake.

It was considered best to present the results from only one case study in detail rather than to present shortened results from both case studies. The decision to focus on the Thailand case study was due mainly to heightened security in Pakistan during the project which prevented the author from visiting the study-site to collect ground data for verification purposes. Results from the Pakistan case study are still referred to in the discussion sections though to 1) describe the transferability of the techniques and 2) to quantitatively compare the patterns of recovery seen in the two countries.

The work in this chapter will form an important contribution to the thesis as outlined in the framework in chapter 1. In particular, retrospective time-series analysis of recovery in Thailand will be used to test the ability of geospatial science to monitor recovery over time. Detailed recovery narratives and quantitative recovery curves will be produced that describe the speed and the quality of recovery over time in a standardised manner. Recovery in Thailand and Pakistan will also be quantitatively compared. This will be the first time this has been done using remote sensing, allowing community recovery to be mapped and analysed remotely for the first time. Previous attempts to produce recovery curves have relied on regional-scale social and economic indicators. The work in this chapter will also allow the

longitudinal recovery in Ban Nam Khem to be recorded in-detail at a time when recovery case studies are still scarce, under-recorded and much-requested by the scientific community.

The chapter starts with a description of the Thailand case study site and the methodology used to prepare the satellite imagery and to conduct ground and household surveys. The rest of the chapter is divided into six sections corresponding to each category of the indicator table. Each section describes the methodology used to extract and analyse the appropriate data and presents a selection of results for each indicator to demonstrate the usefulness of the proposed techniques.

### **3.2. Case Study Sites**

It was important to select the case study sites and satellite imagery carefully to ensure they were suitable for the study of post-disaster recovery. The incorrect acquisition of imagery would be a very costly mistake to make in terms of time and resources. A simple conceptual model was therefore designed to assist the selection of data and case-study sites based on evidence of recovery and the availability of high-spatial-resolution satellite imagery and supplementary data. A comprehensive literature search was first conducted to highlight areas of damage and recovery in a number of countries known to have recently undergone post-disaster recovery. Individual zones were then identified within those areas of interest which were deemed accessible and for which there was auxiliary data available in the form of written reports and geospatial datasets that could be used to help verify the results of the image analysis.

Databases of commercially-available high-spatial-resolution satellite imagery, including Ikonos from Geoeye and Quickbird and Worldview-1 from Digital Globe, were then searched. The geographic extents of any potential satellite images were then imported into ArcGIS and viewed along with important meta-data describing their acquisition date, near-nadir angle and cloud cover. This provided an effective method of analysing the spatial and temporal availability of imagery in different locations. The dates and extents of any suitable images were then compared to the narratives of recovery and key-dates that were derived from the literature review to ensure the images were suitable and likely to coincide with key recovery processes.

The two case study sites were carefully selected so they represented very different hazard-types and different economic and cultural environments to test the transferability of the remote sensing techniques. The first case study, Ban Nam Khem, a fishing village on the West Coast of Phang Nga Province, Thailand, was completely destroyed by the Indian Ocean tsunami in December 2004, while the second site, Chella Bandi, Pakistan, on the outskirts of Muzaffarabad was struck by the Kashmir earthquake in October 2005, again resulting in substantial damage and disruption. The settlements are comparable in size, each containing approximately 2-3,000 buildings. A conscious decision was made to apply the analysis at a scale that could be completed by one analyst as this provided a certain amount of consistency when developing the techniques. It was also deemed preferable to test as many of the indicators as possible over a relatively small area instead of only having time to apply one indicator to a large area. While the study areas were relatively small they still encompassed all of the aspects of recovery in the recovery table including buildings, transitional settlements, livelihoods and services. An attempt to scale-up the remote sensing analysis beyond settlement-scale using semi-automated analysis techniques and a random sampling strategy is presented in chapter 5.

#### *Ban Nam Khem, Thailand*

On the morning of 26 December 2004 an undersea earthquake of magnitude 9.1 on the Richter scale triggered devastating waves that hit many countries bordering the Indian Ocean. This was one of the biggest undersea disturbances ever recorded with an epicenter just off the coast of Sumatra, Indonesia. Many countries were affected by the waves but the hardest hit included Indonesia, Sri Lanka, India and Thailand (USGS, 2004). Thailand was selected as a suitable country to study because there were reports of substantial damage and because colleagues had previously worked in Phang Nga and Phuket to test damage assessment tools (Ghosh et al. 2005). An independent damage assessment by the Pacific Disaster Centre after the 2004 Indian Ocean tsunami helped to identify four potential case study sites in the country: 1. Ban Nam Khem, 2. Khao Lak, 3. Phuket Island and 4. Phi Phi Island (ADPC, 2005a). Phi Phi Island was dismissed because of problems of accessibility and the unavailability of ground data, and Phuket and Khao Lak were not selected - despite the availability of damage assessment data - due to their heavy dependence on the tourism industry, which was assumed might bias the speed and quality of the recovery process. The Asian Disaster Preparedness Centre reported that the other potential study site, Ban Nam Khem was “badly damaged with only a few buildings left standing” (ADPC, 2005a).

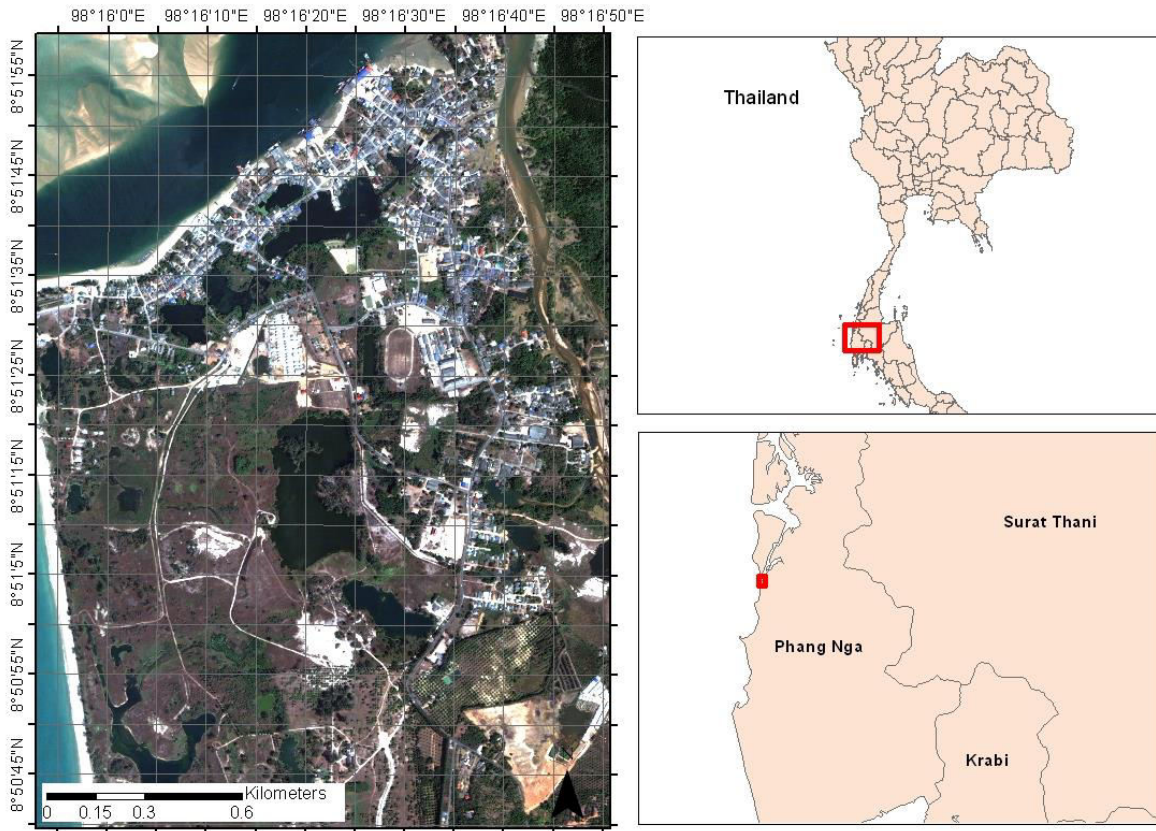


**Figure 3-1: Map of Ban Nam Khem, Phang Nga Province, Thailand in February-2009.**

Ban Nam Khem is a small fishing village located north of Khao Lak, on the Andaman coast. An account by the Thai Government described 4 waves striking Ban Nam Khem between 9:35 am and 10:03 am ranging from 2 to 10 m high. Ban Nam Khem's low elevation and its proximity to the mouth of the Pak Ko River contributed to the loss of over half of its population of 6,000 people and up to 80% of its infrastructure, including fishing fleet, harbour and fish processing facilities (UNDP, World Bank and FAO, 2005). The tsunami also caused psychological trauma, damage to coral reefs and coastal reefs, as well as the degradation of water quality and agricultural land (UN Country Team, 2005).

The state spent £1 million on reconstruction and assistance in the first year in a response that involved the collaboration of the Royal Thai Government, the Thai Private Sector and Non-Governmental Organisations (UN Country Team, 2005). There was no national preparedness plan; instead the disaster was managed by the Prime Minister. Most of the immediate relief efforts were focused at the Bang Muang refugee camp in Takua Pa District, which housed 3,500 people and acted as a central base for 57

relief groups. The camp successfully brought the survivors together and enabled them to control their recovery through group meetings and decisions.

As part of the government's compensation scheme, villagers who lost property to the tsunami were offered either a free house or a lump sum of money. The Thai army used concrete blocks and corrugated-iron roofs for the houses, which had a floor space between 4 x 4 m and 6 x 6 m (Bhumiprabhas, 2005). The size of the government-provided housing was a lot smaller than aid agency housing and was consequently less accepted by the local population (Baumgartner, 2006). The exact material, size and design differed according to the agency's access to funds and expertise. Crucially, the government offered no consultation to beneficiaries on building design or allotment procedures. Interviews and focus groups indicated that most villagers wanted to live near the shore because many of them were fishers and proximity to the sea enhanced their income.

The tsunami brought about complex land-right disputes, which slowed the overall recovery process. Many villagers settled in Ban Nam Khem before it became valuable due to tourism, but did not obtain title deeds or lease contracts. The Centre on Housing Rights and Evictions (COHRE) reported that by 2 and 3 May 2005 there were at least 200 evictions and displacement by the Far East Trading and Construction Company, which planned to build a resort and claimed the occupants were staying on its land illegally (COHRE, 2005).

The livelihoods of the post-tsunami communities were found to be particularly vulnerable due to their reliance on so few forms of income, many of which were based on the region's fragile coastal resources. At least 22 shrimp hatcheries and 12,726 m<sup>2</sup> of cage cultures were lost. A survey conducted by Paphavasit et al. (2006) reported that one-third of respondents and one-quarter of dependants were unemployed after the tsunami and over half of the respondents had to change jobs. Many of the fishers became unskilled labourers and had to move from their homes, which dramatically changed their livelihoods. The people in Ban Nam Khem estimated that they would face economic strain for at least 4 years after the disaster.

### **3.3. Methodology**

The approach used to prepare and analyse the satellite imagery and extract the information required to monitor post-disaster recovery is described here. More information about the individual procedures and algorithms used for each indicator is provided in the appropriate sections of this chapter. The overall image-analysis workflow can be divided into three main components: 1. Pre-processing 2. Feature extraction and 3. Feature analysis. These steps are described below.

#### *Satellite Image Acquisition and Pre-processing*

Recovery was monitored using a time-series of high-spatial-resolution satellite images acquired before the tsunami, immediately afterwards and in the months-and-years thereafter. The choice of imagery was dependent upon their availability in commercially-available image archives. Only images with a maximum ground sample distance of 1.0 m were considered, including Ikonos, Quickbird, Geoeye-1 and Worldview-1, to ensure that relevant features such as buildings and roads would be observable (Cowen and Jensen, 1998).

The timeline of satellite images collected for Ban Nam Khem before and after the tsunami and throughout the recovery process is presented in table 3-1. The satellite images were purchased from DigitalGlobe and Geoeye as *standard ortho ready 4-band bundles* with no topographic relief applied, making them suitable for custom orthorectification. Each package contained a panchromatic image and a multispectral image-file with four bands covering the blue, green, red and near-infrared parts of the electromagnetic spectrum, except for the Worldview-1 image which only consisted of a black-and-white panchromatic image with no multispectral data.

The images were downloaded in GeoTIFF format with 11-bit depth (up-sampled to 16-bit) and all contrast and brightness adjustments turned off. The images all contain no obvious cloud or haze covering the study-area and were collected with an off-nadir angle of less than 30 degrees to minimise the building-lean effect (Hubing, 2012). The satellites have sun-synchronous orbits which mean they all cross a given point on the earth's surface at approximately 10:30 am local time.

	<b>Date</b>	<b>Timeline</b>	<b>Sensor</b>
<b>1</b>	24 June 2002	-30 months	Ikonos
<b>2</b>	02 January 2005	+7 days	Quickbird
<b>3</b>	21 April 2005	+4 months	Ikonos
<b>4</b>	14 July 2005	+7 months	Quickbird
<b>5</b>	28 February 2006	+1 year	Quickbird
<b>6</b>	21 November 2006	+2 years	Ikonos
<b>7</b>	08 February 2008	+4 years	Ikonos
<b>8</b>	05 February 2009	+5 years	Quickbird

**Table 3-1: Time-series of high-spatial-resolution satellite images acquired of Ban Nam Khem, Thailand. Timeline = time before or after the 2004 tsunami event.**

After the images were downloaded they were pre-processed to prepare them for quantitative spectral analysis and thorough visual examination. The pre-processing involved three steps 1. Radiometric correction 2. Pan-sharpening and 3. Geometric correction. First radiometric correction removed the effect of the sensor’s hardware and the atmospheric conditions on the pixel values, which is necessary before conducting spectral analysis or comparing imagery from different sensors. The pre-processing steps are described further below.

*Top-of-Atmosphere Spectral Radiance*

Image data collected by sensors owned by DigitalGlobe and Geoeye are distributed in relative radiance values commonly known as Digital Numbers (DNs). Relative radiometric correction is applied by the distributors when the product is generated to reduce banding and other non-uniformities which obscure the image. Two further radiometric correction steps were applied by the author using ENVI 4.2. Relative radiance was first converted to top-of-atmosphere spectral radiance which is defined as the spectral radiance entering the satellite’s telescope aperture. This removed the effect of the sensor’s hardware and data conversion processes on the radiance values. This ultimately allows images from different

sensors to be quantitatively compared, which is important when using multiple sensors in a single project. Top-of-atmosphere spectral radiance was calculated by multiplying the pixel values with an absolute calibration factor and dividing the result by the effective bandwidth (Updike and Comp, 2010):

$$L_{\lambda Pixel, Band} = \frac{K_{Band} \cdot q_{Pixel, Band}}{\Delta\lambda_{Band}}$$

Where  $L_{\lambda Pixel, Band}$  is the top-of-atmosphere spectral radiance image pixel values ( $W \cdot m^{-2} \cdot sr^{-1} \cdot \mu m^{-1}$ )  $K_{Band}$  is the absolute calibration factor ( $W \cdot m^{-2} \cdot sr^{-1} \cdot count^{-1}$ ) for a given band,  $q_{Pixel, Band}$  are satellite image pixel values and  $\Delta\lambda_{Band}$  is the effective bandwidth ( $\mu m$ ).

The absolute calibration factor was calculated by the image-providers pre-launch by illuminating the focal plane with a known radiance source in a controlled laboratory environment and effective bandwidth was calculated from the relative spectral radiance response for each band. Both parameters were extracted from the metadata files provided with the imagery.

#### *Surface Reflectance (using the FLAASH Atmospheric Model)*

In a second radiometric correction step radiance values were converted to surface reflectance by modelling atmospheric conditions to remove the effect of the atmosphere on the data. This step is recommended when conducting quantitative spectral analysis. The effect of the atmosphere was modelled using the Fast Line-of-sight Atmospheric Analysis of Spectral Hypercubes (FLAASH). FLAASH is a radiative transfer model that performs atmospheric correction to create an image that approximates the reflectance of the earth's surface (Gao and Goetz, 1990). FLAASH is a MODTRAN4-based software package developed by the Air Force Phillips Laboratory, Hanscom AFB and Spectral Science, Inc (SSI) (Adler-Golden, 1999; Matthew et al. 2000).

The model requires input parameters describing the sensor, the time and date that the image was captured and the central coordinates of the image (see figure 3-2). A tropical model was selected and applied to the image to correct for water vapour in the atmosphere. The tropical model assumes a standard column water vapour amount of  $4.11 \text{ g/cm}^2$  or higher and was selected because of the study-site's latitude (less than  $10^\circ N$ ) and average temperature (close to  $27^\circ c$ ) (ENVI, 2009). A maritime aerosol

model was also selected to remove the effect of aerosols in the atmosphere. This model represents the boundary-layer over oceans, or continents under a prevailing wind from the ocean. It is composed of two components, one from sea spray and another from rural continental aerosol (that omits the largest particles) (ENVI, 2009). This was found to slightly reduce the blue and green components caused by aerosol scattering in the atmosphere.

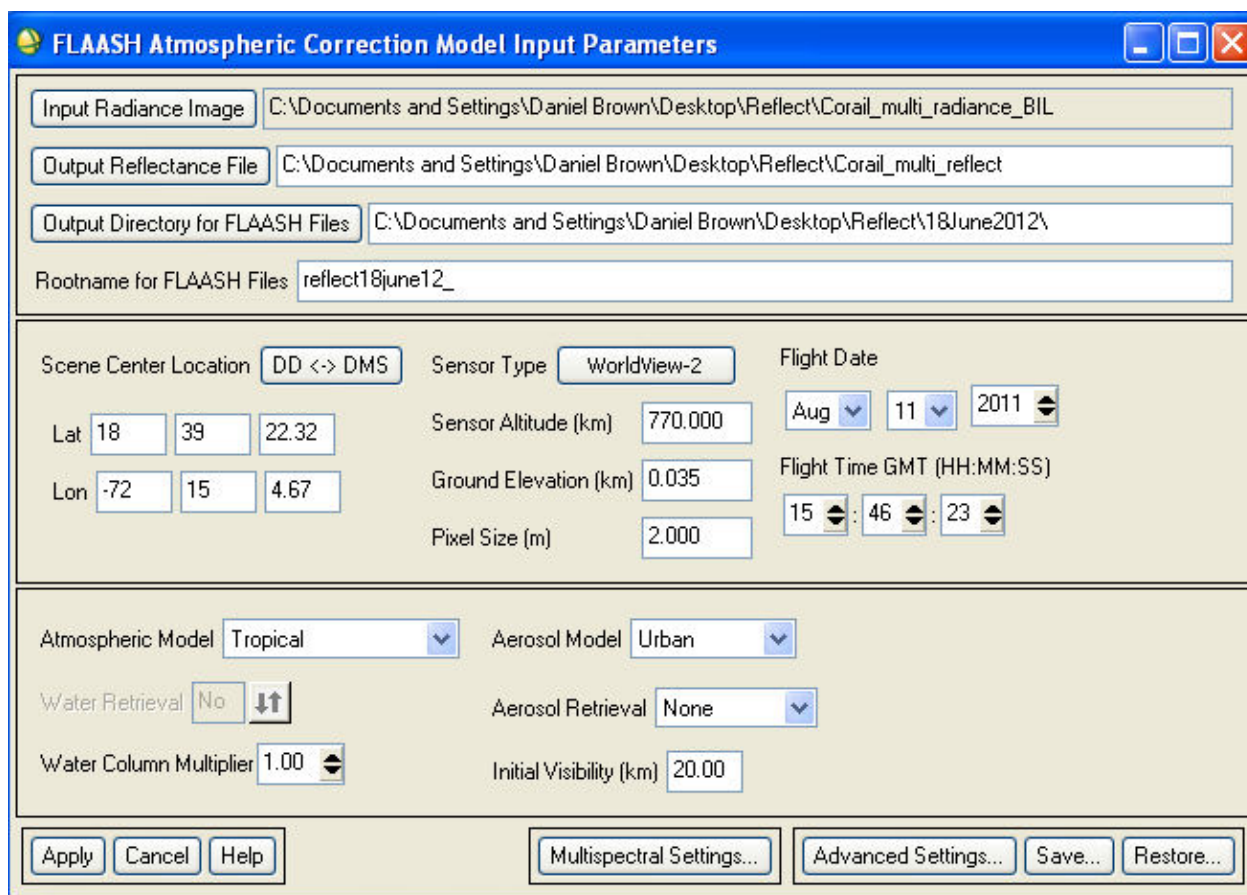


Figure 3-2: FLAASH atmospheric correction model graphic-user interface.

### *Pan-sharpening*

After applying radiometric correction the Ikonos and Quickbird images were pan-sharpened using PCI Geomatica's PanSharpe programme. This technique fused the high-spatial-resolution panchromatic data with the lower-spatial-resolution multispectral bands to produce a high-spatial-resolution multispectral image. The multispectral and panchromatic data were re-sampled by the image-suppliers to the same geographic extent which allowed pan-sharpening to be done reliably before geometric correction

(Cheng & Chaapel, 2009). An automated algorithm developed by Dr. Yun Zhang at the University of New Brunswick was used to do this using the PCI Geomatica software environment. The method approximates the grey level value relationship between the original data and the pan-sharpened image bands using a least-squares technique.

When selecting a suitable pan-sharpening algorithm it was important to find one that produced clear, natural-looking high-spatial-resolution images to aid visual interpretation and to be used in presentations to users and stakeholders. Pan-sharpen algorithms were found to vary significantly, particularly in the way they processed vegetation in imagery. The Gram-Schmidt algorithm available in ENVI for example, produced very light-looking vegetation, with a less prominent red-edge than the other algorithms. In contrast, Pansharpe was found to produce less colour distortion and clearer outlines, particularly on urban features of interest.

#### *Geometric Correction*

Geometric correction involved two steps: 1) orthorectification and 2) image registration. First the images were orthorectified with PCI's Orthoengine using the supplied Rational Polynomial Coefficient (RPC) models. The RPC math model is a mathematical relationship used to correlate the pixels of an image to correct locations on the ground accounting for known distortions caused by the sensor and the terrain. This is necessary when using the images and their derived products in GIS for accurate mapping and length measurements. Orthoengine's RPC technique is based on the block adjustment method, which removes distortions that occur during image capture due to the terrain (Grodecki & Dial, 2003). The technique involved the integration of a freely-available 30 m ASTER Global Digital Elevation Model (DEM) acquired from NASA and ground control points (GCPs). Root Mean Square Errors (RMSE) in the X and Y directions were all within 2.0 m with the use of 5 Ground Control Points acquired in the field with a Garmin GPSmap 62S receiver. These errors were in-line with expectations outlined by the image-suppliers (Digital Globe, 2005).

After the images were orthorectified they were manually registered to a base image so that locations in all of the images aligned accurately with each other. This process is necessary to allow precise change detection analysis to be performed. The images were registered by manually placing Ground Control Points on solid features identifiable in both the base image and the images that were being registered.

ENVI's image registration algorithm iteratively adjusted the image being registered until a Root Mean Square Error (RSME) of no more than 1 pixel was achieved. This means that when multiple images are analysed together the geometric discrepancy between the location of an image feature, such as a building footprint, will not be more than 1 pixel in the X or Y direction.

### *Feature Extraction*

Once the images were pre-processed they were loaded into ArcGIS for manual interpretation analysis and ENVI 4.2 for semi-automatic analysis. As shown in table 3-2, different mapping techniques were used to map different features. Buildings, roads and bridges and other key features were manually delineated to create point, line and polygon vector datasets, while Maximum Likelihood supervised classification in ENVI was used to semi-automatically create land-cover maps marking the extent of the built and natural environment. The Maximum Likelihood classifier applies a statistical decision-rule that examines the probability function of a pixel for each of the classes identified by the analyst, and assigns the pixel to the class with the highest probability. The probability values are based on training statistics provided by the analyst in the form of sample pixels, which represent the classes that are to be classified.

More advanced methods of semi-automating features in the imagery, such as Object-Based Image Analysis (OBIA), were used to extract objects with predictable spatial and reflectance properties, including transitional shelters and shrimp ponds. OBIA is comprised of two main components: it first segments an image into homogenous groups of pixels and then classifies those objects using their spatial, spectral and textural attributes. Maximum Likelihood and OBIA were both used to map a planned camp in Haiti, the results and methodologies of which are described in detail in Chapter 5.

Both manual and semi-automated approaches to analysing satellite imagery were tested for this work as they generally tend to differ in the amount of time and expertise that are required to conduct them and the amount of detail they are able to extract, so are likely to appeal to users with different needs and resources. Manual methods of identifying and delineating individual objects in an image for example, tend to be relatively time-consuming but more reliable than automated approaches.

Mapping Technique	Features
Manual Delineation	Buildings, Roads, Bridges, Boats, Tents, Water Towers etc.
Supervised Classification	Land Cover Extraction, Green Spaces
Object Based Image Analysis	Transitional Shelters, Planned Camps, Shrimp Ponds

**Features Integrated into a Multi-Temporal Geodatabase with standardised Schema**

**Table 3-2: The methodology used both manual and semi-automated remote sensing techniques to map features related to the recovery process.**

Once these features were extracted from the imagery they were integrated into a multi-temporal recovery geodatabase as point, line and polygon vector layers. The analysis was repeated and applied to each of the satellite images. A new temporal layer of the database was derived from the analysis of each satellite image, representing the pre- and post-disaster situation and various *states* in the recovery process. The geodatabase was also divided into six thematic sub-layers, each representing one of the main indicator categories described in the indicator table. The categories encompass a range of physical, environmental, social and economic factors that combine to give a reasonably full picture of the reconstruction process.

### *Feature Analysis*

Once the features in the imagery were mapped and stored in a GIS database the speed of recovery was determined by applying change detection analysis to the geodatabase. This technique calculated the rate that various processes were conducted, including debris removal, building construction, road rehabilitation and vegetation recovery. The method also identified when key features, such as schools and sources of livelihood, appeared and when transitional shelters and planned camps were removed and dismantled. The overall progress of recovery was also inferred by noting the presence or absence of key features at different points in time.

Change detection was used to analyse the change between two different temporal states of the database. Changes in raster imagery, such as land cover maps, were identified using Raster Calculator in ArcGIS to subtract the most recent image (time 2, T+1) from the oldest image (time 1, T). This procedure created a new code for each pixel representing every possible type of land-cover change.

$$T(x,y) - T+1(x,y) = N(x,y)$$

*Where: T = land cover code in time 1; T+1 = land cover code in time 2; N = land-cover change between time 1 and 2; (x,y) = pixel's unique location in the image.*

To analyse change in vector layers over time each feature in the database was allocated a column for each date represented in the database. Unique codes were then added to these columns signifying the features' absence or presence in each image. Change detection was achieved by querying these columns using Structured Query Language (SQL). For example, the following command would select segments of highway constructed between February 2008 and February 2009.

```
SELECT [HIGHWAY_FEB2008 = 0] AND [HIGHWAY_FEB2009=1]
```

*Where: 0 = highway not present or passable, and 1 = highway is present and passable.*

To spatially analyse these temporal changes the datasets were disaggregated by geographic boundaries and other attributes, such as the executing agency in-charge of the project.

For some indicators, the progress of recovery was evaluated by normalising the number of features (number of buildings, length of roads etc.) to base-line statistics, which were constructed using the pre- or post-disaster images. This analysis successfully identified slow projects and gaps in the supply of resources. It was also used to substantiate claims that a region had been 'built back better' by comparing the reconstructed landscape to the one that existed before the disaster.

A minimum of two states in time are required to conduct change detection analysis. Recovery projects may be evaluated using an image acquired before a project commences and another after its completion. Alternatively, a time-series of images may be acquired throughout the duration of the project to provide real-time updates and to monitor changes as they're happening.

Where appropriate, additional information was inferred from the mapped features, including the number of Internally Displaced Persons (IDPs), which was estimated based on the number and size of structures located in planned camps. Information about the quality of recovery was also inferred by looking at changes to the size and shape of buildings and by analysing their spatial and contextual properties. This was achieved using common spatial analyst tools in ArcGIS including Kernel analysis and Nearest Neighbour. More advanced spatial analysis techniques were also employed, such as landscape metrics, which were used to quantify changes to building size, shape and density.

Network analysis was applied to the road network to analyse connectivity and travelling times brought about by the relocation of households and facilities. Spatial analysis and proximity analysis were also applied to planned camps to ensure occupants had sufficient living and covered space, and to measure infrastructure placement. These measurements were compared to minimum standards contained in the Sphere Guidelines and other humanitarian frameworks to ensure that latrines and other features were properly located and that there was adequate accessibility.

Finally, proxy indicators were developed to allow certain social and economic aspects of recovery to be inferred from physical recovery processes. By observing features associated with major sources of livelihood for example, assumptions were made about the speed of livelihood recovery in various sectors.

Technique	Purpose of analysis	Example of questions that might be answered
<b>Change Detection</b>	To measure the speed of recovery processes. Location of change. Absence and presence of particular features of interest.	How fast were houses built at Site A? When was the school built? Is the sea-wall larger than it was before the disaster? What is the progress of project A versus project B?
<b>Buffer Analysis</b>	To measure the proximity of features to one-another.	How many buildings have been built within 200 m of the coast? Have any buildings been constructed beneath slopes over 25 degrees? What is the building density in the immediate vicinity of building A?
<b>Landscape Metrics</b>	To analyse the size, density and distribution of features.	Are the new houses the same size as those that existed before the disaster? Are there now more houses of smaller size at site A?
<b>Network Analysis</b>	To measure the connectivity between features. Travelling times and distances between those features.	How far are households from sources of livelihood? Are sufficient schools available for the new housing development?
<b>Spatial Disaggregation</b>	All data may be disaggregated by geographic boundary, executing agency etc. according to the needs of the users.	How many schools were built in each Province? Has Executing Agency A completed 2,000 houses in Region B?

**Table 3-3: Forms of spatial analysis used to study features related to post-disaster recovery.**

### 3.4. Auxiliary Datasets

At an intermediate stage in the image analysis, field work was carried out to obtain feedback on the recovery indicators and to acquire ground-knowledge from official statistics, key-informant interviews, household surveys and direct ground observations. Geo-referenced results from these tools, including photographs, observations and survey results, were integrated into the recovery database so that direct comparisons to the image analysis could be made as part of the verification process. During the two-week deployment, information was obtained from as many different sources as possible, including a field survey, social-auditing and literature review so that the results from each source could be triangulated against each other and used to verify the proposed narrative of recovery. All of these tools were deployed in February-2009 to provide a snapshot of recovery four years after the tsunami. The Quickbird satellite was also tasked to collect a satellite image on 5 February 2009 to coincide with the field deployment.

### *Household Survey*

The household survey was used to derive a narrative of the recovery process, to infer household's levels of satisfaction and to provide information on key processes and when they happened. The survey was designed by the author and Dr. Steve Platt, a social scientist based at Cambridge Architecture Research Ltd. who had previously designed a number of tools and surveys to analyse social processes related to the built environment.

The survey was piloted once and applied in Thai by Dr. Ratana Chuenpagdee and colleagues based at the Coastal Development Centre, Bangkok. The survey opens with questions about the socio-economic and demographic characteristics of the household. The central part of the survey contains six sections pertaining to each of the indicator categories. In each of these sections the survey contains questions to determine what problems were faced, how the household overcame these issues, if their situation was better, worse or the same as before the disaster, when key events occurred and how the recovery process could have been improved. Due to the complex nature of recovery the majority of the questions were designed as open-ended prompts to invoke discussion about their experiences.

50 households were surveyed in total. They were selected by applying a random geographic sampling strategy to a building database created with the manual analysis of satellite imagery. The sample encompassed households living in both government and agency-provided housing in Ban Nam Khem, as well as households that had relocated to housing developments outside of Ban Nam Khem. Because of time and resource restraints the survey could only be applied to this small group of households. The survey results therefore do not have any great statistical significance but they still provide a very useful dataset to identify key physical, demographic and socio-economic processes that were on-going during the recovery process.



**Figure 3-3: Pilot household surveys conducted in Ban Nam Khem in February-2009.**

### *Key-Informant Interviews*

In addition to the household surveys 11 key-informant interviews were also conducted to provide an overview of the impact of the disaster and the recovery process. The contacts were carefully chosen to represent as many aspects of society as possible. The survey was conducted in the form of a face-to-face interview in people's homes or places of work. The interviewer used a standard set of questions and recorded the answers in the form of hand-written notes that were typed up later. Seven men and four women were interviewed. Seven of these were in Ban Nam Khem at the time of the tsunami, one of whom was in his fishing-boat. The interviewed key-informants include:

- Assistant to the Village Head
- Technical Advisor, Action Aid, Thailand
- President of the Fund for Tsunami Victims, Ban Nam Khem
- Head of sub-district Bang Muang
- President of Housewife Group
- President of TAO Bang Muang
- Committee Member, Mangroves Nature Tourism Group
- Leader of the fish cage culture group
- Vice president of the Centre for Security and Protection Volunteer
- Youth Group Leader
- Vice Principal, Ban Nam Khem School

A copy of the household and key-informant survey forms are provided in Appendix A and B.

### *Ground Survey*

The objective of the ground survey was to capture physical information about the case study site, including buildings, roads, power-lines, water tanks, schools, sources of livelihood and the natural environment. The ground data was then used to validate the satellite image observations. The field survey also recorded detailed information on ground conditions that were not amenable to remote sensing, such as building-use and details about alterations and minor repairs. The field survey was conducted across the whole extent of the satellite image and included areas that were directly and indirectly affected by the tsunami, including a community of prefabricated houses that were built by agencies several kilometres away.

Two methods were used to capture geo-coded imagery on the ground – still photographs taken by a GPS camera (Ricoh Caplio 500SE) and video linked to the VIEWS™ system. The VIEWS system and a GPS camera were used in Ban Nam Khem over four days to capture and store 10 hours of video data and 1,500 geo-referenced photographs. GPS Photomapper software was used to process and view the geo-coded photographs alongside a satellite image. GPS Photomapper is a plug-in for ArcGIS 9.2/9.3. It allows geocoded imagery to be imported into ArcGIS and saved as a Shapefile with a single point representing each individual photograph. A view tool allows a thumbnail of each image to be displayed within the ArcGIS environment, which provides a quick and effective method of validating the satellite imagery with the ground data. Figure 3-4 shows the GPS image points loaded into ArcGIS with a satellite backdrop of Ban Nam Khem. The whole of the inundated area was surveyed using this method.

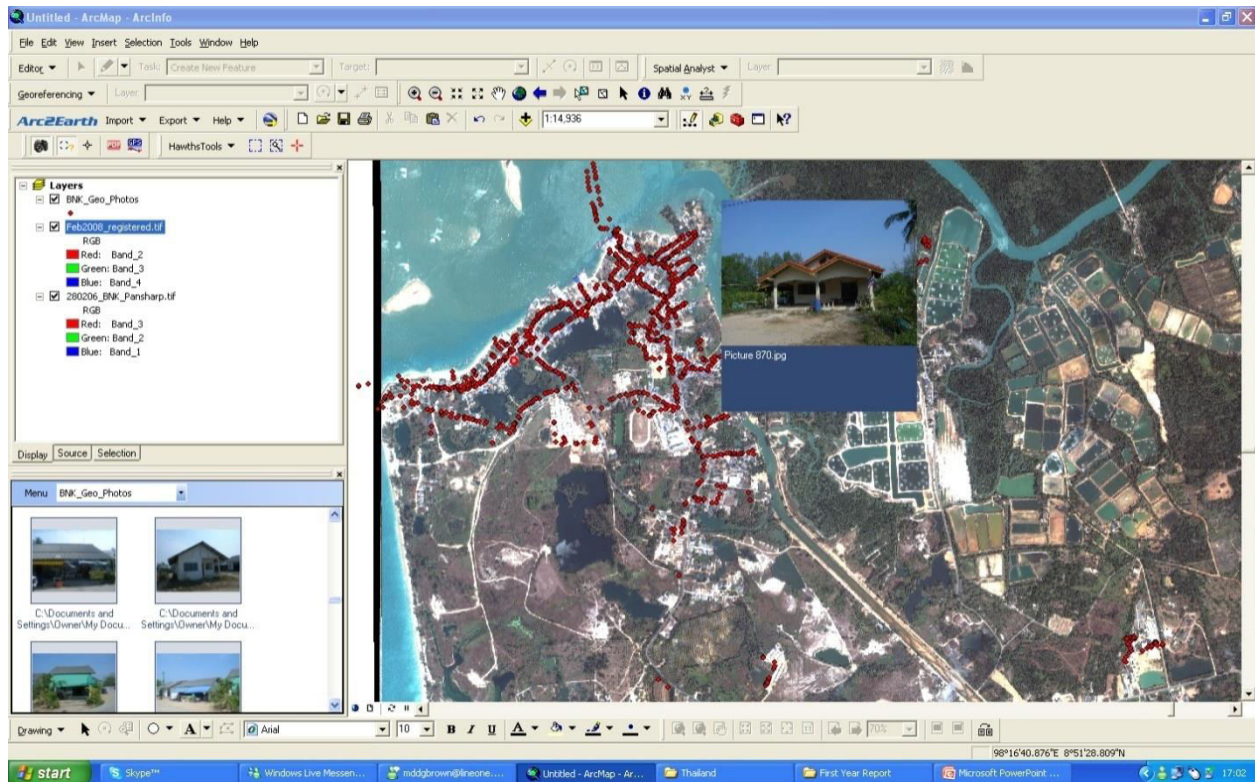


**Figure 3-4: GPS Photomapper used to simultaneously view satellite imagery and GPS photographs. Each red dot represents a single GPS photograph.**

The VIEWS™ (Visualizing Earthquakes with Satellites) system, developed by ImageCat Inc, integrates remotely-sensed imagery with GPS-registered high definition video through a map overlay that draws a track of the recording linked to the video playing in a window next to the satellite image. VIEWS collects continuous video footage from a site using two high definition video cameras on-foot or in a slow-moving vehicle: one camera pointing sideways to record building facades and the other pointing forward to capture building heights and additional information such as road type and power-lines.



**Figure 3-5: The VIEWS system deployed in Ban Nam Khem, Thailand (left) and Sichuan Province, China (right).**

### **3.5. Case Study Results**

The following section presents a summary of the results from the Ban Nam Khem case study. The results have been divided into six sections corresponding to the main indicator categories: 1. Accessibility 2. Buildings 3. Transitional Settlement/Displaced Population 4. Natural Environment 5. Livelihoods and 6. Services and Utilities. Each section contains a summary of the results acquired using remote sensing and spatial analysis for each indicator, focussing on the impact of the disaster and the speed and quality of the recovery effort. The sections are preceded by a summary of information gathered from other sources, including published reports, focus-group meetings, household surveys and key informant interviews. The reliability and usefulness of each analysis is discussed along with any limitations of the proposed approaches. Where appropriate, the process of recovery in the Thailand and Pakistan study sites are compared and the transferability of the techniques is discussed.

#### **Section 1: Accessibility**

##### **Literature Search and Household Survey Results**

Many of the roads near to the shoreline in Ban Nam Khem were badly damaged and had to be closed. The convergence of water over the village from the west and north coasts meant that much of the area was covered in mud and sand deposits 15-20 cm thick (Umitsu et al. 2007). Reports from the area confirmed that all roads within 1 km of the coast were left covered in a layer of mud, rubble and water and were likely to be only partially accessible, making it difficult for rescuers to reach survivors.



**Figure 3-6: Debris and inland water in Ban Nam Khem (left) and pumping equipment (right). (Source: Radarheinrich, 2005).**

It was important to remove the debris quickly to restore accessibility and to clear contaminated land. The Thai government also wanted to restore the region's beaches rapidly to encourage the return of international travellers. Debris and inland water was removed by the army using pumping equipment and diggers. To restore accessibility as quickly as possible the main roads were cleared first. It took approximately one week to clear the light debris in most areas, but the central market area took a further 3 weeks. It would have been difficult for people to move across town during this time.



**Figure 3-7: The army resurfaced the main road (left) but an estimated 34% of houses were still accessible by earth-road (right). (Source: Daniel Brown)**

## Remote Sensing Methodology

### *Delineate the Transport Network*

A digital linear representation of the transport network was created and used to produce statistics to describe the length of road affected by the tsunami and subsequently cleared and resurfaced. The transport network dataset was later used to assess accessibility between different features of interest. To create the transport dataset the roads were first manually-delineated and classified by road-type as main roads, minor roads and earth-roads according to their width and whether they were paved with asphalt or not. Roads paved with asphalt exhibited low reflectance in all four multispectral bands with no major absorption features creating a grey colour, while earth-roads exhibited an increase in reflectance towards longer wavelength giving them a red-brown hue (Herold et al. 2004). Highways were estimated to measure 15 m across, major asphalt and non-asphalt roads 10 m and earth-roads approximately 5-7 m.

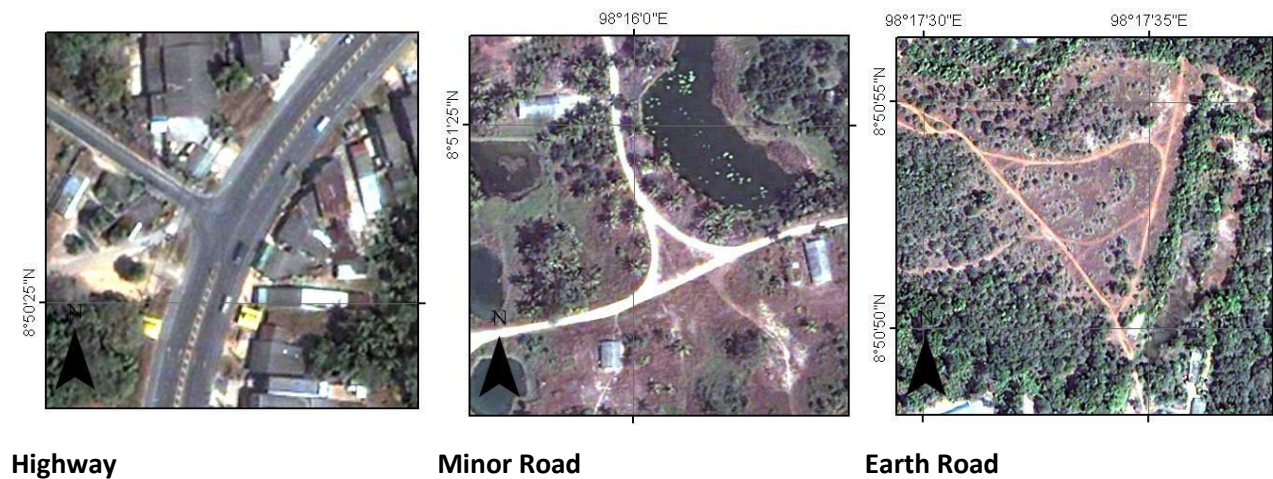


**Figure 3-8: Road types identified in Ban Nam Khem.**

The length of each road-type was measured using ArcGIS and added to the attribute table of the road dataset. The classification scheme allowed statistics to be produced that described the type of roads that were affected. Disaggregating paved and unpaved roads in particular was deemed important for decision-making and budgeting. Assumptions about the access and use of these different road-types

were made by the analyst when conducting accessibility analysis. For example, it was assumed that vehicles larger than cars could not use narrow paths or earth-roads.

The post-disaster road database was further disaggregated into four groups according to the roads' accessibility and status: 1. Unaffected, 2. Blocked, 3. Cleared and 4. Re-surfaced or Reconstructed. This taxonomy was devised so that the length and location of *affected* roads and inaccessible regions could be identified. The blocked roads were further sub-divided into damage categories according to how they were affected again to assist those agencies making decisions about how to clear and prepare the affected roads. Descriptions of the damage classes are provided below.

<b>Damage Category</b>	<b>Description</b>
<b>Debris</b>	Road or track is covered in varying amounts of debris, which is identifiable due to a substantial change in the hue and texture of the road surface. The colour and texture of the debris is likely to differ according to its composition and volume. A road is classed as <i>heavy debris</i> when the original road surface is no longer visible under the debris.
<b>Flooded</b>	Road or track is covered in water, which appears blue-to-black in optical imagery with a very low reflectance across all bands.
<b>Structures in Road</b>	Road or track is blocked by structures such as buildings, boats or cars. The analyst must try to distinguish between vehicles deposited by natural forces and those still in-use by people in the affected area.
<b>Vegetation</b>	Road or track is covered in vegetation, which is identifiable by a mainly green hue and shadowing effects. Vegetation's spectral profile exhibits a higher reflectance in the infra-red band than the red band.
<b>Washed Away</b>	Road or track is present in the pre-disaster image but not in the post-disaster image and is located in the inundated zone so is assumed to have been washed away.

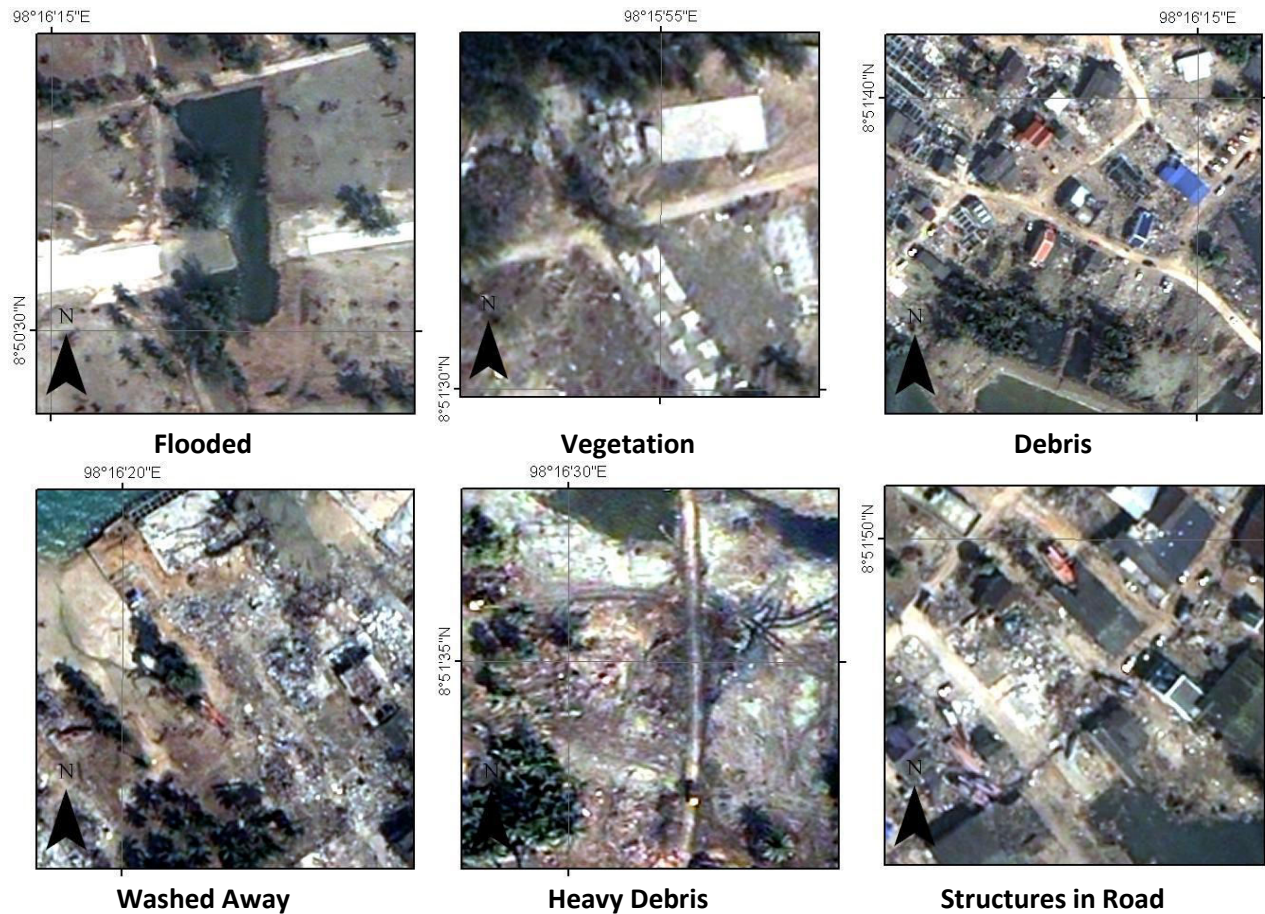
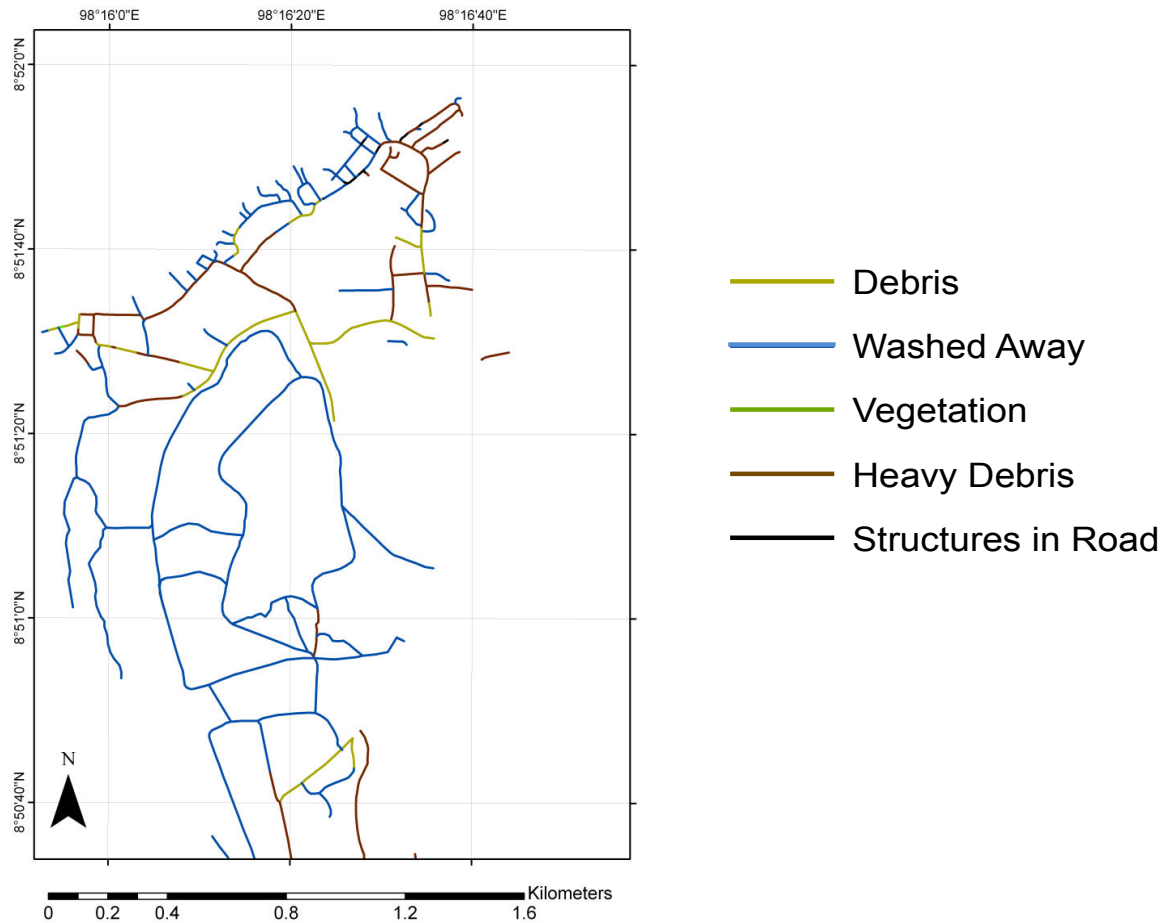


Figure 3-9: Road damage classification after the 2004 Indian-Ocean tsunami.

### Indicator 1. Road Length (Km)

#### *Damage Assessment*

Analysis of the post-disaster satellite image allowed a damage assessment of the road system to be conducted. 29.8 km of road became impassable after the tsunami, mainly due to being washed away (19.4 km) or the presence of heavy debris (7.5 km). Most of the *washed away* roads were either roads located near to the sea-front or non-asphalt roads to the south of Ban Nam Khem.



**Figure 3-10: Damage to the transport infrastructure in Ban Nam Khem.**

### *Clearance of Roads*

After four months all of the roads in the centre of Ban Nam Khem were cleared of debris but not yet resurfaced with asphalt. This allowed access to the affected area to be restored, so that construction of buildings and services could begin. After the roads were cleared, asphalt and earth both exhibited similar spectra to that shown before the tsunami but with a higher reflectance in all bands. The increase in reflectance after clearance is possibly due to the presence of dirt on the surface and/or the loss of oily components and sealing tar that decreased the general object absorption (Herold et al. 2004). 10.4 km of the affected roads were cleared of debris in total and 19.4 km remained blocked or washed away. Most of the roads that remained affected or blocked were minor roads outside of Ban Nam Khem to the south. The heavy debris on these roads was removed later between April-2005 and February-2006, so

that only 184 m remained flooded or covered in debris in February-2006. Figure 3-11 shows the status of the road network four months after the tsunami.

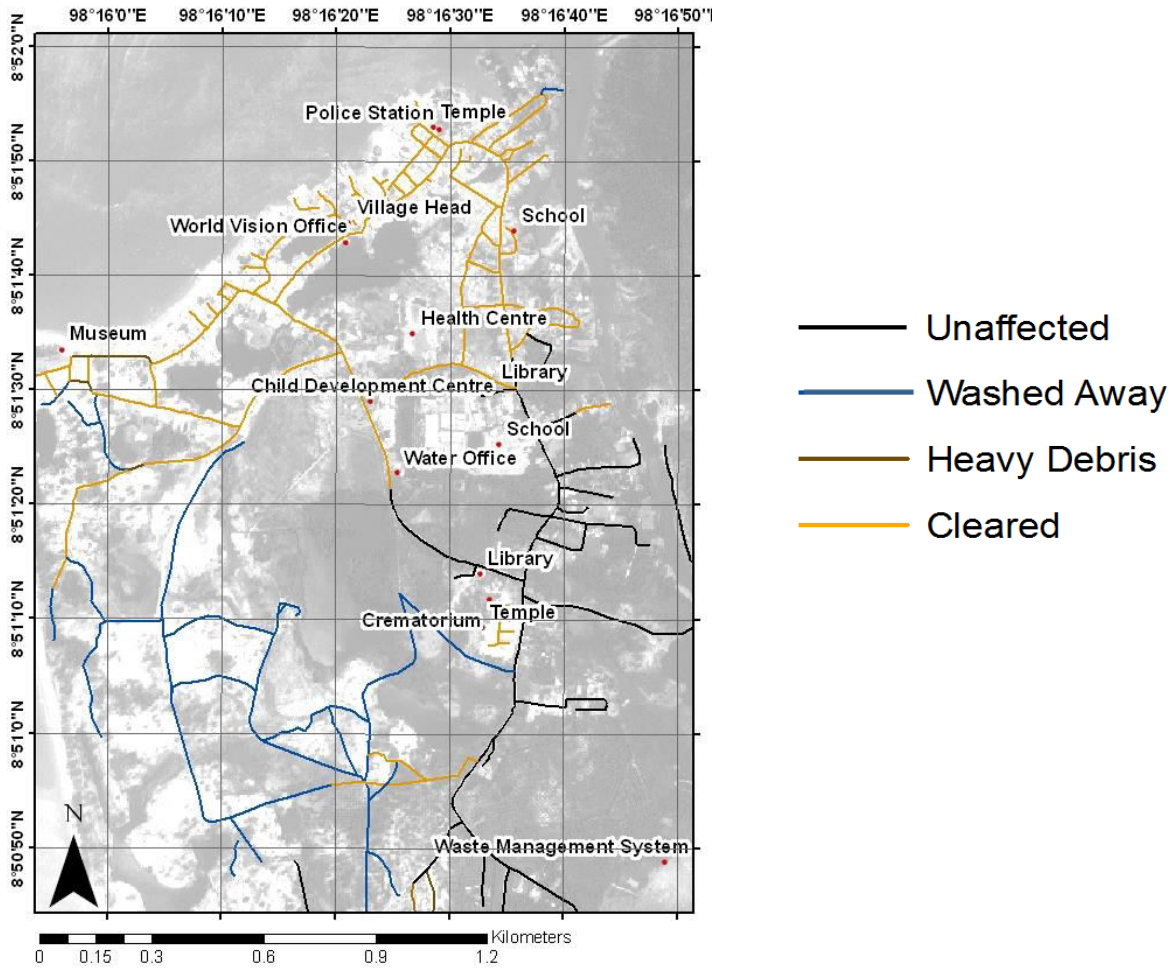


Figure 3-11: Road status in Ban Nam Khem on 21 April 2005, four months after the 2004 Indian-Ocean tsunami.

#### *Reconstruction and Resurfacing of Roads*

After they were cleared many of the roads in the centre of Ban Nam Khem were resurfaced with fresh asphalt. This process was clearly observable in the satellite imagery as the fresh asphalt appeared darker with a lower reflectance in all four bands of the satellite image. The asphalt got lighter with age again matching field observations made by Herold et al. (2004). Most of the reconstruction and resurfacing of roads occurred between April-2005 and February-2006: 13.7 km of paved road and 6.7 km of non-

asphalt road were constructed or resurfaced during this time. Figure 3-12 shows the total length of functioning roads over time by road-type. Functioning road is defined here as any road surface that is not identified as being directly damaged or blocked.

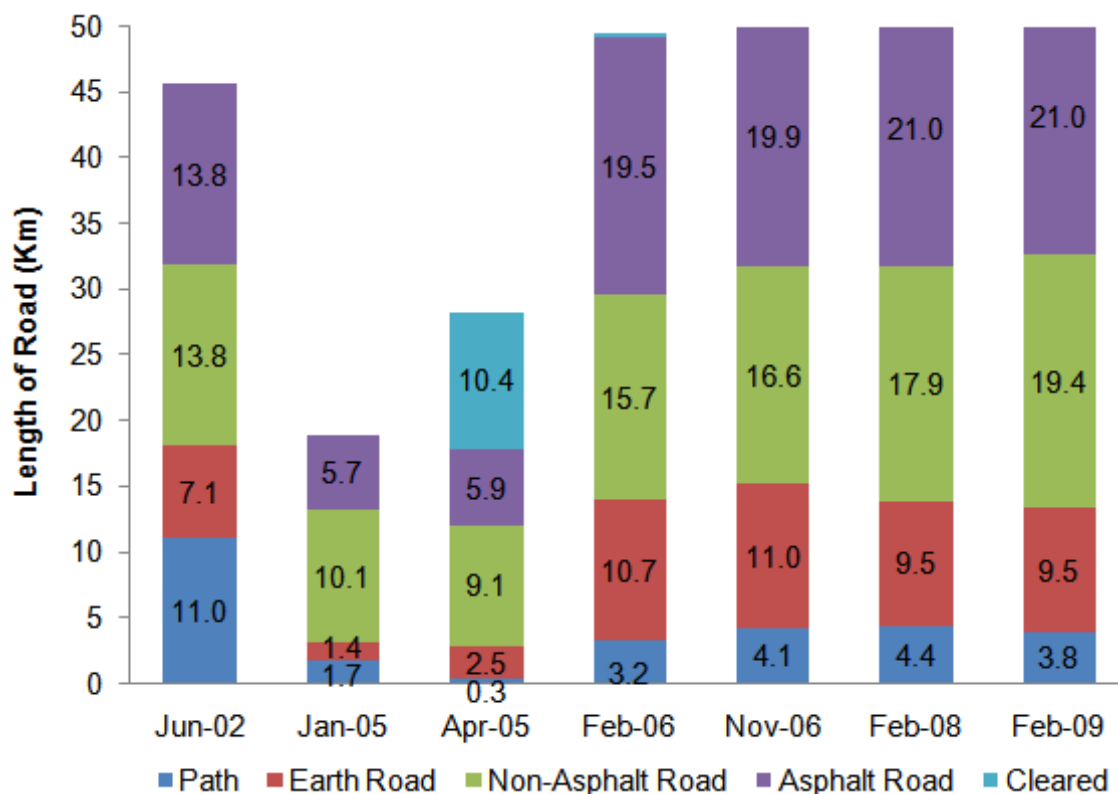


Figure 3-12: Total length of functioning road in Ban Nam Khem by road type.

### Indicator 2. Network Analysis

On completion of the digitised transport database, *Network Analyst* – available as a plug-in for ArcGIS - was used to assess how accessibility had changed between different points of interest due to damage, clearance and reconstruction of the transport infrastructure. The most commonly used Network Analyst tools for this assessment included:

- a) Best Route Analysis: to investigate changes to *travelling time* and *travelling distance* brought about by *changes* to the transport network and relocation of households and services/facilities after reconstruction.

b) Service Area Analysis: to identify households and businesses with inadequate access to key facilities and services and to propose where these services may be constructed or relocated to ensure sufficient access.

### Accessibility around Ban Nam Khem

After the tsunami, the government and various national and international agencies offered residents the opportunity to relocate from Ban Nam Khem to several new housing developments around Takua Pa District. *Best Route* analysis was used to show how moving to these new developments affected peoples' access to services and facilities. As an example, the map in figures 3-13 shows the shortest travelling routes from six of the largest housing developments to Ban Nam Khem School marked with a red star.

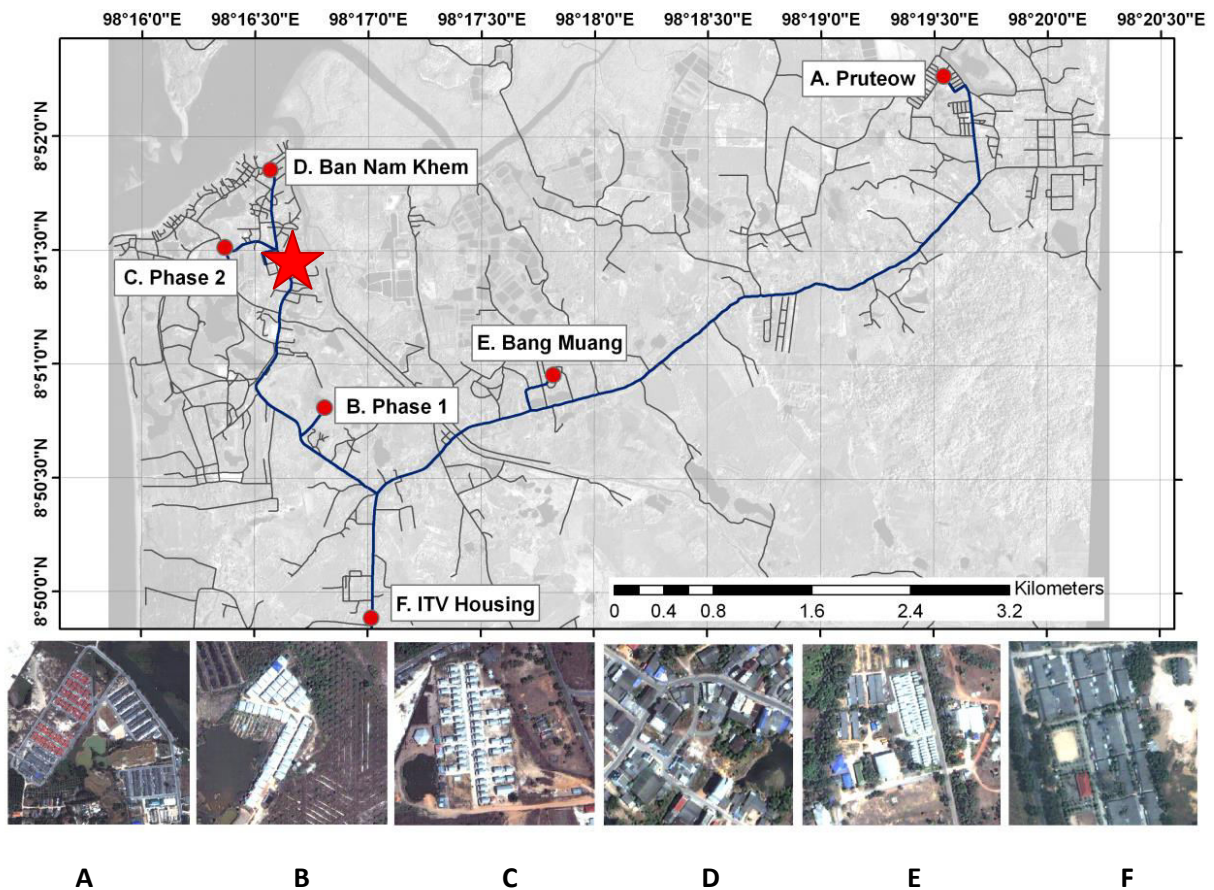


Figure 3-13: Best route from six housing developments to Ban Nam Khem school (red star) showing the shortest distance.

A similar best route analysis was used to assess accessibility between the new housing developments and fishing-piers, a major source of livelihood for many households. Traveling times and walking times were derived based on Thai speed limits and an estimated walking speed of 4.5 km an hour (Knoblauch et al. 1996). Prior to the disaster most homes in Ban Nam Khem were within a 10 minute walk of the piers. Households in Phase 1 agency housing remained close to the shore (13 minute walk), but those in Bang Muang, ITV Housing and Pruteow housing developments had a significantly larger distance to travel (e.g. 19 minutes on a moped from Pruteow) along a very busy road, which is likely to have led to significant changes in their lifestyle and source of livelihood. Reports suggest that residents were at the time of the field study selling their homes in the ITV development and returning to live in Ban Nam Khem permanently so they can continue to work in the fishing sector. Figure 3-14 presents the distance from six housing developments to fishing piers in Ban Nam Khem.

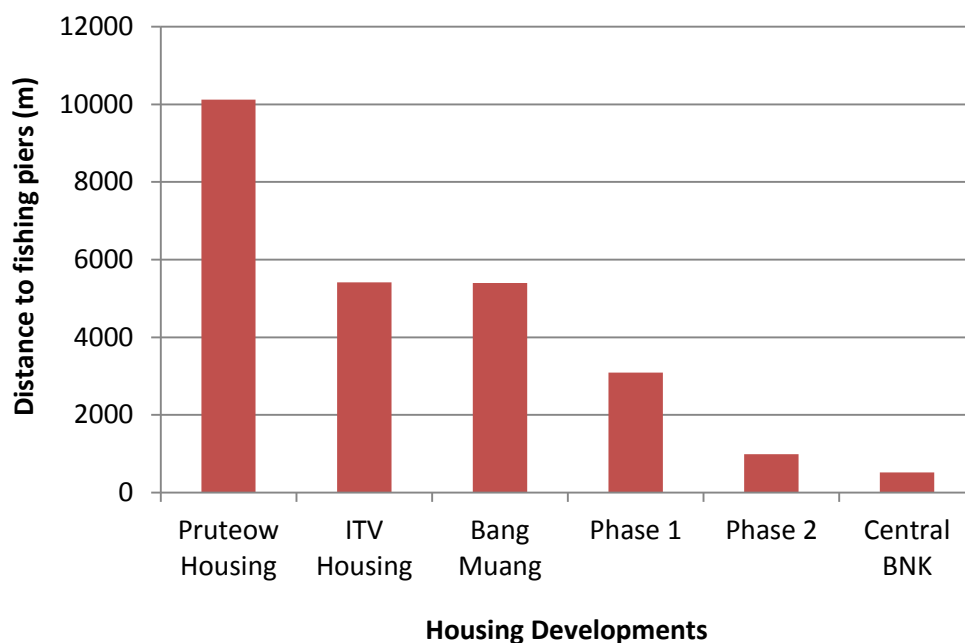
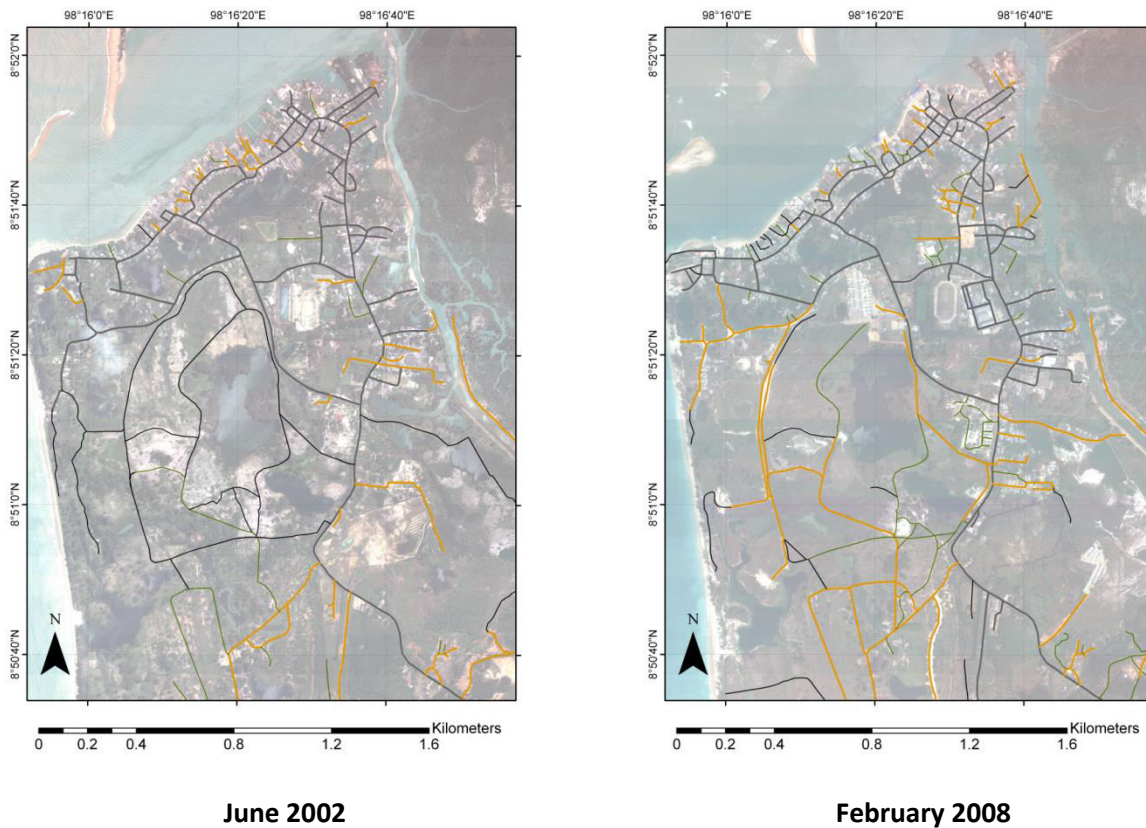


Figure 3-14: Distance (metres) from six housing developments to fishing-piers in Ban Nam Khem.

#### Accessibility within Ban Nam Khem

Allocating time-stamps to each of the road segments allowed the transport infrastructure to be mapped and spatially analysed over time. Pre-disaster maps were compared to post-construction maps to

identify significant changes to the layout of the transport infrastructure as a result of the reconstruction process (see figure 3-15). The maps show that the layout of the roads did not change, despite some planners suggesting changes to the road-layout might help to improve evacuation times (Norwegian Geotechnical Institute 2006). The army did not build new roads or evacuation routes but they did resurface existing roads. Only 2.3 km of new asphalt road were constructed, mainly by agencies linking new housing developments to the main road or by developers on private land to the south of Ban Nam Khem that was due to be developed into resorts. Overall travel-routes and accessibility in Ban Nam Khem itself though were expected to be similar than they were before the tsunami, which was verified by key informants and households on the ground.



**Figure 3-15: Road maps of Ban Nam Khem before the tsunami and after reconstruction. Paved roads are in grey and non-asphalt roads are in yellow.**

### **Indicator 3. Reconstruction of Bridges and Public Transport Facilities**

In addition to monitoring the road network satellite imagery was also used to monitor other features associated with transportation such as bridges and large public transport facilities. Where appropriate, bridge status information was linked to the network analysis work described previously. Conspicuous forms of public transport were also monitored by observing signs of activity or disruption in-and-around appropriate depots or facilities. Traffic activity on the roads was also monitored to infer the use of the transport network at different stages of the recovery process.

#### *Bridges*

A single road-bridge to the north of Ban Nam Khem was totally destroyed by the tsunami. The bridge was one lane wide and formed a link between the mainland and shrimp ponds. Within four months a new single-lane bridge had been constructed. Three months later, a new bridge was three-quarters complete with the middle span still to be constructed. The new bridge was wider and appeared to be made of concrete. It was completed by February-2006 presumably allowing larger vehicles access to the shrimp ponds.

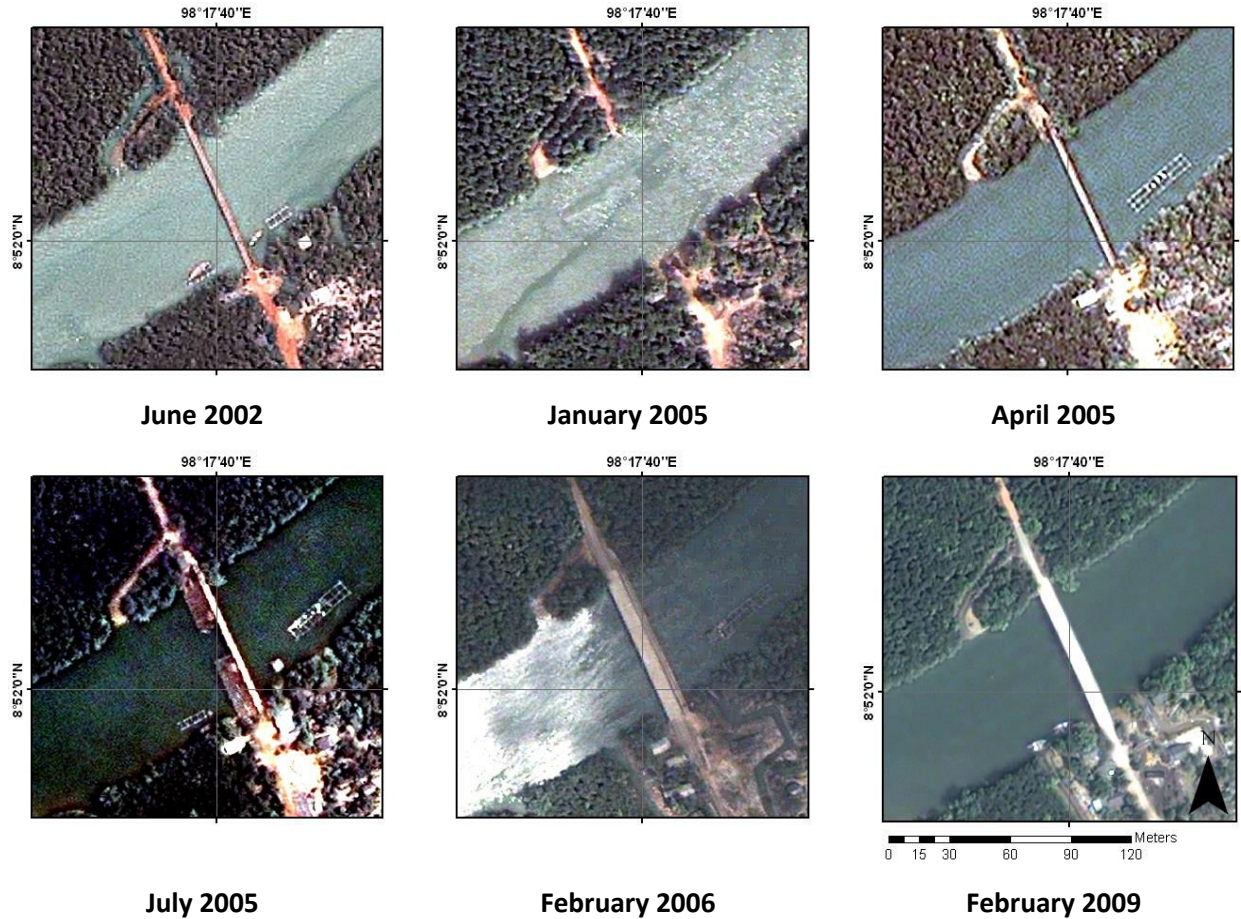


**Figure 3-16: The destruction and construction of a bridge near Ban Nam Khem linking shrimp ponds to the mainland.**

#### *Public Transport: Ferry Service*

The ferry port facilities and the ferry itself were also easily identifiable in the satellite imagery. The presence and absence of the ferry, the pier and the surrounding buildings was used to assess the recovery of the ferry service. The tsunami directly hit the pier and ferry facilities, demolishing all of the buildings in the area. The pier was still standing but the surrounding area was covered in heavy debris. The road surfaces and buildings were all reconstructed between April-2005 and February-2006. The ferry could be seen in the imagery functioning only one week after the tsunami, forming a valuable link between Kho Khoa Island and the mainland.



June 2002



January 2005



April 2005



July 2005



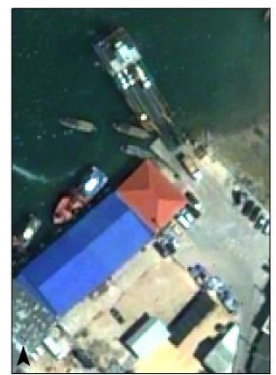
February 2006



November 2006



February 2008



February 2009

Figure 3-17: Analysis of the ferry pier in Ban Nam Khem.



Figure 3-18: The Kho Khoa ferry (left) and in satellite imagery functioning one week after the tsunami (right).

#### **Indicator 4. Presence of Vehicles**

Monitoring traffic activity was used to estimate the extent to which different transport routes and services were being used. This analysis was particularly useful in the immediate aftermath of the disaster to highlight areas of human activity. Figure 3-19 shows the results of the January 2005 image analysis, acquired 7 days after the tsunami at approximately 10:30 am local time. Each visible vehicle was marked with a green point. There are at least four areas of interest visible, which have been enlarged in the figure:

- a) A group of cars parked near to the shoreline, indicating human activity in the worse affected area and the possible presence of emergency relief workers.
- b) A group of cars at Ban Nam Khem school, located just outside of the worse-affected area and the site where Ban Nam Khem camp was later constructed.
- c) Lorries, tents and relief supplies present in the grounds of Bang Muang School, indicating the arrival of relief material to the area.
- d) A significant amount of traffic on the main road from Khao Lak to Takua Pa indicating a possible exodus of people in-and-out of the Province.

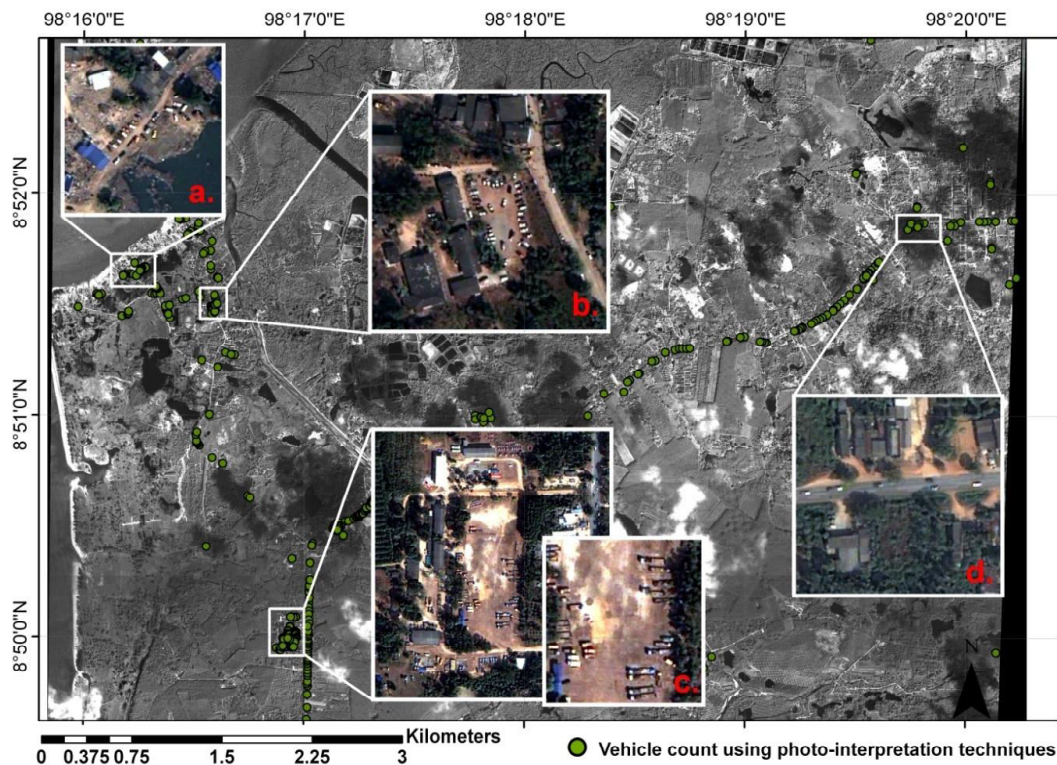


Figure 3-19: Traffic analysis of the post-disaster satellite image acquired on 02 January 2005.

### Discussion

Remote sensing provided a reliable method of extracting detailed statistics on changes to accessibility and the length of affected and reconstructed transport network. The narrative of recovery acquired with remote sensing closely matched ground reports and official statistics. In particular, remote sensing analysis correctly identified that all roads within 1 km of the coast were either washed away or covered by a mixture of mud, rubble and water. Recovery maps after the disaster show the clearance of roads by the army within several months and the resurfacing of main roads within one year. Applying accessibility analysis to the digitised transport network helped to quantify how the relocation of services and residential areas was likely to affect peoples' access to camps and sources of livelihood.

With a skilled image analyst, these indicators provide a high level of information and reliability. High-spatial-resolution multi-spectral satellite imagery such as Quickbird and Ikonos with a ground sampled distance (GSD) between 0.60 m – 1.0 m can reliably map the centrelines of road and distinguish asphalt from non-asphalt road surfaces. The width of the roads can also be accurately measured to classify

tracks, roads and highways. Fifty GPS photographs containing road surfaces were selected at random to check the satellite interpretation results with a 96% accuracy rate. There was confusion in densely-built areas though where road surfaces were obscured by building facades and shadows, but otherwise the results were highly reliable. The analysis of roads in the Delmas 56 slum in Haiti, described in Chapter 4, similarly missed minor roads located in densely-packed areas and resulted in a much lower accuracy.

A limitation of remote sensing is its inability to identify non-structural damage (or local structural failures) to bridges or the transport network. It was also unable to provide reliable information on the quality of the construction work or on the location of road restrictions, such as one-way systems or roadblocks. The method therefore assumes that all cleared and/or reconstructed roads in the imagery are open and accessible to the public. In Ban Nam Khem, some roads were in-fact located on private land and public access was therefore restricted by developers. Some residents complained about the quality of the asphalt used on the roads, but satellite imagery was not able to detect this and the expertise or tools were not available in the field to analyse the quality of the road surfaces.

A major weakness of *Accessibility Analysis* for many users is that it can be time-consuming and expensive to conduct over a large area because the transport infrastructure must first be digitised. This took one day to do for Ban Nam Khem. The preparation time would be dramatically reduced though if a suitable GIS was already available on which the damage and clearance attributes could be added. An analyst therefore needs to weigh-up the potential outputs and results against the time required to create the database. As shown previously, a substantial amount of information can be extracted once the transport dataset has been created. Open-source alternatives to ArcGIS's Network Analyst are now also available with packages such as Grass GIS which can help reduce software costs for those wanting to conduct such analyses.

### *Transferability*

The satellite image analysis of the Pakistan case study area identified 4 km of roads that were directly affected by the earthquake in Chella Bandi, 25 km less than were affected in Ban Nam Khem – presumably because of the nature of the hazards. 74% of the affected roads in Chella Bandi were covered in varying amounts of debris from collapsed buildings and land-slides. Large cracks were even visible in some areas and some roads were flooded after the near-by river burst its banks behind a

landslip. Although individual blockages to roads were small in Chella Bandi they were scattered throughout the settlement so blocked access to many commercial and residential areas.

The road damage classes used here were widely applicable to Ban Nam Khem and Chella Bandi and were also used following the 2008 Wenchuan earthquake to good effect (Brown et al. 2012). However, some of the classes are unique to different hazards and not all of the classes were seen in each case study. For example, there were no landslides or road cracks observed in Ban Nam Khem.

Figure 3-20 shows the length of functioning road in both case study sites normalised to the pre-disaster state – again, *functioning road* refers to the length of road not directly blocked or damaged. The graph shows how less length of road was directly affected by the earthquake in Chella Bandi. Roads were cleared in both case studies very quickly, highlighting the urgency to re-gain accessibility to most central areas. The length of functioning roads in Chella Bandi increased to its highest level in the first year of recovery as people formed temporary access-routes to-and-from transitional settlements but these were later re-claimed by owners of the land. After several years, both case study sites had very similar transport systems and road statistics as were present before the disasters.

The graph highlights some limitations when trying to use this indicator to compare case study sites. In particular, the amount of inaccessibility in Chella Bandi in the aftermath of the earthquake is not fairly represented here. As well as roads *directly* affected by hazards, the indicator might also include roads *indirectly* affected such as roads no-longer reachable because of road-blockages. The line in the graph representing Chella Bandi would then presumably show a steep decline after the earthquake and quick recovery within the first few months, similar to Ban Nam Khem. The results here also highlight the need to distinguish between permanent roads and temporary roads built to provide temporary access-routes to relief or camps.

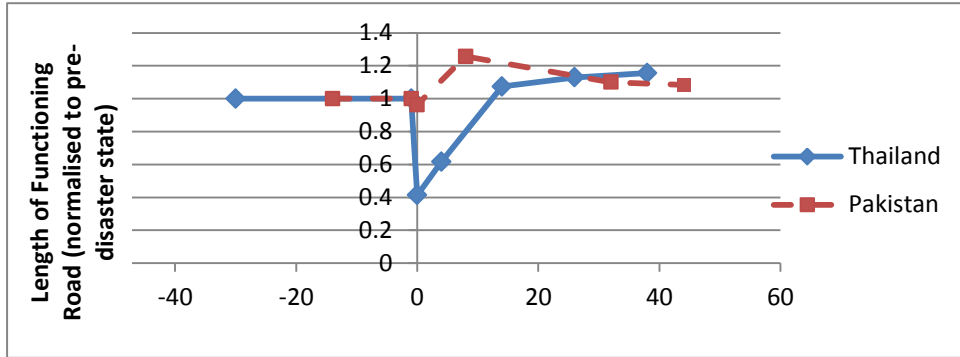


Figure 3-20: Length of functioning road in Ban Nan Khem and Chella Bandi.

## **Section 2: Buildings**

This section of the chapter describes a multi-scale workflow and set of analyses that can be used to monitor recovery of the building stock. The indicators are divided into three spatial tiers – regional, street-level and per-building. A similar multi-scale approach was applied to damage assessments using remote sensing (Ghosh et al. 2007). Tier 1 offers a regional perspective: semi-automatic and rapid manual analysis techniques are used to map the urban extent throughout the recovery process and change detection analysis is then applied to identify areas of building construction and removal. Tier 2 analyses changes in the urban layout and morphology by analysing *groups of buildings* using either density or Nearest Neighbour statistics or a more advanced Landscape Metrics approach. In Tier 3 high-spatial-resolution satellite imagery is analysed to extract detailed information on a representative sample of individual structures by analysing their stage of development, building attributes, location and building context. The three tiers can be applied independently but also collectively to form a logical workflow for the analyst. A regional approach may first be used to highlight areas of interest or areas that show substantial change, which may then be analysed in more detail using the neighbourhood and per-building techniques described.

### **Indicator 5. Removal and Construction of Buildings**

#### **Remote Sensing Methodology**

This indicator tracks the construction and removal of buildings by monitoring their presence and absence throughout the recovery process. The extent of the built environment was first delineated in each image. Two different approaches for mapping the built environment were used for this work: both a manual and a semi-automatic method. The first involved systematically identifying each building in the imagery and marking it with a single point, then repeating this analysis on subsequent images to ‘update’ the point database. The second method involved the use of a supervised classification to classify impervious surfaces at different stages of recovery. Impervious surfaces include pavements, roof-tops and other surfaces made mainly of asphalt, concrete, brick and stone. Maximum Likelihood simultaneously classified 5 land classes – bare ground, sparse and thick vegetation, impervious surfaces and water – based on training pixels manually selected by the analyst. Change detection analysis was then applied to the maps to identify the expansion and contraction of built-up areas between two states

in time. Changes in the point layer were identified by querying the geodatabase using Structured Query Language and changes to the image classification results were identified using raster calculator to subtract one classification image from the other to create a unique code representing each possible land-cover change.

## **Results**

### *Method 1: Manual Delineation of Building Points*

A building database was created manually with a point representing each building visible in the satellite imagery. In total, 621 buildings were washed away by the tsunami or otherwise removed between June-2002 and 02 January-2005. A further 52 buildings were demolished between 02 January-2005 and 21 April-2005. It is assumed that these buildings were demolished because they were deemed unsafe or because they were an obstruction to construction work. The graph in figure 3-21 shows that most of the reconstruction-work was completed by February-2006, but that small amounts of construction were still on-going four years after the tsunami. When plotted, the data forms a recovery curve showing the speed of construction and the number of buildings present both before and after the disaster. The total number of buildings present in Ban Nam Khem increased by 48% from 1,170 to 1,727.

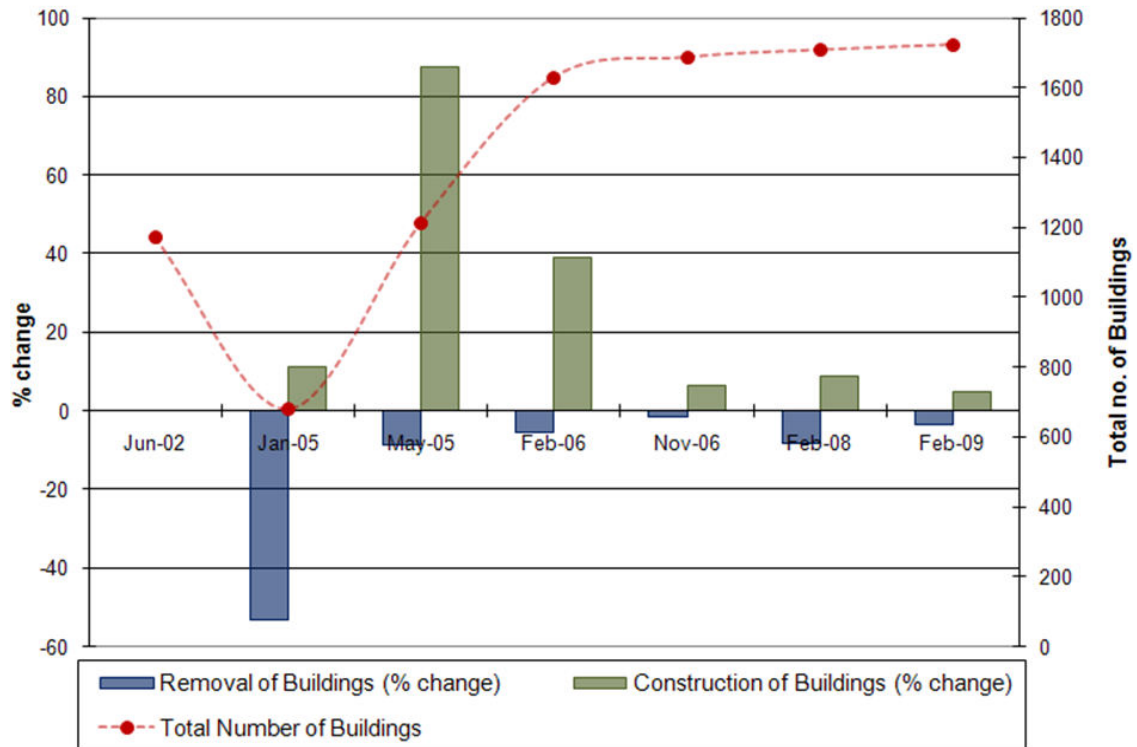


**Figure 3-21: Total number of buildings in Ban Nam Khem.**

The recovery curve in figure 3-21 shows the rate of construction across the whole of Ban Nam Khem. To examine spatial disparity in the reconstruction process maps of building construction and removal were produced by appropriately coding the building point database. When comparing the change between two images, buildings that were present in the older image and not present in the most recent image were marked as 'removed' and buildings that appeared on a previously empty or destroyed plot were marked as 'constructed'. The results show that the majority of buildings in the centre of Ban Nam Khem were constructed within 5 months, while buildings outside of this area were more likely to have been built at a later date.

		
<p><b>June 2002.</b> 1,170 buildings identified two and a half years before the tsunami.</p>	<p><b>June 2002 – January 2005.</b> Almost all of the buildings within 200 m of the shoreline were destroyed, except for a group of concrete buildings in the north-east.</p>	<p><b>January 2005 – April 2005.</b> 592 buildings were constructed, including permanent housing in the centre of town and a new residential area 400 m inland. Transitional shelters were also erected in the grounds of Ban Nam Khem school.</p>

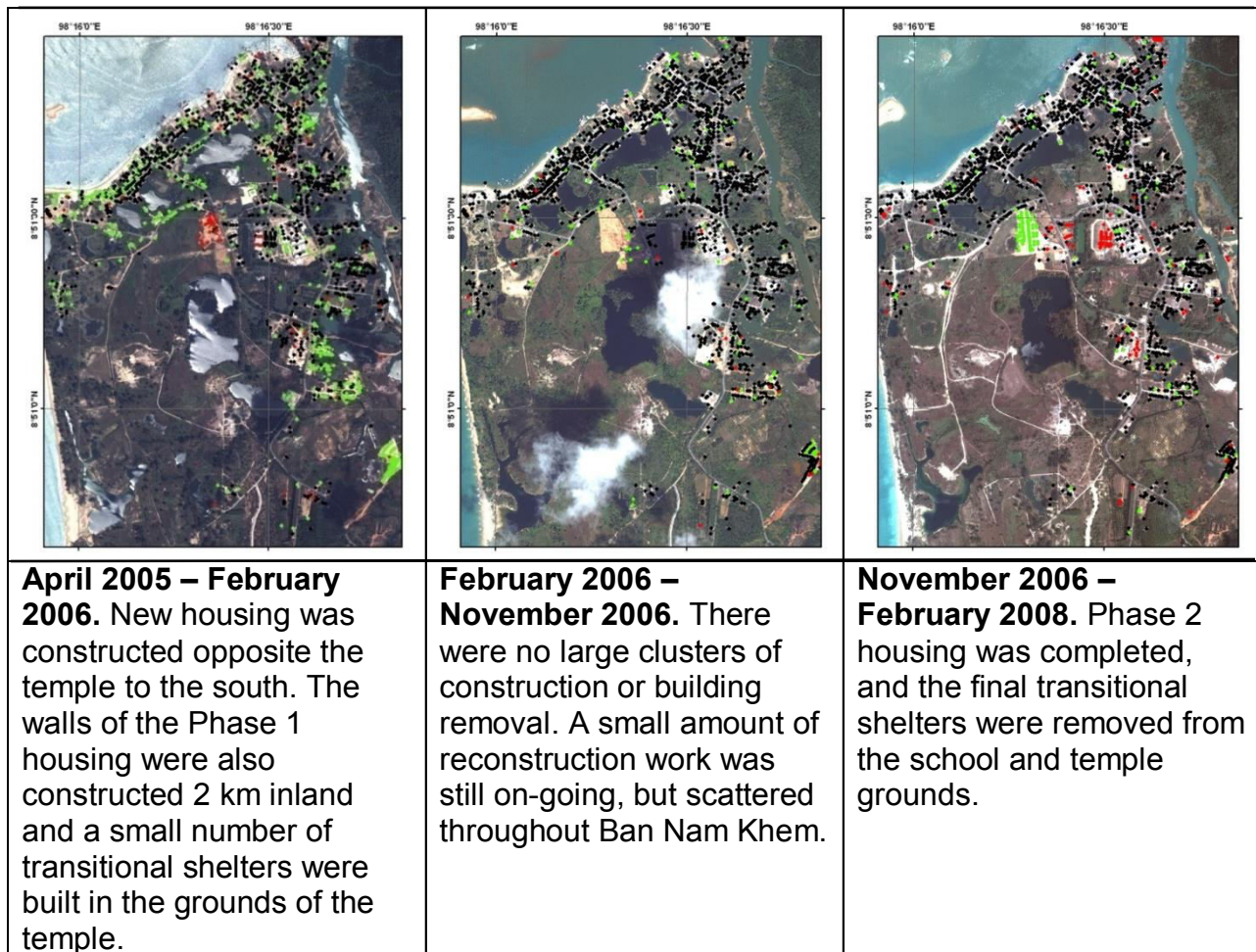


**Figure 3-22: Building point database showing the construction and removal of buildings at different stages of the recovery process (black = pre-existing; red = destroyed or removed; green = reconstructed).**

To further analyse spatial disparity in the speed of construction across Ban Nam Khem, a 250 m grid was placed over the building points and used to disaggregate the data. Building numbers were then plotted over time, producing separate recovery curves for 8 of the grids. The size and shape of the curves characterises the speed and type of reconstruction in each grid (see figure 3-23). Most areas in the centre of Ban Nam Khem were reconstructed to pre-tsunami levels within 1 year of the tsunami ( e.g. grids 1&3), except for some areas on the coast where a 30 m non-construction zone was put in place (grid 2). Outside of Ban Nam Khem curves were produced for new developments (grids 4&7), planned encampments (grid 5) and areas not affected by development (grid 6&8).

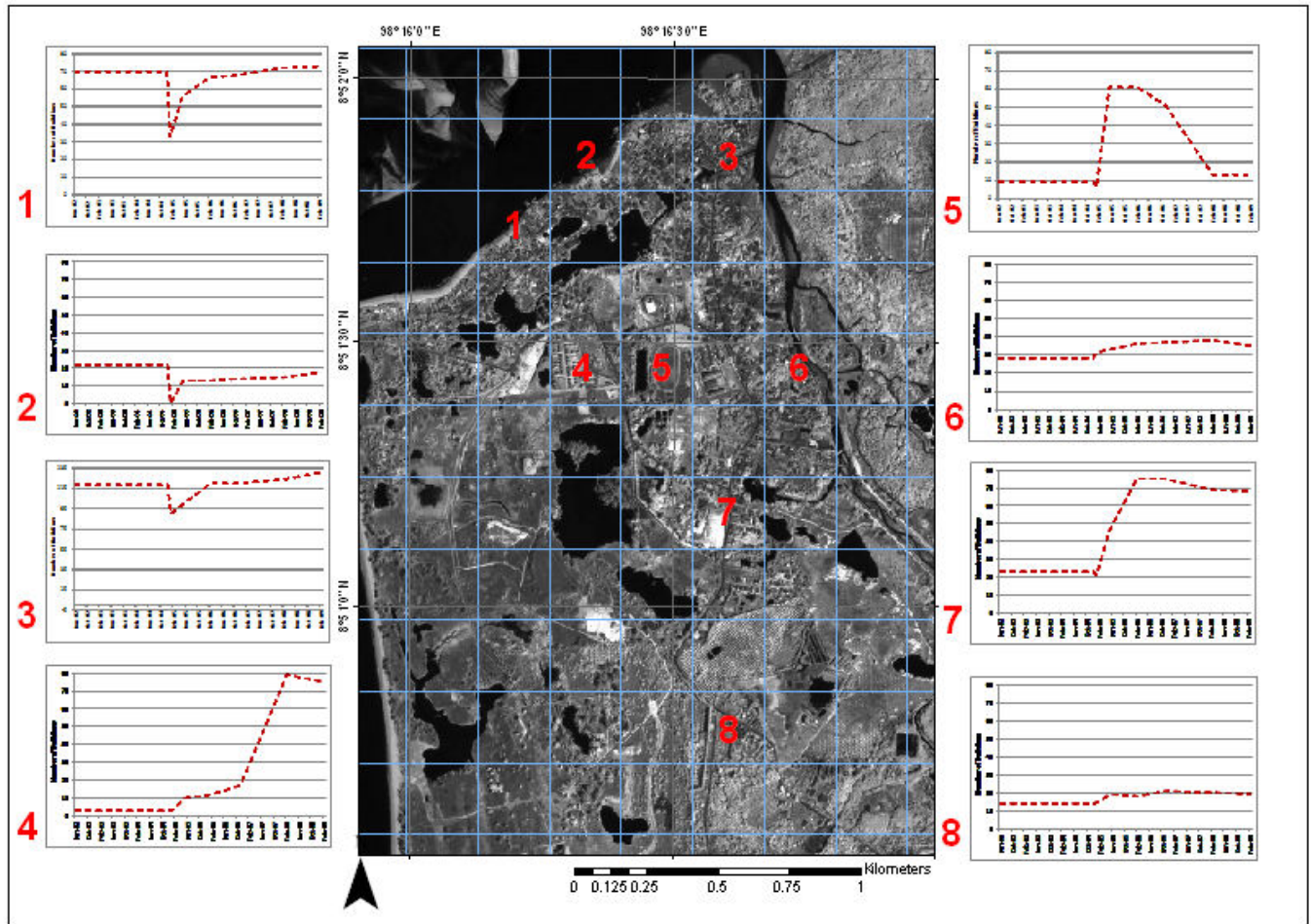


Figure 3-23: Building construction curves for eight 250 m grid cells. The plots show the number of buildings in each grid over time.

#### *Distance to Ocean*

As a mitigation measure, the Ministry of Interior introduced a 30 m non-construction zone for residential buildings by the sea. By overlaying this restriction zone over the building database the enforcement of this policy was monitored. The analysis shows that the tsunami totally destroyed at least 61% of buildings within 30 m of the coast. After four years 109 buildings were still present within the 30 m restriction zone; only 11 less than were there before the tsunami. Integrating ground observations into the building dataset identified the use of these buildings. Approximately 24% were residential and the rest were used for fishing (53%), industry (18%) or tourism (5%). Most buildings were therefore reliant on an ocean-side location and exempt from the policy. Buildings present within 30 m of the coast in February-2009 are shown as a red point in figure 3-24. This example shows how the building point

database may be strategically disaggregated to monitor reconstruction patterns in particular areas of interest.

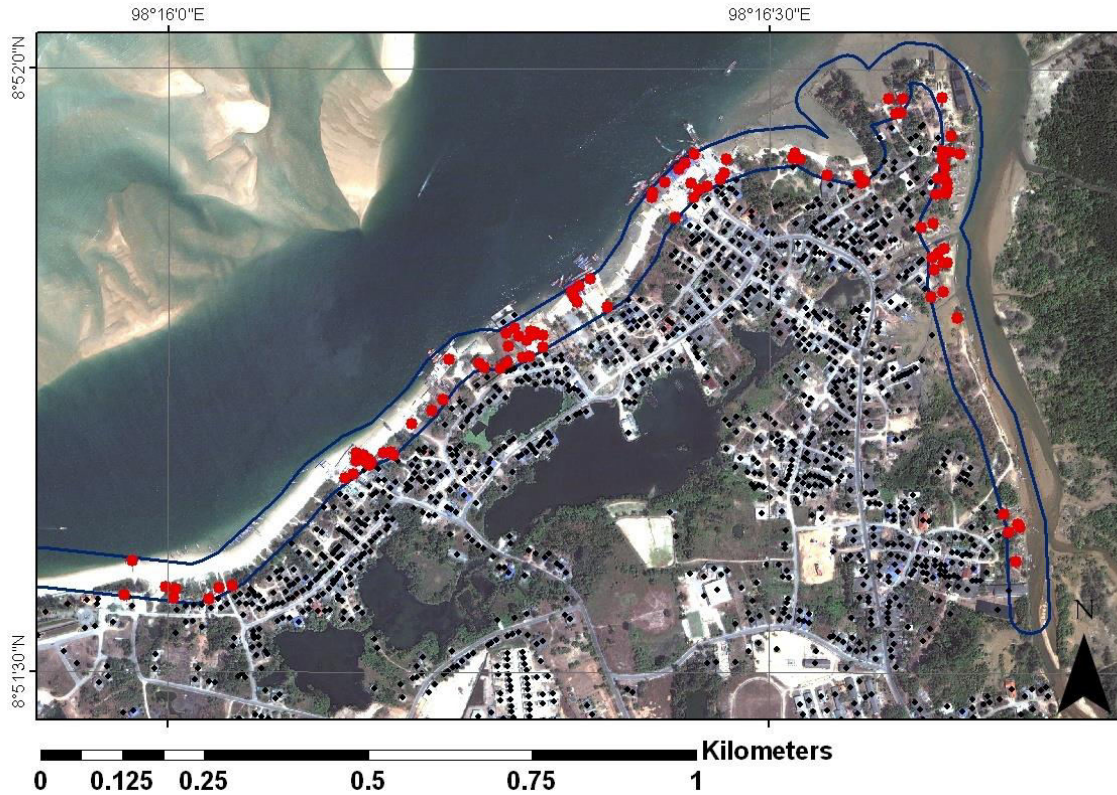


Figure 3-24: Buildings constructed within 30 m of the ocean after the 2004 tsunami.

#### Method 2: Supervised Classification of Impervious Surfaces

Maximum Likelihood classification was also used to classify impervious surfaces as a means of semi-automatically analysing the built environment. ArcGIS's raster calculator was then used to subtract one classification image from another to produce change detection maps that identified areas of construction and degradation. The method and results are described in more detail in the *environment* section of this chapter. A map showing areas of development between January-2005 and May-2005 produced by Maximum Likelihood (left) and the manual identification of buildings (right) are compared in figure 3-25. Pixels that have been converted to impervious land-cover in the classification images are displayed in grey, whilst newly-constructed buildings identified using the manual delineation technique are marked as green points. The two maps correlate well and can be used to identify at least four

clusters of construction work: 1. Army-built housing near to the coast 2. Residential buildings 400 m inland 3. Ban Nam Khem school buildings and 4. A planned camp at the temple.

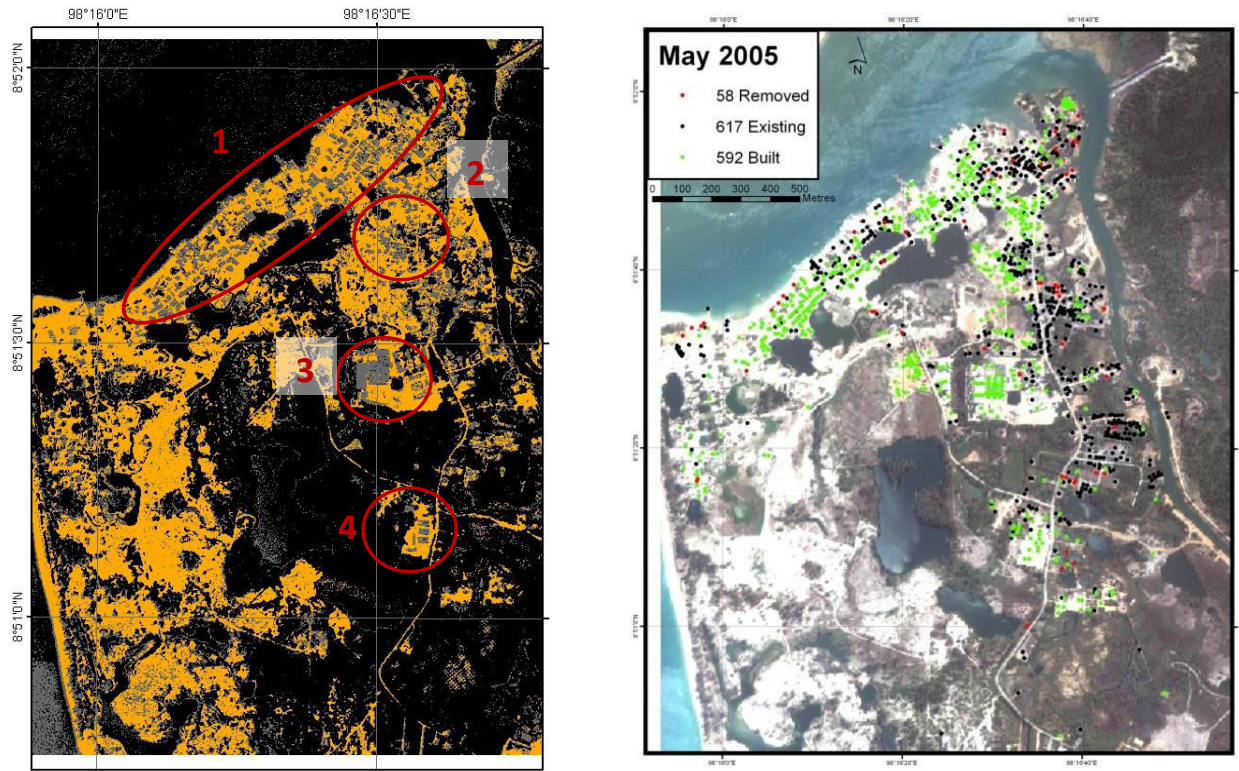


Figure 3-25: Areas of building construction coded grey and bare ground coded yellow using maximum likelihood classification (left) correlate well with a map of building construction produced manually (right).

## Discussion

### *Method 1: Manual Delineation of Building Points*

The manual method provides a relatively reliable way of creating a building database and extracting detailed statistics on the number of buildings that have been constructed and removed. The technique was based on the identification of individual buildings and therefore produced a very detailed output. A rapid version of the manual analysis is conducted across the whole scene by simply identifying the presence and absence of buildings in each image, but extra value may be added to the data by

disaggregating the points by location, structure-type or the stage of construction, according to the needs of the user.

To test the accuracy of the manual building detection the results were directly compared to ground observations made at 50 building locations during the ground deployment. Nine errors were identified: four commission errors and five omission errors, resulting in 82% accuracy. Commission and omission errors occurred when the satellite interpretation incorrectly included or missed buildings respectively from the analysis. Commission errors occurred in Ban Nam Khem when garages, gated-areas or outbuildings were incorrectly counted as permanent-buildings, while omission errors typically occurred when more than one building was located under a single roof.

**Omission Error**



**Two buildings under one roof**

**Commission Error**



**A garage misinterpreted as a dwelling**

**Figure 3-26: Omission and commission errors in Ban Nam Khem.**

Despite the relatively high reliability of the manual method there are a number of limitations that are important to be aware of. Firstly, the remote sensing analysis wrongly assumed that all buildings in the imagery were complete and in-use. However, the ground survey found at least 32 abandoned buildings that were not identified as abandoned using satellite imagery. In hindsight, signs of non-occupation could be observed around some of the structures – such as the presence of overgrown vegetation - but this still relies on some weak assumptions. The manual method of analysis also assumed that most buildings that were removed between the acquisition of the pre-disaster image and the post-disaster image were destroyed by the disaster event, but it is possible that some of the buildings may have been demolished before the first post-disaster image was acquired. To conduct an accurate damage assessment it is therefore important to do so as soon after the disaster as possible and to use pre-event

imagery acquired as close to the disaster date as possible to create a baseline so that non-residential structures can be excluded from the analysis.

#### *Method 2: Supervised Classification of Impervious Surfaces*

In addition to the manual analysis the Maximum Likelihood classifier was also used to test a method of classifying impervious surfaces semi-automatically. The technique provided a relatively quick method of identifying areas of construction and estimating the rate of construction after a tsunami. Figure 3-27 shows the change in building numbers counted manually and the impervious surface area extracted with the Maximum Likelihood classifier. The two plots show a similar trend to each other suggesting that in this example Maximum Likelihood could be used to infer the rate of reconstruction. The biggest discrepancy between the two methods occurs in the post-tsunami image when maximum likelihood overestimates impervious surfaces due to confusion with water-logged soils. The same technique did not work as well in Pakistan, as the changes to the built-environment after the earthquake tended to be more subtle and not as easily recognisable by automated techniques. The spectral classifier did identify areas of new development on bare ground and vegetation though. More work is required to better understand the spectral changes that take place after a building is demolished and reconstructed to automate the classification of construction processes in urban areas.

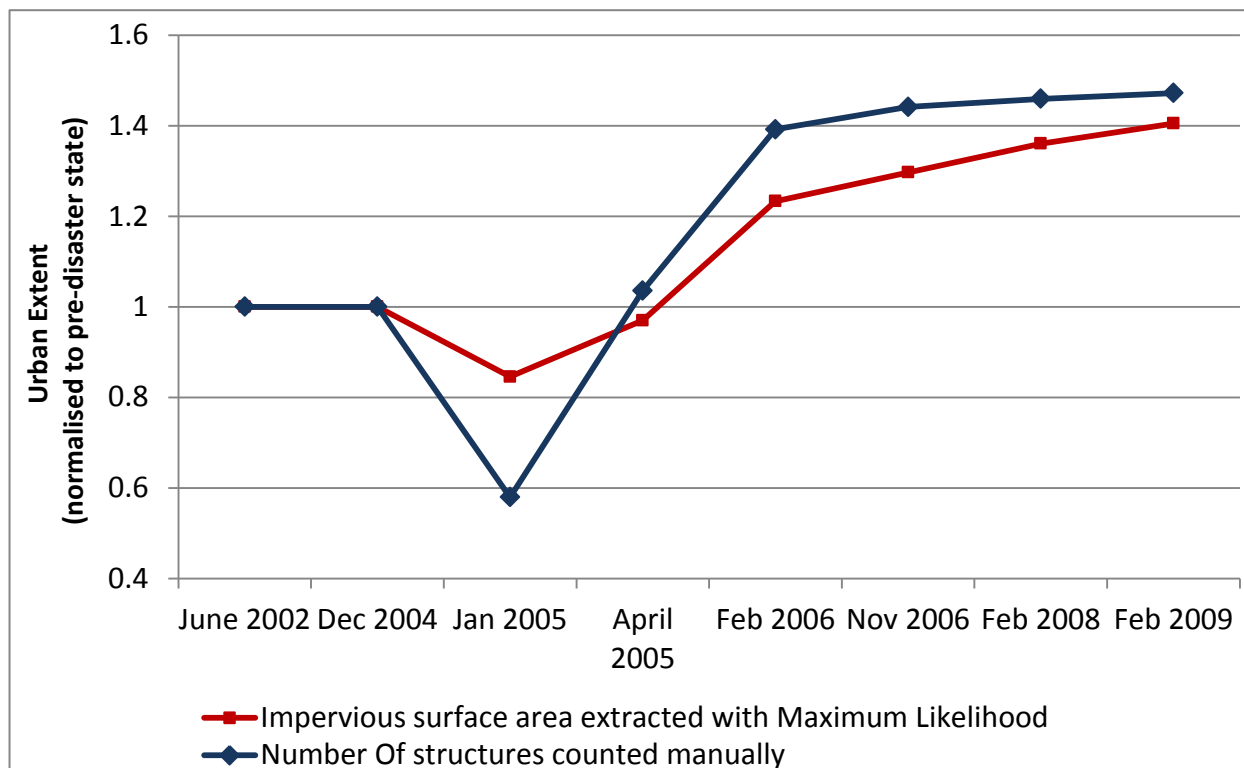


**Figure 3-27: The urban extent normalised to the pre-disaster state measured manually and with Maximum Likelihood classifier.**

To assess the accuracy of the impervious surface classification in Ban Nam Khem, the extent of the impervious surface measured in February-2009 was compared to 1,742 manually-delineated building points leading to an accuracy of 83%. The building points were assumed to accurately represent the *impervious surface class* as they were manually placed in the centre of each building in Ban Nam Khem. Most of the confusion was with bare ground due to their spectral similarity, with 11.5 % of the building points incorrectly classified as bare ground. Impervious surfaces were particularly conspicuous immediately after they were constructed which reduced these types of confusions. However, with time the roofs weathered and became less spectrally prominent by blending with the surrounding bare ground.

The semi-automatic method was a lot less time-consuming than manually delineating individual building points and can be applied quickly across a large geographical extent. Selecting suitable training pixels in the image and applying the classification took approximately 1–2 hours per image while manual delineation took 1-2 days. Manual analysis is a more appropriate method if the user requires a database

of points or polygons representing individual building locations and plots. The user may choose the most appropriate method of analysis based on resources available to them and their data requirements. Alternatively, the two methods may be used to complement each other in the same workflow. For example, the supervised classification method may first be used to identify 'areas of interest' (e.g. areas of significant building removal or building construction), which may then be analysed in more detail at a per-building scale using the manual delineation of satellite images and/or ground survey techniques.

Figure 3-28 compares the number of buildings in Ban Nam Khem and Chella Bandi over time after the two disasters. The results show that the reconstruction of buildings was much faster in Ban Nam Khem than Chella Bandi - the number of buildings plateaus after one year in Ban Nam Khem and after three years in Chella Bandi. Ban Nam Khem saw a quick response because the scale of the disaster was relatively small and the Thai government were prepared strategically and financially to reconstruct rapidly. Despite the fast speed of reconstruction the household survey identified much discontent with the quality of the houses. In Chella Bandi, reconstruction was slow to begin with as attention was focussed on providing shelter before the on-coming winter. Pakistan used an owner-driven approach and it also took time to train households appropriate construction techniques and to supply appropriate materials. The situation in Chella Bandi was further complicated as it is located in a high-risk zone so households were initially prevented from constructing there. Many people moved to Chella Bandi from the surrounding mountains which led to a dramatic increase in the number of buildings there.

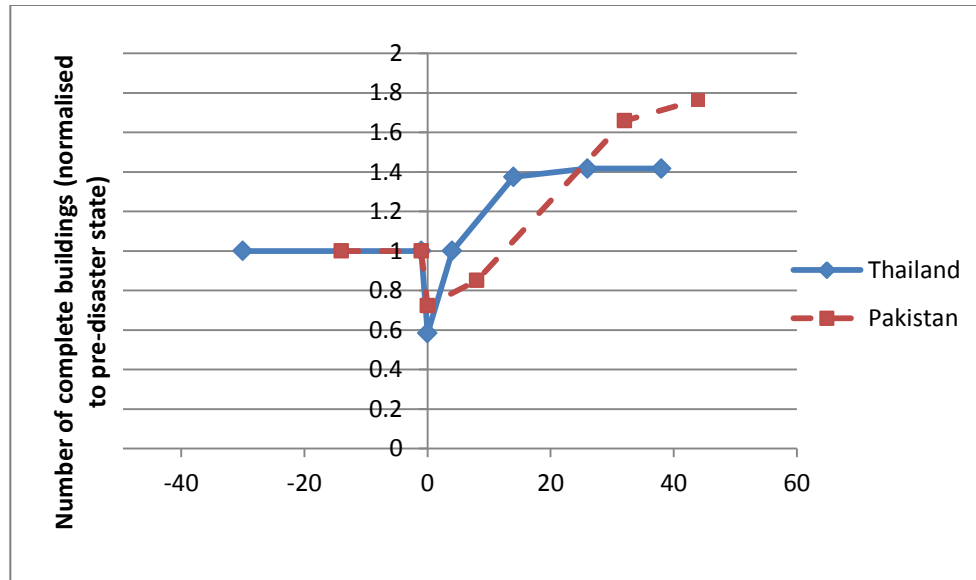


Figure 3-28: Number of buildings in Ban Nan Khem and Chella Bandi.

#### Indicator 6. Change in Urban Layout and Morphology

##### Remote Sensing Methodology

This indicator analyses groups of buildings to monitor spatial-temporal changes to the urban form and morphology of a disaster-affected region. Building density and urban morphology are important issues in urban planning and land management. Densely-built areas may be difficult to redevelop and are commonly associated with smaller dwellings and a lack of green space. A densely-built urban area may also have less space and light, and increased disturbance from neighbouring households. The change in building density may therefore be monitored along with other aspects of the physical environment to indicate a change in people's quality of life (Jackson, 2003). Two methods of quantitatively analysing the built environment are proposed: first, density and nearest neighbour statistics are calculated using the building point database developed in the previous step; second, landscape metrics are applied to manually-delineated polygon datasets representing building perimeters in a subset of Ban Nam Khem.

*Method 1: Density and Nearest Neighbour Statistics*

The building points counted in the June-2002 and February-2009 images were mapped independently and analysed for their density. Building density maps were produced by applying *kernel analysis* to the building point database using ArcGIS. A kernel was passed across the scene one pixel at a time and the number of building-points within the kernel was counted. The pixel at the centre of the kernel was then assigned a building density. The average building dimensions in Ban Nam Khem were used to select appropriate kernel parameters. A kernel width of 30.0 m allowed the kernel to encompass several buildings simultaneously and an output cell size of 10.0 m produced appropriately detailed building density maps. Nearest neighbour is another *Spatial Analyst* tool available in most GIS software and can be used to measure the distance between each building-point, producing a range of outputs in metres. The most complex is a  $N \times N$  distance Matrix showing the distance between every point in the database, but for this purpose, a summary of the distance statistics was sufficient.

*Method 2: Landscape Metrics*

Landscape Metrics are a set of spatial statistics that allow maps to be quantitatively described and compared. They are produced by analysing a series of 'patches' using patch analyst software such as FRAGSTATS (McGarigal & Marks, 1994). A patch corresponds to a polygon or an individual unit on a map. The method was initially developed for ecological applications to quantify landscape patterns, but the method has been adopted and applied here to building footprints and urban maps. This approach may therefore be used to quantify changes to the total built-up area, and to monitor the average building density, shape and size.

The input to the analysis was a binary vector map containing two categories: 1. Buildings and 2. Non-Buildings. The reliability of the Landscape Metrics was dependent upon the accuracy of this vector dataset, so the building-outlines were manually digitised to ensure the highest possible reliability. The Landscape Metrics were applied to a 250 x 250 m subset; the size of the area was selected so that it covered several blocks of buildings and therefore provided an effective overview of that particular area. In total, 20 Landscape Metrics were produced, but it soon became apparent that much of the data produced was redundant. A multivariate factor analysis by Ritters (1999) similarly found that 26 metrics used to measure land use and land cover had six common and orthogonal factors or dimensions that

explained 87% of the variation. For the purpose of this study, 8 indices were selected and grouped into four categories that described different aspects of the built environment’s form and morphology (as shown in table 3-4).

Category	Landscape Metric	Description
<b>Total Building Extent</b>	Class Area (CA)	The total building area.
	Number of Patches (NUMP)	The total number of buildings.
<b>Building Shape</b>	Mean Shape Index (MSI)	The sum of building perimeter divided by the square root of building area, adjusted against a standard square, divided by the number of patches ( <i>NP</i> ) (measures the complexity of average patch shape in the landscape compared to a standard shape).
	Mean Perimeter-Area Ratio (MPAR)	Sum of each patch perimeter/area ratio divided by the number of patches (measures ‘shape complexity’ – amount of edge per area).
<b>Building Size</b>	Mean Patch Size (MPS)	The average building size.
	Mean Patch Edge (MPE)	The average building perimeter.
<b>Building Density</b>	Mean Nearest Neighbour (MNN)	The average distance to the neighbouring building.
	Patch Density (PD)	Building Density.

**Table 3-4: Landscape Metrics from McGarigal & Marks (1994) applied to building polygon maps.**

## Results

Analysis of the building-point database created for Indicator 5 (*removal and construction of building*) identified building-plots that were not rebuilt after the tsunami and building developments that were constructed on new plots. All of these physical changes led to significant transformation in the morphology and layout of the village. Across Ban Nam Khem the mean nearest neighbour statistic fell by 1.3 m and the minimum nearest neighbour dropped from 3.6 m to 0.6 m, suggesting that a lot of the buildings had been built back closer together. Figure 3-29 presents building density maps in June-2002 and February-2009 and a change detection image showing change in density between these dates.

There was an increase in building density throughout most of the army-built developments. Some of the areas near to the coast experienced a decrease in building density. Areas on the coastline that were already well-established though tended to increase in density.

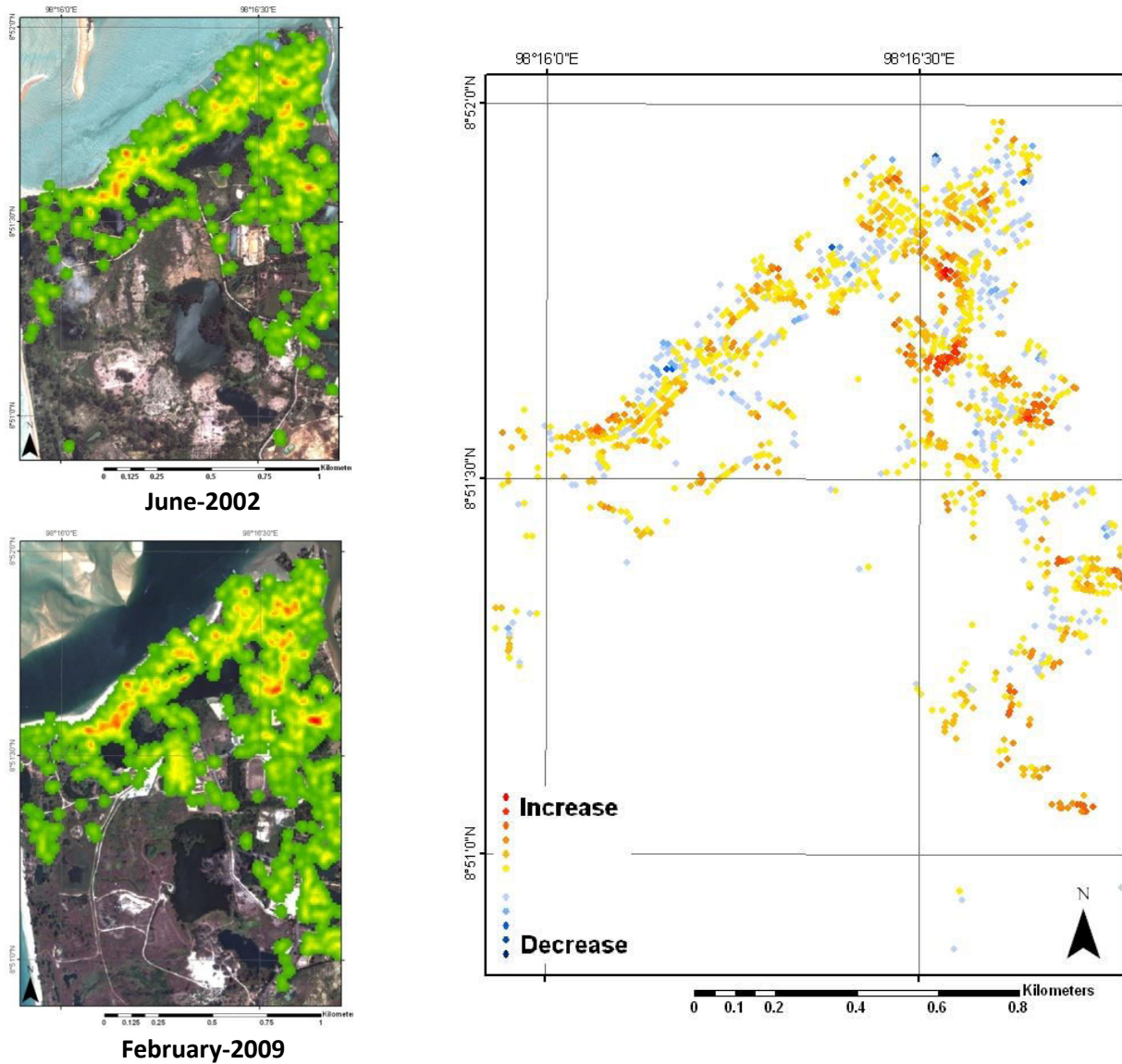
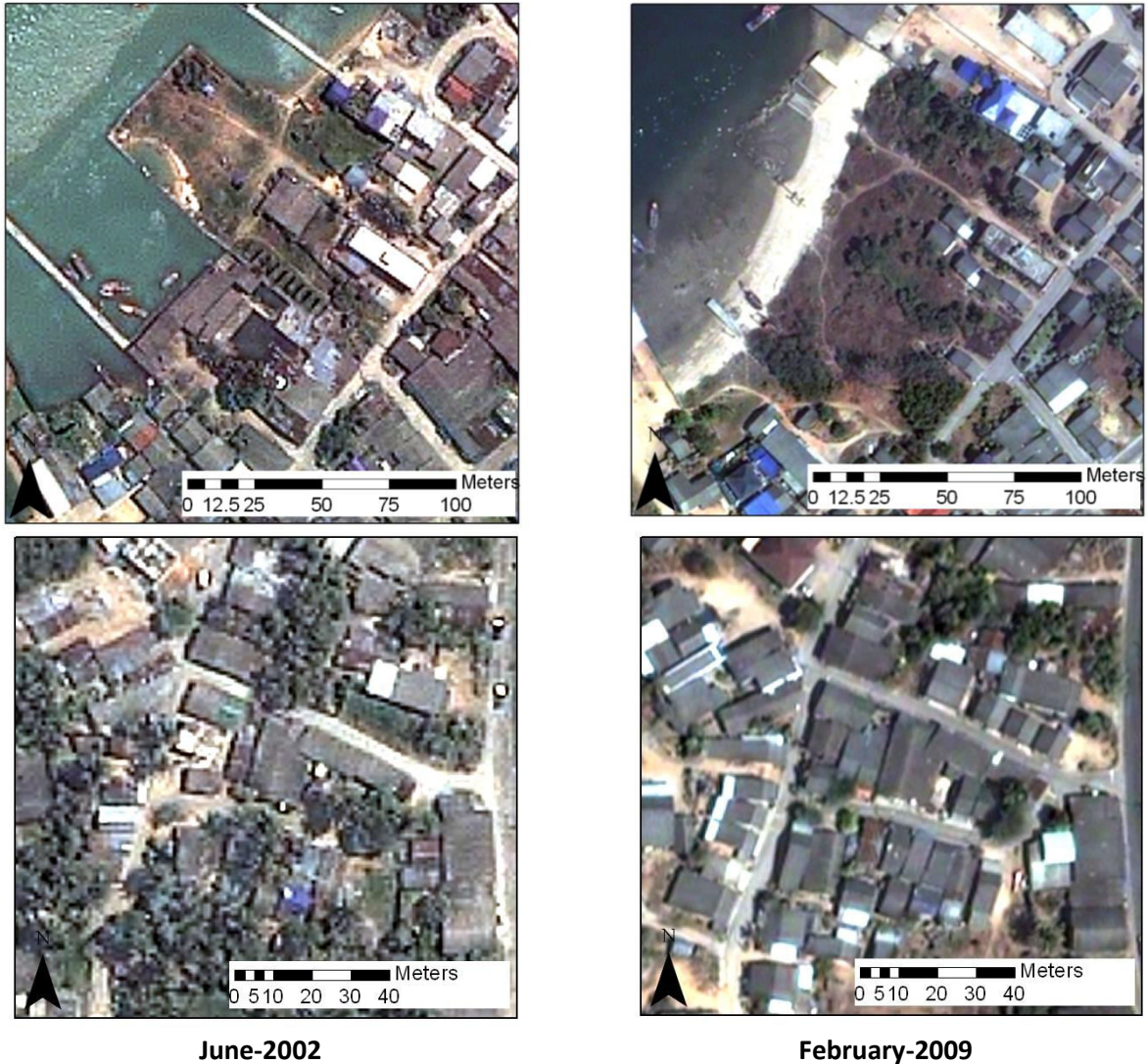


Figure 3-29: Building density maps (left) and building density change between 2002 and 2009 (right).



**Figure 3-30: Some areas near to the coast experienced a decrease in building density (top row), while some army-built areas saw an increase in building density (bottom row).**

### *Landscape Metrics*

To explore change to building morphology in more detail, landscape metrics were applied to building polygons in a 250 m subset in the centre of Ban Nam Khem.

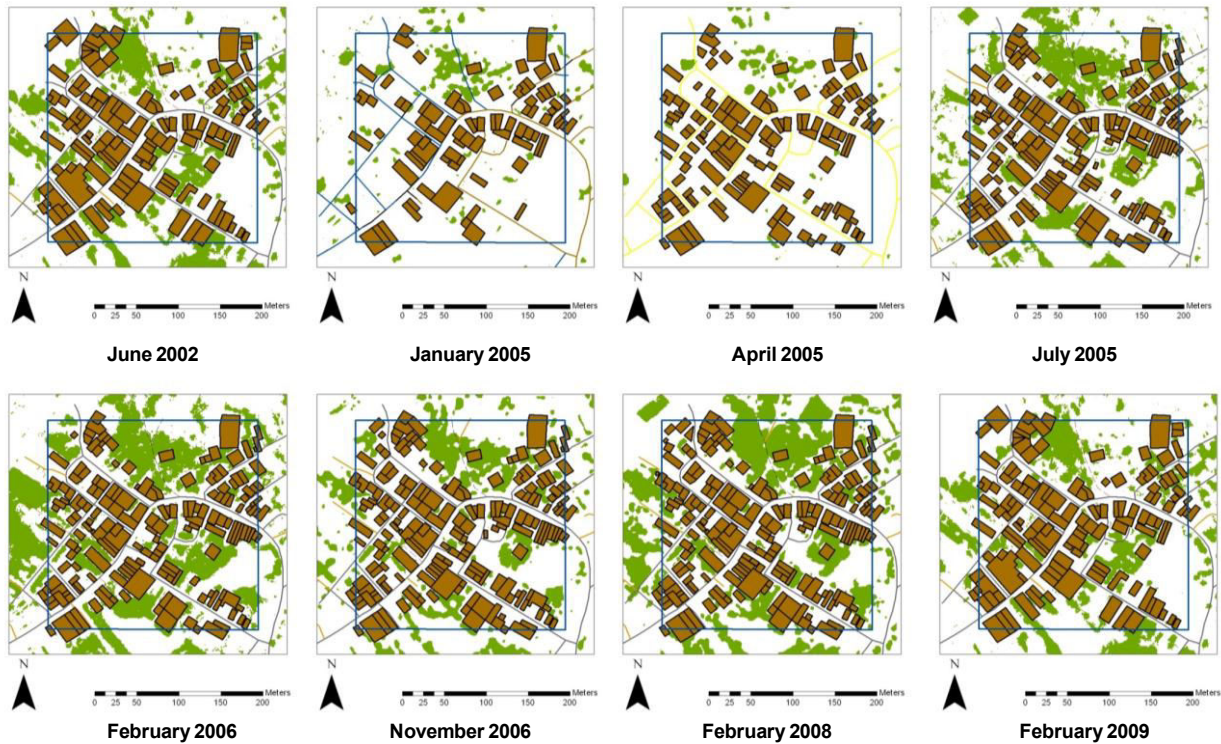


**Figure 3-31: Landscape metrics were applied to building footprints delineated in a 250 m subset in the centre of Ban Nam Khem.**

The results show that the total number of buildings in this subset increased by 46%, but that the total building-area returned to a similar level present before the tsunami. This resulted in a higher density of buildings and a lower mean nearest neighbour. Average building size and building perimeter also decreased, and the perimeter-area ratio increased suggesting more complex building shape (possibly due to increased fragmentation – more buildings of a smaller size). Meanwhile, the Mean Shape Index (MSI) decreased slightly, suggesting less diversity in shape across the subset.

### Discussion

This indicator is used to monitor changes to the urban layout and morphology of a disaster-affected region. Building density maps and nearest neighbour statistics are applied to groups of buildings to describe the distance between buildings, whilst landscape metrics are used to quantify changes to the total built-up area and to monitor the average density, size and shape of the buildings. Urban design affects a building's light, noise and comfort levels, and the layout and morphology of the built

environment can affect an area's overall attractiveness and vibrancy, so these methods may be used as proxies for monitoring living conditions throughout the recovery process.

The creation of building density maps and nearest neighbour statistics both require the building points database created for Indicator 5 (*removal and construction of buildings*). The points database was created by manually delineating individual buildings and so took 1-2 days to create. If the building points are already available though, the building density maps and nearest neighbour statistics may be produced in an hour or so and applied quickly across the whole region. The maps and statistics produced from this method give a synoptic view of the changes to the built environment throughout the recovery process. They may be particularly useful to highlight clusters of density change that might require more detailed ground examination.

The Landscape Metrics method created detailed statistics on the total built-up area, and the average density, size and shape of the reconstructed buildings. Building design is likely to have a significant effect on the occupant's life and their overall perception of recovery. Pivot-table analysis of the results from the household survey suggest that *building size* might be a particularly important factor in determining whether the respondents believed their house was better or worse than before a disaster. The Landscape Metrics method may therefore be used to collect important data on the dimensions of the reconstructed buildings, which may also be used as proxies for monitoring living conditions.

## **Indicator 7. Quality of Dwelling Reconstruction**

### **Remote Sensing Methodology**

High-spatial-resolution satellite images contain a large amount of information about the buildings and the landscape surrounding them. Image analysts may utilize colour, texture, shape, size, orientation, pattern, shadow, site and situation of objects (Jensen, 1996). In a recovery context, this information may be used to determine the rate and pattern of reconstruction and to describe changes in the building-design and the context in which the buildings are situated. This assessment of buildings and reconstruction will focus on four elements: *structural attributes, stage of development, location and spatial context*. These may be analysed individually or collectively.

*Structural attributes:* Information about the structures may be obtained by delineating the buildings' footprint and monitoring changes within the boundary of the building. The size, shape and orientation of the buildings may be established, as well as the roof-colour and roof material. In addition, any modifications or extensions to the building may also be identified. A post-reconstruction environment is often quite sterile due to the standard building designs used and the loss of historic designs, it is therefore very common for households to personalise their properties with decoration or building modifications.

*Stage of Development:* The progress of the construction process at each plot may be determined by monitoring the construction process and by identifying the clearance of land and the construction of foundations. A 6-stage development cycle was created, which can be analysed using high-spatial-resolution satellite imagery with a ground sampled distance of 1.0 m. The development cycle includes a stage where buildings have been seriously damaged and five subsequent stages of construction in chronological order from cleared land (0) to buildings with modifications (4) (see figure 3-32).



**Figure 3-32: Different Stages of the building development cycle observed at different sites across Ban Nam Khem**

*Location:* each building has a unique geographic location which may be mapped using its latitude and longitude. The location of the building is important for various reasons. It affects the environment in which the building is present (e.g. rural, suburban or urban), which ultimately determines its proximity to services, facilities and livelihoods. It also affects its proximity to nuisances and hazards such as busy roads and flood plains. Relocation can divide once strong communities, breaking social bonds and contributing to long-term psycho-social issues. It is therefore important to monitor the relocation of households following a disaster. This may be achieved by monitoring the location of new developments, rebuilds and the location of vacant sites. The position of the building relative to the surrounding facilities and services may be analysed by assessing travelling times, as shown in the Accessibility section.

*Building context:* the state of the built and natural environment immediately surrounding a residential property may also have a large part to play in the household's quality of life (Lo and Faber, 1997). In

particular, the analyst should note the dominant land cover and the morphology of the urban form in which the building is located. In this study this is achieved by semi-automatically extracting the building density, nearest neighbour and vegetation density within a 50 m buffer of each structure. The quality and type of road structure within each buffer is also extracted using a similar semi-automated technique to analyse issues of accessibility. Information about the affluence of a neighbourhood may also be inferred by observing the presence or absence of key features near-by such as: driveways, car parks, crops, external buildings and swimming pools.

### *Analysis of 50 Buildings*

As a proof of concept, the analysis was applied to 50 buildings across Ban Nam Khem which were selected using a random geographic sampling method. The sample included all possible building-types, locations and different levels of damage and loss, and was non-stratified to avoid introducing bias. The sample therefore included government and agency-supplied buildings in the centre and outside of Ban Nam Khem. The occupants of these buildings were also interviewed using the household survey to verify the remote sensing analysis.

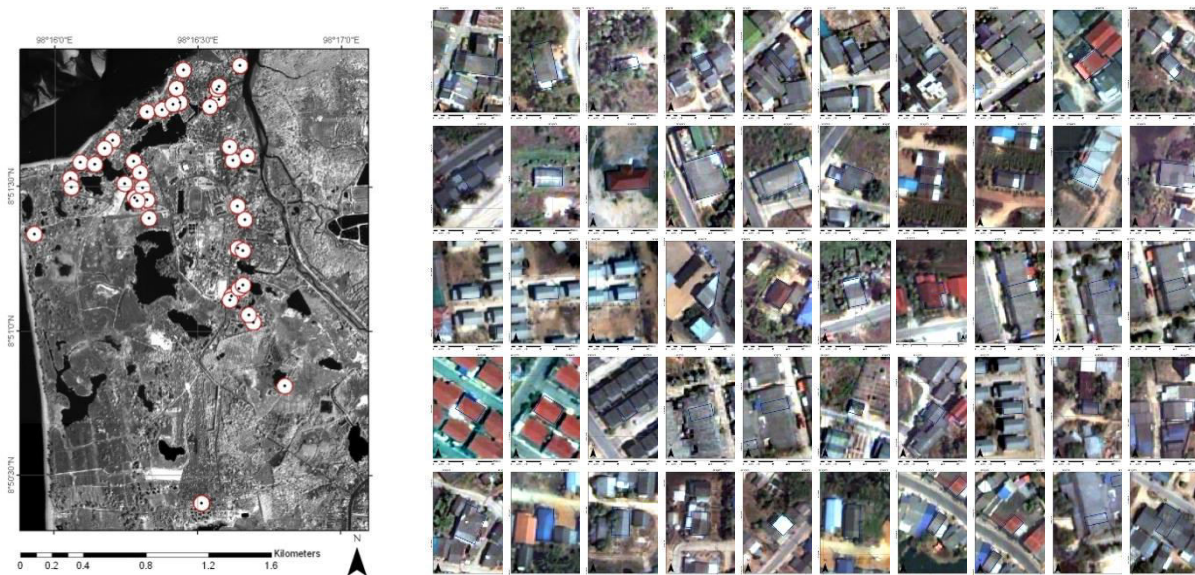


**Figure 3-33: Fifty households were analysed in detail across Ban Nam Khem using remote sensing and the household survey.**

The results of the remote sensing analysis are summarised below:

**Structural attributes:** The average size of the building sample before the tsunami was 98 m<sup>2</sup> (st dev: 63.0 m<sup>2</sup>). After the reconstruction process, in February-2009, it had increased by 18 m<sup>2</sup> to 116 m<sup>2</sup> (st dev: 58.1 m<sup>2</sup>). Of the 15 buildings that were rebuilt, nine were bigger than they were before the tsunami, four the same size; only two were smaller. However, these findings are sensitive to the sample selected. An analysis of a 250 m square subset in the centre of Ban Nam Khem suggested that the average size of residential and non-residential buildings had decreased by 52 m<sup>2</sup>, but that the number of buildings in the same area had increased.

The proportion of buildings with driveways, gardens and extensions increased after recovery, but these features were almost exclusively associated with agency-built structures. Many of the agency structures were also built with 2-storeys compared to the single-storey government-provided structures. These differences led to disparity across Ban Nam Khem with some groups perceived to have benefited more than others which has led to discontent amongst some residents.

The proportion of detached buildings also increased from 58% to 72% because the building designs used by the government were predominantly detached. This might have contributed to greater privacy despite the overall increase in building density.

	Pre-disaster %	Post-disaster %
<b>Detached &amp; Semi-detached</b>	58	72
<b>Grey-tile roofs</b>	92	84
<b>2-storey</b>	0	14
<b>Single-storey</b>	100	86
<b>Driveway</b>	8	34
<b>Garden</b>	0	16

**Table 3-5: Changes in building structure and associated features in Ban Nam Khem.**

Of the 50 sampled houses, half of them had modified or extended their property in some way. 17 households appeared to have built the extensions themselves, 13 of which were in the form of a corrugated-iron overhang to the side of the building built to provide additional cover from the rain and the sun. Eight other extensions were built by Worldvision between November 2006 and February 2008.

They were identifiable in the satellite imagery because of their uniform shape (rectangular) and spatial context (in residential areas, attached to government-built housing) and brighter reflectance than the building to which they were attached.



**Homemade Extension**



**Worldvision Extension**

**Figure 3-34: Building extensions were common features in the post-construction landscape.**

*Stage of Development:* Most of the sampled houses (78%) were constructed within 1 year of the tsunami. This is due to the army's quick deployment and construction approach. The ITV housing, outside of Ban Nam Khem, was also constructed quickly with many structures completed by April-2005. The other agency-built developments, however, took longer with some developments such as the Phase 2 housing not commencing until 2 years after the disaster, presumably because it took time to find and purchase appropriate land for construction and to raise the required capital. Army-built homes were constructed within 7 months of the tsunami while agency-built homes were built 3 to 4 years after the tsunami. Figure 3-35 shows the proportion of buildings at each stage of development throughout the recovery process.

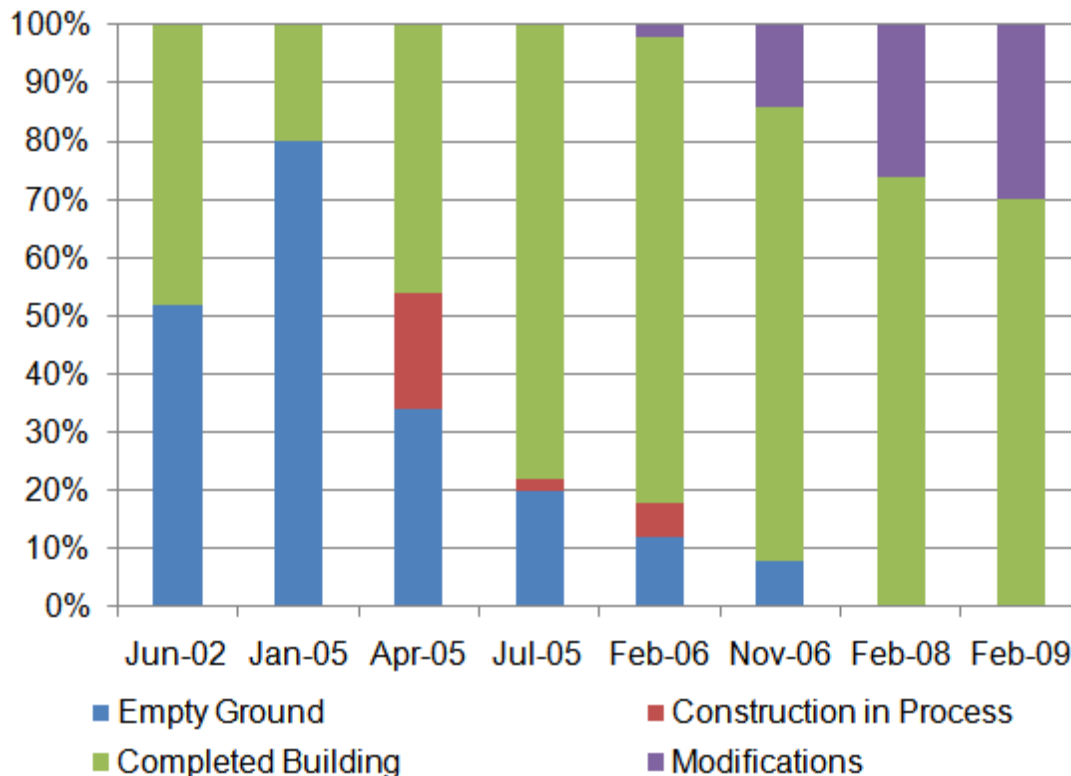


**Figure 3-35: Proportion of buildings at different stages of development throughout the recovery process.**

*Location:* As covered in the *Accessibility* section, the army-built government housing was rebuilt on their original plots, and therefore maintained close proximity to the services and facilities in the centre of Ban Nam Khem, while the agency-structures were built predominantly outside of Ban Nam Khem, leading to significant changes to the lifestyle of a household. However, the vulnerability to future tsunamis has been significantly reduced by living further from the coast and the construction of two-storeys. It remains to be seen if the households remain in the new location in the long run.

### Discussion

This analysis has demonstrated that the detailed information available in satellite imagery throughout the recovery process may be used to quantitatively monitor reconstruction so that the work of the executing agencies may be identified on a map, monitored, evaluated and recorded. The attributes measured by this analysis can be used to describe the building and its location, the speed of construction and the state of the surrounding natural and built environment becoming the new baseline

for future urban planning. Although more work is required to determine how these elements contribute to levels of household contentment, the findings from the household survey suggests that the size of the building, access to facilities and services, the distance to potential hazards and the time taken to reconstruct the building are highly significant.

The household survey obtained information about changes to the socio-economic and demographic make-up of the households. Key information about their registration status and land entitlement was also established. In addition, it was used to produce a recovery narrative describing when key events happened and to infer their perception of recovery by identifying any problems residents faced and how the process of recovery could have been improved. Important information was also obtained about the households' source of livelihood and any support they received, and it highlighted problems with the provision of utilities that were unobservable with remote sensing. In hindsight, there were several important aspects of recovery that were missed from the survey; these include the security of the households, their experience of crime throughout the recovery process and their participation in the community.

The household survey results show that both the size and the location of the buildings (e.g. proximity to fishing facilities) were important factors in the households' perception of recovery. Both of these attributes were objectively measured in satellite imagery in a quantitative manner. In fact, remote sensing was able to quantify changes to the proximity and connectivity of households in both Ban Nam Khem and Chella Bandi and households that were relocated elsewhere. Households that had been relocated outside of Ban Nam Khem have generally found it difficult to continue making a living in the fishing industry and felt disconnected from the village. The small size of the building was also a major factor contributing to the households' discontent with the army-constructed buildings. Remote sensing was able to objectively show that an agency structure had a floor space 68% larger than the government-built structure. Both remote sensing and a household survey were used to estimate when the occupants moved into their houses. Households living in agency-provided housing told us that they moved into their homes in December-2008, which matched remote sensing's estimate of a move in date between February 2008 and February-2009. The households in government-housing told us that they moved in July-2006 while remote sensing estimated a move-in date between April-2005 and July-2005. This shows that the occupancy of a building cannot always be confidently determined with satellite imagery alone.

In summary, the household survey was able to capture unique information that was not possible with remote sensing, such as income, source of livelihood, the date water and power supplies were restored, and overall contentment levels with the recovery process. Assumptions could be made about a household's overall contentment with their house and overall perception of recovery based on key measurements made with remote sensing such as the building size, the presence of a garden and its location and connectivity. For example, households living in bigger structures with a porch, garden and driveway were often the most content. Participation of the household in the construction of the house also appears to have been an important factor in ensuring overall contentment. The results from remote sensing may be used to map the unequal allocation of building size and types across Ban Nam Khem. Recommendations may be made to improve future recovery work based on these results. It is important to recognise that good building design does not automatically equate to a good recovery. A full evaluation should also take into account issues such as affordability, environmental performance and the availability of a mix of building typologies.

### **Section 3: Transitional Settlement/Displaced Population**

#### **Literature Search and Household Survey Results**

The tsunami destroyed hundreds of homes instantly making thousands of people homeless. In the first days and weeks, the homeless population resided in tents, underneath canvas and trees and in nearby temples. Within a week, a grouped settlement approach was adopted in Thailand and five planned camps were constructed in Phang Nga province. The largest camp was the Bang Muang refugee camp, which was organised by Community Planning Network leaders, Community Organisation Development Institute (CODI) and NGO workers.



**Figure 3-36: Tents (left) and relief supplies (right) at Bang Muang camp. (Source: Radarheinrich, 2005).**

The construction of the camp began on 29 December and it was opened on 1 January. Within a week, the camp was estimated to be providing shelter to up to 3,000 people (CODI, 2005). The camp contained tents and other essential needs such as toilets, bathing and cooking facilities. Transitional shelters were later constructed in these camps by a number of organisations each with their own designs. Shelters constructed by CODI and the army consisted of rubber-tree pole frames, plywood or fibre-cement panelled walls and corrugated tin-sheet roofs (Kerr, 2005).



**Figure 3-37: Transitional shelters at Bang Muang Camp (left) and emergency shelters donated by the Friend-in-Need foundation (right). Source: Radarheinrich, 2005 (left) and Daniel Brown (right).**

## **Indicator 8. Transitional Settlement**

### **Remote Sensing Methodology**

Remote sensing was used to map emergency and transitional shelter solutions across the affected area. Tents or owner-constructed shelters are often used in the immediate aftermath of a disaster to provide shelter. As the process progresses into early recovery, shelter may be provided in the form of transitional, often pre-fabricated, shelters arranged in planned camps or dispersed throughout the affected area (Corsellis & Vitale, 2005).

Emergency and transitional shelter outlines were manually delineated in each image and where appropriate, the extent of planned camps was also marked allowing the generation of multi-temporal descriptive statistics. The statistics were used to produce a narrative describing the presence and absence of emergency shelter and transitional settlement throughout the recovery process.

Manual analysis of satellite imagery was also used to produce up-to-date maps of the camps, displaying the location of buildings, roads and other major topographic features and land cover. For a more detailed analysis, small internal features such as food and water distribution points were mapped by ground workers and integrated into the database. Proximity analysis was then used to ensure access to key facilities met agreed standards stipulated in the Sphere Guidelines (Sphere Project, 2011) and the UNHCR's Handbook for Emergencies (UNHCR, 2007) as shown in table 3-6.

The *surface area* available per person was also monitored with satellite imagery by estimating the area occupied by the camp and sub-dividing this by the number of people living there. The camp population may be derived from official statistics or estimated using satellite imagery based on the number and size of the structures as in Indicator 9 (*displaced population*). These standards are important to implement to control the spread of disease and to prevent overcrowding (UNHCR, 2007).

Distance in Metres					
	Dwellings to Water (Max)	Water to Latrine (Min)	Shelter to Latrine (Min/Max)	Living Space m <sup>2</sup> per person (Min)	Surface Area m <sup>2</sup> per person (Min)
UNHCR	100	30	30/100	3.5	30
NRC	150	30	30/100		
Sphere	500	30	30/50	4.5	45

**Table 3-6: Recommended camp standards: UNHCR, Sphere Project and Norwegian Refugee Council.**

The attributes and information obtainable with remote sensing to monitor transitional settlements and displaced populations is summarised in table 3-7.

Attribute	Description	Notes
Coordinates	The camp's geographic position (latitude, longitude).	Required to map the distribution of Internally Displaced People (IDP).
Location	A description of the camp's location and the previous function of the buildings and land it is occupying (e.g. school grounds).	To ensure that the camps aren't occupying important public land, such as school grounds, for longer than is necessary.
Size of camp	The length and width of the camp in metres.	Allows the capacity of the camp to be estimated.
Accessibility	The level of accessibility monitored by mapping road access to and within each camp.	Accessibility is crucial for the import of resources and materials. It is also important that the displaced population are kept close to their original home so they may assist with its maintenance and reconstruction.
Number of structures	The total number of buildings within each camp, and the date that they were constructed and dismantled.	The progress of the recovery process may be inferred from the presence and absence of emergency and transitional shelters.
Building Morphology	Statistics describing the size and distribution of structures throughout each camp.	Living standards may be inferred from building size, camp layout and building density statistics.
Proximity Analysis	Analysis of the camp layout and the distance between structures and other features inside the camp.	With the integration of ground data the spatial distribution of shelters and other features such as water-taps, latrines, health facilities and lighting structures may be analysed and compared to agreed standards.
Contents of the camp	Description of other visible features and services within the camp e.g. boat yard, water tower.	Location of services may also be acquired with ground surveys and integrated with remote sensing-derived maps.
Green Spaces	The presence of vegetation (gardens, parks, crop patches) within the camp.	Trees provide shade and pleasant surroundings and crops provide food and an income for inhabitants.
Environmental Impact Assessment	The condition of the site before and after the camp is dismantled by monitoring signs of erosion, the build-up of waste, the return of vegetation and the removal of materials and structures.	The use of semi-automated techniques such as Normalised Difference Vegetation Index (NDVI) and Maximum Likelihood supervised classification for this purpose is described further in the environment section of this chapter.

**Table 3-7: Attributes of transitional settlement that can be monitored using remote sensing.**

## Results

There were four planned camps present within the study area: Ban-Nam-Khem School camp, Ban-Nam-Khem Temple camp, Bang Muang sub-district camp and Pruteow camp. The map in figure 3-38 shows the location of the camps across the area. Both the school camp and the temple camp were located within 2 km of the village, while Bang Muang and Pruteow camps were located 4.5 km and 9.3 km away respectively.

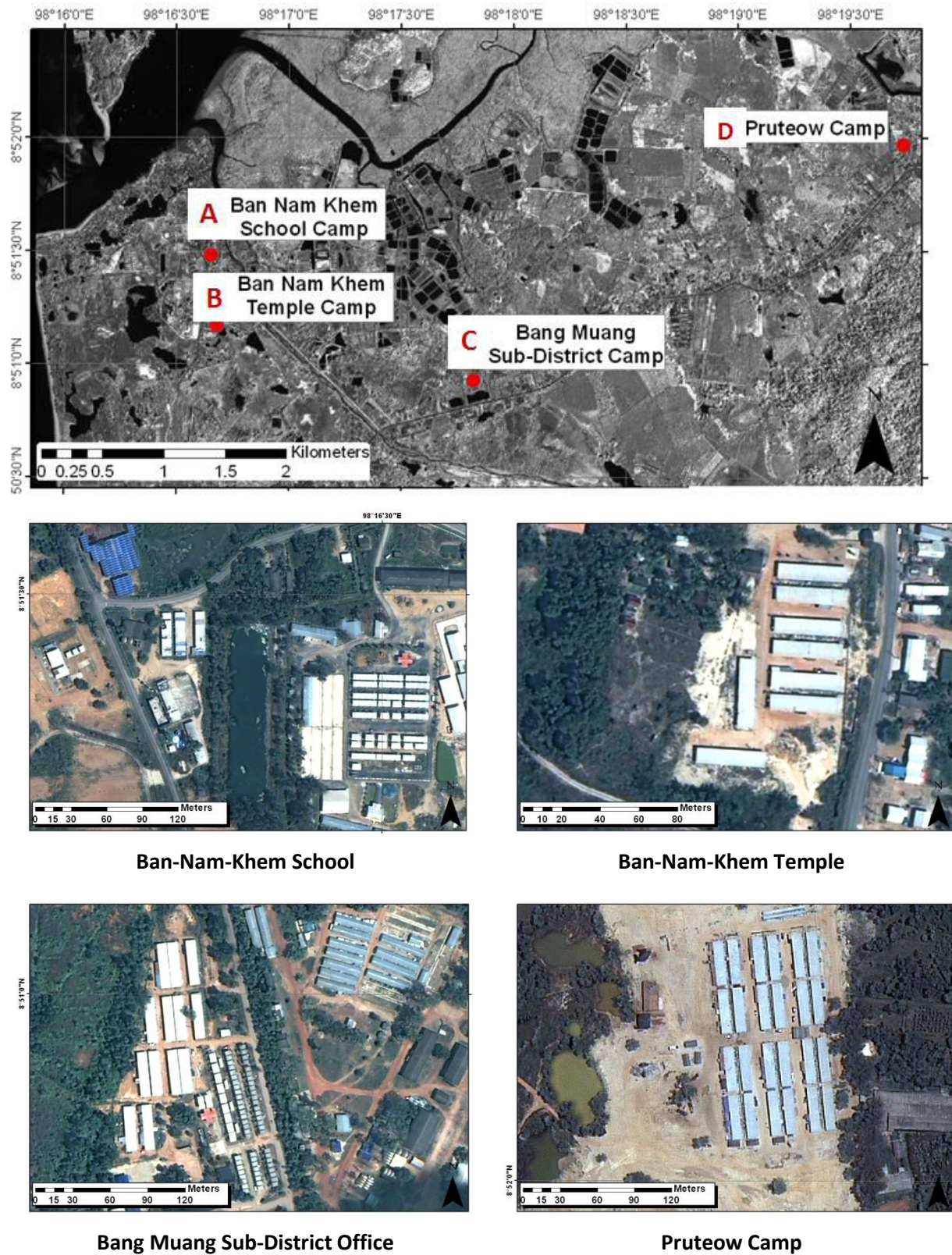


Figure 3-38: Four planned camps in Bang Muang sub-district.

The location, longevity, use and environmental impact of each camp was analysed in detail using remote sensing. Figure 3-39 shows the number of buildings counted at each camp. Ban Nam Khem School and Bang Muang were the largest camps. The buildings at all of the sites were constructed within four months of the tsunami and most were removed within 3 years. A summary of the camp analysis is described below as proof of concept.

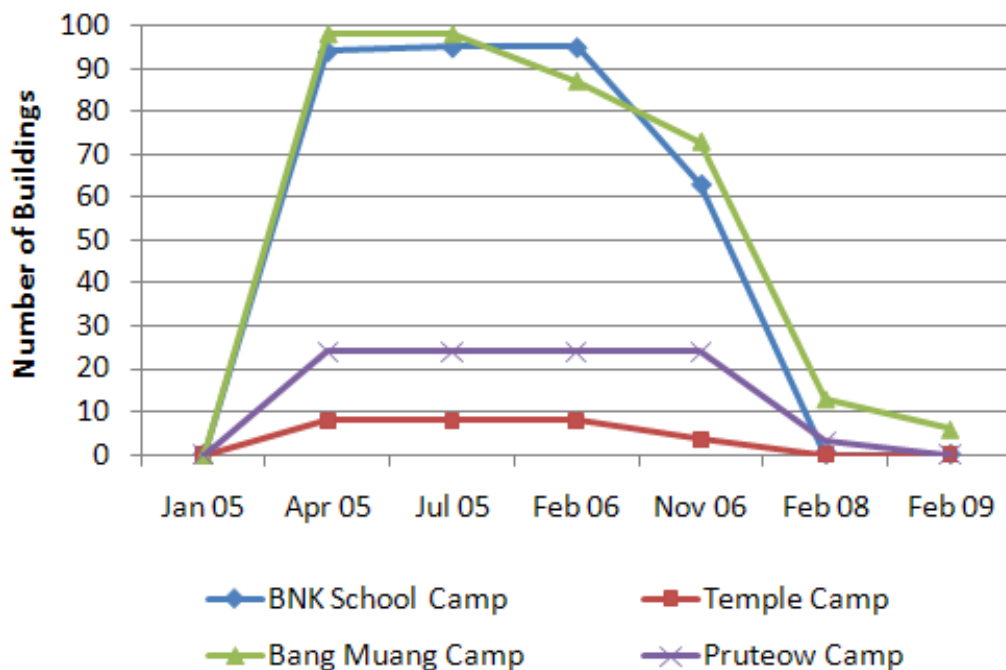


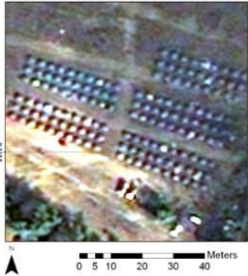
Figure 3-39: The number of buildings present at four planned camps.

#### Location and Accessibility

BNK School camp was erected on playing fields, while the temple camp was contained within the grounds of the local temple and the Bang Muang and Pruteow camps were constructed on land owned by the local administration. All of the camps were located outside of the inundated area. Both the school and temple camps were near to the village and connected by the main road, so were easily accessible. In contrast, Bang Muang and Pruteow camps were situated on the highway to the large town of Takua Pa, so access was difficult for those without a vehicle. Inside the camps, asphalt roads were constructed at the school site to provide accessibility and non-asphalt tracks were provided at the other three sites.

### *Camp Shelters*

A number of organisations constructed transitional shelters at the planned camps resulting in a variety of building designs. Table 3-8 shows information about the different structure-types identifiable in the imagery. The displaced population lived in tents for the first few weeks before being moved to transitional shelters. These shelters were all constructed between January and April-2005, which minimised the amount of time people had to live under canvas. Most of the shelters were dismantled by the end of 2006 which coincided with the completion of the army-built housing in the village.

			
	<b>Tents</b>	<b>Single Dwelling Emergency Shelters</b>	<b>Transitional Shelters</b>
<b>Size (m)</b>	2 x 1.5	4 x 3.5	7 x 35
<b>Area (m<sup>2</sup>)</b>	3	14	245
<b>Height (m)</b>	1.5	4	3
<b>Number of Units</b>	147 (Bang Muang)	50 Bang Muang 64 BNK School	13 Bang Muang 8 BNK School 8 BNK Temple 24 Pruteow
<b>Shape</b>	Square	Square	Rectangular
<b>Roof Colour</b>	Numerous	Grey	Grey
<b>Present</b>	02 January 2005	April 2005 – dismantled in November 2006	April 2005 – February 2006
<b>Provided By</b>	Government	Friends in Need Foundation	World Vision, CODI and the Army

**Table 3-8: Tents and transitional shelters used at planned camps in Phang Nga Province.**

#### *Building-Use*

Ban-Nam-Khem school and Bang Muang were both large camps hosting aid-agencies and other services. Figures 3-40 and 3-41 show detailed maps of the two camps. At the school site, a boat yard was erected between July-2005 and February-2006. A small administration office was also located at the entrance to the camp and the living quarters were divided into two sections: those provided by World Vision and

those provided by the Friends in Need foundation. At the Bang Muang camp, service buildings hosting nursery and medical services were located near to the entrance and transitional shelters were arranged at the back.

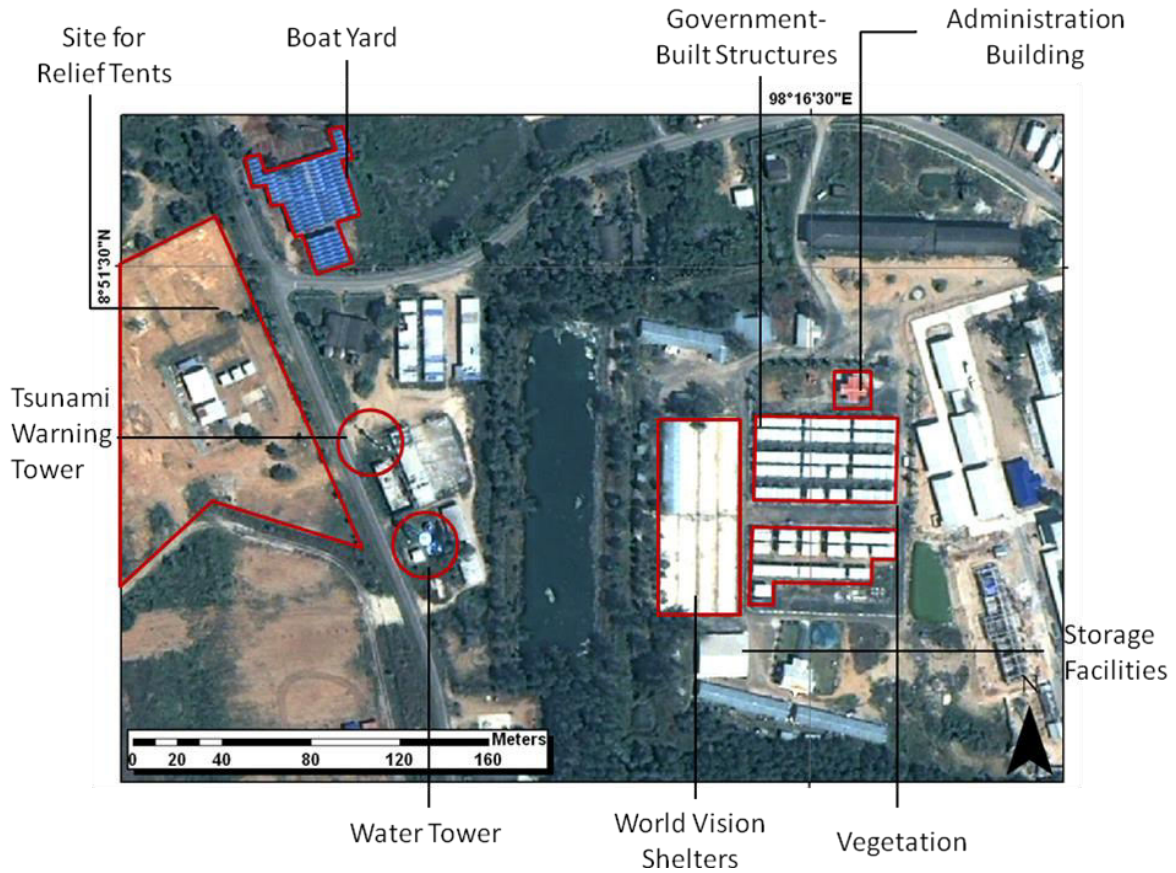
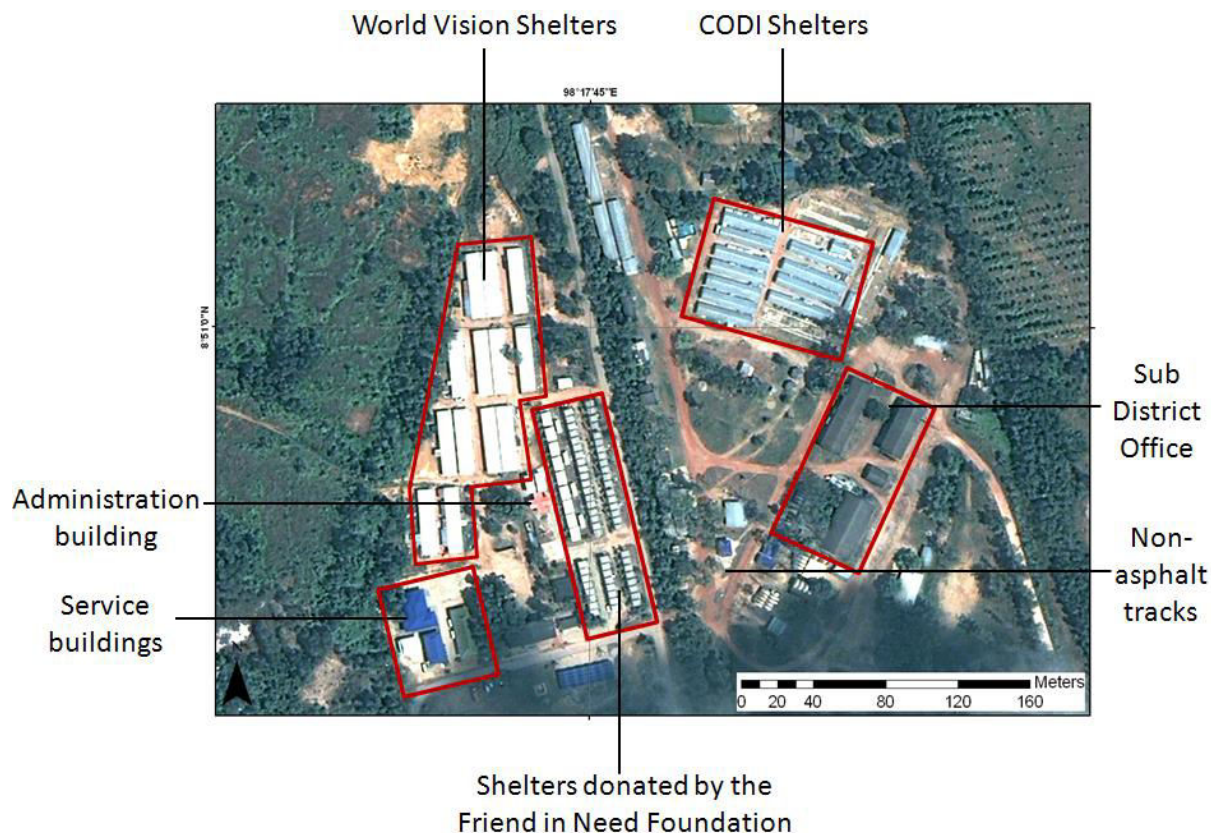


Figure 3-40: Layout of the BNK School camp mapped using information from both remote sensing and local officials.



**Figure 3-41: Layout of the Bang Muang camp mapped using information from both remote sensing and local officials.**

### *Camp Layout*

The school camp measured 50,000 m<sup>2</sup> and contained approximately 95 structures. The number and size of the transitional shelters was used to estimate a population of 720 people, which corresponded well to official data. The camp therefore provided a surface area of 69 m<sup>2</sup> per person, which is over 50% higher than the UNHCR's recommendation. The UNHCR recommends a surface area of 45 m<sup>2</sup> per person to allow space for roads, essential services and administration buildings (UNHCR, 2007). The site could therefore have held up to 1,111 people.

The camps in general are compact, minimising walking distances and appear to be contained within a barrier to reduce potential security risks. All kitchen and sanitation facilities are assumed to be within the main part of the camp, so are no more than 60 m from the residential quarters; other facilities, such as the boat-yard are no more than 200 m away. Figure 3-42 shows camp measurements made using

satellite imagery. The measurement of structure-size using Worldview-2 imagery is validated as part of the work with the Red Cross presented in Chapter 4.

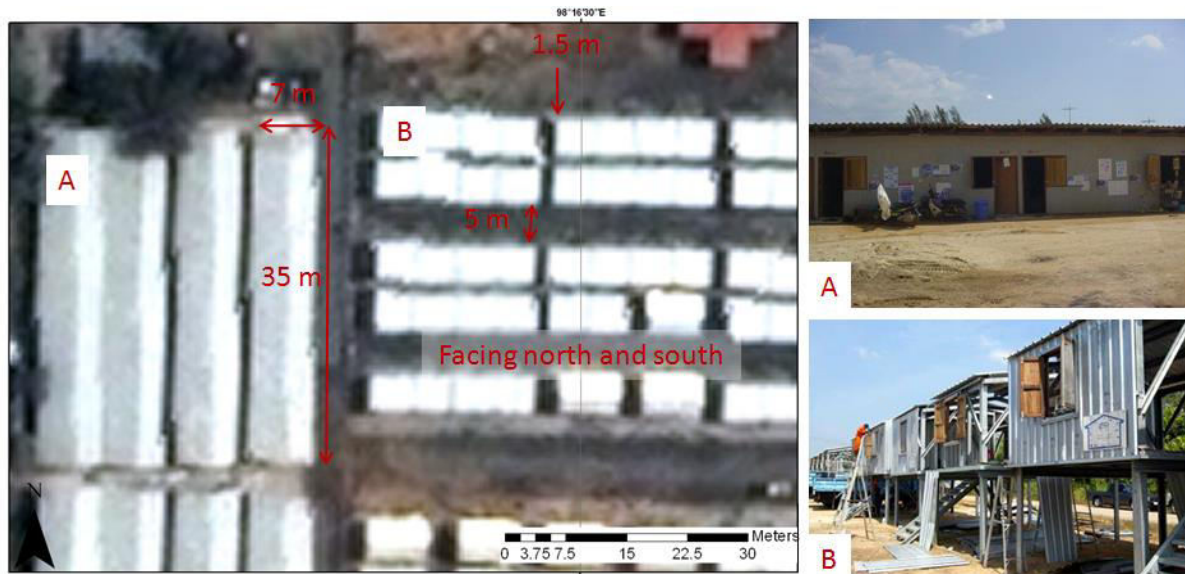
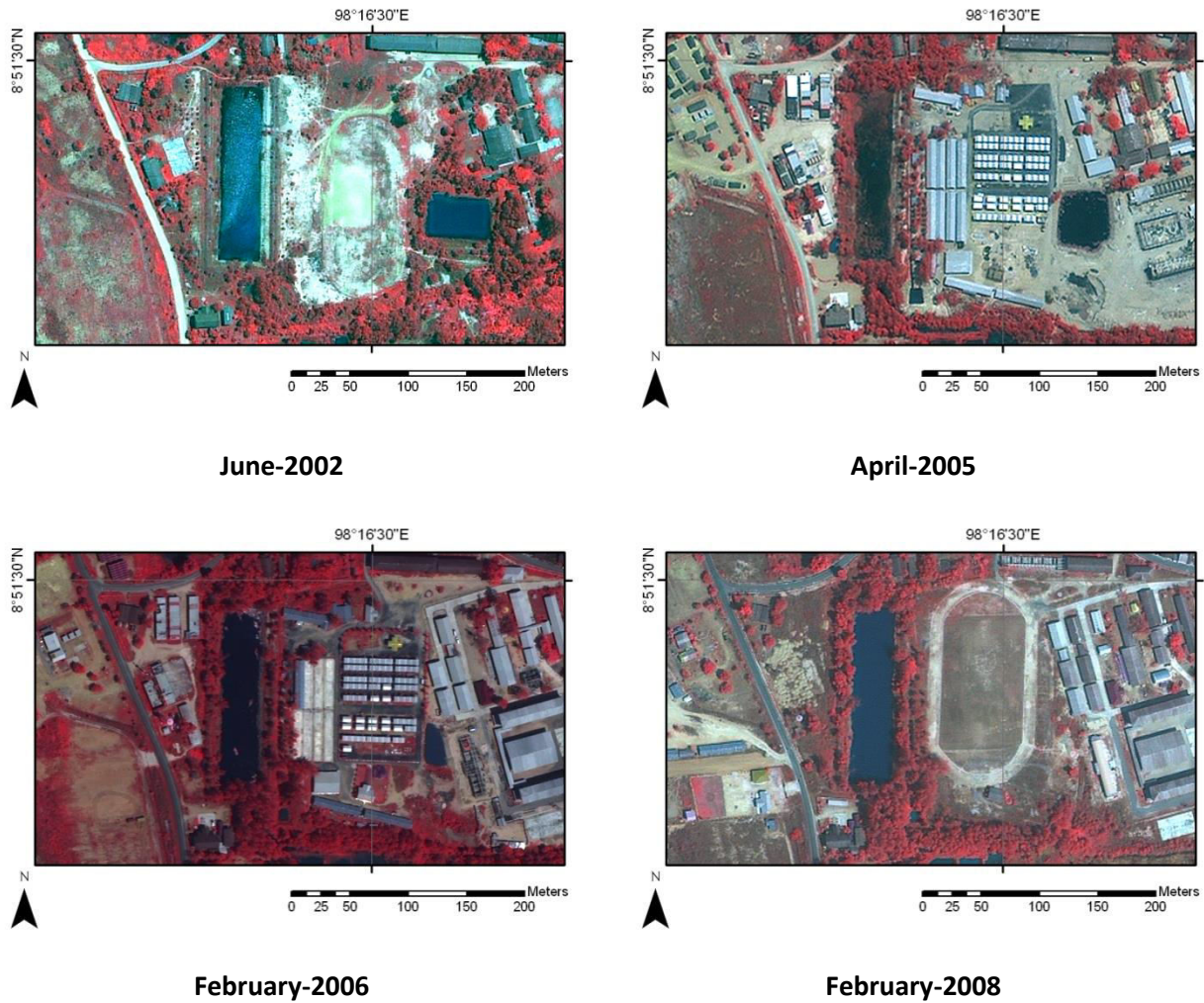


Figure 3-42: Shelter dimensions and layout measured in satellite imagery.

#### *Environmental Assessment*

Vegetation and lines of trees can be seen within the camps, which would have helped to provide a more pleasant, natural environment and could have provided natural shelter from the elements for inhabitants. By February-2008, the school site was restored to its former function as a playing field. All materials and structures were removed and the vegetation remained intact in the surrounding area. Vegetation also began returning where structures once stood. Figure 3-43 shows near-infrared false-colour-composite maps of the camp between 2002 and 2008, with vegetation highlighted in red. The use of Normalised Difference Vegetation Index and supervised classification to monitor land cover change in- and out-side camps is discussed further in the environment section of this chapter.



**Figure 3-43: Near-infrared false-colour-composite images showing removal of transitional shelters and restoration of playing field at Ban-Nam-Khem School Camp.**

### Discussion

Remote sensing was used to identify and map the physical attributes of the camps, such as the number of buildings and their spatial dimensions, and a description of the camps was derived by measuring attributes such as building density, surface area per person and the availability of green space. This data can act as important proxies for living standards, information that is not always easily available from agencies. Remote sensing can therefore provide an independent assessment of the camp size and its contents. However, it cannot always distinguish the occupancy or use of each structure.

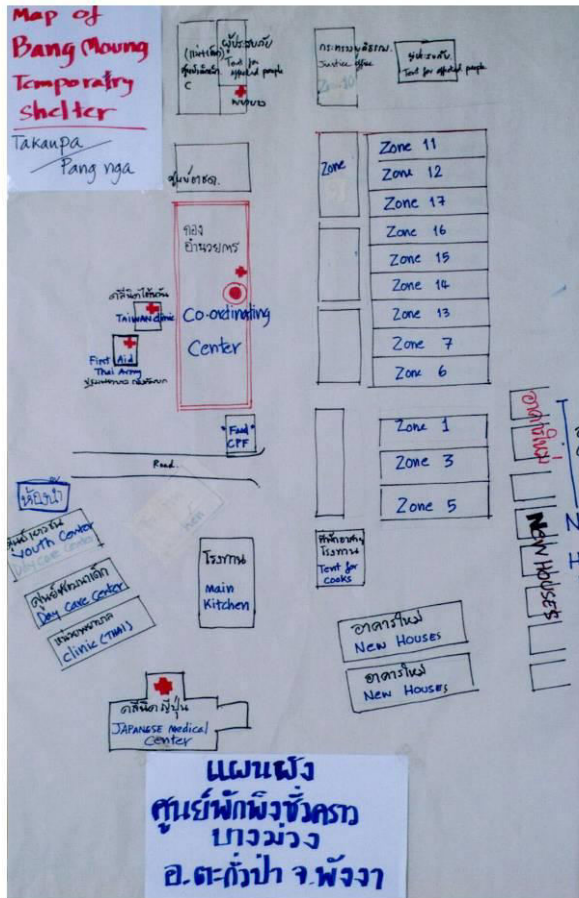
Table 3-9 presents a summary of the results obtained for the Bang Muang Camp by remote sensing and compares them to statistics published by various sources. Remote sensing provides a highly reliable source of data for the description of structural and environmental changes within a camp. The existence of the Bang Muang camp was identified within a day of its official opening date. Remote sensing also identified the same number of tents at the camp as reported in the official statistics and underestimated the number of transitional shelters by only 6%.

	<b>Official Statistics</b>	<b>Remote Sensing</b>	<b>Error</b>
<b>Camp Size</b>	112,000 m <sup>2</sup> (CODI Survey)	135,000 m <sup>2</sup> (300 m x 450 m)	+ 20.5 %
<b>Date Opened</b>	1 January 2005 (300 people registered on the first day) (CODI Survey)	On 2 January 2005, there was evidence to suggest the presence of a camp: 3 large tents and 6 lorries were present and 150 small tents had been erected.	+ 1 day
<b>Tents</b>	500 tents (BNK book)	500 tents	0 %
<b>Small Shelters</b>	80 (Kamsaen, 2005)	75	- 6.3 %
<b>Shelter Dimension</b>	3.5 x 5 m (Kamsaen, 2005)	3.5 x 5 m	0 %
<b>Shelter Material</b>	Transitional shelters were built in long rows with rubber tree pole frames, plywood or fibre-cement panelled walls, corrugated tin sheet roofs and windows of hinged plywood panels (Kerr, 2005).	Buildings in long rows with corrugated roofs.	Building morphology and roof material correctly identified, but a detailed description of building type and quality must be obtained from ground survey work.

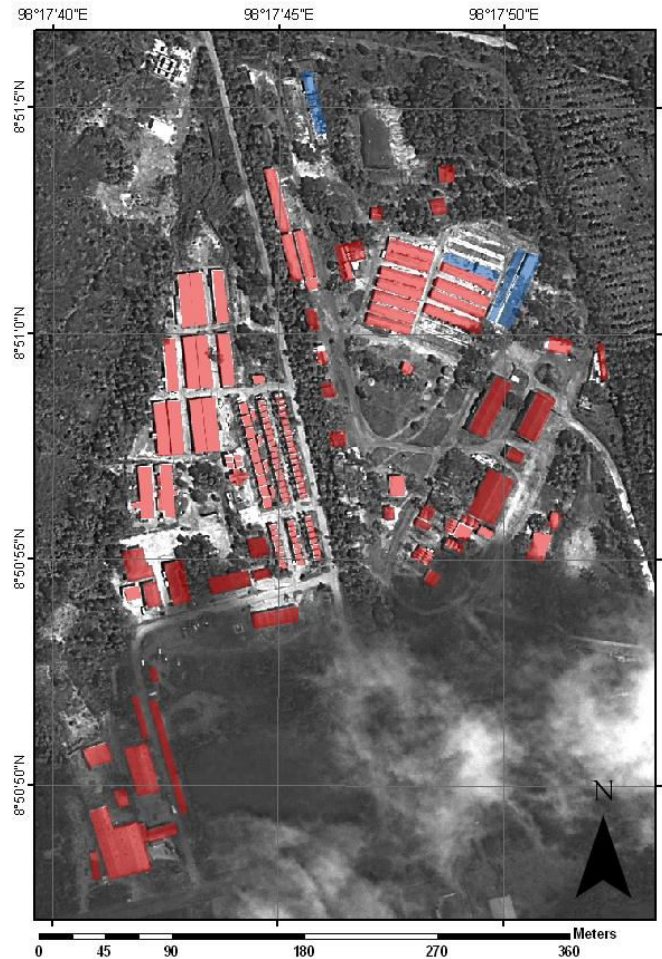
**Table 3-9: Accuracy of remote sensing compared to official statistics for Bang Muang Camp.**

Although the number of buildings in planned camps can be identified with some confidence using remote sensing, establishing building-use with remote sensing alone is more error prone. For example, what seemed like a communications tower and satellite dish were actually a tsunami warning tower and a water tower respectively. Figure 3-44 compares a hand-drawn map of Bang Muang Camp with a map produced with remote sensing. It shows that the remote sensing image more accurately maps the camps layout but that the hand-drawn map contains information about building-use that cannot be

inferred from the remote sensing map, suggesting that satellite image-derived maps must ideally be populated with data from the ground.



Map created by CODI on the ground



Map from remote sensing

Figure 3-44: Map of Bang Muong Camp derived on the ground (left) and using satellite imagery (right).

*Ban Nam Khem and Chella Bandi*

The strategy used to provide transitional settlement in Chella Bandi and Ban Nam Khem was very different - in Thailand, transitional shelters were provided within the confines of planned camps, while in Pakistan transitional shelters and tents were dispersed throughout the city as well as in planned camps. The dispersed tents and shelters had to be identified in the imagery amongst other permanent buildings. The analysis of transitional settlement was therefore much more challenging and time-

consuming in Chella Bandi. In many cases, the transitional shelters were easily recognisable by their detached nature and regular shape and size. Some tents though were indistinguishable from the ground reflectance and/or covered by vegetation. These camps were often very dynamic as well, with the configuration and size regularly changing making them difficult to monitor.



**Figure 3-45: The dispersed settlement approach used in Pakistan (left) was more difficult to reliably monitor than the planned camp approach used in Thailand (right).**

The number of transitional shelters counted in Ban Nam Khem and Chella Bandi is directly compared in figure 3-46. Emergency shelters, mainly in the form of tents and pieces of canvas, were provided to the displaced population within several weeks in both countries. Over 1,000 tents were erected within 2 weeks of the earthquake in Chella Bandi alone. After 8 months, the number of structures increased to 2,053 tents and 353 prefabricated shelters. 40% of the tents were located in a single camp on the grounds of Chella Bandi University.

While the structures in Ban Nam Khem were removed over a period of only a few months, the decrease in structure numbers in Chella Bandi appears to have occurred over a much longer period of time. The number of shelters dropped by 1,278 by 2008 which corresponded with official reports stating that the government was trying to return camp inhabitants to their homes from 2006 onwards. The lack of

imagery between June-2006 and September-2008 makes it difficult to ascertain whether this drop in structure numbers was gradual or immediate.

Almost all of the displaced population in Ban Nam Khem were re-housed within 3 years of the tsunami while the latest satellite image of Chella Bandi, acquired four years after the earthquake, still shows 38 transitional shelters and 830 tents were present. The ground deployment confirmed that these structures were still being lived in although the government had made it clear that no-one should be living in tents beyond 2007 (ERRA-UN, 2007). According to the inhabitants the shelters were uncomfortable, too hot in the summer and did not provide enough protection from the cold in the winter.

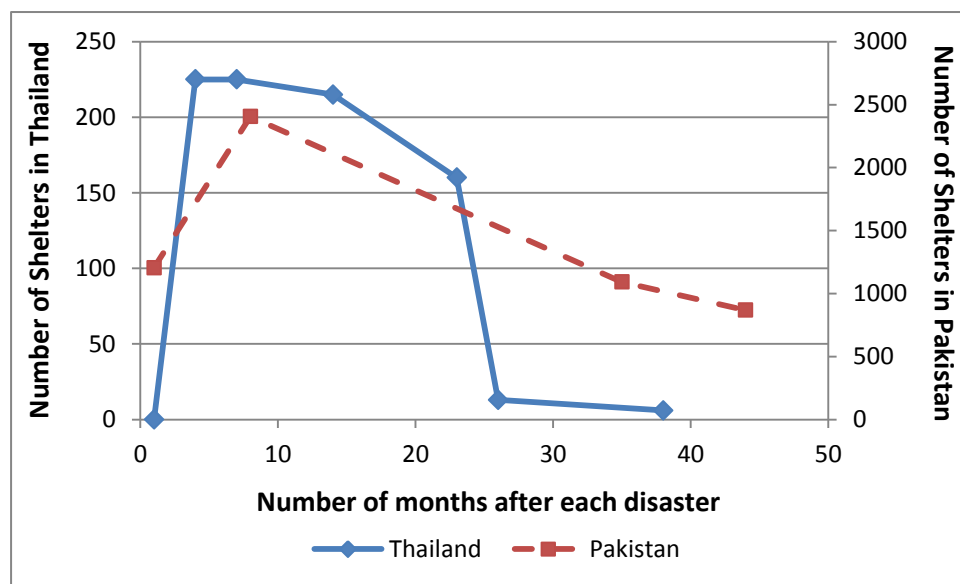


Figure 3-46: Comparative recovery trends in transitional shelter numbers in Ban Nam Khem and Chella Bandi.

The creation of planned camps in Phang Nga province, Thailand was praised because of the way it drew everyone together and allowed people to take control of their own recovery. Logistically, it also allowed the provision of supplies to be made a lot easier. Some people preferred to stay close to their homes to protect and reconstruct them. In Chella Bandi, construction-costs were paid to occupants in stages but they were prevented from building permanent homes there as it was located in a high-risk zone near to a fault-line. As a result, the compensation was subsequently spent on living costs, and in many cases, the temporary shelter has now become permanent.

### **Indicator 9. Displaced Population**

This analysis is used to estimate the number of people residing in transitional settlement throughout the recovery process. The Sphere Guidelines suggest agencies collect demographic data from as many different sources as possible. Supplying agencies with detailed data on the number of transitional shelters may be used to supplement or verify the demographic data they have collected from other sources. The number of people residing at each camp was estimated by multiplying the number of residential dwellings by the number of people estimated to be occupying each dwelling, which used assumptions based on the size of the buildings and the minimum area requirements of the Sphere Guidelines.

Residential buildings were first identified within each of the camps. They were commonly distinguishable from other building-types due to their high density and uniform shape and layout. There were two commonly used building designs in Phang Nga Province: a) elongated, rectangular buildings containing approximately 8 attached dwellings and b) single square units.



**Figure 3-47: Transitional shelters used in planned camps across Phang Nga province.**

The occupancy of each elongated building was estimated based on its width and its length and the integration of some simple ground observations. The width of the structures was measured directly in the satellite imagery as 3.5 m and later verified on the ground. Sub-dividing the length of the structures into individual dwellings was more difficult and required the integration of field knowledge to do so confidently. The average dwelling width was measured on the ground at shelters still-standing inside the Bang Muang site. The average dwelling width was approximately 4 m so the number of dwellings per building was estimated by dividing the total length of the structures by 4 m. For example, a building with a length of 32 m was presumed to contain approximately eight dwellings. Each dwelling was therefore assumed to measure approximately 3.5 m x 4 m (14 m<sup>2</sup>), which is in-line with minimum area requirements described in the UNHCR's Handbook for Emergencies that states dwellings with these dimensions could safely accommodate 4 people (UNHCR, 2007).

## Results

The total population residing in transitional shelters was calculated by accumulating the estimated population at each of the four camps. This estimation was then compared to statistics supplied by the Department of Disaster Prevention and Mitigation (DDPM) for the years 2005, 2006 and 2007. An error was calculated for each of the years by directly comparing the remote sensing estimates to the government statistics. The results appear to correlate well. The camp population after four months was estimated to be 3,200: overestimating the DDPM figure by only 231 (+7.8%), while the February 2008 estimate (3 years after the tsunami) underestimated the DDPM statistics by only 53 (-9.4%). In February 2009, up to 192 people were still estimated to be residing in transitional shelters at the Bang Muang site. The occupation of the site was confirmed by field deployment at the same time. It is unknown whether the occupiers were un-housed victims of the tsunami or dwellers from elsewhere.

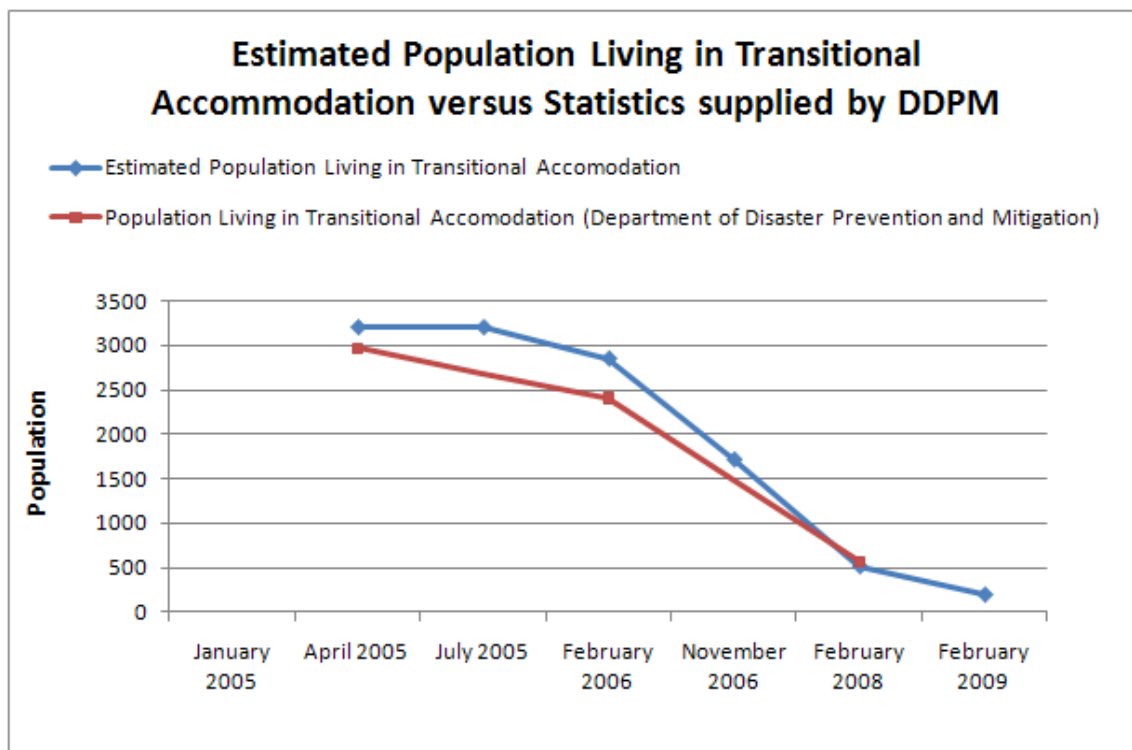


Figure 3-48: Estimated population living in transitional settlement estimated by remote sensing and the Department of Disaster Prevention and Mitigation.

## **Discussion**

This method presents a relatively quick way of estimating the displaced population living in camps. This does not take into account people who are living temporarily with relatives elsewhere, nor people who have moved to other provinces with less damage and more jobs. In this case study populations living in planned camps were estimated to within 10% with the integration of ground knowledge on dwelling size. There are a number of assumptions that have to be made when estimating a planned camp's population. For example, the analysis assumed that all of the buildings were occupied and being used, but the results from Bang Muang camp show that this might not always be the case. In February-2009, 60 small single-unit structures were still standing and were initially included in the analysis, but field deployment found them to be empty. They were emergency shelters and in-fact only used in the first year of the response. At the same time, thirteen large transitional shelters were still standing and occupied by households.

By analysing the features and land cover near to the buildings it is sometimes possible to estimate whether a building is occupied but this is more reliably determined on the ground. For example, in the February-2006 image cars can be seen outside the emergency shelters and the access routes appear well-used. After this date though, there's no further evidence of use in the vicinity of these shelters, so they may be presumed to be vacant from the November-2006 image onwards. In hindsight, the thirteen large shelters in the Bang Muang camp may be presumed to be occupied though as visible extensions were added to the shelters between February-2008 and February-2009.

Despite the high accuracy achieved here the author doesn't recommend remote sensing as a primary source of data for monitoring the displaced population. It could be useful though in situations where access is denied or other data sources aren't readily available. More reliable population estimates are likely to be obtained through ground survey work; in particular, camp registration offers a good opportunity to count the number of Internally Displaced Persons (IDPs), which can then be disaggregated by gender and/or age. Even so, remote sensing offers a useful tool to map and visualise the displaced population across the affected region and to update camp inventories. Up-to-date information is important to prevent overcrowding at camps and to assist resource allocation.

## Section 4: Natural Environment

### Literature Search and Household Survey Results

The force of the tsunami broke coral reefs under the water-line and caused erosion and sedimentation, which smothered seagrass and other aquatic plant-life. On land, the intrusion of seawater led to extensive flooding, eroded soils and caused dramatic changes to the morphology of the coastline. Beach ecosystems in particular were eroded, greatly reducing the sand area used by Turtles to lay their eggs. When the waters receded, large amounts of debris and hazardous waste were deposited up to 2 km inland. Salt water and sewage also infiltrated groundwater, leading to land contamination and the presence of coliform bacteria in drinking-wells (Vaccari et al. 2010). The level of damage to the mangroves in the region ranged from the complete removal of trees to indirect damage caused by root upheaval, debris and salt deposits. Ground surveys estimated that approximately 3.9 km<sup>2</sup> of mangrove forests, 8.9 km<sup>2</sup> of coral reefs and 9.9 km<sup>2</sup> of sandy beaches were affected across Thailand (Paphavasit et al. 2007).



**Figure 3-49. Mangroves species such as *Rhizophora apiculata* and *Avicennia alba* were widely distributed around Ban Nam Khem. Photo: Daniel Brown (February 2009).**

The clean-up operation began on 9 January 2005 with substantial support from the private sector and international organisations (UNDP, World Bank and FAO ,2005). The most urgent tasks were cleaning-up beaches, providing drinking water-sources and setting up sewage and garbage collection (Phuket

Gazette, 2005). Debris was removed by the army and disposed on temporary sites where it was sorted. The government wanted debris to be cleared before the monsoon commenced after three months, but according to a local focus group, the debris continued to accumulate long after the tsunami (ONEP Focus Group, 2005).

A number of government departments worked closely to assess the impact of the tsunami, repair damage and promote rehabilitation. They overturned affected corals and removed 97 tonnes of debris and dead plant material. They also replanted and monitored affected species and provided training to locals so they could assist with the rehabilitation and development of natural resources (ONEP, 2005). Legislation was published by the Office of Natural Resources and Environment Policies and Planning (ONEP) to ensure the recovery process was sensitive to its surroundings. This led to the affected sites being declared 'environmentally protected areas'. For a period of one year, the legislation prohibited trawl-nets within 3,000 m of the coast, controlled infrastructure development in coastal areas and ensured land use was environmentally friendly (ONEP, 2005). Most sites were expected to recover from mild impacts of the tsunami, but some areas including the mangroves in Phang Nga were expected to require long-term rehabilitation work (Paphavisit et al. 2007).

### **Remote Sensing Methodology**

Scientists have been developing techniques since the 1960s to semi-automatically classify vegetation and to extract biophysical information from satellite imagery (Running et al. 1994; Lyon et al. 1998). Vegetation may be classified by analysing the red and near-infrared bands of a multi-spectral satellite image. The spongy mesophyll of a leaf scatters near-infrared energy to protect the cells from overheating (Gates et al. 1965); the subsequent difference in the reflectance between the near-infrared and red parts of the electromagnetic spectrum creates a phenomenon known as the "red-edge". Measuring the steepness of this edge allows changes in the extent and health of vegetation to be assessed: dense, healthy vegetation has a large red-edge, while sparse, unhealthy vegetation has a more subtle red-edge (Jordan, 1969).

Two semi-automatic methods were used during this research to extract information on vegetative land cover: Normalised Difference Vegetation Index (NDVI) and Maximum Likelihood supervised classification. NDVI is a normalised ratio of the red and near-infrared bands and provides a useful

measure of whether a pixel contains live green vegetation or not (Rouse et al. 1974). An appropriate NDVI threshold was determined for each image to effectively mask vegetative and non-vegetative land covers. The threshold amounts were found iteratively by amending the values and visually assessing the results. This method was used to map areas of mangrove rehabilitation and urban green spaces. Spatial metrics were applied to the NDVI maps to quantify changes in the size, distribution and fragmentation of the green spaces over time.

The Maximum Likelihood classifier was used to semi-automatically classify five land cover classes, including sparse vegetation and thick vegetation, based on training areas provided by the analyst. Once the extent of the land covers was mapped, change detection analysis was applied to the classified images to monitor transformations in land cover and in particular, to identify areas of erosion, land degradation, deforestation and the removal of vegetation. A full description of the Maximum Likelihood classifier is provided in Chapter 5 where the technique was used to classify spontaneous settlement and planned camps in Haiti for UN-Habitat.

### **Indicator 10. Land Cover and Urban Green Space Analysis**

#### *Land Cover Area Analysis*

Figure 3-50 shows six Maximum Likelihood classification images focussing on the centre of Ban Nam Khem before and after the tsunami. The Maximum Likelihood classifier applies a statistical decision rule that examines the probability function of a pixel for each of the classes, and assigns the pixel to the class with the highest probability. The probability values are based on training statistics provided by the analyst in the form of sample pixels, which represent the classes that are to be classified.

The maps show that most of the vegetation within 1 km of the coastline was removed by the tsunami and replaced with a layer of mud and debris. From February-2006, much of the coastal vegetation returned but patches of vegetation were removed around construction sites and planned-camps throughout the recovery process.

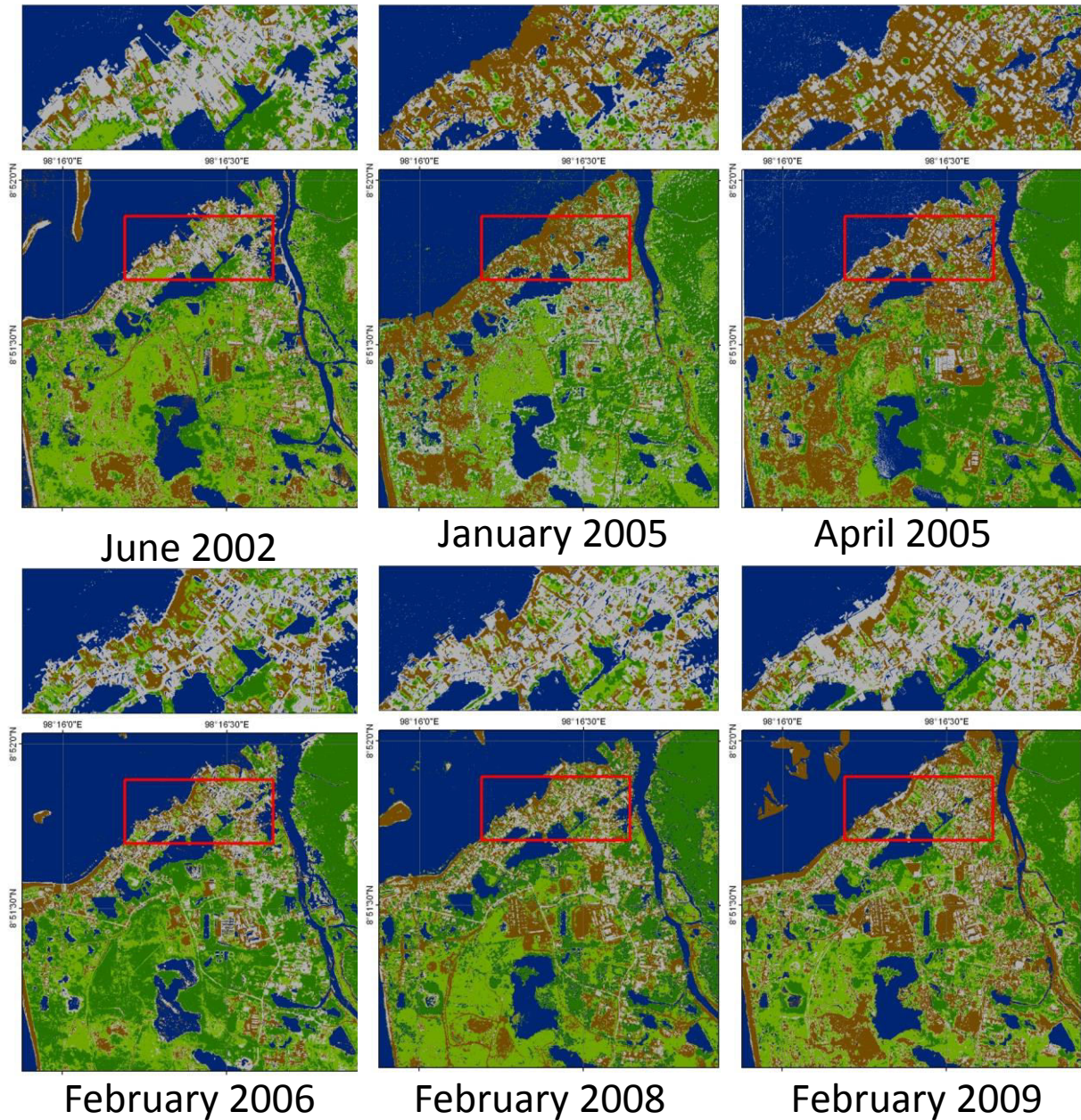


Figure 3-50: Six Maximum Likelihood classification images showing the effect of the tsunami and the recovery process on land cover. The satellite images have been classified into five land classes: bare ground (brown), sparse vegetation (light green), thick vegetation (dark green), urban (grey) and water (blue). The classes - based on the USGS land cover classification system (Anderson et al. 1976) - were selected to show land cover change processes such as land degradation, construction and the re-growth of vegetation. The urban area inside of the red rectangle is magnified to show detail.

The area occupied by each land cover class was extracted from a subset of the classification results. The results are summarised in the histogram in Figure 3-51. Water area varied very little throughout the site because the water-height at the time the images were acquired was fairly constant. Urban area dropped by 15% after the tsunami because much of the impervious surface was either washed away or covered in debris. Debris was classified as bare ground, so bare ground was seen to increase significantly between June-2002 and January-2005. It increased again between January-2005 and April-2005 after the army levelled much of the land with sand. It fell by February-2006 though as vegetation began to return and debris was cleared. After the initial clean-up, urban area increased continually from April-2005 through to February-2009. The results suggest that urban area increased by 30% between June-2002 and February-2009 as a result of new construction. The accuracy of the urban classification is verified in the *building* section of this chapter.

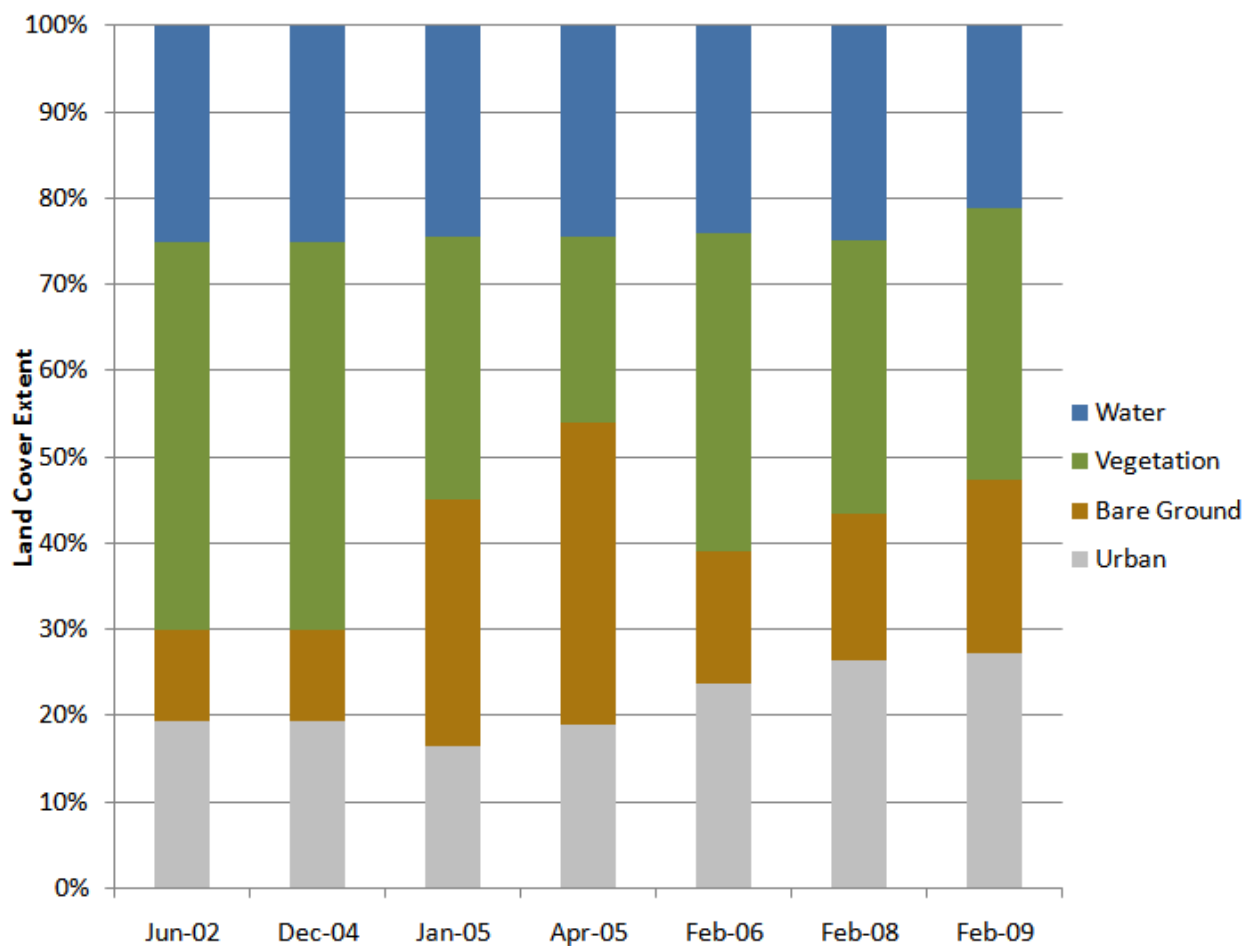


Figure 3-51: Proportion of land-cover in Ban Nam Khem, extracted from Maximum Likelihood classification images.

### *Environmental Degradation*

A series of change detection maps were produced from the Maximum Likelihood classification images that show the transition from vegetation to the other three land cover classes. The maps are referred to as degradation maps as they show the conversion of vegetation to bare ground, water and urban land covers. The objective of these degradation maps is to identify non-urban land cover change caused by erosion, land degradation, deforestation and the removal of vegetation as a result of the disaster and the subsequent recovery activities. Change detection analysis was conducted in ArcGIS by using Raster Calculator to subtract one classified image from the other. The degradation maps were then produced by assigning a unique code and suitable colour-scheme to the change detection images. Pixels that changed from vegetation to bare ground, urban or water were coded brown, grey and blue respectively. Pixels that remained vegetation were coded green. Areas that remained bare ground or urban were coded black.

Figure 3-52 shows the change detection map of Ban Nam Khem generated from the June-2002 and February-2009 Maximum Likelihood images. The result confirms that most of the vegetation damaged or removed by the tsunami has now returned. Area (a) on the map represents new residential buildings that were built by the army within a year of the disaster, Area (b) corresponds to a new agency-built housing development containing 56 houses, and Area (c) shows the main school site that had expanded during the recovery process.



**Figure 3-52: Change detection map of Ban Nam Khem showing at least three areas of new development: (a). New army-built housing (b). Phase 2 housing and (c). Ban Nam Khem school.**

The same method was used to identify areas that had remained urban between June 2002 and February 2009. It is assumed that these are areas where buildings were re-built or repaired on their original plots. Brown and grey pixels in figure 3-53 correspond to areas that remained bare ground or urban respectively between June-2002 and February-2009. The map successfully highlights rebuilt houses, factories and fishing-piers. The re-surfaced road network is also displayed as a grey linear feature.

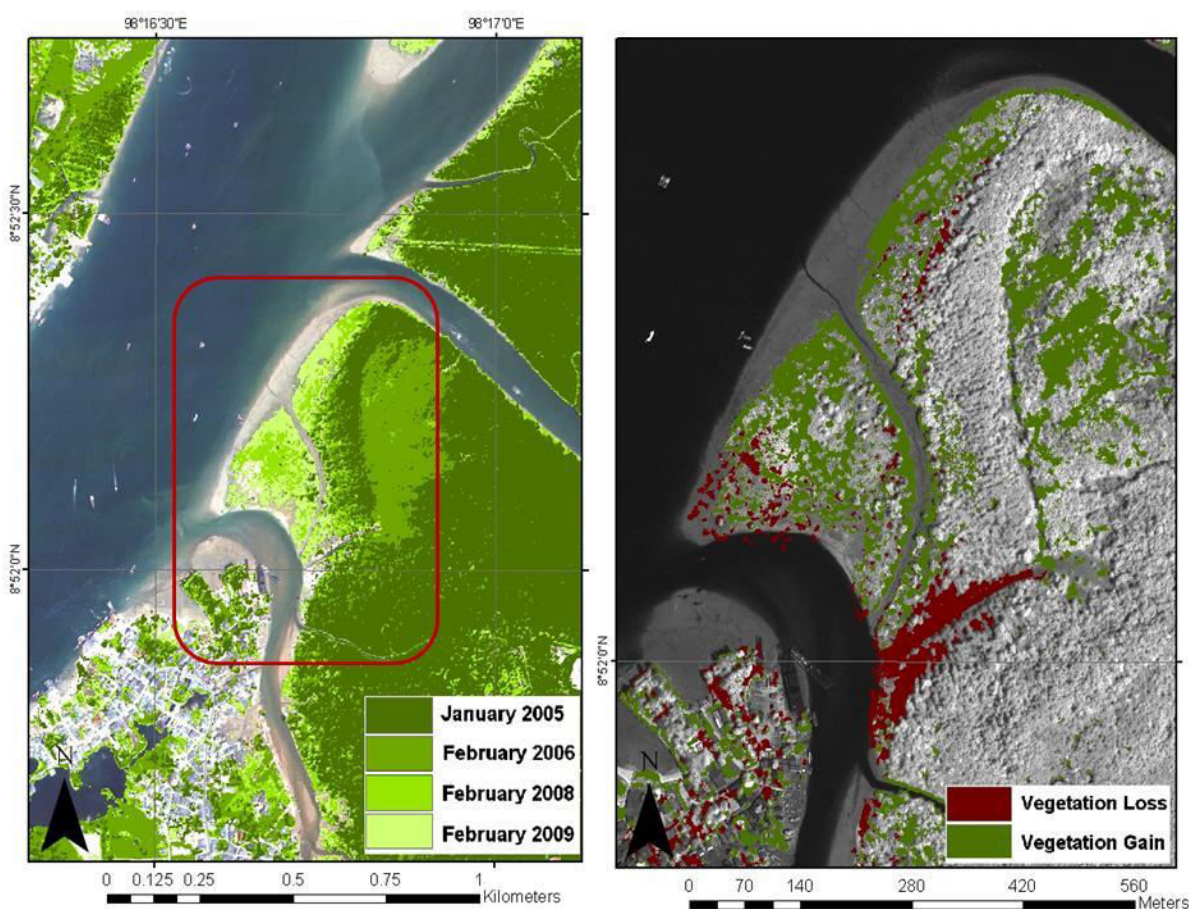


Figure 3-53: Change detection map of Ban Nam Khem showing areas of reconstruction and repair including (a). Fishing Piers (b). Army-built houses and (c). Resurfaced roads.

### *Mangrove Analysis*

The extent of the mangrove forests around Ban Nam Khem were semi-automatically delineated by applying thresholds to a series of NDVI images. Mangrove forests were particularly important to monitor as they can act as an important natural barrier against the impact of a tsunami. They can also trap sediment which prevents coastal erosion and provide important nursery space to shrimp, crustaceans, molluscs and fishes.

The dark green area in figure 3-54 shows the extent of the mangrove in January-2005, immediately after the tsunami, when 0.16 km<sup>2</sup> or 21% of mangrove was destroyed. Most of the mangroves that were destroyed were located on the edge of the forest. The different shades of lighter green show the regeneration of the mangrove forest over time. The area of mangrove forest grew to 0.74 km<sup>2</sup> after only one year - equivalent to 95% of the forest area that existed before the tsunami. The trees on the inside of the forest were the first to recover while the trees on the edge, that took the full force of the waves, took 3 to 4 years. The total area of mangrove forest in February-2009 was 0.87 km<sup>2</sup>, 10% more than existed before the tsunami.



**Figure 3-54: Green mangrove forest at different stages of the recovery process (left) and areas of mangrove forest gained and lost between June-2002 and February-2009 (right). The only extensive area where mangrove forests did not re-grow is an area to the south that contains a channel that was used to remove a stranded trawler.**

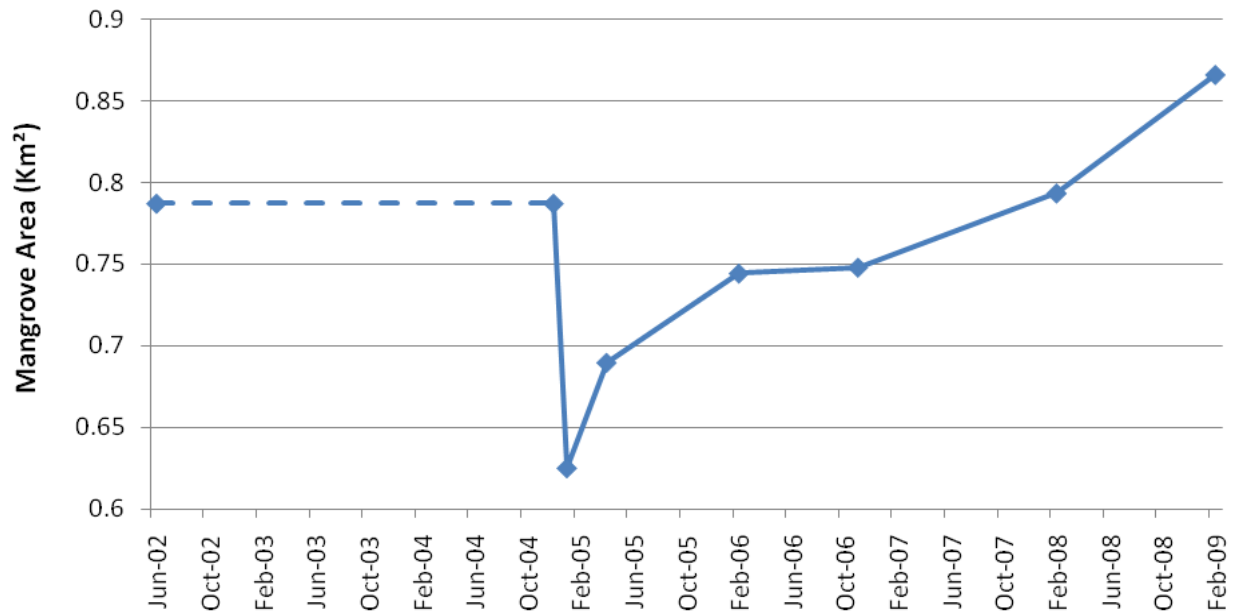
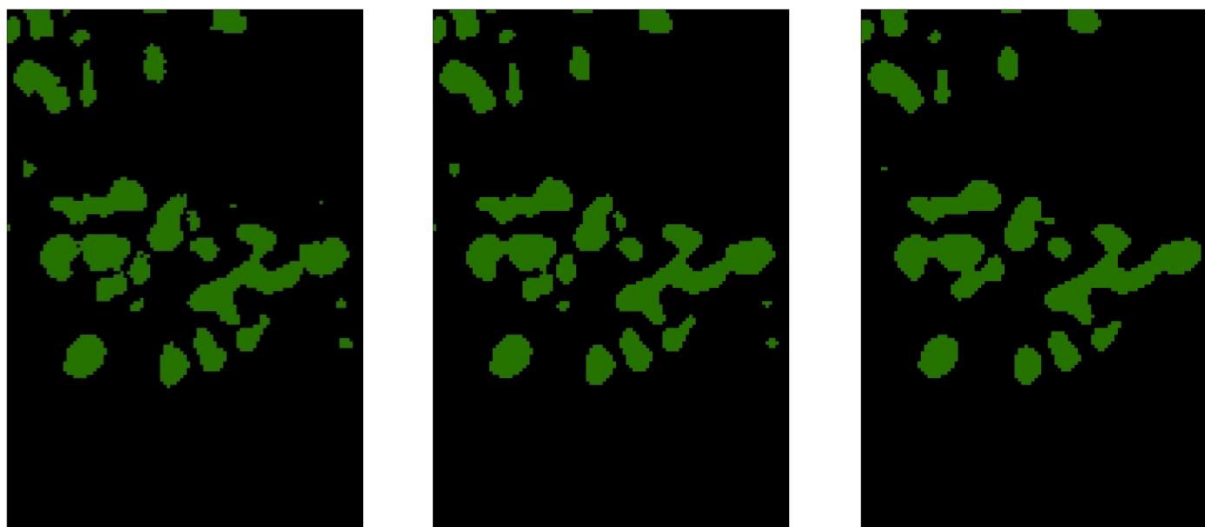


**Figure 3-55: The area of Mangrove forest is seen to recover beyond the extent observed before the tsunami by 10%.**

#### Urban Green Space

The same NDVI threshold technique was applied to an urban subset to map urban green spaces. Spatial metrics were then applied to the maps to quantify the structure and pattern of the green spaces by analysing patches of pixels representing vegetation and their spatial relationship to each-another (Frohn, 1998; Arroyo-Maya et al. 2005).

To prepare the green-space maps for Spatial Metric Analysis, a smoothing Median filter was applied to remove small patches of vegetation only a few pixels in diameter and to smooth the vegetation patch objects. Median 3x3 was found to sufficiently 'clean' the maps without significantly altering the shape of the green space patches.



No Filter

Median Filter 3x3

Median Filter 7x7

Figure 3-56: A Median filter was applied to the urban green space maps to remove noise and smooth the object shapes, which ultimately improved the reliability of the spatial metric results.

A group of spatial metrics were selected to quantify changes in the size, distribution and fragmentation of the urban green spaces. Only 5 metrics were deemed necessary to adequately explain the pattern of recovery as shown in table 3-10. Fragmented green spaces - considered important in built-up areas for quality of life and as habitats for biodiversity - were quantified using the Mean Nearest Neighbour, and the presence of adequately-sized spaces - necessary for parks and recreational activities – were monitored with the Large Patch Index.

Metric	Description
Large Patch Index (LPI)	The size of the largest green space.
Mean Nearest Neighbour (MNN)	The average distance between the green spaces.
Patch Density (PD)	The density of green patches.
Total Edge (TE)	The length of green edge exposed to the built environment.

Table 3-10: Spatial metrics used to characterise the size, distribution and fragmentation of urban green spaces.

The Spatial Metrics show that 72% of urban green space in terms of area was removed as a result of the tsunami. The green spaces that remained were small and highly fragmented, characterised by a low *Large Patch Index* (LPI) and a high *Mean Nearest Neighbour* (MNN). A further 0.02 km<sup>2</sup> of green space was removed between January-2005 and April-2005, during the clearance work, leaving only 0.03 km<sup>2</sup>, which further increased the MNN and reduced the *Patch Density* (PD).

Between April-2005 and November-2006 vegetation began to recover, with the green space area reaching 0.15 km<sup>2</sup> in November-2006 – the same as was present before the tsunami. During this time, *Large Patch Index* and *Total Edge* (TE) both increased. *Patch Density* also increased between April-2005 and February-2006 as the vegetation re-grew in fragmented patches, but dropped again by November-2006 as the patches began to aggregate.

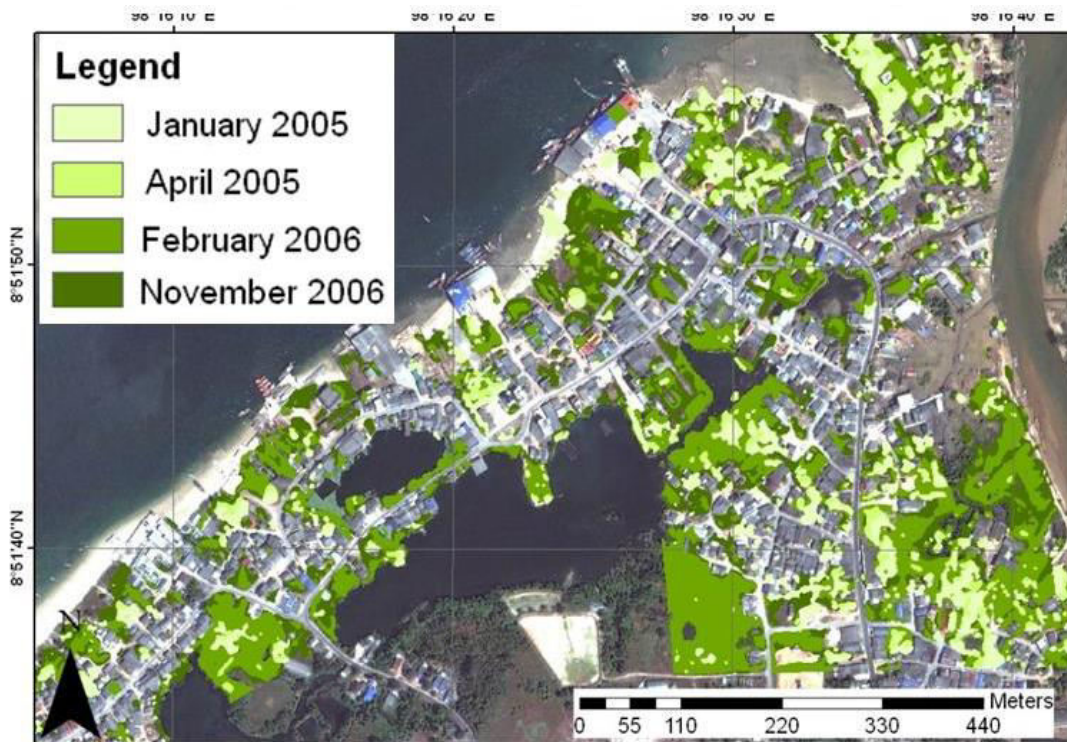


Figure 3-57: Green Space in Ban Nam Khem classified using NDVI Threshold technique.

### Discussion

Satellite imagery is particularly well suited to the monitoring of the natural environment. Satellites can acquire data covering large geographic areas and the presence of red and near-infrared bands on high-

resolution sensors means vegetation may now be extracted easily and reliably. Remote sensing was used to monitor land cover using two commonly-used semi-automatic techniques. NDVI was quick and reliable and provided results which were used to monitor vegetation growth and to identify areas of degradation throughout the recovery process. Maximum Likelihood supervised classification was used to classify five land-cover classes and to monitor instances of land degradation, construction and vegetation rehabilitation.

### *Reliability and Accuracy*

To determine the accuracy of the Maximum Likelihood technique, on which the change detection maps and area statistics were derived, the results were directly compared to the manual classification of land cover. 50 random points were generated in ArcGIS and each of the points were manually assigned to one of 5 land cover classes by zooming to the point in the image and noting the underlying land cover - where possible, geo-coded ground photos and video data was used to assist the identification of the land cover at these points.

The average accuracy of the six classification-images was 82.2 % with individual accuracies ranging from 68.0% for the January-2005 image to 89.4% for the April-2005 image. All of the classifications obtained accuracy greater than 80.0%, except for the post-disaster image collected in January-2005. Disturbance to the land cover caused by the tsunami appears to have reduced the accuracy of the classification as there was frequent confusion between bare ground, sparse vegetation and urban; in particular, between the wet, inundated, water-logged soil and urban land cover, leading to an overestimation of urban area.

In contrast, the April-2005 image acquired in the early phases of recovery achieved the highest accuracy with 89.4%. The buildings in this image were accurately classified because they were newly-built and therefore more conspicuous. With time though, the buildings weathered and became less dissimilar than the background reflectance surrounding the buildings. Bare ground was also particularly conspicuous in this image as it had just been re-surfaced and took a particularly smooth texture and sandy hue.

Analyst must be aware of such errors and limitation when attempting this form semi-automated analysis. There are other factors that analysts must consider when purchasing satellite imagery and conducting classifications that might increase the overall reliability. The timing of the images is particularly important when monitoring vegetation and knowledge of the plants' phenological growth cycle is important to understand the growth stage of the vegetation in the images. Seasonal differences can significantly alter the results of a classification study. The water height and tide may also affect the exposure of different amounts of vegetation and bare ground.

### *Transferability*

Maximum Likelihood was used to classify the same 5 land cover classes in Chella Bandi and Ban Nam Khem. This technique successfully classified planned camps and access routes as urban land cover and identified land-slides as a conversion from vegetation to bare ground. Degradation maps were also produced in Pakistan to show where settlements and camps had expanded over time. Training datasets need to be created for each image being classified to accommodate the differences caused by atmospheric conditions, satellite position and seasonality. As such, it isn't yet possible to produce a fully automated methodology that can be applied to different locations or the same location in different images.

The steep terrain and ground movement after the Pakistan earthquake led to poor geographic registration in some areas which created alignment errors. These errors were not significant when conducting a regional-level analysis but were important when attempting to analyse individual street-building level. Overcoming these registration issues in mountainous terrains is a significant issue that needs to be addressed.

The trends for each land cover in Ban Nam Khem and Chella Bandi are presented in figure 3-58. In Ban Nam Khem there was a large increase in the amount of bare ground caused by the tsunami and subsequent clearance work followed by a rapid *re-greening* of the landscape after a year as vegetation returned. Thereafter bare ground increased and vegetation decreased gradually as more buildings were developed. In contrast, in Chella Bandi there was little change in bare ground immediately after the earthquake despite the presence of small landslides. The biggest increase in bare ground in Chella Bandi was observed 8 months later due to the erosion of the ground in-and-around spontaneous camps and

also the presence of fallow fields. Compact planned camps in Thailand appear to have caused less degradation than dispersed camps in Pakistan.

There was a linear increase in urban land cover observed at both sites throughout the recovery process as a result of development and the presence of transitional settlement. The overall increase in urban area is slightly larger in Chella Bandi, possibly because many households moved to Muzaffarabad from surrounding mountainous areas to seek assistance. Water levels were relatively constant in Thailand but in Pakistan a large increase in water was observed after the earthquake caused by the accumulation of water behind a large landslide which later dispersed.

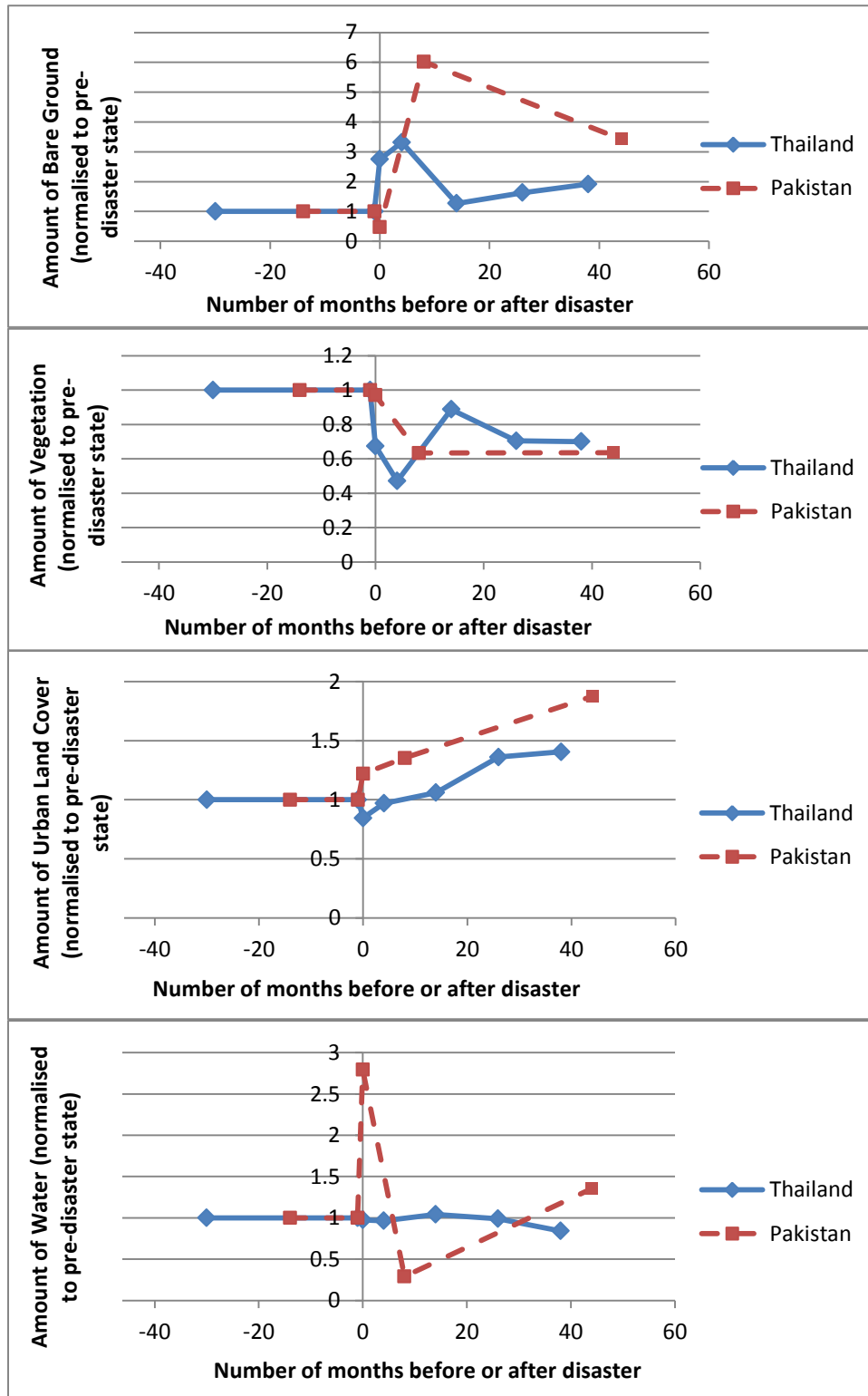


Figure 3-58: Comparative trends in land cover for Ban Nam Khem and Chella Bandi.

## **Section 5: Livelihoods**

### **Indicator 11: Recovery of Livelihoods**

#### **Literature Search and Household Survey Results**

The tsunami had an enormous impact on livelihoods in Thailand through the loss of income, productive assets and marine and coastal natural resources (ADPC, 2005b). Fishing-fleet, harbours and fish-processing facilities were all destroyed, including 1,807 hatcheries, 1,876 fishing boats and 991 fishing gears (UN Country Team, 2005). Many of Khao Lak's hotel resorts also received major damage, including two large complexes within the case study site. Tourism and fisheries were the hardest hit sectors, losing \$321 million and \$43 million respectively including loss of assets and income. Thailand lost \$2.09 billion because of the tsunami, making it the second-worst affected country in terms of financial loss (UN Country Team, 2005).

A walking ground survey in Ban Nam Khem in 2009 identified at least 22 forms of livelihood encompassing a wide range of sectors, including agriculture, fishing and manufacturing. The ground survey and analysis of satellite image suggest that both shops and fish processing facilities are significant livelihood providers. The majority of the 64 shops identified in Ban Nam Khem sell food, drinks and basic household items. A small number sell clothes, while stores near to the coast cater primarily for tourists. 32 fish processing facilities were also identified covering over 10,000 m<sup>2</sup>. Other forms of livelihood include 12 restaurants, 12 swallow-nest factories, 12 bars and cafes, 12 mechanics and 11 small factories.

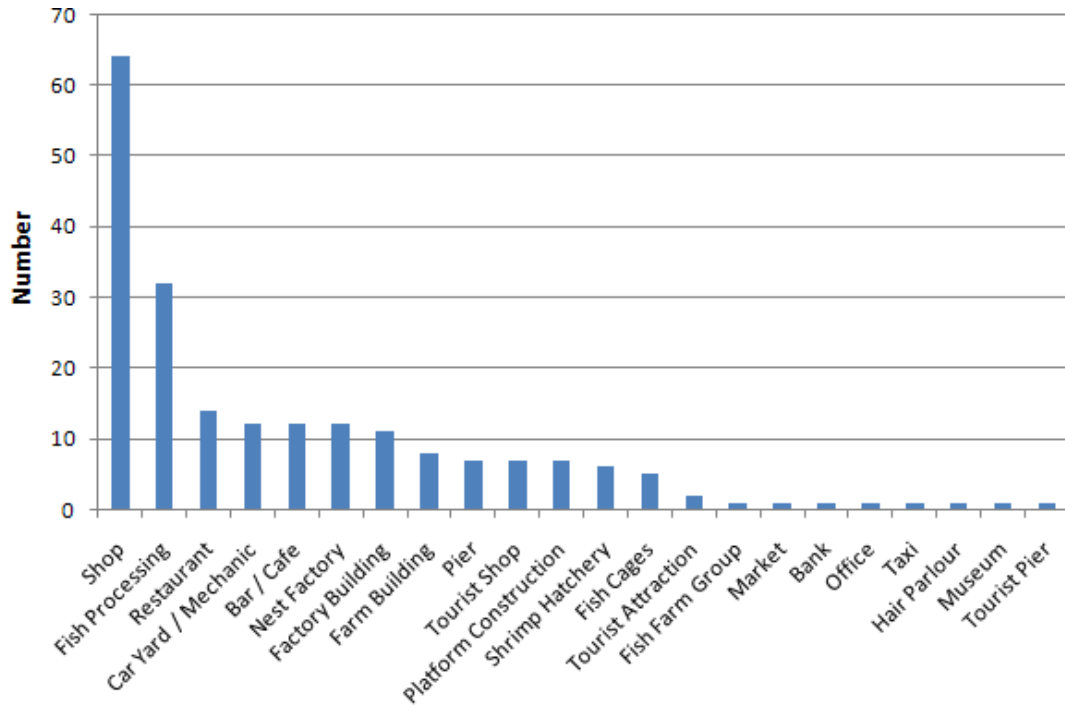


Figure 3-59: Sources of livelihood identified on a walking-survey of Ban-Nam-Khem in February-2009.

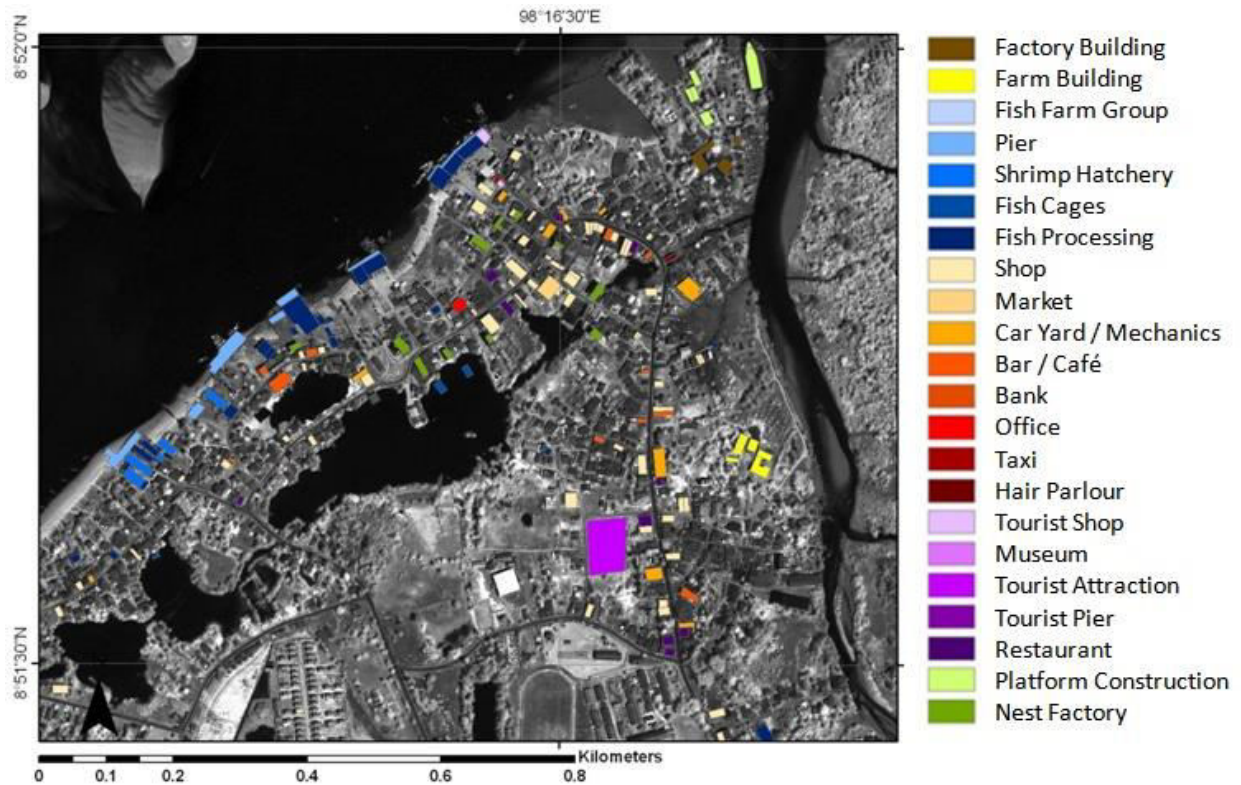


Figure 3-60: Livelihood map of Ban Nam Khem populated using satellite image analysis and ground survey observations acquired in February-2009.

Remote sensing was used to identify large, conspicuous forms of livelihoods without the use of ground knowledge. Both fish processing facilities and other factories were instantly identifiable from their size and location. Fish processing facilities were located along the shore-line and factories were located in a small manufacturing zone to the east of Ban Nam Khem. Other conspicuous forms of livelihood, such as a construction area for mining-platforms, were visible in the satellite imagery but required ground knowledge to verify their use.

As the fishing industry is one of the main sources of income in the region and associated features are clearly visible in satellite image, the following results-section focuses on fishing-related indicators, including the use of shrimp-hatcheries and grow-out ponds, pier length and the presence of boats.



**Figure 3-61: Shrimp farming. Derelict shrimp hatcheries (left) and functioning grow-out ponds (right) in Ban Nam Khem. Source: Daniel Brown.**

## **Remote Sensing Methodology**

### *Shrimp Hatcheries*

Thailand is a major exporter of shrimps, producing over quarter a million tonnes a year (Cai et al. 2009). The cultivation of marine shrimps and prawns for human consumption comprises two phases: shrimp hatcheries and grow-out ponds. Both facilities were identified in satellite imagery and monitored throughout the recovery process. The hatcheries consist of a series of concrete tanks while the grow-out

ponds are large aerated pools where the juveniles are left to grow to marketable size. At least 14 hatcheries were identified from their large size and proximity to the ocean.

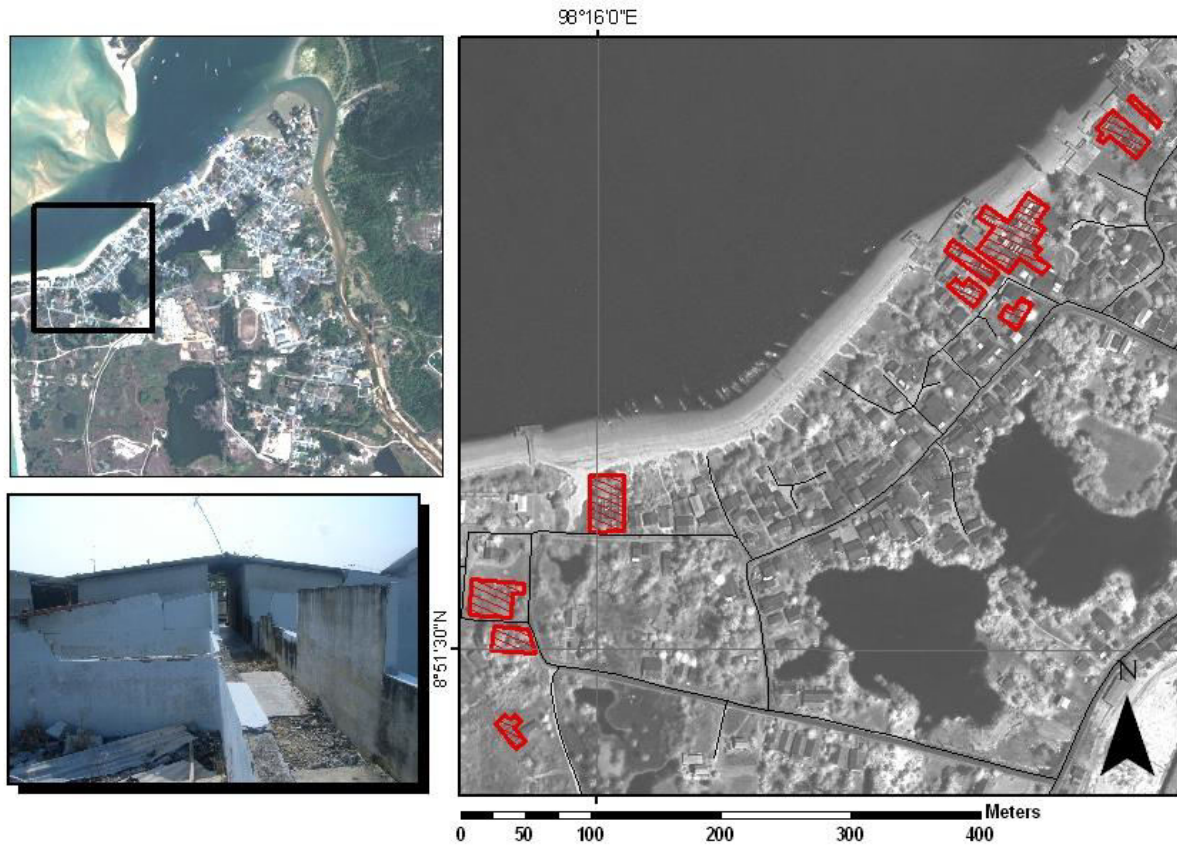


**Figure 3-62: Shrimp hatcheries in Ban Nam Khem mapped with satellite imagery.**

Before the tsunami, the hatcheries were more difficult to identify without ground knowledge because the tanks were covered with roofing to provide a protected environment for the larvae. The tsunami destroyed the walls and roofs of the hatcheries leaving only the concrete tanks behind, which were clearly identifiable in the imagery. Figure 3-63 shows a medium-scale hatchery in Ban Nam Khem before and after the tsunami.



**Figure 3-63: A medium-scale hatchery in Ban Nam Khem in June 2002 (left) and January 2005 (right).**

Remote sensing can be used to count the number of hatcheries affected by the tsunami and to estimate the maximum production capacity destroyed by calculating the area and number of tanks affected. The hatchery shown above contains approximately 40 tanks. All 14 hatcheries in Ban Nam Khem were situated by the coast and were totally destroyed by the tsunami. The remote sensing analysis shows none of these hatcheries were reconstructed and no new hatcheries were built. This was validated with ground-data collected in February 2009 and confirmed by a UNDP, World Bank and FAO report (2005). One of the hatcheries was demolished and the other 13 hatcheries were left derelict. These shrimp hatcheries ceased to operate in Ban Nam Khem because of high investment costs, low shrimp prices and low levels of compensation (Arunmas, 2007).

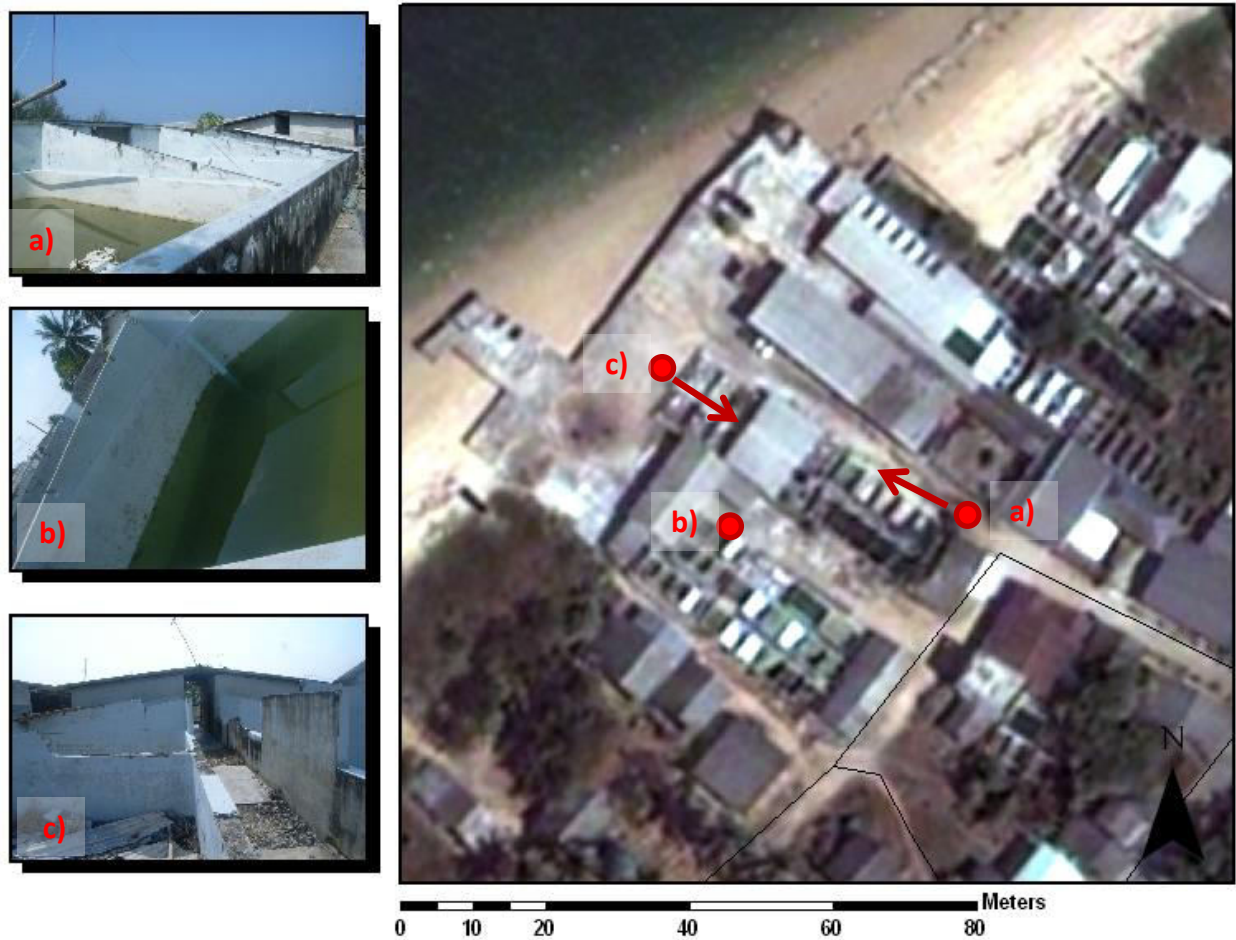


**Figure 3-64: Derelict shrimp hatcheries identified in satellite imagery and verified in field photographs in February-2009.**

#### *Grow-out Pools*

Unlike the hatcheries, the grow-out ponds on the outskirts of the village were unaffected by the tsunami as they were protected from the waves by a stretch of mangrove forest. The ponds were manually delineated and classified according to whether they were full of water or not. The ponds full of water were further disaggregated according to whether there were pumps present or not and whether those pumps were aerating the water. Rotating pumps and aerated water were assumed to signify that a pond was being used at the time the imagery was collected.

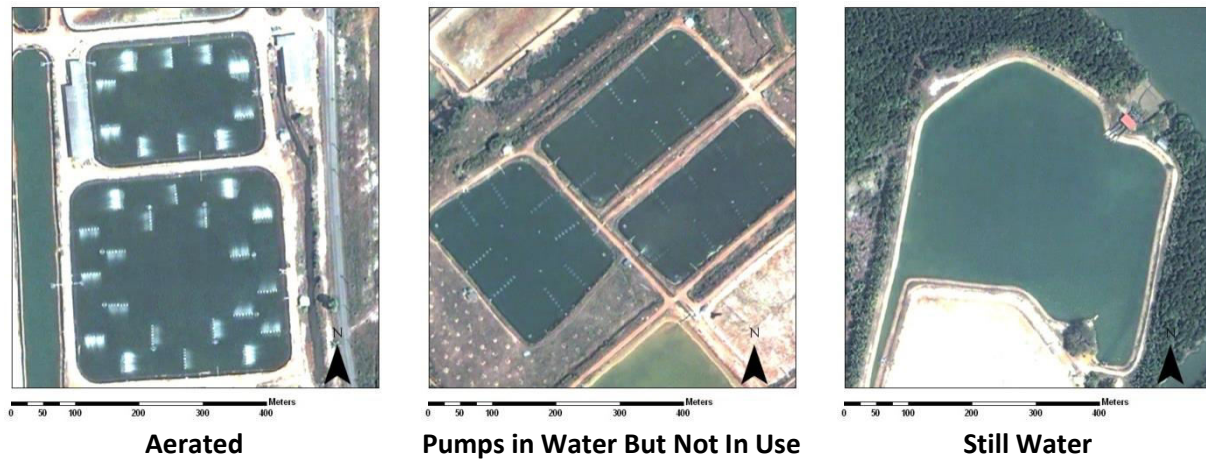


**Figure 3-65: Classification of shrimp ponds full with water.**

The proportion of ponds full of water did not vary very much, with approximately 55 % full of water at any one-time, except in February-2008 when 70 % of ponds were full. The area of ponds being aerated never dropped below the pre-disaster level, suggesting that their productivity was not affected. Significantly, 206 km<sup>2</sup> of pools were being aerated within a week of the tsunami. A new complex containing 20 ponds was later constructed between February-2006 and February-2008, a sign of continued investment in the area.

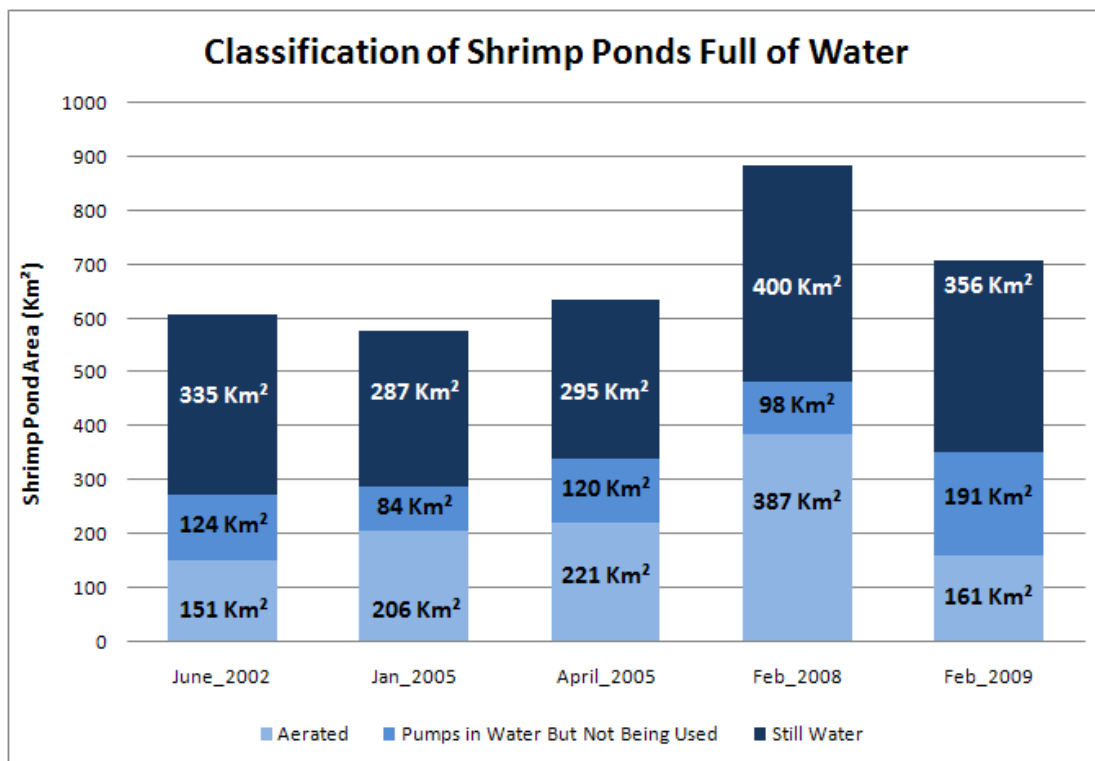


Figure 3-66: Area of functioning shrimp ponds.

### Piers

The northern part of Ban Nam Khem faces the Andaman Sea and almost half of the seafront contains piers for mooring trawlers and long-boats. Large yards are located near to the piers for fish storage and other materials, such as timber. The number of harbours and jetties was an indicator adopted by TRIAMS as part of their infrastructure monitoring. For this study *length of piers* was deemed to be a better measure as it gives an indication of mooring capacity. The number and length of piers was measured in the satellite imagery and the functionality and use of each pier was also gauged from the presence of boats and the condition of the piers.

Before the tsunami, there were 25 piers measuring 539 m in length. These were all totally destroyed by the tsunami, with only 1 pier (12 m) remaining. Pier reconstruction was rapid. The satellite imagery showed that by July-2005 many of the piers had been restored and were being used by 67 boats. By February-2009, there were 27 piers. According to Bang Muang Sub-District Office, the fishing piers in Ban Nam Khem were rebuilt in about 6–7 months and the fishmongers started trading in June-2005.

DDPM statistics also report that 100% of harbours and jetties in Phang Nga Province were constructed by 2006. These reports validate the remote sensing observations and vice-versa.

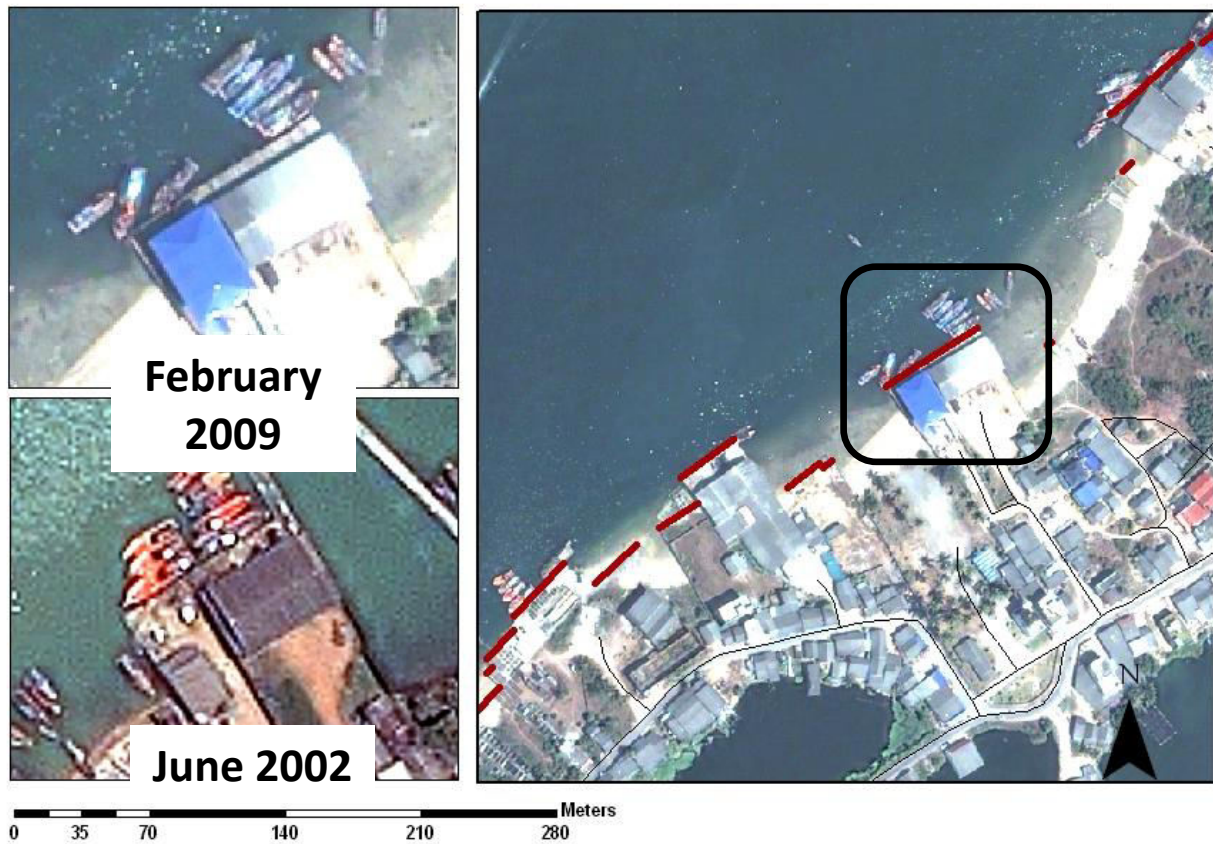


Figure 3-67: Piers monitored in June-2002 and February-2009.

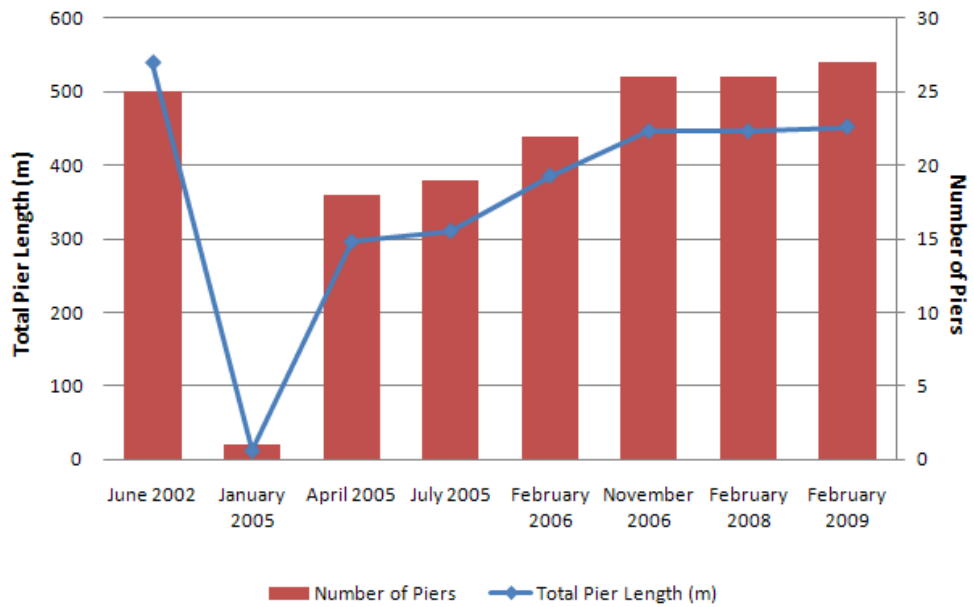


Figure 3-68: Pier length in Ban Nam Khem, calculated from Remote Sensing.

### Boats

Two types of boat are used in Phang Nga Province: long-tail boats and fishing trawlers. Figure 3-69 shows boats in ground survey photography and satellite imagery. The long-tail boats are approximately 10 m long. Trawlers are wider and measure between 15 to 20 m. Both boat types are used predominantly for fishing, but the long-boats are also used as ferries. Individual boats were identified in satellite imagery and statistics on the number of boats, their location and proximity to harbour and pier facilities were extracted.



**Long-Tail Boats**

**Trawlers**

**Figure 3-69: Long-tail boats and trawlers in ground photography and satellite imagery in February-2009.**

The number of boats is used here as a proxy for livelihood recovery. The imagery analysis shows that after the tsunami boats disappeared across the whole of Ban Nam Khem and returned between January-2005 and February-2006. A point was manually placed on each boat visible in the imagery. This dataset was converted to a series of density maps as shown in figure 3-70 to show clusters of boats throughout the recovery process.

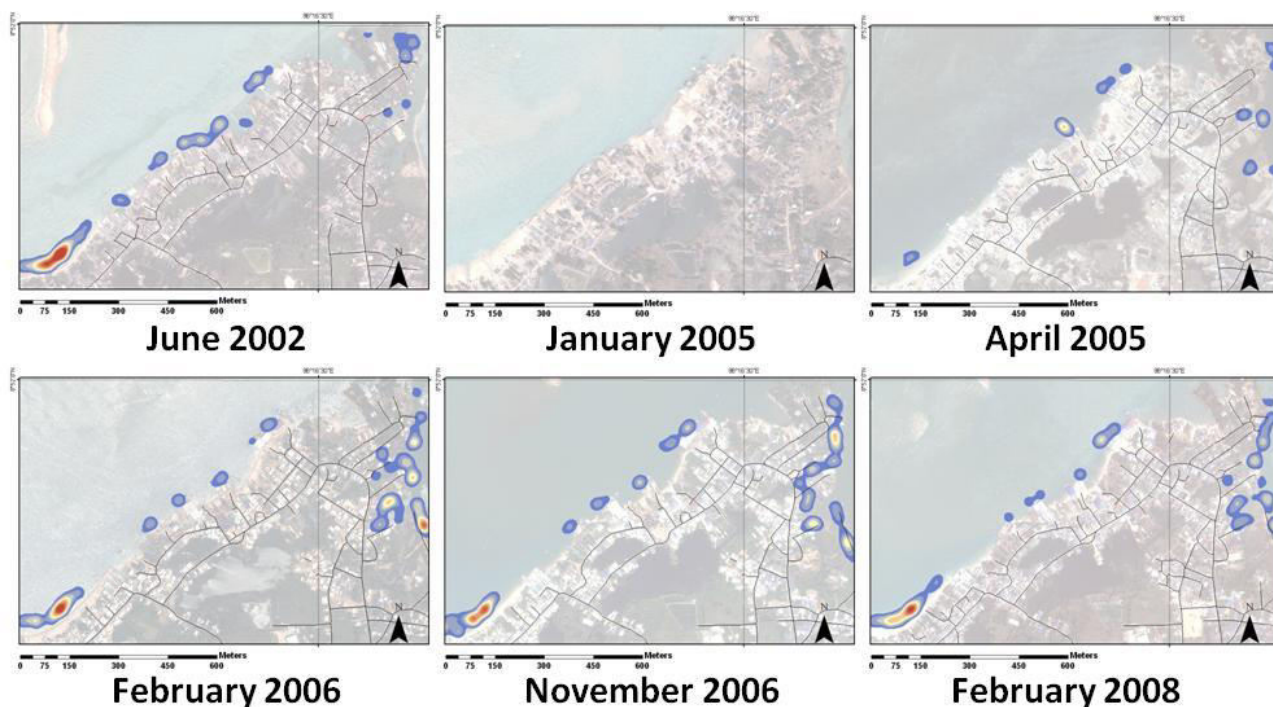


**Figure 3-70: Boat density in Ban Nam Khem throughout the recovery process, calculated from visual observation of satellite imagery.**

At least three clusters of boats were identified in Ban Nam Khem as shown in figure 3-71. Many long-tail boats were situated on the beaches at site (a). The tsunami destroyed all boats here, but they reappeared between April-2005 and February-2006, with numbers returning to approximately 70-80% of those seen in June-2002. At site (b), trawlers were tied to piers near to large fish processing facilities. Despite their large size, all of the trawlers disappeared. The number of trawlers gradually recovered, reaching 80% of the pre-disaster state by February-2009. This gradual recovery reflects the high cost of replacing trawlers. At site (c), there was an increase in the density of long-tail boats until February-2006, when the number dropped dramatically. The rise and fall of boat-numbers at this site was due to the temporary presence of new boats outside a boat yard there.

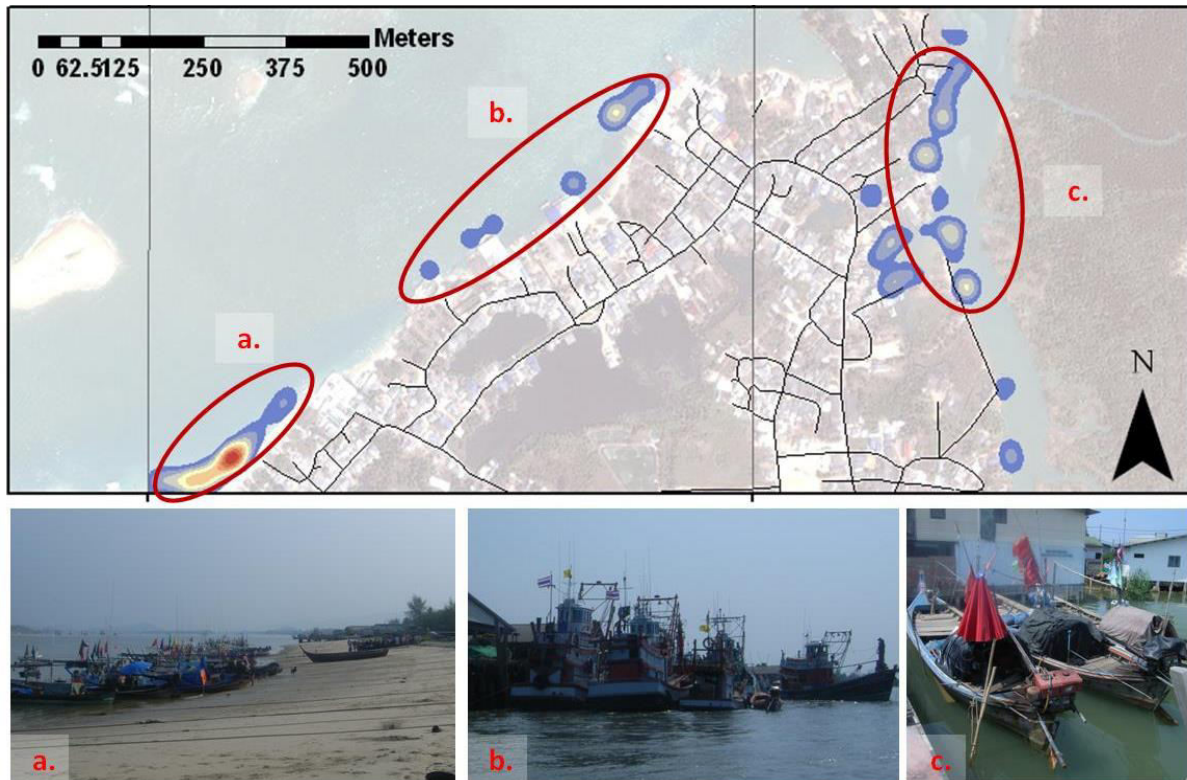


**Figure 3-71: The location of boats observed in satellite imagery acquired in February-2009: site (a). long-tail boats, (b). large trawlers and (c). mangrove fishers and boat repair yard.**

Care must be taken when interpreting these results. The Department of Fisheries warned about interpreting absolute boat numbers as an indicator of livelihood and a focus group meeting in Ban Nam Khem highlighted that although there are now many more boats than before the tsunami, there were still people who used to have boats that now don't.

Most of the new long-tail boats were provided by local and national NGOs but government compensation was insufficient to repair or replace many boats and gear (Roberts, 2005). Unregistered boats were also not eligible for state compensation and fuel prices increased by 40% preventing many people from continuing to earn a living by fishing.

## Discussion

Both remote sensing and ground surveys were used to identify and describe the spatial disparity and abundance of major sources of livelihood in Ban Nam Khem. The ground survey identified at least 22 forms of livelihood encompassing a wide range of sectors, including agriculture, fishing and manufacturing. The presence of so many businesses throughout Ban Nam Khem suggests that there is a comfortable economy there, with less reliance on few, vulnerable sectors of the economy. Remote sensing was used to monitor some of the more conspicuous forms of livelihood such as shrimp hatcheries, grow-out ponds, piers and boats. In summary, it showed that shrimp hatcheries were destroyed by the waves and not built back, while grow-out ponds were protected by mangrove forests; the presence of pumps in the ponds throughout the recovery process suggest that the productivity remained constant. Piers were also totally destroyed by the waves but were built back within one year and were being used by long-tail boats, trawlers and a car ferry. Tourist resorts in the area were also reconstructed within a year of the disaster.

Despite the level of detail obtainable with remote sensing, it is still very difficult to translate the remote sensing observations into actual employment figures. At best, it can be used to comment on the timing and extent of recovery of various conspicuous sectors. The household survey, in contrast, was able to estimate the proportion of households working in particular sectors at various points in time. It also identified various issues being faced by workers in different sectors. The focus group meetings and key informant surveys were also useful to identify general issues faced by workers in Ban Nam Khem. For example, the focus group meeting informed us that despite the large number of boats available in Ban Nam Khem there were still many households without access to one.

Despite the limitations associated with the use of satellite imagery, it was still able to provide a significant amount of information and it is possible that some remote sensing observations may be used to infer the overall level of recovery in certain sectors. For example, the household survey results suggest that approximately 57% of fishers were working again within one year of the tsunami. At the same time, 67% of boats had returned to fishing piers. Figure 3-72 shows the proportion of fishers working and the length of pier both normalized to the pre-disaster state. The *number of fishers* was obtained from the household survey, while *pier length* was acquired from satellite imagery. The results match each other relatively well, which suggests that *pier length* might be used to infer the recovery of

the fishers' livelihood. During the household interviews, the fishers told us that it took several years for them to return to their jobs. The recovery was relatively slow for a number of reasons including high oil price, low fish resources and a decrease in the price of products.

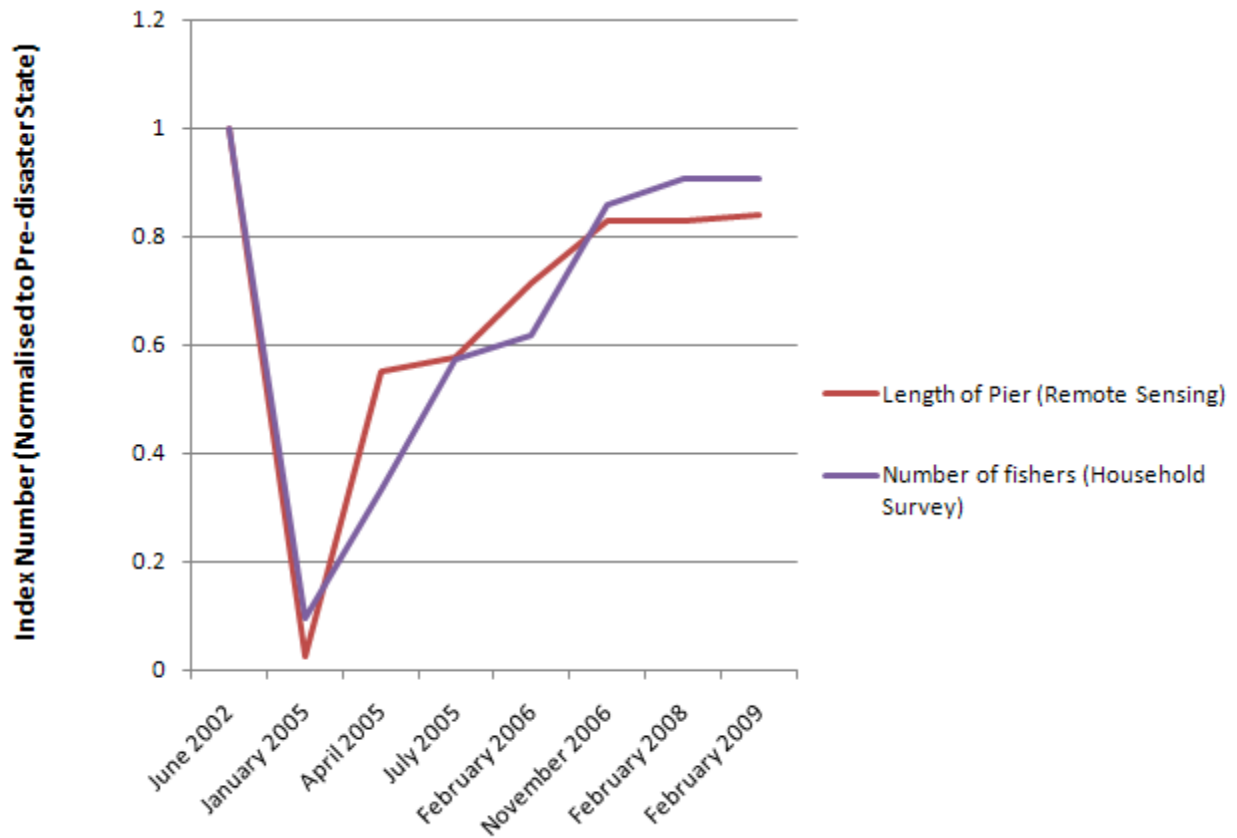


Figure 3-72: The number of fishers and the length of pier after the 2004 tsunami normalized to the pre-disaster state.

## Section 6: Services and Utilities

This section describes a range of techniques that can be used to monitor services and facilities in an area. Services and facilities are defined here to include all aspects of the built-up environment that contribute to the functioning of a successful and cohesive community - for example, health and education facilities, emergency services and places of worship. They are monitored by observing changes to structures and other features that contribute to their operation; power was additionally inferred by measuring night-time light radiance.

### Indicator 12. Services and Facilities

#### Remote Sensing Methodology

Monitoring services and facilities first requires features or groups of features associated with the services to be mapped across the affected region. Services and facilities often have a unique *cultural signature* in satellite imagery, defined as the assemblage of specific materials and structures, that allow them to be identified (Jensen, 2007). Large schools and temples for example may often be identified using satellite imagery alone by analysing the buildings' structural attributes, decoration and clues in the immediate environment. These cultural signatures can be generalised but are likely to vary from culture-to-culture. Table 3-11 lists some of the physical attributes visible in clear, high-spatial-resolution satellite imagery that can be used to indicate some building's use in many U.S. and European built-up areas.

Building Type	Cultural Signature Attributes
Commercial	Variable building size Densely-packed buildings Air vents Near-by car park Sometimes on a main high street (often straight)
Education Facilities	Playground Playing Field Parking Area Road Markings
Factories	Chimneys Lorries / heavy vehicles Warehouse structures Other handling equipment (e.g. plant equipment, bulldozers, cranes) Transportation near-by to move raw materials around the site (e.g. conveyors, pipelines, railroads)
Hospital	Large Building(s) Helipad Ambulances Car park
Homes	Regular building size and shape Driveway Garden Garage
Hotels	Multi-storey building(s) Swimming pool Tennis Court

**Table 3-11: Physical attributes used to indicate building use.**

Many services lack these unique cultural signatures – especially if they are accommodated in a non-descript building with no visible clues in the immediate vicinity, in which case their use is often indecipherable in satellite imagery without the integration of ground data. The creation of a comprehensive GIS database of services and facilities therefore requires the integration of other in-situ datasets, such as geo-referenced notes and images and/or the location of features incorporated from existing paper or electronic maps.

Once a service’s location has been established, information about its abundance, speed of recovery and location, in particular its proximity and accessibility to households and businesses, can be analysed using remote sensing. In some cases, effective data standards have been produced by leading agencies that can be used to determine their data requirements after a disaster, such as the PAHO’s data model for health facilities (PAHO, 2010b).

## Results

A detailed geodatabase of services and facilities in Ban Nam Khem was first created using satellite image analysis and ground deployment. As expected, some buildings had a distinctive cultural signature and their use was identifiable in the satellite imagery, for example temples had large pitched red roofs and school buildings were located near to playing fields. The use of non-descript buildings though, such as the police station, health centre and other services, were identified by ground surveys and by officials during the key informant interviews. The resulting service database contained 30 features representing 18 different services, including a temple, church, school, water office, library and police station (figure 3-73).

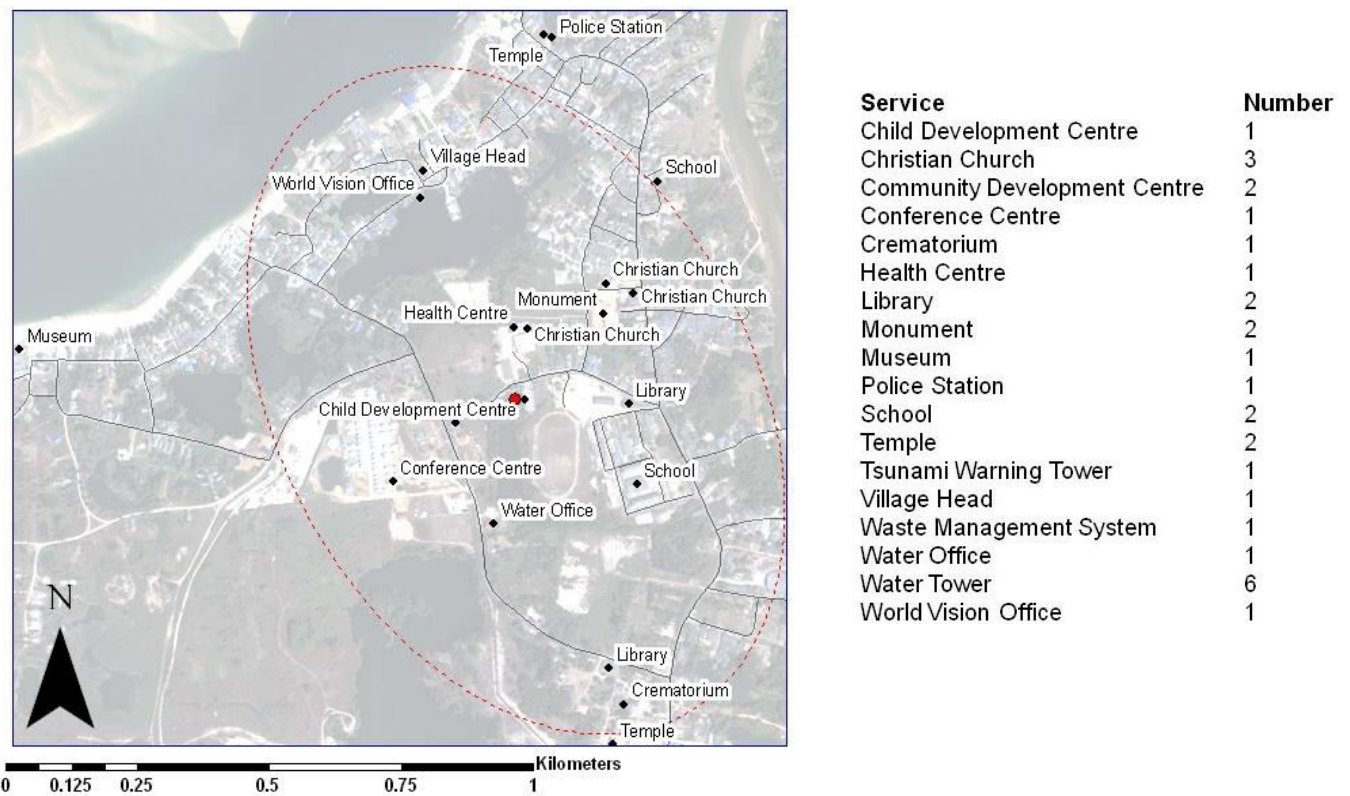


Figure 3-73: Ban Nam Khem's service and facility database.

The results show that a diverse range of facilities are now available in the village with good access for most households. The number and distribution of services before the tsunami is not available for comparison, but the pre-disaster image was used to establish that several new services had appeared during the recovery process, including the community development centre, the conference centre and several Christian churches. The presence of these religious buildings as a result of the NGO-led recovery process was highly controversial, with a number of people complaining about their dominant presence in a predominantly Buddhist country.

The service map in figure 3-73 shows the distribution of the services throughout Ban Nam Khem. A new temple and school building were constructed on their original sites, while health facilities were transferred to a new location slightly further from the coast. Many of the key services present, such as the community centre and the school, are located in the centre of the village - 1.0 km from the coastline in an area that is slightly elevated and considered to be relatively less vulnerable to flooding.

The speed of reconstruction and other detailed attributes were measured for 5 of the main services in Ban Nam Khem using remote sensing, including the temple, school, community centre, police station and museum. The results of the detailed analysis were then verified using ground photography. Figure 3-74 shows the site of the temple and the main school in Ban Nam Khem in February-2009 with field photographs collected at the same time highlighting particular features of interest.



**Figure 3-74 Site of Ban Nam Khem temple (left) and school (right) surveyed with satellite imagery and ground photography.**

All of the service buildings in Ban Nam Khem were reconstructed between April-2005 and February-2006 (14 months after the tsunami), except for the temple which was not completed until 4 years after the tsunami. The construction of the school was particularly rapid, with all of the walls and part of the roof already constructed by April-2005 (only 4 months after the tsunami). Figure 3-75 shows a time-line of key events at Ban Nam Khem school collected with satellite imagery only.

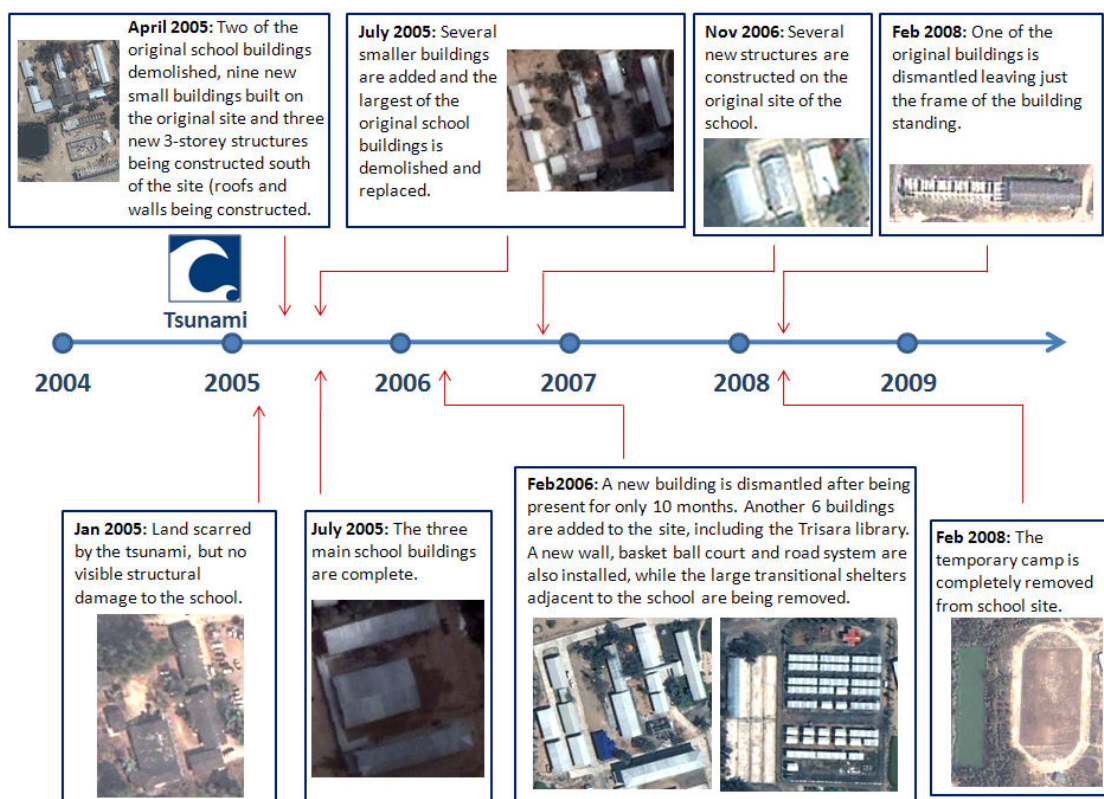
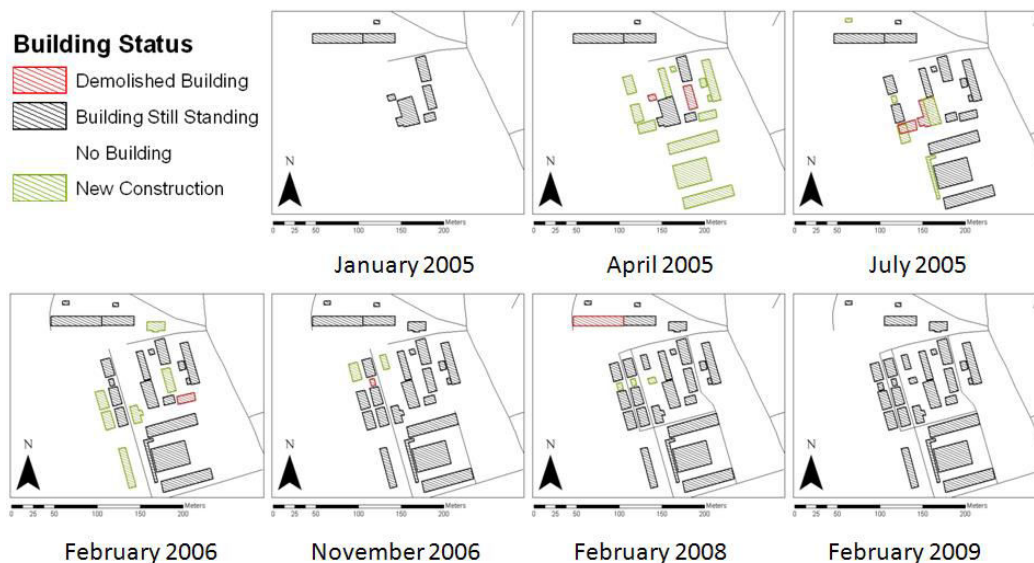


Figure 3-75: Time-line of events at Ban Nam Khem School.

Although the damage to the school was not visible in the satellite imagery, published reports suggested that the lower floor of the 2-storey school was destroyed along with teaching resources – highlighting weakness of remote sensing as a primary damage assessment tool. Key informants claimed that Ban Nam Khem School reopened after one month and that volunteers helped with the teaching in the school-yard. These reports match remote sensing analysis which shows several temporary structures on the school grounds in April-2005. These structures were presumably being used for teaching, but their use could not be identified in the satellite imagery alone. Agency reports suggest that the new school building was finished in six months by the military. These reports again match the remote sensing

analysis which showed most of the school-buildings were near completion in April-2005 and that the buildings appeared to be in-use from February-2006 onwards. There are now more buildings than there were before the tsunami, including two 3-storey buildings and a multi-purpose building containing a kindergarten, library and activity room.



**Figure 3-76: Building analysis of Ban Nam Khem School site throughout the recovery process shows the construction of permanent and temporary structures.**

## Discussion

This work shows how remote sensing may be used to create a geospatial database and framework that can host service and facility information across an affected region. Such a system is vital when monitoring the status of key services across an affected area and can be used to assist decision-making on the ground.

Some prominent services were identified using satellite imagery analysis alone, such as the temple and the school. Certain generalisations can be made about the cultural signatures of some services that allow them to be identifiable in satellite imagery. These signatures can often be very sensitive to the culture of the region being studied though so it is particularly important that the analyst is fully aware of these cultural nuances before conducting the analysis (Jensen et al., 2002).

Some services in Ban Nam Khem were missed or misclassified by the image analysis including the police station and community centre. The satellite image analysis of services was certainly found to be more effective with the integration of in-situ datasets. This was also the case after the 2010 Haiti earthquake where volunteers used many inventive ways of logging the location of 150 health facilities, including public internet searches, ground surveys on mopeds as well as aerial imagery analysis (WikiProjectHaiti, 2010; PAHO, 2010a).

After a facility or service was identified in the imagery in Ban Nam Khem, remote sensing was used to monitor changes to the features associated with the service, their accessibility, location, vulnerability and the speed of reconstruction. Remote sensing was not always able to explain the physical changes on the ground, but in these cases the observations were often quickly verified and explained by a carefully-selected key informant.

Of course detailed aspects of a service may be monitored more reliably with a mixed-method approach using household surveys and published statistics (USAID *et al.* 2004). The household survey in particular, proved to be a significant source of detailed, valuable information on the restoration and quality of services available in Ban Nam Khem. The work presented in this chapter though has still shown that remote sensing can provide a substantial amount of useful information to monitor and verify the recovery of key services.

### **Indicator 13. Utilities – Power, Water and Sanitation<sup>1</sup>**

#### **Remote Sensing Methodology**

Automated mapping/facilities management (AM/FM) and geographic information systems (GIS) have been used to manage right-of-way corridors for various utilities in the past (Jadkowski et al. 1994). The ground sample distance (GSD) of the imagery strongly determines what features associated with utilities may be identified and delineated. Satellite imagery with a GSD of 1.0 m is capable of displaying power facilities, such as power stations, transformers and substations. Imagery with a spatial resolution of 0.5 m is capable of showing the presence of local power supply equipment, such as solar panels and wind

---

<sup>1</sup> Due to space constraints only a selection of the Ban Nam Khem remote sensing analysis is included in this thesis. The full analysis results – including the monitoring of water supply features - are available in a set of guidelines written by the author at the end of the Recovery Project (Brown, Platt and Bevington, 2010).

turbines, while smaller features such as utility-poles and cables require a spatial resolution of at least 0.25 m to be visible. Figure 3-77 shows the presence of shadows and cables in 0.25 m aerial imagery of Haiti that indicate the presence of utility-poles and power-lines.



**Figure 3-77: Features required for power-supply observed using aerial imagery of Port-au-Prince after the 2010 Haiti Earthquake.**

While remote sensing can be used to map features associated with the supply of power, night-time light datasets are likely to provide a more informative means of monitoring power by measuring radiance levels over time. Night-time lights have previously been used to monitor a number of processes, including economic activity and CO<sup>2</sup> emissions (Doll *et al.* 2000) and the provision of electricity (Elvidge *et al.* 2010). The data can be acquired by the Operational Linescan System (OLS) on-board a series of satellites belonging to the US Air Force Defense Meteorological Satellite Program (DMSP). Night-time light imagery is currently only available at a resolution of 0.5-2.7 km though, which means the centre of Ban Nam Khem for example would be represented by only 2 pixels.

## Results

As a proof of concept, a time-series of DMSP-OLS annual composite images, covering the Thai and Pakistan case study sites from 2000 to 2009, were acquired from NOAA's National Geophysical Data Center. To create these composite products, cloud-free single orbits were collected for each calendar year, then rectified and aggregated to generate stable light mosaics. The images therefore contain average night-time light values on a relative scale for each year. The Ban Nam Khem composite-images for the years 2002, 2004, 2006 and 2008 are presented in figure 3-78.

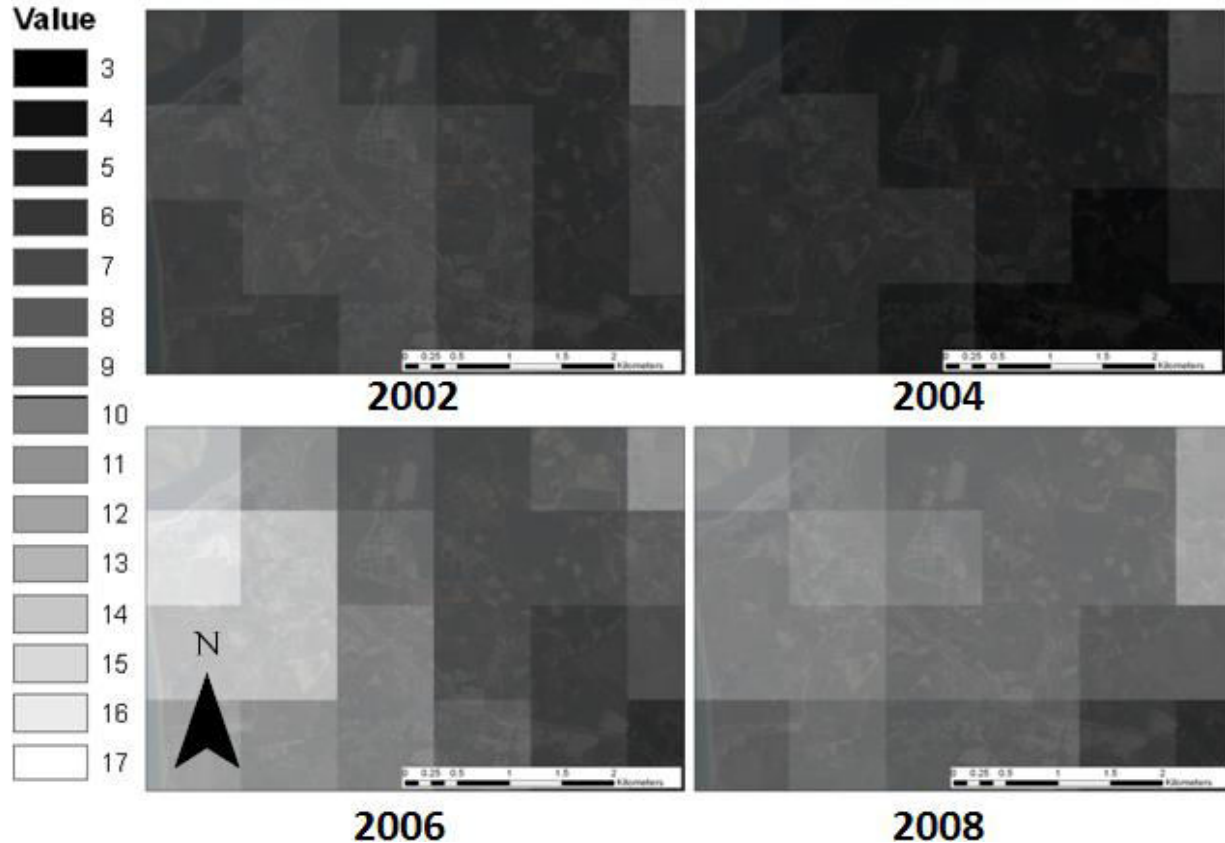


**Figure 3-78: Annual composite night-time light data over Ban Nam Khem before and after the 2004 tsunami.**

The average night-light values in Ban Nam Khem increased after the tsunami peaking during the reconstruction process in 2006, then dropped slightly but remained higher than it was before the disaster. Meanwhile, data from Chella Bandi showed less variability in night-time light values after the 2005 earthquake, possibly due to the bright lights from the near-by city of Muzaffarabad. The increased radiance intensity in Ban Nam Khem after the tsunami is likely to have been caused by increased human activity due to reconstruction and the presence of brightly-lit planned camps during this period. The DMSP-OLS satellites acquire global imagery every 24 hours, so changes in night-time lights over a much shorter period of time may also be monitored but the appropriate data was not accessed for this project. Figure 3-79 shows a comparison of annual composite night-time light values in Ban Nam Khem and Chella Bandi between 2004 and 2009, normalised to pre-disaster conditions.

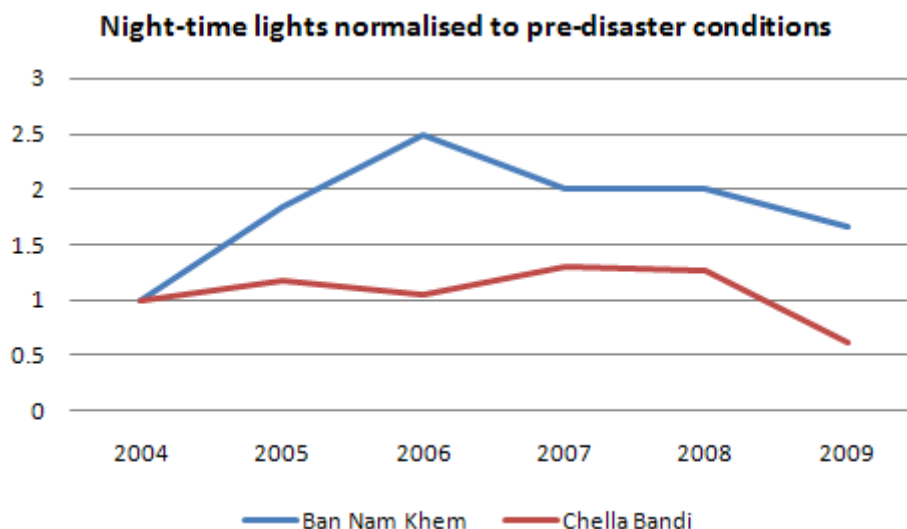


**Figure 3-79: Average night-time lights in Ban Nam Khem and Chella Bandi normalised for pre-disaster condition.**

Households reported that electricity supply was restored to some areas within 3-4 days. Power was supplied to residents of planned camps at no cost for the first year. The key informants separately reported that the mains power was restored after 12 months on average. These observations match the date when a lot of the households had moved into government-supplied properties and also coincides with the peak in radiance observed in the night-time light composites shown above. Apparently temporary and often dangerous measures were adopted by some households that didn't already have access to electricity, by extending electrical cables from the army-built houses. According to the household survey, the supply of power in Ban Nam Khem was not consistent for all households, with 16% complaining of power cuts and others complaining that the current was low and unstable – something that could not be confidently identified with remote sensing alone.

### Discussion

In Ban Nam Khem, optical imagery could not be used to directly monitor the return of power to the village. Individual night-time light images have the potential to show changes in the provision of power but currently at a very low spatial resolution only. Annual night-time light composites, as shown previously, appear to show an increase in radiance during the reconstruction process – an observation that might warrant further investigation using a dataset with greater temporal resolution. The household survey and the key informant interviews acquired useful information on the provision of

power, including the date when mains power was restored to households and businesses, quality and reliability of supply, how a lack of power may have affected households and/or their livelihoods and about price changes.

Remote sensing was also used to monitor features related to the supply of water. In Ban Nam Khem, satellite image analysis identified several features associated with the over-ground supply of water. This over-ground supply of water was of concern to many residents in the village, with many calling for a permanent underground system. Where possible, in-situ data is required to monitor these facilities adequately but using remote sensing to monitor utilities can be particularly useful in difficult-to-access regions such as the Right Bank Drinking Water Treatment Plant in Iraq (SIGIR, 2007) and the Fukushima power facilities after the 2011 Tōhoku earthquake.

## **Conclusion**

This chapter presents a framework and set of remote sensing analyses that can be used to monitor post-disaster recovery. The indicators were developed and applied to Ban Nam Khem, Thailand - which suffered substantial damage after the 2004 Indian Ocean tsunami - and then verified by comparing the results to data acquired with ground survey and social-audit techniques. The remote sensing analyses are divided into six categories based on existing humanitarian frameworks and the needs of users described in chapter 2: accessibility, buildings, transitional settlement/displaced population, natural environment, livelihoods and services/utilities.

To assess changes to the transport network - as a result of damage and subsequent clearance and resurfacing efforts - road length statistics and road maps were produced. A taxonomy consisting of blocked, cleared and reconstructed/resurfaced roads was developed for this purpose. Cleared and resurfaced roads were found to have unique spectral and textural properties that allowed them to be identified in the imagery reliably. Disruption to bridges and conspicuous transport facilities, such as ferry facilities, were also inferred by monitoring their physical-status and activity in the immediate vicinity. Network analysis was then applied to the digitised transport network to monitor changes to accessibility between households, businesses and services, brought about by their relocation and/or changes to the road network.

A multi-scale approach was used to monitor buildings at regional, street and per-building level. A rapid manual analysis and separate semi-automatic Maximum Likelihood classifier were first used to identify the presence of buildings and areas of impervious surface in each satellite image and then change detection was applied to monitor areas of construction and demolition. Standard spatial analyses, such as Kernel Analysis and Nearest Neighbour and more advanced Spatial Metrics, were then applied to groups of buildings to monitor changes to morphology and layout of the built-environment. Information regarding occupants' quality of life and vulnerability were then inferred from these measures. Detailed analysis was also applied to individual buildings selected using a random geographic sampling technique across the whole area – focusing on their physical attributes, spatial context, location, accessibility/connectivity and speed of development.

Emergency and transitional shelters were monitored separately from permanent buildings by monitoring dispersed and planned camps and estimating the displaced population living inside them. Living conditions were also inferred in planned camps and areas of transitional settlement by monitoring density of the camp, placement of infrastructure and the presence of vegetation. The displaced population was estimated based on the type and size of shelters present. Re-settlement in Ban Nam Khem was assumed to be near completion when the camps were dismantled and sufficient numbers of permanent housing were reconstructed in the village to house the displaced population.

Maximum Likelihood and Normalised Difference Vegetation Index (NDVI) were both used to monitor degradation and recovery of the natural environment after the disaster and throughout recovery. In particular, the 5-class Maximum Likelihood classification results successfully highlighted areas of development and areas of degradation as a result of the tsunami and subsequent recovery processes. Landscape metrics were then used to monitor the distribution and fragmentation of green space over time. To improve the reliability of supervised classification in urban environments the author recommends a thorough spectral, spatial and textural analysis of the construction process as it appears in satellite imagery at different stages of development. A detailed spectral and spatial analysis of planned camps and spontaneous settlement is provided in Chapter 5.

A series of proxy indicators were then developed for the final two categories to monitor the recovery of livelihoods, services and utilities. Conspicuous forms of services were identified using their unique cultural signature and their recovery was then inferred by monitoring physical attributes, spatial context, location and connectivity of associated features. The recovery of livelihoods was also inferred here to good-effect by monitoring associated features such as pier length, number of boats and functionality of near-by shrimp ponds. Only a limited number of livelihoods and services were monitored with remote sensing.

Many of the analyses presented here were first conducted by *manually* identifying and mapping features of interest. Where possible, *semi-automated* techniques were used as well as they can often be quicker, and while they generally provide less detail and reliability they can still be very useful for certain applications – in particular, to highlight areas of substantial change for more detailed examination. Maximum Likelihood was particularly useful at identifying different land-cover changes. Object-based image analysis was also used to map features using their spectral, textural and spatial attributes such as

transitional shelters and shrimp ponds. An in-depth examination and comparison of spectral, object-based and textural methods to map a planned camp for UN-Habitat is presented in Chapter 5.

The results presented in this chapter show that remote sensing was used to produce reliable datasets for the first four categories in the table. For example, roads were mapped with 96% accuracy, buildings identified with 82% accuracy, the displaced population in planned camps were estimated to within 10% and the accuracy of the Maximum Likelihood classifications was above 80% for each image except for the post-tsunami image where there was substantial confusion with water-logged soils. In contrast, remote sensing could not be used as reliably to directly monitor aspects of socio-economic recovery – remote sensing could be used to provide proxy indicators for these categories though to infer their recovery. These sectors in particular depend on the integration of ground knowledge derived from social-auditing techniques with that from remote sensing.

The work in this chapter also highlighted a number of limitations and assumptions in each category that are important for analysts to be aware of. Road interpretation for example was less reliable in dense urban areas where road-surfaces were obscured by buildings and shadows. A number of commission and omission errors were also identified when creating the building point database. And without the integration of appropriate ground knowledge the remote sensing analysis wrongly assumed that all roads and buildings in the scene were being used and had not been abandoned. Sometimes clues in the immediate vicinity of these features may indicate their possible use, such as parked cars. If a client requires more detailed or more reliable products then ground techniques may be conducted alongside, before or after the remote sensing analysis.

The deployment of ground survey and social-audit tools here highlighted many processes not identifiable using remote sensing, including social and political processes related to land disputes, as well as educational and nutritional standards, gender equality and other aspects of social recovery. The cross-comparison of results from each of the tools also helped to highlight each tool's strengths and weaknesses stressing the need for a multi-tool approach to monitoring recovery. A suggested workflow for the use of these various tools is provided in the conclusion of this thesis based on the experiences in Thailand, Pakistan and Haiti.

After the completion of this work the indicators were presented to staff at the British Red Cross who then chose appropriate indicators for their reconstruction project in Haiti. The indicators were then applied in real-time in an operational environment which allowed their suitability to a particular type of project to be thoroughly tested. The use of remote sensing during the response, planning and monitoring phases of the Red Cross project, including the use of the indicators developed here, is mapped and described in detail in the next chapter.

## **Bibliography**

ADPC (2005a). *Thailand - Post rapid assessment report: Dec 26th 2004 tsunami*. Asian Disaster Preparedness Center. Available at:  
[http://www.adpc.net/v2007/ikm/ONLINE%20DOCUMENTS/downloads/TsunamiRapidAssessmentReport\\_15Feb.pdf](http://www.adpc.net/v2007/ikm/ONLINE%20DOCUMENTS/downloads/TsunamiRapidAssessmentReport_15Feb.pdf)

ADPC (2005b). *The economic impact of the 26 December 2004 earthquake & Indian Ocean tsunami in Thailand*. Asian Disaster Preparedness Center.

Adler-Golden, S. M., Matthew, M. W., Bernstein, L. S., Levine, R. Y., Berk, A., Richtsmeier, S. C., Acharya, P. K., Anderson, G. P., Felde, G., Gardner, J., Hoke, M., Jeong, L. S., Pukall, B., Ratkowski, A. and H.-H. Burke (1999). Atmospheric correction for short-wave spectral imagery based on MODTRAN4. *SPIE Proceedings on Imaging Spectrometry*: **3753**, 61-69.

Anderson, J. R., Hardy, E. E., Roach, J. T. and Witmer, R. E. (1976). A land use and land cover classification system for use with remote sensor data. *Geological Survey Professional Paper*: **964**. USGS, Reston, Virginia.

Arroyo-Moya, J.P., Sanchez-Azofeifa, G.A., Rivard, B., Calco, J.C. and Janzen, D.H. (2005). Dynamics in landscape structure and composition for Chorotega region, Costa Rica from 1960 to 2000. *Agriculture, Ecosystems and Environment*: **106**, 27-39.

Arunmas, P. (2005). No Relief in Sight. *Bangkok Post*. 03 July 2005.

Baumgartner, M. D. a. P. (2006). *Under construction: A descriptive report on the post-tsunami reconstruction processes in Khao Lak, Thailand and Banda Aceh, Indonesia*. P. S. G. O. D. Research.

Bevington, J., Adams, B. and Eguchi, R. (2010) GEO-CAN debuts to map Haiti damage. *Imaging Notes*: **25** (2).

Bhumiprabhas, S. (2005). A second wave hits Baan Nam Khem. Tsunami. One Year On. *The Nation Newspaper*. 13 December, 2005. Available at:

<http://www.nationmultimedia.com/specials/tsunami/tsunami2.php>

Brown, D., Platt, D. and Bevington, J. (2010). Disaster recovery indicators. Centre for Risk in the Built Environment. Cambridge University, UK.

Brown, D. Saito, K., Liu, M., Spence, R., So, E. and Ramage, M. (2012). The use of remotely sensed data and ground survey tools to assess damage and monitor early recovery following the 12.5.2008 Wenchuan earthquake in China. *Bulletin of Earthquake Engineering*: **10** (3), 741-764.

Cai, J., Leung, P. and Hishamunda, N. (2009). *Assessment of comparative advantage in aquaculture. Framework and application on selected species in developing countries*. Food and Agriculture Organisation of the United Nations (FAO). Rome, Italy.

Cheng, P. and Chaapel, C. (2009). *Pan-sharpening and geometric correction. WorldView-2 satellite*. PCI Geomatics. Available at: [http://www.pcigeomatics.com/pdf/GeoInformatics\\_WorldView-2.pdf](http://www.pcigeomatics.com/pdf/GeoInformatics_WorldView-2.pdf)

COHRE (2005). Asian tsunami, evictions and land rights monitoring. Centre on Housing Rights and Evictions.

CODI. (2005). *Relief and rehabilitation activities for tsunami affected communities in south Thailand: a report on the activities of CODI*. Original report in Thai. Community Development Organisation. December 2005.

Corsellis, T. and Vitale, A. (2005). *Transitional settlement - displaced populations*. The University of Cambridge, Shelter Project & Oxfam GB.

Cowen, D.J. and Jensen, J.R. (1998). Extraction and modelling of urban attributes using remote sensing technology. In *People and Pixels*. Liverman, D., Moran, E.F., Rindfuss, R.R. and Stern, P.C. (eds.) National Academy Press. Washington D.C.

Digital Globe (2005). *Quickbird Imagery Products FAQ*. 22 May 2005.

Doll, C.N.H., Muller, J.P. and Elvidge, C.D. (2000). Night-time imagery as a tool for global mapping of socioeconomic parameters and greenhouse gas emissions. *Ambio*: **29**, 157-162.

Elvidge, C.D., Baugh, K.E., Sutton, P.C., Bhaduri, B., Tuttle, B.T., Ghosh, T., Ziskin, D. and Erwin, E.H. (2010). Who's in the dark: Satellite based estimates of electrification rates. In: Yang, X. (ed). *Urban Remote Sensing: Monitoring synthesis and modelling in the urban environment*. Wiley-Blackwell, Chichester.

ENVI. (2009). *Atmospheric correction module: QUAC and FLAASH User's Guide. Version 4.7*. August 2009 edition.

ERRA-UN. (2007). *ERRA-UN Early recovery plan – final report*. June 2006 – May 2007. Available at: <http://www.china-up.com:8080/international/case/case/890.pdf>

Frohn, R.C. (1998). *Remote Sensing for Landscape Ecology. New metric indicators for monitoring, modelling, and assessment of ecosystems*. Lewis Publishers, Boca Raton.

Gao, B. and Goetz, A. (1990). Column atmospheric water vapor and vegetation liquid water, retrievals from airborne imaging spectrometer data. *Journal of Geophysical Research*: **95** (D4), 3549-3564.

Gates, D.M., Keegan, J.J., Schleter, J.C. and Weidner, V.R. (1965). Spectral properties of plants. *Applied optics*: **4** (1), 11-20.

Ghosh, S., Huyck, C.K., Adams, B.J. and Eguchi, R.T. (2005). *Preliminary field report: Post-tsunami urban damage survey in Thailand, using the VIEWS reconnaissance system*. MCEER, University of Buffalo.  
<http://mceer.buffalo.edu/research/Reconnaissance/tsunami12-26-04/page1.asp>

Ghosh, S., Adams, B.J., Womble, J.A., Friedland, C. and Eguchi, R.T. (2007). Deployment of remote sensing technology for multi-hazard post-Katrina damage assessment. *The 2<sup>nd</sup> International Conference on Urban Disaster Reduction*. Taipei, Taiwan. November 27-29, 2007.

Grodecki, J. and Dial, G. (2003). Block adjustment of high-resolution satellite images described by rational functions. *Photogrammetric Engineering and Remote Sensing*: **69** (1), 59-68.

Herold, M., Roberts, D.A., Gardner, M.E. and Dennison, P.E. (2004). Spectrometry for urban area remote sensing – development and analysis of a spectral library from 250 to 2400 nm. *Remote Sensing of Environment*: **91**, 304-219.

Hubing, N. (2012). Buying optical satellite imagery? *Earth Imaging Journal*. June 12, 2012. Available at:  
<http://eijournal.com/2012/buying-optical-satellite-imagery>

Norwegian Geotechnical Institute. (2006). *Tsunami risk mitigation measures with focus on land use and rehabilitation*. Oslo, Norway. Available at:  
[http://www.ccop.or.th/download/pub/tsunami\\_final\\_report.pdf](http://www.ccop.or.th/download/pub/tsunami_final_report.pdf)

Jackson, L.E. (2003). The relationship of urban design to human health and condition. *Landscape and Urban Planning*: **64**, 191-200.

Jadkowski, M.A., Convery, P., Birk, R.J. and Kuo, S. (1994). Aerial image databases for pipeline rights-of-way management. *Photogrammetric Engineering & Remote Sensing*: **60** (3), 347-353.

Jensen, J.R. (1996). *Introductory Digital Image Processing: A Remote Sensing Perspective*. Prentice-Hall, Saddle River, New Jersey

Jensen, J. R., Botchway, K., Brennan-Galvin, E., Johannsen, C., Juma, C., Mabogunje, A., Miller, R., Price, K., Reining, P., Skole, D., Stancioff, A. and Taylor, D. R. F. (2002). *Down to Earth: Geographic Information for Sustainable Development in Africa*. National Research Council, Washington D.C.

Jensen, J.R. (2007). *Remote sensing of the environment. An earth resource perspective. 2<sup>nd</sup> edition*. Pearson, New Jersey.

Jordan, C. F. (1969). Derivation of leaf area index from quality of light on the forest floor. *Ecology*: **50**, 663–666.

Kamsaen, S. (2005). World Vision World Wide shares the responsibility in aftershock tsunami. Feature Story. *World Vision Newsletter*. Available at: [http://www.worldvision.or.th/newsletter/index\\_t.htm](http://www.worldvision.or.th/newsletter/index_t.htm)

Kerr, T. (2005). The Relief Camp at Bang Muang. *Housing by People in Asia*: **16**, 33. Asian Coalition for Housing Rights Website. Available at: [http://www.preventionweb.net/files/2077\\_VL108806.pdf](http://www.preventionweb.net/files/2077_VL108806.pdf)

Knoblauch, R., Pietrucha, M. and Nitzburg, M. (1996). Field studies of pedestrian walking speed and start-up time. *Journal of the Transportation Research Board*: 1538, 27-38.

Lo, C.P. and Faber, B.J. (1997). Integration of Landsat Thematic Mapper and census data for quality of life assessment. *Remote Sensing of Environment*: **62**, 143–157

Lyon, J.G., Yuan, D., Lunetta, R.S. and C.D. Elvidge. (1998). A change detection experiment using vegetation indices. *Photogrammetric engineering and remote sensing*: **64** (2), 143-150.

ONEP (2005). Emergency Relief. Office of Natural Resources and Environmental Policy and Planning. Available at: [http://www.onep.go.th/tsunami//Tsunami\\_Eng/menu5.asp](http://www.onep.go.th/tsunami//Tsunami_Eng/menu5.asp)

Matthew, M. W., Adler-Golden, S. M. Berk, A., Richtsmeier, S. C. Levine, R. Y., Bernstein, L. S., Acharya, P. K., Anderson, G. P., Felde, G. W., Hoke, M. P., Ratkowski, A., Burke, H.-H., Kaiser, R. D. and Miller, D. P. (2000). Status of atmospheric correction using a MODTRAN 4-based algorithm. *Proceedings of SPIE – The International Society for Optical Engineering*: **4049** (11), 199-207.

McGarigal, K. and Marks, B.J. (1994). *FRAGSTATS: Spatial pattern analysis program for quantifying landscape structure. Version 2*. USDA Forest Service. Washington D.C.

ONEP Focus Group (2005). Conclusion of the focus group meeting of Bang Muang Sub-district, Takua Pa District, Phang-nga Province. Bang Muang TAO Conference Room. 20 September 2005.

PAHO (2010a). Haiti Health Facility Data, MSPP Haiti. Cartography: UN/MINUSTAD, 2010. Pan American Health Organisation (PAHO).

PAHO (2010b). *Field Definitions and Master Data*. Updated March 11 (Version 6). Pan American Health Organisation (PAHO). Available at: <http://sites.google.com/a/netspective.org/haiti-health-facilities/home/field-definitions--master-data>

Paphavasit, N., Chotiyaputta, C. and Siriboon, S. (2007). Pre-and post-tsunami coastal planning and land-use policies and issues in Thailand. In: *Proceedings of the workshop on coastal area planning and management in Asian tsunami-affected countries*. 27-29 September 2006, Bangkok, Thailand. Food and Agriculture Organisation (FAO). <http://www.fao.org/docrep/010/ag124e/AG124E00.HTM>

Phuket Gazette. (2005). Patong clear of tsunami debris. *Phuket Gazette*: **12** (3).

Radarheinrich (2005). Tsunami Achieve & Storm Chasing. 4 April 2005. Available at: <http://www.radarheinrich.de/wbblite/thread.php?threadid=347>

Ritters, K.H. O'Neill, R.V., Hunsaker, C.T., Wickham, J.D., Yankee, D.H., Timmins, S.P., Jones, K.B. and Jackson, B.L. (1995). A factor analysis of landscape pattern and structure metrics. *Landscape Ecology*: 10 (1): 23-39.

Roberts, J. (2005). Thai government puts tourism ahead of the poor in tsunami relief effort. World Socialist Web Site. Available at: <http://www.wsws.org/articles/2005/jan2005/thai-j17.shtml>

Rouse, J.W., Haas, R.H., Schell, J.A. and Deering, D.W. (1974). Monitoring vegetation systems in the Great Plains with ERTS. *Proceedings of the Third Earth Resources Technology Satellite-1 Symposium*: **1**, 309. NASA, Washington D.C.

Running, S. W., Justice, C.O., Salomonson, V., Hall, D., Barker, J., Kaufmann, Y.J., Strahler, A.H., Huete, A.R., Wan, Z.M., Teillet P. and Carneggie, D. (1994). Terrestrial remote sensing science and algorithms planned for EOS/MODIS. *International Journal of Remote Sensing*: **15** (17), 3587-3620.

SIGIR (2007). *Right Bank Drinking Water Treatment Plant Rehabilitation*. Commander's Emergency Response Program. Ninewa Governorate, Iraq. Sustainment Assessment. Office of the Special Inspector General for Iraq Reconstruction. SIGIR PA-07-106. Available at:  
<http://www.dtic.mil/dtic/tr/fulltext/u2/a529182.pdf>

Sphere Project. (2011). *Sphere Handbook: Humanitarian Charter and Minimum Standards in Disaster Response*. Practical Action Publishing, Rugby, UK.

Taubenböck, H., Post, J., Roth, A., Zosseder, K., Strunz, G. and Dech, S. (2008). A conceptual vulnerability and risk framework as outline to identify capabilities of remote sensing. *Natural Hazards and Earth Systems*: **8**, 409-420.

Umitsu, M., Tanavud, C. and Patanakanog, B. (2007). Effects of landforms on tsunami flow in the plains of Banda Aceh, Indonesia, and Nam Khem, Thailand. *Marine Geology*: **242**, 141-153.

UN Country Team. (2005). *Tsunami Thailand — one year later: national response and contribution of international partners*. Joint publication by the United Nations Country Team with lead support from UNDP and the World Bank.

UNDP, World Bank and FAO (2005). *Livelihood Recovery and Environmental Rehabilitation*. Thailand. Joint Tsunami Disaster Assessment Mission. Available at:  
<http://reliefweb.int/sites/reliefweb.int/files/resources/1A86FCEBEA89413685256F8E006830A1-undp-tha-10jan.pdf>

UNHCR. (2007). *UNHCR Handbook for Emergencies*. Third edition. Geneva, Switzerland.

Updike, T. and Comp, C. (2010). *Radiometric Use of WorldView-2 Imagery*. Technical note. Digital Globe Inc., Longmont, Colorado.

USAID, ORC Macro, UNICEF and FASAF (2004). *Guide to the Analysis and Use of Household Survey and Census Education Data*. Washington D.C. Available at:

<http://www.uis.unesco.org/Library/Documents/hhsguide04-en.pdf>

USGS (2004). *Magnitude 9.1 – off the west coast of Northern Sumatra*. U.S. Geological Survey, California.

Ushahidi (2010). Available at: <http://www.usahidi.com/>

Vaccari, M., Collivignarelli, C., Tharnpoophasiam, P. and Vitali, F. (2010). Wells sanitary inspection and water quality monitoring in Ban Nam Khem (Thailand) 30 months after 2004 Indian Ocean tsunami. *Environmental Monitoring and Assessment*: **161**. 123-133.

WikiProjectHaiti (2010). *WikiProject Haiti/Status/Hospitals*. Available at: [http://wiki.openstreetmap.org/wiki/WikiProject\\_Haiti/Status/Hospitals](http://wiki.openstreetmap.org/wiki/WikiProject_Haiti/Status/Hospitals)

## **Chapter 4: Mapping the use of geospatial tools during the planning and implementation of a British Red Cross Integrated Recovery Programme after the 2010 Haiti earthquake**

### **4.1. Introduction: Aims and Content of the Chapter**

The development of an indicator table for monitoring post-disaster recovery with remote sensing is described in Chapter 2. After its development, these indicators were applied retrospectively to areas in Thailand and Pakistan that had experienced post-disaster recovery, the results of which are presented in Chapter 3. A follow-up to the original Recovery Project took place between 2011 and 2012 and allowed geospatial tools to be applied to recovery projects in real-time to explore their usefulness and how they might be operationalized (Brown, Platt and Bevington, 2010).

This chapter and the next describe work conducted for the follow-up Recovery Project, which included a 3-month deployment to Port-au-Prince, Haiti between September and November 2011. The aim of the work was to verify who the users of the techniques were likely to be and to establish when and how geospatial data and techniques might be used. To help answer these questions geospatial and information management support was provided to humanitarian and non-government agencies responding to the 2010 Haiti earthquake.

Technical and capacity support was provided to an integrated recovery programme in Delmas 19, Port-au-Prince led by the British Red Cross, focusing on 1) the use of remote sensing as a needs assessment tool and 2) GIS as a planning and monitoring tool and 3) Community mapping to assist the participatory process. This allowed the information needs and decision-making processes of an aid agency to be mapped and better understood. This work will provide a unique insight into the sector and will show how the proposed indicators in Chapter 2 align with current operational thinking. This is deemed important to ensure uptake of the proposed indicators. As outlined in the framework in chapter 1, this chapter will also contribute knowledge to the mapping of humanitarian information needs, which is an important and growing area of scientific interest in itself. In this chapter the assessment of a complex urban slum using manual analysis of satellite imagery is also verified by comparing the results of the remote analysis to accurate cadastral maps created on the ground. Three forms of semi-automatic

analysis were used to monitor planned camps and instances of spontaneous settlement for UN-Habitat, the results of which are described in Chapter 5. Through these various case studies the reliability of manual and semi-automatic analysis of satellite imagery is tested thoroughly in multiple recovery contexts and across several geographic scales.

The British Red Cross (BRC) and UN-Habitat represent two very different agencies in Haiti, operating at different geographic scales with very different objectives and data needs. BRC can be thought of as an *implementing* agency conducting recovery and construction work on behalf of beneficiaries. Their integrated recovery project was for a community of around 500 households and consisted of shelter, livelihood, water and sanitation components. A remote assessment of the site was conducted using remote sensing techniques between April and August 2011. A ground deployment by the author then coincided with the aggregation of enumeration and cadastral datasets and a series of internal planning and project design meetings.

UN-Habitat represents a *coordinating* agency as well as an implementing agency, providing support to the government and agencies involved in the response to the earthquake. UN-Habitat is mandated by the UN General Assembly to promote socially and environmentally sustainable towns and cities with the goal of providing adequate shelter for all. To realise this mandate UN-Habitat requested up-to-date information on 1) the size, condition and content of camps, and 2) the location and extent of on-going reconstruction processes including spontaneous settlement.

The research presented in this chapter and chapter 5 was demand-led by the agencies involved and provides an example of a successful collaboration between academic and humanitarian institutions.

## **4.2. The 2010 Haiti Earthquake**

The 2010 Haiti earthquake of 7.0 Mw occurred at 4:53pm on 12<sup>th</sup> January 2010 at a depth of 10 km. The epicenter was located 25 km west of Port-au-Prince. No strong motion records were available for the main quake so ground motion intensity – such as those displayed in the USGS Shakemap in figure 4-1 – was inferred from observed damage and estimations based on the earthquake magnitude, distance and ground geology. Damage assessment teams identified instances of surface faulting, coastal uplift and liquefaction as a result of the earthquake. Significant liquefaction was observed near to the port which

lies on reclaimed land (Booth et al. 2011). Surveys conducted for the British Red Cross also identified low soil bearing capacity and signs of liquefaction damage near to canal and drainage systems running throughout the Delmas Commune (Potangaroa, Neri and Brown, 2011).

The earthquake caused major damage to residences and commercial buildings across the city of Port-au-Prince and surrounding settlements. Substantial economic, social and physical vulnerabilities that existed in Haiti before the earthquake contributed to its enormous impact. The Port-au-Prince metropolitan area is characterized by high-density, poorly-built slums and a lack of adequate building standards which led to substantial building damage and subsequent injuries and deaths. The government reported that an estimated 315,000 people died while international agencies claim it is more likely to have been around 220,000 people.

The Camp Coordination and Camp Management cluster estimated that 1.5 million people were displaced and living in planned and spontaneous camps several months after the quake. Two years after the earthquake, 550,560 people remained in camps occupying many of the capital's open spaces and thousands of others continued to live in poverty in shantytowns and slums, often exposed to weather and health risks and lacking access to basic services. Reconstruction and repair continued to progress slowly, hampered by a lack of tools, materials and capacity and by the hurricane season. Agencies were put into emergency mode following a major cholera epidemic and security restricted the movement of staff across the capital. Two years after the earthquake, many of the businesses in the downtown area remained closed and the buildings were still in a derelict state waiting to be repaired or demolished.

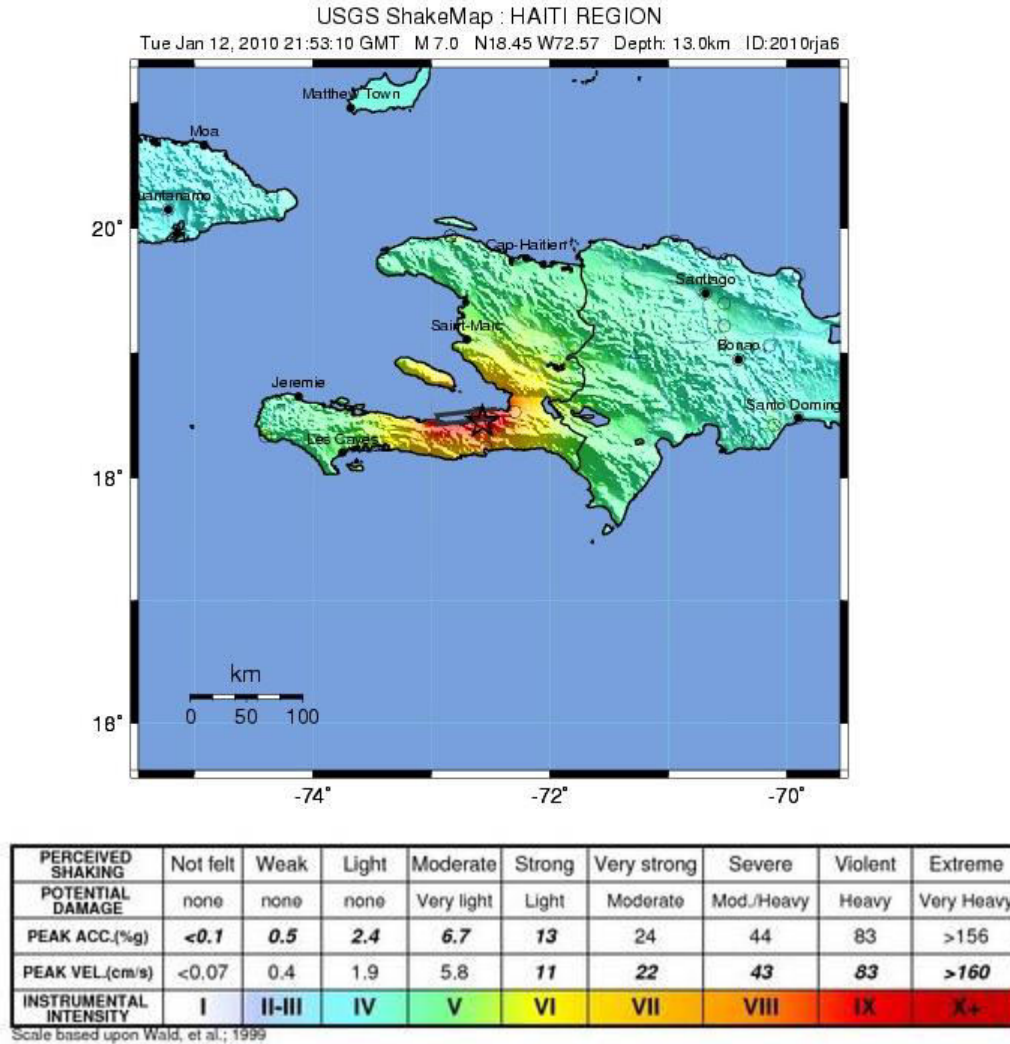


Figure 4-1: USGS Shakemap of the 2010 Haiti earthquake

### 4.3. The Recovery Process in Haiti

#### 4.3.1. Post-Disaster Needs Assessment (PDNA)

The earthquake effectively crippled the Haitian government and it wasn't until 25 January 2010 that the President requested a Post-Disaster Needs Assessment (PDNA). The PDNA measured the economic impact of the disaster across a number of cross-cutting themes and sectors and resulted in a recovery framework outlining early to long-term needs, priorities and resource requirements (Haiti PDNA, 2010). The PDNA arrangement was overseen by the Haitian government but administered by a tripartite agreement between the World Bank, United Nations and European Commission. Substantial support

was also provided by the Inter-American Development Bank (IADB) and other institutions and practitioners worldwide.

The PDNA estimated that the total value of needs amounted to US\$ 11.5 billion over three years, which was broken down to 52% for the social sector, 15% for infrastructure (including housing) and 11% for the environment and risk and disaster management. Following the release of the PDNA report, United Nation member states and international partners pledged \$5.3 billion over 18 months at a donor conference in New York on 31 March 2010. UNOCHA's Financial Tracking Service reported one and a half years later that only US\$ 3.5 billion had been contributed or legally committed to the response<sup>1</sup>. To coincide with the release of the PDNA the Government produced the *Action Plan for National Recovery and Development in Haiti*. In this document the Government called for structural changes across the entire nation, a reverse of the spiral of vulnerability and a stimulation of the economic environment in the country. The report is based around four areas of work: territorial, economic, social and institutional rebuilding with cross-cutting themes for each field. The plan is also divided into two temporal phases. The first is the immediate response, which lasted for 18 months, encompassing the end of the emergency period and the preparation of projects. The full recovery stage was allocated a window of ten years, allowing it to take into account three programming cycles of the National Strategy for Growth and Poverty Reduction (Government of the Republic of Haiti, 2010).

#### *4.3.2. Reconstruction: Design and Planning*

Relief and recovery support was provided by a range of different organisations: government ministries, private entities, NGOs and multilateral agencies, many of whom were providing support in the country before the earthquake. In October 2011, 427 agencies had reported to the Shelter cluster alone that they were operating in Haiti. Of these, 202 were national partners, 189 international NGOs, 16 international organizations, 11 government partners and 9 UN agencies<sup>2</sup>.

The Cluster system was established in Haiti in 2009 by the UN's Inter-Agency Standing Committee (IASC) to provide support and coordination to the agencies working there. Table 4-1 lists the 12 cluster groups

---

<sup>1</sup> Financial Tracking Service: <http://fts.unocha.org/> (last viewed on 8 December 2011).

<sup>2</sup> More information on the organisations working in Haiti is available from OCHA's Who What Where section of the Humanitarian Response website: <http://haiti.humanitarianresponse.info>

operating at the end of 2011. In October 2011 the Shelter cluster and Camp Coordination and Camp Management (CCCM) cluster were merged to form the *CCCM/Shelter/Non Food Items* cluster led by the International Organisation for Migration (IOM). The focus of the cluster was to support the camp population and the return of the remaining camp population to their homes through the use of rental subsidies, host family grant support, permanent housing repair/reconstruction, and the provision of transitional shelters.

Cluster	Coordinator(s)	Cluster	Coordinator(s)
Agriculture	FAO	Health	PAHO/WHO
CCCM/Shelter/NFI	IOM	Inter-cluster	OCHA
Early Recovery	UNDP	Logistics	WFP
Education	UNICEF	Nutrition	UNICEF
Emergency Telecom	WFP	Protection	ONCHR
Food	WFP	Water	UNICEF

**Table 4-1: Cluster groups and cluster coordinators operating in Haiti two years after the earthquake.**

The CCCM-Shelter-NFI cluster reported in August 2012 that 17,222 houses had been repaired (Shelter Cluster, 2012). Support for permanent construction was predominantly being provided by agencies at a community scale. CARE for example, were operating in Carrefour to repair 310 damaged houses of families who agreed to accommodate households from nearby camps for a period of one year. Many of the agencies— such as the British Red Cross and Habitat for Humanity – were and continue to work on small projects in separate communities. Others have combined their support in multi-donor efforts. For example, the Inter-American Development Bank (IDB), United Nations and World Bank established the Haiti Reconstruction Fund to support the *Action Plan for the Recovery and Development of Haiti*. 19 donors contributed US\$335 million to finance 14 different reconstruction initiatives. US\$30 million was also reserved to finance President Martelly’s 6 camp/16 neighbourhood reconstruction programme designed to help camp dwellers rebuild and return to their homes.

#### 4.4. Study Site: Delmas 19

This chapter focuses on support provided to BRC’s Integrated Recovery Programme in the Delmas 19 slum. The *target area* is an informal settlement bounded by major roads and buildings in the central

business district of Port-au-Prince. BRC described Delmas 19 as ‘extremely densely populated, lacking access roads, visibly run down, and with buildings that suffered high levels of damage during the earthquake’ (IFRC, 2011a). The area measures only 200 m by 200 m but it contains almost 500 building plots.

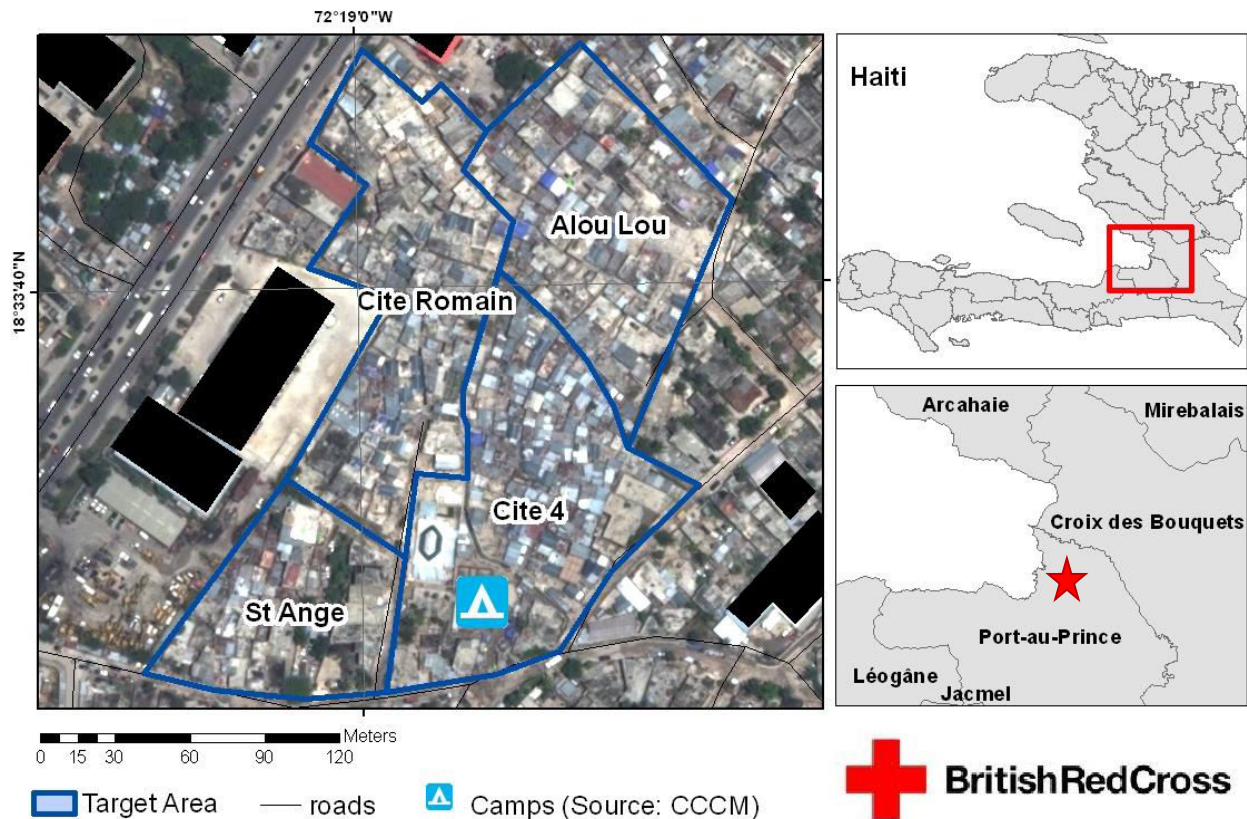


**Figure 4-2: Location of the British Red Cross Integrated Recovery Programme. Delmas 19 is split into four zones marked by blue lines.**

The settlement sits at the bottom of a canal system that carries water and rubbish from higher neighbourhoods. The land in Delmas 19 was reclaimed from marshland in the early 1980s through a process of land-fill using stones and other construction material. The original plots have since been subdivided or ‘sold’, though formal land tenure was never issued.

Most of the buildings in the neighbourhood are built with concrete block masonry walls and corrugated-iron roofs. The dimension and height of each dwelling varies enormously. There are no parks or open

public areas, only narrow alleyways – less than a metre wide - which are used for recreation and for washing. Only a few houses have city water supply and drainage is by gutters built into the alleyway. The neighbourhood is split into four quarters: Cite 4, Romain, St Ange and Alou Lou. Cite 4 is by far the most densely-built part of the area with some buildings measuring not much more than 35 m<sup>2</sup> and containing approximately 10 people each.



**Figure 4-3: Panoramic photograph of Delmas 19 slum characterized by small buildings and narrow access-ways. (Source: Daniel Brown).**

#### **4.5. BRC's Integrated Recovery Programme**

One of BRC's first responses to the earthquake was to provide cash grants to nearly 4,000 households occupying Automeca Camp. In September 2010 around 3,330 of those households were evicted by the landowner. A BRC survey in the camp found that many evictees were returning to the nearby neighbourhood area of Delmas 19, where they were previously living. Initial ground assessments in the neighbourhood highlighted a need for housing repair, reconstruction and livelihood support. A long-term integrated recovery programme was therefore established at the end of 2010 in line with the government recovery strategy encouraging people to return from the camps back home. Owner-driven shelter and livelihood activities were core to the programme from the beginning. A BRC concept note published in September 2011 stated that the aim of the programme was 'to help the community gain safe housing which is resistant to reasonably predictable events by repairing damaged houses and reconstructing unsafe or collapsed houses'.

#### 4.6. Mapping the Decision-Making Processes

A key step towards understanding how geospatial technology may be used throughout a recovery programme is to map the likely data needs and decision-making processes. Figure 4-4 shows the key monitoring and evaluation activities in a programme cycle according to the International Federation of the Red Cross (IFRC), which provides a useful framework to start with. The activities are divided into three main phases: initial assessment, planning and implementation. The initial needs assessment determines what type of programme might be appropriate in the target area. Planning then involves detailed programme scheduling and design alongside a baseline study to capture the current state of the site. Monitoring takes place once the project has commenced with a mid-term evaluation at the half-way point to reflect on-going processes and a final evaluation survey at the end of the project.

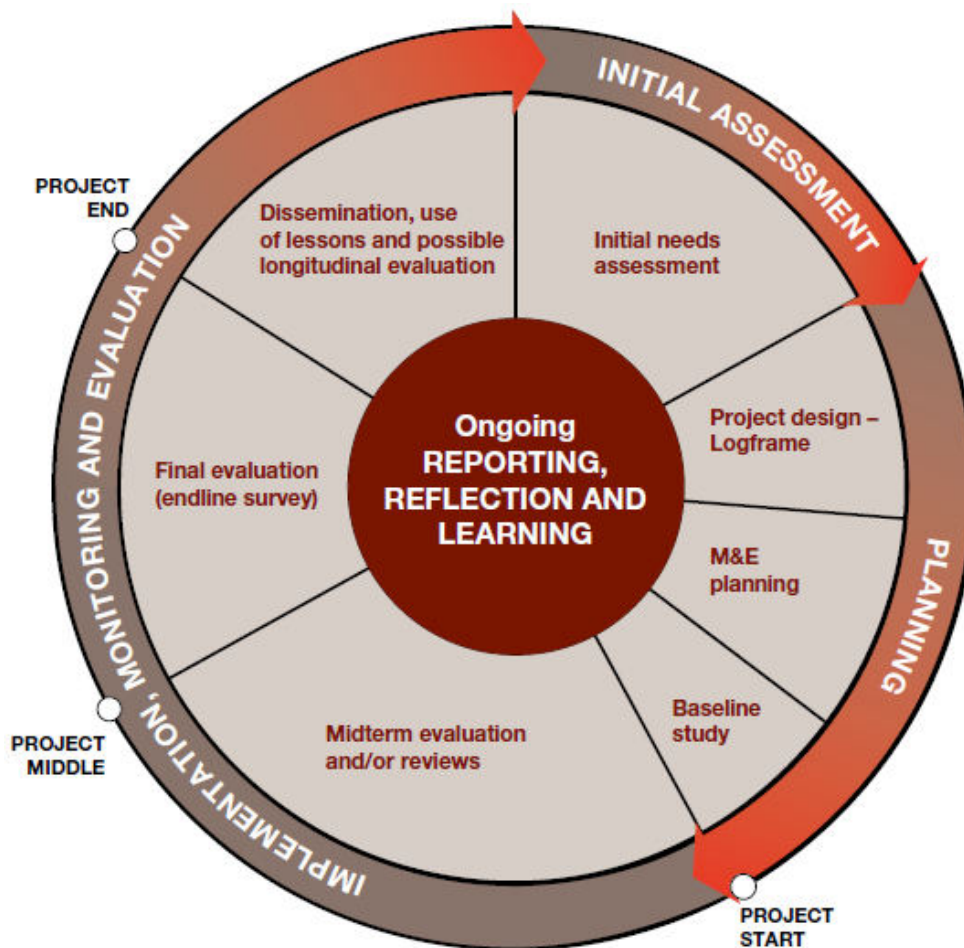


Figure 4-4: Key monitoring and evaluation activities in a Red Cross programme cycle (IFRC, 2011b).

The following section briefly reviews the key data collection exercises that were implemented during the needs assessment and planning phases of the BRC's integrated recovery programme. These tools and surveys are described in more detail throughout the rest of the chapter.

#### *4.6.1. Initial Needs Assessment*

The post-disaster needs assessment (PDNA) was conducted within 3 months of the earthquake to quantify physical damages and economic losses and to select response options for early to long-term recovery. The statistics in the assessment were estimated using a range of methodologies that used techniques including remote sensing and statistical sampling. During the first year of the response, between February 2010 and January 2011, an in-depth engineering assessment of buildings led by the Ministry of Public Works, Transport and Communication (MTPTC) was also conducted; 382,000 buildings were surveyed by 300 local engineers to measure the safety of individual building plots. The aim of the survey was to identify dangerous buildings, promote reoccupation of safe buildings and to create a geo-referenced inventory for recovery planning.

There was very little data available to agencies following the earthquake: the National Action Plan derived from the PDNA contained no master-plan and the aforementioned MTPTC building survey was deemed incomplete and unreliable by engineers working for BRC (Potangaroa and Neri, 2011). Agencies wanting to operate in Haiti largely had to collect their own data to plan and design their programmes. BRC conducted a house-to-house baseline survey at the beginning of 2011 to collect data on household economic situation, shelter, water-sanitation and livelihoods. At the same time, the remote assessment of Delmas 19 using aerial imagery, Lidar and Pictometry was conducted by the author focusing on accessibility, built environment, population movement and flood risk.

#### *4.6.2. Planning and Design*

As the project entered the planning and design stage, various data collection techniques were deployed to collect the data required for decision-making and project design. The data collection techniques can be divided into two broad groups: 1) participatory and 2) non-participatory. The non-participatory tools include the collection of socio-economic information and technical observations on the ground: a) Cadastral Survey – recorded the location and size of the owners' plots using high-accuracy GPS

equipment; b) Enumeration survey – collected detailed information on ownership/legal status, family situation and social-economic vulnerability; c) Engineer survey and observations (also referred to as the retrofittability survey– identified the damage type and the repair/reconstruction options that were available and d) architect observations recorded information on living conditions and how families used the space around them.

Alongside these non-participatory methodologies, BRC also used a participatory process known as Participatory Approach to Safe Shelter Awareness (PASSA). This is a series of meetings that allows communities to improve their living environment, build safer shelters and design better settlements by identifying problems and solutions, and ultimately results in the development of a community action plan.

The author's deployment to Haiti coincided with the completion of these various surveys. The results from these tools were integrated into a single GIS by the author. This allowed data from the non-participatory and participatory techniques to be triangulated against each other for validation purposes. The database also provided a baseline representation of the post-quake community and a tool for costing and beneficiary selection in time for the project's internal planning meetings where key decisions were made about the structure of the programme.

Figure 4-5 shows a flow diagram that summarises how geospatial tools were used at various points in the BRC project. The tools were found to be useful at all phases of the British Red Cross project: 1) as a needs assessment tool after the disaster 2) to support baseline damage assessments and beneficiary profile creation and 3) as a GIS database to store, analyse and visualise cadastral and enumeration ground datasets and 4) as a platform for monitoring data. This thesis will describe each of these processes in detail, focussing on how geospatial tools were used at each stage of the project and outlining any problems that arose.

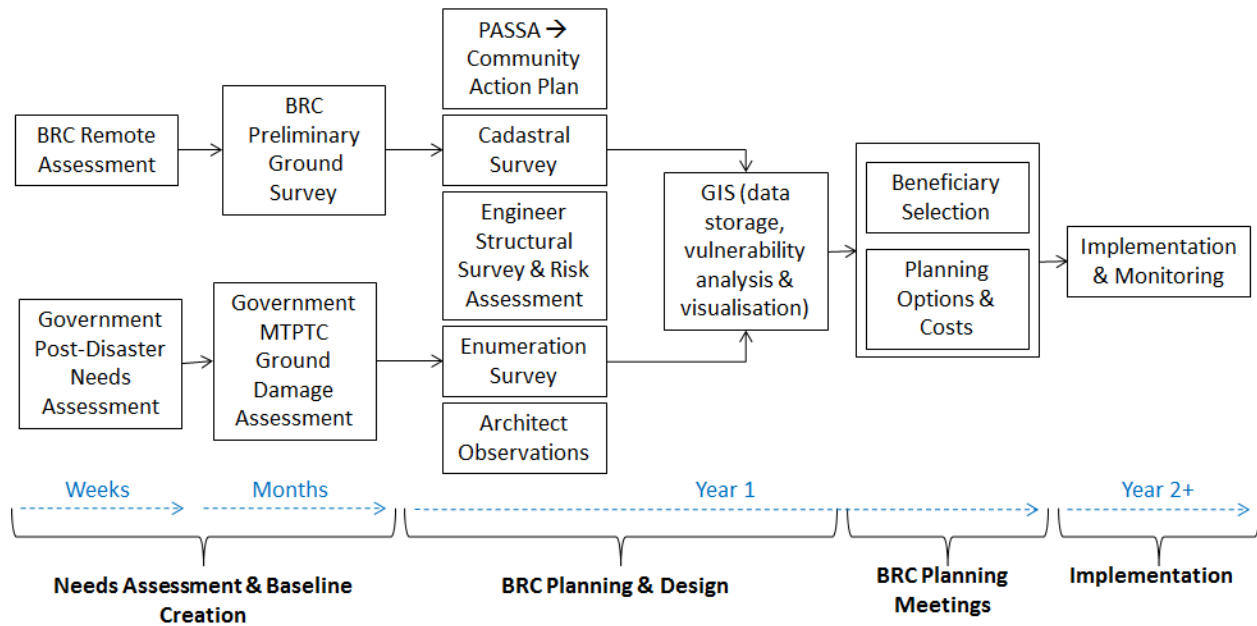


Figure 4.5: Flow diagram showing how geospatial tools were used at each stage of a British Red Cross project in Haiti.

#### 4.7. Remote Sensing in Support of Post-Disaster Needs Assessment

Post-Disaster Needs Assessments (PDNAs) are conducted after disasters to measure losses and to inform the creation of a recovery framework. The Damage and Loss Assessment (DALA) methodology, on which the PDNA is based, recommended in 2003 that remote sensing be used to highlight affected areas and to identify major building damage. A review of 29 PDNA reports by the author found that 11 directly referenced the use of *satellite imagery*. The review found that satellite imagery was mainly used after flood and storm events to map flood extents. Damage to buildings, agriculture and transport infrastructure was sometimes validated and rationalized by comparing results to satellite image maps showing the extent and duration of flooding. The team responding to the 2009 floods in Namibia found geospatial information to be important in three phases of PDNA: 1. Planning of reference data and field mission logistics 2. To perform spatial disaggregation of data to relevant administrative units and 3. to extrapolate and validate field observations (Government of the Republic of Namibia, 2009).

The immediate aftermath of the Haiti earthquake saw an enormous response from the remote sensing community to support the PDNA process and other large-scale mapping needs, accelerated by an unprecedented amount of free datasets, distributed through on-line outlets such as Google Earth and

OpenStreetMap. Results from the analysis of Geoeye satellite imagery covering Port-au-Prince were available within 3 days of the earthquake and satellite image analysis of areas outside of Port-au-Prince were ready before the first PDNA planning meeting on 20 January. The results from the satellite image analysis were used at the planning stage of PDNA to highlight highly damaged areas, but only the results from the analysis of aerial imagery were used in the PDNA report itself.

When compared to aerial image-based assessment the satellite analysis was found to underestimate the amount of damage considerably (Haiti PDNA, 2010). The aerial and Lidar imagery, with a spatial resolution of 20 cm and 2 points/m<sup>2</sup> respectively, was collected between 18-21 January and analysed in the second week of the response. The results of the aerial analysis were then used to estimate the economic losses and damage to buildings for the PDNA. The results were presented in the 'Building Damage Assessment Report' on 11 March in time for the Donor conference in New York on 31 March. The analysis estimated that there were 90,000 damaged buildings covering over 26 million m<sup>2</sup> and costing over US \$6 billion to repair (Haiti PDNA, 2010).

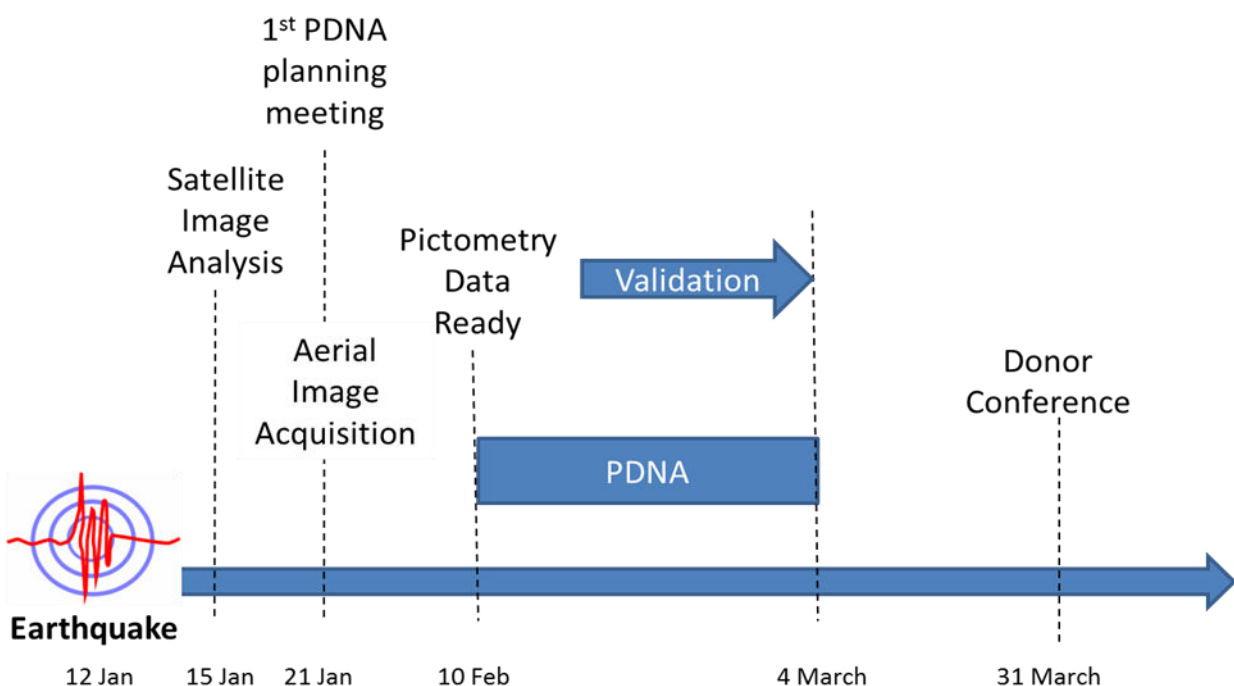


Figure 4-6: Acquisition and analysis of imagery in the first three months after the 2010 Haiti earthquake.

Crowd-Sourcing – the act of outsourcing large tasks to lots of people - emerged as an effective method of data-mining information to support emergency management. Platforms such as Ushahidi were used to integrate, locate and map vast amounts of information from the affected population collected via email, voicemail, SMS, Twitter and other social media, while the Global Earth Observation Catastrophe Assessment Network (GEOCAN) used crowd-sourcing as an approach to manage the manual analysis of large amounts of satellite and aerial imagery.

Pictometry data was also used to validate the aerial image analysis before ground data became available. The data, consisting of oblique angle imagery and nadir imagery with a 10 cm spatial resolution, was collected on an aircraft at the beginning of February 2010. When viewed in the Pictometry online viewer<sup>3</sup> buildings were analysed from above, and from the north, south, east and west. Booth et al. (2011) used Pictometry data to analyse 1,247 buildings selected randomly using a stratified sampling approach based on land-type and neighbourhood damage levels. The accuracy of the Pictometry assessment was estimated by comparing the results to ground survey data collected by the Earthquake Engineering Field Investigation Team (EEFIT). 63% of the worst damaged buildings (damage levels 4 and 5 on the EMS-98 damage scale) were identified with this system. In contrast, GEOCAN observations using aerial imagery correctly identified only 40% of very heavy damage and structural damage (Spence & Saito, 2010).

A full review of the use of remote sensing in the different stages of the disaster management cycle – including damage assessment – is beyond the scope of this thesis but is available as a paper on the Cambridge Architectural Research Ltd. website (Brown, 2017).

---

<sup>3</sup> Pictometry website: <http://www.pictometry.com/>

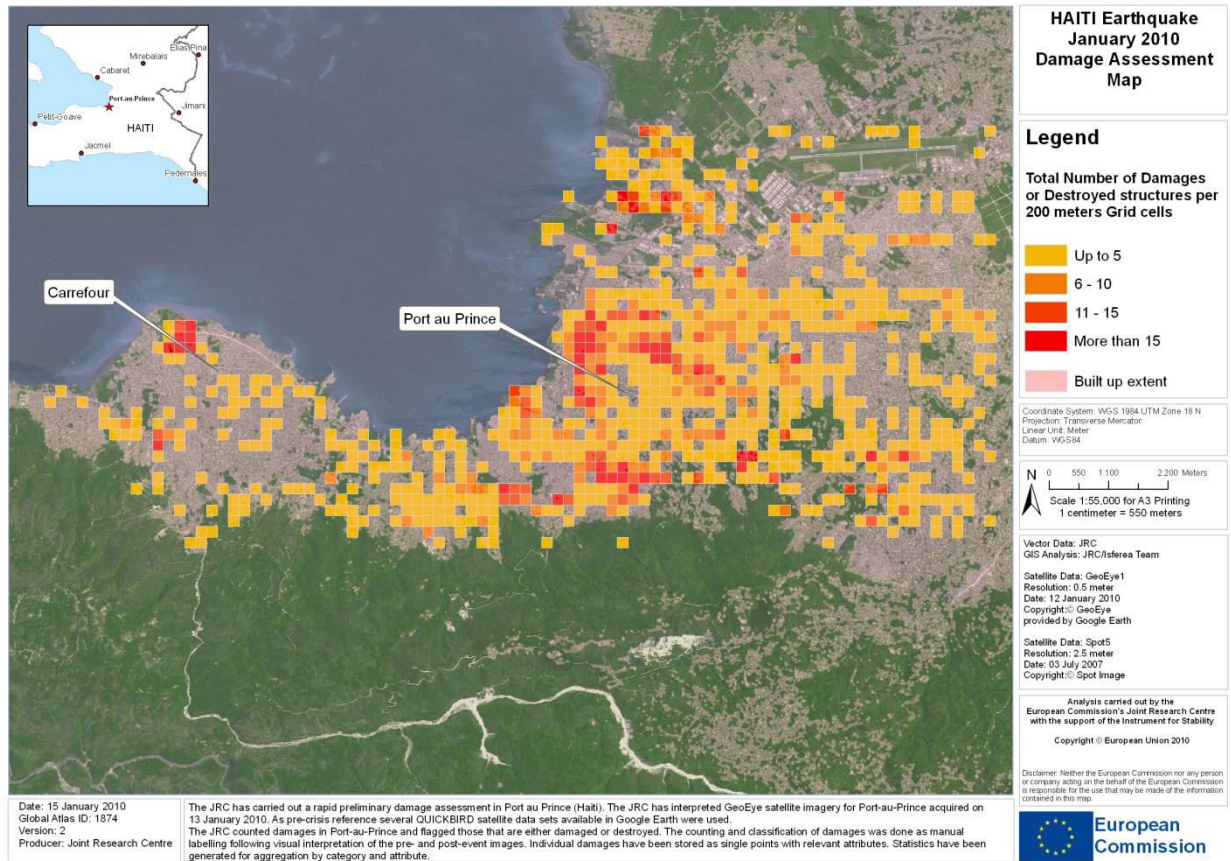


**Figure 4-7: Result of a rapid damage assessment across the Port-au-Prince metropolitan area using remote sensing technology by the European Union’s Joint Research Centre.**

#### 4.8. MTPTC Building Safety Ground Assessment

Two months after the earthquake a ground assessment took place across the whole of Port-au-Prince to assess buildings’ level of safety. The main motivation for the survey, led by the by Ministère des Travaux Publics Transport et Communications (MTPTC), was to protect citizens by identifying damaged and dangerous buildings and to identify safe structures to support the return of people from camps. The assessment used an ATC-20-2 technical questionnaire that was modified for the Haitian building stock (ATC, 2005). Approximately 300 engineers were trained to apply the assessment and to tag the buildings with spray-paint either red (unsafe, do not enter), yellow (restricted use) or green (lawful occupancy permitted).

The engineers evaluated 382,256 buildings between February 2010 and January 2011, marking 205,539 buildings green (54%), 99,043 yellow (26%) and 77,674 red (20%) (Schwartz, 2011). The MTPTC safety tags sprayed on buildings in Delmas 19 were recorded by BRC during the enumeration survey. 98 buildings were untagged and 400 buildings were tagged: 20% green, 29% yellow and 52% red. There are proportionally more red-tagged buildings in Delmas 19 than in the MTPTC's complete database for Port-au-Prince. The Delmas site is thought to contain relatively more red tags due to the presence of water channels throughout the site and subsequent liquefaction during the earthquake.

The BRC's original shelter strategy suggested that the MTPTC safety tags be used as a measure of vulnerability and to determine the type of shelter support suitable for each household; in particular, households in yellow-tagged buildings were to receive support for repairs and red-tagged houses were to be reconstructed. The engineers on the BRC project questioned this approach though as the MTPTC classification is not a structural assessment and it does not consider issues of code compliance; instead the assessment is based only on visible damage. The ATC guideline (on which the MTPTC survey is based) states that "the tagging process is not a damage survey, but an assessment of whether the building is safe for entry or occupancy" (in Potangaroa and Neri, 2011). As a result green-tagged buildings can be deemed 'safe' but might still be damaged and/or seismically vulnerable when another earthquake occurs (Potangaroa and Neri, 2011).

The reliability of the MTPTC tags was also called into question. To verify the damage tags Dr. Regan Potangaroa and Rafael Mattar Neri carried out a study of structures in Delmas 19 on 23 September 2011. They found that out of 10 red-tagged buildings 3 were confirmed as red, 4 were in fact yellow and 3 were green. These results suggest that the tagging in this neighbourhood was not accurately applied by MTPTC and/or the status of some buildings had changed since the survey. A more detailed technical survey was therefore advised both to assign more descriptive damage levels and to survey untagged buildings.



Reassigned Red to Green

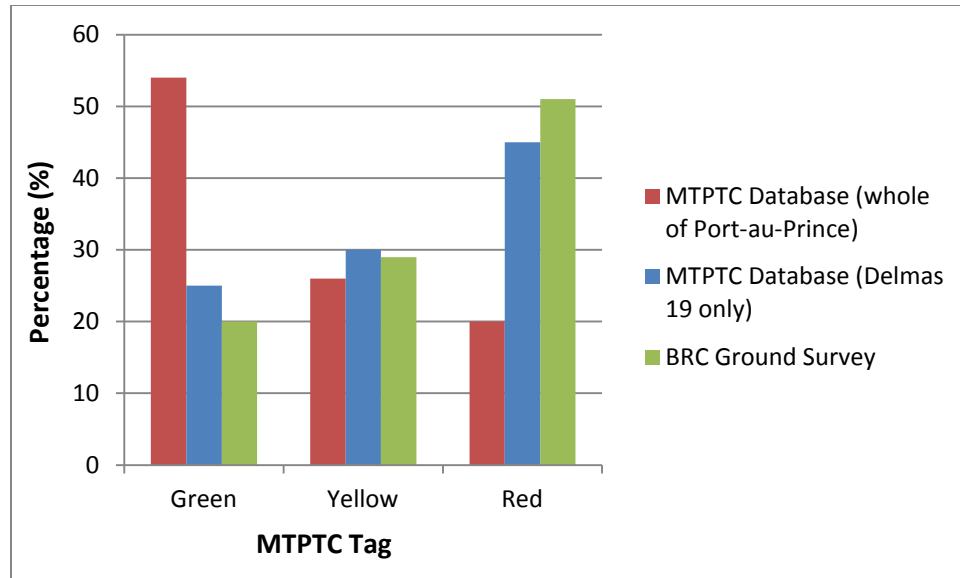
Reassigned Red to Green

Remained Red

**Figure 4-8: MTPTC-tagged buildings re-assigned tags by BRC engineers in September 2011.**

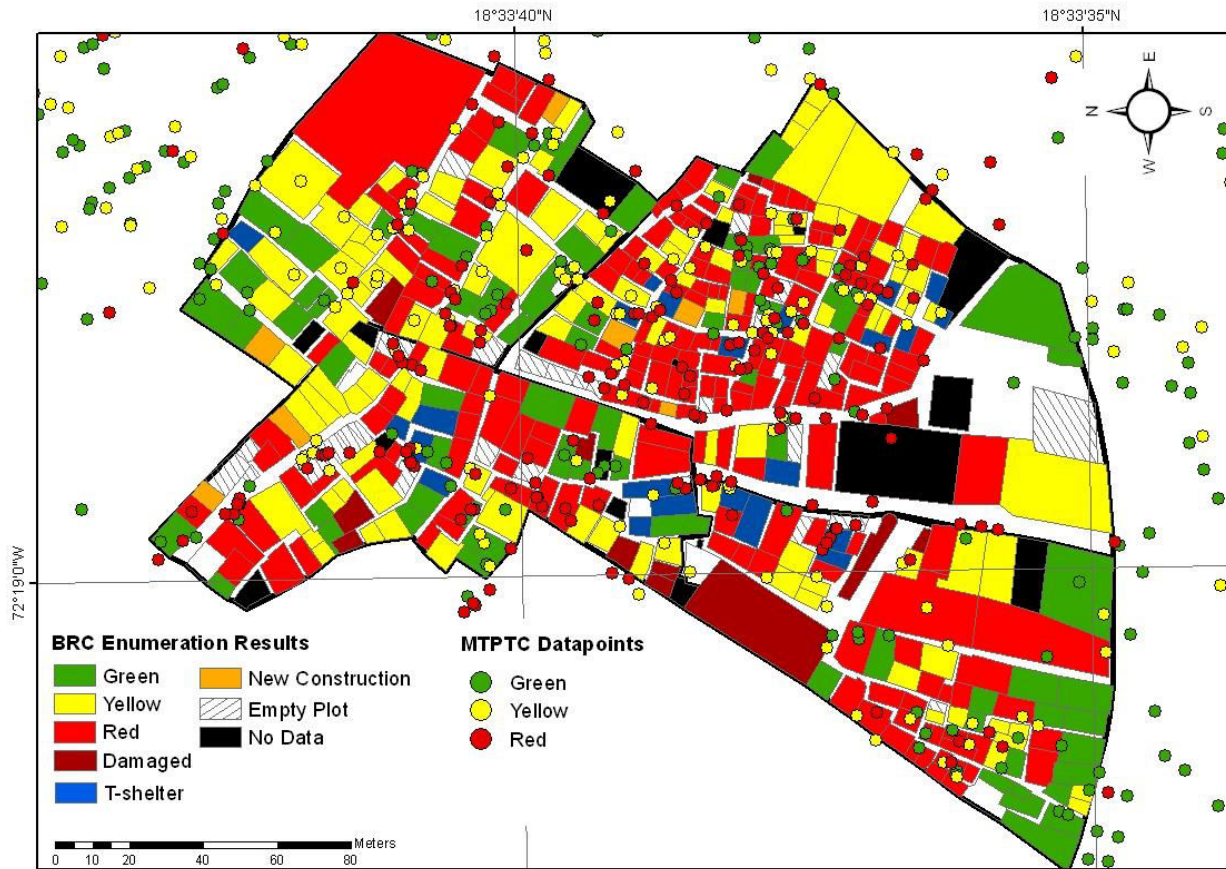
When conducting each building assessment the MTPTC engineers collected a GPS coordinate and a photograph of the surveyed buildings. This allowed the results to be saved as a KML file and distributed to agencies in a spatial dataset to view in Google Earth. Each point in the dataset contained a XY coordinate and an appropriate colour tag. To assess the usability of the MTPTC spatial dataset for Delmas 19 it was directly compared to the MTPTC spray-tags recorded by BRC on the ground.

Figure 4-9 shows the percentage of red, yellow and green-tagged buildings recorded by BRC staff on the ground (green bars) and in the MTPTC spatial dataset (blue bars) for Delmas 19. The results show that the proportion of each colour-tag recorded by BRC and the MTPTC spatial dataset match closely (blue and green bars), but that the proportion of red-tagged buildings in Delmas 19 is substantially higher than the average recorded by MTPTC for the whole of Port-au-Prince (red bars).



**Figure 4-9: Comparison of the proportion of MTPTC tags in Delmas 19 recorded in the MTPTC database and the BRC's enumeration survey.**

A spatial join procedure in ArcGIS was used to link and directly compare plot-by-plot the points in the MTPTC database with the MTPTC tags recorded on the ground in the BRC enumeration survey. The majority of plots (329, 66%) did not intersect with a MTPTC point; this included 139 buildings identified as having a red-tag in the ground survey, while 59 building plots (12%) contained more than one MTPTC point. By analysing instances where a MTPTC point intersects with a ground-recorded tag, 62 are correct matches and 79 are incorrect, resulting in an accuracy rate of 44%. Figure 4-10 shows the MTPTC database (points) overlaying the MTPTC tags recorded in the BRC's enumeration survey (polygons).



**Figure 4-10: Spatial analysis of MTPTC database (points) and MTPTC tags recorded on the ground by BRC (polygons).**

It is clear from this simple analysis that the majority of MTPTC data points do not appear to align properly with the building outlines. There are several reasons why this might be the case. The first is likely to be due to limitations with the GPS equipment used. Poor GPS reception in dense urban environments in particular, is likely to have led to poor placement accuracy. In the map above it seems that many of the points are clustered around the access ways in Delmas 19 – this might have happened if engineers were not able to access some buildings and instead took a GPS reading some distance away from the plot.

Errors with the reliability of the engineering surveys and the location-information associated with them appear to be a common problem. It was also an issue with field survey data acquired from the county council after the 2011 Christchurch earthquakes (Foulser-Piggott et al. 2012; Foulser-Piggott, Spence and Brown, 2013). It highlights the need for a common damage assessment protocol and protocols in

collecting and recording geospatial locations in general. Instead of relying on GPS readings, engineers would be better to locate themselves manually either on a paper map or handheld GIS device. This process would be more accurate if building polygons and imagery were ready at the start of the survey.

#### **4.9. BRC's Baseline Survey in Delmas 19**

In January and February 2011 BRC carried out a house-to-house survey to capture a baseline 'snapshot' of the beneficiaries and to assess the household economic security, livelihood, shelter and water-sanitation situation; the results were intended to support the development of the programme's strategy and implementation plan.

948 family heads were surveyed across the whole Delmas 19 area. The questionnaire was divided into three sections, one for each component of the programme. The shelter part of the questionnaire asked about the households' shelter situation now and before the earthquake. It also asked for descriptions of the dwellings on the plot and any damage they sustained, as well as the households' home and land ownership status. The water-sanitation team asked for information describing their access to water and toilet facilities, the cost of water and their method of household waste disposal, while the Livelihoods team asked for a combined household income, livelihood-type and how best the households thought they might be assisted with their income.

On completion of the survey it was apparent that there were substantial errors with its design and results which affected how the data could be used and updated. In particular, the results highlighted the need to clearly define the scale at which the data should be collected and in particular, the need to correctly define the concepts of 'house', 'household' and 'family'. It was established after the completion of the survey that the Livelihood and Shelter teams required the data at different geographic scales. Livelihoods were interested in the number of unique family units within the target area (both inside and outside of structures), while Shelter needed the data aggregated to plot level. Shelter also required precise geographic locations for each household to allow them to assess geographic risks, and precise plot size information to calculate construction and repair costs.

A survey was conducted with the head of each household but there were often multiple households living on a single plot and unfortunately the results could not be aggregated afterwards to plot-level as

there was not sufficient location or address information available. It was also not clear if the households were living on their permanent plot or if they were currently displaced. Although the aggregated results of the survey were interesting the content on the baseline survey was largely of not much use to the shelter team. As a result, they designed and implemented a new Enumeration survey which was conducted at plot-scale in May 2011 and is described later in the chapter.

The Livelihood team intended to continue using the Baseline survey dataset by adding Milestones to show the status of each household and in particular, to mark when each had received appropriate grants or other support. The process of finding each household in the field though was time-consuming as they only had the GPS coordinate and street name of each household and there was substantial population movement in and out of the site at the time. The coordinates in the database were full of errors and it took several days of data cleaning to get them to a state where they could be mapped. The GPS coordinates were also only accurate to within 10-15 m which did not allow the data to be linked adequately to individual plots.

The use of appropriate geospatial tools and protocols during the implementation of this survey could have prevented the waste of substantial time and resources and also saved the Livelihoods team a considerable amount of time in the field locating households.

#### **4.10. Remote Sensing Assessment of Delmas-19**

After the completion of the baseline survey a detailed assessment of Delmas 19's road and built environment was conducted by the author by manually analysing remote sensing data, including nadir and oblique aerial imagery, and Lidar data. The remote sensing analysis coincided with the planning and design phase of the BRC project but in theory it could have been applied as soon as the data became available i.e. satellite imagery within 24 hours, aerial, Lidar and Pictometry within a few weeks. The key objectives of the remote assessment were similar to those of the PDNA: to identify losses and needs and to assist the design of a suitable recovery programme but it was conducted across a much smaller area and in a lot more detail. The main outputs from the work included maps of the site for navigational purposes, a preliminary GIS database for enumeration and spatial analysis and statistics to describe the size and morphology of the site.

Two aerial images were acquired after the earthquake by different agencies, subsets of which are shown in figure 4-11. National Oceanic and Atmospheric Administration (NOAA) collected an image on 17 January using an Applanix digital sensor system frame camera and Rochester Institute of Technology (RIT) collected an image on 21 January for Imagecat, funded by the World Bank, using a KCM-11 high-spatial-resolution optical camera. Both NOAA and RIT images have a spatial resolution of approximately 20-30 cm and a horizontal accuracy within 1-2 metres. The RIT image was selected for this analysis as it appears brighter and the colours and contrast are substantially clearer. A third aerial image was also acquired by Google on 09 November 2010 which was later used to update the status of buildings and shelters in the area ten months after the earthquake.



**NOAA (17 January 2010)**



**WB-Imagecat-RIT (21 January 2010)**

**Figure 4-11: Two aerial images acquired after the earthquake vary in their contrast and clarity.**

In addition to the optical sensor the RIT's airplane also carried a Leica ALS60 Lidar laser system. The Lidar cloud points were made publicly available after the earthquake as LAS points and as an interpolated 1 m Digital Surface Model (DEM) and Surface Elevation Model (SEM). The ALS60 system collected four range returns as well as intensity return measurements which allowed the laser points to be classified as isolated low points, ground classification points and below surface points. It's important to note that the

Lidar acquisition was not optimised for many applications including hydrology and wall-to-wall coverage as the plane was flying at approximately 2,500 ft to optimise the collection of aerial imagery. Despite the likely inefficiencies the Lidar dataset was used in this analysis to estimate both building height and to map the topography across the site.

Within days of the earthquake, a separate aircraft owned by Pictometry International Corporation captured 45,000 oblique aerial images. This was the first time such data had been collected systematically after an earthquake. The data covered the whole of Port-au-Prince and provided users with 4 oblique views of each point on the ground with a 40 degree angle, which allowed building facades to be examined and measured in detail.



**Figure 4-12: Oblique Pictometry imagery was used to observe the facades of buildings.**

#### **4.11. Selecting Appropriate Geospatial Analyses with BRC**

The first task was to choose appropriate analyses to conduct by asking BRC staff to select suitable methods and products. This was an iterative process that involved describing potential analyses and also suggesting new analysis based on the objectives and work of the recovery programme being described. After initial discussions and inspection of the remote sensing data a list of indicators and techniques was developed based on the indicator table introduced in chapter 2. When asked to identify measures in the list they thought would be useful for their project the BRC staff selected a broad range of indicators encompassing most sectors - similar to the results of the user-needs survey also described in chapter 2. Environmental measures were deemed not necessary though as the management of debris was being conducted on a larger scale than the target area. The list of proposed techniques is shown in table 4-2. Note that some new measures were developed due to the availability of Lidar and Pictometry data such as the number of storeys.

<b>Accessibility</b>	<ul style="list-style-type: none"> <li>Total length of road network by road type (m)</li> <li>Length of damaged and blocked roads (m)</li> <li>Length of cleared and reconstructed roads (m)</li> <li>The distance from each building to the nearest road surface (m)</li> <li>Travel distance and routes to key services</li> </ul>
<b>Buildings</b>	<ul style="list-style-type: none"> <li>Number and location of buildings</li> <li>Number and location of damaged buildings</li> <li>The number and location of removed, rebuilt &amp; newly-built buildings</li> <li>Building Size (m<sup>2</sup>)</li> <li>Building Density</li> <li>Building Height</li> <li>Land use mapping (industrial, residential and commercial)</li> </ul>
<b>Environment</b>	<ul style="list-style-type: none"> <li>Presence of vegetation</li> <li>Presence of debris</li> </ul>
<b>Population Movement</b>	<ul style="list-style-type: none"> <li>Number and location of tents</li> <li>Number and location of transitional shelters</li> <li>Size and layout of tents and shelters</li> </ul>
<b>Hazard and Risk</b>	<ul style="list-style-type: none"> <li>Topography analysis</li> <li>Proximity of buildings to drainage channels</li> </ul>

**Table 4-2: A list of proposed techniques given to BRC based on the indicator table introduced in Chapter 2 and preliminary discussions with the team.**

With the BRC staffs' agreement the analysis focused on three sectors **accessibility, buildings and population movement**. Very basic **risk and hazard mapping** was also conducted by mapping water channels, catchment areas and likely drainage across the site. A transport and building database containing 2.5 km of roads and 568 building plots was first produced by manually analysing the aerial imagery. Spatial analysis of this database then provided statistics on road length and building numbers that were not previously available to the Red Cross. After the building footprints were mapped and verified with Pictometry imagery, collapsed and demolished buildings were identified as were tents and transitional shelters.

The statistics derived from this analysis were later used in the BRC's design and planning report to help justify a need for the project and to characterize the existing built environment. Information on the number of storeys and the shape and size of plots was particularly useful for initial costing and design work. Six regular-shaped house footprints commonly found in Delmas 19 were defined based on the morphology measurements. Density statistics were also used during the BRC's planning meetings to visualise discrepancies in living space across the site.

A summary of the results from the road and building analysis are presented in the following section focussing on the accuracy and reliability of the results. A validation of these datasets was conducted by comparing the results to 'ground-truth' datasets created from the cadastral survey which was produced in the field using sub-metre accurate GPS equipment.

Note that manual analysis of the imagery was used for the remote assessment to ensure maximum accuracy. Automated techniques were not used but were later tested across large geographic extents for UN-Habitat, the results of which are presented in Chapter 5.

#### **4.12. Accessibility**

Manual analysis of aerial imagery was used to identify 2.5 km of roads within Delmas 19. The road-type was assigned to the database using the same classification definitions used in Chapter 3: highway, asphalt, non-asphalt and lanes. Once complete, the road database was used to calculate statistics that described the length of road by road-type in each neighbourhood and accessibility to building plots and key services. Manual analysis of the November 2010 aerial imagery was also used to identify damaged and blocked roads and to map newly constructed and cleared roads.

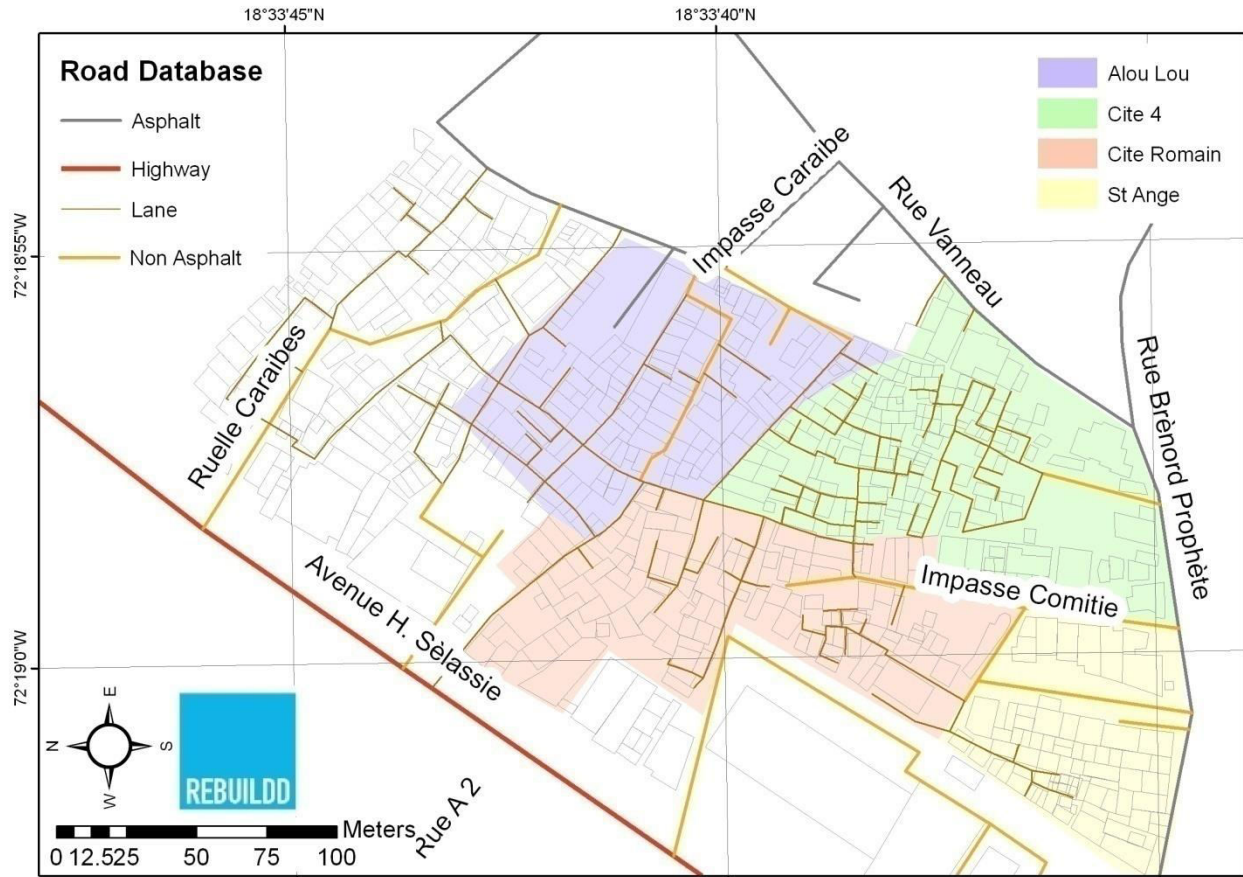
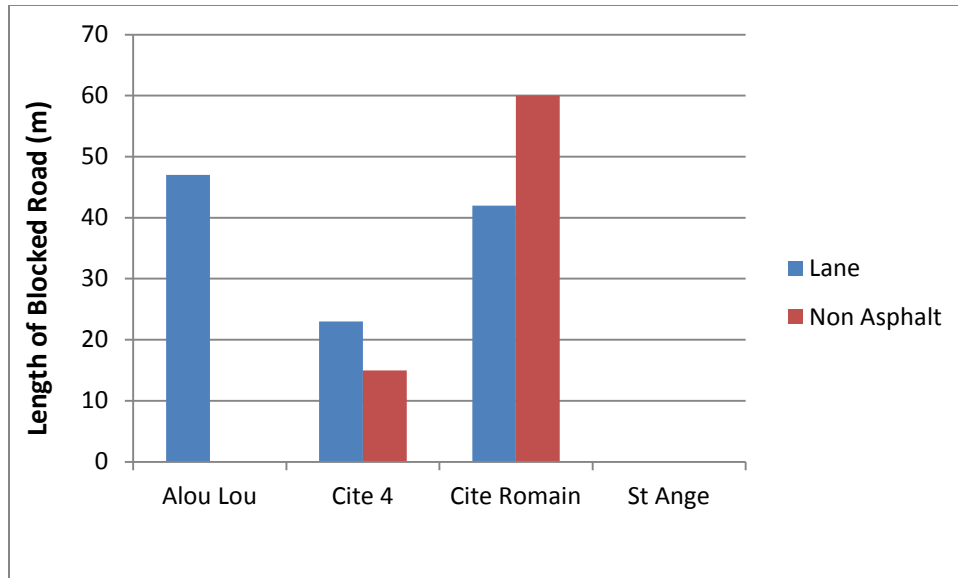


Figure 4-13: The road database created using the manual analysis of aerial imagery.

75% of the roads delineated in the database were either small paths or narrow lanes providing access to housing across the whole of Delmas 19. Only 119 m of the roads in the scene were classified as asphalt. After the earthquake 187 m of roads were marked as being covered in rubble or debris from near-by building collapses. This included a 75 m section of the Impasse Comitie which affected access to parts of Cite Romain. Debris clearance in the area was completed by the end of the first year. All roads appeared to have been cleared by November 2010 but no new roads were constructed between January and November 2010, which matched ground reports from BRC.



**Figure 4-14: Length of blocked roads in four neighbourhoods of Delmas 19 measured using aerial imagery.**

Figure 4-15 below shows two other uses of the road database. The distance from each building footprint to the nearest road surface was measured as an indicator of accessibility and is displayed on the left. Distances ranged from 0 to 21 m with a mean of 2.0 m across the whole site. Buildings more than 4m away from a road surface are shaded yellow or green in the diagram. 76% of all buildings though were within 4 m of a road surface and only 52 buildings were over 10 m away from a road. The road network was also used to measure travel routes and distances to key services including health facilities and water wells – the locations of which were obtained from a Pan American Health Organisation (PAHO) and UN-Minustah dataset respectively.

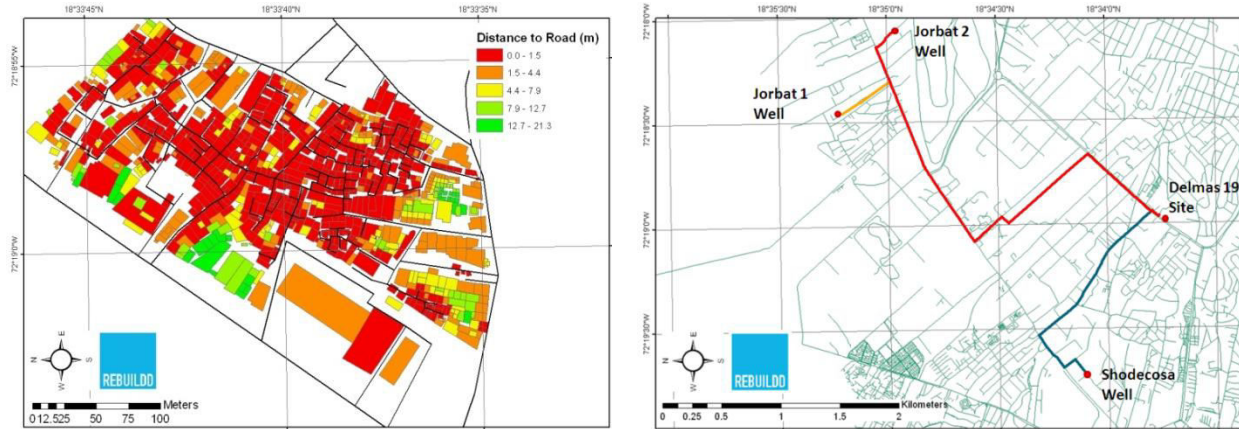


**Figure 4-15: The road network used to measure the distance from each building to the nearest road surface (left) and the shortest route to water wells and other facilities (right).**

#### 4.12.1. Validation of the Road Database

The road database was validated by comparing it directly to a road map created in the field by Haitian surveyors using precise sub-metre accurate GPS equipment. The two road datasets were overlaid in ArcGIS and the road segment in the remote assessment was assumed to be correct if the centroid of the road layer was within 3m of the ground truth dataset.

Figure 4-16 shows the correctly delineated roads (black line), areas that were mistakenly delineated as roads (red) and roads that were missed by the remote analysis (blue). 1,827 m of roads were mapped correctly by the remote analysis, 316 m were wrongly delineated and 1,235 m were missed by the analysis. The results show that roads were mapped with high accuracy but that a significant length of road was missed by the analysis.

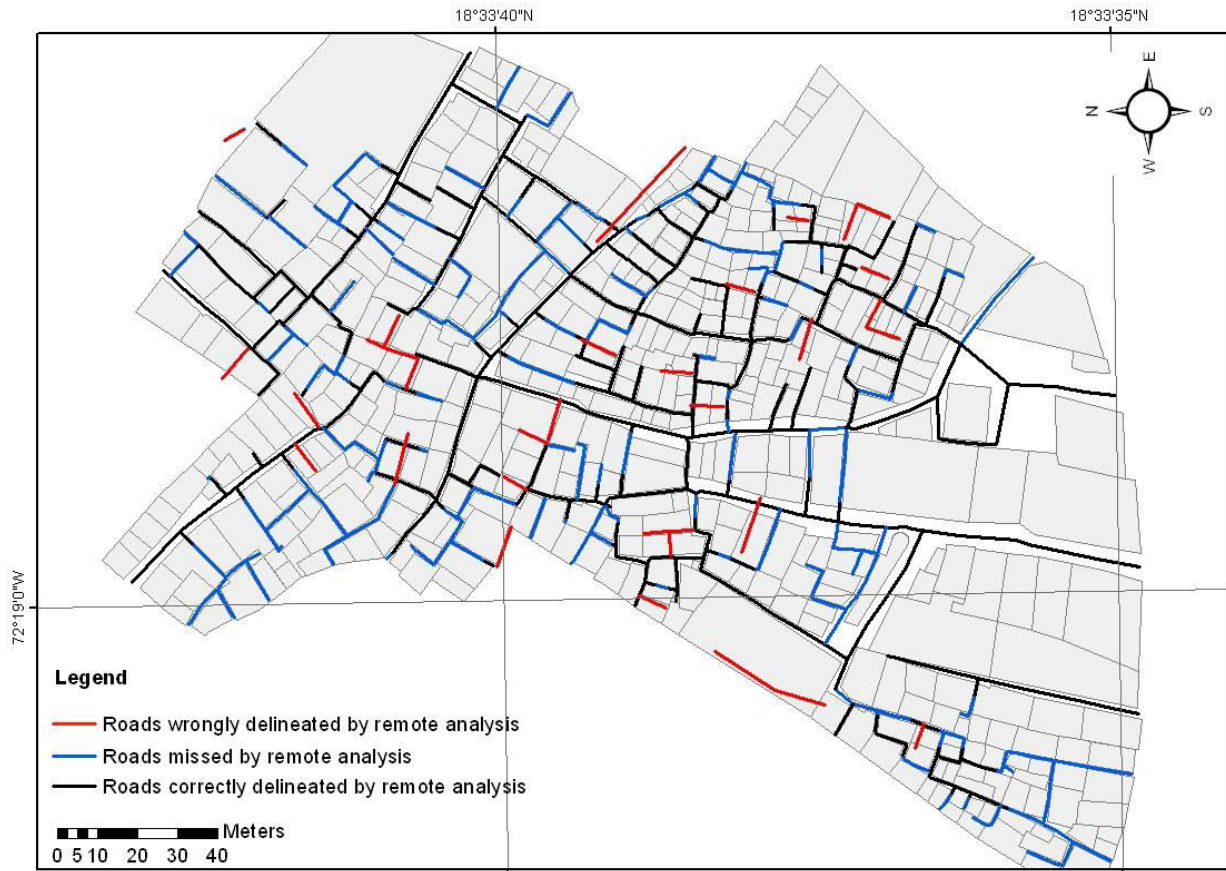


**Figure 4-16 Validation of remote mapping of roads in Delmas 19 slum using aerial imagery.**

Close inspection of the results show that highways and other asphalt roads were mapped with high confidence – in-fact, all the main roads were mapped correctly, but smaller lanes were often difficult to identify – especially those in particularly high-density areas to the south of the scene. In these cases, the presence of vehicles, shadows and building facades was used to identify spaces between buildings and likely access routes. The more prominent lanes were mapped using these techniques, but the smaller lanes were missed from the analysis, especially those located underneath corrugated-iron roofing.



**Figure 4-17: Highways and asphalt roads were delineated with high confidence in the aerial imagery but narrow lanes were often missed.**

#### 4.13. Building Database

To map the built environment, building outlines were manually delineated using post-earthquake aerial imagery. This was a challenging task in a high-density slum area. Where buildings were attached and clear building outlines were not visible, shadows and patterns in the corrugated-iron were used to estimate where building edges were likely to be located. The following part of the report describes the building database and the products derived from it. The database was used to count the number of buildings and later as a spatial framework to host a survey of structural damage, to monitor removed, rebuilt and newly-built buildings and to calculate urban morphology statistics such as building size, density and height.

To verify the building database it was directly compared to the cadastral survey, both datasets are presented in figure 4-18. While the cadastral database conducted in summer 2011 contained 536 individual buildings the remote assessment counted 578 buildings (+8%) in the January 2010 image and 529 buildings (+1%) in the November 2010 image. This suggests very-high accuracy in a particularly difficult area to map. According to BRC, very minimal amounts of construction were known to have taken-place between the date the aerial image was acquired and the date of the cadastral survey.

To assess how accurately individual buildings had been delineated the cadastral and remotely-derived datasets were overlaid, joined and compared. The results show that 334 building outlines (67%) correctly overlapped with one remotely-identified building. 78 buildings (16%) did not intersect with a remotely-derived building polygon – so are assumed to have been missed by the remote analysis. The remaining 84 building plots (17%) were counted more than once by the remote analysis.

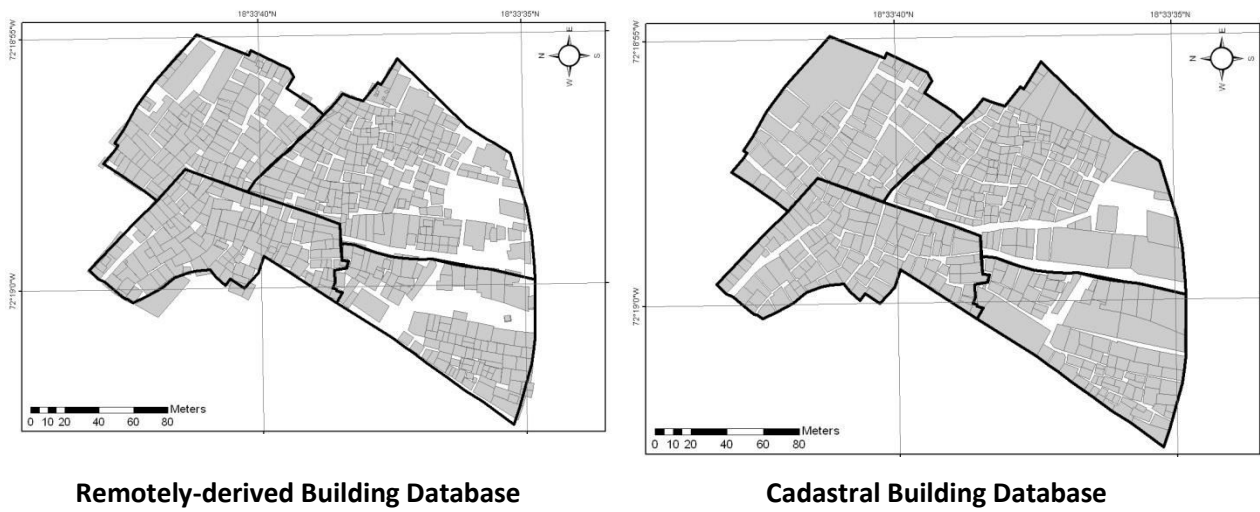


Figure 4-18: Comparison of building database created using aerial imagery (points) and ground GPS surveying (polygons).

The plot-to-plot comparison with the cadastral survey found that two-thirds of plots were correctly delineated and that approximately one-third of the plots were either over or under-segmented by the analyst. Remote sensing was therefore not reliable as a tool for accurate cadastral survey. Multiple attached buildings were often counted as one structure if they were under one roof. In some cases, a single building was placed on multiple plots so they were only counted once. Conversely, a roofless building was over-counted when an internal wall was incorrectly delineated as a building outline. Buildings were more often counted more than once when extensions or roof panels were mistakenly interpreted as a separate dwelling. Similar omission and commission errors were encountered during the analysis of Ban Nam Khem, described in Chapter 3.

#### *4.13.1. Assessment of Structural Building Damage*

At the time the remote assessment of Delmas 19 had started no engineering survey had been conducted on the ground other than the MTPTC safety survey. The number and location of heavily damaged buildings was important to know for effective programme design. To provide BRC with information on the extent and distribution of damage each building footprint was classified as having structural damage or no structural damage. The assessment focussed only on structural damage that could be identified confidently remotely. Structural damage included signs of damage to roofs and external walls and the presence of rubble.

Two ground-derived damage datasets were used to validate the remote assessment of structural damage: the MTPTC safety survey tags which were collected from households with the enumeration survey in May 2011 and the results of a retrofittability survey conducted by BRC engineers in September 2011. In the retrofittability survey buildings were marked according to whether they were likely to require 'low', 'medium' or 'high' retrofit costs. Figure 4-19 compares the results of the MTPTC safety survey, the engineer retrofittability survey and the remote assessment of structural damage; buildings identified as having structural damage are highlighted in red.



**Figure 4-19: Comparison of structural damage results from engineer retrofittability survey, remote assessment and ground-derived MTPTC tags.**

The remote assessment using aerial and Pictometry images identified 338 buildings thought to have structural damage, which equates to 58% of the building stock. For this validation exercise, buildings were assumed to have structural damage in the MTPTC dataset if they were tagged red or yellow or if the site was marked as already cleared or containing a transitional shelter. Using these assumptions 383 buildings were marked as damaged. Buildings were assumed to have structural damage in the retrofittability survey if they were tagged as requiring 'high cost retrofit', already demolished or already an empty plot or plot containing a transitional shelter. Using these assumptions the retrofittability

survey contained 311 buildings with structural damage. The results suggest that aerial imagery can identify *the number of buildings with structural damage* with an accuracy of at least 12%.

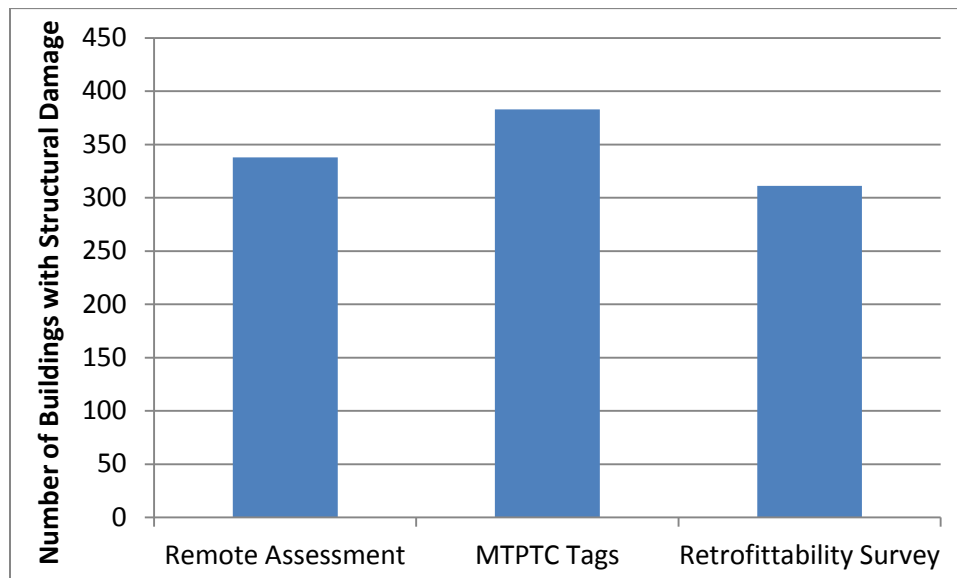


**Figure 4-20: Number of buildings with structural damage derived on the ground and remotely.**

Comparing the remotely-derived damage assessment to the retrofittability assessment plot-by-plot was difficult as the two datasets used different building outlines. Validation was done by linking the two spatial datasets using a spatial join procedure. The remote assessment data was converted to points and joined to the building plots in the retrofittability survey they intersected with. Of the 338 damaged buildings identified remotely 216 (64%) intersected with a building plot marked as damaged by the retrofittability survey. Similarly, of the 311 damaged buildings in the retrofittability database 216 (65%) intersected with a building polygon identified in the remote assessment as being damaged. These results suggest two-thirds of heavily damaged buildings were correctly identified by the analysis of aerial and pictometry data. This observation matches that of Spence and Saito (2010) who found that 63% of buildings with structural damage (EMS-98 Levels 4 and 5) were identified with Pictometry data.

#### 4.13.2. Building Morphology

Upon completion of the building database spatial analysis was applied to the building polygons to calculate statistics to describe the size and layout of the structures. ArcGIS was used to calculate the length, width and area of each plot. The building height and dimension statistics were later used by BRC to develop six typical plot-types in Delmas 19 for preliminary cost calculations and logistics planning. The density of buildings was also visualised and used at the main planning meeting as a means of comparing covered living space across the site.

The building heights were estimated using the Lidar laser data collected by the Centre for Imaging Science at Rochester Institute of Technology. The data was downloaded as a Surface Elevation Model (SEM) and a Digital Elevation Model (DEM), both with 1 m spatial resolution. The SEM represents the height of the earth's surface including all objects on it such as buildings, while the DEM represents the bare ground surface elevation without any objects. A building height model was calculated using raster calculator in ArcGIS by subtracting the DEM values from the SEM for each pixel in the scene. No further processing was necessary to distinguish buildings from other above-ground objects as the scene was covered exclusively by buildings. The building height model and hill shade image represent the height of buildings across the scene and are presented in figure 4-21.

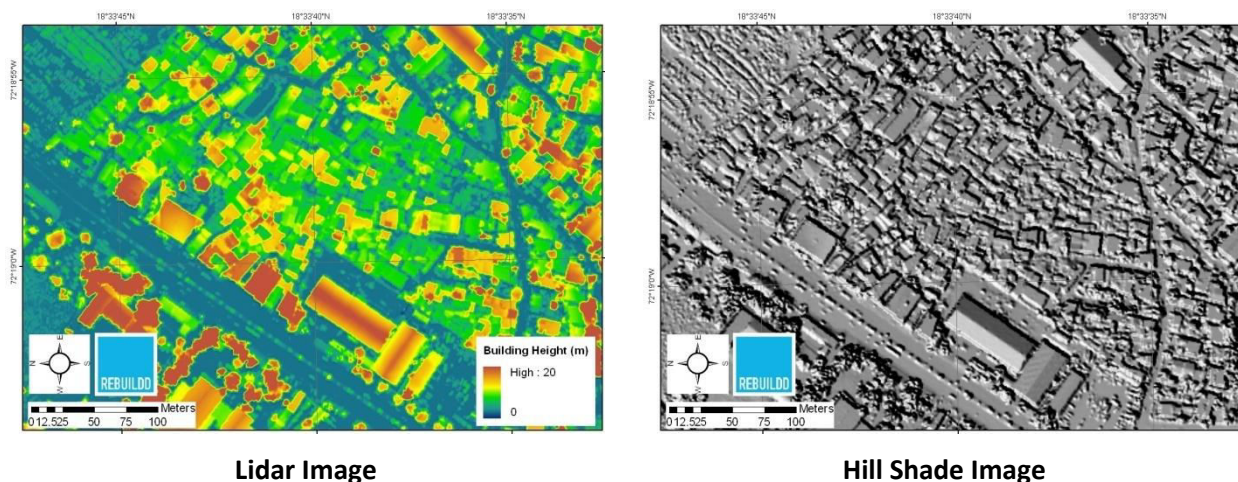


**Figure 4-21: Surface Elevation Model (left) and Hill-Shade Image (right) representing building height were both derived from RIT's Lidar data.**

The mean building height was estimated for each building polygon in the cadastral database using zonal statistics. The procedure estimated the height by calculating the mean value of the height model pixels intersecting with each building polygon. Importing the height data into ArcScene allowed a 3D model of Delmas 19 to be created. The number of storeys was estimated for each building by assuming an average storey is at least 3 m high based on BRC observations. The 3D model shows that most of the buildings are either 1 or 2 storeys, though there are some 3-storey buildings lining the main road to the north-west of the site.

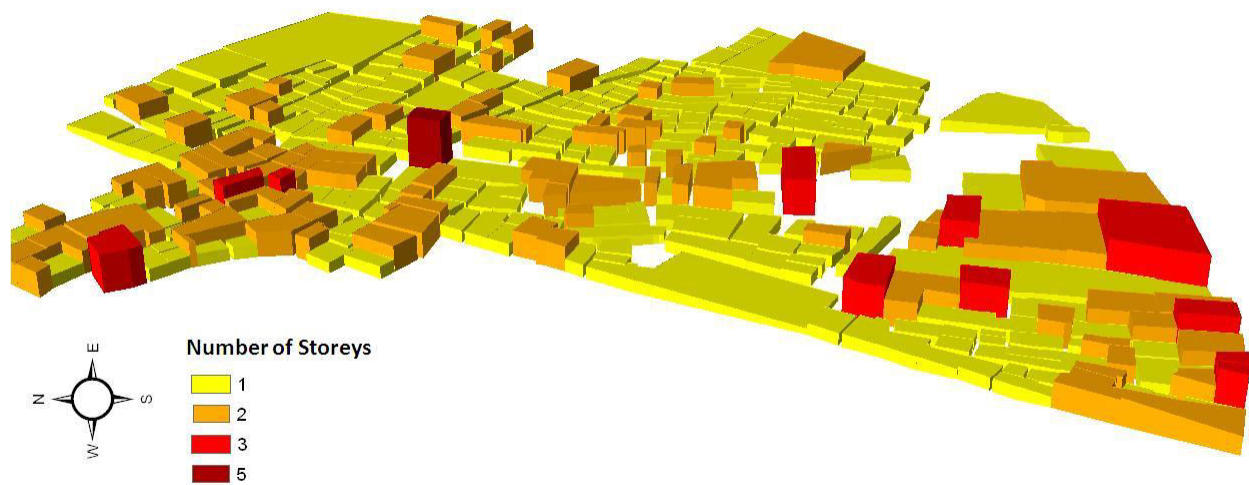


**Figure 4-22: Three-dimensional model of Delmas 19 derived from Lidar height data.**

The accuracy of the building height model was validated by comparing it directly to the ground-derived observations of building storeys. Figure 4-23 shows the results of the two assessments side-by-side and the pivot table displayed in table 4-3 shows the result of the direct plot-by-plot comparison between Lidar observations and the ground assessment. Crucially, of the 463 buildings containing height information 348 were assigned the correct number of storeys using Lidar resulting in 75% accuracy.

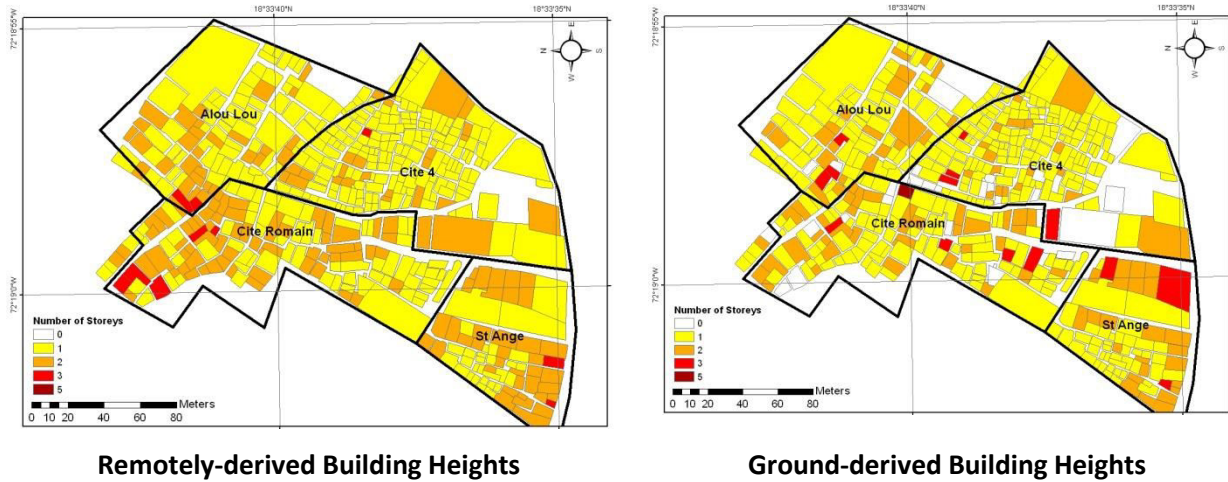
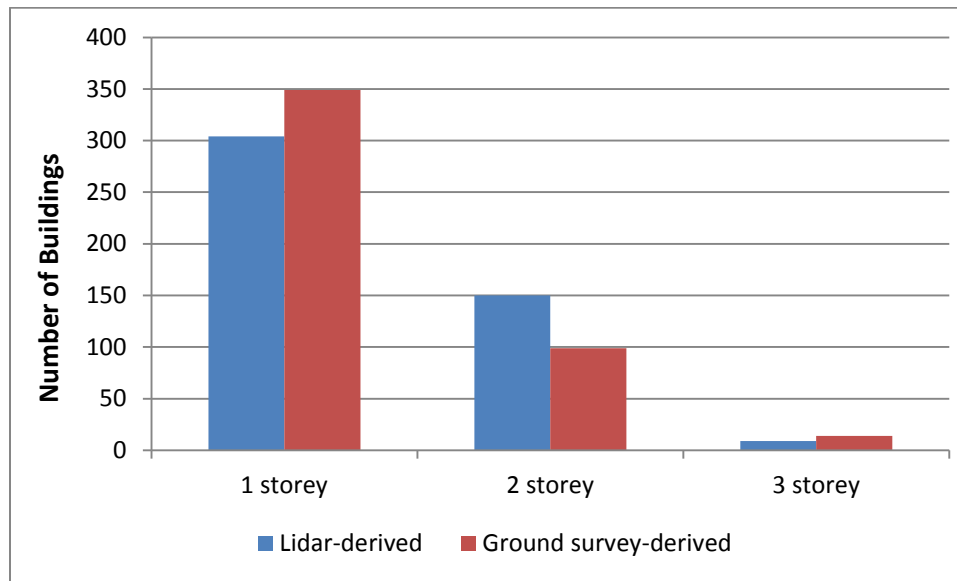


Figure 4-23: Comparison of building height model derived using Lidar data and ground survey.

		Number of Storeys – Lidar-derived			
		1	2	3	Grand Total
Number of Storeys – Ground-derived	1	275	72	2	349
	2	21	72	6	99
	3	7	6	1	14
	5	1			1
	Grand Total	304	150	9	463

Table 4-3: Comparison of building height statistics derived using Lidar data and ground survey.

Of the 114 errors recorded, two-thirds occurred when a 1-storey building was incorrectly tagged as a 2-storey which resulted in an overestimation of 2-storey structures. Ground assessments confirmed that the majority of single-storey buildings were less than 3.0m high but that some structures with pitched roofs were as high as 3.5 m. Buildings with one storey higher than 3.0 m were likely to have been classified as 2-storey. Some residents also temporarily placed tarpaulin on flat roofs which artificially raised the height of the building leading to errors. The results show surprisingly high accuracy though considering the flight route and altitude of the airplane were optimised for the acquisition of aerial imagery and not Lidar. The total number of buildings estimated to have 1, 2 and 3-storeys using Lidar and ground assessments are presented in figure 4-24.



**Figure 4-24: Comparison of the number of buildings with 1, 2 or 3 storeys derived with Lidar and ground survey.**

#### 4.13.3. Building Size Statistics

On completion of the building database each building's dimensions were calculated. The results of this analysis were particularly useful for BRC's preliminary design work and initial cost calculations. The amount of covered space available per person was also calculated by integrating household size statistics from the enumeration survey, which was a useful proxy social-economic indicator.

The maps in figure 4-25 compare the size of each building estimated using aerial imagery and ground survey techniques. The aerial survey estimated that the average building size across the whole site is 43.0 m<sup>2</sup>, with building size varying substantially from 5.4 m<sup>2</sup> to 338.2 m<sup>2</sup>. The cadastral ground survey data shows that 54% of buildings are over 33 m<sup>2</sup> and 17% under 19 m<sup>2</sup>. The biggest building (338.2 m<sup>2</sup>) is a factory located on the east side of Alou Lou. The two maps show similar clustering of small structures in Cite 4 and St Ange. 72% of buildings under 19 m<sup>2</sup> are located in Cite 4 alone.

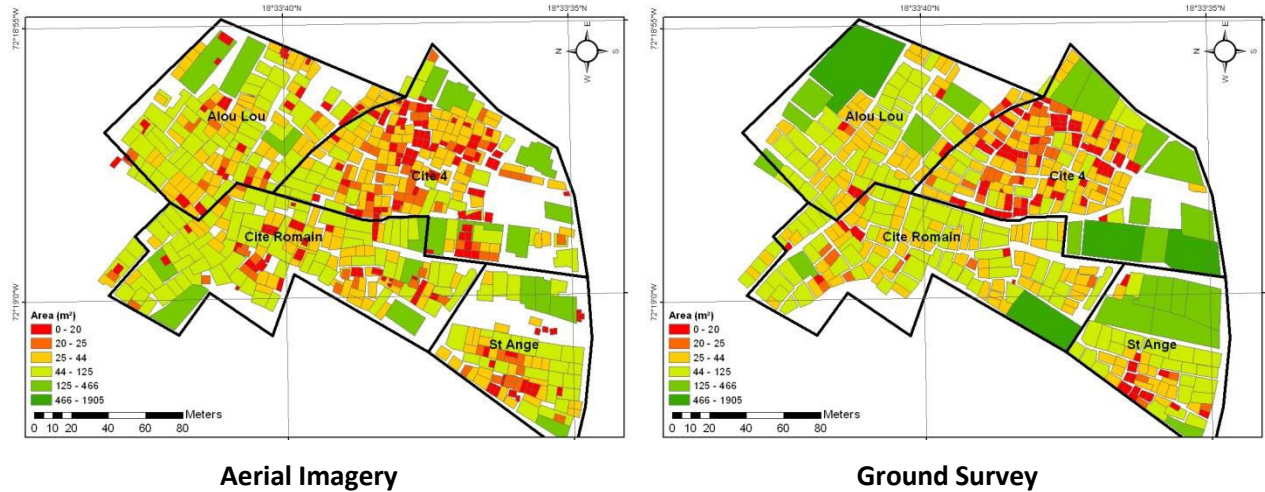


Figure 4-25: Comparison of building size estimates derived using aerial imagery and ground survey.

To validate the size statistics acquired from the aerial image analysis the graph in figure 4-26 shows the number of buildings in Delmas 19 disaggregated by six size categories. The statistics estimated with both aerial imagery and ground field work match very closely suggesting that remote sensing was used with high confidence to produce a profile of the building size in the area.

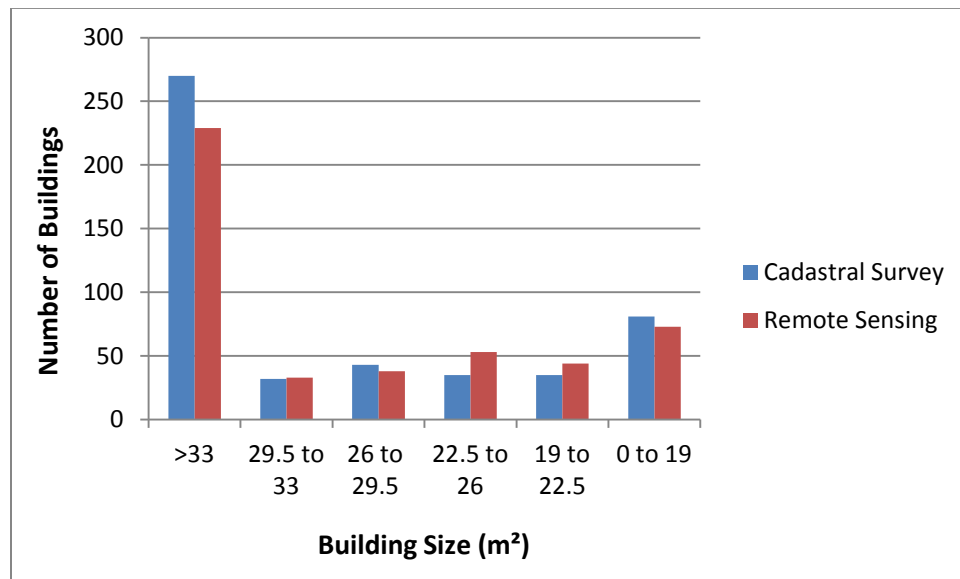


Figure 4-26: The number of buildings disaggregated by size estimated using aerial imagery and ground survey.

Satellite imagery was used to measure lengths and distances for this work and the analysis of Ban Nam Khem (Chapter 3). The accuracy of the distance measurements made using a pan-sharpened Worldview-2 satellite image with 46 cm spatial resolution were verified by comparing the length and width of four buildings measured in the field and in the satellite imagery. The buildings used in this validation exercise included a transitional shelter, permanent structure, an empty plinth and a makeshift shelter. The results are presented in table 4-4. All of the measurements were correct within 50cm and 75% of the measurements were correct within 30cm (equivalent to two-thirds the length of a pixel).

	<b>Ground Measurements (m)</b>	<b>Satellite Measurement (m)</b>	<b>Difference (m)</b>	<b>Difference (%)</b>
<b>T-shelter width</b>	3.68	3.81	0.13	3.5
<b>T-shelter length</b>	4.90	5.11	0.21	4.3
<b>Permanent Structure width</b>	10.31	10.70	0.39	3.8
<b>Permanent structure length</b>	13.36	13.64	0.28	2.1
<b>Plinth width</b>	4.32	4.33	0.01	0.2
<b>Plinth length</b>	4.50	4.59	0.09	2.0
<b>Makeshift Shelter width</b>	5.16	5.65	0.49	9.5
<b>Makeshift Shelter length</b>	7.21	7.37	0.16	2.2

**Table 4-4: Comparison of building dimensions measured on the ground and using satellite imagery.**

#### 4.13.4. Building Density

The final building morphology analysis was *building density* which was calculated and mapped by applying a point density algorithm to the building database. Each pixel in the map was coded by measuring the number of buildings within a 17 m radius. This parameter was selected based on the size and distribution of buildings in the target area. A similar kernel size was used for the density analysis of

Ban Nam Khem in Chapter 3. The density maps allow areas of high and low building density to be identified. Population density can also be calculated using this method by assigning the estimated number of individuals living in each building to the algorithm. The highest building density in the scene is 44 buildings per 900 m<sup>2</sup>, which occurs in the centre of Cite 4. Not unsurprisingly, the high density areas correlate closely with the areas also containing small buildings.

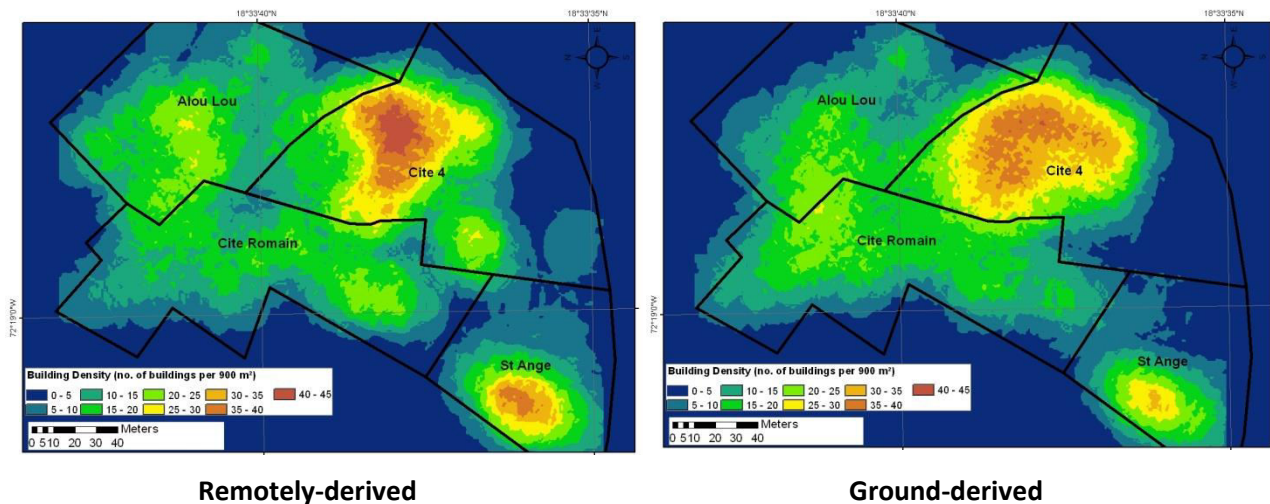
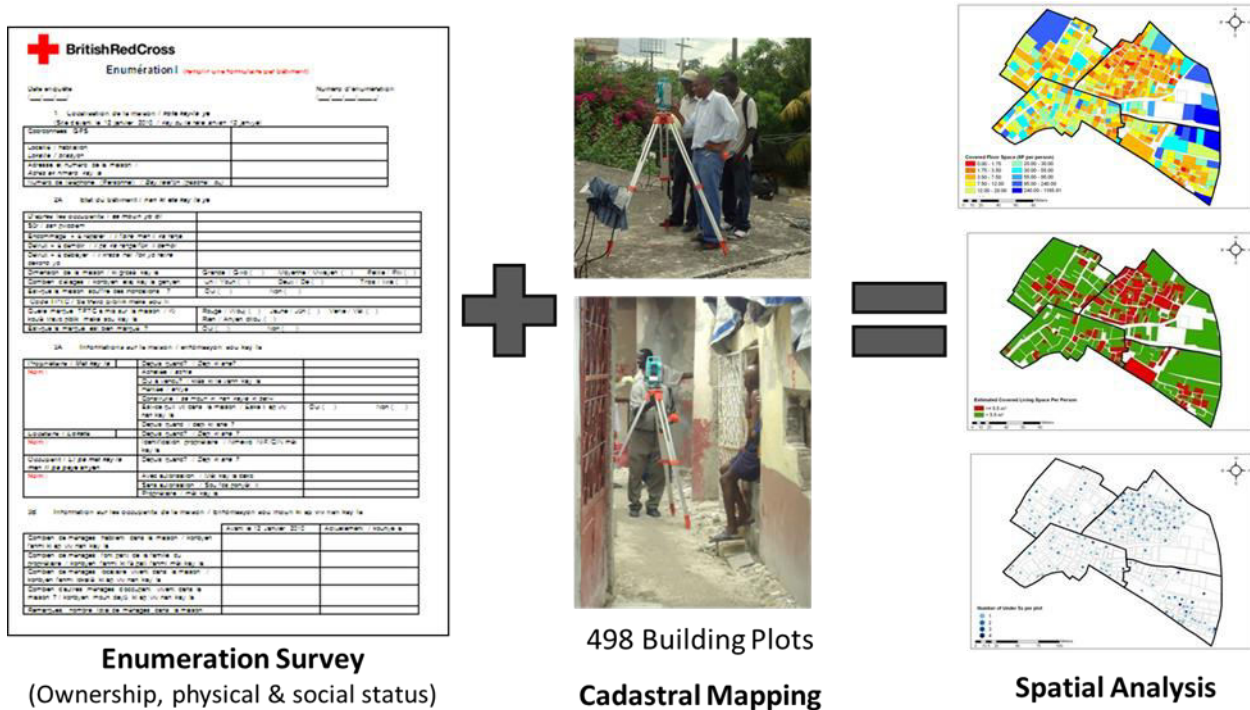


Figure 4-27: Comparison of building density statistics derived remotely and using ground survey.

#### 4.14. GIS Enumeration and Cadastral Survey

After the decision was made to implement a recovery programme the process soon moved to the planning and design phase. House-to-house cadastral and enumeration surveys were first conducted to collect accurate, up-to-date information on Delmas 19 and the people living there. The cadastral survey mapped the location and boundaries of each land plot while the enumeration survey collected data on the physical status of the buildings and the legal and social-economic status of the occupants. The two datasets were later linked by the author to form a comprehensive GIS database of the target area which allowed detailed analysis and visualization of building plot and enumeration attributes. These detailed ground datasets replaced much of the remote survey data and results reported in the previous section such as the building and road database and topographic information.



**Figure 4-28: Cadastral and enumeration surveys were linked in the GIS to produce maps of the target area.**

The surveys both started in May 2011 and took around 7-8 months to complete and verify. The cadastral survey was conducted by a local team of surveyors called SAGESS. The surveyors mapped each building plot using Starfire GPS equipment with sub-metre accuracy. At each plot the team also acquired the occupant's name and ownership information, and they assigned a unique enumeration code using their own pre-fix system e.g. HAITI-PAP-D19-221. The code was tagged onto the side of the building and later used as an identification number by the surveyors conducting the enumeration survey.

The enumeration survey consisted of a questionnaire designed to collect information on the owner, the physical status of the plot and the legal and social-economic status of the occupants. The survey form was based on a template provided by the Committee Interministeriel d'Aménagement and Territoire (CIAT) but was adapted to accommodate information needs for the integrated recovery programme.

The location of the plot was first marked by a GPS coordinate and street address. The survey team then asked for information on the size and state of the building followed by the house and land ownership status, focussing on the location of the owner and the status of the occupants (renters, owner's family

etc.). In the final section of the survey, socio-economic information was collected for each individual living on the plot. Back in the office the data was split between two worksheets. The first worksheet contained information on the plot and the owner with a unique row for each building plot. The second sheet contained socio-economic information for the occupants with a unique row for each inhabitant. The enumeration-code was used to link each individual to the plots they were associated with.

#### *4.14.1. Validation Process*

On completion of the surveys both had to be verified and signed-off by the community. This process was very time-consuming – when changes were made to one survey care had to be taken to ensure the other survey reflected those changes too. Having the two datasets in ArcGIS allowed the process of comparing them easier. In particular, maps were produced that highlighted the plots that needed to be re-visited. Initial analysis identified substantial discrepancies between the two surveys so another independent field survey was conducted by BRC national staff to verify the plots and the enumeration data associated with them. Once the datasets looked to be consistent with each other, each block in Delmas 19 had to be agreed and signed-off by the community and affected households given the opportunity to appeal. To assist this process paper maps from the GIS were taken to the community and used to communicate the proposed changes.

The independent checks in the field revealed that mistakes were made when conducting both the cadastral and enumeration surveys. The cadastral survey missed some plots altogether while other plots overlapped incorrectly and needed to be re-plotted. The process of validating these changes was further complicated as some households were attempting to divide their plots hoping it would double the aid they might receive. Aerial and Pictometry imagery was therefore useful during this process to validate these claims by providing a snap-shot of the urban landscape, showing what existed before and immediately after the earthquake.



**Figure 4-29: Pictometry was used to confirm the presence of three structures in the centre of Delmas 19 that had since been demolished. This figure shows the demolished buildings, viewed from four different directions.**

#### **4.15. Photographic Survey**

After the plots were signed-off a separate ground survey deployment collected a GPS photograph of each plot which was used as baseline material to show the state of the sites prior to the commencement of the project. The surveyors used a Ricoh 500SE GPS camera with a horizontal accuracy of around 10 metres to capture the images. Because of the poor location accuracy of the camera the GPS coordinates alone could not be used to link each photograph to the appropriate plot. The surveyors were therefore asked to note the photograph's ID for each plot onto paper maps as they took the photograph. Each individual photograph was then re-named in the office using each plot's unique enumeration code and then linked to a point dataset containing the centroid coordinates of each building plot. After the data was loaded into ArcGIS clicking on the point in the middle of each plot opened a box containing the survey photograph and other essential information about the building.

Once the photographic survey was complete the results were exported as a KML file so the photographs could be viewed by advisors in the London office using Google Earth. Figure 4-30 shows the KML file

opened in Google Earth. To create the KML file, each photograph was compressed to reduce its size and uploaded to an image hosting website. Each point in the KML contains a HTML link to the appropriate photograph so it may be viewed on-line. This method means the KML file itself is extremely small (375 kb) so may be quickly and easily shared amongst Red Cross colleagues and other stakeholders.

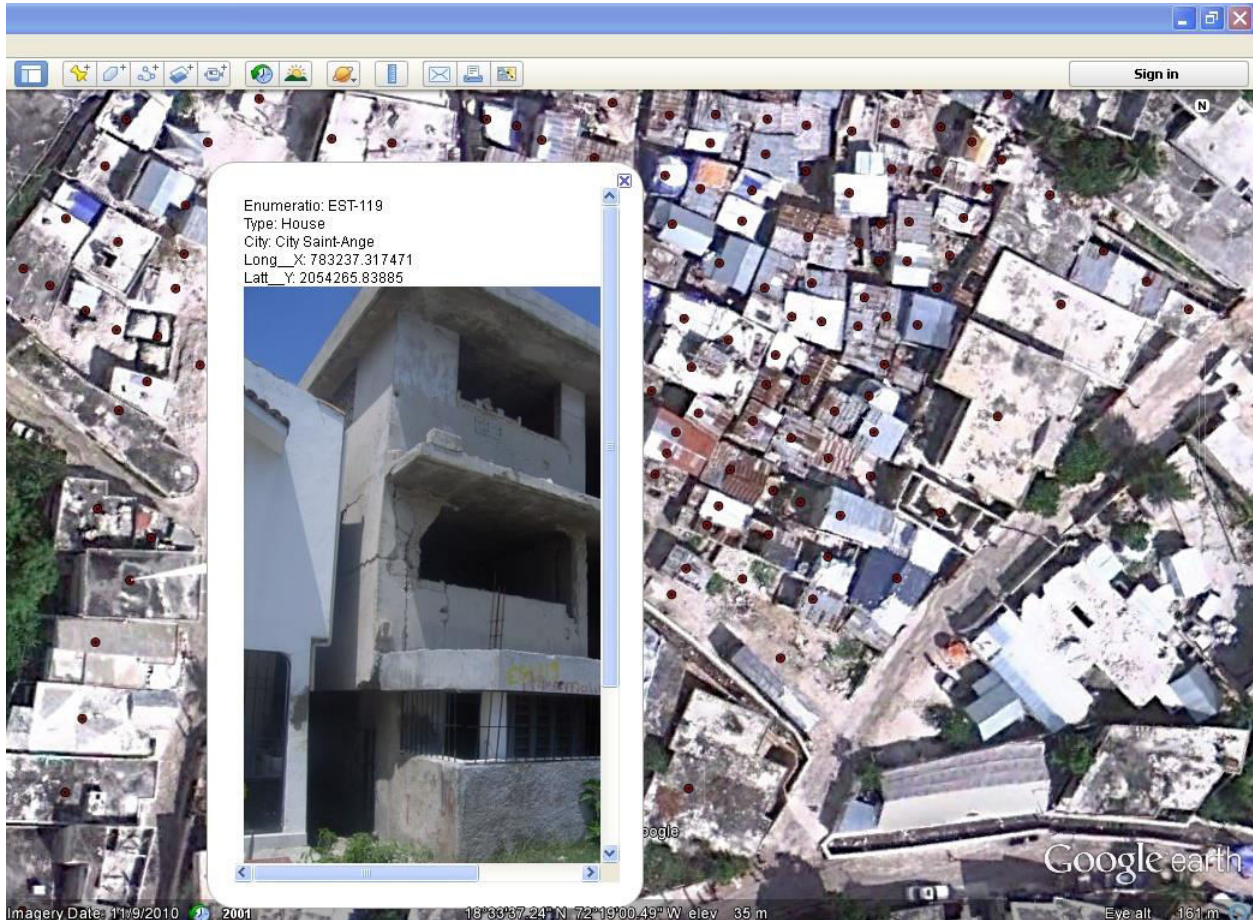


**Figure 4-30: GPS photographs of each building plot were shared and viewed internationally using Google Earth.**

#### **4.16. Integration and Analysis of Data in ArcGIS**

On completion of the ground surveys the ownership information, social vulnerability indicators and building status data were all loaded into a single ArcGIS project. The BRC's GIS Officer was then trained and given responsibility to store, analyse and visualise these datasets. Integrating the data into a single system allowed information to be easily triangulated and analysed collectively. The plots mapped for the

cadastral survey formed the physical framework of the database and the enumeration data was linked to each plot using the unique enumeration code. The *baseline survey* results collected at the beginning of the project were linked to the GIS by matching owner name, identification number and telephone number to data in the enumeration survey. Not all of the baseline survey entries could be linked to a plot using this method due to mismatches in the data entries and a lack of accurate location information, so the dataset is incomplete.

To summarise, the survey results integrated into the GIS at this point included:

- a) BRC's baseline survey conducted in January-2011 to collect **household information** on shelter, livelihoods and WATSAN.
- b) Shelter's enumeration survey conducted in May-2011 to collect information about **house ownership, social-economic status** of the occupants and the **physical status** of the plots.
- c) Shelter's building retrofittability survey conducted by engineers in October-2011 to classify each permanent structure according to their size and roof material to allow **retrofit costs** to be estimated. It was assumed that larger structures and buildings with a concrete roof would cost more to retrofit. The engineers also identified clear plots, transitional-shelters, makeshift shelters and buildings deemed dangerous and in need of demolition.
- d) **Cost information** acquired from a bill of quantities (BOQ) exercise conducted by the engineers and integrated into the GIS as a separate table.

A number of community-scale datasets were also incorporated into the GIS. This included maps of the road and canal system, topographic information and an analysis of open public spaces using Syntax's Depthmap software. The location of water facilities and sources of livelihood, which had been mapped for the Livelihood and WATSAN teams, were also loaded into the database. Data representing slope and the canal system were particularly useful for basic hazard analysis. By incorporating the building plot maps into the analysis of water flow, buildings that might be at risk from heavy flooding were identified for further investigation. Soil bearing capacity measurements taken on the ground were also interpolated and mapped using the GIS to identify areas that might not be able to support heavy load amounts.

#### *4.16.1. Costing and Beneficiary Selection*

After the data was loaded into the GIS the database provided an accurate representation of the target area prior to the project's commencement. The next step was to use the GIS as a tool to assist preliminary beneficiary selection and costing prior to a series of internal planning and design meetings. A workflow was developed that allowed the team to apply a number of selection criteria to analyse the building plots using the legal, social and physical attributes available. Using this algorithm, the database was able to locate and count the number of plots that met different criteria and to provide dimension statistics and cost information for those different scenarios.

This exercise was expected to help the group better understand the large amount of information that had been collected and how it may inform future decision-making by analysing and visualising a number of different scenarios. In particular, the results were expected to show which indicators of vulnerability and physical status might be useful as part of the beneficiary and work selection process. The results were also likely to highlight any gaps in the BRC's database that might need to be filled in the future. The indicators and ranges used in this analysis were only meant to provide an initial insight into how useful the indicators might be and to review the physical and social status of the target area. The community will ultimately decide who the most vulnerable are based on recommendations.

The following section reviews the results from the social, economic and physical analyses applied to the GIS during the planning and design phase.

#### *4.16.2. Social Vulnerability*

Social indicators were collected with the enumeration survey. The Shelter team selected three indicators of social vulnerability after reviewing the *Household Composition and Social Analysis* report produced by the author, which reviewed the results of the enumeration survey using the GIS. The indicators selected included: 1) single or multi-headed households 2) Covered living space (m<sup>2</sup> per person) and 3) % of dependents (under 5s and over 60s) per household.

### Single or multi-headed household

Single-headed households only have a single adult to provide financial and physical security and support to the occupants. Single-headed households were therefore assumed to be significantly more vulnerable than multiple-headed households. The indicator was initially applied irrespective of gender, but can be later disaggregated by gender if deemed appropriate by the community. 162 households across Delmas 19 were found to be single-headed and 189 were multi-headed.

### Covered living space (m<sup>2</sup> per person)

*Covered living space* is an important measure of vulnerability that quantifies the amount of covered floor space available per person. It was calculated for each plot using the following equation:

$$\frac{\text{Plot Area (m}^2\text{)} \times \text{Number of Storeys}}{\text{Number of Occupants}}$$

It was assumed that households with less covered living space per person live in more cramped conditions, which is likely to lead to other issues such as lack of privacy, increased health risk and a generally lower quality of life. The Sphere Guidelines recommend that at least 3.5 m<sup>2</sup> of covered space is available per person. The covered floor space indicator in Delmas 19 is visualised in figure 4-31; 89 plots provide less than the Sphere guidelines recommend and these are shaded red and dark orange. 71% of the buildings that provide less than 3.5 m<sup>2</sup> covered space per person are located in in Cite 4 to the east of the site.

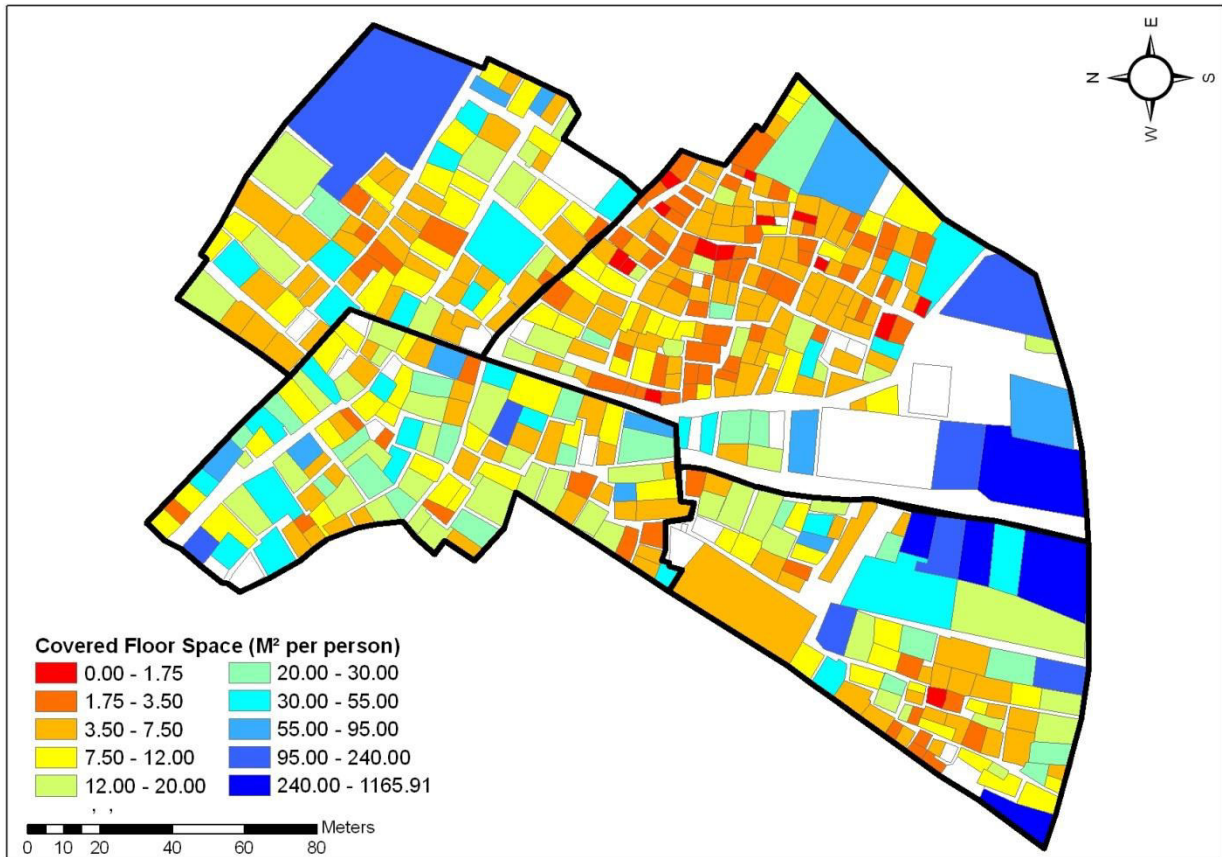


**Figure 4-31: Amount of covered living space (m<sup>2</sup> per person).**

#### Proportion of dependents (under 5s and over 60s) per household

It was assumed that under 5s and over 60s were likely to be dependent upon the surrounding household due to their inability to work or provide assistance to the household. The age ranges were selected after reviewing the demographic statistics for the target area but are likely to need revising by the community. The data shows that 35% of plots have children under 5 living on them and 70% have children aged 5-18. The indicator was calculated as the **number of dependents as a percentage of the owner's household size** and is presented in figure 4-32. 68 plots were identified with more than 20% of dependents as a percentage of the total household size.



**Figure 4-32: Location of plots containing more than 2.5%, 5%, 10% and 20% of dependents as a percentage of the owner's total household size shaded in pink.**

#### 4.16.3. Economic Vulnerability

The economic vulnerability of the household determines their ability to afford any necessary repair or reconstruction costs and is crucial to determine at a household level. Livelihood statistics were collected in the BRC's baseline survey in January 2011. Unfortunately, the cadastral survey was not ready when the baseline survey was conducted and adequate location information was not collected with the baseline survey so it was not possible to confidently link the data to individual building plots. An automatic method was developed to link as many baseline survey entries as possible to building plots

after the cadastral survey was complete using owner name, ID number and phone number information. This procedure successfully linked 284 building plots (57%) to at least one baseline survey entry.

The incomplete results of the baseline survey are still useful and show that as of January 2011 36% of families did not have an income and 28% reported not having any working members of the family. 84% also described themselves as 'in debt'. The reported monthly household income ranged from 0 to 55,000 gourdes; the most frequent response was 0 gourdes and the average was 2,300 gourdes. The most common form of livelihood was street selling, following by skilled and unskilled casual labour.

Figure 4-33 shows the results of two livelihood indicators from the baseline survey mapped in the GIS.

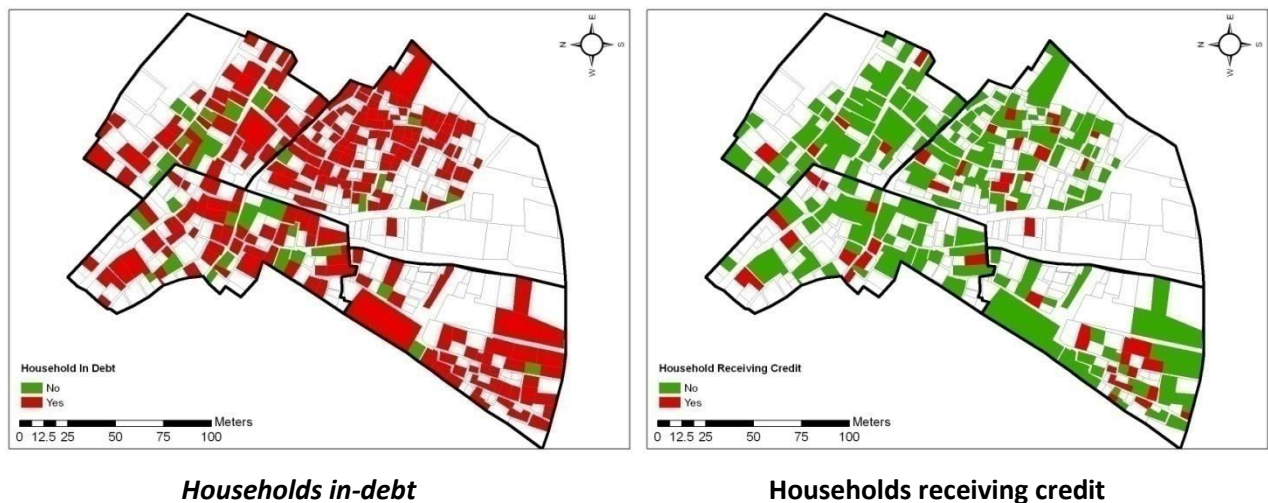


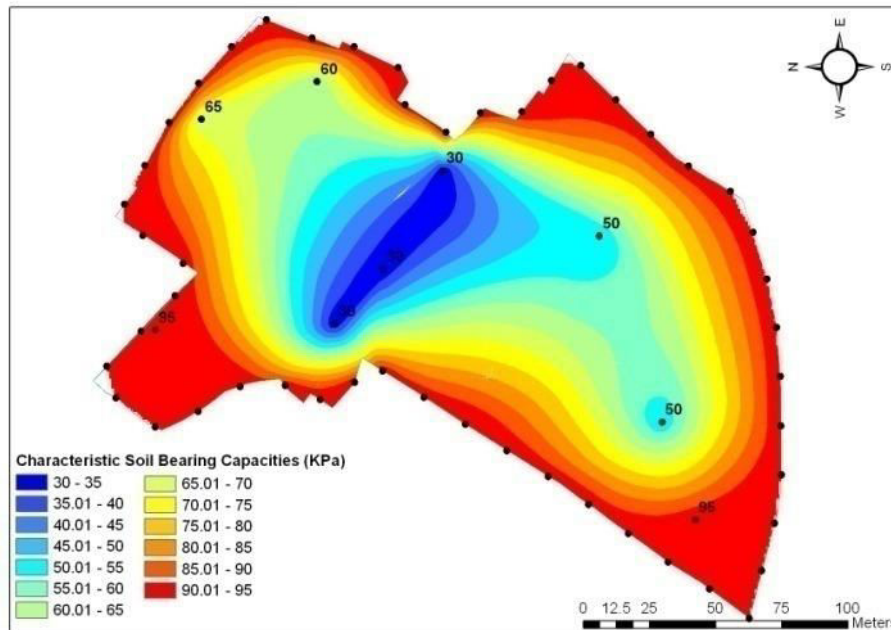
**Figure 4-33: Livelihood indicators from the baseline survey linked to Shelter’s GIS database. Households in-debt or receiving credit are shaded red.**

#### 4.16.4. Physical Vulnerability

Alongside the above-mentioned ground surveys other observational work and analysis was conducted to identify plots that were in particularly poor condition or located in hazard zones. Buildings that appeared to be in poor physical state or prone to flooding were identified by engineers during the retrofittability survey. 66 plots were also flagged by the GIS as they were adjacent to water channels running across the site. Flood risk was further analysed by mapping water flow across the site using the

Digital Elevation Model produced from the Lidar data. Unfortunately accurate height information from ground GPS equipment was not available to adequately validate the Digital Elevation Model. The results of the flow analysis suggested that water was likely to accumulate in Cite Romain due to the topography of the area – an observation which was later verified by community members as part of the participatory process. It was suggested that in future the community mark water levels in different parts of the settlement during heavy rains to better understand the flood process in those areas.

Because of the swampy conditions it was also important for the engineers to determine the load that the ground across the settlement was capable of holding. The soil bearing capacity was established using a scala penetrometer test which involved dropping a weight over a known height and measuring the depth of penetration. This test was conducted at 9 points across the site that were considered to be representative of the area by the engineers. Using more points was not possible due to the extensive coverage of concrete and the lack of exposed bare ground. Maps of soil bearing capacity were produced in the GIS by interpolating these ground measurements. Potangaroa, Neri and Brown (2011) assumed that the minimum required bearing pressure under dead and live loads was 50 kPa. The results of the soil bearing capacity test are presented on the left in figure 4-34 with areas of low bearing capacity shaded blue. This area corresponds to the location of at least 52 plots which will require more detailed investigation. It is also interesting to note that the areas of low soil bearing capacity correlate with areas of substantial damage identified after the earthquake.



Soil Bearing Capacity

**Figure 4-34: Soil bearing capacity was mapped to highlight high-risk zones.**

#### 4.16.5. Scenario Analysis of Beneficiaries and Project Costs

A preliminary list of beneficiaries and project costs were produced for BRC as proof of concept and to better understand the data by analyzing the indicators and other datasets collectively using the GIS. In step one, buildings marked as dangerous in the retrofittability survey were assumed to require demolition irrespective of the vulnerability level of the households living in them. These buildings were automatically added to the list of plots that were likely to be reconstructed irrespective of the vulnerability status of their inhabitants. 10 plots in total were marked as 'dangerous' and fell into this category.

In the next step the remaining plots were disaggregated by owner-type. The recovery strategy for each plot was likely to differ depending on the owner's location and their ownership status. For this exercise, plots were selected only if the owner was living on the plot. Renters were to be analysed separately. The social and economic vulnerability indicators were then applied to the selected plots - in this case, plots

were included only if they contained a single-headed household AND provided less than 10 m<sup>2</sup> covered living space per person.

The locations of these plots were then mapped and statistics produced to describe the size and status of the plots that met the criteria. Table 4-5 shows the status of the 108 selected plots – 27 have been marked as dangerous or unretrofitable because of their size, amount of damage or location. 42 plots have been marked as retrofittable and the remaining 39 plots contain a shelter, rebuilt house or empty plot.

Plot Category	Number
Can't be retrofit (including 10 tagged dangerous)	27
Retrofittable – low cost	21
Retrofittable – medium cost	14
Retrofittable – high cost	7
Transitional Shelter	3
Repaired or rebuilt house	1
Makeshift Shelter	13
Empty Plot	21
Other	1
<b>Total</b>	<b>108</b>

**Table 4-5: Number of plots that meet the selection criteria disaggregated by plot-type.**

After the selection criteria were applied to the plots, the engineer's Bill of Quantities cost estimates for new housing and retrofitting were integrated into the analysis to estimate how much each selection criteria might cost to implement. The engineers assigned each plot to one of three cost categories during the retrofittability survey. Buildings with more than one storey and/or a concrete roof were assumed to cost more to retrofit. Based on the upper cost estimates for each category the retrofit work for this test scenario was estimated to cost in the order of \$70,000. The analysis also identified 64 plots that met the criteria that couldn't be retrofitted, or that contained a shelter or nothing at all. Full reconstruction of these plots might be an option. The engineer's house design, including the

foundations and walls to the first floor, was estimated to cost \$6,557 per structure but this did not include demolition costs which would have to be calculated on a case-by-case basis. As the project moves into the logistics phase of the project the GIS was anticipated to support the planning of demolition and access to individual plots. The images in figure 4-35 show a selection of the plots that met the selection criteria.



**Retrofittable – low cost**



**Retrofittable – high cost**



**Makeshift Shelter**



**Empty Site**



**Transitional Shelter**



**Transitional Shelter**

**Figure 4-35: A sample of plots that met the selection criteria analysis.**

#### **4.17. Monitoring of Project Progress**

The Red Cross work was frequently being monitored throughout the planning phase through weekly reports, phone conversations with London and more formal evaluations such as the mid-term review. A review conducted in September 2011 for example, evaluated each component of the project (Water-sanitation, Livelihoods and Shelter) by considering the project's progress, lessons learned and efficiency in terms of output and cost.

After the planning and design phase of the project is finished and the logistics have been organised the GIS was to be used to host the enumeration data and to support the management and monitoring of the proposed recovery work. A geodatabase capable of monitoring change over time can be built manually or with existing tools such as the Tracking Analyst in ArcGIS. The GIS Officer in Haiti was trained by the author to manually update the existing database by adding 'milestones', which can be ticked off for each plot once each target had been reached.

In addition to monitoring recovery a well-designed GIS database can be used to centrally manage the tasks, costs, timing and location of the improvement work. The progress at each plot may also be measured relative to expected timeframes to highlight areas of slow progress that require further assistance. This requires each job to be assigned a geographic location and a description of essential tasks – each task can then be linked to subtasks, timeframes and information about those responsible. Budgets and project schedules are likely to change throughout the project as a result of this information so the system must be flexible enough to deal with these potential changes.

Most of the monitoring data will be collected by members of the community and independent assessors working in the field. The field teams will need to aggregate the plot-level data on a regular basis and geographically locate any relevant community-scale changes in the project area. As long as changes to plots have an associated plot ID they can be easily added to the GIS by the database team.

In its current form the GIS system is similar to existing management systems for construction work but with the benefit of using a spatial map framework. The system can therefore be used to produce maps and statistics to show progress over time. Ultimately the GIS can help the team to visualise

improvements and communicate progress and issues to the community, local authorities and other stakeholders, which will help encourage their involvement and engagement as the project progresses.

#### *4.17.1. Using Satellite Imagery to Monitor Construction and Transitional Shelters*

Most of the monitoring data will be collected using community participation and by assessors on the ground. The Red Cross's *Owner-Driven Housing Reconstruction Guidelines* (IFRC, 2010) provide guidance on this including recommendations on what aspects of construction need to be monitored. The appropriate indicators are selected once a project plan and log framework has been finalised. Trained individuals will then need to monitor things such as the quality of construction techniques and the materials used. Satellite imagery can be a useful secondary dataset at this stage of the recovery process to verify ground survey results and to monitor the progress of recovery.

To verify the claim that satellite imagery can be used to monitor recovery in Haiti, Worldview-2 imagery was collected in September 2011 and used to monitor construction and the provision of transitional shelters across Delmas 19. The results of the satellite monitoring were then directly compared to the engineer's retrofittability survey conducted in October 2011 and verified again using the plot-by-plot photographic survey results available in the GIS.

After the Worldview-2 satellite image was pan-sharpened and geometrically corrected using the methodology described in Chapter 3, the building plot dataset from the cadastral survey was placed over the satellite image. Each plot was then individually analysed and tagged as either containing 1) a pre-existing building 2) a transitional-shelter 3) an incomplete building under construction 4) a complete new building or 5) an empty plot. Where necessary, to distinguish between existing buildings and new buildings the satellite image was compared to historic imagery collected in January and November 2010. The rectangular transitional shelters in the region were built by UNOPS and had unique spectral and spatial attributes that were used to distinguish them from other features in the imagery. In particular, the roofs were made with corrugated-iron which appeared dark with distinct white stripes at the joins. Most of the shelters also had corrugated-iron verandas over their entrances which reflected brightly in the imagery.

The results of the validation exercise show that satellite imagery was used with high confidence to identify the transitional shelters because of their predictable size and distinctive features but empty plots were less reliably distinguishable from other features such as flat concrete roofs. There was very little new construction in the area but four new buildings marked in the engineer survey were all correctly identified using satellite imagery.

In total, 34 transitional shelters were identified out of 35 resulting in 97% accuracy. Only one permanent building was mistakenly classified as a transitional shelter because it also had a corrugated-iron roof and a similar shape and size to the shelters. In two cases, the image analyst correctly identified shelters on plots that were not identified in the engineer's ground survey, thus verifying and updating the ground survey results. Mistakes with the ground surveys were not unexpected though due to the density and complexity of the urban environment. Overall, these results suggest that satellite imagery can be used as a secondary data-source to verify and support ground assessments.

Empty plots were not so easily identifiable and sometimes confused with other categories. Of the 54 plots marked as empty in the satellite imagery, 7 contained a building or makeshift shelter resulting in 87% accuracy. These errors occurred when flat concrete roofs appeared like bare ground or where the site was partly empty. In addition, of the 62 empty sites in the target area 15 (24%) were wrongly assumed to contain a building. These sites often contained features that were mistaken for permanent buildings including tents, ruined walls, shadows from adjacent buildings and materials such as blocks or concrete. The satellite imagery did not contain enough spatial detail to confidently identify these small features.

It must be noted that this analysis was completed by an analyst with years of experience. The reliability of the results depends on a number of factors but is particularly dependent on the spatial and spectral uniqueness and clarity of the features of interest. Monitoring using satellite imagery is not likely to be cost-effective for small sites but grass-root mapping initiatives can be used to acquire cheaper aerial imagery using balloons and kites. A more detailed examination of the use of remote sensing as a monitoring tool is presented in Chapter 5; in particular remote sensing datasets were used to monitor the location of tents, tarpaulins and shelters across large geographic areas and a planned camp for UN-Habitat.

#### **4.18. Maps to Support the Participation Process**

To increase the likelihood of a successful shelter project it is important to acquire the input and agreement from the beneficiaries themselves. That is why every step of the process in Haiti has been overseen and ultimately signed-off by the community themselves. PASSA (Participatory Approach to Safe Shelter Awareness) is a knowledge-sharing technique, developed by IFRC and BRC in Bangladesh and Uganda that allows communities to improve their living environment by identifying priority needs and building the capacity within the community to plan for change.

During the planning and design phase of the project a group of 32 community representatives were selected to represent each zone in Delmas 19. A series of 8 activities were conducted over a 3-4 month period to identify and prioritize key problems in the community and develop suitable solutions. The groups developed a historical profile of the neighbourhood and identified and prioritized the risks and needs. Everyday problems and risks were highlighted that the community felt threatened their health and safety. Cite 4 in particular was highlighted as an area of high-risk during earthquakes due to the narrow access routes and particularly poor building quality and Cite Romain due to its relatively low level and subsequent risk of flooding. These observations matched the results of the remote aerial image analysis of accessibility and the built environment.

The third activity of PASSA titled *Community mapping and visiting* allowed members of the community to map the settlement's main infrastructure and to identify both safe and unsafe shelter conditions. Maps can be extremely important tools in any planning process to visualise and analyse spatial information but also as data collection tools. The main aim of the PASSA mapping exercise was to get the community to think about the space they live in by creating their own maps and spatial representations of Delmas 19. It is hoped as a by-product of this that the results will provide a useful insight into how the community perceive the space around them and also provide the community with confidence and knowledge to approach local authorities with their ideas for development.



**Figure 4-36: Satellite imagery and maps provided throughout the session are used as prompts for discussion and to give the participants something they can compare their own map against.**

The risks and solutions identified during the PASSA process were turned into a Community Action Plan focusing on public health, housing, water management and drainage. Solutions suggested by the community groups were affordable and feasible to implement in the near future. To deal with rubbish for example the community suggested clearing the canals and developing a management plan for community bins. In the future, BRC will work with community groups to establish how this may be supported. A community team was created for each of these issues to plan and implement suitable solutions in the future. The maps and data will continue to be useful during the implementation stage to organize and monitor the work of these groups. The community will also continue community mapping initiatives such as measuring flood levels, waste mapping, livelihood mapping and emotional mapping (where they feel safe).

Most of the inhabitants of Delmas 19 had never seen a map or plan of their community and needed the concepts of scale and proportion to be explained to them, so when asked to map their community what they produced was a rather abstract perception of their space. Many members of the community also needed the purpose of the mapping to be explained to avoid suspicion and confusion. The maps were still very legible though and contained key features that were positioned in the correct position relative to each other often linked by a series of corridors. These maps were given to a local artist who worked with the community to produce more realistic spatial representation of the area.

The final map contains building blocks with the names of owners, as well as corridors, churches and other key facilities. The map also highlighted tall, damaged buildings and areas affected by flooding and garbage. The results showed that flooding was likely to occur in Cite Romain. Paths carrying water in St Ange and Alou Lou are also marked. Maps have been converted to canvas to be used for the planning phase. It seems that the satellite imagery is difficult for most participants to interpret without guidance, but that the GIS map of building plots was used frequently as reference material.

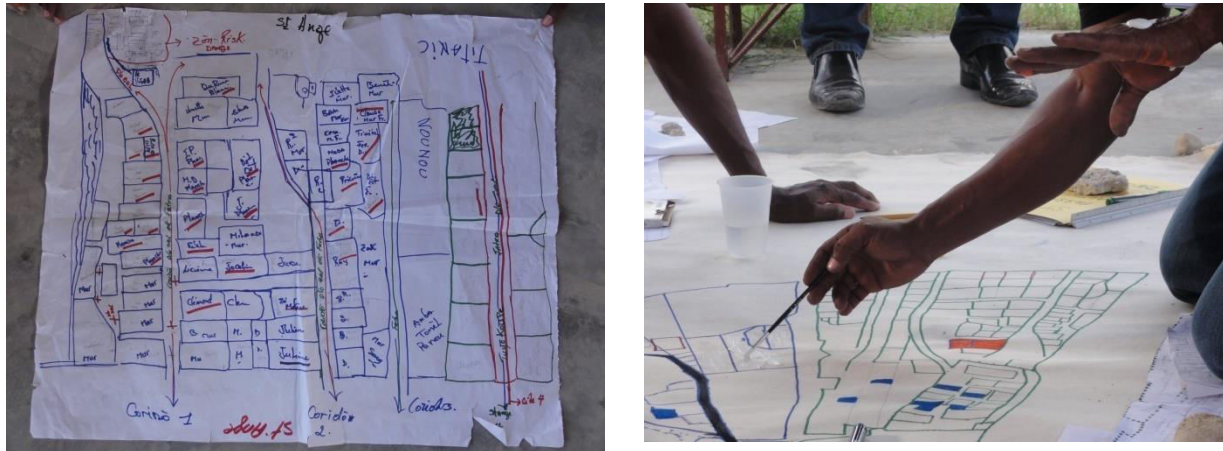


**Figure 4-37: The abstract community maps (left) were converted to real plans of the community to support the community action plan (right).**

#### 4.19. Conclusion

The work presented in this chapter shows how some of the geospatial protocols developed in Chapter 3 were used in an operational setting with the British Red Cross. Specifically, there are three broad post-disaster phases of data collection where geospatial tools were found to be useful: 1) rapid needs assessment 2) planning/design and 3) recovery monitoring. These phases closely match common components of a reconstruction programme identified by Jo Da Silva in her book *Lessons from Aceh*. Jo Da Silva's framework is presented in figure 4-38; the components that were assisted with geospatial technology are marked by the author with blue stars.

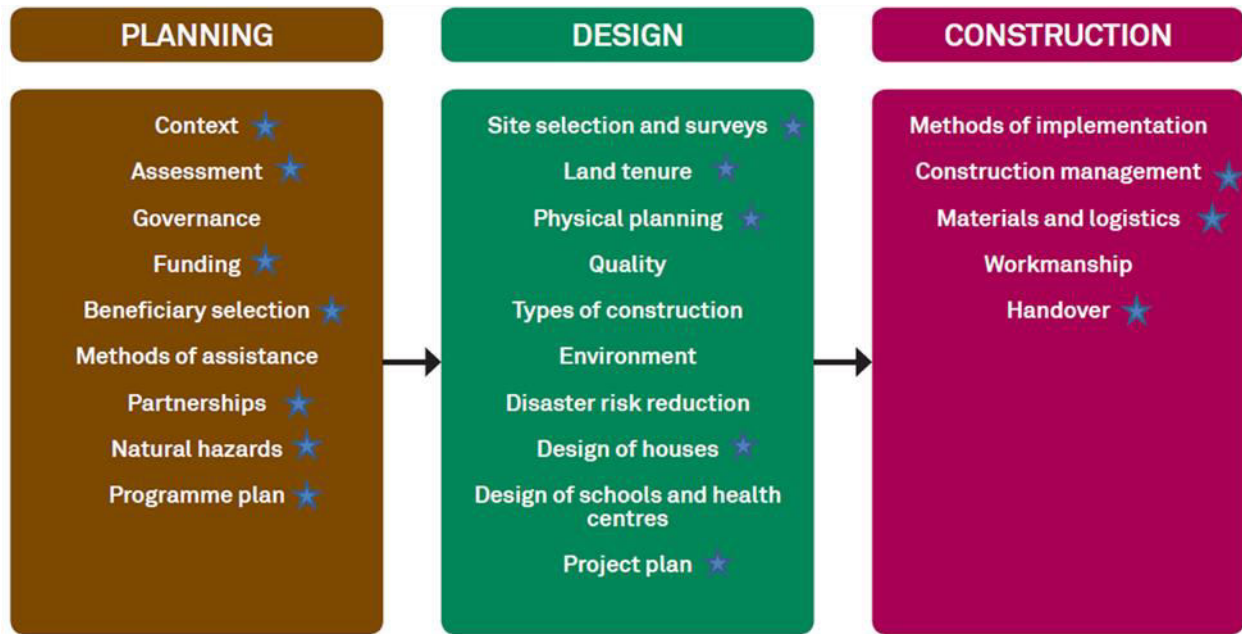


**Figure 4-38: The common components of a reconstruction programme (adapted from Da Silva, 2010). Blue stars represent components of the BRC project that were assisted with geospatial tools. Note that this framework does not include needs assessment.**

#### 4.19.1. PDNA and Rapid Remote Assessment

In the weeks and months after the earthquake geospatial tools were very valuable to the PDNA process, before ground work was possible, by estimating the extent and distribution of damage across large areas. Later in the process geospatial tools were used to support ground assessments by highlighting particular areas of interest and later mapping and analysing the ground-derived results. Identification of structural damage across Delmas 19 using Pictometry images resulted in 64% accuracy, similar to results produced by Spence and Saito (2010).

Remote sensing was also used in the early stages of the BRC project to perform a rapid assessment of the Delmas 19 settlement. Verification highlighted some of the limitations of using remote sensing in a dense, slum environment which are important to be aware of. All of the main roads in Delmas 19 were mapped correctly but almost half the length of small lanes was missed as they were covered or obscured by buildings. And approximately one-third of the 536 buildings were over-counted or not counted by remote analysis. This suggests remote sensing is not a reliable tool for accurate cadastral mapping.

Building dimensions were correct though within 50 cm and despite the limitations, the building database was still used to produce a useful profile of the built environment, to calculate building morphology statistics and as a framework on which an assessment of structural damage and the monitoring of recovery was conducted. The provision of transitional shelters and other physical changes, such as the identification of open plots, were also monitored with high confidence after the earthquake and in some cases were used to correct the ground survey results.

#### *4.19.2. Planning and Design Work*

GPS receivers and GIS systems brought significant value to planning and design work by recording, storing and analysing spatial data. The GIS system successfully stored social, physical and legal information required to plan and implement a recovery project. The database was also used to assist beneficiary selection and costing work. The maps produced with this system were also used to support logistical decision-making, to promote the programme and to assist the participatory process.

While geospatial tools have become more commonly used in the immediate aftermath of large disasters, geospatial tools are less commonly found supporting the subsequent planning and monitoring stages. And frustratingly many of the datasets produced for the needs assessment are not being passed on and used as baseline material for the subsequent phases. It's important that damage and needs assessments are designed with recovery planning in mind and that the results from these assessments are reliable and disseminated widely.

#### *4.19.3. Strengths and Weaknesses*

The BRC database was still being used in Haiti one year after its creation, managed by a single national staff member and a team of data collectors. The Head of Mission reported that he would like to see geospatial support provided to other development projects and agreed that the GIS would lead to improved efficiency, better understanding of data and improved decision-making. Other agencies such as Habitat for Humanity also expressed an interest in deploying a similar system but unfortunately the time was not available to do so.

The technology helped provide a systematic overview of the situation and manage information in a complex, dynamic situation where there was a lack of data and capacity. Aerial imagery was valuable in the first months of the response because of the speed it became available. It was also able to provide information even when ground restrictions were in place. It's important to be aware of remote sensing's limitations though in this sort of urban environment.

Later the GIS brought value because of its ability to visualise, store and analyse large amounts of data. The use of a single GIS system also helped to integrate the different elements of the recovery programme so they were all using the same platform. A substantial amount of time was also saved by logging the location of beneficiaries and their statuses - this allowed re-surveying to be conducted much quicker and also prevent fraudulent behaviour. The GIS and mapping can also be seen as an output of the programme in itself which can be provided to the community to help them apply for funding and manage their community themselves in the future.

Users must be realistic about the amount of time required to collect and analyse such data though. It took several weeks to put together the building database but once completed it was able to produce results and information relatively quickly. And it was substantially quicker than the ground survey which took seven months. To help speed up the data collection process the Red Cross would like to see standardised protocols produced and the use of advanced handheld technology incorporated.

An independent final evaluation of the BRC programme was published five years later (Advisem, 2016). It acknowledged that appropriate research and analysis was conducted to understand the technical requirements of building in Delmas 19, but unfortunately it would seem the database was not maintained for the duration of the project. The data management teams were overwhelmed as the cadastral survey contained mistakes and there were disputes amongst the community. The three components of the programme also continued to work and collect data independently of each other (Advisem, 2016). This suggests that somebody with technical ability needs to be on-hand to ensure the continued use of the technology. Issues surrounding the reliability of remote sensing and the institutional and staffing options available are discussed in the conclusion chapter.

## Bibliography

Advisem Services Inc. (2016). Final evaluation of the British Red Cross' Haiti earthquake 210 response and recovery programme: achievements, challenges and recommendations. Ottawa, Canada.

ATC. (2005). ATC-20-2.Detailed Evaluation Safety Assessment Form. Available at:  
<https://www.atcouncil.org/products/downloadable-products/briefing-papers/45-downloadable/downloads/107-atc-20-download>

Booth, E., Saito, K., Spence, R., Madabhushi, G. and Eguchi, R.T. (2011). Validating assessments of seismic damage made from remote sensing. *Earthquake Spectra*: **27**, 157-177.

Brown, D. Remote Sensing and Disasters (2017). Cambridge Architectural Research Ltd.

Brown, D., Platt, D. and Bevington, J. (2010). Disaster recovery indicators. Centre for Risk in the Built Environment. Cambridge University, UK.

Clermont, C., Sanderson, D., Sharma, A. and Spraos, H. (2011). *Urban disasters – lessons from Haiti. Study of member agencies' responses to the earthquake in Port-au-Prince, Haiti, January 2010*. Report for the Disasters Emergency Committee (DEC), London.

Corbane, C. and Lemoine, G. (2010). *Standard Operating Procedures Collaborative Spatial Assessment (CoSA). Release 1.0*. JRC Scientific and Technical Reports, Ispra, Italy.

Da Silva, J. (2010). Lessons from Aceh. Key considerations in post-disaster reconstruction. Practical Action Publishing. Rugby, Warwickshire.

Foulser-Piggott, R., Spence, R., Saito, K., Brown, D.M. and Eguchi, R. (2012). The use of remote sensing for post-earthquake damage assessment: lessons from recent events, and future prospects. *15th World Conference of Earthquake Engineering (WCEE)*. Lisbon, Portugal.

Foulser-Piggott, R., Spence, R. and Brown, D. (2013). *The use of remote sensing for building damage assessment following the 22nd February 2011 Christchurch earthquake: the GEOCAN study and its validation*. Report for Global Earthquake Model (GEM). Cambridge Architectural Research Ltd.  
<http://www.carltd.com/sites/carwebsite/files/GEOCAN%20Christchurch%20Report.pdf>

Ghosh, S., Huyck, C.K., Greene, M., Gill, S.P., Bevington, J., Svekla, W., DesRoches, R. and Eguchi, R.T. (2011). Crowdsourcing for rapid damage assessment: the Global Earth Observation Catastrophe Assessment Network (GEO-CAN). *Earthquake Spectra*: **27**, 179-198.

Government of the Republic of Haiti (2010). *Action Plan for National Recovery and Development of Haiti. Immediate Key Initiatives for the Future*. Port-au-Prince, Haiti.

Government of the Republic of Namibia (2009). *Post-disaster needs assessment*. A report prepared by the Government of the Republic of Namibia, with support from the international community. Available at:  
[http://www.recoveryplatform.org/assets/submissions/201211102240\\_pdna\\_flood\\_namibia2009\\_english.pdf](http://www.recoveryplatform.org/assets/submissions/201211102240_pdna_flood_namibia2009_english.pdf)

Haiti PDNA. (2010). *Haiti Earthquake PDNA: assessment of damage, losses, general and sectoral needs*. Government of the Republic of Haiti, Port-au-Prince.

IFRC. (2010). *Owner-driving housing reconstruction guidelines*. The International Federation of Red Cross and Red Crescent Societies. Geneva, Switzerland.

IFRC. (2011a). *Haiti earthquake operation – first 12 months*. Red Cross Red Crescent Societies. Shelter Technical Brief. January 2011.

IFRC. (2011b). *Project/programme monitoring and evaluation (M&E) guide*. International Federation of Red Cross and Red Crescent Societies, Geneva, Switzerland.

Meier, P. (2011). *OpenStreetMap's new micro-tasking platform for satellite imagery tracing*. iRevolution Blog. September 7 2011. Available at: <http://irevolution.net/2011/09/07/osm-micro-tasking/>

Potangaroa, R., Neri, R.M. and Brown, D. (2011). *The design development and costs of several key housing issues for Delmas 19, Port-au-Prince, Haiti*. Consultant report for British Red Cross. December 2011.

Potangaroa, R. and Neri, R.M. (2011). *A review of the red tagging of buildings in Delmas 19*. Consultancy report for British Red Cross. 22 Sept 2011

Schwartz, T.T. (2011). *Building assessments and rubble removal in quake-affected neighbourhoods in Haiti*. BARR Survey Final Report. USAID. May 13, 2011.

Shelter Cluster. 2012. Emergency Shelter and CCCM Cluster. Minutes from Meeting on 9 August 2012, 11:30am-1:00pm. UCLBP – Bourdon.

Spence, R. And Saito, K. (2010). Port-au-Prince earthquake damage assessment using Pictometry. A report for Imagecat Inc. Cambridge Architectural Research Ltd. June 2010.

## **Chapter 5: Comparing the use of manual and semi-automated remote sensing techniques to monitor camps and spontaneous settlement for UN-Habitat after the 2010 Haiti earthquake**

### **5.1. Introduction: Aims and Content of the Chapter**

Geospatial tools were applied in real-time as part of the follow-up to the Recovery Project to explore how they might be useful in an operational setting. The British Red Cross's decision-making process and the validation of manual image analysis of a complex urban slum is described in Chapter 4. In this chapter, three forms of semi-automatic analysis of satellite imagery were used to monitor planned camps and instances of spontaneous settlement for UN-Habitat. This allowed image analysis techniques and sampling procedures to be tested thoroughly across large geographic extents, which was something the original Recovery Project highlighted as a particular need (Brown, Platt and Bevington, 2010). The conclusion to this chapter will summarise the accuracies, strengths and weaknesses of each technique with recommendations on what to use and when.

Extensive data on camp status and spatial distribution was already available from the Camp Coordination and Camp Management's (CCCM) Displacement Tracking Matrix (DTM), but limited data was available on the process of spontaneous settlement. Remote sensing will be used to validate the existing DTM camp datasets and to provide new information on spontaneous urban processes.

This study was conducted at the end of October 2011 at the request of the United Nations Human Settlements Programme (UN-Habitat) to test the effectiveness and reliability of remote sensing as a tool to monitor camps and spontaneous settlement in areas affected by the 2010 Haiti earthquake. The work formed a contribution to the project '*Programme to support the reconstruction of housing and neighbourhoods*' managed by the United Nations Development Group. The objectives of this UN programme were to develop an inventory of homes in the most-affected areas, to develop a mechanism for on-going monitoring and evaluation of reconstruction and to create a platform for the analysis and dissemination of information.

The programme's outputs were expected to support decision-making and enable recovery actors in Haiti to work more coherently and effectively with each other. UN-Habitat recognised that the Haitian government required information to plan, coordinate and quality-control reconstruction and that national and international agencies operating in the country needed information to help with programming and for monitoring purposes. Sixteen months after the earthquake the country still did not have detailed ground knowledge on the location of the affected population and the status of their properties, tenure situation and level of basic service provision.

The work presented in this chapter focuses on how effectively remote sensing tools can be used to support the monitoring and evaluation of reconstruction by providing information on the size and layout of *planned camps* and the location and extent of on-going reconstruction processes including *spontaneous settlement*. Manual and semi-automated remote sensing techniques were used to monitor two sites, each with very different layouts, spatial characteristics and building-types, to test the versatility of the remote sensing tools in different post-disaster environments. The chapter is split into two studies:

Study 1) Spectral and manual techniques were applied to Canaan to monitor a large area of spontaneous settlement covering over 5 km<sup>2</sup>

Study 2) Mathematical morphology, object-based image analysis and spectral semi-automated techniques were applied to Corail Sector 4, a planned camp containing identical transitional shelters arranged in blocks

The characteristics of the two study areas are summarised in table 5-1.

	Study 1: Canaan	Study 2: Corail Sector 4
<b>Camp Type</b>	Spontaneous Settlement	Planned Camp
<b>Spatial Characteristics (m<sup>2</sup> per person)</b>	Not very dense (136.4)	Dense (47.6)
<b>Main Building Type</b>	Makeshift shelters & Concrete structures	Wooden transitional shelters
<b>Remote Sensing Techniques Applied</b>	Manual & spectral	Manual, morphological, object-based & spectral
<b>Aerial Image</b>		

Table 5-1: A summary of the camp characteristics and techniques applied to each camp.

## 5.2. Study Background

### 5.2.1. Camps in Haiti

After the 2010 Haiti earthquake 1,555 camps were established accommodating over one-and-a-half million people. Most of the camps were created spontaneously in small open public spaces, located across a stretch of land 84 km wide from Petit-Goave in the west to Port-au-Prince in the east. In August 2011, nineteen months later, 802 official camps were registered with an estimated population of 550,560 people (CCCM, 2011a).

At the time of the study, most of the camp population still lived in makeshift shelters made with wooden frames, tarpaulin and corrugated-iron. These shelters were often attached to each other and were erected in small spaces with poorly organised layouts. Most of the camps lacked permanent road surfaces and the inhabitants commonly did not have access to basic services or sources of livelihood.

Monitoring the status of camps was necessary to inform decision-making surrounding exit and development strategies. The strategy for return in Haiti was based on the closure of camps and returning displaced families back to their neighbourhoods of origin (ICCG, 2011). UN-Habitat required information to track the status of camps and in addition, they wanted to be able to identify camps that might be considered for development as permanent settlements because residents had made considerable physical and financial investment there.

### *5.2.2. Spontaneous Settlement in Haiti*

Outside of the documented camps was an evolving process of new settlement and housing construction which included land invasion, sale and development of plots, and unregistered shelter and housing construction. UN-Habitat believed this process represented the majority of housing reconstruction efforts by Haitian families with their own resources, rather than those families and houses being assisted by donor funding or agency assistance (UN Internal Document, 2011).

Despite this, the numbers of new houses under construction through this process, the locations, services available, financial investment, building standards and other information had not been comprehensively monitored or analysed to date. Decisions on how to strategically support, guide, limit, control or intervene in this spontaneous development process required information on the extent of construction taking place and were important in terms of housing reconstruction policies.

### *5.2.3. CCCM's Displacement Tracking Matrix (DTM)*

The Displacement Tracking Matrix (DTM) offered the most comprehensive dataset on the size and condition of camps in Haiti. The CCCM cluster developed the DTM in March 2010 to provide information on the movement of the camp population and the condition of camps and camp-like settlements

(CCCM, 2011a). The objective of the dataset was to provide timely and accurate information to advise the humanitarian response and transition towards return and recovery (CCCM, 2011b.)

Data was collected bi-monthly from approximately 1,000 camp locations. The first version of the DTM (DTM v1.0) was designed to record and maintain a list of all camp sites and to collect data on the situation in these sites on a regular basis. In October 2010 the DTM was revised – and was thereafter known as DTM v.2.0 - to meet changing information needs as the camp situation evolved and as the capacity of agencies to collect data expanded.

According to the DTM strategy document the DTM v2.0 sought to collect the most accurate and updated data identified in table 5-2.

<b>Database Category</b>	<b>Database Attribute</b>
<b>IDP camp identification</b>	Site name, geographic coordinates and address
<b>Camp management</b>	Classification of site, name of camp management agency and camp committee, and owner of the land
<b>Service provision</b>	Basic indicators on water and sanitation, names of service providers
<b>Demographics</b>	Population: number of households and individuals
<b>Population tracking</b>	Timeline of camp site establishment, place of origin of the population, movement in and out of camp and reasons for stated movement
<b>Security</b>	Security provision
<b>Shelter</b>	Type of shelter and number of empty shelters

**Table 5-2: Attributes contained in the DTM v2.0 dataset. Source: (CCCM, 2011b).**

#### *5.2.4. DTM Data Collection Methodology*

The method of data collection used by CCCM varied depending on the size and layout of each camp – meaning the data was not standardised. Two-person field teams were assigned to approximately 40-50 camp sites within the same geographical area. The field teams then used a variety of data collection methodologies, including key informant interviews and physical counting to estimate the population.

On 7 November 2011, a field visit was arranged to see first-hand the data collection methods CCCM used to collect the DTM information. The author joined Joanna Dabao from the Data Management Team while her team surveyed Canaan, a large spontaneous camp to the north of Port-au-Prince. A group of 10-15 surveyors were used to conduct the building counts. Canaan was estimated to contain over 35,000 people; because of its enormous size a comprehensive building-by-building survey was conducted only every 4 months with a follow-up survey 2 months in-between to identify any significant changes in the number of households.

The survey method relied heavily on the surveyors' knowledge of the camps and assumed they could recognise any change in the camp structure and layout. No maps or information from the previous survey was taken into the field for validation. The survey form had been designed to collect International Organisation for Migration (IOM) number, serial number, name and phone number of occupants. The number of people and families per structure was also recorded as well as structure-type. The structure-type categories used in the survey included 'makeshift shelter', 'transitional shelter', 'tent' and 'other'. There was not a category for concrete structures; these were instead recorded in the 'other' category.



**Figure 5-1: Building-by-building survey techniques used by International Organisation for Migration in Canaan to count shelter numbers. Left: discussion with camp coordinators about recent arrivals and departures. Right: surveyor recording the presence of a new structure.**

During the data collection stage, information was also collected and validated by talking to community representatives and the camp managers. The bi-monthly DTM datasets took approximately 6 weeks to collect, analyse and disseminate. Figure 5-2 shows how long each stage of the process was expected to

take. Data collection for Canaan alone took about a week and another week to validate. Once the data was verified it was entered into the database during weeks 3-4. If necessary, the data was verified again with further visits and consultation with key informants such as CCCM Camp Management Operation teams and other service providers.

Activity	Wk 1	Wk 2	Wk 3	Wk 4	Wk 5	Wk 6
Data Collection						
Data Entry						
Analysis						
Validation with key CCCM actors						
Formal Release of Report						

**Figure 5-2: The bi-monthly cycle undertaken at each camp site to collect and update the DTM dataset lasted about six weeks.**

Once the data was ready, the information was disseminated in bi-monthly reports through the CCCM Cluster and was posted on the CCCM website. The reports focused on the current status of the camps as well as an analysis of trends such as population movement. In addition to written reports, the raw data was published as a spreadsheet and a KMZ Google Earth file to allow users to conduct further analysis and visualisation.

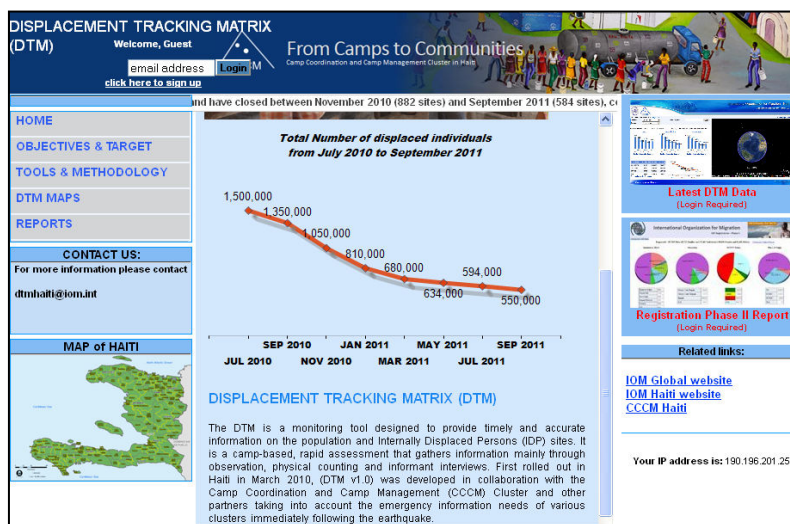


**Figure 5-3: Results of the DTM were published online at the CCCM website.**

### **5.3. Methodology**

#### *5.3.1. Building Schema*

The first step of the study involved the creation of a suitable building classification schema listing buildings likely to be found in the study area. This was devised after several field trips to the region, preliminary analysis of aerial imagery and after consulting existing survey protocols including the CCCM's DTM. The schema contained a list of building types likely to be found in areas of spontaneous settlement and camps across Haiti. The classification system is split into two parts: non-concrete and concrete buildings.

Part one contains non-concrete structures found in Haiti's camps including tents, makeshift shelters and transitional shelters. Makeshift shelters were by-far the most common non-concrete structure in Canaan. These were made with a combination of corrugated iron, plywood panels and tarpaulin in both the walls and roof. Transitional shelters commonly consisted of plywood walls and corrugated iron roofs with a standard size and shape.

Part two contains concrete structures at various stages of completion (e.g. foundations dug, plinth/columns laid, walls built, part of the roof complete and fully complete). Identifying the different levels of construction was necessary to allow UN-Habitat to more accurately estimate the amount of investment made by households in areas of spontaneous settlement. The ability of remote sensing to identify these various stages of construction was tested when analysing the Canaan site.

Definitions and visual examples of each building class are presented in Appendix C. The general appearance of each building-type is also described based on a preliminary analysis of aerial imagery. The descriptions focus on the hue, shape and texture of the structures.

### 5.3.2. Image Selection and Pre-Processing

A preliminary manual assessment of the site was made using an aerial image that was acquired by Google in November 2010. This aerial image was used in the work with the British Red Cross and is described in Chapter 4.

The semi-automatic analysis was undertaken upon a single 25 km<sup>2</sup> Worldview-2 image acquired on 11 August 2011 over one and a half years after the earthquake. The attributes of the image are presented in table 5-3. The satellite image was purchased as a *standard ortho ready 4-band bundle* with no topographic relief applied, making it suitable for custom orthorectification. The package contained a panchromatic image and four multispectral bands located in the blue, green, red and near-infrared parts of the electromagnetic spectrum. The image was selected to coincide with field deployment. The image was pre-processed before any analysis was conducted. The pre-processing involved three steps 1. Radiometric correction 2. Pansharpening and 3. Geometric Correction. These steps are described in detail in Chapter 3.

<b>Sensor:</b>	<b>Worldview-2</b>
<b>Central Lat/Lon:</b>	18.661, -72.271
<b>Acquisition Date:</b>	11 August 2011
<b>Sensor tilt (view) angle:</b>	18.8 degree
<b>Satellite azimuth angle:</b>	178.1 degrees
<b>Solar azimuth angle:</b>	98.9 degrees
<b>Satellite elevation:</b>	68.3
<b>Solar elevation:</b>	73.4

**Table 5-3: Worldview-2 image attributes.**

**Study 1: The mapping and enumeration of spontaneous settlement across a large geographic extent using semi-automatic analysis of high-spatial-resolution satellite imagery**

**5.4. Introduction**

The objective of this study is to test how reliably semi-automated analysis of high-spatial-resolution satellite imagery can be used to monitor urban processes, such as spontaneous settlement, across large geographic areas. The work focuses on the Canaan region of Port-au-Prince, Haiti. Tens of thousands of people moved there towards the end of 2010 in an attempt to benefit from free services and jobs promised at the near-by planned camps. This area of spontaneous settlement was officially recognised as a 'camp' by the CCCM Cluster and as such, was subject to the government's strategy for return based on the closure of camps and the return of displaced families to their neighbourhoods of origin (ICCG, 2011). UN-Habitat believed that a strategy of development should be considered for some camps, including areas of spontaneous settlement, where substantial personal investment in construction was believed to have already taken place. To support decision-making and in particular, to develop suitable development and exit strategies for these areas, the organisation required data on the number and type of structures already constructed.

*5.4.1. Study Summary*

A building-by-building ground survey was first conducted in a subset of Canaan to characterise the site and to classify the building stock. 48% of the surveyed buildings were complete and incomplete *concrete* structures with concrete-slab or corrugated-iron roofs. The rest of the structures were makeshift shelters made with a combination of wood, tarpaulin and corrugated-iron. Spectral analysis of the materials found that corrugated-iron and concrete have sufficient spectral separability from each other and the surrounding bare ground and are therefore suitable for spectral classification.

Maximum Likelihood supervised algorithm, one of the most commonly used spectral classifiers, was used to map corrugated-iron and exposed concrete across the whole of Canaan. The number of buildings with corrugated-iron roofs was then estimated using two methods: 1) the total area of corrugated-iron mapped by maximum likelihood was divided by an average building size statistic and 2)

a regression approach was used to link the number of automatically and manually-counted buildings in 73 randomly-selected grids across Canaan.

The following section introduces Canaan and its key characteristics. The results of a ground survey are reviewed to reveal information about the building-types in the area. Manual analysis of aerial imagery, corresponding to the ground survey site, is then validated to identify likely errors and confusions, and a spectral analysis of the satellite imagery is conducted to better understand the spectral separability between different classification classes. The results from these analyses are then used to develop a suitable methodology.

#### 5.4.2. Study Site: Canaan

The analysis focuses on the Canaan site, located west of the Corail Sector 4 planned camp, 12 miles to the north of Port-au-Prince. The camp was selected by UN-Habitat as an area representing spontaneous settlement after reviewing the CCCM's DTM dataset and several field visits. Occupants began to settle in these areas in the hope that they would receive the free aid and services being provided at the near-by planned camps.

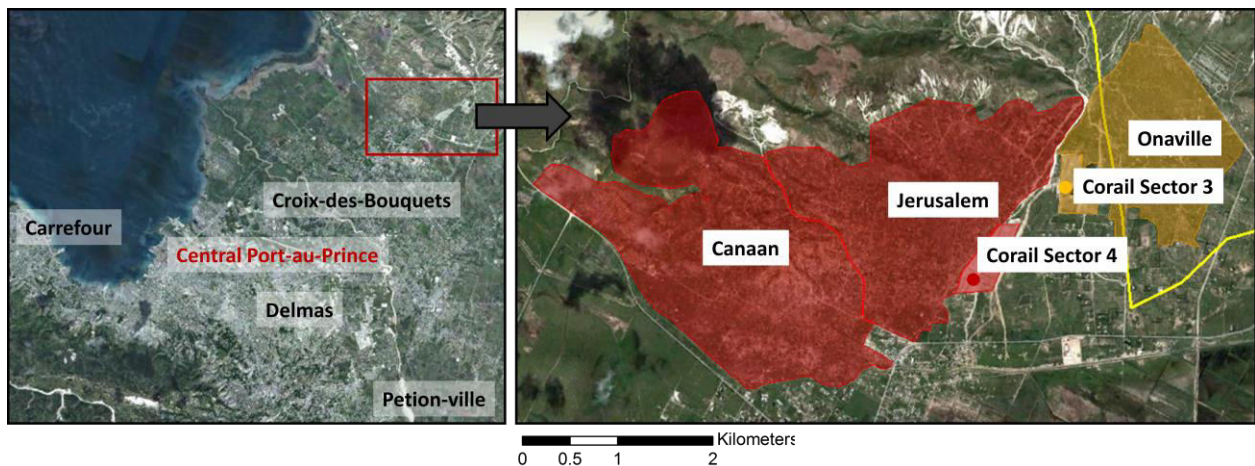


**Figure 5-4: Canaan is located west of the Corail planned camps, 12 miles north of central Port-au-Prince.**

The DTM classified Canaan as a 'spontaneous settlement' covering over 5 km<sup>2</sup> of private scrubland and vegetation. In August 2011, CCCM used ground techniques to estimate that the site contained 5,929

makeshift units, 790 tents and 707 transitional-shelters, hosting a total of 36,015 people. The site was very large and spacious, providing 136.4 m<sup>2</sup> per person. The buildings were almost all detached and the land immediately surrounding each dwelling was often enclosed and owned by the inhabitants. There was limited service and utility provision across the site: according to the DTM there was no water or waste management in Canaan and only 23 toilet facilities, suggesting that open defecation was common.



**Figure 5-5: Makeshift shelters in Canaan.**

### **5.5. Ground Survey Results**

In October 2011 a building-by-building survey was conducted within a 350 m x 500 m subset of Canaan in the south-east of the site. The subset was selected because of its accessibility and because in aerial imagery the building-type and layout appeared to be representative of the whole Canaan area. The site was also deemed big enough to contain both road-side and non-road side structures; according to visual interpretation of Google Earth aerial imagery before the field visit, the area contained 401 structures as of November 2010, including a combination of tents, makeshift shelters and concrete buildings.

The purpose of the ground survey was to collect observations to allow a suitable building typology to be developed and to create a database of geocoded photographs and observations that could be used to verify the satellite image analysis. It was conducted on foot by a group of five people, including the author, Professor Ian Davis (Independent Consultant), Maggie Stephenson (UN-Habitat) and Victoria Batchelor (ARUP). A building-by-building approach was used so that every building along a 1 km route was surveyed. This resulted in 61 individual building surveys. Half of the survey took place along a primary or secondary road and the other half away from the roadside. The November 2010 aerial image of the area was viewed on an iPhone in the field with the GPS activated so the location of the team

could be cross-referenced with the results of a preliminary assessment of the study area. A Ricoh GPS camera was also used to collect 114 photos of the structures. At each plot, the type of building was recorded, the main material-type of the walls and the roof, and the stage of construction.



**Figure 5-6: GPS-encoded photographs were taken for each building surveyed along a 1 km route and are displayed here as red dots.**

The subset in Canaan was found to contain both concrete and non-concrete structures, including tents, transitional shelters and makeshift shelters. Concrete structures were found at various stages of construction including at foundation, plinth/column, wall and incomplete roof level. Figure 5-7 presents the number and proportion of building-types observed in the Canaan subset during the ground survey.

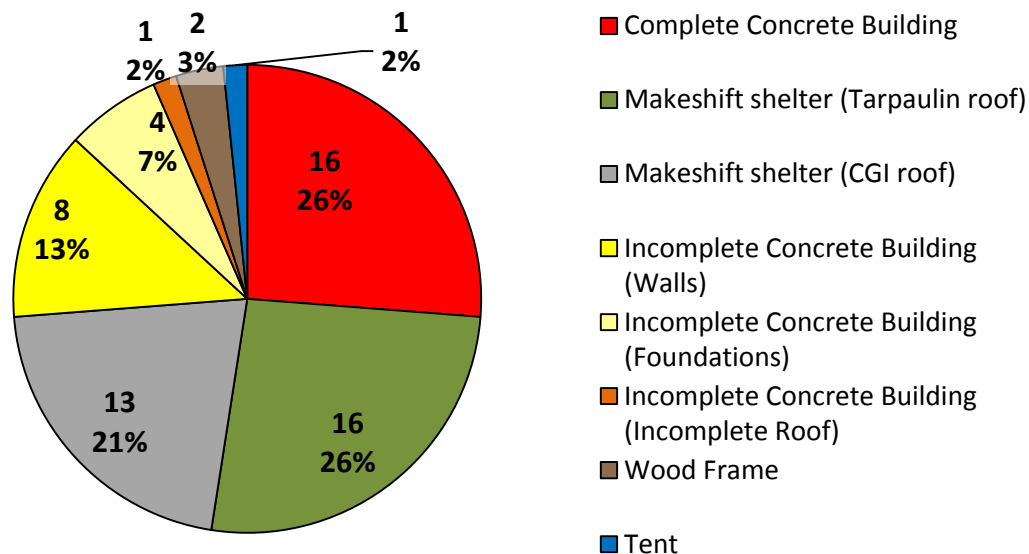


Figure 5-7: The proportion of building-types surveyed in the Canaan subset in October 2011.

Note: CGI = Corrugated-Iron.

#### 5.5.1. Concrete Structures

26% of the buildings surveyed in Canaan were *complete* concrete structures. All were made with concrete blocks and concrete columns. Two had concrete-slab roofs but most were made with corrugated-iron roofs. Three re-bars were commonly used per column and the exposed foundations had all been dug two ft for the wall and three ft for the columns. The concrete structures came in different shapes and sizes ranging from one-room structures (measuring approximately 4 x 4 m) to multi-room structures (measuring 10.5 x 9 m).

Incomplete concrete structures at different stages of construction comprised 22% of the total building sample. Complete and incomplete concrete structures therefore made up 48% in total. It must be noted though that many of the walls and foundations appeared to have been abandoned and many looked as though they had not been worked on since the Google Earth aerial image was acquired - almost 12 months earlier in November 2010. This suggested that some people arrived in Canaan in the middle of 2010, began constructing concrete structures but left the structures abandoned before the end of the year. Interviews and other social-audit techniques were conducted by UN-Habitat to understand more about the reasons for this phenomenon.

### **5.5.2. Non-Concrete Structures**

Makeshift shelters made up 47% of the sample. The most common non-concrete structures had tarpaulin or corrugated-iron roofs, though it was noted that the material used for the roof did not always match the wall material. Most of the shelters appeared to have been made with wooden tree-pole frames. Canvas tents were relatively rare and only made up 2% of the structure sample. Detailed descriptions and examples of the building-types are presented in Appendix C.

## **5.6. Manual Analysis of Aerial Imagery Corresponding to the Ground Survey Site**

Aerial imagery corresponding to the area visited in the field was analysed before the field visit by manually assigning a building classification to each of the structures visible in the image. Aerial imagery was used for this part of the study as the Worldview-2 satellite image had not been purchased in-time for the ground survey. There had been very little development work done in the study area between the date the aerial image was acquired (November 2010) and the ground survey was conducted (October 2011) which meant a verification of the manual analysis of aerial imagery was still possible. The location of the concrete and non-concrete structures, as identified in the aerial imagery, is presented in figure 5-8. The map on the left shows the location of completed concrete structures and concrete structures at various stages of construction, and the map on the right shows non-concrete structures including tents, makeshift shelters and wooden frames.

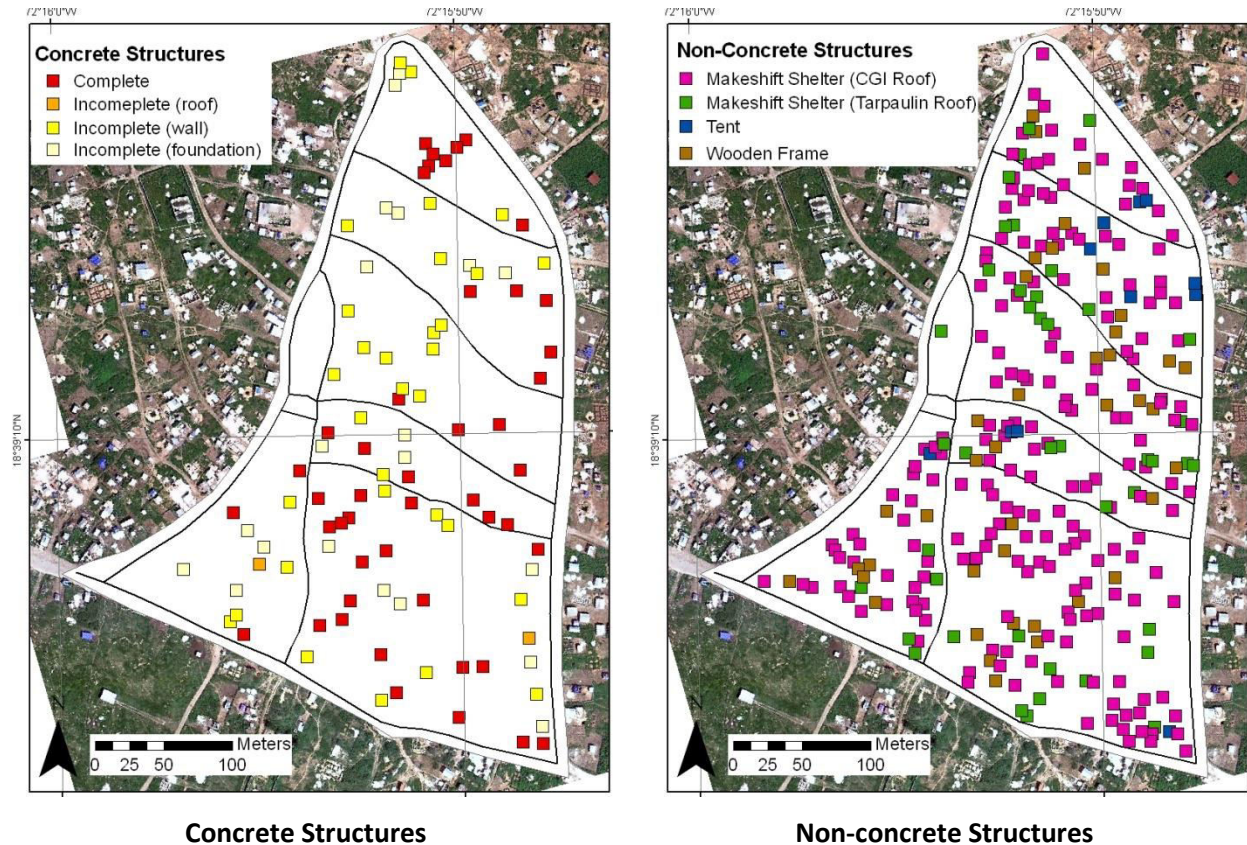


**Figure 5-8: The location of concrete and non-concrete structures identified in aerial imagery representing a subset of Cnaan in November 2010.**

To assess the accuracy of the manual image analysis and to identify likely errors and confusions a contingency matrix was created to directly compare the results of the manual analysis to the 61 ground-derived observations. Three of the ground-surveyed buildings were not present in the imagery as they were removed between the image acquisition date and the ground survey, so were not included in the analysis. Care must be taken when interpreting the results of the matrix due to the small sample size but the results are still useful to highlight likely errors and confusion between building-types. The contingency matrix is presented in table 5-4. It directly compares the results of the ground survey and manual image analysis: for example, the first column shows that 13 corrugated-iron roof structures were counted in the ground survey. 11 of those were correctly classified in the image analysis and 2 were misclassified as concrete structures.

Omission and commission errors occur when a classification incorrectly misses or adds a building to a class respectively. Omission and commission errors for each building class were calculated as percentages for each class and are presented in table 5-5. For example, out of 19 buildings remotely classified as corrugated-iron 42% were incorrectly classified as concrete, canvas or tarpaulin. Of the 13 corrugated-iron structures identified by ground survey 15% were misclassified as concrete structures by remote sensing.

		Ground-derived Observation								
Building Category		CGI	Pc	Pf	Pr	Pw	T	Tp	Wf	Grand Total
Remotely-derived Observations	CGI	11	3				1	4		19
	Pc	2	12							14
	Pf			3		1				4
	Pr				1					1
	Pw		1			5				6
	T									0
	Tp							12		12
	Wf								2	2
Grand Total		13	16	3	1	6	1	16	2	58

Table 5-4: Contingency matrix comparing 58 ground observations to manual aerial image analysis.

Building Category	Commission Error (%)	Commission Error (pixels)	Omission Error (%)	Omission Error (pixels)
CGI	42	8/19	15	2/13
Pc	14	2/14	25	4/16
Pf	25	1/4	00	0/3
Pr	00	0/1	00	0/1
Pw	17	1/6	17	1/6
T	00	0/0	00	1/1
Tp	00	0/12	25	4/16
Wf	00	0/2	00	0/2

Table 5-5: Omission and commission errors for each building category.

Key: CGI = Makeshift shelter (corrugate-iron roof), Pc = Complete Concrete Structure, Pf = Incomplete Concrete Structure (foundation), Pr = Incomplete Concrete Structure (Incomplete roof), Pw = Incomplete Concrete Structure (walls), T = Tent, Tp = Makeshift shelter (tarpaulin roof), Wf = Wooden frame.

This exercise resulted in an overall accuracy of 79%. Note though that the manual analysis was conducted with substantial ground knowledge acquired during the ground survey. Large concrete buildings with concrete slab roofs were identified with high confidence (commission error, 14%; omission error, 25%), but there were significant errors associated with the identification of corrugated-iron: 8 out of 19 corrugated-iron shelters classified in the imagery were in-fact concrete or tarpaulin structures resulting in a commission error of 42%. Concrete, corrugated-iron and canvas all appear very similar in the imagery but have subtle spectral differences in the electromagnetic spectrum which it is expected can be exploited by spectral classifiers. One of the most common confusions occurred between makeshift shelters and concrete structures both of which had corrugated-iron roofs. The size of the building did not appear to correlate with structure type, but in some cases the presence of concrete or sand near to a structure did indicate that the building was likely to be concrete.

The various stages of construction were identified with high confidence in the aerial imagery due to their unique linear formations. The foundations and walls of a building commonly appeared to divide the ground into easily recognisable grids. Walls were often distinguishable from foundations by the shadow they cast. There was one misclassification of a site at wall level though which was in fact at foundation level.

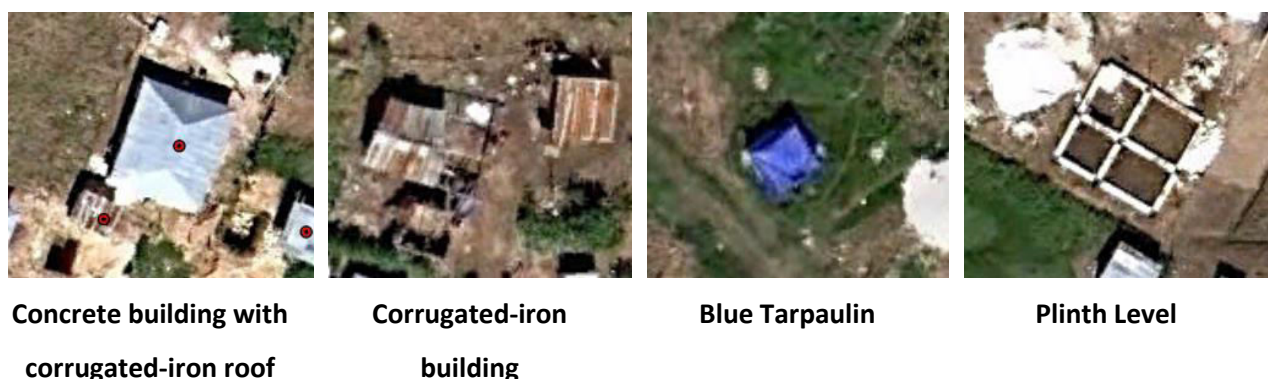


Figure 5-9: Different building classes visible in Canaan aerial imagery.

### 5.7. Spectral Analysis of Satellite Imagery

The ground study established that most buildings in Canaan were composed of corrugated-iron, concrete or tarpaulin. A spectral analysis of these materials is necessary to determine if and how they may be automatically identified in the satellite imagery. Ten spectral samples were taken from the imagery for each of the three roof materials and for bare ground. The samples were collected from flat roof surfaces across the whole of Canaan to minimize atmospheric or shadowing effects. The materials' spectral profiles show their reflectance in each of the four worldview-2 bands and are presented in figure 5-10.

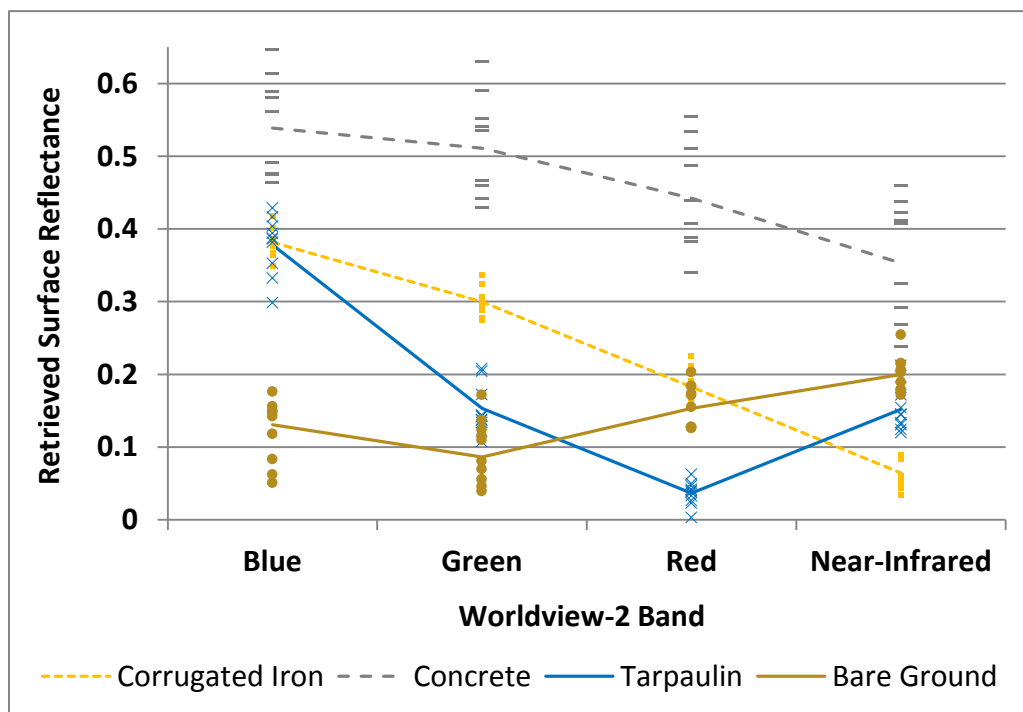


Figure 5-10: Retrieved surface reflectance for 3 roof materials in Canaan.

Concrete and corrugated-iron show a similar spectral pattern to each other, highest in the blue band and lowest in the near-infrared band. Blue tarpaulin peaks in the blue band and reflects substantially less in the green and red bands, which gives it its strong blue hue in the imagery. In contrast, bare ground has a slightly higher reflectance in the red band. Concrete has the highest reflectance overall in all four bands and its profile is quite distinct from the other three. Corrugated iron and tarpaulin spectral profiles overlap substantially in the blue band but are more distinct from each other in the other bands.

Bare ground has a distinctive low reflectance in the blue band but overlaps with tarpaulin in the green band and in the near-infrared band.

To classify the buildings successfully there must be significant disparity between the reflectance of the structures and the ground surrounding them. Figure 5-11 shows how a corrugated-iron and concrete roof appears in each band of a Worldview-2 image. Concrete appears white due to its strong reflectance in all four bands, but shows the least distinction with bare ground in the near-infrared band. Corrugated-iron shows less disparity with the surrounding ground than concrete in all bands, but reflects relatively strongly in the blue band. Note though that weathered corrugated-iron appears to reflect a lot less than non-weathered corrugated-iron, especially in blue and green bands, which might lead to increasing confusion with bare ground over time (Herold et al. 2004).

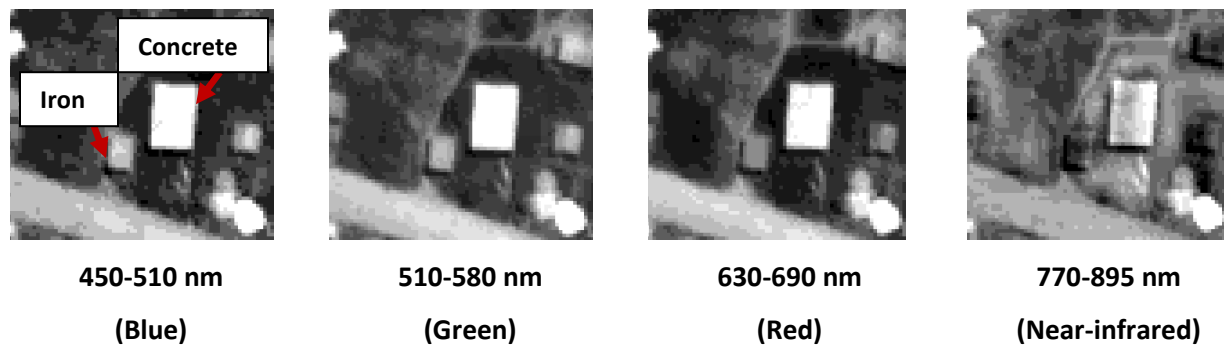


Figure 5-11: Corrugated-iron and concrete roof in four bands of a Worldview-2 satellite image.

### 5.7.1. Jeffries-Matusita Spectral Separability test

To measure the spectral separability between shelter materials and background pixels the Jeffries-Matusita Separability test was applied to pixel samples from the Canaan subset. There are two common measures of separability available: *divergence* and the *Jeffries-Matusita distance*. A problem with the *divergence* measure arises because it increases quadratically as the distance between classes increases, which can lead to misleading interpretation of the results (Richards, 1999). This problem is overcome with the Jeffries-Matusita measure due to the introduction of an exponential factor which leads to exponential decreasing weight with increasing separation. The test measures the average distance between two class density functions using the following formula (Richards, 1999):

$$\alpha = \frac{1}{8} (\mu_i - \mu_j)^T \left( \frac{C_i + C_j}{2} \right)^{-1} (\mu_i - \mu_j) + \frac{1}{2} \ln \left( \frac{|(C_i + C_j) / 2|}{\sqrt{|C_i|} \times |C_j|} \right)$$

$$JM_{ij} = \sqrt{2(1 - e^{-\alpha})}$$

Where:  $i$  and  $j$  = the two classes being compared;  $C_i$  = the covariance matrix of class  $i$ ;  $\mu_i$  = the mean vector of class  $i$ ;  $\ln$  = the natural logarithm function;  $T$  = transposition function;  $|C_i|$  = the determinant of  $C_i$  (matrix algebra).

The presence of the exponential factor gives an exponentially decreasing weight to increasing separations between spectral classes. The output value for the test ranges from 0-2. In this study, all three shelter materials and bare ground scored over 1.9 which suggests high spectral separability and means spectral classification may be used to classify them with confidence (Richards, 1999).

The class separability is visualized in figure 5-12 as a series of scatter-plots showing the distribution of four spectral classes in each combination of the Worldview-2 satellite's four bands. As expected, the results show good separability between bare ground, corrugated-iron and concrete in each band combination. The cluster of points representing these classes appear clumped and distinct from each other.

The tarpaulin class is split into two distinct clusters that represent both blue and white tarpaulin. Blue tarpaulins are the most common form of tarpaulin in the study area and are represented as a large cluster of points to the bottom of the scatter-plots. White tarpaulin is less common so the clusters representing them are smaller. The white tarpaulin points appear towards the top and right of the scatter-plots, just below concrete in the spectral space.

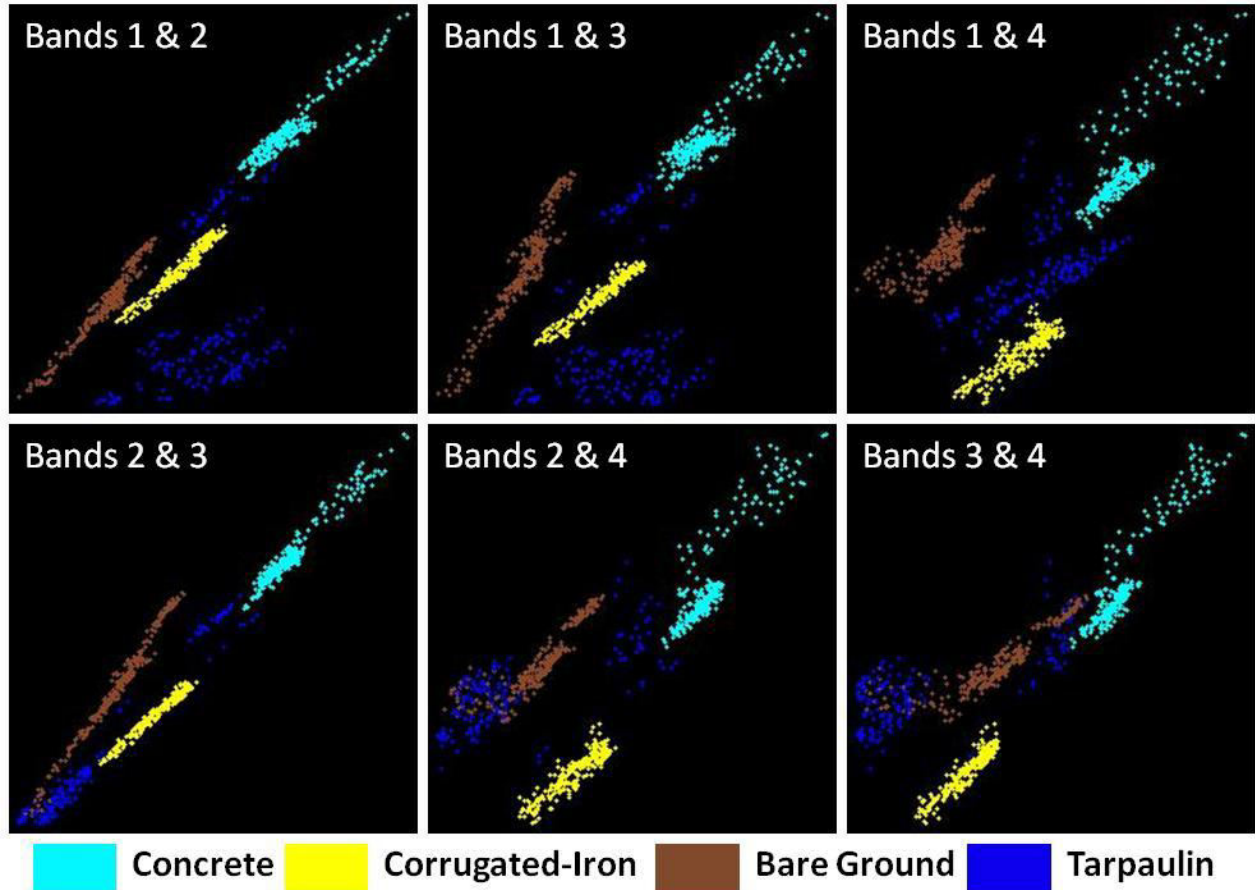


**Figure 5-12: Scatter-plot of class points displaying the separability between four classes in Worldview-2's four bands. The x-axis of each scatter plot represents the first band's reflectance values and the y-axis represents the second band's reflectance values.**

The spectral separability analyses show that there is sufficient spectral contrast between corrugated-iron, concrete and bare ground, but that there could be some confusion between concrete and white tarpaulin. Warner, Nelis and Foody (2009) states that spectral approaches should not be used when land-types have similar spectral signatures or when a single land-type has multiple signatures. These results suggest that there is likely to be some confusion between concrete and white tarpaulin resulting in commission errors in the concrete class. These errors are expected to be minimal though as white tarpaulin is not commonly used in the region.

In summary, the results of the ground survey and spectral analysis were used to identify and characterize the features likely to be classified in the scene. The spectral analysis shows that corrugated-iron and concrete is likely to be classified with high confidence using semi-automated spectral

classification. Maximum Likelihood classification will therefore be used to map these two materials. Morphological approaches were tested but they were deemed not suitable as the fixed kernel sizes were not able to process the large variation in makeshift shelter size across Canaan. And Object Based Image Analysis (OBIA) did not work effectively as the segmentation algorithm in ENVI's<sup>1</sup> feature extraction software did not detect the edge of buildings reliably enough. These two approaches to image analysis are tested thoroughly though in study 2.

Incomplete buildings at foundation and wall level were also not classifiable using spectral or object-based techniques due to the complex arrangement of reflectance patterns within each building plot so a manual approach was developed to classify foundations and walls. The contingency matrix produced in the validation exercise showed that manual analysis of aerial imagery could likely identify these features with high confidence.

### **5.8. Study 1 Method: Mapping Corrugated-Iron and Concrete Using the Semi-Automatic Maximum Likelihood Classifier**

Maximum Likelihood is a parametric spectral classifier that works by estimating a probability density function for each class and then assigning each pixel in the image to the class with the highest probability. It is one of the most commonly used supervised classification techniques and was used to map corrugated-iron and concrete in this study. The multivariate probability functions for four classes are displayed in Figure 5-13. The vertical axis is associated with the probability of a pixel value being a member of one of the classes. Note that concrete has a high probability of reflecting strongly in both bands 3 and 4.

---

<sup>1</sup> ENVI. Exelis Visual Information Solutions. Boulder, Colorado, United States.

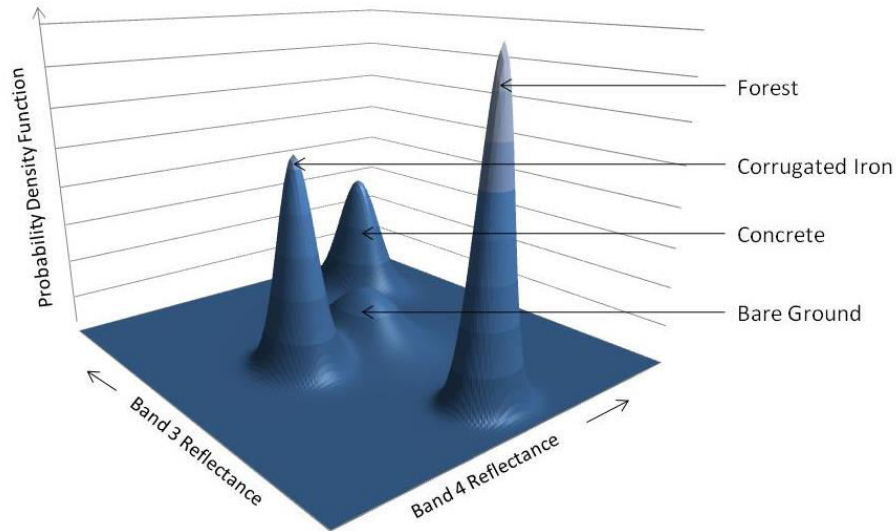


**Figure 5-13: Probability density functions for 4 land cover classes in Canaan calculated using the class mean and standard deviation statistics.**

Although confusion with vegetation was unlikely due to its unique reflectance in the red and near-infrared bands, a vegetation mask was created using a normalized difference vegetation index (NDVI) image with a threshold of 0.53. NDVI techniques were described in the environment section of Chapter 3. Maximum likelihood was then applied to the non-vegetation pixels and used to classify three land cover classes: corrugated-iron, concrete and bare ground. Maximum Likelihood is a *supervised* classifier, so requires the analyst to select groups of pixels known to represent each class. The method therefore assumes the analyst has knowledge about the land cover in the area of study. Ground knowledge for this study was acquired through the ground survey and subsequent spectral analysis of the imagery, described in the previous sections of this report.

Ground photographs and observations were also used to assist the selection of training pixels. When selecting the training areas it was important to select pixels that fully represented the variation found in each class – for example, when training the corrugated-iron class, pixels were selected from both the sunny and shaded side of a pitched roof. Between 757 and 1,198 pixels were selected for each class. Richards (1999) recommended 10 to 100 training pixels per class, but Warner, Nelis and Foody (2009) recommended at least 30 to 100 pixels for each *parameter* in the problem being solved, corresponding to 210 to 700 pixels for a classification with 4 bands and 3 classes.

The following section uses Matrix Mathematics to describe the Maximum Likelihood approach in more detail. Each training pixel selected by the analyst is assigned to a particular class (e.g. corrugated-iron or concrete) and is represented by a measurement vector ( $X_c$ ) as shown below. The average of all training pixels for a single class is called the Mean Vector ( $M_c$ ) and the covariance between bands is represented as a covariance matrix ( $V_c$ ).

$$X_c = \begin{bmatrix} BV_{i,j,1} \\ BV_{i,j,2} \\ BV_{i,j,3} \\ \cdot \\ \cdot \\ BV_{i,j,k} \end{bmatrix} \quad M_c = \begin{bmatrix} \mu_{c1} \\ \mu_{c2} \\ \mu_{c3} \\ \cdot \\ \cdot \\ \mu_{ck} \end{bmatrix} \quad V_c = \begin{bmatrix} COV_{c11} & COV_{c12} & \dots & COV_{c1k} \\ COV_{c21} & COV_{c22} & \dots & COV_{c2k} \\ \cdot & \cdot & \dots & \cdot \\ \cdot & \cdot & \dots & \cdot \\ COV_{ck1} & COV_{ck2} & \dots & COV_{ckk} \end{bmatrix}$$

Where:  $BV_{i,j,k}$  is the brightness value for the  $i, j^{\text{th}}$  pixel in band  $k$ ;  $\mu_{ck}$  represents the mean value of all pixels obtained for class  $c$  in band  $k$ , and  $Cov_{ckl}$  is the covariance of class  $c$  between bands  $l$  through  $k$ .

The Maximum Likelihood decision rule calculates the probability that each pixel vector belongs to each class and then assigns each pixel to the class with the highest probability. The probability density function of each class is modeled as a multivariate normal distribution based on statistics from the training pixels. The procedure assumes that each training class in each band is normally distributed (Gaussian); an assumption of normality is generally reasonable for common spectral response distributions (Lillesand Kiefer and Chipman, 2008). The estimated probability density function for class  $w_i$  for example, is computed with the mean and variance using the equation:

$$\hat{p}(x | w_i) = \frac{1}{(2\pi)^{\frac{1}{2}} \hat{\sigma}_i} \exp \left[ -\frac{1}{2} \frac{(x - \hat{\mu}_i)^2}{\hat{\sigma}_i^2} \right]$$

Where:  $\exp [ ]$  is  $e$  (the base of the natural logarithms) raised to the computed power;  $x$  = a single brightness value on the  $x$ -axis;  $\hat{\mu}_i$  = estimated mean of all the values in a single training class;  $\hat{\sigma}_i^2$  = estimated variance of all the measurements in this class.

When multiple bands of remote sensing data are used, a n-dimensional multivariate normal density function is calculated for the classes of interest. Because the distributions of the class samples are assumed to be normally distributed they can be characterised by the mean vector and covariance matrix using the equation below:

$$p(X | w_i) = \frac{1}{(2\pi)^{\frac{n}{2}} |V_i|^{\frac{1}{2}}} \exp\left[-\frac{1}{2}(X - M_i)^T V_i^{-1}(X - M_i)\right]$$

Where:  $|V_i|$  is the determinant of the covariance matrix;  $V_i^{-1}$  is the inverse of the covariance matrix, and  $(X - M_i)^T$  is the transpose of the vector  $(X - M_i)$ . The mean vectors ( $M_i$ ) and covariance matrix ( $V_i$ ) for each class are estimated from the training data.

After the training phase the algorithm begins the classification and assigns each pixel to the class with the highest probability value. The results were then processed with a 5x5 majority filter to remove isolated pixels incorrectly classified. Finally, the classes were converted to a vector layer for further analysis within ArcGIS.

## 5.9. Sampling Approach to Estimate the Number of Corrugated-Iron Roofs

The number of buildings with corrugated-iron roofs was estimated by dividing the total area of corrugated-iron classified using maximum likelihood by the average building size statistic derived from the manual analysis. A separate statistical regression approach was also used to estimate the total number of buildings with corrugated-iron roofs. A regression coefficient was calculated by linking the number of buildings automatically extracted by the maximum likelihood classifier (independent variable) to the number of manually-delineated buildings (dependent variable) in a random sample across Canaan.

### 5.9.1. Sample Selection

The sample for the analysis was selected using a random geographic sampling technique. A 75 m x 75 m grid containing 869 cells was first placed over the Canaan site. Maximum likelihood and manual analysis was used to count the number of buildings present in a sample of these grids. A minimum required

sample size of 73 grids was estimated using the formula below accepting an error of +/- 1 building with a confidence of 95% (Byrkit,1972):

$$\text{Minimum Required Sample Size} = \frac{Z^2 * p * (1 - p)}{C^2}$$

Where: Z is the Z-value 1.96 for 95% confidence level; p = population proportion (0.5) and C = confidence level expressed as decimal (+/- 1 building).

The random geographic sampling approach was used to ensure an even coverage across the site to create a fully representative sample. Each grid measured 75 m by 75 m, large enough to contain a *block* of buildings and thus be representative of each area's built environment.

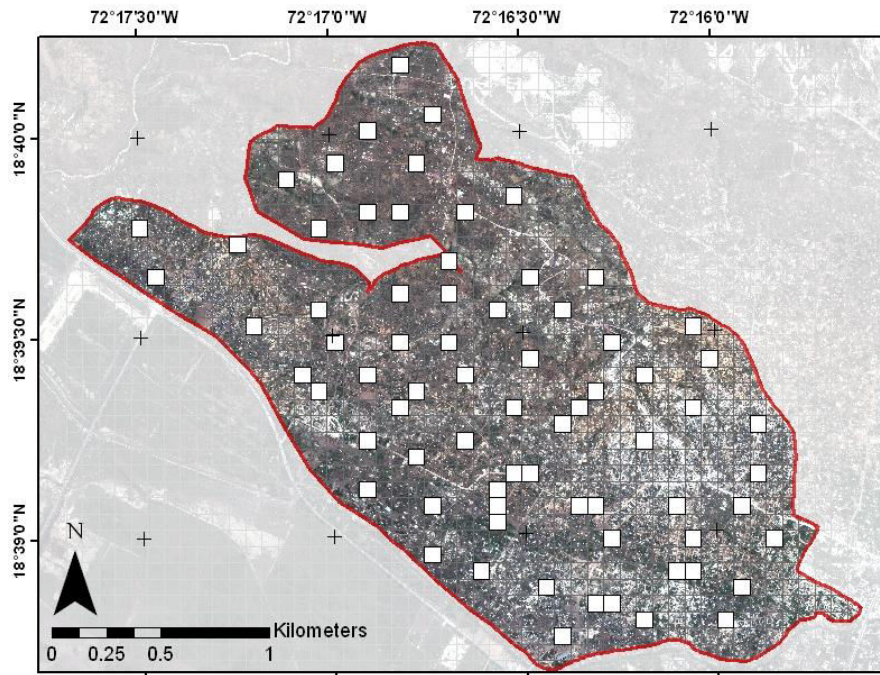


Figure 5-14: Location of the 73 randomly-selected grid cells.

The sample contained a total of 673 buildings counted manually. To minimise error with the manual analysis the results were validated by independent analysts and structural engineers at Imagecat Ltd. The Imagecat analysts noted that the assumption of construction material based on roof material did not seem to be a valid relationship. They also noted that in many cases a tarpaulin can cover the actual

roof; corrugated-iron roofs can cover either concrete or makeshift structures and that tents can give the appearance of tarpaulin.

### 5.9.2. Regression Analysis

The relationship between the dependent and independent variables is expressed as an equation in the form:  $Y = b_1X_1 + b_2X_2$  (where Y is the dependent variable,  $X_1$ ,  $X_2$  are independent variables and  $b_1$ ,  $b_2$  are coefficients that describe the size of the effect of the independent variables on the dependent variable). The regression analysis was applied twice: 1) to compare the number of manually-counted buildings to the number of corrugated-iron polygons created by maximum likelihood and 2) to compare the number of manually-counted buildings with the area of corrugated-iron delineated by maximum likelihood. The area of corrugated-iron was anticipated to have a closer relationship as it potentially overcomes issues of polygons merging or splitting which can happen if buildings are close together or roofs are spectrally heterogeneous. Table 5-6 shows that both regression results produced a high r-square value ( $> 0.80$ ), so over 80% of the dependent variable is explained by the regression models. The *number of buildings* actually has a slightly higher r-squared value than *area of building* so more variation is explained by that relationship.

Coefficient	Regression 1: Number of CGI buildings	Regression 2: Area of CGI buildings
Intercept	0.667 (0.596)	2.176 (0.679)***
Number of CGI buildings automatically delineated	0.786 (0.045)***	
Area of CGI buildings automatically delineated		0.036 (0.003)***
R-squared	0.883	0.814

Table 5-6: Two regression results show the relationship between the number of manually-counted buildings and 1) number of automatically-delineated buildings and 2) area of corrugated-iron automatically-delineated. Standard errors are reported in parentheses. \*, \*\*, \*\*\* indicate significance at the 90%, 95% and 99% level respectively.

The scatter-plot in figure 5-15 shows the strong positive relationship between visually counted and automatically-derived numbers of structures. The relationship has an r-square of 0.883 which means that 88% of the variation of the dependent variable is explained by the independent variables.

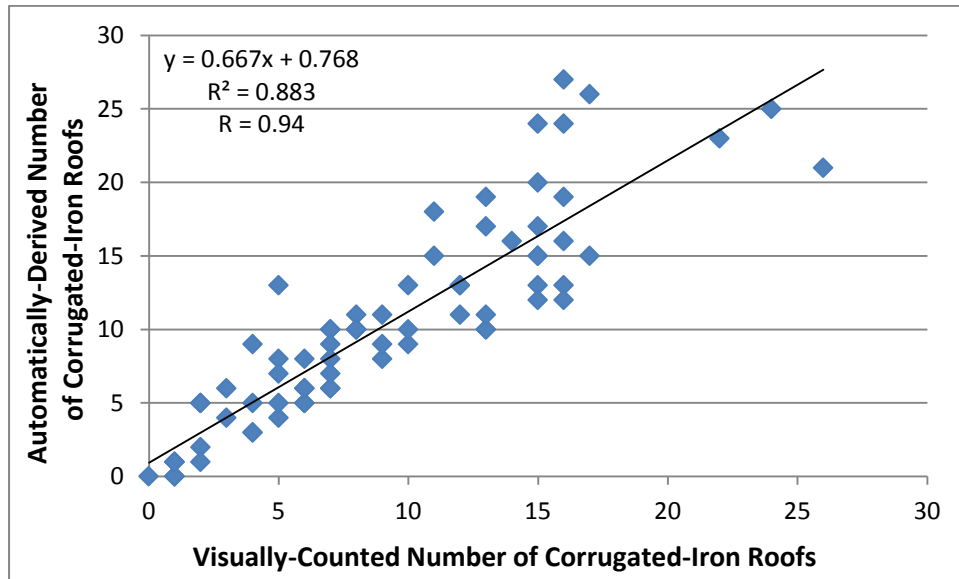


Figure 5-15: Comparison between automatically-derived number of structures and visually-counted number of structures for the 73 randomly selected cells across Canaan.

### 5.9.3. T-Test and Probability Statistics

A T-score can be used to determine whether to reject or accept the null hypothesis that the coefficient of change is zero. It is calculated by dividing the coefficient by the standard error. A p-value is then calculated by comparing the t-statistic to values in the Student's t-distribution. The Student's t-distribution describes how the mean of a sample with a certain number of observations is expected to behave.

The p-value therefore tells us how confident the independent variable correlates with the dependent variable. The regression result has a p-value of  $1.11 \times 10^{-20}$  which allows the null hypothesis to be rejected with very high confidence ( $p < 0.00005$ ). This shows that there is very small chance that the results would have been derived in a random distribution. Alternatively, we can say with a probability of 99% that the variable is having some effect.

## **5.10. Manual Identification of Building Walls and Foundations**

Manual analysis of aerial imagery was used to map incomplete concrete structures at foundation and wall level. Various automated attempts were tested to map these features, including object-based and textural approaches, but all produced unsatisfactory results. This is partly due to the large variation in size, shape and reflectance of the building sites. More work is required to better understand the common spectral, spatial and contextual characteristics that these features all share.

The contingency matrix, shown in table 5-4, comparing manual analysis of aerial imagery to ground survey results established that visual interpretation could be used to identify building foundations and walls with high confidence. This is due to their unique appearance in the imagery. Manual analysis was therefore used to map walls and foundations across the whole of Canaan. Full descriptions of the classes are provided in the building schema in Appendix C. Foundations commonly consist of dark linear features caused by shadow within the trenches, while plinths and walls can generally be seen as white lines with a shadow cast away from the sun. The outer edge of each feature was delineated with a single polygon so the total area of the sites could be calculated.

## **5.11. Results**

The results in terms of the number and area classified by each method are presented below. The reliability of the semi-automatic methods are then assessed in detail by comparing the extents of the classification results to the manually delineated buildings in the 73 grids selected randomly for the regression analysis.

### *5.11.1. Corrugated-Iron*

Semi-automatic classification of high-spatial-resolution satellite imagery estimated that the site contained 175,230 m<sup>2</sup> of corrugated-iron roof corresponding to 5,653 buildings (assuming an average building size of 31 m<sup>2</sup>). A second method, using a statistical regression model based on the relationship between visually-interpreted structures and automatically-extracted structures, estimated that there were 6,189 buildings with corrugated-iron roofs.

The CCCM used ground methods to estimate that there were 5,929 makeshift shelters and 707 transitional shelters, equalling 6,636 structures in total. The accuracies of the two remote sensing methods are therefore -15% (using average building size statistics) and -7% (using regression analysis). It must be noted though that the accuracy of the CCCM's estimate is unknown. The CCCM figure is likely to be an overestimation of the number of corrugated-iron roofs as it also includes concrete structures, which would increase the accuracy of the remote sensing results.

The regression method took longer to implement than maximum likelihood classification alone as it involved the manual delineation of over 600 buildings. In this study the greater time investment has been rewarded though with more accurate results. A map of corrugated-iron created by the semi-automatic maximum likelihood classifier is presented in figure 5-16.

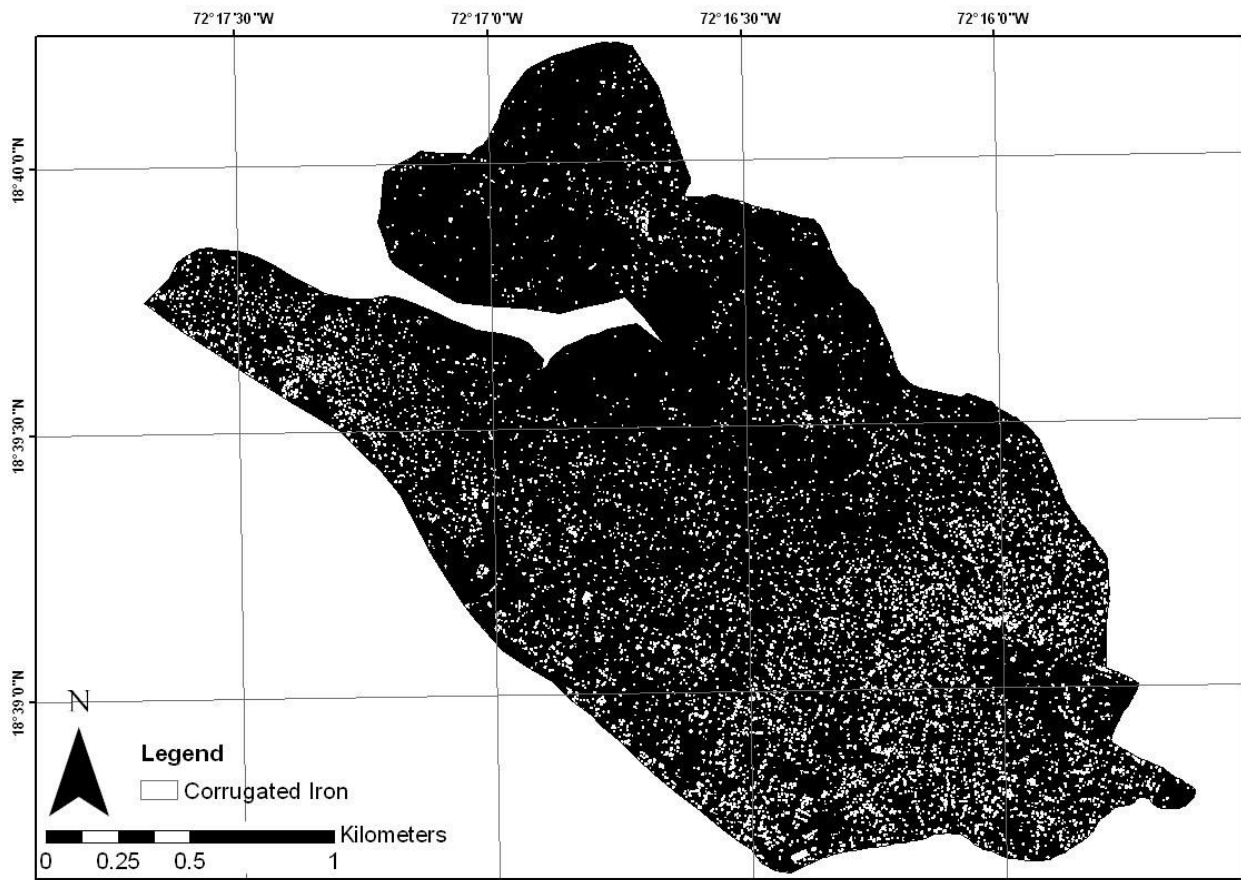


**Figure 5-16: 175,230 m<sup>2</sup> of corrugated-iron in Canaan automatically mapped using the maximum likelihood classifier.**

### 5.11.2. Exposed Concrete

Maximum Likelihood was also used to classify exposed concrete as it was found to be spectrally dissimilar to corrugated-iron and bare ground. Concrete was a lot less prevalent than corrugated-iron. The technique estimated that there was 44,977 m<sup>2</sup> of exposed concrete. The technique produced a total of 5,150 objects with an average size of 8.7 m<sup>2</sup>. The process classified features including concrete-slab roofs and piles of concrete material located near to new constructions. A ground survey is required to estimate the proportion of exposed concrete that is occupied by each of the feature types. Figure 5-17 shows a map of exposed concrete produced using Maximum Likelihood.

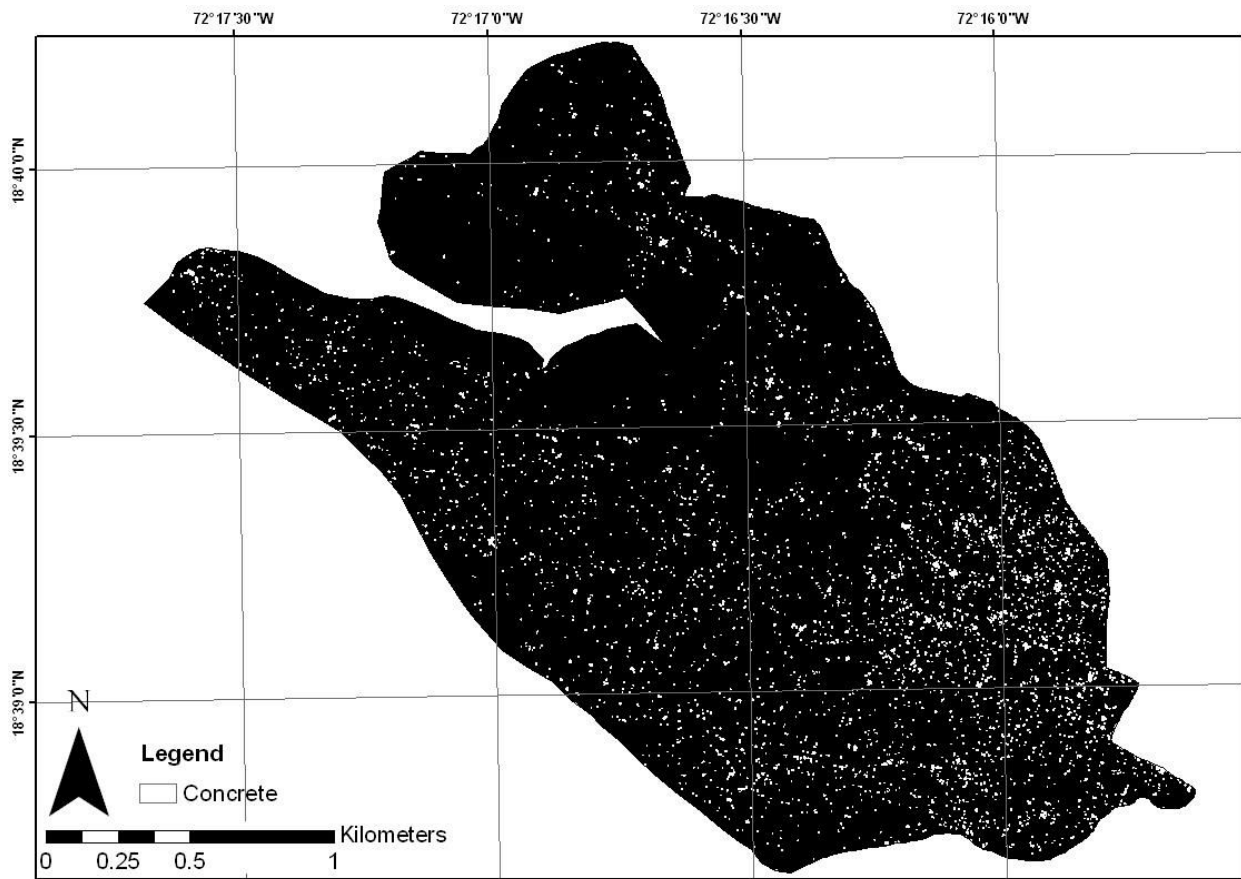


**Figure 5-17: Map of exposed concrete in Canaan automatically mapped using maximum likelihood classifier.**



**Figure 5-18: Examples of exposed concrete in Canaan: piles of concrete material near to a construction site (left) and a vacant building with concrete-slab roof (right).**

### 5.11.3. Walls and Foundations

Automated techniques were less successful at classifying the different stages of construction, including foundations and walls, but these features were both classified with high confidence using manual techniques due to their unique form. Manual analysis of the Canaan site classified 479 sites with foundations only (covering 29,710 m<sup>2</sup>) and 521 sites with walls (covering 33,640 m<sup>2</sup>). The size of the sites ranged from 8.4 m<sup>2</sup> to 324.0 m<sup>2</sup> with an average size of 63.4 m<sup>2</sup>.

Figure 5-19 shows a map of foundations and walls that were derived manually. The features were located mainly on flat land near to roads. Many of the features looked like they might have been abandoned as they were overgrown with vegetation. A UN-Habitat household survey suggests that some households may return to build upon the foundations once they have acquired the necessary financial resources to do so.

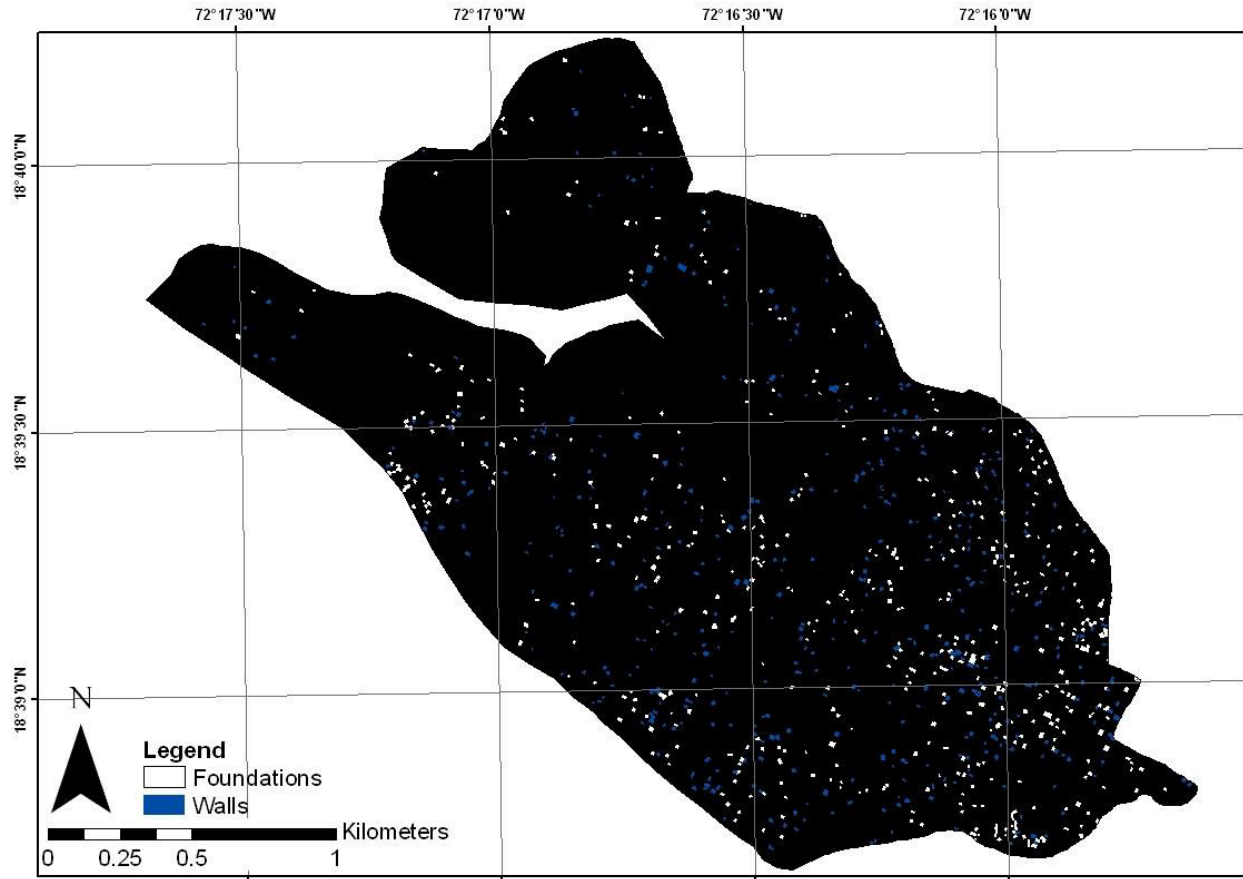


**Figure 5-19: Map of incomplete concrete structures (foundations and walls) in Canaan mapped manually using aerial imagery.**

#### 5.11.4. Distribution of Building-Types across Canaan

The relative distribution of corrugated-iron, concrete and walls/foundations across the area are presented as density maps in figure 5-20. Orange and red colours represent areas where there are large amounts of each class and greens and yellows represent areas where there are small amounts. The maps were produced by passing a kernel with 178 m radius across the classification images shown in figures 5-16, 5-17 and 5-19. All classes appear to be prevalent to the south of the scene. In particular, there appears to be a large amount of concrete to the south-east of Canaan on the border with Jerusalem. The region to the north is the least populated area as it has steep slopes and limited access.

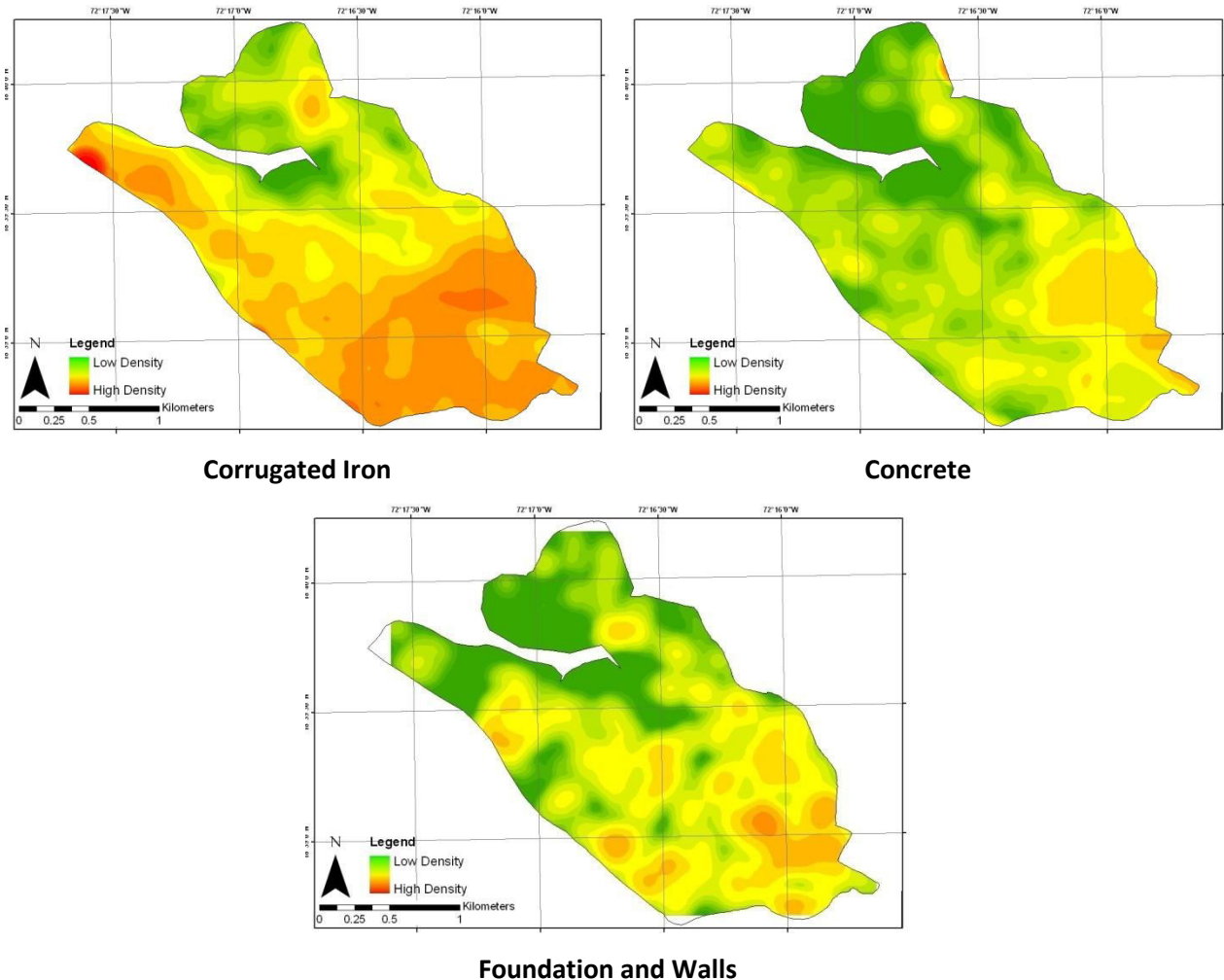


Figure 5-20: Density of corrugated iron, concrete and incomplete concrete structures. Measured using a kernel 178.41 m radius (100,000m<sup>2</sup> area) and 15 m cell size.

### 5.12. Accuracy of the Maximum Likelihood Classifier

The accuracy of the maximum likelihood classification of corrugated-iron and concrete was analysed at pixel-level by directly comparing the pixels classified both manually and automatically in the 73 randomly-selected grids across Canaan. Corrugated-iron produced a correlation coefficient of 0.96 and concrete 0.89 suggesting that the total area automatically classified was very accurate for both materials.

The overall accuracy of each class was calculated again as the *proportion of pixels correctly classified*. This technique also highlighted commission and omission errors in the classification results. Commission

and omission errors occur where the manual and automatic results do not overlap: commission errors occur where the classifier has classified pixels not believed to be part of a building and omission errors occur where the classifier has missed pixels believed to be part of a building. This is shown graphically in figure 5-21. The *commission error* is the proportion of automatically-delineated building pixels that do not overlap with the manually-delineated building pixels and the *omission error* is the proportion of manually-delineated building pixels that do not overlap with the automatically-delineated building pixels.

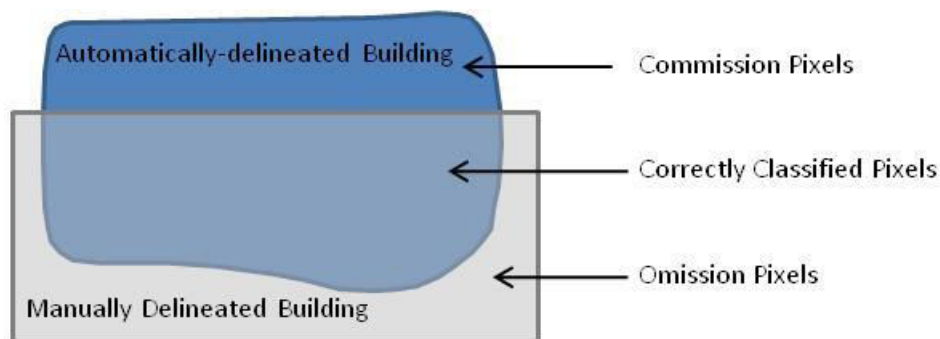


**Figure 5-21: How to calculate correctly-identified pixels, commission and omission errors by directly comparing manually-delineated polygons (grey) and automatically-delineated polygons (blue).**

A total of 27,835 pixels representing corrugated-iron were delineated manually and 22,009 were “correctly” classified with the maximum likelihood classifier resulting in an overall accuracy of 79.1%. The omission error was 20.9% and the commission error 35.8%. Commission errors occurred when bare ground patches, building sites, tarpaulin, and to a lesser extent car windows were mistakenly classified as corrugated-iron.

The classification of concrete was less successful with an overall accuracy of 55.6%, an omission error of 44.4% and commission error of 26.3%. Commission errors occurred when concrete was confused with partly-constructed buildings at wall or plinth level or other exposed impervious surfaces. As expected, there were also commission errors when white tarpaulin was mistakenly classified as concrete due to their spectral similarity.

Omission errors commonly occurred around the edge of both corrugated-iron and concrete features due to the mixed-pixel effect. Omission errors were particularly high for the concrete class leading to a low

overall accuracy. This is because the pixels on the edge of concrete features contain both concrete and bare ground creating a unique spectral reflectance that were not represented in the training pixels. This issue can be overcome by adjusting the training pixels sample to include those on the edge of concrete features but this risks increasing commission error if more bare ground is incorrectly classified as concrete. The accuracy of the classification is ultimately dependent on the quality of the training pixels as well as the spectral separability of the classes.

### **5.13. Conclusion**

This study shows that remote sensing can be used to monitor spontaneous settlement reliably and rapidly over large areas. Semi-automatic spectral classification was used to map corrugated-iron and concrete while manual techniques were used to monitor walls and foundations. Manual methods generally provide more reliable results than automated approaches but take more time to conduct. The manual mapping of walls and foundations took around 10-12 hours to complete while a maximum likelihood classification can be completed in 1 or 2 hours depending on the complexity and number of classes. More time may be required to validate the results of the classification though and to refine the training pixels.

The number of corrugated-iron roofs was estimated correctly to within at least 7% of CCCM ground-derived estimates. The accuracy of the CCCM statistics is unknown though and likely to overestimate the number of corrugated-iron structures. A large reason for this high accuracy was the detached nature of the structures and because the buildings were made with identical roof material with a high contrast to the background reflectance. The accuracy would certainly be lower in a denser, more complex urban environment, as was seen in the Red Cross study in Chapter 4. A per-pixel analysis identified common commission and omission errors which need to be overcome to increase the accuracy and reliability of this technique further.

Limitations of the remote sensing approach were also identified by comparing the results of manual analysis of aerial imagery to ground observations. In particular, remote sensing analysis was not able to distinguish between makeshift shelters and concrete buildings under corrugated-iron roofs using imagery alone. Sampled ground knowledge was therefore required to supplement the maps and datasets produced from this work to estimate the proportion of each building-type present across the

site. Despite this an overall accuracy of 79% was calculated for manual analysis with substantial ground knowledge based on a building typology containing eight classes.

This study shows that there has been substantial personal investment in construction across Canaan in the form of incomplete and complete concrete structures and makeshift shelters. The results were presented to UN-Habitat at the end of 2011 who then estimated the amount of personal investment in Canaan and surrounding region to be approximately US\$64 million. The statistics and maps from this work were then presented by the UN to the Prime Minister's Office who has since agreed to recognize and regularize Canaan as part of the Municipality. This will result in a provision of basic services, the regularizing of tenure and the provision of technical support to the area. Remote sensing played a significant role in this policy decision and was useful as a means of collecting, analyzing and visualizing building statistics across a large geographic region (Maggie Stephenson, Personal Communication).

## **Study 2: The Mapping and Enumeration of Planned Camps using Semi-Automatic Analysis High-Spatial-Resolution Satellite Imagery: Comparing Spectral, Morphological and Object-Based Approaches**

Planned camps are constructed after or during an emergency situation to provide a support system to homeless households. This includes a space where displaced populations can find shelter and full service infrastructure, including water supply, food distribution, non-food item distribution, education and health care (Corsellis & Vitale, 2005). Mapping planned camps is important for many applications including site planning, population estimation and monitoring of spatial standards (UNHCR, 2007). Manual methods of analysing camp features using satellite imagery can be time-consuming so the development of automated workflows is necessary to operationalise the process (Wimmer et al. 2009).

The objective of this study is to compare spectral, mathematical morphology and object-based approaches to mapping transitional shelters in Corail planned camp. The shelters and features within planned camps are often arranged in blocks and rows according to spatial standards set by guidelines such as those found in the Sphere handbook (Sphere Project, 2011). The advantage of a grid layout is that it provides good access and consistency between camps for logisticians and aid workers.

Statistics describing the regular building shapes and morphologies common in planned camps were incorporated into rulesets and used to analyse satellite imagery using mathematical morphology (MM) and object-based image analysis (OBIA) (Giada, Groeve and Ehrlich, 2003; Kemper et al. 2011). *OBIA* is a semi-automatic technique that segments adjacent pixels in an image into homogenous zones (*image-objects*) and then classifies them using their spatial, textural and spectral attributes; while, mathematical morphology refers to a series of operators used to isolate image components of known *shape* and *size*. This is achieved by passing a kernel, known as a structural element, across the image to analyse pixels and their neighbours.

While MM and OBIA both allow spatial and contextual attributes to be incorporated into the analysis traditional pixel-based methods of classification use only the reflectance information contained in individual pixels. The shelters in Corail camp exhibit a similar reflectance across the site due to the common geometry, material composition and weathering conditions. The Spectral Angle Mapper (SAM)

classifier was used to map corrugated-iron roofs found on transitional shelters by identifying pixels with a similar reflectance vector to corrugated-iron reference pixels.

The three classification techniques were used to estimate both the *number* of transitional shelters in the camp and the total *area* covered by these structures. The accuracy of the techniques was analysed by comparing these statistics and results to manually-derived maps of the camp. The discussion focuses on the type of errors produced by each method and the amount of work involved to implement each of the techniques.

#### **5.14. Corail Planned Camp**

To design suitable analytical processes and protocols a detailed understanding of the reflectance characteristics, size, shape and context of the features of interest is required. The following section introduces Corail camp and then reviews the spatial and spectral characteristics of the site focusing on attributes that are likely to be exploitable by the proposed image analyses.

Corail is a planned camp located approximately 12 km from the centre of Port-au-Prince and was managed by the International Organisation for Migration. Households were relocated to the site 3 months after the earthquake when a spontaneous camp in Delmas 48 was vacated after it was found to be at risk of flash flooding. Occupants initially resided at the site in tents before being transferred to transitional shelters 15 months later. The project was criticised as the occupants were relocated up to 15 km from their homes and because the camp itself was far from services and sources of livelihood and was also thought to be at risk from wind and flooding (UN-Habitat, UNHCR and IFRC, 2010).



**Figure 5-22: A typical streetview in Corail camp (Source: Daniel Brown, October 2011).**

## 5.15. Spatial Characteristics of Corail Camp

### 5.15.1. Content and Layout

According to the DTM dataset the Corail site measured 300 m by 800 m (212,916 m<sup>2</sup>) and contained 1,120 transitional shelters accommodating 4,470 individuals. The boundaries of the site were determined by existing natural drainage and the transitional shelters were positioned in rows and blocks for ease of access. In addition to the transitional shelters the site also contained education and health facilities to the north made with wood and brick and small latrine blocks along a road running through the center of the camp. The DTM database states that the site had 202 toilets in total and received de-sludging, bathing and waste management support by Oxfam. Occupants had more recently developed a market selling food and household items and many small businesses had been established within or alongside the transitional shelters themselves including restaurants, a carpentry workshop and an art gallery.



**Figure 5-23: Aerial image of Corail camp on 5 June 2010 shows structures in regular rows and blocks with large spaces between them. (Source: Timo Luege. IASC Haiti Shelter Cluster).**

### 5.15.2. Transitional Shelters

The floor plan and elevation of the transitional shelters in Corail camp are presented in figure 5-24. The shelters measure 4.97 m by 3.75 m and have an area of 18.64 m<sup>2</sup> and a height of 2.44 m. The shelters

are made with plywood walls and corrugated-iron roofs. Each shelter includes a raised concrete finished plinth and a small veranda area covered by an extended truss roof. As stated in IASC (2010) the Haiti Shelter Cluster is using principles and minimum standards from the UNHCR Emergency Response Handbook for Emergencies (UNHCR, 2007) and the Sphere Project Handbook (Sphere Project, 2011). These guidelines recommend that 45 m<sup>2</sup> is available per person (including garden space). A 30 m wide firebreak is also recommended for every 300 m of built-up area. Measurements from the author's own analysis of satellite imagery estimate that the site provides approximately 47.6 m<sup>2</sup> per person and that there is at least 5 m between shelters side-by-side and 3m between the top and bottom of shelters.

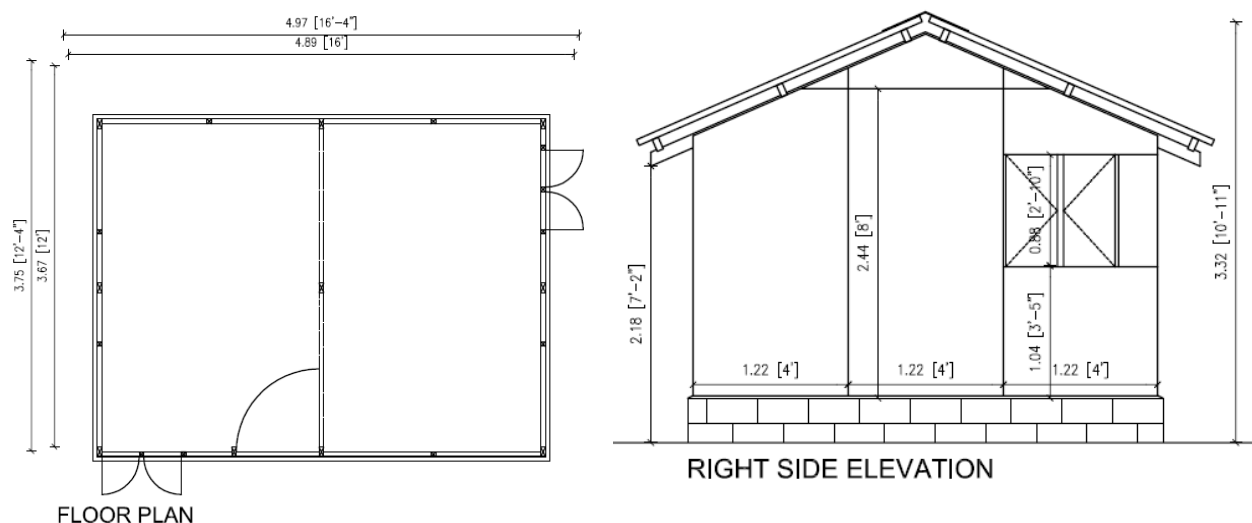


**Figure 5-24: Floor plan and elevation of the transitional shelter used in Corail planned camp (Source: Haiti Shelter Cluster, 2010).**

### 5.16. Spectral Characteristics of Camp Features

Materials each have their own unique reflectance characteristics and absorption patterns at different wavelengths. The *spectral reflectance signature* of a material can be visualised as a two-dimensional plot displaying the fraction of radiation reflected as a function of the incident wavelength. The reflectance signatures for camp structures (sunny and shaded) and background land cover are plotted in spectral profiles shown in figure 5-25. The structures' reflectance peaks in the blue band of the Worldview-2 satellite sensor corresponding to wavelengths between 450 nm and 510 nm. Reflectance can be seen to decrease as the wavelength increases with reflectance lowest in the red and near-infrared bands. These observations match the spectral profiles presented in Study 1 of this chapter.

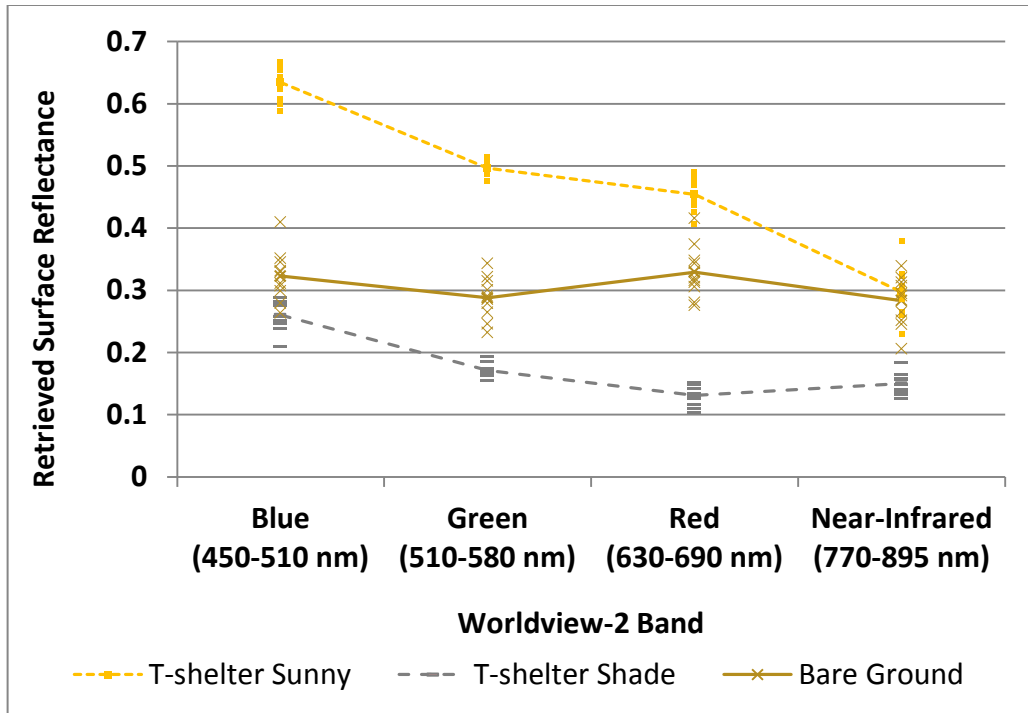


**Figure 5-25: Reflectance of shelter roofs and background land cover estimated from a Worldview-2 image using the FLAASH Atmospheric Model.**

The geometry of the camp structures relative to the solar incidence angle dramatically affects the spectral patterns observable in the imagery. The rectangular shelters have all been built at approximately 26 degrees with their entrances facing north-east or south-west. The sun azimuth angle at the time the image was acquired was 98.9 degrees, so the sun is shining across the site from the east. The pitched roofs of the shelters are therefore exposed to sun on the east side and shaded on the west. As expected, the reflectance of the shaded roof panels is lower than the sun-lit panels in each band. The shelters also cast 1 m shadows on the ground around them. Because the minimum distance between structures is 3 m though the shadows do not overlap with the surrounding shelters.



**Figure 5-26: Detailed view of transitional shelters in Worldview-2 satellite imagery.**

Several published studies present spectral reflectance signatures from common roof materials acquired with field spectrometers. These 'laboratory' observations help to validate and explain the spectral profiles measured using satellite imagery. The reflectance of an object is related to its physical condition and chemical properties, as well as its geometry and surface morphology. For example, Nasarudin and Shafri (2011) noted that the reflectance of metal decking is lowest between 500 and 850 nm – the part of the electromagnetic spectrum measured by the Worldview-2 satellite - and increases in the near-infrared and short-infrared parts of the spectrum. These observations correlate with observations of galvanized metal sheeting made by spectroscopy scientists at USGS (Clark et al. 2007). Herold et al (2004) note that many roof materials exhibit iron-oxide absorption at 520 nm, 670 nm and 870 nm, which coincides with the green, red and near-infrared bands of most high-spatial-resolution optical satellites including Ikonos, Quickbird and Worldview-2. This might partly explain the lower reflectance in these bands. Other spectral features described by these papers occur in the short-infrared part of the electromagnetic spectrum which is outside the spectral range of most high-spatial-resolution satellites.

Note that the reflectance statistics presented in the spectral plots in figure 5-25 were acquired from relatively new and unweathered corrugated-iron roofs. The reflectance of a material can actually change substantially over time with different materials exhibiting increases and decreases in reflectance. A decrease in reflectance can be caused by the accumulation of dirt or dust on the surface of the material. Nasarudin and Shafri (2011) show that older metal decking increases reflectance in the shortwave near-infrared and decreases elsewhere in the electro-magnetic spectrum.

### 5.17. Method 1: Spectral Angle Mapper (spectral analysis)

Spectral Angle Mapper (SAM) is a supervised per-pixel classifier that classifies pixels using their spectral reflectance information only. SAM was used to map corrugated-iron roofs found on transitional shelters in Corail camp by classifying pixels with a similar spectral vector to corrugated-iron reference pixels. Much like the Maximum Likelihood classifier used to monitor spontaneous settlement in Study 1, SAM measures spectral similarity by comparing image pixel spectra to a reference spectra that is provided as a training dataset by the analyst. While Maximum Likelihood compares the means of the spectra using a probability rule, SAM processes the spectra as vectors in an n-dimensional space where the number of dimensions (n) is equal to the number of spectral bands. The measure of spectral similarity is the *angle* between the vectors in units of radians (Kruse et al. 1993).

A training dataset was created by selecting pixels that were known with high confidence to represent corrugated-iron in the scene. These pixels were selected from the center of rooftops across the whole of the site. SAM then processed each pixel in the image and defined multidimensional vectors for each spectrum. The algorithm then determined the spectral similarity between each pixel spectra vector and the reference spectra vector by calculating n-dimension angles ( $\alpha$ ) between the vectors in radians, with smaller angles representing a closer match to the corrugated-iron training data. A threshold of 0.14 radians was found to be appropriate for the Corail camp image. Pixels with angles less than 0.14 radians were therefore classified as corrugated-iron. A hypothetical example of the SAM technique using a sensor with only two bands is presented in figure 5-27.

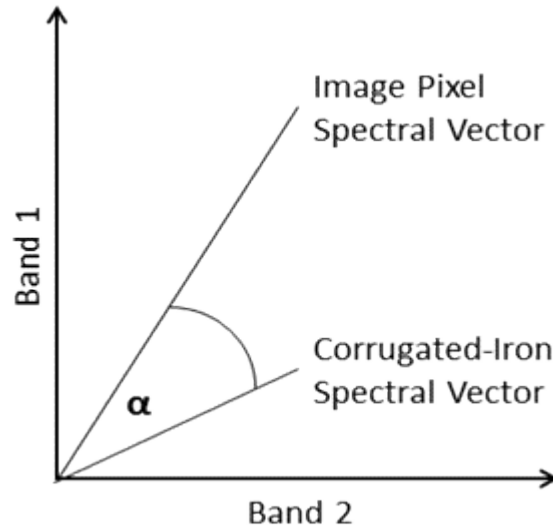


**Figure 5-27: Spectral Angle Mapping compares the vector for an unknown feature type to a known material spectral vector. The two features match if the angle ( $\alpha$ ) is smaller than the specified tolerance value (from Kruse et al. 1993).**

SAM was considered a suitable spectral classifier for this application for two key reasons: 1. The analyst only needs to provide training data for the target material and not for the background material, which ultimately leads to an easier and more rapid workflow and 2. The classifier is relatively insensitive to the effect of illumination and albedo caused by shadowing effects when applied to calibrated reflectance values. This was deemed a particularly important characteristic as the spectral analysis in section 5.16 highlighted that the west-facing roof panels in the camps are obscured by shade. As the diagram in figure 5-27 demonstrates, the vectors in the n-dimensional multispectral space have both an *angle* and a *magnitude* which is represented by the length of the lines. When the level of illumination of a feature varies the length of the vector increases or decreases accordingly but the vector angle remains the same. Crucially, SAM only compares the angle between the spectra and not the length of the vectors, so is not affected by varying illumination.

After the image was classified the output binary image was filtered using a 5x5 majority filter. This process was used to smooth the edges of the image objects and to fill in any gaps smaller than the size of the structural element. Figure 5-28 shows the grey-scale rule image produced using the SAM workflow. The different shades of grey correspond to the different angles in radian with white shades

corresponding to low angles and a closer match to the corrugated-iron reference spectra. The image in the bottom-right shows the classified SAM image after being processed with the majority filter.

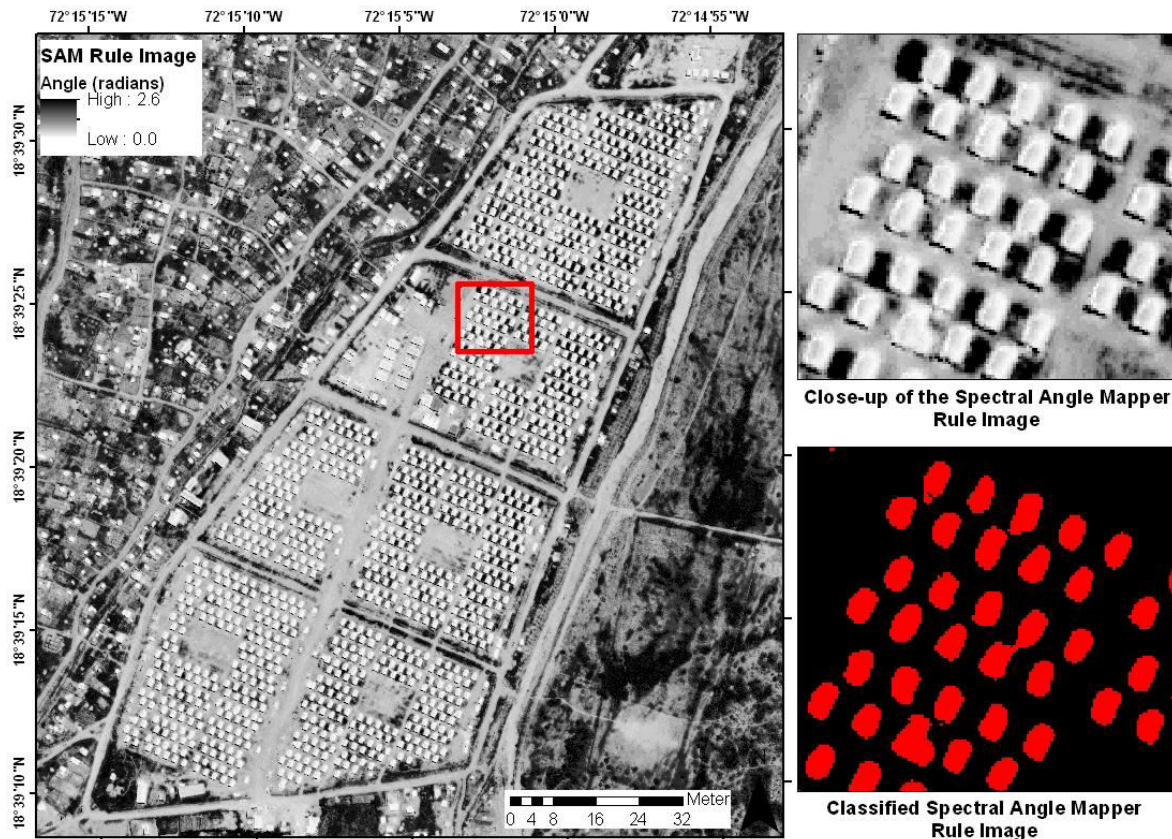


Figure 5-28: SAM grey-scale rule image. White shades are pixels that have a close spectral similarity to corrugated-iron reference pixels.

### 5.18. Method 2: Top-Hat Transformation (mathematical morphology analysis)

In remote sensing literature, *mathematical morphology* refers to a set of image processing operations that are commonly used to extract image components based on their *form and structure* and to simplify image data while preserving their essential shape characteristics (Haralick, Sternberg and Zhuang, 1987). Unlike per-pixel based methods of classification such as SAM, morphological operators work by analysing *groups* of pixels in an image. The size and shape of the neighbourhood that is analysed at any one time is defined by the size and shape of the *structural element* or array of cells that is passed across the input image.

A workflow using opening and closing operators and top-hat processing was developed to extract transitional shelters from the imagery by exploiting their common shape and size characteristics. Unlike SAM and OBIA, the morphological process did not use the spectral characteristics of corrugated-iron and was in-fact applied to 8-bit greyscale imagery not multispectral imagery. The shaded and sun-lit roof panels were analysed separately because their brightness differed substantially.

The opening operator followed by the white top-hat operation was first applied to worldview-2's blue band to extract the sun-lit roof panels. The closing operator followed by the black top-hat operator was then applied to the near infrared band to extract the shaded side of the roofs. The results from these processes were then filtered and merged.

The blue and near infrared bands were used because sunny roof panels were found to be brightest and most spectrally distinct in the blue band and shaded roof panels were darkest and most spectrally distinct in near-infrared. The workflow for the morphological analysis is summarised in the flow diagram in figure 5-29 and described in more detail afterwards.

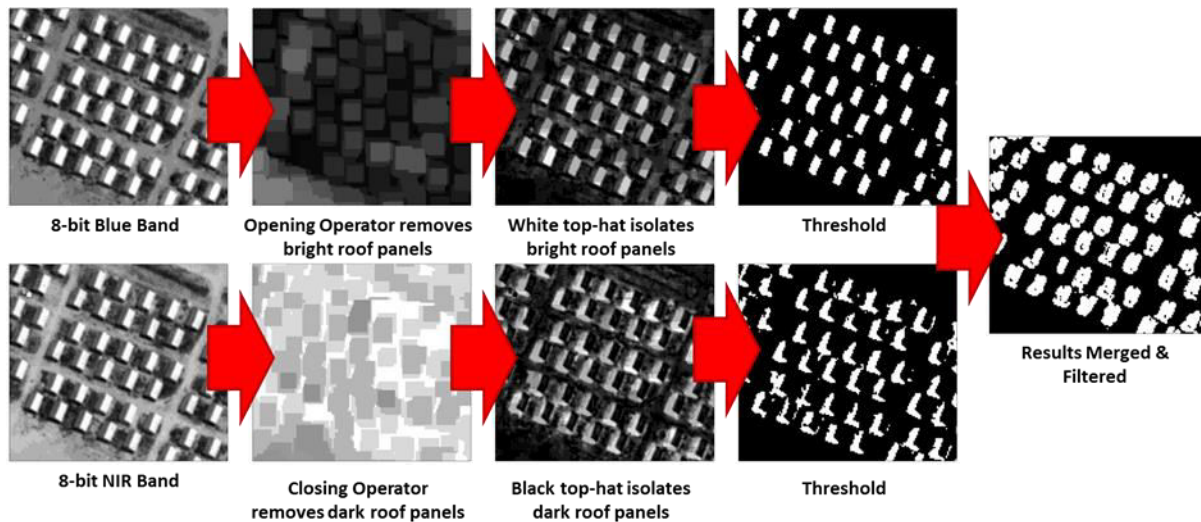
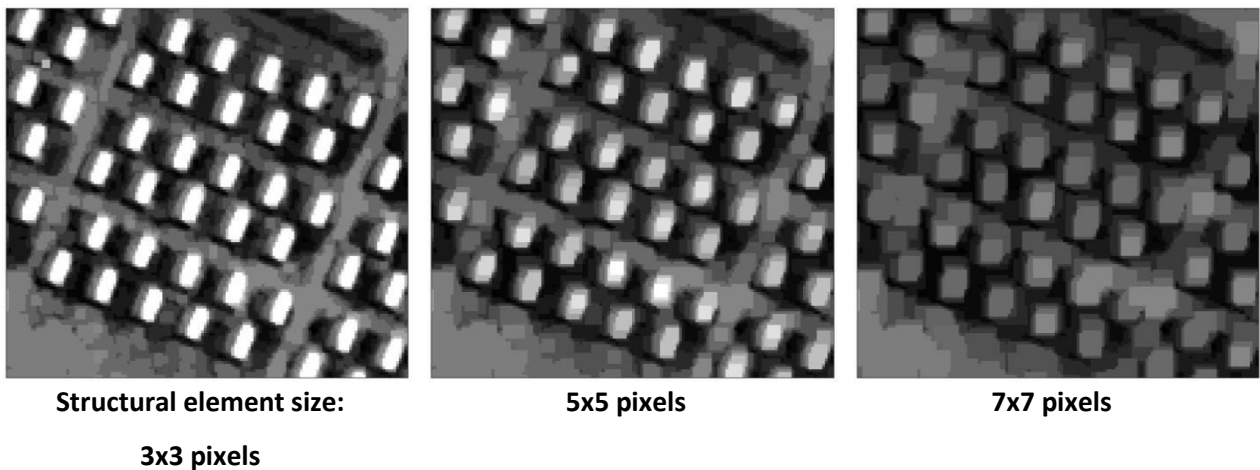


**Figure 5-29: Mathematical morphology workflow used to extract sunny and shaded roof panels in Corail planned camp.**

### 5.18.1. The Structural Element

In mathematical morphology each operator uses a unique rule to alter the pixels of an image. The rules are applied to the image using a structural element, which is an array of cells that contains the relative coordinates of a pixel's neighbourhood. The operator applies the rule to all the pixels within the boundaries of the structural element and assigns a value to the output pixel based on the results of the rule. The structural element repeats this process for every pixel in the image.

The size and shape of the structural element closely determines the features that are filtered. A square structural element was appropriate here to isolate rectangular features. The size of the structural element determines the minimum size of the features that are removed or preserved by the filtering. As an example, figure 5-30 presents the blue band image after it was filtered with the opening operator using a square structural element of varying size. Bright objects smaller than the structural element are expected to be removed by the process. The bright building roof panels are still present in the output image when the square structural element measures 3x3 pixels. The roof components are partially removed with an array measuring 5x5 or 7x7 and completely removed with a structural element measuring 11x11 pixels or more. These observations correlate with the size of the shelters which are 4.97 m or approximately 10 pixels in a Worldview-2 image.



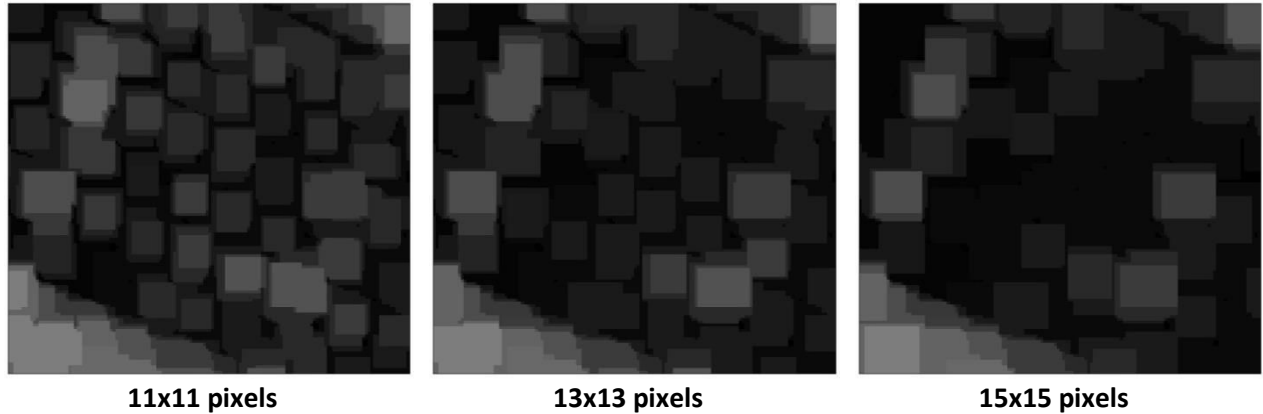


**Figure 5-30: The Opening operator applied to the blue band of a Worldview-2 image using a square structural element of varying size.**

### 5.18.2. Erosion and Dilation Operations

*Erosion* and *dilation* are two of the most fundamental operators in mathematical morphology. Many other morphological algorithms are based on them including the opening and closing operators used in this study (Soille, 2003). The rule for the dilation operator is that *the value of the output pixel is the MAXIMUM value of all the pixels within the confines of the structural element*. A grey-scale image after being processed with the dilation operator appears brighter and dark objects are reduced or eliminated. Gonzalez & Woods (2002) define grey-scale dilation ( $f \oplus b$ ) as follows:

$$(f \oplus b)(s, t) = \max \{f(s - x, t - y) + b(x, y) \mid (s - x), (t - y) \in D_f; (x, y) \in D_b\}$$

Where  $D_f$  and  $D_b$  are the domains of the input image ( $f$ ) and the structural element ( $b$ ). And  $f(x, y)$  and  $b(x, y)$  are functions that assign distinct gray level values to each pair of coordinates. The condition that  $(s-x), (t-y)$  need to be in the domain of  $f$  and  $(x, y)$  in the domain of  $b$ , establishes that the two sets need to overlap by at least one element.

The rule for the erosion operator is *the output pixel is the MINIMUM value of all the pixels in the input pixel's neighbourhood*. Gray-scale erosion ( $f \ominus b$ ) is therefore defined as:

$$(f \ominus b)(s, t) = \min \{f(s + x, t + y) - b(x, y) \mid (s + x), (t + y) \in D_f; (x, y) \in D_b\}$$

Figure 5-31 shows the dilate and erosion filters applied to a subset of the Corail camp.

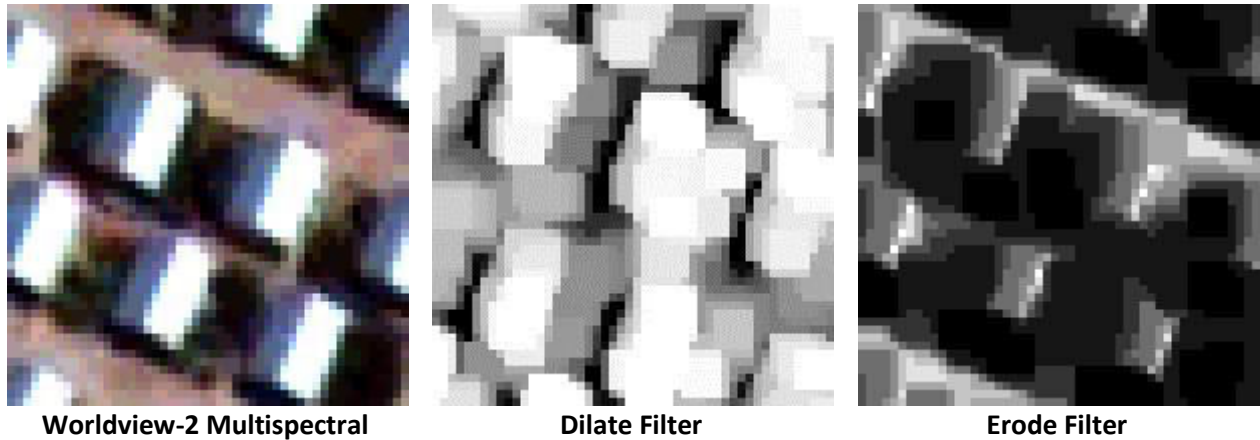


Figure 5-31: Erosion and dilation filters applied to blue and near-infrared Worldview-2 bands respectively.

### 5.18.3. Opening and Closing Operations

Morphological opening is defined as a sequence of one erosion followed by one dilation ( $(f \ominus b) \oplus b$ ) and the morphological closing as one dilation followed by one erosion ( $(f \oplus b) \ominus b$ ). The opening operator can be used to remove light features of the image with little effect on dark features and the closing operator to remove dark features with little effect on light features. Figure 5-32 shows how the opening and closing operators were applied to 8-bit blue and near-infrared bands of the Worldview-2 image to remove sun-lit roof panels and shaded roof panels respectively.

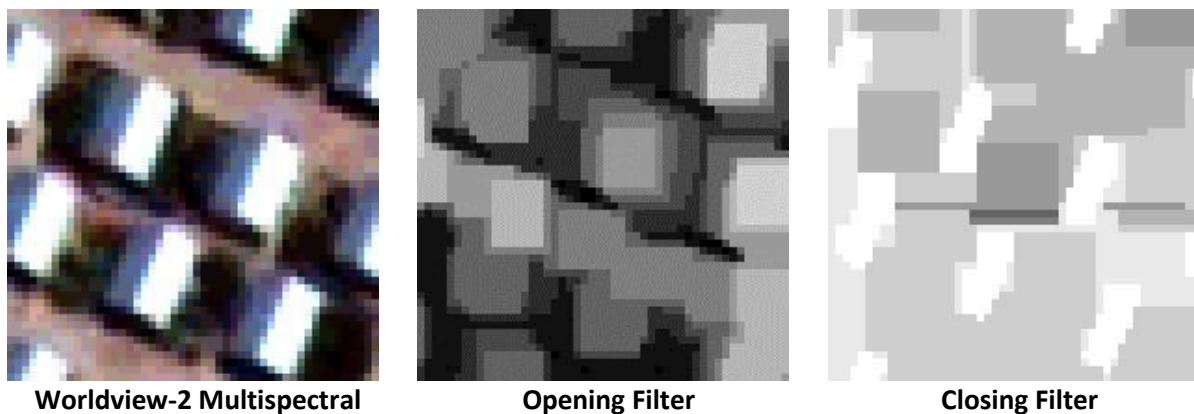


Figure 5-32: Opening and closing filters applied to blue and near-infrared Worldview-2 bands respectively.

#### 5.18.4. Top-Hat Transformation

After applying the opening and closing operators top-hat processing was used to isolate and extract the dark and light roof features (Serra, 1982). This was achieved by computing the difference between the original image and the transformed images. Two types of top-hat operation were applied: the *white top-hat transformation* which is the difference between the input blue band and its opening by a structural element and the *black-hat transformation* which is the difference between the input near-infrared image and its closing operator. The white top-hat operator returns objects in the input image that are brighter than the surroundings and smaller than the structural element and the black-hat operator returns objects in an image that are darker than the surroundings and smaller than the structural element.

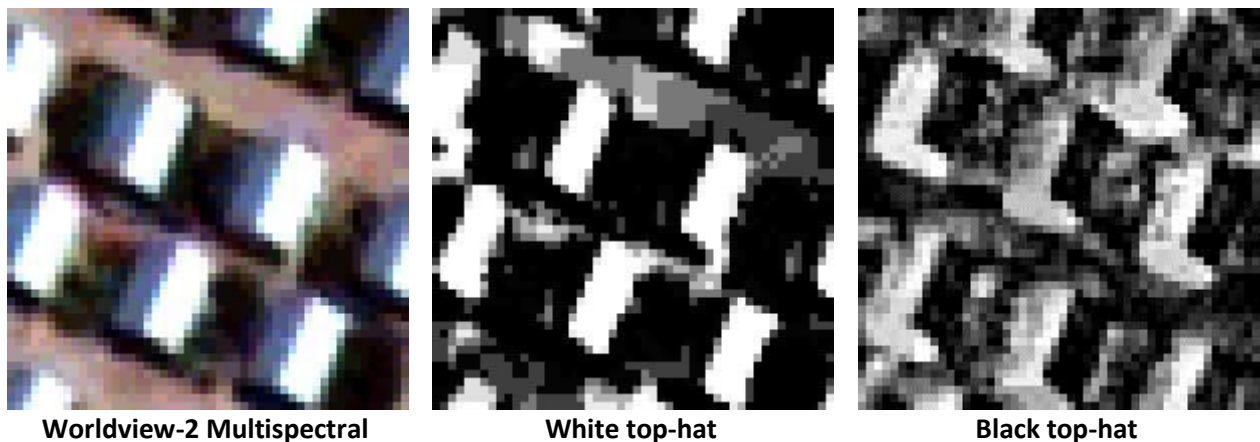


Figure 5-33: Top-hat processing applied to the results of the opening and closing filters.

#### 5.18.5. Post-Processing

To isolate and extract the shaded and sun-lit roof panels a threshold was applied to the top-hat transformation results. A threshold of 125 was applied to the white top-hat transformation results and 150 to the black top-hat operator so that pixels with values above the threshold were assigned to the transitional shelter class. The binary top-hat images were then filtered with an opening filter to remove small objects and a dilate operator to fill gaps in the final objects. The two filtered threshold images representing dark and light roof panels were then merged using the union operator to create the finished map.

### **5.19. Method 3: Object-Based Image Analysis (OBIA)**

Object-Based Image Analysis (OBIA) divides an image into homogenous zones which are then classified using their spectral, spatial and textural attributes. Two methods of classifying the objects is tested in this study: 1. Rule-based method that uses rulesets developed by the analyst and 2. A supervised classification method based on the selection of representative sample objects. The OBIA workflow can be thought of as a 4-step process comprised of pre-processing, segmentation, classification and post-processing. These steps are described in detail below.

#### *5.19.1. Pre-Processing*

Segmentation reduces the scene's heterogeneity by dividing groups of adjacent pixels into homogenous image objects (Cross & Mason, 1988; Flanders et al. 2003). The objective of segmentation in this application is to create image objects that accurately represent the shape and size of the transitional shelters in the scene; for the segmentation algorithm to work most effectively the structures must have clear edges and homogenous roof pixels to avoid segmentation within the roofs and significant contrast with the ground to avoid merging between buildings. The segmentation algorithm was applied to 4-band pan-sharpened images. An erode filter with 1.5 m radius was used to remove noise within the building outlines and around the edge of the roofs to produce cleaner edges.

#### *5.19.2. Feature Extraction*

The feature extraction process itself involves two methodological procedures: 1. Image segmentation and 2. Object classification. A single ruleset controls both of these processes by applying specially-selected image processing techniques, thresholds and parameters; for this study, suitable rulesets were created and saved using ENVI EX software developed by ITT and the image objects were analysed using ArcGIS's Spatial Analyst tools. Figure 5-34 shows each stage of the feature extraction workflow applied to a camp subset containing transitional shelters.

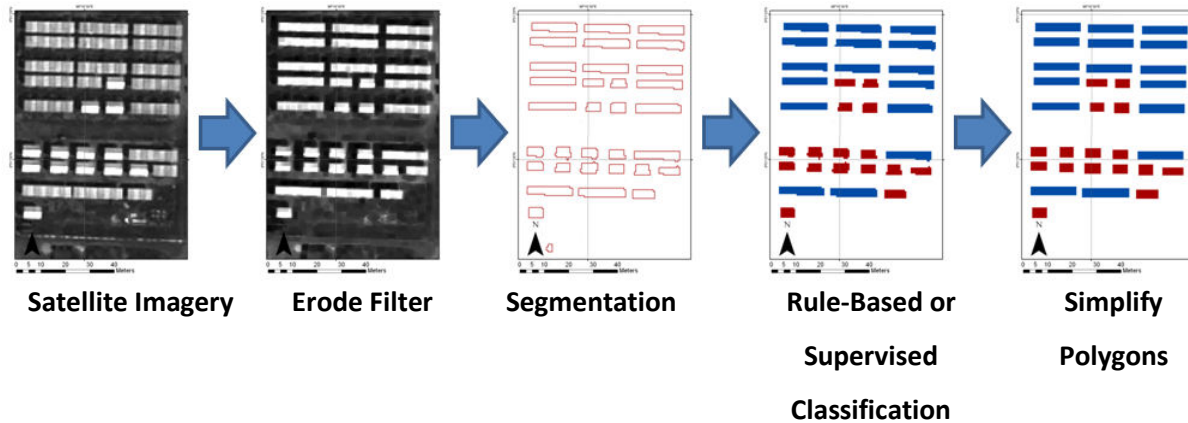


**Figure 5-34: Object Based Image Analysis workflow applied to transitional shelters. In this example two different shelter shapes have been extracted and coded red and blue.**

#### 5.19.2.1. Image segmentation

Segmentation is the process of portioning an image into non-intersecting regions. Gonzalez and Woods (2002) identify two categories of segmentation algorithm. The first, known as edge-detection technique, creates partitions based on abrupt changes in intensity while the second group divide an image into similar regions according to a set of predefined criteria.

A patented edge-based segmentation algorithm was used to divide the image (Xiaoying, 2009). The algorithm defines homogenous zones in the imagery using reflectance values as well as a scale factor that is defined by the analyst making it particularly useful. The segmentation algorithm first normalises each of the input bands and then calculates a gradient image for each. It fuses the gradient images together to produce a single gradient map. A relative level threshold is then set by the analyst and a 'modified gradient map' is produced by setting all gradient values below the gradient magnitude to be the same as the gradient magnitude. The relative level threshold ranges from 0.0 to 100.0 and is adjusted by the analyst: a larger scale value suppresses weak edges and areas with weak contrast, resulting in larger objects and vice-versa. After a suitable threshold level is selected, a watershed algorithm is applied to the modified gradient map using a FIFO queue data structure (Vincent and Soille, 1991). The pixels on the waterlines are then labelled 0 and the watershed lines used to divide the image into multiple regions which are each given a unique label.

Inspection of the results established that the segmentation algorithm over-segmented some groups of pixels, particularly around the edge of the structures. The Full Lambda-Schedule algorithm was therefore applied in an additional step to merge adjacent objects based on their spectral and spatial characteristics. Adjacent objects,  $i$  and  $j$ , are merged if the merging cost ( $t_{i,j}$ ) is less than the threshold lambda value defined by the analyst. The Full Lambda-Schedule algorithm is defined by Robinson, Redding and Crisp. (2002) as follows:

$$t_{i,j} = \frac{|O_i| \cdot |O_j|}{|O_i| + |O_j|} \cdot \|u_i - u_j\|^2$$

*length*( $\partial(O_i, O_j)$ )

Where  $O_i$  is object  $i$  of the image,  $|O_i|$  is the area of object  $i$ ,  $u_i$  is the average value in object  $i$ ,  $\|u_i - u_j\|$  is the Euclidean distance between the spectral values of objects  $i$  and  $j$ , *length*( $\partial(O_i, O_j)$ ) is the length of the common boundary of  $O_i$  and  $O_j$ .

Image objects were created and the parameters refined until they accurately represented the size and shape of the building footprints. The process involved an initial segmentation of the image followed by iterative amendments to the inputs and segmentation parameters until the buildings' boundaries were effectively delineated. The final relative level threshold used in the analysis was 24.9. This was the highest value to effectively delineate the boundaries of the shelter. The threshold lambda value was 89.6. The high lambda parameter effectively merged any objects that were spectrally and spatially similar to one another. Figure 5-35 presents a preview of the Corail camp objects after the segmentation algorithm was applied.



Figure 5-35: Groups of pixels were converted to image objects using an edge-detection algorithm.

### 5.19.2.2. Analysing Image Object Attributes

The segmentation procedure produced a total of 16,073 objects. Once an acceptable segmentation was achieved the attributes of the image objects were calculated and analysed in detail by applying queries to the dataset using Structured Query Language (SQL) expression and then monitoring the statistics of the selected objects. A class model was created for transitional shelters that accurately characterised the structures' spatial, textural and spectral attributes. Spatial indices such as area and main direction were found to be particularly useful at 'describing' the objects representing the structures. Figure 5-36 shows three spatial indices applied to objects representing a subset of Corail camp. Note that the shaded and sun-lit roof panels were segmented as separate objects so must be classified separately in the next step.

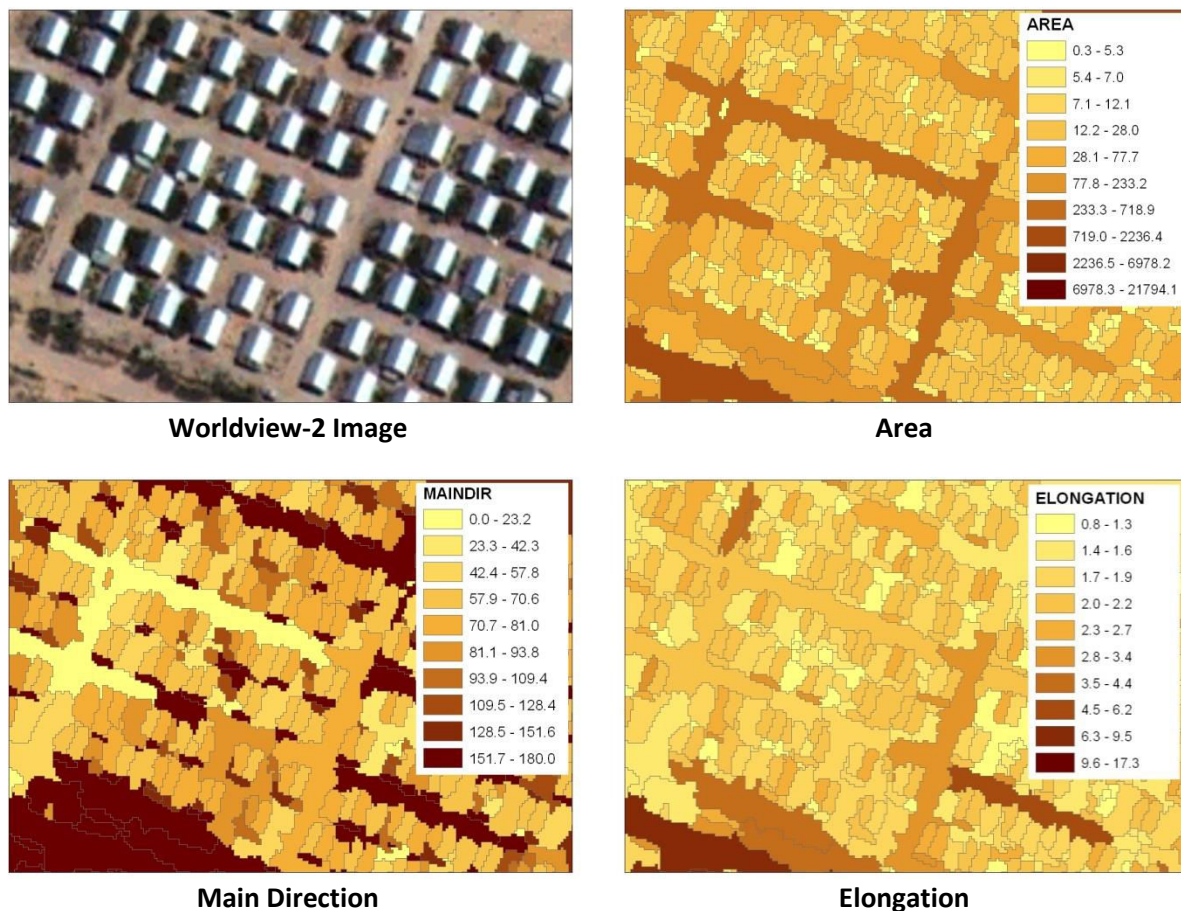


Figure 5-36: Three spatial indices applied to objects representing Corail camp.

### *5.19.2.3. Object Classification*

Classification is the process of allocating image objects to suitable classes based on their feature values. Two methods of classifying image objects were tested in this study: a) rule-based classification and b) nearest neighbour supervised classification. The former performs the classification based on a series of rules defined by the analyst while the later classifies the objects using statistics calculated from a sample of objects.

#### *5.19.2.3.1. Rule-Based Classification*

Rule-based classification is an advanced method of classification that lets the analyst define features by creating sets of rules using the objects' spatial, textural and spectral attributes. Rule-based classification is based primarily on human knowledge and reasoning about specific feature types (Jin & Paswaters, 2007). Suitable rules and rule parameters were developed based on the measurements and observations made when analysing the image characteristics at the beginning of the study and when analysing the results of the segmentation in the previous step.

Due to differences in reflectance the edge-based segmentation algorithm divided the shelter roofs into two parts: one object representing the shaded roof panel and the other the sun-lit panel. The two sides of the roofs were classified independently due to the significant difference in reflectance values produced by each.

The sun-lit roof panels were classified by simply identifying objects with a bright reflectance. An average reflectance above 1953.00 in the blue band was found to be appropriate. The ruleset for the shaded roof panels used area and direction attributes as well as spectral descriptors. The main direction attribute is defined as the "angle subtended by the major axis of the polygon and the x-axis in degrees". To distinguish shaded roof panel objects from bare ground objects the ruleset incorporated a spectral rule that selected objects with a low standard deviation in the green band. This exploited the characteristic that each roof panel exhibited a lower standard deviation in reflectance than bare ground because of its relatively flat surface. The full ruleset for shaded roof panels was:

- Objects with an area between 2 and 24 m<sup>2</sup> AND
- Objects with a direction between 52 and 101 degrees AND
- Objects with Average NIR band value less than 0.25 AND
- Objects with Average NIR band value more than 0.5 AND
- Objects with Green Band Standard Deviation less than 0.05

The ruleset was applied using fuzzy-logic instead of the traditional binary-based approach. This technique uses a membership function to represent the degree that an object belongs to a class instead of a binary rule. Fuzzy logic approach therefore allows for variation in object attributes which might be produced by the segmentation process (Benz et al. 2004). The output of each fuzzy rule is a confidence map containing values that represent the degree to which each object belongs to the class. Each object is ultimately assigned to the feature type with the maximum confidence value. This means that objects not complying exactly with the rules might still be considered in the classification depending on the results of the other rules. This is important as sometimes variation is introduced in the imagery by atmospheric and geometric differences and through processing such as pan-sharpening, causing the segmentation to work differently across the image.

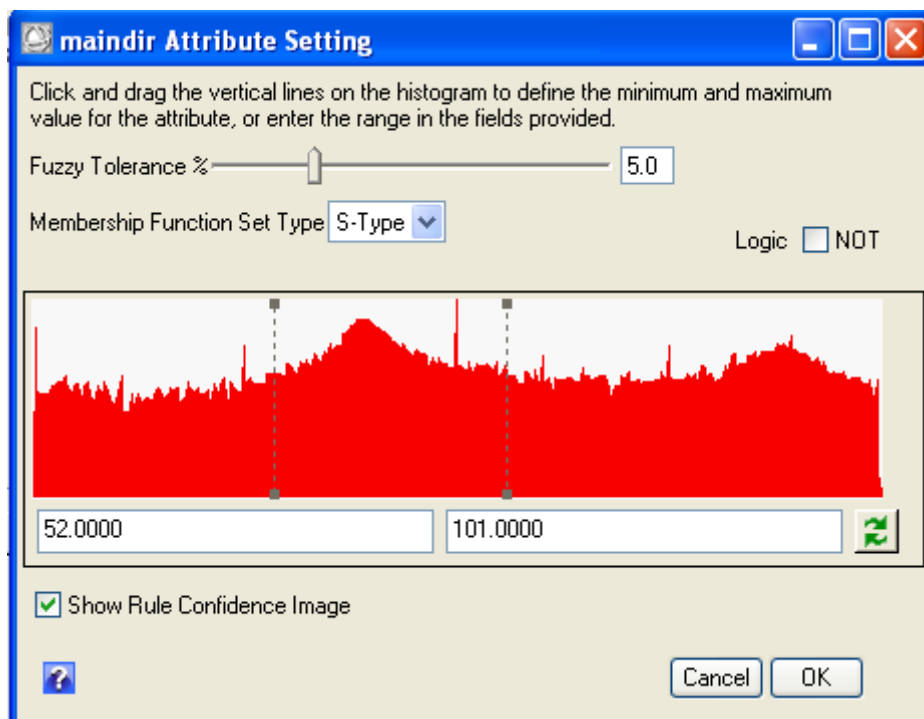


Figure 5-37: Fuzzy rules for the main direction defined.

Fuzzy logic was introduced into the workflow by defining rulesets using fuzzy versions of the traditional concepts 'greater than', 'less than' and 'in-between'. Membership functions, such as S-type and linear, model the amount of fuzziness applied (Jin and Paswaters, 2007). The S-type membership function was found to be convenient for this application as it introduced a small amount of fuzziness. The fuzzy tolerance parameter determines the amount of fuzzy logic applied to each rule. 5% was found to be sufficient to model uncertainty in the classification by using information from all rules and not rejecting objects using a single binary condition.

#### *5.19.2.3.2. K Nearest Neighbour Classification*

K Nearest neighbour (KNN) is a form of supervised classification that classifies objects based on their similarity to training data provided by the user. The KNN algorithm assumes unclassified objects and training data are points in a feature space and it classifies the objects by identifying the most common class amongst its nearest neighbours.

KNN is a non-parametric instance-based machine learning algorithm and is one of the most commonly used data mining tools (Duda, Hart and Stork. 2001). It is known as an instance-based algorithm as it does not generalise the training datasets. Instead, all of the training data is stored during the learning phase; the classification then assigns class labels to unclassified objects after measuring the distance to nearby training data. As a result, the learning phase is commonly quick while classification can be computationally intensive, especially when large training datasets are being used.

The training phase first requires the analyst to identify a set of objects that are known to represent each of the classes with high confidence. In this study, 10 object samples were selected for each of the three classes used in the classification: shaded roof panel, sun-lit roof panel and bare ground. The training data points consist of a set of vectors in a multidimensional space each with a class label. The feature space is n-dimensional, where n equals the number of object attributes used during the classification. The data points all have a position in the feature space so distances can be computed by Euclidean distance using the following formula:

$$d(p, q) = \sqrt{\sum_{i=1}^n (q_i - p_i)^2}$$

Where  $p_i$  and  $q_i$  are two points in Euclidean  $n$ -space.

After the Euclidean distances were calculated the classification was performed by assigning the class to an unclassified object which is most frequent among the  $k$  training samples. The user-defined  $k$  parameter determines the number of neighbours considered when performing the majority voting procedure. A  $k$  value of 1 means that the object is assigned the class of its nearest neighbour in the feature space. A heuristic approach was used to select 3 as a suitable  $K$  parameter for this classification. Larger values of  $K$  are known to reduce the effect of noise on a classification but a  $K$  of 3 was found to be appropriate because the noise in the data was minimal.

Figure 5-38 presents a hypothetical example of the nearest neighbour algorithm in a two-dimensional feature space. If  $k=1$  is defined by the user than the unclassified object (black circle) is assigned to the red class as a red point is closest to the object in the feature space. When  $k=3$  the object is classified as green because of the closest three points two are green and when  $k=5$  three of the five points are red and two are green.

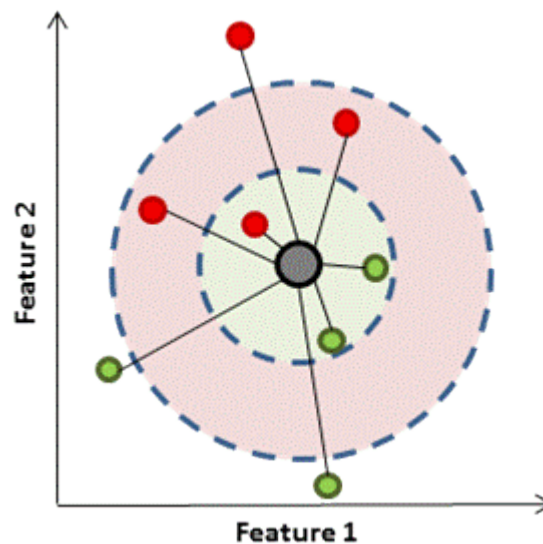


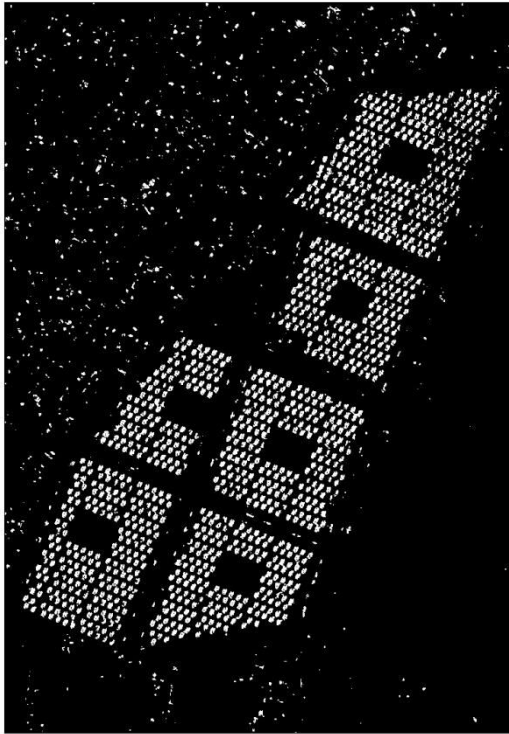
Figure 5-38: Nearest neighbour classification in the two-dimensional feature space.

## **5.20. Results**

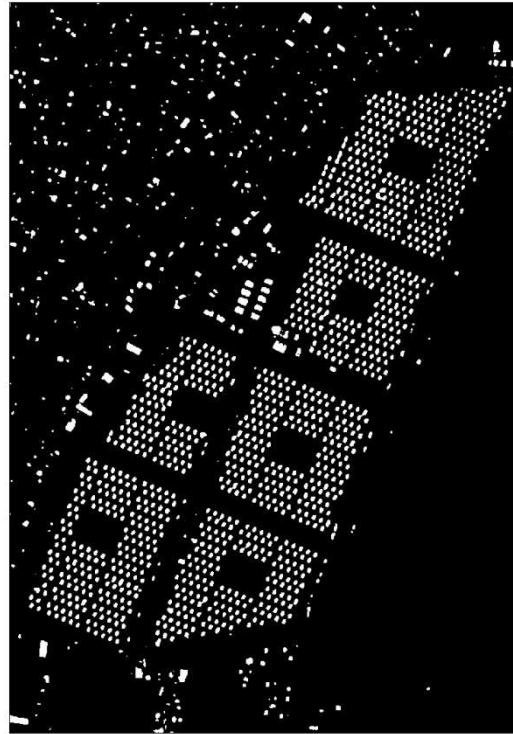
The reliability of the four classification results was first assessed by comparing both the number of shelters and the total area calculated by each method to statistics created from the manual delineation of transitional shelters. The outlines of all 1,120 transitional shelters were manually delineated to produce a validation dataset. Paper maps and ground observations from the camp and camp workers were used to verify the manually-derived maps.

Like in Study 1, the accuracies of the classifications were then calculated at pixel level by comparing the amount of overlap between the manually-delineated building outlines and the extents of the individual classifications. Maps created from this validation exercise highlight exactly where and why classification errors occurred, allowing commentary on the strengths and weaknesses of each method and recommendations on how the techniques may be improved.

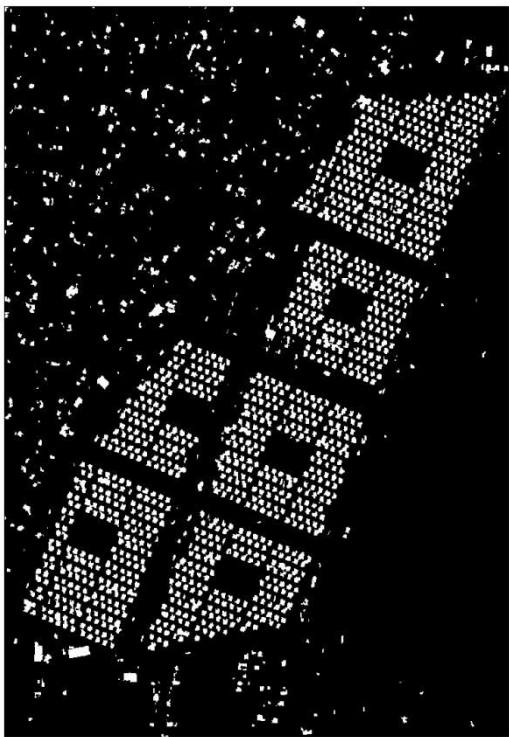
Figure 5-39 shows the classification image results produced from each of the four techniques. The outline of the transitional shelters and the layout of the camp is immediately recognisable in each of the maps. Closer inspection of the maps reveals subtle differences in the classification results; these differences will be explored in detail below.



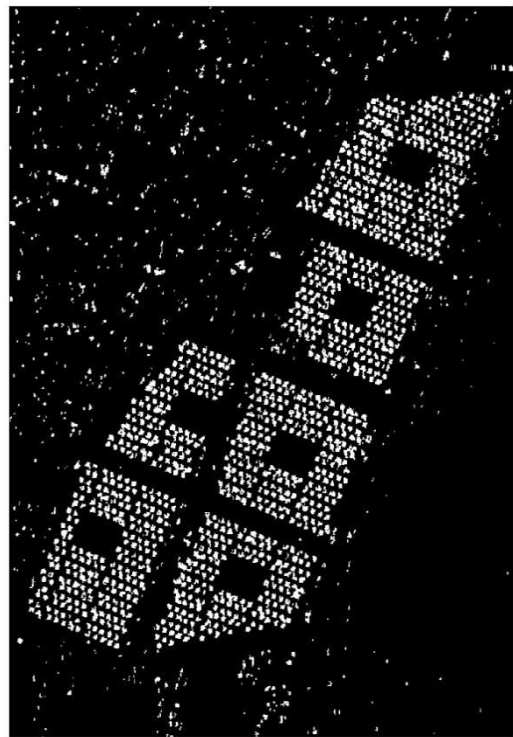
Mathematical Morphology



Spectral Angle Mapper



OBIA (Nearest Neighbour)



OBIA (Rule-Based)

Figure 5-39: The classification of Corail camp using four semi-automatic workflows.

The number of shelters and the area occupied by those shelters is important for camp managers to know for enumeration purposes. The estimated number of transitional shelters was first assessed by counting the number of objects produced by each method within the confines of the camp, assuming that each object represents a single transitional shelter. The area occupied by the image objects representing transitional shelters was also calculated in m<sup>2</sup> and summed for the whole camp.

Table 5-7 show the number of objects and the total area classified with each of the methods. OBIA provides the closest estimate of the number of structures. The number of shelters is estimated to within 3% by both rule-based and supervised OBIA approaches and to within 10% by the spectral angle mapper. Mathematical morphology performs the least well and overestimates both the number of the shelters and the area by over 30%.

Each of the four methods overestimated the area occupied by shelters. Spectral classification provides the closest estimate of area with a result within 10.5% while the OBIA methods overestimated area by between 20-25%.

	Number Objects	%	Total Area	%
Manual	1,195	---	29,374	---
Morphology	1,622	+35.7	38,649	+31.6
OBIA (supervised)	1,190	-0.4	36,655	+24.8
OBIA (rule)	1,227	+2.7	35,458	+20.7
Spectral	1,305	+9.2	32,450	+10.5

**Table 5-7: The number and area of shelters estimated by each classification method.**

Overlay analysis was conducted to better understand these results and the sources of error. This was achieved by overlaying the results of each individual classification with the manually-derived map. This analysis identified pixels that were correctly classified, pixels that were missed by the classification (omission error) and pixels that were incorrectly classified (commission error). These results are

analysed with a series of contingency matrixes and error images, and they are used to calculate an overall accuracy, kappa coefficient, and errors of commission and omission.

The overall accuracy is calculated as the number of correct pixels divided by the total number of pixels, while the Kappa coefficient reflects the difference between actual agreement and the agreement expected by chance. As shown in table 5-8 the Kappa coefficient correlates with overall accuracy. The Kappa coefficient is defined as follows (Lillesand et al. (2008):

$$\hat{k} = \frac{N \sum_{i=1}^r x_{ii} - \sum_{i=1}^r (x_{i+} \cdot x_{+i})}{N^2 - \sum_{i=1}^r (x_{i+} \cdot x_{+i})}$$

*Where: r = number of rows in the contingency matrix,  $x_{ii}$  = number of observations in row i and column i (on the major diagonal),  $x_{i+}$  = total of observations in row i,  $x_{+i}$  = total of observations in column i, N = total number of observations included in matrix.*

Contingency matrixes were created to directly compare the number of pixels correctly and incorrectly classified. A summary of the results extracted from the contingency matrixes is presented in table 5-8. Analysis of commission and omission errors helped to identify where each method had overestimated and underestimated the number and area of buildings. The commission error is the proportion of classified pixels not overlapping with manual polygons and the omission error is the proportion of manually-delineated pixels not overlapping with the classification.

There is a high correlation between the overall accuracy and the area results reported previously, spectral analysis has the highest overall accuracy (94%), followed by OBIA (91-92%) and MM (88%).

	Overall Accuracy (%)	Kappa	Error of Commission (%)	Error of Omission (%)
Morphology	88.01	0.5989	41.10 (63451/154385)	22.20 (25941/116875)
OBIA (rule)	90.77	0.6782	33.02 (46713/141448)	18.94 (22140/116875)
OBIA (supervised)	92.22	0.7321	29.70 (43083/145061)	12.75 (14897/116875)
Spectral	94.12	0.7866	21.71 (28012/129043)	13.56 (15844/116875)

**Table 5-8: Summary of the overlay analysis results. Errors of commission and omission in terms of the number of pixels are presented in parentheses.**

The next section discusses the errors identified for each classification method in more detail, where and why they occurred and how they can be rectified. The discussion focuses on four types of error that were found in the results.

The error types are shown in figure 5-40 and consist of two types of commission error and two types of omission error. The red lines in the figure are the manually delineated shelter outlines and the black polygons show the area classified by Mathematical Morphology. Commission error 1 and omission error 1 occur when the extent of the classification is beyond or short of the building outline leading to overestimation or underestimation of the shelter area respectively. Commission error 2 occurs when isolated objects outside of the shelter outline are incorrectly classified as transitional shelters leading to overestimation of the number of structures and omission error 2 occurs when there are gaps inside of the shelter objects.

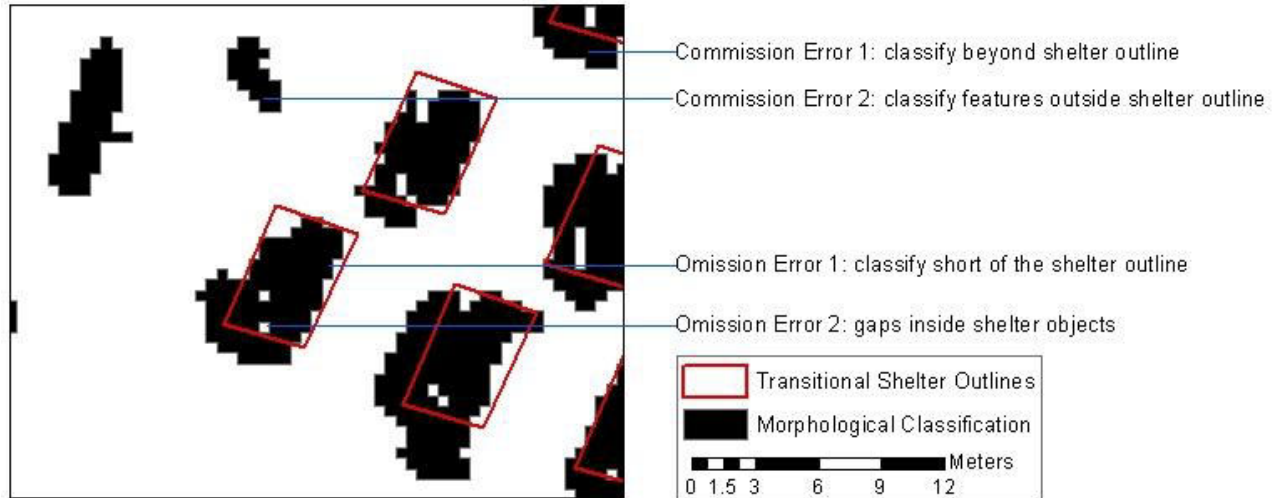


Figure 5-40: Types of commission and omission errors.

### 5.20.1. Commission Error 1: classify beyond shelter outline

The most common commission error occurred when the classifier incorrectly classified beyond the edge of the building outlines leading to an overestimation of the building area. Examples of these commission errors are shown in figure 5-41.

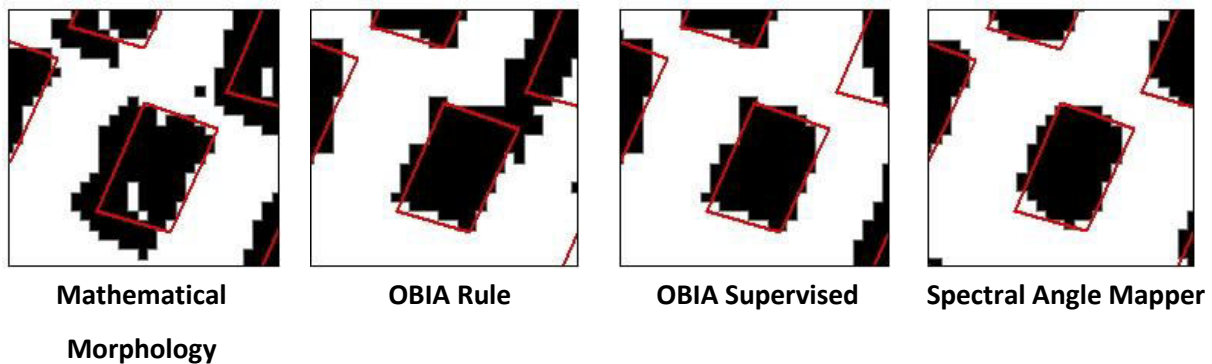


Figure 5-41: Examples of commission error 1 in Corail camp.

MM consistently classified beyond the edge of every shelter in the camp which led to the high overall commission error and the high area estimation. The errors occurred on the southern and western sides of the structures where shadows were being cast by the shelters. These shadows were incorrectly classified as part of the shaded roof panels due to their adjacency and similarities in brightness. This error is very difficult to prevent or minimise due to the brightness similarity of the cast shadows and the

shadow on the shelter roofs. The error could be minimised though by introducing an additional post-processing step to clip the roof objects by a known amount according to the expected length of shadow based on the shelter's height and the sun's position.

OBIA was less likely to produce this sort of commission error; while OBIA tended to overestimate the shelter area in places, the error was not consistent around every shelter as it was for MM. The shape and size of the commission error caused by OBIA also varied substantially in its shape around each shelter. The error occurred when the segmentation algorithm failed to segment cleanly around the edge of the shelters. Instead of creating rectangular objects around the edge of the buildings the segmentation incorrectly added various obtrusions to the objects. This commonly occurred when the edge-detection algorithm incorrectly segmented around features adjacent to the shelters such as areas of dark scrub and shadowed ground.

This error highlights a weakness with the edge-detection segmentation approach. The effectiveness of segmentation is important as the results of the classification are directly dependent upon the results of the segmentation stage. Other, more advanced, segmentation procedures are available including a multi-resolution segmentation algorithm available with Definiens Developer. This is a bottom-up method that clusters smaller homogenous objects into larger ones. The process allows the user to determine the objects' maximum homogeneity using criteria such as colour, shape, smoothness and compactness (Cruse and Hempel, 2005).

#### *5.20.2. Commission error 2: classify features outside shelter outline*

Commission errors also occurred when isolated features outside of the shelter outlines were incorrectly classified as transitional shelters leading to an overestimation of the number of transitional shelters. MM and OBIA both produced this error when small dark structures and clumps of vegetation were mistaken for shaded roof panels due again to their similarity in brightness and shape. The vegetation error may be minimised by applying a vegetation mask in the pre-processing stage. Figure 5-42 shows examples of both types of commission error in a subset of Corail camp.

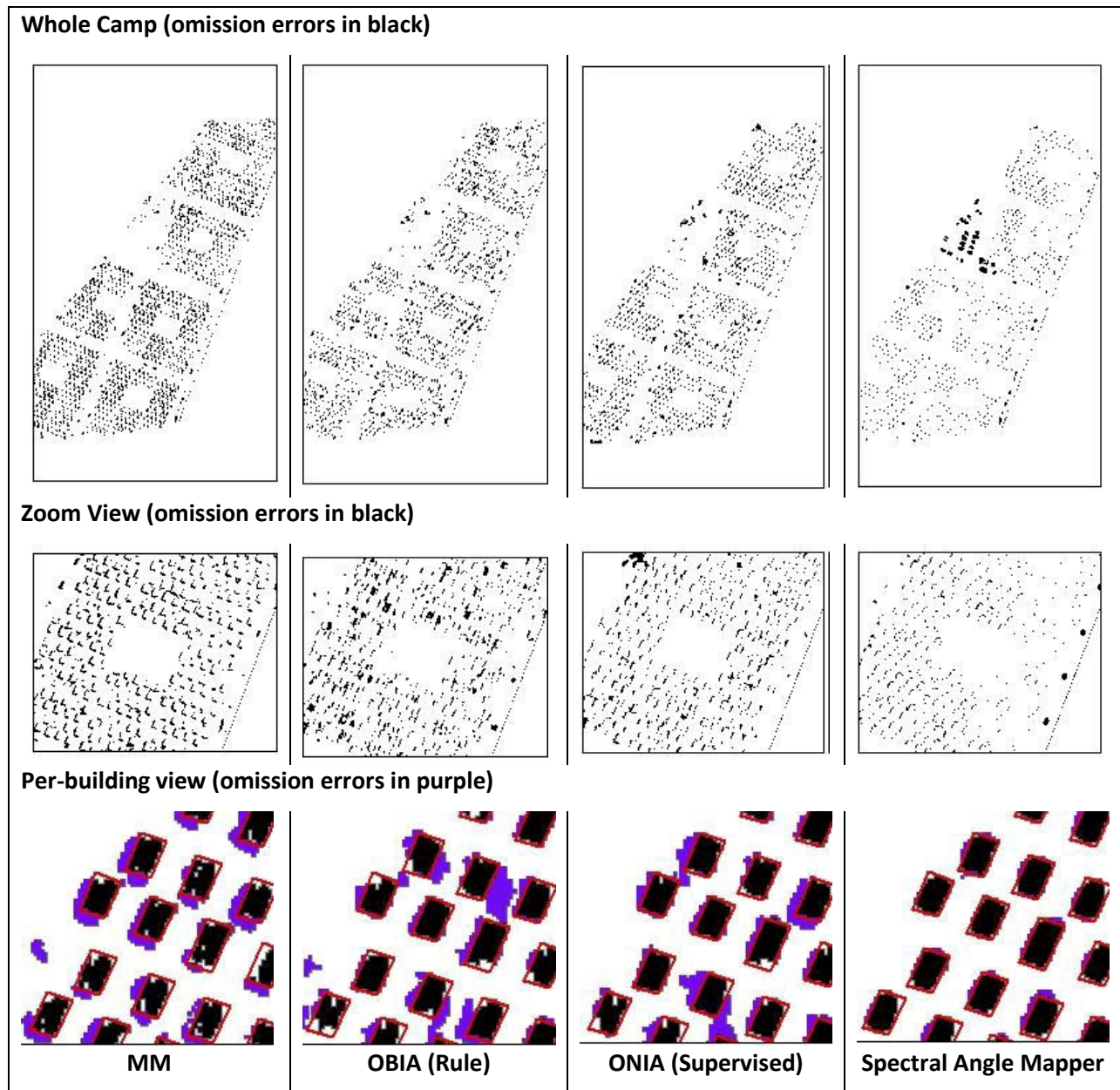


Figure 5-42: Commission errors shown in black across Corail camp and in purple on the bottom row.

The spectral classifier was very successful at only classifying corrugated-iron. The commission error (22%) occurred mainly where buildings other than transitional shelters were classified. This included 30 functional and storage buildings to the north of the site and a series of elongated toilet blocks along the central roadway. The large functional buildings classified by SAM are visible as black polygons in figure 5-42 . MM and OBIA did not classify these buildings as the methods both incorporated spatial rules that

allowed them to recognise that these buildings were a different shape and size to the transitional shelters.

SAM was unable to distinguish between buildings with corrugated-iron roofs based on their spatial attributes. This ultimately led to SAM overestimating the number and area of transitional shelters in the camp. Despite misclassifying these large buildings SAM still produced the lowest overall commission error because it did not classify beyond the edge of the transitional shelter outlines. MM produced the highest commission error as it consistently misclassified shadow around every transitional shelter.

### *5.20.3. Omission errors 1 and 2: classify short of the shelter outline and gaps inside shelter objects*

Mathematical Morphology and OBIA (rule) both produced the highest omission errors: 22% and 19% of shelter pixels were missed by these techniques respectively, while OBIA (supervised) and SAM missed between 12-13% of pixels. Figures 5-43 shows omission errors across the Corail camp. The detailed building-level images on the bottom row show that MM and OBIA (rule) missed large sections of the shelters. OBIA (supervised) was also susceptible to omission errors, but the results of the SAM classification appear to closely match the outlines of the shelters.

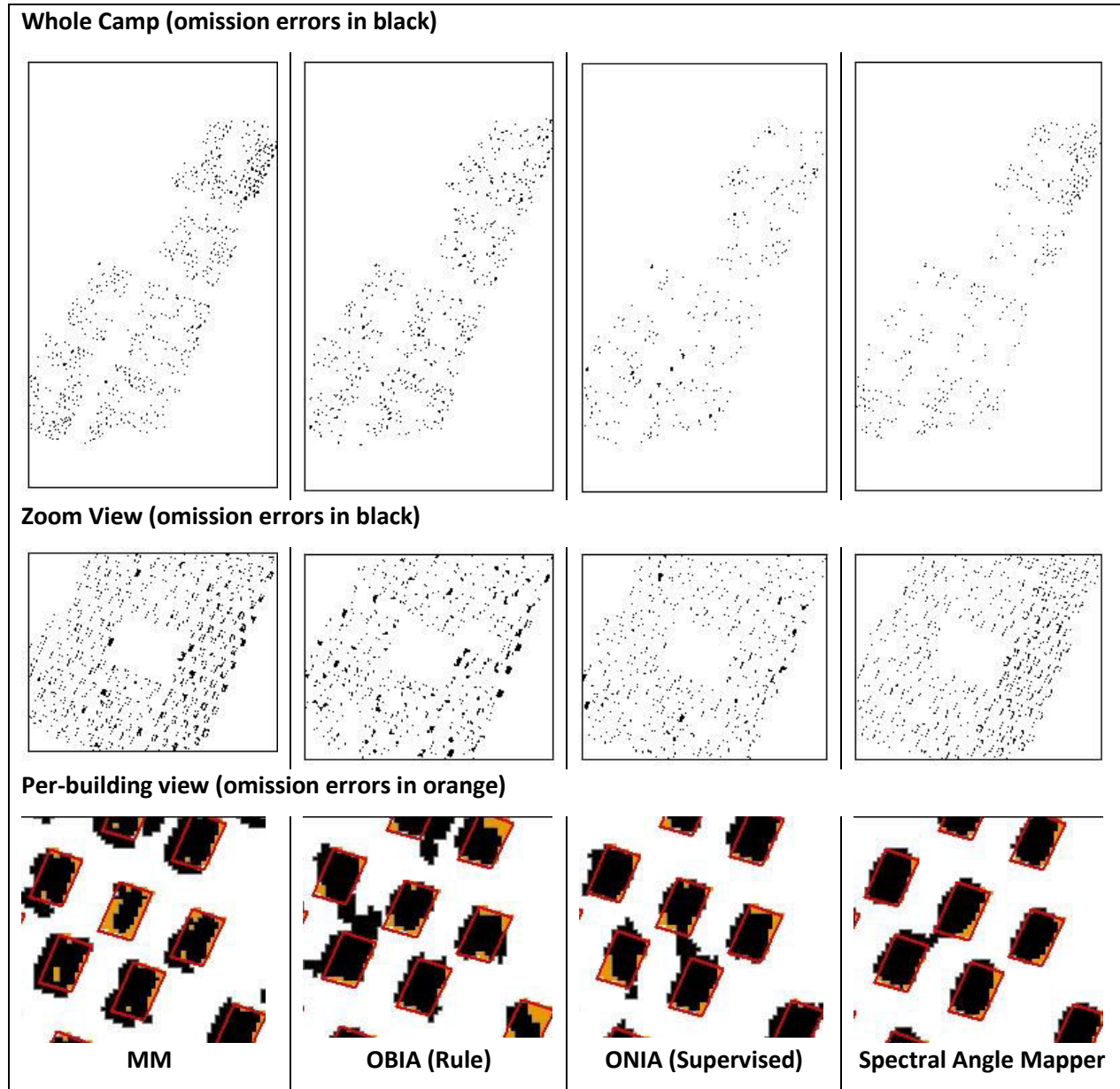
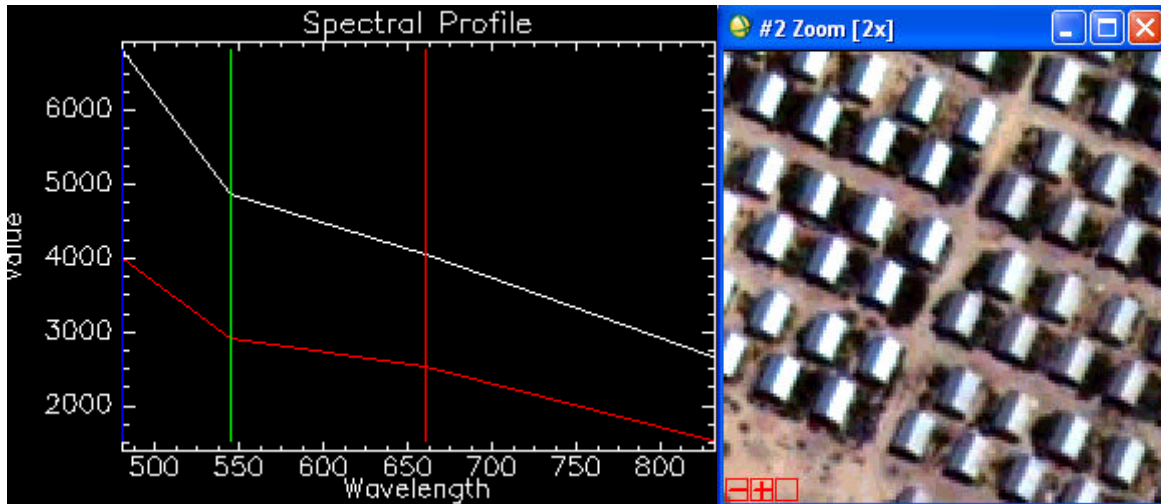


Figure 5-43: Omission errors shown in black across Corail camp and in orange on the bottom row.

The maps highlight exactly where omission errors occurred across the Corail site. The images show that MM and SAM struggled to classify a block of buildings to the north of the site. Studying the locations where these errors occurred revealed that there are subtle differences in the reflectance of the shelters across the site, with some blocks of shelters reflecting brighter than others. Figure 5-44 shows two blocks of shelters: the block to the left appears brighter than the shelters on the right. The spectral

profile shows that the brighter shelters reflect higher in all bands. This difference in reflectance might occur if the buildings were constructed long before the others or if they were exposed to dust or other weathering agents. It's also possible that the roofs may have been treated with a protective substance or that the material used was from a different source.



**Figure 5-44: Transitional shelters with different reflectance values contributed to omission errors. The spectral profile on the left shows the brighter shelter reflectance profile (white line) and the darker shelter reflectance profile (red line).**

These differences in reflectance appear to have been one of the main causes of omission error. MM in particular failed to classify some of the darker sun-lit roof panels, presumably as the brightness of the pixels was not distinct enough from the surrounding background pixels to be captured by the filtering procedure. OBIA (rule) often failed to classify the same darker sun-lit panels while OBIA (supervised) classified this area better suggesting that OBIA (supervised) is flexible to these differences in object attributes as long as the different object types are represented in the training class.. To reduce the omission error for OBIA (rule) the ruleset will need to be amended to reduce the minimum NIR band reflectance threshold. This will ensure the darker roof panels are classified but might lead to more commission errors.

SAM produced the lowest omission error overall due to its accurate classification of corrugated-iron. Figures 5-42 and 5-43 show how closely the extent of the SAM classification matched the shelter outlines. Any omission or commission errors caused by SAM may be rectified by masking areas of high

confusion or by altering the pixels used in the training dataset but this was not necessary due to the high accuracy of the results. The small omission errors that were produced by SAM are likely to have done so because pixels on the edge of the shelters contain reflectance from both corrugated-iron and bare ground. Pixels representing this unique spectrum may be added to the training class but are likely to lead to more misclassification of bare ground as corrugated-iron.

## **5.21. Discussion**

The two studies in this chapter show how remote sensing can be used to monitor planned camps and spontaneous settlement over large geographic extents and provide useful information to recovery organisations such as UN-Habitat. In study 1, a semi-automatic Maximum Likelihood method was used to estimate the number of corrugated-iron structures across 5 km<sup>2</sup> to within 15% accuracy of CCCM ground-derived estimates and to within 7% accuracy with the use of regression analysis. Manual analysis across this whole area is estimated would have taken approximately 50 hours, whilst Maximum Likelihood took 2 hours (not accounting for the ground analyses that were completed before). The regression analysis required buildings in 73 randomly-selected grids to be manually delineated and for those results to be directly compared to the Maximum Likelihood results which took a further 16 hours to conduct and increased the accuracy from 15% to 7%. This gives analysts a number of options depending on the time available and accuracy required. Its important analysts recognise limitations in the areas they are working. In this case ground survey work was required to estimate the proportion of buildings under corrugated-iron roofs that were made of concrete or corrugated-iron as the wall-types were not decipherable using remote sensing.

In study 2, four semi-automatic approaches to mapping a planned camp were tested thoroughly. Spectral Angle Mapper was the easiest and quickest to implement and produced the most accurate estimation of shelter area. The high accuracy was largely because SAM overcame shadow issues caused by the shelters' pitched roofs and was flexible enough to allow for brightness variation between shelters too. The other approaches struggled with both these factors. Mathematical Morphology was work intensive and produced poor results as it incorrectly classified shadows adjacent to the shelters and nearby patches of vegetation. Object-based Image Analysis counted the number of transitional shelters accurately (within 3%) but was less successful at estimating the total shelter area, due mainly to

limitations with the segmentation algorithm used. The supervised OBIA produced slightly better accuracy and was quicker and easier to implement than the rule-based OBIA method.

In summary, there are a large number of approaches and algorithms available to remote sensing analysts. In areas where the spectral and spatial attributes of the structures are regular, then spectral classifiers such as Maximum Likelihood and Spectral Angle Mapper can be deployed successfully. OBIA can be used in more complex landscapes to utilise images' spatial, contextual and spectral information. Mathematical Morphology was found to be time-consuming and inaccurate, even in this relatively simple context. This chapter shows how the approaches take different lengths of time to conduct and produce different levels of accuracy. It has also shown how different approaches may be useful for particular applications. To choose the best tool for their application the analyst must have a good understanding of the landscape they are studying and the tools available to them. Lessons from this chapter and others will be summarised and outlined as guidelines in the concluding chapter.

## **Bibliography**

Benz, U.C., Hofmann, P., Willhauck, G., Lingenfelder, I. and Heynen, M. (2004).

Multi-resolution, object-oriented fuzzy analysis of remote sensing data for GIS ready information. *ISPRS Journal of Photogrammetry and Remote Sensing*: **58**, 239–258.

Brown, D., Platt, S. and Bevington, J. (2010). *Disaster recovery indicators*. Centre for Risk in the Built Environment. Cambridge University, UK.

Byrkit, D.R. (1972). *Elements of statistics. An introduction to probability and statistical inference*. Van Nostrand Reinhold Company, London.

CCCM (2011a). *Displacement Tracking Matrix V2.0 Update*. Camp Coordination Camp Management (CCCM) Cluster. Port-au-Prince, Haiti.

CCCM (2011b). *Displacement Tracking Matrix (DTM). Strategy – Version 2.0*. Camp Coordination Camp Management (CCCM) Cluster. Port-au-Prince, Haiti. May 2011.

*Chapter 5: Comparing the use of manual and semi-automated remote sensing techniques to monitor camps and spontaneous settlement for UN-Habitat after the 2010 Haiti earthquake*

Clark, R.N., Swayze, G.A., Wise, R., Livo, E., Hoefen, T., Kokaly, R. and Sutley, S.J. (2007). *USGS digital spectral library*. U.S. Geological Survey, Digital Data Series 231. Virginia, USA.

Corsellis, T. and Vitale, A. (2005). *Transitional Settlement: Displaced Populations*. Oxfam Publishing, Oxford, UK.

Cruse, B. and Hempel, C. (2005). Object based land cover mapping for Groote Eylandt: a tool for reconnaissance and land based surveys. *Proceedings of NARGIS 2005. The North Australian Remote Sensing and GIS Conference*. 4<sup>th</sup>-7<sup>th</sup> July. Darwin, Australia.

Cross, A. M., Mason, D. C. and Dury, S. J. (1988). Segmentation of remotely sensed images by a split and merge process. *International Journal of Remote Sensing*: **9**, 1329-1345.

Duda, R.O., Hart, P.E. and Stork, D.G. (2001). *Pattern classification* (second edition). John Wiley & Sons inc, Chicester.

Flanders, D., Hall-Beyer, M. and Pereverzoff, J. (2003). Preliminary evaluation of eCognition object-based software for cut block delineation and feature extraction. *Canadian Journal of Remote Sensing*: **29**: 441-452.

Giada, S., Groeve, T.D. and Ehrlich, D. (2003). Information Extraction from Very High Resolution Satellite Imagery Over Lukole Refugee Camp, Tanzania. *International Journal of Remote Sensing*: **24(22)**, 4251-4266.

Gonzalez, R.C. and Woods, R.E. (2002). *Digital Image Processing (second edition)*. Prentice Hall, New Jersey.

Haiti Shelter Cluster (2010). *Transitional shelter designs*. IASC Haiti Shelter Cluster Website. (Last visited 20 July 2012): <https://sites.google.com/site/shelterhaiti2010/technical-info/tshelter/t-shelter-designs>

Haralick, R.M., Sternberg, S.R. and Zhuang, X. (1987). Image analysis using mathematical morphology. *IEEE Transactions on Pattern Analysis and Machine Intelligence*: **9, 4**, 532-550.

Herold, M., Roberts, D.A., Gardner, M.E. and Dennison, P.E. (2004). Spectrometry for urban area remote sensing – development and analysis of a spectral library from 350 to 2400 nm. *Remote Sensing of Environment*: **91**, 304-319.

IASC (2010). *Summary of principles of response and minimum standards from UNHCR emergency response handbook for emergencies and sphere project handbook*. Inter-Agency Standard Committee.

ICCG (2011). *Return and relocation Strategy. Draft 13*. Approved by the Inter-Cluster Coordination Group. Port-au-Prince, Haiti. January 18, 2011 (In French)

Jin, X. and Paswaters, S. (2007). A fuzzy rule base system for object-based feature extraction and classification. In: Kadar, I. (ed). *Signal Processing, Sensor Fusion, and Target Recognition XVI. Proceedings of SPIE*: **6567**.

Kemper, T., Jenerowicz, M., Gueguen, L., Poli, D. and Soille, P. (2011). Monitoring changes in the Menik Farm IDP camps in Sri Lanka using multi-temporal very high-resolution satellite data. *International Journal of Digital Earth*: **4**, 91-106.

Kruse, F. A., Lefkoff, A. B., Boardman, J. B., Heidebrecht, K. B., Shapiro, A. T., Barloon, P. J. and Goetz, A.F. H. (1993). The Spectral Image Processing System (SIPS) - Interactive Visualization and Analysis of Imaging spectrometer Data. *Remote Sensing of the Environment*: **44**, 145 - 163.

Lillesand, T., Kiefer, R.W. and Chipman, J.W. (2008). *Remote sensing and image interpretation*. John Wiley & Sons, New Jersey.

Nasarudin, N.E.M. and Shafri, H.Z.M. (2011). Development and utilization of urban spectral library for remote sensing of urban environment. *Journal of Urban and Environmental Engineering*: **5 (1)**, 44-56.

Richards, J.A. (1999). *Remote Sensing Digital Image Analysis*. Springer-Verlag, Berlin.

Robinson, D.J., Redding, N.J. and Crisp, D.J. (2002). Implementation of a fast algorithm for segmenting SAR imagery. Scientific and Technical Report. Defense Science and Technology Organisation, Australia.

Serra, J. (1982). *Image analysis and mathematical morphology*. Academic Press, New York.

Soille, P. (2003). *Morphological image analysis: principles and applications*. Springer-Verlag, New York.

Sphere Project (2011). *Humanitarian Charter and Minimum Standards in Disaster Response*. The Sphere Project. Oxford, OXFAM Publishing.

UN-Habitat, UNHCR and IFRC (2010). *Shelter projects 2010*. A.9 Haiti 2010 - Earthquake. Corail –Sector 4. [www.sheltercasestudies.org](http://www.sheltercasestudies.org)

UNHCR (2007). *Handbook for emergencies (third edition)*. United Nations High Commissioner for Refugees, Geneva, Switzerland.

UN Internal Document (2011). *Analysis of camps and spontaneous settlement*. Port-au-Prince, Haiti. This document formed a TOR, drawn up by UN-Habitat before commencing the project. 12 October 2011.

Xiaoying, J. (2009). *Segmentation-based image processing system*. US Patent 20,090,123,070, filed Nov. 14, 2007, and issued May 14, 2009.

Vincent, L and Soille, P. (1991). Watersheds in digital spaces: an efficient algorithm based on immersion simulations. *IEEE Transactions on Pattern Analysis and Machine Intelligence*: **13 (6)**, 583-598.

Warner, T.A., Nellis, M.D. and Foody, G.M. (2009). *The SAGE Handbook of Remote Sensing*. SAGE Publications Ltd. London, UK.

Wimmer, A., Lingenfelder, I., Beumier, C., Inglada, J. and Caseley, J. (2009). Feature Recognition Techniques. Chapter 8 in: Jasani, B., Pesaresi, M., Schneiderbauer, S. and Zeug, G. (2009). *Remote Sensing From Space. Supporting International Peace and Security*. Springer.

## Chapter 6: Conclusion

### 6.1. Introduction: Aims and Content of the Chapter

This conclusion chapter will first briefly review the development of a table of indicators and the need for research on monitoring post-disaster recovery as identified in the literature review (both from Chapter 2). How the indicators were applied with remote sensing to monitor recovery in Thailand is then described and provides a succinct review of the technical methodology (from Chapter 3). A discussion on the timing and duration of recovery events and processes and when to purchase satellite imagery then follows. This includes a review of the British Red Cross's decision-making process during their community reconstruction project in Haiti and when and how remote sensing was found to be useful in an operational context (from Chapter 4).

Recognising that a mixed-method approach to monitoring and evaluating is often the most effective strategy, the benefits of direct observations and social-audit techniques are then discussed and protocols to integrate remote sensing are proposed. The final part of the conclusion reviews operational considerations when using remote sensing to monitor post-disaster recovery. This begins with a review of the reliability of remote sensing in Thailand and Haiti. It continues with a discussion on appropriate scales of analysis and methodologies, including a review of the four semi-automatic methods used to map planned camps and instances of spontaneous settlement for UN-Habitat in Chapter 5, the transferability of the analyses to different contexts, the staff/institutional context necessary, overcoming users' uncertainties, and issues surrounding data security, privacy and dissemination.

Throughout the conclusion broad recommendations will be provided on *what* to measure, *when* to measure and *how* to measure. The chapter will consider how timely, reliable and relevant the techniques are and how manageable, realistically applicable and transferable to different contexts they are. The conclusion will finish with a summary directly addressing the main research question (*'can remote sensing and geospatial tools be used to support the spatial analysis, planning and monitoring of post-disaster recovery and reconstruction?'*) and some suggestions for further research.

## 6.2. The Need for Monitoring and Evaluation of Post-Disaster Recovery

The literature review in Chapter 2 identifies the need for a systematic approach to monitoring and evaluating recovery and reconstruction following a disaster for both operational and strategic reasons. The World Bank for example calls for a “rigorous yet participatory and flexible approach to monitoring and evaluation in all aspects of housing and community reconstruction” (Jha et al. 2010, p269). Previous monitoring systems have been too complicated or time-consuming for agencies to use sustainably, so recovery data has been either lacking or not timely. The post-disaster scenario can also be confusing and dangerous, so collecting data is often challenging, with numerous agencies working across large, hazardous areas. Remote Sensing was expected to offer a systematic method of collecting independent and quantitative datasets rapidly and non-intrusively across large, dynamic geographic regions.

The main objective of this thesis is to assess the feasibility and reliability of using remote sensing and geospatial tools to support the planning and monitoring of post-disaster recovery and reconstruction. To test the hypothesis that remote sensing and GIS can be used to support post-disaster recovery a series of indicators and techniques were developed and applied retrospectively to case study sites in Thailand and Pakistan and later in real-time to support humanitarian operations in Haiti.

## 6.3. Recovery Indicator Table

A full table of indicators for monitoring and evaluating post-disaster recovery using high-spatial-resolution satellite imagery is presented in chapter 2. It was created after reviewing existing humanitarian frameworks and consulting affected communities and relevant stakeholders through a user-needs survey and a series of focus-group meetings. The indicators are therefore assumed to be *relevant* for a wide-range of stakeholders. As requested by the user-needs survey respondents, the table is small and manageable yet encompasses a wide range of categories. The indicator table consists of six categories: accessibility, buildings, transitional settlement/displaced population, natural environment, livelihoods and services. These categories can be independently analysed or combined to provide a holistic representation of the recovery process.

The indicators and sectors of interest will likely differ according to the type of user (e.g. coordinator or implementer) and the objectives of the programmes they are overseeing as well as constraints such as the data and resources available for M&E. Coordinating agencies will likely require a *holistic*

approach to monitoring recovery that encompasses multiple sectors. Managers of the British Red Cross's integrated recovery programme for example requested information about the three sectors they were supporting (housing, water and livelihoods) plus they requested information on access, building morphology and local hazards to inform project planning and logistics. UN-Habitat (lead agency for the Camp Coordination cluster after the 2010 Haiti earthquake) required information specifically on planned camps and spontaneous settlement processes in-and-around urban areas.

#### **6.4. The Application of Indicators to Ban Nam Khem, Thailand: Review of Technical Methodology**

The application of these indicators to monitor recovery in Ban Nam Khem, Thailand (Chapter 3) showed that remote sensing could be used to directly monitor physical signs of recovery, especially those associated with accessibility, buildings, the displaced population and the natural environment. Some conspicuous signs of service, utility and livelihood recovery were also visible but comprehensive monitoring of these categories was not possible with remote sensing alone and was more reliant on the integration of ground observations and data from social-audit methods such as focus group meetings and household surveys.

Recovery was monitored using a time-series of high-spatial-resolution satellite images acquired before the disaster, immediately afterwards and in the months-and-years thereafter. The overall methodology is comprised of four components: 1. Image pre-processing 2. Image Mapping / Database Creation 3. Data Analysis and 4. Product Creation.

Buildings, roads and bridges and other key features were manually delineated, while Maximum Likelihood Supervised Classification was used to create land cover maps marking out the extent of the built and natural environment. More advanced mapping techniques, such as Object Based Image Analysis, were used to extract objects with known spectral or spatial characteristics including transitional shelters and shrimp ponds. These features were then integrated into a multi-temporal recovery geodatabase as point, line and polygon vector files. A new temporal layer of the database was created from each satellite image, representing a different state in the process of recovery. Each temporal layer was further divided into 13 thematic sub-layers, each representing one of the main indicator categories.

Once the features in the imagery were mapped and stored in a GIS database the speed of recovery was determined by applying change detection analysis to the geodatabase. This technique calculated the rate that various processes were conducted, including debris removal, building

construction, road rehabilitation and vegetation recovery. The method also identified when key features, such as schools and sources of livelihood, appeared and when transitional shelters and planned camps were removed and dismantled. The overall progress of recovery was then inferred by noting the presence or absence of key features at different points in time. Where appropriate, the datasets were disaggregated by geographic boundaries or executing agency, allowing disparity in the speed of recovery to be assessed. The progress of recovery was further evaluated by normalising the numbers of features (number of buildings, length of roads) in each region to base-line statistics, which were constructed using the pre-disaster image or the objectives of each recovery project (where known). This analysis was successful at identifying slow projects and gaps in the supply of resources. It was also used to substantiate some aspects of claims that a region had been 'built back better'.

Additional information was estimated based on the mapped features, such as the number of Internally Displaced Persons (IDPs), which was calculated based on the number and size of structures located in planned camps. Information about the quality of recovery was also inferred by looking at changes to the size, shape and density of the features and by analysing their spatial and contextual properties. This was achieved using common spatial analyst tools in ArcGIS such as landscape metrics and kernel analysis. Network analysis was also used to monitor connectivity and travelling times brought about by the relocation of households and facilities. Building density might be used as a proxy indicator to signify changes in quality of life or social vulnerability (Cutter, Boruff and Shirley, 2003) and relocation of households was thought could break social ties and affect access to services and livelihoods. These theories were later verified in the field with the use of social-audit methods.

Spatial analysis and proximity analysis were also applied to planned camps to test occupants had sufficient living and covered space and to measure infrastructure placement. These measurements were compared to minimum standards contained in the Sphere Guidelines and other humanitarian frameworks to ensure that latrines and other features were properly located and that there was adequate accessibility. In addition, conspicuous forms of services, utilities and livelihoods were assessed by monitoring their activity, location and speed of recovery. Proxy indicators were also developed to allow certain social and economic aspects of recovery to be inferred from physical recovery processes. By observing the restoration of features associated with major sources of livelihood for example, assumptions were made about the speed of livelihood recovery in relevant sectors.

Table 6-1 lists some of the key analyses used to monitor post-disaster recovery in this thesis.

Technique	Purpose of analysis	Example of questions that might be answered
<b>Change Detection</b>	To measure the speed of recovery processes. Location of change. Absence and presence of particular features of interest.	How fast were houses built at Site A? When was the school built? Is the sea-wall larger than it was before the disaster? What is the progress of project A versus project B?
<b>Buffer Analysis</b>	To measure the proximity of features to one-another.	How many buildings have been built within 200 m of the coast? Have any buildings been constructed beneath slopes over 25 degrees? What is the building density in the immediate vicinity of building A?
<b>Landscape Metrics</b>	To analyse the size, density and distribution of features.	Are the new houses the same size as those that existed before the disaster? Are there now more houses of smaller size at site A?
<b>Network Analysis</b>	To measure the connectivity between features. Travelling times and distances between those features.	How far are households from sources of livelihood? Are sufficient schools available for the new housing development?
<b>Spatial Disaggregation</b>	All data may be disaggregated by geographic boundary, executing agency etc. according to the needs of the users.	How many schools were built in each Province? Has Executing Agency A completed 2,000 houses in Region B?

**Table 6-1: Forms of spatial analysis used to study features related to post-disaster recovery.**

### 6.5. When to Purchase Images

To avoid costly mistakes it is important for analysts to know when to monitor each indicator and how frequently to acquire satellite imagery. Evaluations must ultimately be conducted when impacts are likely to be visible and measurable. So the timing of when a user acquires a satellite image depends on the progress of recovery and the processes occurring on the ground at the time. It also depends on the questions the users are trying to answer and the spectral, spatial and temporal limitations of satellite data as this determines which features and processes may be observed. Technical limitations of current high-spatial-resolution satellite sensors are reviewed in Chapter 2.

It also depends on whether the data is intended to be used to monitor on-going recovery projects or to evaluate completed projects. To facilitate detailed monitoring of a project, data might need to be collected every few days or weeks throughout the emergency relief phase to keep track of the constantly changing situation, while imagery may only be required every 6-12 months in the long-term recovery phase to track construction and development projects. Project evaluations may be carried out using just two images: a pre-project image (baseline) and a post-project image to identify

changes that have occurred as a result of the intervention. Monitoring a series of images captured over time allows changes in a variable to be monitored, as was done in Thailand and Pakistan (Chapter 3). The length of a longitudinal study and the frequency that the images are required will depend on the processes being assessed. A longitudinal study will likely have to be at least 4 or 5 years long though to encompass all relief and reconstruction processes

#### *6.5.1. Timing of Events – Relief and Recovery*

As analysts decide *when* to collect satellite imagery it's important they consider the timing and duration of key recovery events and processes. A study by the Independent Evaluation Group (IEG) found that disaster-related projects, funded by the World Bank, varied significantly in their implementation time, from two to seven years, while Emergency Recovery Loan projects took on average 3.9 years (IEG, 2006).

While there is likely to be a lot of variation in the timing and duration of recovery events and processes, certain assumptions can be made about when these activities might happen. Figure 6-1 shows some of the key processes and events visible in satellite imagery with an estimation of when they are likely to appear relative to each other, based on observations from this thesis. When selecting imagery, analysts will want to consider what phase of recovery they are investigating (i.e. emergency relief, early recovery or long-term recovery) as the relevance and importance of different indicators is likely to vary throughout the recovery process.

Emergency relief is very time-sensitive and decisions often have to be made with no or limited information. Remote sensing can provide estimates of the magnitude of damage, the impact the disaster has had on accessibility and the location of the displaced population relatively quickly at this stage in the process. Between emergency relief and long-term recovery is early recovery, during which it is important to restore normality (clear debris, demolish vulnerable buildings) and restore lifelines quickly to avoid further disruption to households and businesses. Long-term recovery will likely involve processes such as the reconstruction of infrastructure and the dismantlement of camps. Other issues, such as environmental rehabilitation and reduction in natural hazard risk, are cross-cutting issues that need to be considered throughout recovery.

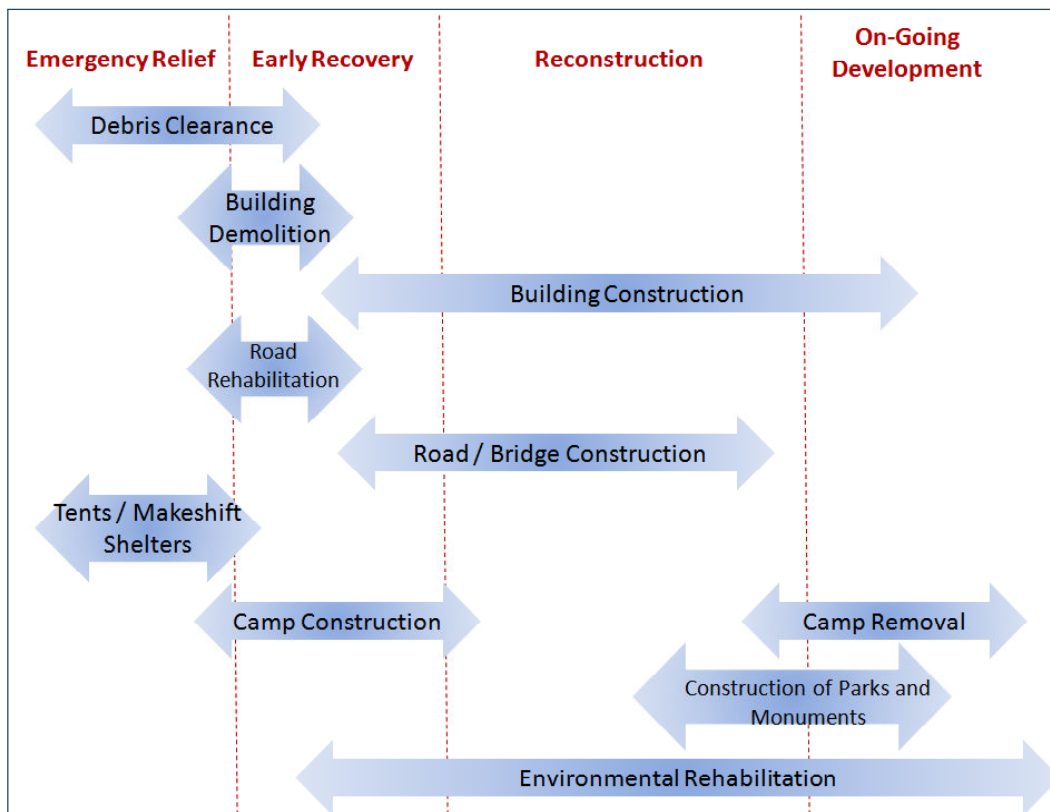


**Figure 6-1: Estimated timing and duration of key recovery activities and processes.**

### 6.5.2. Mapping the British Red Cross's Operational Decision-Making Process

Whilst discussing timing issues it's useful to review users' operational decision-making process. Chapter 4 describes work done in support of the British Red Cross's (BRC) Integrated Recovery Programme in Haiti. This chapter was useful because firstly, it allowed remote sensing analyses to be further validated, this time in a dense, complex, urban slum environment. And second, the BRC's operational decision-making process was mapped and recommendations made on where remote sensing could bring particular value by itself and in support of other tools. The geospatial tools were found to be useful at all phases of the BRC project cycle: 1) as a rapid assessment tool after the disaster, 2) as a GIS database during the design/planning phase to store, analyse and visualise cadastral and enumeration ground datasets (thus helping both strategic and operational decision-making) and 3) as a platform for monitoring data.

The process of recovery often starts with preliminary discussions with key informants and site visits and later the release of the National Government's needs assessment and recovery plan, for which remote sensing has already proved itself useful (Haiti PDNA, 2010). Where possible these early processes should include discussions with the community to establish the need and feasibility of a

project from their perspective and culminate in the signing of a MOU. Remote sensing of aerial imagery was used in the early stages of the BRC project to perform a preliminary assessment of the Delmas 19 settlement. After reviewing the indicator table the BRC staff asked for the analysis to focus on three sectors: accessibility, buildings and population movement. Very basic hazard mapping was also conducted by mapping water channels, catchment areas and likely drainage across the site. A transport and building database consisting of 2.5 km of roads and 568 building plots was produced by manually analysing the aerial imagery using the methodology described in Chapter 3.

The statistics derived from this analysis were later used in the BRC's design and planning report to help justify a need for the project and to characterize the existing built environment. Information on the number of storeys and the shape and size of plots was particularly useful for initial costing and project design work. Maps and other datasets were also produced to assist navigation and for logisticians to locate and move materials into the site and to support the participatory process with the community. The BRC Project Manager also believes there might be potential to use the early remote sensing-derived maps as part of a preliminary registration of beneficiaries (where formal land ownership documents don't already exist) by logging their approximate locations thus improving the efficiency of subsequent ground-survey work.

As the BRC project progressed to the design/planning stage a ground cadastral survey was necessary with sub-metre accuracy GPS equipment as well as a detailed enumeration of the plots and the households living on them. A GIS system was used to store, analyse and visualise enumeration and cadastral datasets, this included social, legal and physical information on each plot and its owners and occupants, as well as engineer reports and architectural observations. Community-wide datasets on livelihoods, services and utilities were also stored in the GIS. The database was used for scenario and costing analysis prior to an internal planning meeting, for beneficiary selection and acted as a baseline for subsequent monitoring. Maps derived from satellite imagery were used to support this process by assisting navigation and in some cases verifying the ground-derived data.

## **6.6. What Tools to Use**

A number of tools are already used by agencies to collect monitoring data and were used throughout this thesis. The tools may be divided into two broad categories: 1) direct observation (e.g. remote sensing and ground survey) that can be used to count features and observe their condition and 2) social-audit techniques (e.g. focus group meetings, household surveys and key informant interviews) which can be used to gather qualitative information. The following section

summarises the relative strengths and weaknesses of each group of tools and provides recommendations on how the tools may be integrated based on observations for this thesis.

#### *6.6.1. Direct Observations*

Direct observations can be used to note the abundance and layout of physical features in the recovery landscape. An advantage of these techniques is that they are often quantitative and objective. The techniques have traditionally been conducted on foot with the use of a structured form or survey to complete. The arrival of high-spatial-resolution satellite imagery now allows some forms of direct observation to be conducted remotely. Results from this thesis show that remote sensing can reliably build a profile of the built environment by mapping buildings, roads and land cover without ground assistance.

Remote sensing can also be used to extract information to infer the impact that physical changes might have had on peoples' lives. For example, remote sensing can be used to monitor the clearance and rebuilding of roads and subsequent changes to accessibility and connectivity. And it can monitor changes to the size, shape, arrangement, location and context of buildings and other large features that might be brought about by different recovery strategies. From this information, basic assumptions can be made about changes to household contentment, quality of life and quality of recovery. For example, the findings from the Thailand household survey suggest that household contentment was likely affected by the size of the building, access to facilities and services, the distance to potential hazards and the time taken to reconstruct the building. Further research on this topic is recommended.

Due to the non-oblique look angle of most satellite sensors and the limited spatial resolution of satellite imagery, ground surveys will likely be required to verify or calibrate some of the remote sensing-derived measurements and assumptions. Comprehensive identification and monitoring of services, utilities and livelihoods in particular is not possible without the integration of ground knowledge. Ground surveys may be used to verify building occupancy, building materials, building use (residential, service or business) and the number of storeys. They can also be used to identify or verify the presence of small features not visible in satellite imagery such as water towers, power lines and tsunami-warning towers. Ground surveys can also be used to acquire information that is not available with remote sensing such as the condition/physical vulnerability of the feature or the quality of minor repair work and the cultural appropriateness of reconstruction work.

The recent integration of GPS into many camera and video systems now means ground survey analysts can collect detailed, geocoded street view data which allows spatial disparities to be mapped and input directly into a GIS system whilst in the field. The data from ground surveys is often more detailed and accurate than remote sensing but can be very time-consuming and expensive to conduct and analyse – especially across large, often insecure geographic regions. It's important to recognise that ground surveys in post-disaster context are often very challenging, time-consuming and can be prone to errors too. For example, the cadastral and enumeration survey of 500 plots took BRC a year versus a few weeks to build a profile using remote sensing.

### *6.6.2. Social Audit Techniques*

Indicators are commonly developed during the design phase of a project, often through a logic framework process that links project inputs and objectives to project outputs and outcomes. While direct observation is useful to measure the physical outputs from a recovery programme (number of buildings, length of road etc.) as part of an on-going monitoring system, social-audit techniques are useful to look at the larger outcomes and indirect impacts that happen as a result of a recovery project. There are various social-audit techniques available to the analyst, including semi-structured interviews, surveys and focus groups. A significant amount of time and skill is required to design semi-structured interviews and to translate, code and analyse the results but they can be used to collect important information about many aspects of recovery.

The Recovery Project's household survey acquired information about the socio-economic and demographic make-up of the households (the survey form is available in Appendix A). It was also used to produce a recovery narrative describing when key events happened and to infer perceptions of recovery. Focus group meetings were similarly used to measure perceptions, levels of satisfaction and to identify when and where key events occurred. Focus groups are very prone to bias though and reliability is difficult to determine, so it is important that they are carefully planned and moderated to ensure a balanced and non-threatening environment is created. Key informant interviews were also used to gain a holistic view of recovery (see Appendix B). A sample of strategically-selected individuals, representing all sectors of recovery, was asked questions about the progress of recovery. The technique was found to be quick, efficient and capable of obtaining a brief but synoptic review. The results of which can be used to determine where and when imagery and other detailed survey data might be required.

There are many important aspects of recovery that can only be captured using social-audit tools, these include but are not limited to: community participation, the incorporation of local peoples' culture and traditions into programming, gender equality, governance and aspects of vulnerability reduction. The OECD-DAC guidance encourages evaluators to consider each programme's relevance, effectiveness, efficiency, impact and sustainability. Furthermore, the *handbook on owner-driven housing reconstruction* by the International Federation of Red Cross (IFRC) recommends teams monitor programme management, programme design and collaborations with partners, as well as the participatory process and the inclusion of vulnerable households (IFRC, 2010). It's also important for evaluators to look for unintended changes (e.g. environmental degradation or increase in prices) and also to capture differing perspectives on the situation (Comerio, 2005). Quarantelli (1999) suggests that government and administration have more realistic concepts about recovery, whilst individual household or businesses are more idealistic.

Participatory methods are increasingly used, as a way to involve beneficiaries in the monitoring process, as a form of empowerment and as a means of obtaining feedback and complaints. Satellite image-derived maps were found to be useful during the focus group meetings in Thailand, Pakistan and Haiti. Attendees were asked to identify features on the maps and to estimate when key events in different areas occurred. Maps can act as a geographic framework for communities, to instigate debate about their needs and priorities and to locate issues, solutions and monitor progress. Maps can also assist communication between community and programme managers and can be used by communities after agencies leave, when communities want to organise and make project applications themselves. Not everybody will understand or trust maps though so this process must be explained properly with training.

### 6.6.3. Mixed Methods

Mixed-method approaches to monitoring and evaluation, encompassing both direct observation and social-audit methods, are increasingly used and recommended; for example, 90% of respondents to a recent ALNAP survey used a mixed-method approach. The most common reason for using mixed-methods is to allow results to be verified and cross-checked (Proudlock et al. 2009). Each data collection tool can gather different types of data and has its own strengths and weaknesses - revolving around issues of cost, accuracy and technical requirement - which determine when and how frequently it may be deployed. The classic trade-off between time/cost requirements and the amount of detail/accuracy achievable often applies. The nature of the data produced by each method also determines when each tool may be most appropriately used. In general, quantitative

approaches permit the estimation of magnitude and distribution by establishing ‘what’ and ‘where’ things happened, while qualitative approaches permit in-depth analysis and description of ‘why’ patterns occurred.

When deployed in an effective work-flow, the tools can supplement each other to provide richer detail and a more in-depth understanding of the issues from numerous perspectives. To create such a work-flow, the tools must be deployed at the right time and in an appropriate order. For example, direct observations might initially be deployed to determine community welfare, which can later be verified and explored in more detail using focus group meetings. Similarly, direct observations may initially identify unexplainable patterns that can be explored in more detail later during interviews and meetings. When time is limited, well-designed key informant interviews may acquire data that will allow a team to become acquainted with the status of an area relatively quickly and efficiently.

Figure 6-2 illustrates how the various forms of data may be integrated and used in a manner that is complementary. In summary, maps and images from satellite image analysis may be used to invoke discussion, inform survey design and to direct teams to appropriate study sites. Similarly, observations made using ground surveys and participatory methods may be geo-coded, integrated into a geodatabase and used to verify remote sensing and to identify gaps in the analysis. Mixed methods are particularly valuable as they allow different sources of information to be cross-checked or ‘triangulated’. Triangulation is the process of using two or more methods of data collection or sources of data in order to check on the validity of the data that is being gathered.

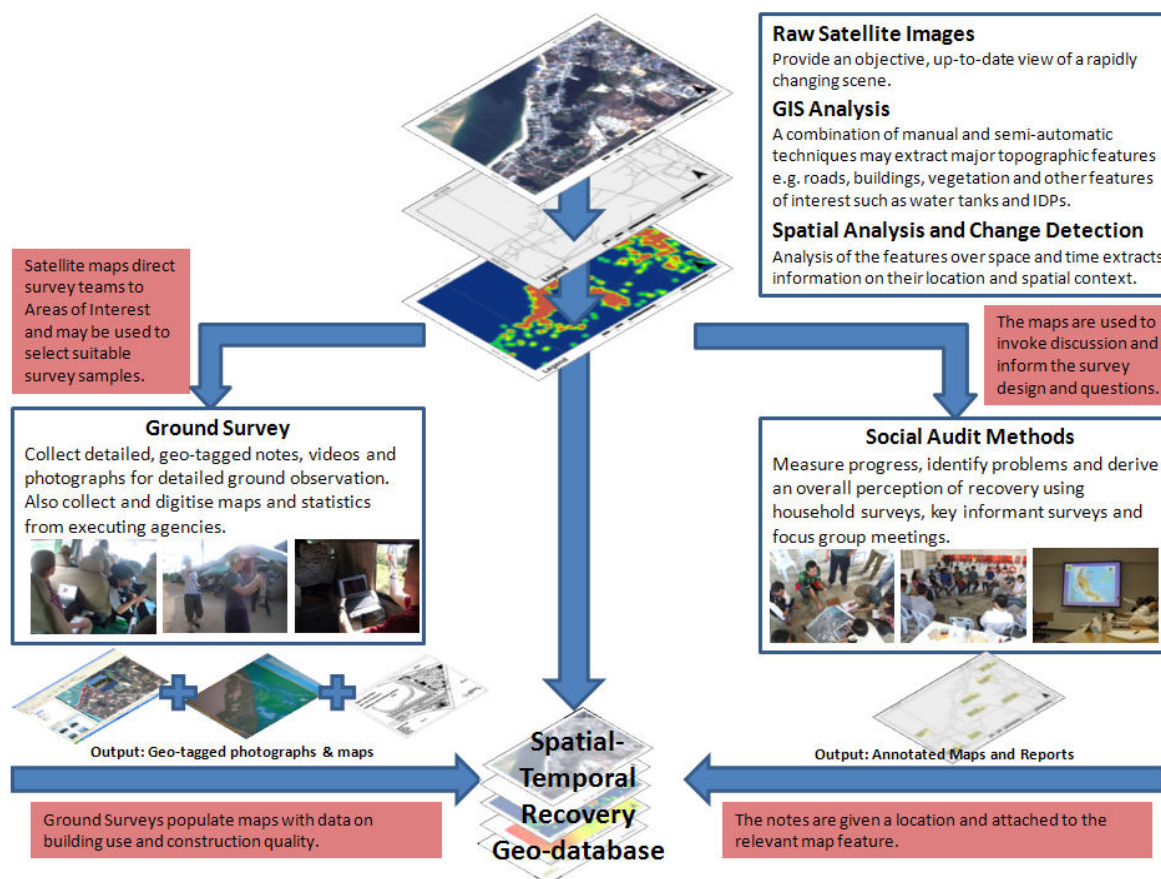


**Figure 6-2: Direct observation and social-audit datasets may be integrated and used to supplement each other throughout the recovery process.**

If an analyst is to evaluate recovery with a single visit the following protocol is suggested. This is repeated at suitable intervals, perhaps every six months, during the period of recovery.

*Pre field deployment*

1. Key informant interviews allow a team to become acquainted with the status of the area and provide an overview of the timing of different aspects of recovery. These might be conducted remotely over the telephone.
2. Published information including official statistics may be obtained from the Internet, recovery agencies and national and local government offices.
3. Initial imagery analysis and mapping of key indicators, for example accessibility and temporary camps, can be conducted before a field deployment.

## *Chapter 6: Conclusion*

*Field work (imagery and initial assessment results used in field to design surveys, navigate to and record survey locations)*

4. Once in the field, focus group meetings and further key informant interviews can explore and verify these initial results.

5. Ground survey, using GPS cameras, is used to survey buildings, probably choosing a random sample of building points. This data can be incorporated into the geodatabase (GIS) and used to inform subsequent imagery analysis.

6. Household surveys can also be conducted, perhaps in parallel to the ground survey by a different team. Information from talking to affected families then allows the analysts to infer what the mapping means in terms of people's lives and their experience of recovery.

*Detailed imagery analysis*

7. Detailed imagery analysis is conducted back at base using insight and information from the information sources above.

### **6.7. Operationalisation of Remote Sensing and Overcoming User's Uncertainties**

Before remote sensing can be fully embraced by the humanitarian community it is necessary to address any uncertainties users might have with the technology. Following Imagecat's involvement in Haiti's Post Disaster Needs Assessment, they found reluctance amongst users to fully embrace remote sensing products because 1) they were not sure how to integrate the products into existing workflows; 2) a lack of trust in data; 3) poor communication between data providers and users; 4) tendency not to share data between agencies and 5) a lack of metadata to go alongside of key datasets (World Bank, GFDRR and Imagecat, 2010). It can also be difficult for users to actively engage with any new technology, especially in a post-disaster context. Hodgson, Davis and Kotelenska (2010) survey of US Emergency Management Agencies (EMAs) found a lack of uptake was due to cost/time constraints and staff technical limitations. A similar lack of uptake has been observed in urban remote sensing (Donnay, Barnsley and Longley, 2001).

Interest in the monitoring and evaluation of recovery and development has grown in the past decade, culminating in the release of ALNAP's *Evaluation of Humanitarian Action Guide* (Cosgrave

and Buchanan-Smith, 2016). At an ODI-hosted event called 'accountability in the humanitarian system' Paul Knox-Clarke (Head of Research and Communications, ALNAP) compared accountability in 2003 and 2011. He noted that there had been many initiatives to improve the efficiency with which the humanitarian community supports disaster-affected populations including two major revisions of the Sphere guidelines (2004 & 2011). Paul Knox-Clarke had a sense that programmes are increasingly willing to incorporate accountability in very sophisticated ways to ensure they better understand the needs and to ensure they're meeting required standards.

It's also getting easier to convince users of the value of remote sensing as more examples of its use become available. After the 2007 Hurricane Katrina in New Orleans for example agencies quickly saw the value of remote sensing when products were provided to them in real-time (Hodgson, Davis and Kotelenska, 2010). Similarly after the 2010 earthquake in Haiti a number of agencies – including the American Red Cross and Habitat for Humanity - wanted the author to replicate the British Red Cross work with them after they saw the results that were possible.

Education is needed to show agencies how to get the full potential from remote sensing and how to integrate remote sensing with existing systems. In Haiti, agencies appeared to recognise the value of remote sensing for their projects but didn't know how to use it to its maximum potential. Most were using out-of-date images on GoogleEarth. The protocols and recommendations in this thesis provide a good starting point for thinking about how remote sensing may be used by academics and managers of recovery projects. It's important that analysts are realistic though about what can be achieved with remote sensing alone and that its advocates promote the use of remote sensing as a tool to support and complement other forms of analysis. It's also important that analysts are clear about the reliability and limitations of remote sensing.

The next section of the conclusion focuses on some of the concerns raised by users, specifically the reliability and accuracy of mapping ground features. Some of the more practical elements of its use are also discussed including time and resource requirements, different methodologies and approaches available, and some of the practical considerations when trying to operationalize remote sensing in a post-disaster recovery context.

### **6.8. Transferability**

The approach described in this report has been designed to be replicable and to be non-country or hazard specific. To test the transferability of the indicators they were applied to two case studies in

Chapter 3: Ban Nam Khem, Thailand and Muzaffarabad, Pakistan. The case study sites differed dramatically in terms of their dominant cultures and economies, the type of hazard they were affected by and the recovery frameworks and approaches that were adopted afterwards. The work demonstrated that the same indicators and similar approach can be applied in widely differing situations though the accuracy of the mapping may vary depending on the area being analysed (as discussed in the 'reliability' section 6.9).

The nature of the hazards meant they had very different impacts on the case study sites. In Ban Nam Khem, the tsunami removed most of the coastal building stock, transport network and natural environment within a kilometre of the shoreline. The impact of the tsunami was enormous but it remained relatively localised. In contrast, the 2005 earthquake in Pakistan caused widespread damage and changes across the country, which affected the government and its ability to respond. The physical signs of recovery were also more apparent, condensed geographically and reliably monitored with remote sensing after the tsunami than they were after the earthquake.

The localised nature of the tsunami is also likely to have contributed to the faster recovery in Thailand than in Pakistan. The Thai Government's relative wealth and its approach to recovery also affected the pattern of recovery and how it may be monitored. For example, in Ban Nam Khem, planned camps were successfully used to host displaced persons. They were removed and people rehoused within three years of the tsunami. In Muzaffarabad the structures were dispersed across the affected region and people were still residing in them four years after the earthquake. This is partly because residents had migrated to the cities from surrounding mountainous areas. The organised, planned camp approach used in Thailand was easier and quicker to monitor than the scattered shelters used throughout most of Pakistan.

When conducting cross-disaster comparisons there are often many cultural and economic differences to be aware of. For example, much of the economy in Ban Nam Khem is based on the fishing industry, while households in Muzaffarabad are more reliant upon farming and the public sector. The main religious structures in each country also differed, with Thai communities based around the Temple and Pakistani communities around the local mosque. It is imperative that image analysts are aware of such cultural matters before embarking on image analysis.

For other natural hazards (e.g. river flooding, windstorm and landslide) the list of recovery indicators is likely to be the same, and the same techniques for monitoring them are likely to be applicable, though this needs to be tested in other studies.

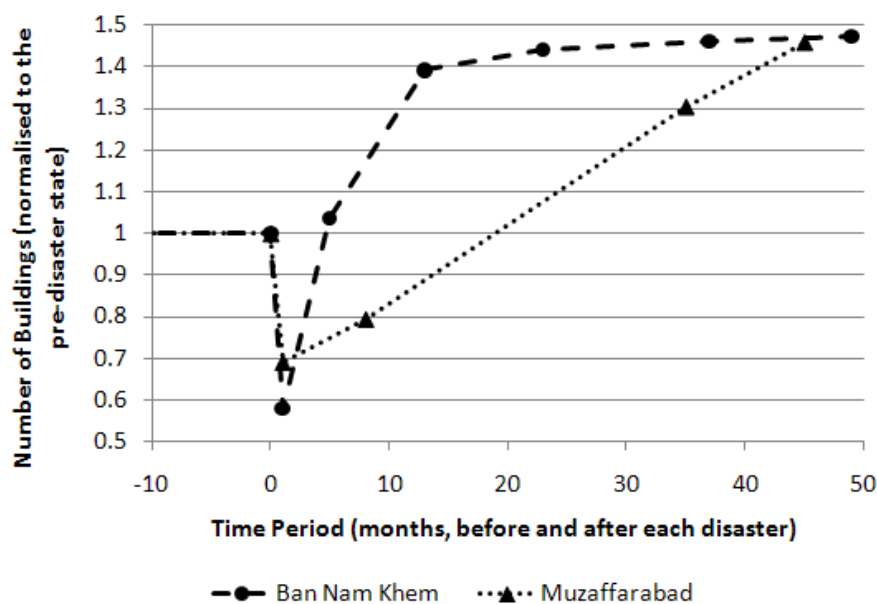


Figure 6-3: Recovery curves for the two case study sites, produced by normalising the number of buildings present using the pre-disaster building number.

### 6.9. Reliability/Accuracy

The *reliability* of remote sensing was assessed by looking at its overall accuracy in Thailand and with the work done for British Red Cross and UN-Habitat in Haiti. The remote sensing analysis applied to Ban Nam Khem (Chapter 3) was found to closely match narratives from key informant interviews, focus group meetings and household surveys, and it was also found to be accurate when compared to detailed ground data collected using VIEWS™ video system and a GPS camera.

For verification, the remote sensing analysis of Ban Nam Khem was compared to ground data at 50 randomly-selected points. The results show that manual remote sensing was used to produce reliable datasets for the first four categories in the indicator table, namely accessibility, buildings, displaced population and natural environment. For example, roads were mapped with 96% accuracy, individual dwellings identified with 82% accuracy, the displaced population in planned camps were estimated to approximately 90% of government statistics and the accuracy of the Maximum Likelihood classifications was above 80% for each image except for the post-tsunami image (68%) where there was substantial confusion with water-logged soils.

The Ban Nam Khem case study provided a relatively uncomplicated landscape to analyse with remote sensing though, with detached buildings and transitional shelters neatly arranged in planned

camps. The analysis of aerial imagery for BRC (Chapter 4) focussed on a complex, dense urban slum so provided a more challenging test. All of the main asphalt roads in Delmas 19 were mapped correctly but almost 50% of small lanes were missed as they were covered or obscured by buildings. An analysis of building plots showed that approximately two-thirds of the buildings were correctly delineated; the other third were either counted twice (commission error) or missed altogether (omission error).

Despite this, rapid assessment with aerial imagery was still able to provide a good profile of the project area, providing accurate estimates of the number and size of buildings, which was useful for initial planning and costing exercises. Satellite image-derived building measurements with a Woldview-2 image were correct within 50 cm. And during recovery monitoring, 34 transitional shelters were correctly identified on the BRC site out of 35. Such a high accuracy was achieved because of the shelters' predictable size and distinctive features. Empty plots were not so easily identifiable though; 24% were wrongly assumed to contain a building.

It must be noted though that this analysis was completed by an analyst with years of experience. The reliability of the results depends on a number of factors but is particularly dependent on the spatial and spectral uniqueness and clarity of the features of interest. An analyst may test the spectral separability of different features of interest and choose appropriate analytical tools before conducting a full analysis, as was done with the Jeffries-Matusita Spectral Separability test in Chapter 5.

#### **6.10. Assumptions and Limitations**

This work has highlighted a number of limitations with remote sensing data. It is important that these limitations and accuracies are clearly communicated to potential users of the data. A limitation of remote sensing is its inability to identify non-structural damage (or local structural failures) to buildings and infrastructure or to provide reliable information on the quality of construction work or the occupancy or use of those features of the built environment.

The method used in Chapter 3 wrongly assumed that all buildings are visible – some might be obscured by vegetation, resulting in omission errors. Service or utility buildings might be wrongly assumed to be residential, resulting in commission errors. The analysis also wrongly assumed that all cleared and/or reconstructed roads in the imagery were open and accessible to the public. In Ban

Nam Khem, some roads were in-fact located on private land and public access was therefore restricted by developers.

Whilst remote sensing can detect the recovery of features related to community services and utilities this in itself doesn't confirm the services or utility is being delivered adequately to the affected population. As was covered previously, ground surveys are required to confirm these details and to assess the quality of such work. It's possible remote sensing observations can be used to infer other information such as the satisfaction and perception of recovery. This is an important topic for further research. If a client requires more detailed or more reliable products then it is recommended that ground techniques are conducted alongside, before or after the remote sensing analysis.

### **6.11. Work at Multiple Scales**

Recovery can be analysed at a range of geographic scales, including individual, household, community or national. The level of damage and the progress of recovery may be interpreted differently depending on which of these scales is used. For example, whilst business or household elements may fail, the return of the economic and labour markets may suggest a successful recovery at community level. Ideally, all of these scales should be analysed collectively: a study of individual households should include information about their context within the environment and a study of the community should involve an understanding of the actions and behaviours of individual elements. Analyses are likely to tell us different stories – the challenge is triangulating them and using each data scale to explain the patterns observed in the other and vice-versa. Work in Ban Nam Khem showed how a tiered approach might be used, starting at a small scale and then focussing in on areas of interest.

### **6.12. Monitoring Large Areas**

Recovery often takes place over large geographic areas. There are various approaches to monitoring large areas. Random geographic sampling can be used to build a picture of recovery without the need for a full, comprehensive assessment as was done with the household survey in Thailand and Pakistan. Remote sensing analysis can also be applied to a sample of buildings or neighbourhoods using this method. Another approach is to use semi-automated image analysis which is usually less work intensive than manual methods, and while they generally provide less detail and reliability they can still be very useful for certain applications – in particular, to highlight areas of substantial change for more detailed examination. Such a tiered-approach to image analysis was demonstrated for the building category in Chapter 3 where Maximum Likelihood was used to identify areas of land-cover

change which were then followed-up with more detailed manual analysis at a neighbourhood and per-building level of analysis.

The two studies in Chapter 5 show how remote sensing was used to monitor planned camps and spontaneous settlement for UN-Habitat over large geographic extents. In study 1, a semi-automatic Maximum Likelihood method was used to estimate the number of corrugated-iron structures across 5 km<sup>2</sup> to within 15% accuracy of official ground-derived estimates and to within 7% accuracy with the use of regression analysis. Manual analysis across this whole area is estimated would have taken approximately 50 hours, whilst Maximum Likelihood took 4 hours (which includes time taken for ground and spectral analyses that were completed before). The regression analysis required buildings in 73 randomly-selected grids to be manually delineated and for those results to be directly compared to the Maximum Likelihood results which took a further 16 hours to conduct and increased the accuracy from 15% to 7%. This gives analysts a number of options depending on the time available and accuracy required. It is important analysts recognise limitations in the areas they are working. In this case the buildings were detached and clearly visible so easy to count, but ground survey work was required to estimate the proportion of buildings under corrugated-iron roofs that were made of concrete or corrugated-iron as this was not decipherable with satellite imagery alone. For more complex images containing multiple building types and densities the analyst may consider dividing the image and analysing these areas independently. Larger areas are likely to add more complexity so will require more flexible training classes (likely to lead to less accuracy) or more time to divide the image or analyse the image appropriately.

#### *6.12.1. Choosing an Appropriate Semi-Automatic Approach*

In study 2 of Chapter 5, four semi-automatic approaches to mapping shelters in a planned camp were tested. Spectral Angle Mapper was the easiest and quickest to implement and produced the most accurate estimation of shelter area. The high accuracy was largely because SAM overcome differences in shadow caused by the shelters' pitched roofs and was flexible enough to allow for brightness variation between shelters too. The other approaches struggled with both these factors.

Mathematical Morphology was work intensive and produced poor results as it incorrectly classified objects with similar shape and brightness to the roofs such as adjacent shadows and nearby patches of vegetation. Object-based Image Analysis counted the number of transitional shelters accurately (within 3%) but was less successful at estimating the total shelter area, due mainly to limitations with the segmentation algorithm used.

In summary, there are a large number of approaches and algorithms available to remote sensing analysts. In areas where the spectral attributes of the features being analysed are regular and known, then spectral classifiers such as Maximum Likelihood and Spectral Angle Mapper can be deployed successfully. OBIA can be used in more complex landscapes to utilise images' spatial, contextual and spectral information but it is important to ensure the segmentation algorithm extracts relevant objects reliably. Mathematical Morphology was found to be time-consuming and inaccurate, even in this relatively simple context. The work in Chapter 5 shows how the approaches take different lengths of time to conduct and produce different levels of accuracy. It also shows how different approaches may be useful for particular applications. To choose the best tool for their application the analyst must have a good understanding of the landscape they are studying and the tools available to them.

Due to the substantial variation in camp types, layouts and contexts and the variation in image conditions it is not possible to recommend a single tool. The analysts must first look at the image they have and make a decision based on what they are trying to achieve. Every image is different with variations in satellite and solar parameters (e.g. look angle, sun height) as well as spectral and spatial variations in the camps' composition and layout. This means one approach may work in one camp and another in a second camp. It's important to understand how each of the tools work and the strengths and weaknesses of each approach.

### **6.13. Time Requirements**

The time and budget requirements for satellite analysis are well-known and can be calculated at the outset of a project. Mapping a previously unmapped area for the first time is the most time-consuming work but can be done with relatively basic skills and software. The image processing (purchasing, pan-sharpening and geographic registration) requires a day's work. For the Ban Nam Khem case study, it took approximately one day to delineate 50 Km of roads and one day to draw 1,700 building footprint polygons across a 2 km x 3 km area. Another couple of days are necessary for the subsequent spatial analysis and report writing<sup>1</sup>.

Once the initial mapping of features has been completed, the time needed to update the database is significantly less. This highlights the importance of constructing pre-disaster databases of high-risk urban areas that are updated regularly. For example, in 2012 the author worked with the Nepal Red

---

<sup>1</sup> All these assumed time requirements are based on the author's high levels of skill and experience.

Cross to create a suite of datasets covering the Kathmandu valley that would be useful in the event of an earthquake (Brown, 2012). Large teams of people will likely be required to map large areas where maps weren't created before a disaster. This might be coordinated through the use of crowdsourcing platforms as was done after the 2010 Haiti earthquake. After a baseline dataset has been created subsequent updates and analyses may presumably be conducted by a smaller team of staff.

#### **6.14. Financial Requirements**

Most of the analysis budget will likely be spent on staff time (discussed above) and to a lesser extent, on the purchase of satellite imagery. The cost of imagery will vary in direct relation to the size of the area. Most automated analysis can only be performed on imagery with multiple spectral bands including a near infra-red band. The average cost of archive multispectral Quickbird imagery in 2009 was \$24 per km<sup>2</sup> with a minimum area of 25 km<sup>2</sup>. So a single image was \$425 (with 25% education or humanitarian discount applied) and an image covering the central areas of Port-au-Prince (approximately 100 km<sup>2</sup>) would cost \$1,700. To task a satellite to collect a new image at a time selected by the analyst is more expensive than purchasing one from the archives. At the time of the project this cost \$28 x 64 km<sup>2</sup> = \$1,792. This still makes commercial satellite imagery an affordable option for most large agencies. The cost of imagery can also be shared between agencies by adding them to the image contract. Image analysis can be completed on most personal laptops with widely-available image analysis software and a geographic information system. All image classification work in this thesis was done using the ENVI software and the analysis of vector datasets was achieved using ArcGIS. Free alternatives are available such as the GRASS software.

Both the British Red Cross and UN-Habitat reported that remote sensing was of great use and value to their projects. BRC felt the work saved the project time and money and would like to see it applied to other projects. The tools assisted the management and communication of information (both to staff, head-quarters and to beneficiaries) and subsequently improved decision-making. The BRC mid-term review states that remote sensing data was useful at a time when there were difficulties with all ground survey results. The remote sensing products also have significant value in themselves and can be considered an important output of a project. The maps and data can be handed to the community who can then use them to assist their own projects after the agencies have left. In Chapter 5, the work with UN-Habitat helped to estimate the amount of investment communities had made in construction in Canaan. As a result the Prime Minister's Office agreed to

recognise the area as part of the Municipality which was valuable and useful both to households living there and to agencies seeking funding for development projects.

### **6.15. Collectors of Data**

Implementers of large programmes might consider hiring an Information Management (IM) delegate to oversee the collection, quality control and submission of data. The three components of the BRC project (shelter, livelihoods and sanitation) worked and collected data independently of each other and in the opinion of the author would have benefited from a central IM delegate to coordinate data collection and avoid duplication of effort. The Red Cross Owner Driven Housing Reconstruction Framework recommends the following staff set-up is established: 1. Database operator (field level) who logs in day-to-day for operational use and can input data, analyse data and produce reports 2. Head of Mission can log into the system and modify if necessary and 3. Finance manager can login to the finance section only (IFRC, 2010).

Some aid agencies might not have the expertise required to analyse satellite imagery or build a database. The analysis might also divert energy and focus from delegates who have other important roles to serve. It's important not to underestimate the time and effort required to do any form of image analysis. Analysts with less experience may ask the image distributor to do pre-processing for them but this can be expensive. In some cases it might make sense for a single agency to take overall responsibility for image analysis. This might be the government or private entities (REACH, UNOSAT) providing assistance. Either way a strong linkage is required between image analysis team and a ground team to verify the results and ensure the best possible accuracies.

### **6.16. Dissemination**

Once data is available it is important to share it. The Sphere Guidelines recommend systems are in place to ensure monitoring information is disseminated amongst humanitarian agencies, affected populations, local authorities and other actors. Ensuring everybody has access to the results will mean producing them in formats suitable for those users. For example, the Red Cross raw data was provided as Excel worksheets and Word documents. The shapefiles and raw images were also provided along with KMLs so the spatial data could be viewed in Google Earth. JPGs and paper maps were also provided for field teams and the offices.

Data is now also commonly linked to the internet via data portals. An increasing problem as more systems are developed is that of duplication. After the 2010 Haiti earthquake, 169 maps were published in the first 5 days (Foody, G.M. 2014). “Too many maps generated by too many actors, showing too similar things in too many different ways (Voigt et al. 2011, page 929)”. This thesis provides a good starting-point, but more work is recommended to standardise the monitoring of recovery to avoid the production of too much unnecessary information.

### **6.17. Responsibility and Accountability of Data Management**

To ensure proper management of data and dissemination of results it is important to identify who is responsible for the information management (IM) system. Sometimes a recovery management agency with a central data system is established by the Government or United Nations to manage, track and evaluate the whole process. Monitoring systems and protocols should be established for each individual programme – ideally, with indicators defined by the coordinating body so data may be integrated smoothly into the national monitoring system. The government system should provide guidance and tools to agencies so that a standard means of collecting, analysing and inputting the data is established and data isn’t duplicated. The monitoring system is more likely to be successful if rooted in an appropriate institutional context, it is set-up before the disaster and the agencies clearly see the benefit of the system (Amin and Goldstein, 2008).

Several initiatives to standardise post-disaster datasets have already been produced to assist humanitarian actors. The Inter-Agency Standing Committee (IASC) created the Common Operational Datasets (CODs) which are the core datasets needed to support humanitarian response. The CODs include administrative boundaries, populated places, transport network and hydrology, and their guidance material include recommendations on data preparing, naming and use of metadata, storing and sharing (OCHA, 2010). P-Codes are also available from OCHA to ensure all agencies are using standardised place names.

### **6.18. Data Security and Legalities**

As the level of detail obtainable with remote sensing increases the privacy of beneficiaries becomes a more relevant consideration. Maps containing private information should never be made public and in fact individuals’ names are only ever needed during a sign-off procedure. Any socio-economic or vulnerability information in a database should be password-protected to control who has access

to it. Ideally the central database is managed and maintained by the Government and local maps and databases are handed-over to local community groups.

### **6.19. Summary Statement**

In conclusion, time-series analysis of remote sensing data, combined with field work, can be used to monitor many aspects of recovery and provide a host of useful information. Its main strengths include its ability to monitor large areas, its non-intrusiveness and the fact that it minimises the need for access to the study site by the survey teams. It can be used to visualise spatial disparity and progress thus providing accountability to stakeholders, and provide situational understanding to those on the ground, ultimately helping quicker and more effective decision-making.

It can be used to supplement other tools by highlighting areas that need further investigation and by providing suitable samples and data to ground workers. It may also be used to verify other data sources and to identify data gaps as part of a process of triangulation. The images and information extracted from them may form the base of a geospatial database capable of storing datasets collected using both participatory and non-participatory methods. It therefore has the potential to provide a useful spatial framework for tracking and analysing post-disaster recovery data and on which data may be shared between stakeholders working in numerous sectors and geographic locations.

The results suggest remote sensing is particularly well-suited to assist the analysis of accessibility, buildings, internally displaced persons and the natural environment. It can also be used to assist the monitoring of other important sectors including livelihoods and services. The results suggest it might also be used to infer information about the quality of recovery. The approach requires high-spatial satellite imagery with a maximum spatial resolution of 1.0 m. It may be used to provide a holistic or selective view of recovery according to the needs and interest of the user.

This thesis has shown how remote sensing has supported two very different recovery projects. It helped to rapidly map BRC's project area which acted as a baseline of the physical environment to support planning and design as well as operational decision-making. It supported communication between implementers, local authorities and the community throughout the process, and it was used to support the cadastral, enumeration and participation processes. It was also useful as a monitoring tool. With UN-Habitat it helped to quantify the amount of money spent on spontaneous settlement which affected strategic and funding decision-making at government-level. In both cases

remote sensing was useful to justify the need for project funding and to communicate the situation on the ground to different stakeholders and actors.

The data is rapid, independent and reliable; attributes which are particularly valuable in a dynamic post-disaster situation, where security is often an issue and data is hard to obtain. Satellite imagery is available to all and has been shown to be cost-effective. The time and budget requirements for the analysis are also well-known and can be provided at the outset of a project. Once the initial mapping has been finalised and the database constructed, the time and resources necessary to update and query the data are significantly reduced. In contrast, passive systems have been shown to be unreliable and field work is relatively expensive and time-consuming (Amin and Goldstein, 2008). This is not to say remote sensing can replace these existing tools, but should be considered as a complementary method capable of acquiring detailed data throughout a project's duration.

## **6.20. Further Research**

### *6.20.1. New Data Collection Methods*

There has been a dramatic advancement in the development of image-collecting hardware since the commencement of this research. Unmanned Aerial Vehicles (UAVs) offer a new, now widely-available approach to collecting remote sensing information. The flexibility to decide when and where to fly a UAV gives analysts more control over when and how images are collected but there is still wariness over UAV use and permission to fly is not always granted. Most of the indicators presented in this work are very likely to be applicable to UAV data. The ability to fly lower and collect higher-spatial-resolution imagery and to collect off-nadir images and to view the sides of buildings means UAVs have the ability to overcome many of the short-comings associated with satellite imagery, such as the inability to view the sides of buildings and to determine the building's use. The inclusion of radar or lidar on UAVs can also allow the creation of 3D models. More research is recommended to test how this new technology can be used to support post-disaster recovery. Researchers might use the indicator table presented in Chapter 2 as a starting point for such research.

### *6.20.2. Crowdsourcing*

Crowdsourcing the analysis of satellite imagery has also developed during the lifetime of this project. There are now multiple crowdsourcing initiatives – such as Tomnod, Zooniverse, Planetary Response

Network (PRN) and Standby Volunteer Task Force (SBTD) – but they tend to focus on assistance to crisis rather than long-term recovery and development. It would be interesting to see how crowdsourcing could be used to support the monitoring and evaluation of post-disaster recovery both through the analysis of image data and the collection of observations on the ground. In the past, people from around the world have been drawn to assist the immediate aftermath of disasters by identifying damage and displaced people in satellite images. It remains to be seen whether volunteers' interest could be sustained or roused to support the monitoring or evaluation of recovery. Another approach might be to get the affected community themselves involved in the crowdsourcing effort assuming that they are more likely to want to help because of their vested interest in it. This could act as another means of overall engagement and participation of the affected communities in their own recovery.

### *6.20.3. Classification of Imagery*

Despite the recent rise of UAVs, satellite imagery is still an important data source. It has high spatial resolution and crucially has global coverage without restrictions. As this thesis has shown, the accuracy of satellite image analysis varies according to the context being analysed but rarely reaches higher than 80%. To improve the reliability of supervised classification in urban environments the author recommends a thorough spectral, spatial and textural analysis of the construction process as it appears in satellite imagery at different stages of development. This might help to determine which tools might be most suited to extracting features associated with construction such as the laying of foundations. Research is also suggested on how the availability of new spectral bands on satellites, such as Worldview-2 and -3, affect the reliability of semi-automated analysis. Early research also suggests Machine Learning might offer an opportunity to increase the reliability of semi-automatic image analysis (Millow, 2016). It has yet to be tested for post-disaster recovery.

### *6.20.4. Decision-Making Process*

Research to date has tended to focus on the development of new methodologies and algorithms to analyse data instead of looking at how these technologies may be integrated into existing work-flows. The work with the British Red Cross and UN-Habitat (Chapters 4 and 5) provide examples of how remote sensing was useful for two very different users of remote sensing products. More work like this is recommended to bridge the gap between the academic remote sensing and humanitarian communities. It's especially important to determine which products are important and when, to avoid the production of unnecessary information.

*6.20.5. Perceptions/Proxy Indicators*

Finally, work in this thesis has shown there might be potential to use remote sensing indicators to infer information about the quality of recovery or as proxy indicators for social or economic processes. For example, in chapter 3 it was proposed that household contentment could be inferred by looking at variables including the size and location of a reconstructed home. More research is suggested to better understand these associations. Figure 6-4 shows four remote sensing indicators plotted against key informant's perception of recovery 6, 12, 24 and 36 months after recovery. The results show a close correlation (correlation coefficient: 0.96) between the number of buildings counted in satellite imagery over time and the perceptions of housing recovery. There's a slight deviation between length of accessible road (Km) and perceptions of access recovery one year after the earthquake, possibly as there was discontent with the quality of the road surfaces. And there was no correlation between vegetative area (%) and perception of environment recovery because vegetative area was affected by factors such as seasonality and crop abundance. Vegetative areas were also degraded in-and-around camps. It's possible key informants interpreted 'environmental recovery' to include factors other than just vegetative land cover, including dust and pollution. And finally, the night-time light radiance drops in the third year of recovery, possibly due to the removal of planned camps and the subsequent reduction in relief activity. More research is recommended to better understand these patterns and to see if remote sensing can indeed be used to estimate the perceived level of recovery.

## Chapter 6: Conclusion

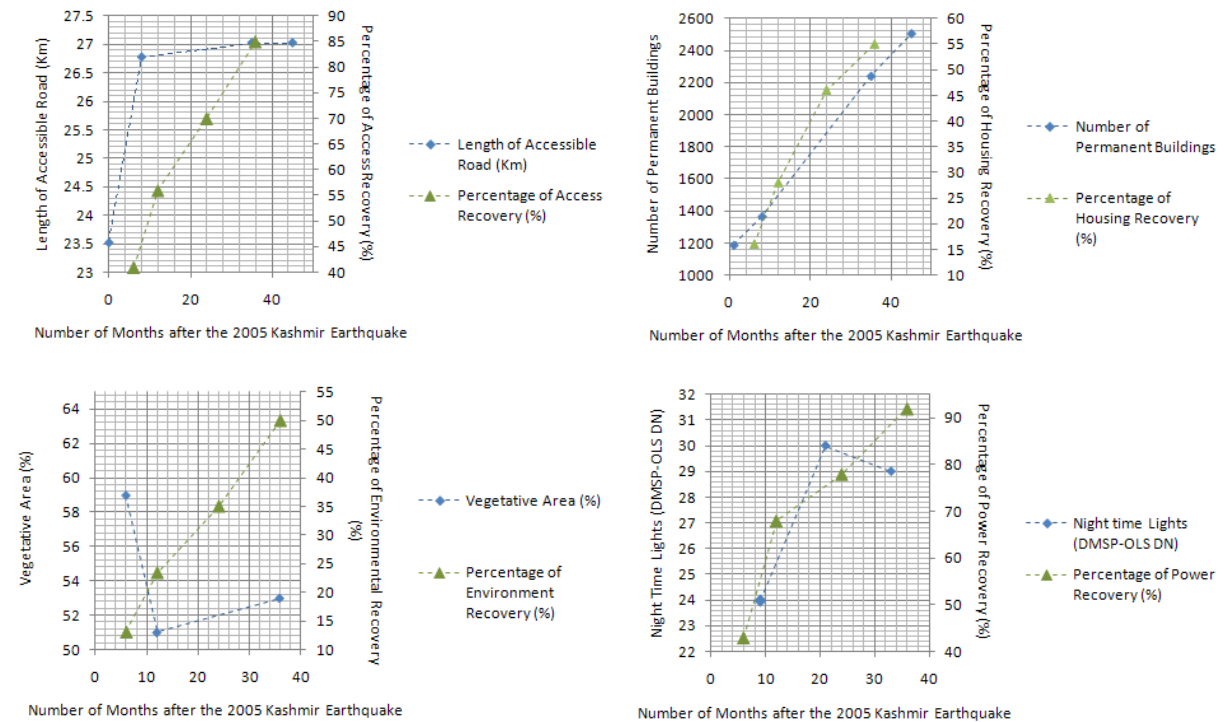


**Figure 6-4: The average percentage of access, housing, environment and power recovery according to key informants plotted against appropriate remote sensing-derived indices.**

## Bibliography

Amin, S. and Goldstein, M. (eds.) (2008). Data against natural disasters. Establishing effective systems for relief, recovery and reconstruction. The World Bank. Washington, DC.

Brown, D. (2012). Geospatial support to Nepal Red Cross' Earthquake Preparedness for Safer Communities project. Consultant report to the British Red Cross, London.

Comerio, M. (2005). Key elements in a comprehensive theory of disaster recovery. *First International Conference on Urban Disaster Reduction*. Kobe, Japan.

Cosgrave, J. and Buchanan-Smith, M. (2016). Evaluation of Humanitarian Action Guide. ALNAP, London.

Cutter, S. L., Boruff, B. J., & Shirley, W. L. (2003). Social vulnerability to environmental hazards. *Social Science Quarterly*: 84, 242–261.

## Chapter 6: Conclusion

Haiti PDNA. (2010). *Haiti Earthquake PDNA: assessment of damage, losses, general and sectoral needs*. Government of the Republic of Haiti, Port-au-Prince.

Donnay, J P., Barnsley, M. and Longley, P. (2001). *Remote Sensing and Urban Analysis*. Taylor and Francis, London.

Foody, G.M. (2014). Rating crowdsourced annotations: evaluating contributions of variable quality and completeness. *International Journal of Digital Earth*: 7(8), 650-670.

IEG (2006). Hazards of nature, risks to development. An IEG evaluation of World Bank assistance for natural disasters. Independent Evaluation Group. The World Bank, Washington DC.

IFRC. (2010). *Owner-driving housing reconstruction guidelines*. The International Federation of Red Cross and Red Crescent Societies. Geneva, Switzerland.

Jha, J.K., Barenstein, J.D., Phelps, P.M., Pittet, D. and Sena, S. (2010). *Safer Homes, Stronger Communities : A Handbook for Reconstructing after Natural Disasters*. World Bank, Washington DC.

Millow, C. (2016). What happens when you combine artificial intelligence and satellite imagery. *Fortune online magazine*. [http://fortune.com/2016/03/30/facebook-ai-satellite-imagery/?xid=for\\_fb\\_sh](http://fortune.com/2016/03/30/facebook-ai-satellite-imagery/?xid=for_fb_sh)

OCHA (2010). *Manual of Geospatial Data*. OCHA, Geneva.

Proudlock, K., Ramalingam, B. and Sandison, P. (2009). *Improving humanitarian impact assessment: bridging theory and practice*. ALNAP, London

Quarantelli, E.L. (1999). The disaster recovery process: what we know and do not know from research. Preliminary Paper #286. University of Delaware. Disaster Research Center.

Hodgson, M.E., Davis, B.A. and Kotelenska, J. (2009). Remote sensing and GIS data/information in the emergency response/recovery phase. In: Showalter, P.S. and Lu, Y. (Eds.) (2009). *Geospatial techniques in urban hazard and disaster analysis*. Springer Science and Business Media, London.

## *Chapter 6: Conclusion*

Voigt, S., Schneiderhan, T., Twele, A., Gahler, M., Stein, E. and Mehl, H. (2011). Rapid damage assessment and situation mapping: learning from the 2010 Haiti earthquake. *Photogrammetric Engineering and Remote Sensing*: 77(9), 923-931.

World Bank, GFDRR and Imagecat (2010). Post-disaster building damage assessment using satellite and aerial imagery interpretation, field verification and modelling techniques. World Bank, GFDRR and Imagecat.

**UNIVERSITY OF CAMBRIDGE UNIVERSITY OF PESHAWAR**

ID  Indicators for Recovery post Kashmir and N Pakistan 2005 Earthquake

**Household Survey**

Introduction : Assalam –o– Alikum

My name is \_\_\_\_\_ We are the M.Sc students from Peshawar University doing titled research with Cambridge University. The information you provide will be confidential, no name and address is written or disclosed. You can refuse to answer a question you don't like. If you want to stop you can. Do you understand the purpose of survey? y/n Do you agree to participate y/n It will take 15-20 minutes. May I start? y/n

Have you been interviewed about the disaster before: y/n How many times? \_\_\_\_ By whom? \_\_\_\_\_

**1. Socio-economic and demographic characteristics of household**

1.1 How many people are in your household now? \_\_\_ Please gives their detail

No.	Relationship to HH	M / F	Age	Marital status & (age at time of marriage)	Education	Occupation	Income
YOU							
2							
3							
4							
5							
6							
7							

1.2 How many people in your household before the disaster? \_\_\_ 1.3 Number of lives lost? \_\_\_ and injured \_\_\_

1.4 After the disaster, did any move away? y/n

1.5 If so, where did they go and why did they move? \_\_\_\_\_

1.6 After the disaster, did any members of your family join you? y/n

1.7 If so, where did they come from and why did they move? \_\_\_\_\_

1.8 When did you move into? (month/year) Tent \_\_\_\_\_ Temporary Shelter \_\_\_\_\_ Permanent House \_\_\_\_\_

**2. Housing** 2.1 What damage did the disaster cause to your home? \_\_\_\_\_

2.2 What happened to your house after the disaster? \_\_\_\_\_

2.3 What financial help did you get for your housing? \_\_\_\_\_

2.5 What technical help did you get? \_\_\_\_\_

2.6 Did you have a say in the design? \_\_\_\_\_

2.7 In what ways is the new home better or worse than before? \_\_\_\_\_

2.8 Did you own the house and/or land prior to the disaster? y/n

2.9 Please describe any problems you suffered with land ownership after the disaster:

.....  
 .....

**3. Location**

3.1 Are you local? y/n 3.2 If you migrated, district of origin \_\_\_\_\_

3.3 Were the members of your household registered at the time of the disaster? y/n

3.4 Did you want to move from your town before the disaster? y/n Why \_\_\_\_\_

3.5 Do you want to move from your town now? y/n Why \_\_\_\_\_

**4. Accessibility and transport**

- 4.1 What problems did you have immediately after the disaster? \_\_\_\_\_
- 4.2 What difficulties do you have now? \_\_\_\_\_
- 4.3 How did you overcome these problems? \_\_\_\_\_
- 4.4 Is your accessibility better or worse now than it was before the disaster? better/worse/remain same
- 4.5 How could the recovery of accessibility have been improved? \_\_\_\_\_

**5. Health**

- 5.1 From the most serious, what health problems have your household suffered as a result of the disaster?
- .....

- 5.3 Did you have any other problems getting treatment? \_\_\_\_\_

**6. Education**

- 6.1 What schools did your children attend? \_\_\_\_\_
- 6.2 What are main problems? (Was the school damaged etc? \_\_\_\_\_
- 6.3 How did you overcome them? What assistance was provided? \_\_\_\_\_
- 6.4 When did your child or children return to school permanently? \_\_\_\_\_
- 6.5 How could the recovery of education have been improved? \_\_\_\_\_

**7. Food**

- 7.1 What problems did you have getting food after the disaster? \_\_\_\_\_
- 7.2 How long were you provided with food aid? \_\_\_\_\_ was it to your liking? \_\_\_\_\_
- 7.3 Has your diet changed since the disaster? \_\_\_\_\_
- 7.4 How could food aid food distribution have been improved? \_\_\_\_\_

**8. Water**

- 8.1 What problems did you have getting clean water? \_\_\_\_\_
- 8.2 How did you overcome these problems? \_\_\_\_\_
- 8.3 When were the following reinstated? (month/year) Temporary supply \_\_\_\_\_ Permanent supply \_\_\_\_\_
- 8.4 How could the recovery of water have been improved? \_\_\_\_\_

**9. Sanitation**

- 9.1 What problems did you suffer from unsanitary conditions? \_\_\_\_\_

**10. Power**

- 10.1 What problems did you suffer with the electricity supply? \_\_\_\_\_
- 10.2 When was your mains power restored? (month/year) \_\_\_\_\_
- 10.3 How could the recovery of power following God forbidden another disaster be improved?

**11. Environment**

- 11.1 In what ways has the surrounding natural environment changed? \_\_\_\_\_
- 11.2 How has this impacted on your life? \_\_\_\_\_

**12. Lifestyle**

- 12.1 In what ways has your lifestyle changed? \_\_\_\_\_
- 12.2 What new appliances have you got? \_\_\_\_\_

**13. Livelihood**

13.1 What were your household's main sources of income? Note if you were unemployed.

	Before	6mths after	1 year after	>2 years after	Now
HH main bread winner Occupation					
Income					

13.2 If you were unemployed, please explain why: \_ \_ \_ \_ \_

13.3 Was there a time when you could not afford the basics? \_ \_ \_ \_ \_

13.4 How did you overcome these problems? \_ \_ \_ \_ \_

13.5 How long did you receive compensation? From who? \_ \_ \_ \_ \_

13.6 Did you receive any advice, retraining or equipment? \_ \_ \_ \_ \_

13.7 Are you trying to find a new job now? y/n Why? \_ \_ \_ \_ \_

**14. Community Recovery**

14.1 God forbidden If the disaster happened again, what aspects should have priority? '1' for immediate '2' can be dealt with later.

Accessibility		Administration and services (fire, police)		Education	
Environment		Food Security		Healthcare	
Housing		Livelihood		Power	
Vulnerability/Safety		Water			

14.2 Are you happy with the speed and quality of recovery as it concerns you? y/n \_ \_ \_ \_ \_

14.3 How could recovery have been made more successful? \_ \_ \_ \_ \_

14.4 Any other comments or observations:

.....

.....

**UNIVERSITY OF CAMBRIDGE UNIVERSITY OF PESHAWAR**

ID  Indicators for Recovery post Kashmir and N Pakistan 2005 Earthquake

**Key Informant Survey**

Name .....

Job title .....

Organisation .....

Where were you at the time of the disaster? .....

**1 Accessibility and transport**

1.1 What locations were difficult to access? Why? .....

1.2 When was reliable access restored to the following locations? (month/year)

Shops/Markets		Health facilities		Schools	
---------------	--	-------------------	--	---------	--

1.3 Were there any other problems with accessibility? .....

1.4 How could the recovery of accessibility have been improved? .....

**2 Health**

2.1 At which hospital, clinic or health facility did most people get treatment? .....

2.2 Did anything prevent people from receiving necessary treatment? .....

**3 Education**

3.1 What problems were there? .....

3.2 What temporary schooling was provided after the disaster? .....

**4 Food**

4.1 What problems were there? .....

4.2 How were these problems overcome? .....

4.3 How could food aid food distribution have been improved? .....

**5 Water**

5.1 What problems were there getting clean water? .....

5.2 Was supply rationed? y/n 5.3 For how long? .....

5.4 When was temporary supply installed? (month/year) \_\_\_\_\_ 5.5 When was permanent supply reinstated? \_\_\_\_\_

5.6 How could the recovery of water have been improved? .....

**6 Sanitation**

6.1 What problems were there from unsanitary conditions? .....

6.2 When were the following services reinstated? (month/year)

Access to a toilet	Removal of rubble and debris	Regular waste collection

**7 Power**

7.1 What problems were there with the electricity supply? -----

7.2 When was mains power restored? (month/year) -----

**8. Community Recovery**

8.1 What percentage impact did the disaster cause to each of the following?

No	Services/amenities	Before (if assumed at)	Immediately after
1	Access to shops and services	100%	
2	Environment around home	100%	
3	Housing	100%	
4	Feeling of safety	100%	
5	Local administration	100%	
6	Schooling	100%	
7	Healthcare	100%	
8	Power	100%	
9	Water and sanitation	100%	
10	Food	100%	
11	Job and livelihood	100%	

8.2 What percentage recovery has been achieved in each of the following?

No	Services/amenities	Before (if assumed)	6mths after	1 year after	2 years after	3 years after	
1	Access to shops and services	100%					
2	Environment around home	100%					
3	Housing	100%					
4	Feeling of safety	100%					
5	Local administration	100%					
6	Schooling	100%					
7	Healthcare	100%					
8	Power	100%					
9	Water and sanitation	100%					
10	Food	100%					
11	Job and livelihood	100%					

8.3 How satisfied are you with the following features of the recovery process. Tick relevant box.

	Very satisfied	Satisfied	Nether satisfied nor dissatisfied	Dissatisfied	very dissatisfied
Access to shops and services					
Environment					
Housing					
Safety					
Administration and Local Services					
Education					
Healthcare					
Power					
Water and Sanitation					
Food					
Livelihood					

Appendix B: Key Informant Survey Form

8.4 God forbidden if the disaster happened again, what aspects should have priorities? Mark '1' for aspects that are immediate priorities and '2' for those that can be dealt with later.

Accessibility		Administration and services (fire, police)		Education	
Environment		Food Security		Healthcare	
Housing		Livelihood		Power	
Vulnerability/Safety		Water			

8.5 Overall, are you happy with the speed and quality of recovery as it concerns you and your community?

.....

8.6 How could the recovery process have been made more successful?

.....

.....

8.7 Any other comments or observations:

.....

.....

.....

.....

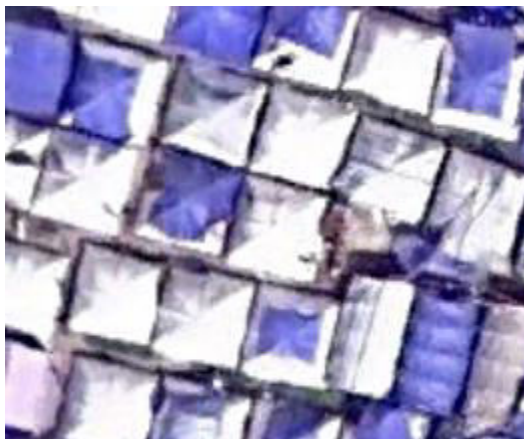
.....

**Non-concrete structures**

**Tents**

Tents are generally made of canvas material and are visible in various shapes, sizes and colours. Tents can be discriminated from corrugated-iron roofs in the imagery due to the presence of non-straight edges and shadows within the roof structure where the material has folded, dipped or where there are ridges. Some tents also have rounded ends and/or small porches at the entrance.

Note: the occupants often cover or extend their tents using pieces of tarpaulin and other loose material. The tarpaulin and canvas material are both likely to weather quickly and thus change colour and shape in the imagery over time.



**Makeshift Shelter**

Makeshift shelters are commonly made by the occupants with tree-pole frames and a combination of plywood panels, corrugated iron sheets and tarpaulin in both the walls and the roof. The tarpaulin roofs differ in colour and generally have a less rigid or regular shape than tents and often do not have pitched roofs.

These structures are commonly seen positioned to the side of construction sites, so it may be assumed that they are providing a temporary shelter solution to households constructing more solid structures.



**Transitional Shelter**

Transitional shelters are one or two room semi-permanent structures located in some planned camps and scattered across the affected region. The structures were constructed by agencies such as UNOPS and use a common building design with plywood panel sheets and corrugated iron sheet roof. The transitional shelters commonly measure 18 m<sup>2</sup> and each include a raised concrete finished plinth and a small veranda area covered by an extended truss roof.



<b>Concrete Structures</b>		
<p><b>Construction Stage 0: Ground Cleared</b></p> <p>The clearance of ground is often (but not always) a precursor to the construction of a building. This process is characterised by the removal of vegetation to leave exposed bare soil, which tends to have a brown-yellow hue and rough textural appearance. The cleared areas are often square or rectangular shape with straight edges. In many cases, the edge of the cleared area represents the extent of the owners' plot of land.</p>	 An aerial photograph showing a rectangular area of cleared, brownish soil in the center of a green, vegetated plot. The cleared area has straight edges and is surrounded by dense green grass and some scattered debris. A small structure is visible in the bottom right corner of the cleared area.	 A ground-level photograph of a cleared plot of land. The soil is brown and uneven. A simple wooden fence made of vertical posts and horizontal rails runs across the foreground. In the background, there are several small buildings with colorful roofs, trees, and hills under a blue sky with scattered clouds.

**Construction Stage 1: Foundations Dug**

Trenches are dug into the ground and if deep enough cast shadows away from the direction of the sun. The shadows and linear features caused by the trenches commonly divide the land into square or rectangular shapes.

Concrete or other materials might be observed near to the trenches due to their bright reflectance, but no concrete or blocks are visible within the trenches at this stage.



**Construction Stage 2: Plinth/Wall Constructed**

Plinth and/or wall material has been laid on top of the trenches. Plinths and walls are identifiable due to their bright reflectance, smooth texture and straight edges. The height of the plinth/wall may be estimated using the length of the shadow and parameters' describing the height of the sun and the position of the satellite at the time the image was acquired.

Note also that in some high-spatial-resolution imagery (<20cm) the re-bars are visible as lines or shadows rising up from the plinths.



**Construction Stage 3: Incomplete Roof**

In some cases a frame might only be half-covered with roof material. The hollow frame is observable at one end of the structure and fixed roofing material at the other end.

Roofing is easily identified as a solid, bright reflecting surface with almost no variation in reflection within the boundaries of the structure. Corrugated iron roofs tend to be pitched which is visible due to differences in reflectance caused by various shading effects. Concrete slab roofs tend to be flat and are therefore more uniform in reflectance and texture.



**Complete Structure**

The structure appears to be complete with a full roof. The height of the building is confirmed by a shadow cast away from the sun.

Note that almost all structures in the study area appear to have corrugated iron roofs.

